ISSN: 2028-9324
CODEN: IJIABO
Impact Factor: 3.456

INTERNATIONAL JOURNAL OF INNOVATION AND APPLIED STUDIES

Vol. 3 N. 4 August 2013

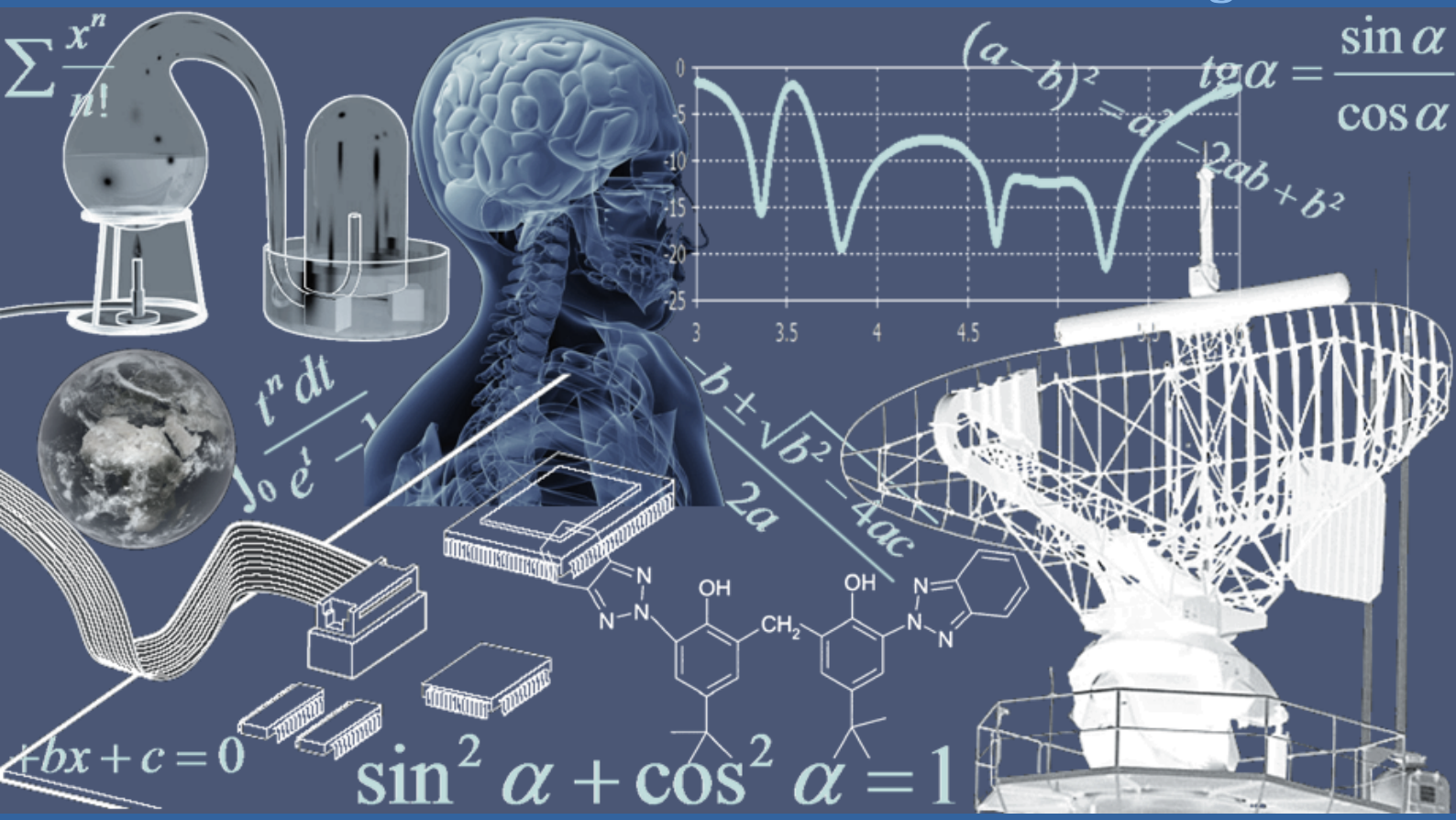

International Peer Reviewed Monthly Journal

Innovative Space of Scientific Research Journals
http://www.issr-journals.org/

International Journal of Innovation and Applied Studies

International Journal of Innovation and Applied Studies (ISSN: 2028-9324) is a peer reviewed multidisciplinary international journal publishing original and high-quality articles covering a wide range of topics in engineering, science and technology. IJIAS is an open access journal that publishes papers submitted in English, French and Spanish. The journal aims to give its contribution for enhancement of research studies and be a recognized forum attracting authors and audiences from both the academic and industrial communities interested in state-of-the art research activities in innovation and applied science areas, which cover topics including (but not limited to):

Agricultural and Biological Sciences, Arts and Humanities, Biochemistry, Genetics and Molecular Biology, Business, Management and Accounting, Chemical Engineering, Chemistry, Computer Science, Decision Sciences, Dentistry, Earth and Planetary Sciences, Economics, Econometrics and Finance, Energy, Engineering, Environmental Science, Health Professions, Immunology and Microbiology, Materials Science, Mathematics, Medicine, Neuroscience, Nursing, Pharmacology, Toxicology and Pharmaceutics, Physics and Astronomy, Psychology, Social Sciences, Veterinary.

IJIAS hopes that Researchers, Graduate students, Developers, Professionals and others would make use of this journal publication for the development of innovation and scientific research. Contributions should not have been previously published nor be currently under consideration for publication elsewhere. All research articles, review articles, short communications and technical notes are pre-reviewed by the editor, and if appropriate, sent for blind peer review.

Accepted papers are available freely with online full-text content upon receiving the final versions, and will be indexed at major academic databases.

Table of Contents

International Journal of Innovation and Applied Studies
ISSN 2028-9324 Vol. 3 No. 4 Aug. 2013, pp. 879-892

http://www.issr-journals.org/ijias/

The effect of soil pH on photo-catalytic oxidation of polycyclic aromatic hydrocarbons (PAHs)

Rakesh M. Pawar, Avice M. Hall, and David C. Naseby

Department of Biotechnology and Pharmacology Health Science,
School of Life Sciences, University of Hertfordshire,
Hatfield, Hertfordshire, England, United Kingdom

ABSTRACT: The environmental fate of polycyclic aromatic hydrocarbons (PAH) is a significant issue, raising interest in its clean up using remediation. However, the physical, chemical, and biological properties of soils can drastically influence degradation of pollutants. The effect of soil pH on degradation of PAHs with a view to modify soil pH to enhance the degradation of PAH's was studied. The degradation rate of key model PAHs was monitored in topsoil modified to a range of pH 4 to 9 at half pH intervals. Photo-oxidation of PAHs in presence of catalyst under UV light at two different wavelengths was studied. The degradation of PAHs during photo-oxidation was carried out at varying soil pH, whilst the degradation rate of individual PAH was monitored using HPLC. Photo-degradation of PAHs at 375 nm showed higher rate of degradation compared at 254 nm. Higher degradation was observed at pH 6.5, whilst in general, acidic soil had greater photo-degradation rates than basic pH of soil. pH 7.5 and pH 8 had slowest photo-degradation. Phenanthrene at both the wavelengths had highest degradation rate and pyrene had slowest degradation rate. Therefore, photo-catalysis can be used as alternative process to eliminate PAHs by manipulating soil pH to enhance remediation.

KEYWORDS: Photo-catalytic oxidation, polycyclic aromatic hydrocarbons, phenanthrene, pyrene.

1 INTRODUCTION

In the natural environment, PAHs undergo an important reaction called photolysis [10], [11]. Photocatalysis (also called photolysis) is a process which uses catalysts such as Titanium dioxide (TiO_2) which facilitates photoreaction in order to degrade the toxic compound. TiO_2 a photo-catalyst is a chemical compound that, in presence of various wavelengths of UV light becomes highly reactive. TiO_2 induced photo-catalytic degradation of a variety of organic substrates is gaining attention due to its potential to degrade PAHs, specifically the PAHs in the environment [13].

Photo-catalytic oxidation (PCO) of PAHs occurs either in solution or in solid phase and also when catalyst is adsorbed onto solid substances. However, recently it has been investigated that photo-catalytic degradation of PAHs may occur in aqueous TiO_2 suspensions [13]. It has been found that when aromatic compounds are exposed to UV light, partially oxidized intermediates of the aromatic compounds are produced which are more susceptible to degradation than their parent compounds. Because of this property of aromatic compounds, photo-degradation has been recommended as an early stage strategy for biodegradation [9]. Photo-degradation of PAHs in the presence of a catalytic solution is considered as an oxidative process which has been further augmented in the presence of photo-inducers. The polarity of the solvent is directly proportional to the rate of the degradation process hence, the higher the polarity of the solvent, the faster the degradation process.

Thus, PAH photo-decomposition initiated by photo-ionization results in the production of PAH radical cations and hydrated electrons which further destroy PAH in the presence of water [15], [16]. PCO, one of the many advanced oxidation processes, relies on the generation of •OH by photo-catalysts (e.g. titanium dioxide semiconductor, TiO_2) to trigger oxidative

Corresponding Author: Rakesh M. Pawar (rakesh.pawar29@gmail.com)

degradation [17]. TiO_2, a semiconductor can be used in photo-catalysis when exposed to ultraviolet (UV) light irradiation, due to its ability to transfer electrons and promote oxidation or reduction which plays a vital role in photo-catalysis [17].

A number of studies on the adsorption of PAHs on silica, alumina and other surfaces have been reported. However, the present work focuses on the possible advantages of various photo-catalytic processes using TiO_2 for the degradation of PAHs present in soil.

However, very few studies have investigated the photo-catalytic degradation of PAHs on soil surfaces using TiO_2 as the catalyst under UV irradiation. Investigating photo-catalytic degradation using a catalyst under varying abiotic conditions particularly soil pH, to enhance the degradation process is one of the objectives of this particular study.

2 MATERIALS AND METHODS

2.1 CHEMICALS

The test PAHs, namely phenanthrene (PHE), anthracene (ANT), fluoranthene (FLU) (Sigma) and pyrene (PYR) (Fluka) were used throughout the experiment. Acetonitrile (HPLC grade), n-hexane (Fisher Scientific, UK). Particles of TiO_2 (Sigma Aldrich), UK.

2.2 STANDARD CURVE FOR PHOTO-CATALYTIC OXIDATION

2.2.1 PAHS STANDARD SOLUTION

A standard curve was made using the different concentrations in ppm of each PAH. 100 mg of each of these individual PAHs were dissolved in 1000 ml of acetonitrile to make 100 ppm of standard stock solutions which were further diluted to produce a standard curve for HPLC analysis. Carbazole (Sigma Aldrich) was used as the internal standard.

2.3 PHOTO-CATALYTIC DEGRADATION OF PAHS

See figure 1 for a schematic representation of the experimental design.

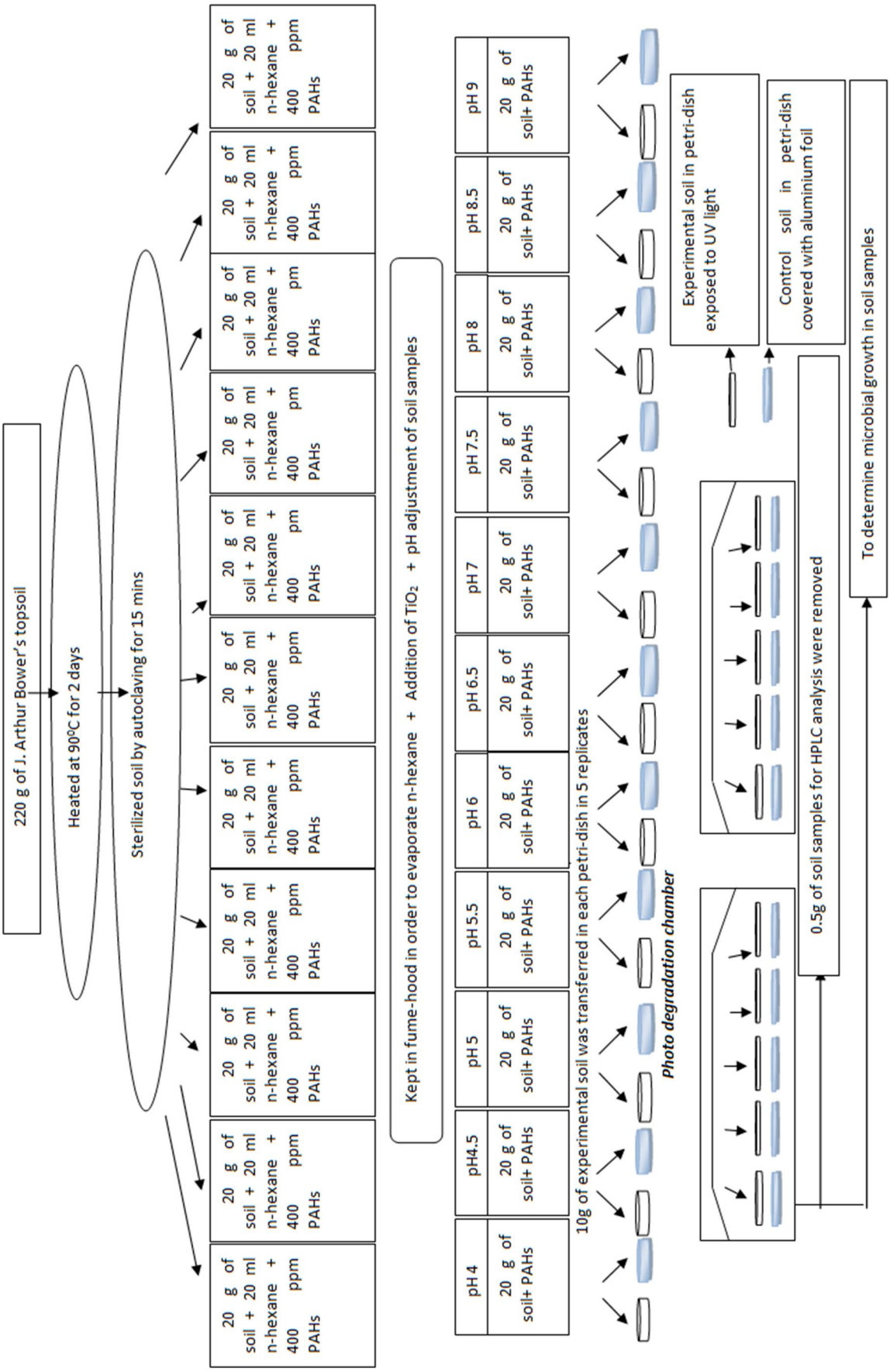

Fig. 1. Schematic representation of experimental design

2.4 PHOTO DEGRADATION CHAMBER

Photo degradation studies were performed in a chamber as shown in figure 1. The UV irradiation intensity was 1041_Wcm^{-2}. The UV lamps (Phillips ATLD 20W, Model UVA, UVB and UVC) were set at wavelengths of 254, and 375 nm. 90 mm plastic petri dishes containing the experimental soil samples were placed under the UV light for photo irradiation. The distance between the lamps and soil samples was 120 mm. Temperature within the chamber was maintained at 20^0C throughout all the experiments.

2.5 DISSOLUTION OF PAH COMPOUNDS AND TiO_2 AS CATALYST IN J. ARTHUR BOWER'S TOPSOIL

20 mg of each PAH was added to 20 ml of n-hexane in 500 ml sterile conical flask and used to contaminate 20 g of J. Arthur Bower's topsoil giving a final concentration of 100 ppm and 2% aqueous TiO_2 (Sigma Aldrich) was added. The weight of the pots containing J. Arthur Bower's topsoil was measured to confirmation evaporation of n-hexane.

2.6 MONITORING PH AND MOISTURE CONTENT OF THE EXPERIMENTAL SOIL

40 g of soil was transferred to seven different pots in order to monitor the pH of the soil along with PAH. Furthermore, deionised water was added to maintain a 30% moisture content of the soil and the pH was adjusted as half interval. From the eleven different pots containing soil of each pH treatment, 20 g of soil was transferred into five petri-dishes resulting in 5 replicates. All replicates were maintained at 20^0C in UV light chamber throughout the experiment. Treated samples from the Petri-dish were removed at 0, 24, 48, 72, 96, 120 hours respectively.

2.7 SAMPLES FOR HPLC ANALYSIS AND PAH EXTRACTION

0.5 g of treated sample, from the 5 replicates of petri-dishes was transferred into 1.5 ml Eppendorf tubes. PAHs were extracted in the eppendorf containing 200 ppm carbazole as an internal standard to 0.5 g of soil before analysis by HPLC. Samples were mixed well using round vortex mixer fitted with multi sample holder which holds a total of 12 samples (Sigma Aldrich) for 5 minutes and extract was filtered using sterile mill pore filter (HPLC grade) prior to HPLC analysis.

2.8 STATISTICAL ANALYSIS

Data obtained from experiments were used for statistical analysis. The final graphed values are represented as mean SD (Standard deviation). Statistical analysis was carried out performing calculations, analyzing and visualizing data in SPSS Statistic 16.0 version. Least significant difference and Tukeys HSD between two different wavelengths was calculated using variance post hoc test in SPSS analysis. And all the graphs were plotted in Microsoft office Excel 2007.

3 RESULTS

3.1 HPLC ANALYSIS OF PAH

To study the effect of abiotic factors particularly soil pH on the rate of photo-degradation, HPLC analysis was employed.

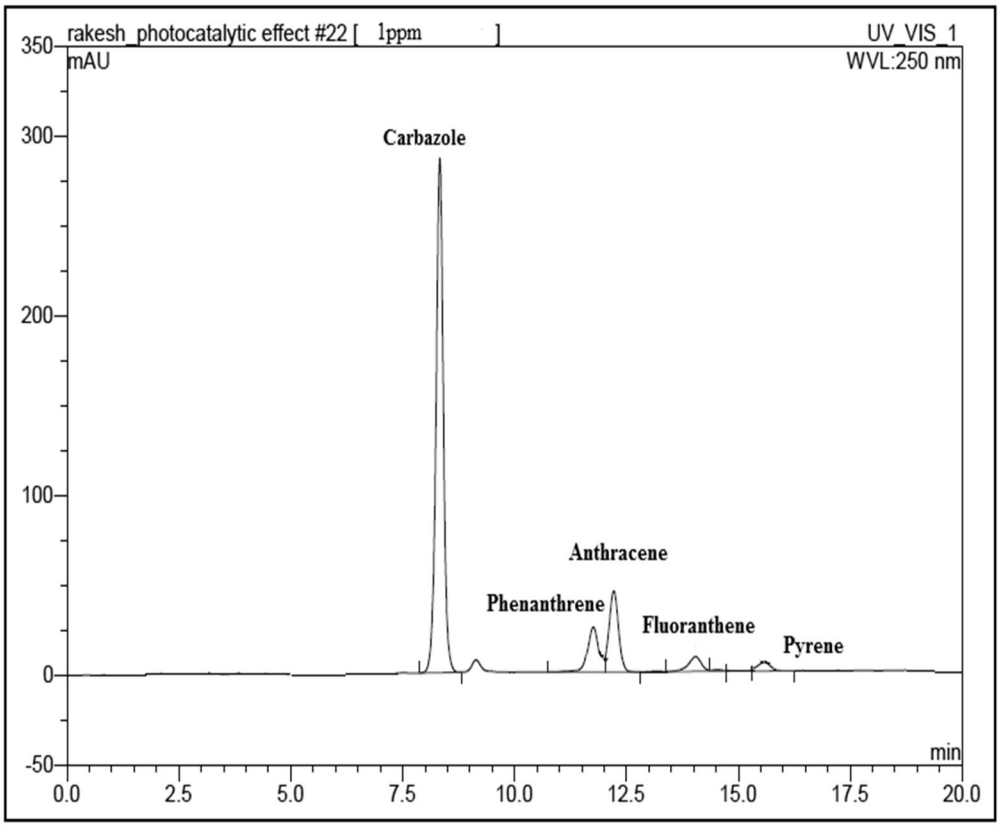

Fig. 2. Standard Chromatogram for HPLC analysis of four PAHs (concentration 1 ppm) and carbazole (20 ppm) with peak height against time

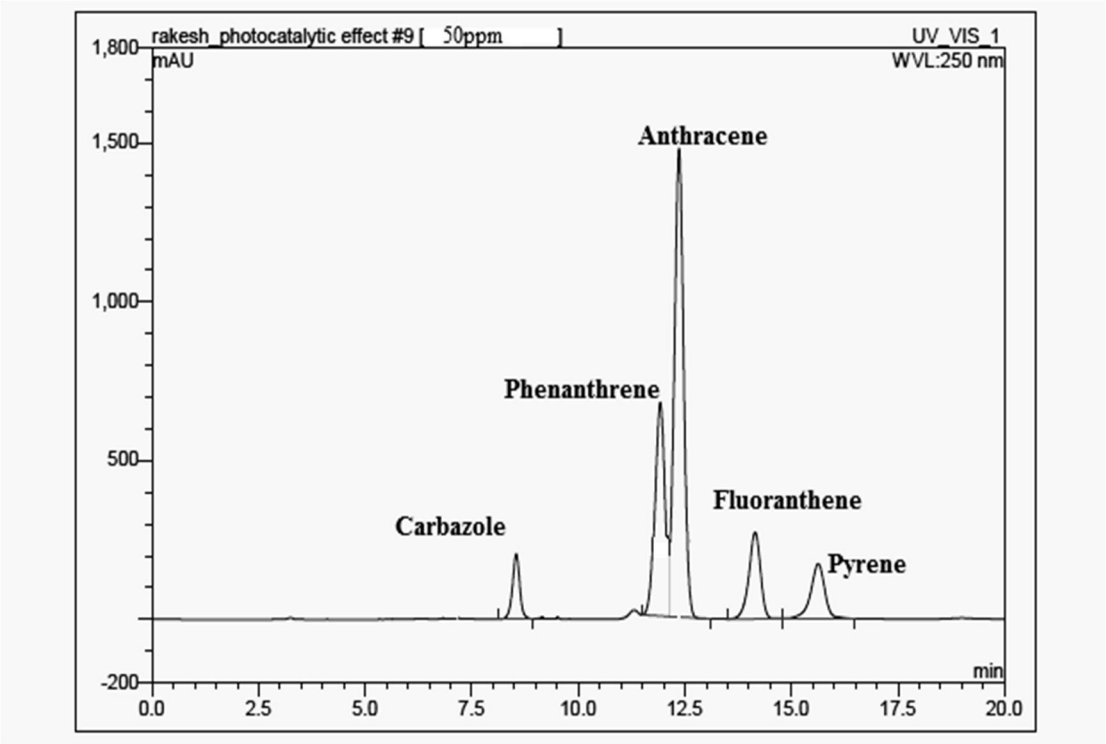

Fig. 3. Standard chromatogram for HPLC analysis of four PAHs (concentration 50 ppm) and carbazole (20 ppm) with peak height against time

Figures 2 and 3 show HPLC standards for 1 ppm and 50 ppm concentration of the four different PAHs dissolved in acetonitrile. The four PAHs present in the contaminated soil were also extracted using acetonitrile. Carbazole was the internal standard representing the first peak in both chromatograms at 20 ppm with a retention time of 8min. In figure 2 carbazole peak area was 300 mAU/min; similarly the peak area in figure 3 was 300 mAU/min with no difference in retention time. Therefore, constant results were found for carbazole. Phenanthrene follows carbazole with a retention time of 11 min and peak area of 30 mAU/min for 1 ppm and 700 mAU/min for 50 ppm. Anthracene is the third peak and second PAH to elute with a retention time of 12.5 mins. Anthracene, and phenanthrene peaks merge in both chromatograms before reaching the x axis. The split peak facility of the chromeleon software was implemented to statistically attribute peak area to these two PAHs. Anthracene at 1 ppm resulted in a peak area of 50 mAU/min and 1500 mAU/min for 50 ppm. The fourth peak and third PAH to elute was fluoranthene at 13 mins with a peak area of 20 mAU/min for 1 ppm and peak area of 300 mAU/min for 50ppm with no differences seen in retention time. The final PAH to elute was pyrene with a peak area of 10 mAU/min for the 1 ppm concentration whereas the peak area for pyrene in 50 ppm concentration was 200 mAU/min.

3.2 STANDARD GRAPH FOR POLYCYCLIC AROMATIC HYDROCARBONS

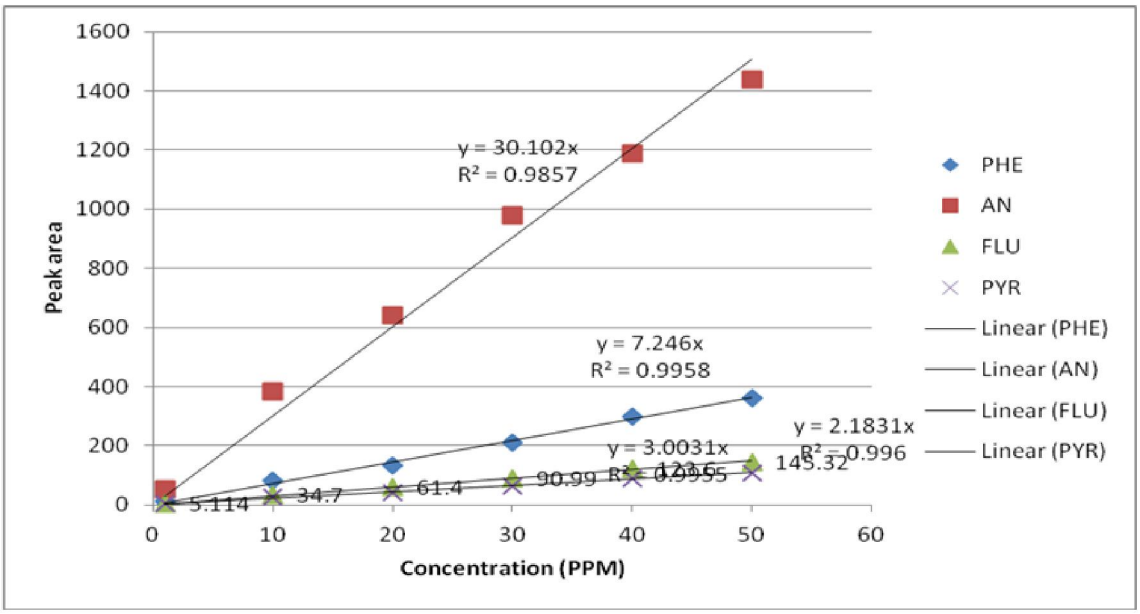

Fig. 4. HPLC standard curve of four PAH showing peak area against concentration. PAH used and their symbol abbreviations are (PHE) Phenanthrene; (AN) Anthracene; (FLU) Fluoranthene; (PYR) Pyrene

The peak areas obtained from running standards of the four PAHs at 1 ppm, 10 ppm, 20 ppm, 30 ppm, 40 ppm, 50 ppm were used to plot standard curves of peak area against the PAH concentration (figure 4). The chromeleon software was used to calculate a linear regression for each PAH (figure 4.). All PAH have r^2 (regression coefficient) values above 0.97 whilst the slope was estimated and displayed as Y values. The r^2value was 0.987 for phenanthrene, 0.978 for fluoranthene, 0.979 for pyrene and r^2 values for anthracene was 0.983 respectively. The Y value was around 35x for anthracene, 14x for phenanthrene, whilst fluoranthene and pyrene were much lower at 6.42x and 4.08x respectively.

In order to have a full evaluation of the extraction efficiency of the four PAHs, 100 ppm of each individual PAH was added to J. Arthur Bower's topsoil and extracted with acetonitrile. The re-extraction efficiency of the four PAHs obtained from these samples ranged from 52.81 to 74.69 % (table 1).

Table 1. Extraction efficiency of four PAHs from J. Arthur Bowers topsoil

PAH used	Amount of PAH added (ppm)	% efficiency for experimental values
Phenanthrene	100	74.69
Anthracene	100	68.42
Fluoranthene	100	64.98
Pyrene	100	52.81

3.3 DEGRADATION OF POLYCYCLIC AROMATIC HYDROCARBONS OVER TIME

Figures 5 to 12 exhibit the degradation curves obtained for the four different PAH in treated soil samples at varying pH under UV irradiation at 254 nm and 375 nm. PAH remaining is displayed as a percentage of the HPLC quantification results obtained after re-extraction at time 0. The control at both wavelengths exhibited little degradation figure (5 to 12 A) in contrast to the samples exposed to UV light figure (5 to 12 B). Greater degradation was more evident at 375 nm (figure 5 B to 9 B) than 254 nm (figure 10 to 12) for all PAHs with a significance value of $P<0.05$ obtained (Post hoc test including LSD and Tukey's test). Phenanthrene showed the highest degradation followed by anthracene, pyrene and fluoranthene. At 375 nm phenanthrene was 80-85% degraded and around 60- 65% degraded at 254 nm. The photo-catalytic degradation rate of anthracene was slower than phenanthrene whilst its degradation rate generally increased at acidic pH with most rapid rate evident at pH 6.5. At 375 nm anthracene was 75-80% degraded and at wavelength 254 nm degradation was 65-70%. Fluoranthene followed after anthracene was 70% degraded at 375 nm and 65% at 254 nm. Around 65% degradation was observed for pyrene at 375 nm and 60% degradation observed at 254 nm.

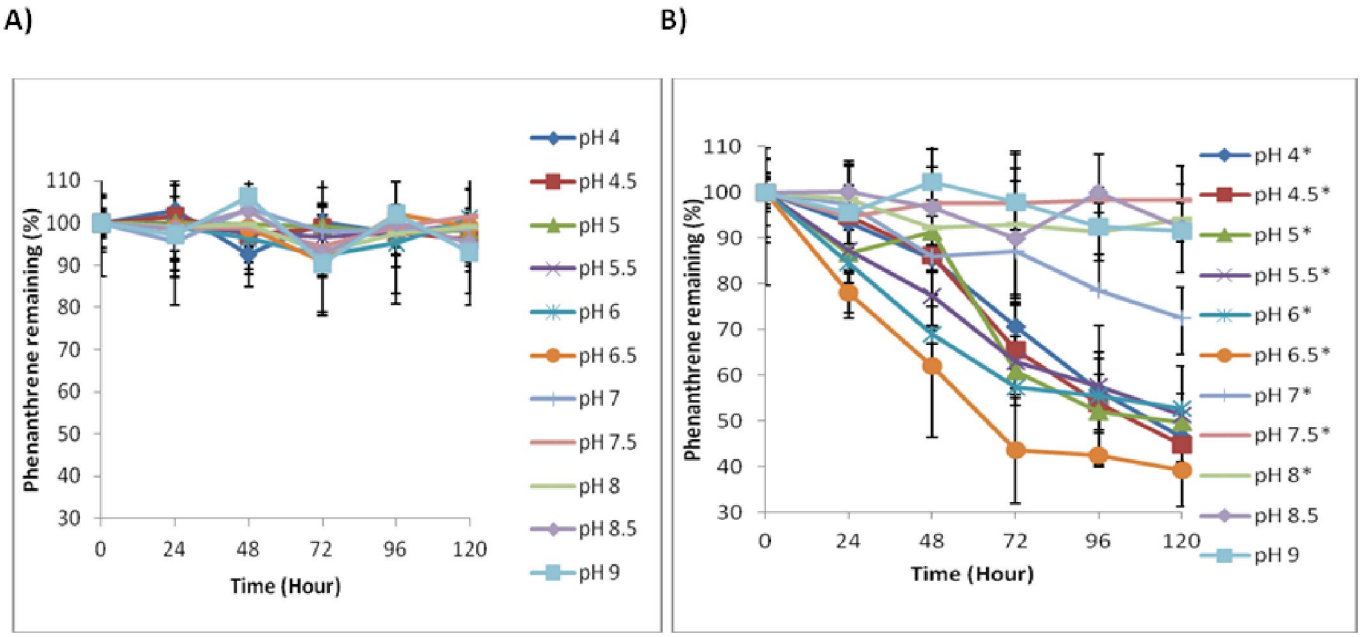

Fig. 5. Percentage phenanthrene remaining in J. Arthur Bower's topsoil at different pH over time during exposure to UV light at 375 nm in the presence of TiO_2

A): Percentage phenanthrene remaining in control samples not exposed to UV light. B): Percentage phenanthrene remaining in experimental sample exposed to UV light at 375 nm. *P<0.05 indicates significant difference between control and experimental sample.

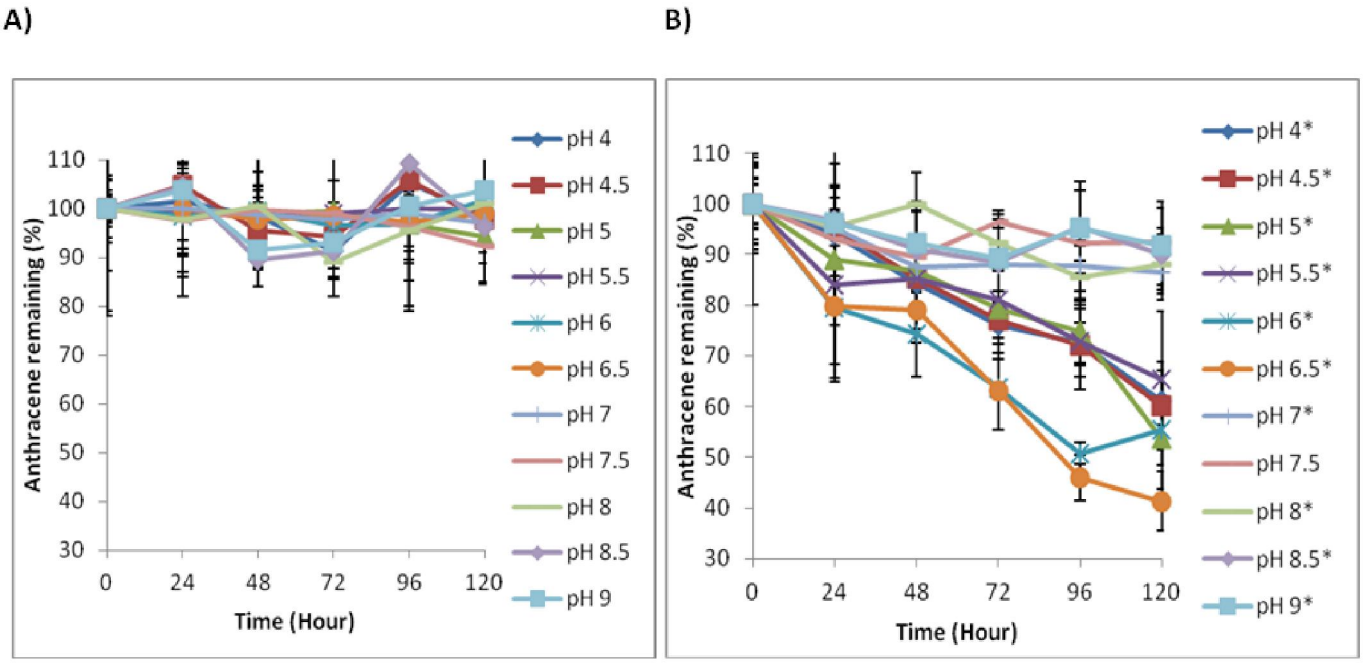

Fig. 6. Percentage anthracene remaining in J. Arthur Bower's topsoil at different pH over time during exposure to UV light at 375 nm in the presence of TiO_2

A): Percentage anthracene remaining in control samples not exposed to UV light. B): Percentage anthracene remaining in experimental sample exposed to UV light at 375 nm. *P<0.05 indicates significant difference between control and experimental sample.

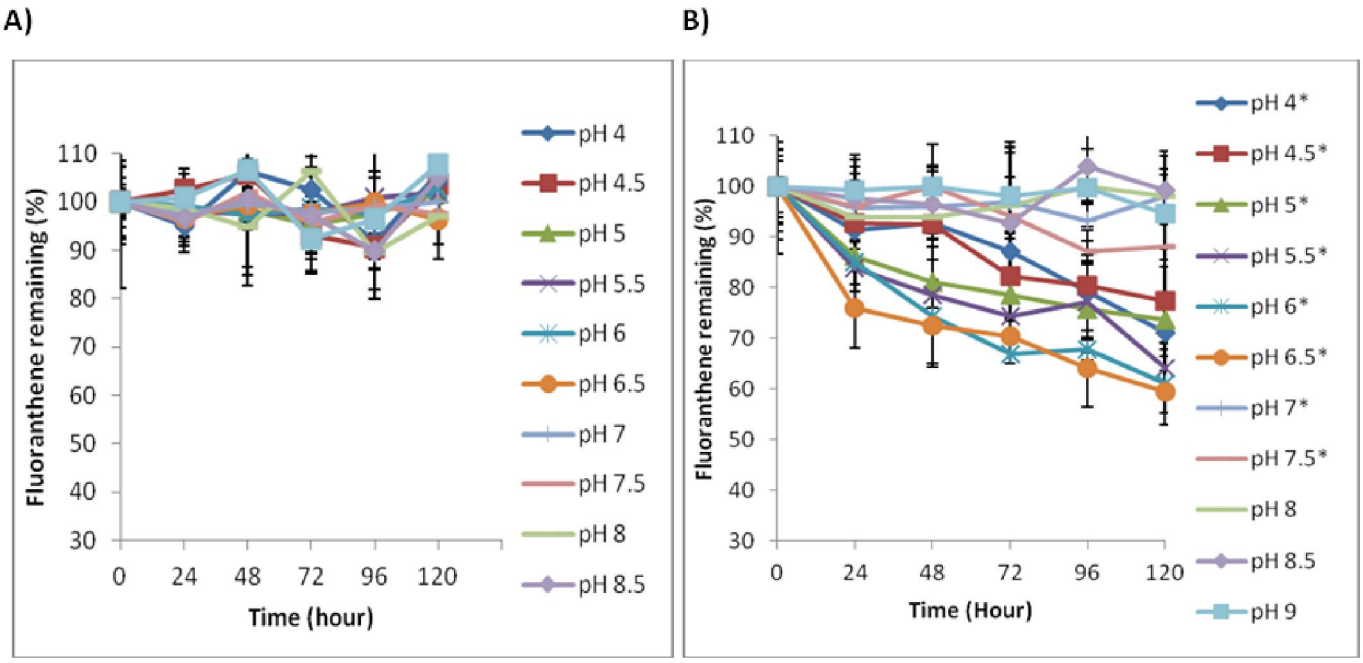

Fig. 7. Percentage fluoranthene remaining in J. Arthur Bower's topsoil at different pH over time exposure to UV light at 375 nm in the presence of TiO_2

A): Percentage fluoranthene remaining in control samples not exposed to UV light. B): Percentage fluroanthene remaining in experimental sample exposed to UV light at 375 nm. *P<0.05 indicates significant difference between control and experimental sample.

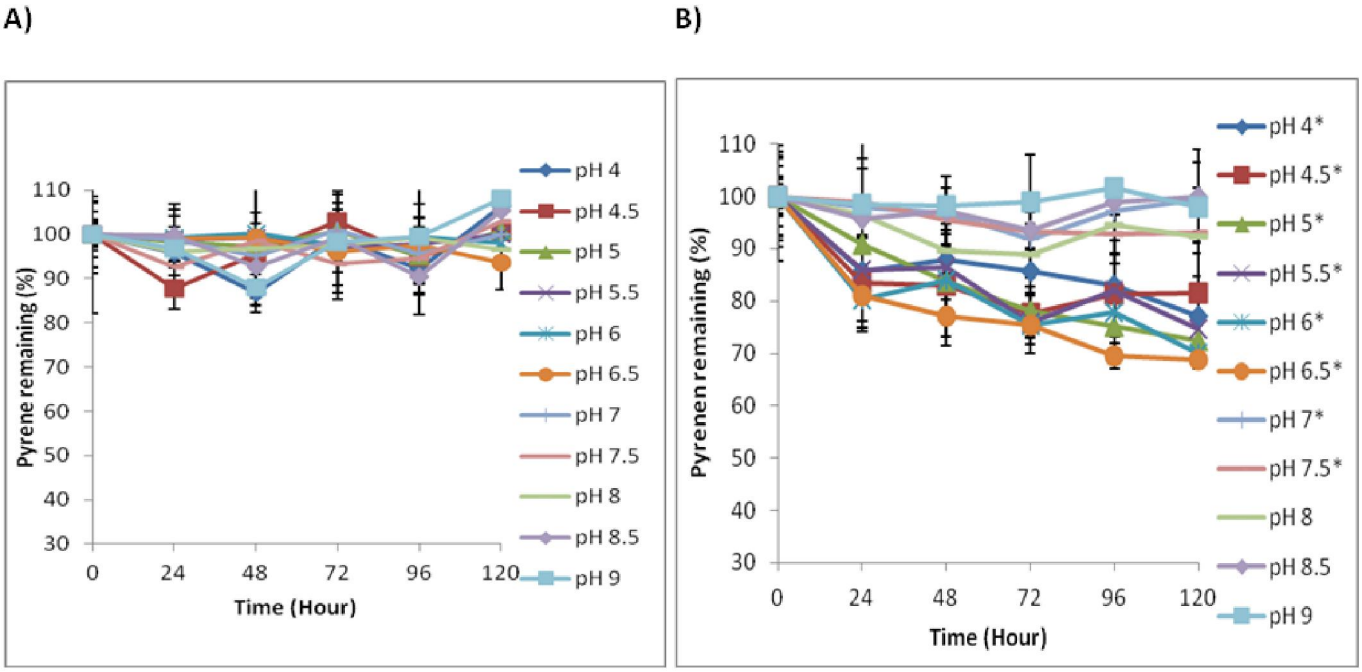

Fig. 8. Percentage pyrene remaining in J. Arthur Bower's topsoil at different pH over time during exposure to UV light at 375 nm in the presence of TiO_2

A): Percentage pyrene remaining in control samples not exposed to UV light. B): Percentage pyrene remaining in experimental sample exposed to UV light at 375 nm. *P<0.05 indicates significant difference between control and experimental sample.

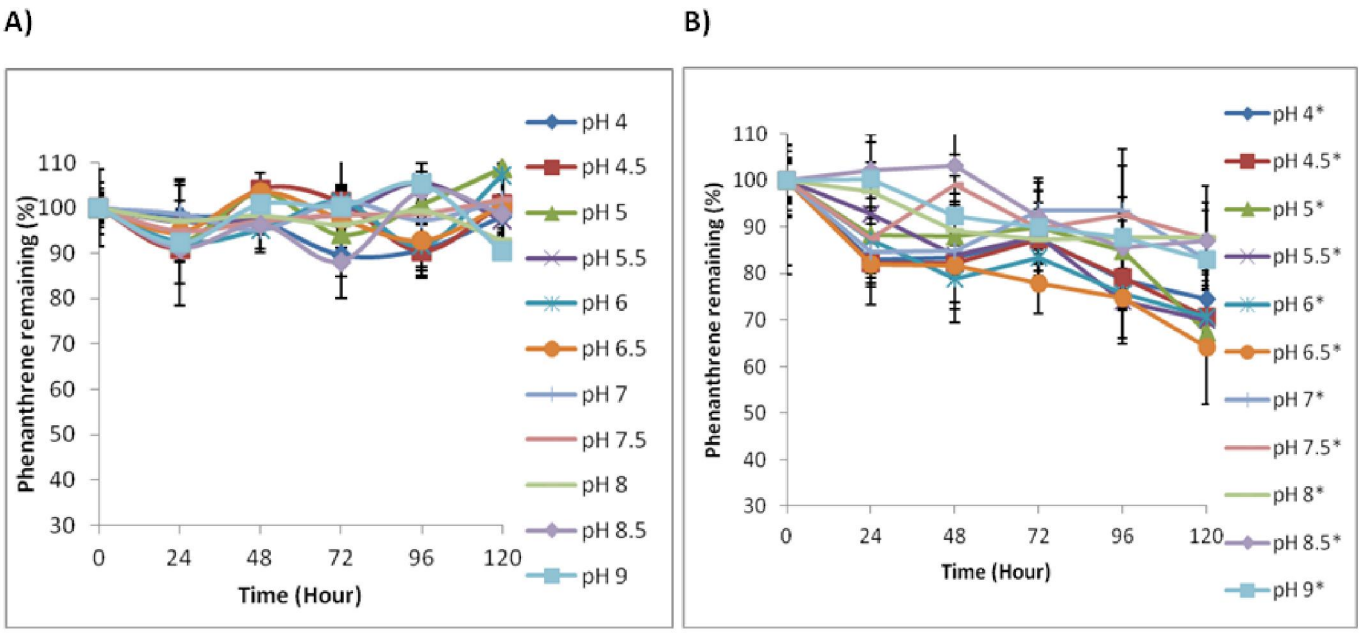

Fig. 9. Percentage phenanthrene remaining in J. Arthur Bower's topsoil at different pH over time during exposure to UV ligh at 254 nm in the presence of TiO_2

A): Percentage phenantherene remaining in control samples not exposed to UV light. B): Percentage phenantherenemaining in experimental sample exposed to UV light at 254 nm. *P<0.05 indicates significant difference between control and experimental sample.

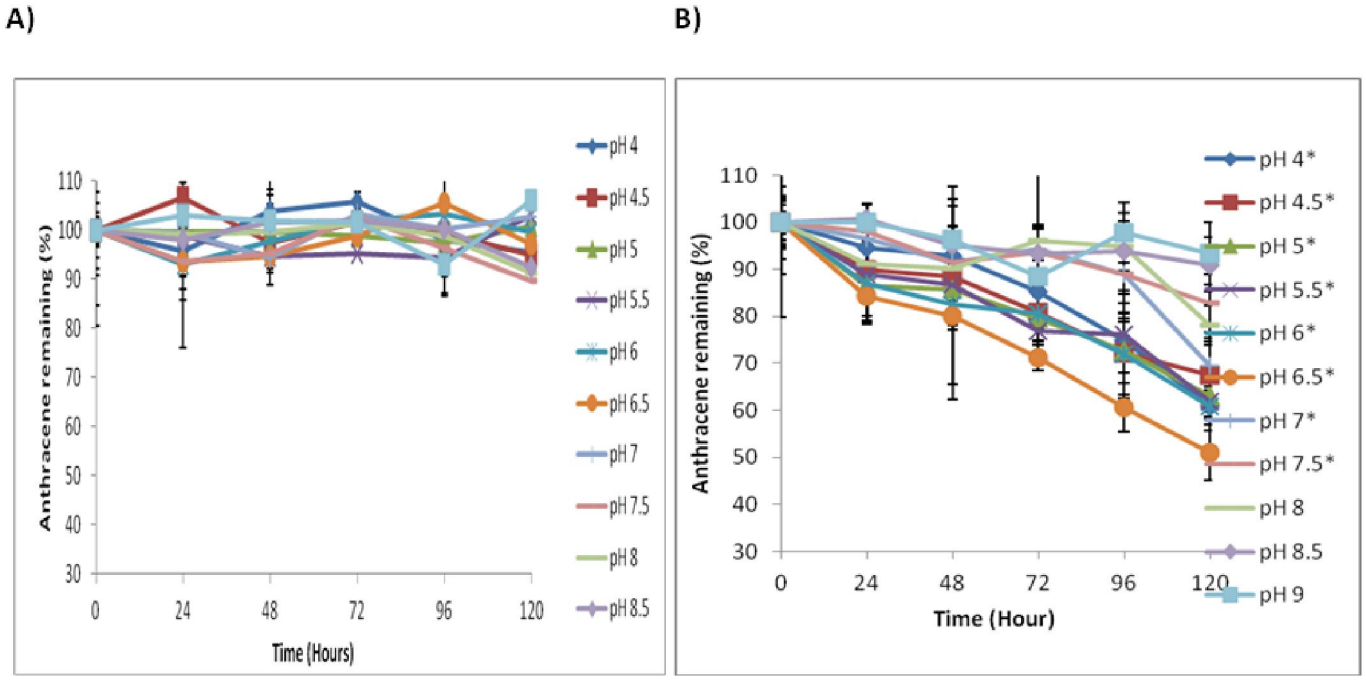

Fig. 10. Percentage anthracene remaining in J. Arthur Bower's topsoil at different pH over time during exposure to UV light 254 nm in the presence of TiO_2

A): Percentage anthracene remaining in 254nm control samples not exposed to UV light. B): Percentage anthracene remaining in experimental sample exposed to UV light at 254 nm. *P<0.05 indicates significant difference between control and experimental sample.

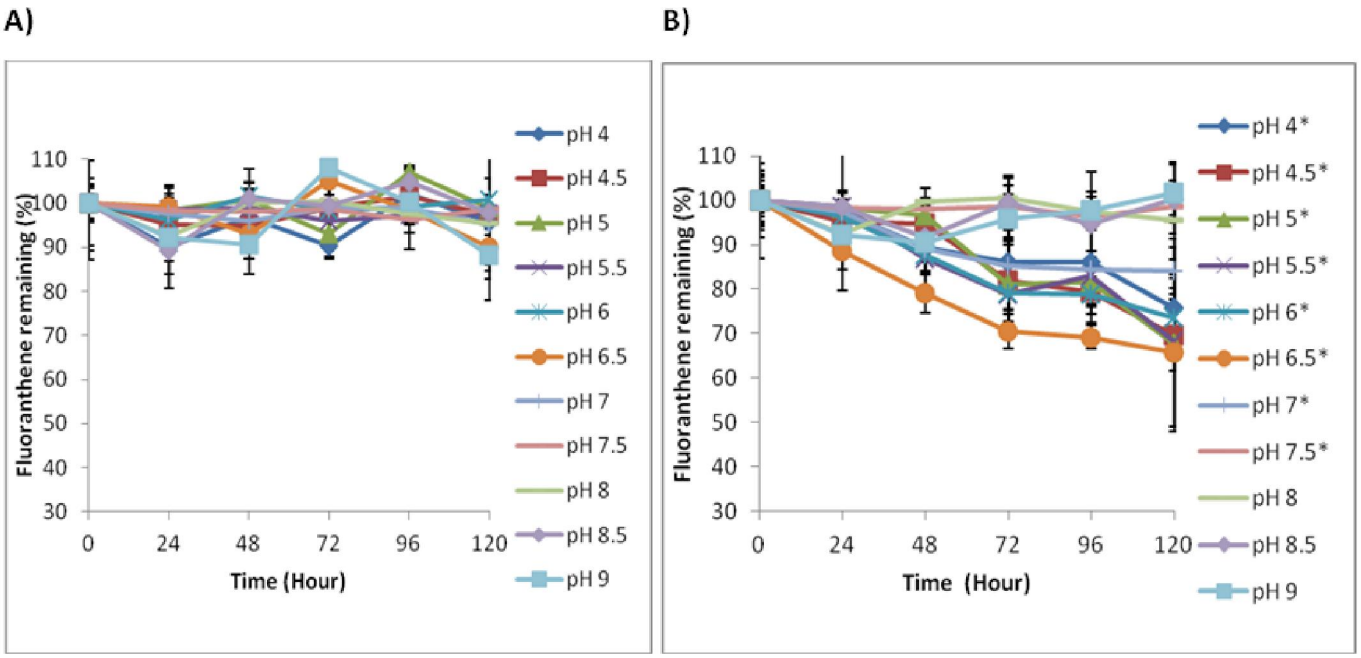

Fig. 11. Percentage fluoranthene remaining in J. Arthur Bower's topsoil at different pH over time during exposure to UV light 254 nm in the presence of TiO_2

A): Percentage fluoranthene remaining in control samples not exposed to UV light. B): Percentage fluoranthene remaining in experimental sample exposed to UV light at 254 nm. *P<0.05 indicates significant difference between control and experimental sample.

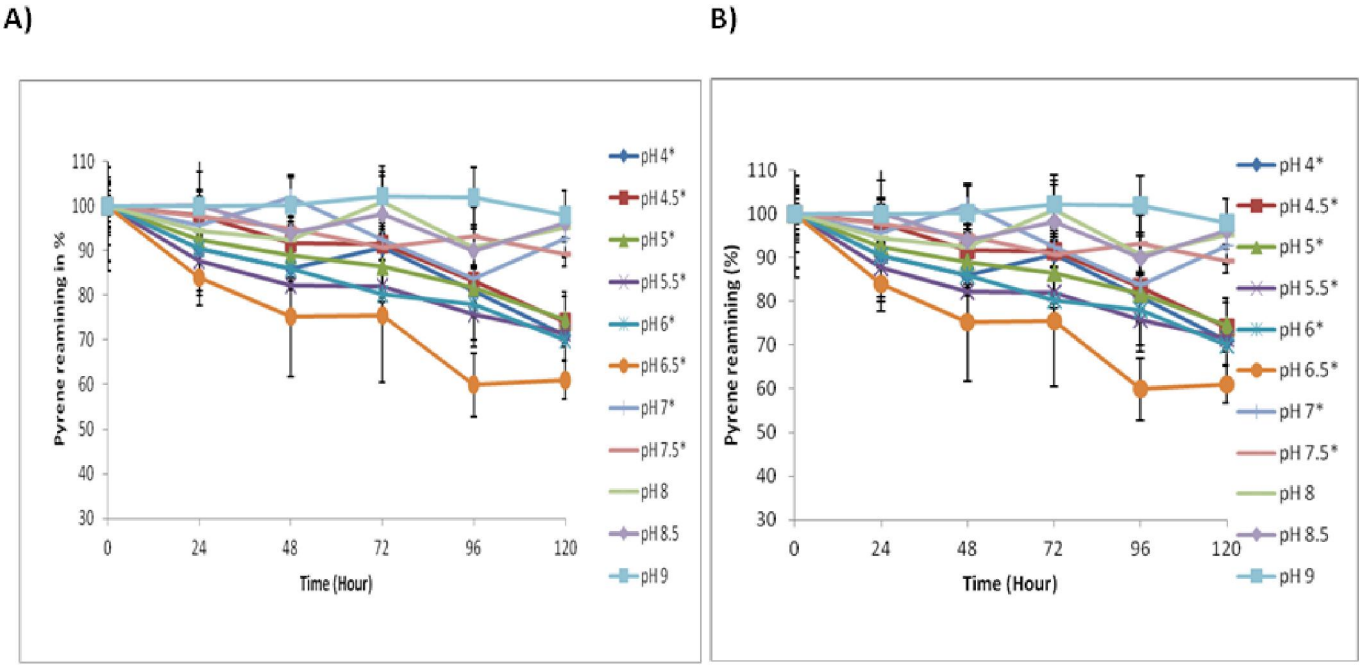

Fig. 12. Percentage pyrene remaining in J. Arthur Bower's topsoil at different pH over time during exposure to UV light at 254 nm in the presence of TiO_2

A): Percentage pyrene remaining in control samples not exposed to UV light. B): Percentage pyrene remaining in experimental sample exposed to UV light at 254 nm. *P<0.05 indicates significant difference between control and experimental sample.

Degradation rate was studied using HPLC for each PAH by calculating the remaining percentage of individual PAH. Phenanthrene, anthracene, fluoranthene and pyrene percentage were constant in all controls with very low degradation rates observed not exposed to UV irradiation. Greater degradation was observed at 375 nm compared to 254 nm with significance P<0.05. Time 0, was plotted at 100% in order to show the remaining percentage of individual PAHs in soil pH.

It was demonstrated in this study that photo catalytic degradation rates were greater in acidic soil pH (pH 5.0, 5.5, 6.0, 6.5) when compared to alkaline soil pH (7.5, 8.0, 8.5, and 9.0) and neutral soil pH (7.0) for each of individual phenanthrene, anthracene, flouranthene and pyrene. In figure 5-12 B, pH 6.5 exhibits greater degradation rate followed by pH 5.5, pH 6.0, pH 5.0, pH 4.5 and pH 4. However, at alkaline soil pH lower degradation rates were evident. Among alkaline soil pH greater degradation was measured in pH 7.5 followed by pH 8.5, pH 8.0 and pH 9.0.

Thus, UV irradiation by two different wavelengths in experimental soil in the presence of TiO_2 resulted in greater degradation at soil pH<6.5, whereas lower degradation resulted under alkaline conditions pH>6.5.

In general, results obtained during photo-catalytic degradation exhibited high influence on soil pH with highest rate of degradation obtained for low-molecular weight (LMW) PAH (phenanthrene and anthracene) when compared to high molecular weight PAH (fluoranthene and pyrene).

4 DISCUSSION

4.1 STANDARD CHROMATOGRAMS FOR HPLC

Standard curves were prepared using the HPLC analysis. Carbazole was used at the same concentration (20 ppm) in all experiments as an internal standard to monitor reproducibility of results. Concentrations of PAHs used for standard curves were 1 ppm, 10 ppm, 20 ppm, 30 ppm, 40 ppm, 50 ppm respectively; as the concentration in experimental samples would not reach levels above 50 ppm and the lower limit of detection is in the region of 1 ppm.

The peaks appearing on the chromatogram were observed based on the number of rings and molecular weights of the PAHs. The order of peaks was phenanthrene followed by anthracene, fluoranthene and at last pyrene. The peak of

phenanthrene and anthracene appear to be merged in the chromatogram (section 3.1 in figure 2 & 3). The split peak facility of the chromeleon software was implemented to separate the peaks of the two PAHs (phenanthrene and anthracene) and was reproducible with standard PAH solutions. Anthracene resulted strong signals and appeared with larger peaks due to the linearity of the molecule as UV detection is greater for linear molecules [7].

Phenanthrene and anthracene are three ring compounds with molecular weight of 178.23 and appear before fluoranthene and pyrene (molecular weight 202.26) [5]. Although, anthracene and phenanthrene are stereoisomers, anthracene is a linear molecule while phenanthrene is non-linear, resulting in an anthracene being more hydrophobic and thus eluting from the column a little slower in the 90:10 acetonitrile: deionised water mobile phase. Peak area of anthracene at a particular retention time gives better symmetry to the molecule which consequently leads to less solubility in extraction solution. Therefore, in general anthracene is expected to degrade slower than phenanthrene followed by fluoranthene and then by pyrene based on their solubility/ hydrophobicity and molecule size [12].

In addition to this, phenanthrene has low molecular weight and is a three ring compound with high solvent solubility [7]. Whereas, fluoranthene and pyrene have lower solvent solubility [5]. Pyrene is a fused four ring compound with very low extractability. The low solvent extractability of pyrene might be due to its high hydrophobicity (sorption partition coefficient log K_{oc}: 4.88; water solubility= 0.13 mg l^{-1}) [7].

4.2 STANDARD CURVE

With respect to chromatogram obtained in the results displayed in figure 2 & 3, a standard curve was constructed to study the PAHs peak area in the standard solution based on their retention time. A linear standard curve (figure 4) was produced for each PAH with the regression coefficient of 0.97 for phenanthrene, 0.97 for fluoranthene, 0.97 for pyrene and 0.98 for anthracene. The value of the regression coefficient obtained for each calibration curve shows that the correlation between relative peak area and concentration was linear and reproducible within selected concentration range. The Y value representing linear regression equation for phenanthrene was 14.32x and for anthracene was 35.12x, whilst for fluoranthene and pyrene the values were much lower at 6.42x and 4.08x respectively. Thus, the data obtained from standard chromatogram were reliable and accurate (figure 4).

4.3 EXTRACTION EFFICIENCY

Contaminated J. Arthur Bower topsoil was used to examine the extraction efficiency (table 1) of the PAHs using HPLC analysis. All four PAHs were extracted with the greatest extraction rate found for phenanthrene. The total PAH recovered was phenanthrene 74.69%, anthracene 68.42%, fluoranthene 64.98%, and pyrene 52.81%. The extraction efficiency of phenanthrene was highest and of pyrene was the lowest. Reference [1] has suggested different extraction efficiency might be due to the poor contact of solvent and soil. PAHs with high-molecular weight may have stronger adsorption and formation of non-extractable residues especially within a complex substrate such as soil [12]. Recovery obtained for phenanthrene and pyrene was consequentially different. In general, relative recovery rates obtained for each PAH were as expected as the molecular weights of phenanthrene and anthracene are the same and for fluoranthene and pyrene are the same. However water solubility and molecular structures are different with greater linearity for anthracene and pyrene resulting in reduced solubility compared to phenanthrene and fluoranthene respectively [12]. Phenanthrene and anthracene are three ring compounds with molecular weight of 178.23 and fluoranthene and pyrene are four ring structures (molecular weight 202.26) [5]. Recovery rates obtained for each individual PAH correlates with the number of aromatic rings and molecular weight of the PAHs.

4.4 PHOTO-CATALYTIC DEGRADATION

Soil pH is considered as an important parameter due to amphoteric nature of most semiconductor oxides. The surface-charged particles present in the soil in presence of catalyst are influenced by the photo-semiconductor particles [8]. Therefore, the effect of pH on rate of photo catalytic degradation needs to be considered.

UV irradiation accelerated the photo degradation of phenanthrene, anthracene, fluoranthene and pyrene in this study. Some studies suggest that naphthalene, acenaphthene, anthracene, fluoranthene all undergo efficient photo-catalytic degradation by TiO_2 [2], [13]. Studies reported in [6] indicated that when TiO_2 is irradiated with light energy greater than its band gap energy (3.2eV), induction (b) and electron (e^-) and valence band holes (h^+) are generated. Thus, organic compounds reduces or react with electron acceptors such as O_2, reducing it to superoxide radical anion $O_2^{\bullet-}$ with the help of the photo-generated electrons. The H_2O molecules which are photo-generated holes are adsorbed to OH^- radicals at the surface of TiO_2

[6]. On the basis of adsorption of H_2O molecules photo-catalytic processes using TiO_2 could be an effective photo catalytic detoxification method for PAH contaminated soil.

This study demonstrated that photo-catalytic degradation rates were higher in acidic soil and lower in alkaline soil than in neutral soil for phenanthrene, anthracene, fluoranthene and pyrene. This is supported by the work reported in [17] suggests that H^+ was favorable for high molecular weight PAH degradation using TiO_2 under UV light, however the same study also suggested that OH^- made low molecular weight PAHs (example: phenanthrene) become more degradable. Similar results for PAH photo-catalytic degradation was found by reference [3].

Moreover, the lack of degradation at high pH is supported by the work in reference [17] who reported that in pesticide contaminated soil, "raising soil pH by adding Ca $(OH)_2$ did not significantly alter the photo-catalytic degradation of Diuron when compared to the soil that received no lime."

In this study, higher degradation rates were obtained of phenanthrene and lower degradation rates of pyrene. Similar results were indicated exhibiting high molar absorptivity and disappearance quantum yield for phenanthrene and pyrene as suggested by reference [6]. The most efficient degradation of PAHs in various contaminated sites is recorded with UV irradiation in presence of the catalyst, TiO_2 [14]. In these studies, photo-catalytic oxidation degradation was carried out at varying soil pH at 375 nm and 254 nm respectively. The control (soil samples with TiO_2 not exposed to UV light) at both wavelengths exhibited little degradation (figure 5 A to 12 A) in comparison to the samples exposed to UV light (figure 5 B to 12 B). During photo-catalytic degradation, 375 nm resulted in greater degradation of each individual PAH compared to 254 nm. Phenanthrene had the highest degradation followed by anthracene, pyrene and last fluoranthene at 375 nm. Phenanthrene exhibited 65% of degradation after five days and 60- 65% was degraded at 254 nm.

The photo catalytic degradation rate of anthracene was slower than phenanthrene whilst its degradation rate generally increased with acidic pH with most rapid rate evident at pH 6.5. At 375 nm anthracene exhibited 55-60% degradation and at 254 nm degradation was 55-60%. Degradation of fluoranthene followed after anthracene exhibiting 60% degradation at 375 nm and 45% at 254 nm. Around 45-50% degradation rate was observed for pyrene at 375 nm and 45% degradation observed at 254 nm.

5 CONCLUSION

For photo-catalytic oxidation, it was observed that soil pH 6.5 gave the fastest rate of photo catalytic degradation in comparison to all other pH. The second greatest rate of degradation was found at pH 6.0. Acid pH resulted in higher degradation rates compared to alkaline pH of soil. Comparatively acidic pH from 4 to pH 6.5 exhibited greater degradation as OH^- and OOH^- radicals which plays important role are highly generated, whilst little degradation was evident at neutral and alkaline pH 7.0 to pH 9.0 where, OH^- and OOH^- radicals might be less. Similarly, [4] reported consistently greater degradation of phenol in acidic soil pH during investigating photo-catalytic oxidation. However, the current investigation suggests soil pH is an important parameter that needs to be monitored in order to control the degradation as high pH led to low photo-catalytic degradation rates.

ACKNOWLEDGMENT

This project was performed in University of Hertfordshire, department of biotechnology, Hatfield, Hertfordshire, UK. I take this opportunity to thanks all my family members and lab colleagues Dr. Zohreh Korasanizadeh, Dr. Arjomand Gharghani and all who have encouraged and supported me throughout my PhD for their valuable help.

REFERENCES

[1] Alef, K. and Kleiner D., "Applicability of Arginine Ammonification as Indicator of Microbial Activity in Different Soils," *Biology and Fertility of Soils* 5(2): 148-151, 1987.

[2] Das, S., Muneer, M. and Gopidas, K.R., "Photocatalytic degradation of wastewater pollutants. Titanium-dioxidemediated oxidation of polynuclear aromatic hydrocarbons," *Journal Photochemistry Photobiology A: Chemistry*: 77-83, 1994.

[3] Funk, G. D., Johnson, S. M., Smith, J. C., Dong, X. W., Lai, J. and Feldman, J. L., "Functional respiratory rhythm generating networks in neonatal mice lacking NMDAR1 gene," *Journal of Neurophysiology* 78(3): 1414-1420, 1997.

[4] Han, M. J., Choi, H. T. and Song, H. G., "Purification and characterization of laccase from the white rot fungus Trametes versicolor," *Journal of Microbiology* 43(6): 555-560, 2005.

[5] Haritash, A. K. and Kaushik, C. P., "Biodegradation aspects of Polycyclic Aromatic Hydrocarbons (PAHs): A review," *Journal of Hazardous Materials* 169(1-3): 1-15, 2009.
[6] Hoffman, M. R., Martin, S. T., Choi, W. and Bahnemann D. W., "Environmental application of semiconductor photocatalysis," *Chemical Reviews* 95: 69-96, 1995.
[7] Irwin, R. J., Vanmouwerik, M., Stevens, M., Seese, L. and Basham, N. D., "Environmental contaminants encyclopedia," National Park Service, *Water Resources Division*, Fort Collins, Colorada, 1997.
[8] Kot-Wasik D., Dabrowska D. and Namiesnik J., "Photodegradation and biodegradation study of benzo[a]pyrene in different liquid media," *Journal of Photochemistry Photobiology A: Chemistry* 168: 109-115, 2004.
[9] Mueller, J. G., Devereux, R., Santavy, D. L., Lantz, S. E., Willis, S. G. and Pritchard, P. H., "Phylogenetic and physiological comparisons of PAH-degrading bacteria from geographically diverse soils," *Antonie Van Leeuwenhoek* 71(4): 329-343, 1997.
[10] Sigman, M. E., Schuler, P. F., Ghosh, M. M. and Dabestani, R. T., "Mechanism of pyrene photochemical oxidation in aqueous and surfactant solutions," *Environmental Science & Technology* 32(24): 3980-3985, 1998.
[11] Sigman, M. E. and Zingg, S. P., "Aquatic and Surface Photochemistry," *CRC Press*: 197-206, 1994.
[12] Song, Y. F., Jing, X., Fleischmann, S. and Wilke, B. M., "Comparative study of extraction methods for the determination of PAHs from contaminated soils and sediments," *Chemosphere* 48(9): 993-1001, 2002.
[13] Wen, S., Zhao, J., Sheng, G., Fu, J., Peng, P., "Photocatalytic reactions of phenanthrene at TiO2/water interfaces," *Chemosphere* 46(6): 871-877, 2002.
[14] Wilson, S. C. and Jones, K. C., "Bioremediation of soil contaminated with polynuclear aromatic hydrocarbons (PAHs): a review," *Environmental Pollution* 81(3): 229-249, 1993.
[15] Zepp, R. G., "Experimental approaches to environmental photo-chemistery (Ed.), Hand Book of Environmental chemistry," *Springer Verlag* 2(B): 19-41, 1982.
[16] Zeep, R. G. and Schlotzhauer, P. F., "Photoreactivity of selected aromatic hydrocarbons in water. Polycyclic aromatic hydorcarbons," *Ann Arbor Science Publisher*: 141-158, 1979.
[17] Zhang, L. H., Li, P. J., Gong, Z. Q. and Li, X. M., "Photocatalytic degradation of polycyclic aromatic hydrocarbons on soil surfaces using TiO2 under UV light," *Journal of Hazardous Materials* 158(2-3): 478-484, 2008.

International Journal of Innovation and Applied Studies
ISSN 2028-9324 Vol. 3 No. 4 Aug. 2013, pp. 893-907

http://www.issr-journals.org/ijias/

Un mécanisme de traces pour interactions téléphoniques utilisant VoiceXML

[A trace mechanism for telephone interactions using VoiceXML]

José Rouillard

LIFL Laboratory,
University of Lille 1,
59655, Villeneuve d'Ascq Cedex, France

ABSTRACT: The research that we present here are related to a study for the design and implementation of a follow-up survey of students via an interactive voice response (IVR) using VoiceXML, a W3C standard language. We present a corpus of questions and answers obtained in natural language, and we validate scientific hypotheses concerning the use of modes of interaction (voice versus direct manipulation). Then, we explain how we passed from a mechanism of exogenous traces (with a monitoring system performed by external tools recordings) to an endogenous mechanism (with a monitoring system made from within the IVR) to provide tools and instruments more adapted to the evaluation of multimodal applications that use speech and gesture (telephone keypad or mouse click on hyperlink). The trace mechanism for telephone interactions using VoiceXML presented here increases the quality of the evaluation of human-machine telephone interactions, because these traces are automatically recorded and reusable. Furthermore, we show that it is possible to get instant statistics (histograms and graphs made in real time, in PHP) using the method presented here. Thus, we have shown that pedagogical surveys, which traditionally are laborious, complex to implement and very time consuming can be facilitated through the methods and tools we recommend.

KEYWORDS: VoiceXML, Interactive Voice Response, traces, corpus, audio recording.

RESUME: Les travaux de recherche que nous exposons ici sont relatifs à une étude pour la conception et la réalisation d'une enquête de suivi d'étudiants, via un serveur vocal interactif (SVI) utilisant le langage VoiceXML, standard du W3C. Nous présentons le corpus de questions et de réponses en langue naturelle obtenu, et nous validons des hypothèses scientifiques, quant à l'usage des modes d'interactions (vocal versus manipulation directe). Puis, nous expliquons comment nous sommes passés d'un mécanisme de traces exogène (avec un système d'écoute effectué par des outils d'enregistrements externes) à un mécanisme endogène (avec un système d'écoute effectué au sein même du serveur vocal interactif), afin de fournir des outils et instruments mieux adaptés à l'évaluation d'applications multimodales permettant un usage de la parole et du geste (touche clavier téléphonique ou clic souris sur hyperlien). Le mécanisme de traces pour interactions téléphoniques utilisant le langage VoiceXML que nous exposons ici permet d'augmenter la qualité de l'évaluation des interactions hommes-machines téléphoniques, du fait que ces traces sont automatiquement enregistrées et réutilisables. Par ailleurs, nous montrons qu'il est ainsi possible d'obtenir des données statistiques instantanées (histogrammes et représentations graphiques effectuées en temps réel, en langage PHP) grâce à la méthode que nous présentons. Ainsi, nous avons montré que des enquêtes de suivi pédagogique, qui traditionnellement sont laborieuses, complexes à mettre en œuvre et très chronophages peuvent être facilitées grâce aux méthodes et outils que nous préconisons.

MOTS-CLEFS: VoiceXML, Serveur Vocal Interactif, traces, corpus, enregistrement audio.

Corresponding Author: José Rouillard (jose.rouillard@univ-lille1.fr)

1 INTRODUCTION

Depuis quelques temps, nous assistons à l'émergence de nouveaux outils de communication mobiles et ubiquitaires. Les usages des blogs, wikis, téléphones portables, smartphones et tablettes sont de plus en plus étudiés par la communauté scientifique. C'est le cas, par exemple, pour l'usage des « blogs mobiles », permettant de consulter ou de déposer une information sur un blog, grâce notamment à un téléphone mobile, en plus des autres moyens traditionnels d'accès à Internet [7]. Cela permet par exemple, pour un étudiant, de rester en contact avec l'équipe enseignante (son tuteur de stage notamment) lorsque l'usage des outils classiques (ordinateur relié à Internet) est temporairement impossible.

De ce fait, la récolte et l'analyse des traces d'interaction avec un environnement d'apprentissage est un thème de recherche en forte évolution. Tracer l'usage des outils employés permet essentiellement de pouvoir croiser différents critères permettant une meilleure adaptation des outils aux utilisateurs. Il s'agit de mieux cerner les populations d'usagers (apprenant ou groupe d'apprenants, tuteur, concepteur, administrateur, agents virtuels…), de faciliter les manipulations des larges volumes d'informations numériques recueillies et de permettre une meilleure étude des modalités de communication avec les systèmes informatiques supportant l'interaction avec les utilisateurs.

Nous exposons dans cet article la notion de traces numériques dont nous avons besoin pour tester et évaluer des systèmes informatiques permettant à des utilisateurs de dialoguer avec un automate en langue naturelle. Nos études abordent la flexibilité des serveurs vocaux interactifs (SVI) ainsi que la traçabilité des interactions lors de dialogues homme-machine téléphoniques. En effet, devant le développement rapide de nouvelles formes d'usages de l'informatique et des réseaux (mobilité, informatique ubiquitaire[1]), il devient difficile de réaliser des expérimentations valides, *in situ*, afin de déterminer la qualité des systèmes produits du point de vue de l'efficacité, de l'utilisabilité et de l'acceptation des solutions envisagées. C'est particulièrement vrai lorsque les utilisateurs peuvent interagir « sans contraintes », grâce au langage naturel ou avec des gestes, par exemple, et cela n'importe où, n'importe quand, avec une grande variété de modalités d'interaction et de multiples canaux d'accès aux systèmes interactifs. Il est alors quasiment impossible d'utiliser des méthodes et outils classiques d'évaluations des systèmes étudiés, notamment pour l'observation et la capture de traces d'interactions.

Dans cet article nous présentons dans un premier temps nos travaux relatifs à une enquête de suivi des étudiants du CUEEP[2] de Villeneuve d'Ascq, en France, réalisée au sein du laboratoire d'informatique de Lille. Nous expliquons tout d'abord le contexte et la motivation quant à ces travaux de recherche, puis nous présentons le système que nous avons mis en œuvre pour réaliser des enquêtes de suivi d'étudiants-stagiaires : il s'agit d'un serveur vocal compatible avec le langage VoiceXML [1], [14] et capable d'interagir avec l'utilisateur sur la base d'un réel dialogue homme-machine (DHM). Le protocole d'expérimentation est ensuite exposé, ainsi que les principaux résultats obtenus.

Dans un second temps, nous nous basons sur ces premiers résultats pour montrer que les traces ainsi recueillies ne sont pas suffisantes pour évaluer convenablement les systèmes de dialogue étudiés, principalement parce qu'il n'était pas possible jusqu'ici d'enregistrer de manière automatique et endogène (c'est-à-dire grâce à un mécanisme interne propre au système) ce que l'utilisateur prononçait réellement lors des différents tours de parole ; la machine enregistrait ce qu'elle croyait avoir compris, et non pas ce qu'y avait réellement été dit par l'utilisateur. Nous montrons ensuite que nous avons réussi à mettre en œuvre un système permettant de récolter des traces provenant de différentes modalités d'interactions au sein d'une même application multimodale (parole, appui d'une touche du clavier téléphonique, clic souris sur un hyperlien dans une page web).

Enfin, nous tirons des leçons de ces études et exprimons un ensemble de règles à suivre, utiles, selon nous, pour améliorer la qualité des corpus recueillis selon ce mode de communication avec l'utilisateur (vocal et/ou touches du clavier téléphonique).

[1] L'informatique ubiquitaire, telle qu'elle a été décrite il y a 15 ans par Mark Weiser, postule un monde où les individus sont entourés de terminaux informatiques interconnectés via des réseaux qui les aident dans tout ce qu'ils entreprennent.
[2] CUEEP : Centre Université - Economie d' Education Permanente

1.1 LES ENQUETES A SIX MOIS : UN TRAVAIL LABORIEUX COMPLEXE ET CHRONOPHAGE

Le CUEEP est un institut pédagogique de l'Université des Sciences et Technologies de Lille. En tant que prestataire de commande de la Région Nord Pas-de-Calais, il effectue le suivi de ses anciens étudiants-stagiaires, six mois après qu'ils aient terminé leur formation. Cela représente un travail important, dont l'expérience a montré qu'il est laborieux, complexe et chronophage (coûteux en temps de travail) :

- laborieux : après avoir effectué un premier repérage dans les listes régions de celles et ceux qui ne sont plus inscrit(e)s au CUEEP depuis 6 mois (diplôme obtenu ou non), il faut appeler ces anciens étudiants-stagiaires grâce aux coordonnées qu'ils ont laissé (numéro de téléphones fixes ou mobiles, personnel ou des parents, etc.) ;

- complexe : il y a toute une organisation à mettre en place dès l'instant où la personne visée n'a pas répondu (changement de numéro de téléphone, absence avec répondeur ; absence sans répondeur : quand rappeler, combien de fois ? …) ; complexe également par l'exploitation des résultats, même quand le questionnaire comporte assez peu de question, car cela demande un travail de retranscription, d'analyse, de statistiques … ;

- chronophage : ce travail, même bien organisé, prend du temps de secrétariat et suppose un relationnel de qualité que la fatigue et l'agacement risque de compromettre, d'autant que pour joindre efficacement les anciens stagiaires il faut très souvent les appeler en dehors des horaires de bureaux.

Nous pensons que ce travail pourrait être mené à bien grâce à un serveur vocal interactif supportant le langage VoiceXML.

1.2 LE LANGAGE VOICEXML

Il existe sur la planète beaucoup plus de téléphones que d'ordinateurs ! C'est à partir de cette constatation que les premiers projets de recherche d'accès à Internet par téléphone ont débuté dans les années quatre-vingt-dix. L'idée consiste à proposer l'accès au réseau Internet par le moyen d'un DHM en langue naturelle. Cette tendance se confirme aujourd'hui avec l'essor considérable que connaît depuis quelques années la téléphonie mobile. Les efforts de standardisation vers un langage non propriétaire, permettant non seulement la gestion des aspects téléphoniques mais également, pour partie, du DHM (relance, aide, reformulation, sous-dialogue, etc.) ont amené à la spécification du langage VoiceXML (pour *Voice Extensible Markup Language*).

Le VoiceXML [16] est donc un langage standard, à balises, permettant d'accéder à Internet grâce à un navigateur vocal via un téléphone fixe ou portable. Il est basé sur XML et s'articule autour de la reconnaissance et de la synthèse vocale, des grammaires de dialogue, et facilite la mise en œuvre de DHM sur serveurs vocaux interactifs. La version actuellement en vigueur est la version 2.1 [17]. D'ici quelques temps, le langage VoiceXML devrait pouvoir supporter les interactions multimodales, selon [2]. Le W3C travaille d'ailleurs sur d'autres langages comme EMMA[3] [3] ou X+V[4] [18] qui partagent certaines balises avec le langage VoiceXML.

Nous présentons ci-après le système que nous avons développé en VoiceXML, afin de tenter d'apporter une solution aux problèmes évoqués précédemment, concernant le suivi des étudiants, six mois après leur départ du CUEEP. Nous étudions également par ce biais les avantages et les inconvénients du VoiceXML, et faisons apparaître, en se basant sur des usages réels, des points à améliorer, comme par exemple, la notion de traces, ou bien encore l'écoute discrète de la part d'un tiers.

2 UN SYSTÈME DE QUESTION/RÉPONSES PAR SERVEUR VOCAL

Le recours à ce que l'on appelle communément un « corpus » s'est généralisé dans de nombreux domaines scientifiques (sciences humaines et sociales, sciences du langage, de l'information et de la communication, etc.). Cependant, le terme « corpus » peut être employé pour désigner deux types de données : ce peut être soit un ensemble de documents, sous forme écrite, orale ou audiovisuelle brute, soit, la somme des informations élaborée à partir de ces sources brutes que l'on vient de citer.

[3] EMMA : Extensible MultiModal Annotation markup language
[4] X+V : XHTML+Voice Profile

Comme le font remarquer [4], à propos de leur projet RITEL[5], « *Un projet riche et complexe doit faire face à plusieurs points épineux. Les plus évidents sont : la reconnaissance de la parole qui doit être à grand vocabulaire et sur laquelle une contrainte temps réel s'applique, la gestion d'un dialogue en domaine ouvert, la communication et l'échange d'informations entre un système de question-réponse et le dialogue, la génération de la réponse.* »

Même si nous avons déjà travaillé, par le passé, sur des problématiques de recherche documentaire de manière électronique, et sur la base de DHM en langue naturelle [12], ou grâce à l'interaction avec des agents animés [13] (voir par exemple les travaux du Groupe de Travail sur les Agents Animés Conversationnels à ce sujet [5]), notre approche est sensiblement différente des travaux classiques de dialogues pour de la recherche d'information dans des bases de données (type renseignements SNCF [10], accès à des base de données médicales ou documentaires (système COALA [8], système AMI [9]) par exemple), dans le sens où, ici, ce n'est pas l'utilisateur qui pose une question relativement ouverte à la machine, mais le contraire. L'effort est moins porté sur la gestion du dialogue et de son fonctionnement, à l'inverse de travaux comme ceux de [6] pour l'application ARISE du LIMSI afin de délivrer des informations ferroviaires via un serveur vocal interactif.

En revanche, ces travaux s'inscrivent plus dans une optique d'usages en contexte, de traces et d'évaluations des IHM, que nous menons dans notre laboratoire.

Nous avons également travaillé sur des dialogues de type pédagogique, dans lesquels la machine interroge l'apprenant dans différentes situations : exercices générés aléatoirement (révision en mathématiques, par exemple), tutorat (la machine accompagne l'étudiant et l'aide en lui fournissant des indices si la réponse donnée est fausse ou incomplète), contrôle des connaissances (par QCM[6] notamment). Les constatations scientifiques demeurent les mêmes : les corpus ainsi que les moyens d'observer les usages *in situ* sont peu nombreux. Il faut donc trouver de nouveaux outils pour modéliser, concevoir et réaliser des systèmes informatiques capables de fournir des traces (à la fois bas niveau et d'un degré de complexité plus élevé) au moment de leur utilisation. Il sera alors très pertinent de capturer également des informations relatives aux contextes d'usages (état des réseaux, niveau de stress de l'usager, niveau sonore ambiant, luminosité, etc.), de manière à pouvoir reproduire ces situations, plus tard, si l'on veut comprendre ce qu'il s'est passé au moment de l'interaction.

Dans l'étude que nous présentons ci-après, l'objectif était double :

1) Nos voulions, dans un premier temps mettre en place un système de DHM permettant d'obtenir de manière semi-automatique des réponses de la part des personnes contactées, afin de livrer les réponses obtenues (ainsi les statistiques qui les accompagnent) à la région Nord Pas-de-Calais, commanditaire de cette étude.

L'ensemble des questions et des réponses possibles était connu à l'avance. Les questions posées n'étaient pas forcément les mêmes pour tous les personnes, car l'ordre et l'enchaînement des questions dépendait des réponses aux questions précédentes. L'automate suivait donc un algorithme particulier, pour ne poser que les questions adéquates à la situation. Par exemple, il ne fallait pas poser la question « *Suivez-vous vos cours en école ou en université ?* » si la personne venait juste de répondre, à la question précédente, qu'elle avait arrêté ses études.

L'ensemble des réponses possibles était également connu à l'avance, puisque sans cela, il ne serait quasiment pas possible de récolter les réponses des personnes interrogées. En effet, en VoiceXML, l'utilisateur peut répondre à une question de deux manières possibles : soit en prononçant un mot ou une phrase prévue par le concepteur du système (on parle alors de grammaire vocale), soit en utilisant les touches de son clavier téléphoniques (on parle alors de grammaire DTMF[7]).

Dans un cas comme dans l'autre, si l'on n'indique pas à l'avance à la machine ce que l'utilisateur est susceptible de répondre, la poursuite du dialogue est difficilement réalisable, sauf si l'on enregistre ce que dit l'utilisateur, et qu'on le soumet à un système de reconnaissance vocale indépendant de celui utilisé sur la plate-forme VoiceXML. Dans d'autres travaux, nous avons étudié cette dernière approche [15], mais pour l'instant, les temps de réponses ainsi que les résultats obtenus sont encore insuffisants pour pouvoir réellement utiliser des systèmes se passant totalement de grammaires vocales.

[5] L'objectif du projet RITEL est de réaliser un système de dialogue homme-machine permettant à un utilisateur de poser oralement des questions, et de dialoguer avec un système de recherche d'information généraliste.
[6] QCM : Question à Choix Multiple.
[7] DTMF : Dual Tone Multi Frequency

2) Dans un second temps, nous souhaitions étudier le corpus de données ainsi recueilli et l'analyser pour valider des hypothèses de travail.

Nous formulons les hypothèses suivantes :

H1 : l'interaction vocale sera plus utilisée que la manipulation directe, lorsque les deux usages seront possibles, car selon la littérature scientifique relative à la multimodalité, ce mode est en général, plus naturel, plus facile à utiliser et reste moins contraignant que tout autre mode [11].

H2 : le type de téléphone (fixe ou portable) qui sera utilisé par les personnes appelées n'aura pas d'influence sur la qualité audio de la communication, et plus particulièrement sur la qualité de la reconnaissance vocale.

H3 : le type de synthèse vocale générée (Homme versus Femme) n'influencera pas les résultats obtenus. C'est-à-dire que nous envisageons le même taux de « bonnes » interactions, quel que soit le type de voix utilisé pour la génération des phrases que devra prononcer le serveur vocal en TTS (Text To Speech).

Enfin, nous voulons, sur la base des résultats obtenus, proposer à la communauté scientifique un guide et/ou des règles ergonomiques facilitant la mise en œuvre de telles études sur le canal téléphonique (sondage d'opinions, avis de consommateurs, QCM pour des apprenants, etc.).

2.1 PRINCIPE ET RÉALISATION

Un ordinateur équipé d'une carte téléphonique et supportant le langage VoiceXML peut dialoguer avec un interlocuteur humain, afin de recueillir des données le concernant (ici : diplôme obtenu, activité depuis six mois : salarié dans quel secteur, pour quel emploi, demandeur d'emploi, en formation, ou encore quelle tranche d'âge, etc.). Pour cela, il faut disposer d'une base de données comportant toutes les informations que l'on possède déjà, à propos des personnes concernées (nom, prénom, adresse, numéro de téléphone...), ainsi que celles que l'on souhaite obtenir lors de « l'entretien téléphonique automatisé ».

Nous avons mené une expérimentation au sein de notre laboratoire, pour tester la faisabilité technique, les contraintes, ainsi que les avantages et les inconvénients d'une telle démarche. Il s'agissait donc d'étudier, de concevoir et de réaliser une application vocale permettant de questionner, via un téléphone, des anciens étudiants-stagiaires du CUEEP, afin d'obtenir de manière automatique des informations précises les concernant. Les différentes étapes du projet furent les suivantes :

1. Etudier les données à analyser (quelles sont les données déjà connues ? celles à recueillir lors de la conversation téléphonique homme-machine ? quels sont ces types de questions, ouvertes ou fermées ?, etc.

2. Etudier la base de données existantes et déterminer quelles étaient les améliorations ou modifications nécessaires à lui apporter.

3. Concevoir l'algorithme d'enchaînement des étapes sur le serveur vocal : salutations, explication du mode de fonctionnement du système, séries de questions/réponses, obtention de l'accord (de la part de la personne interrogée) pour enregistrer les résultats recueillis, formule de politesse et salutations finales. Que faire en cas d'erreurs ou d'incompréhensions ? Comment reformuler la question ?

4. Réaliser l'application vocale en langage VoiceXML ; avec connexion à un langage dynamique (PHP) pour accéder à la base de données (MySQL).

5. Mise en œuvre de l'application sur le serveur vocal de notre laboratoire.

6. Tests et évaluations (temps de réponses, intelligibilités de la synthèse vocale, ambiguïtés lors de la reconnaissance vocale, préférences des entrées DTMF – clavier téléphoniques – pour les données sensibles, etc.).

7. Prévenir les futurs sortants du dispositif de formation de l'appel d'un serveur vocal, et, au besoin, exécuter une démonstration en public.

8. Exploiter les informations recueillies sur la base de données.

9. Transférer les informations requises aux commanditaires, de manière électronique.

En résumé, afin d'alléger cette tâche, anciennement exécuté manuellement par des secrétaires, l'étude devait amener des éléments permettant de juger de la pertinence et de la réalité des arguments prônant l'utilisation d'un serveur vocal, à savoir, qu'il ne se fatigue pas, ne s'énerve pas, peut rappeler plusieurs fois les personnes absentes à différents moments de la journée et il génère automatiquement les statistiques associées aux informations recueillies dans des base de données.

2.2 PROTOCOLE DE RECUEIL DE DONNÉES POUR LE CORPUS SEC

Le protocole suivi pour l'enregistrement du corpus SEC (Suivi des Etudiants du CUEEP) fut le suivant :

1. Activer la fiche de l'étudiant n° X, en appelant une page web du type :

http://svr/suivi_etudiants/ questionnaire_pour_une_personne.php?numero=X

Cela permettait au système de générer pour la personne indiquée (clé primaire numéro X dans la base de données) un dialogue VoiceXML personnalisé, à partir d'un patron. Par exemple, la première question devenait : « Etes-vous bien Monsieur Patrice Martin ? », au lieu de « Etes-vous bien <Titre> <Prénom> <Nom> ? »

2. Lancer l'enregistrement audio. Cela consistait à mettre en route l'enregistrement vocal de l'audioconférence, à partir d'un microphone posé à côté du téléphone de l'expérimentateur. L'intégralité des conversations était enregistrée sur un PC, dans un fichier audio au format WAV.

3. Appeler l'étudiant. Cette opération manuelle, était donc effectuée par l'expérimentateur.

4. Lui expliquer la démarche (sondage d'opinion qui ne durera que quelques minutes, grâce à une machine, avec reconnaissance vocale et/ou DTMF, etc.).

5. Sans raccrocher, appeler le serveur vocal grâce à un numéro interne du laboratoire (le 31.02).

6. L'expérimentateur doit alors appuyer sur la touche « conférence » de son téléphone et rester discret. Le mode audioconférence est activé, et la personne appelée entend la voix de synthèse du serveur vocal. Le dialogue entre eux commence.

7. Une fois la conversation terminée, sauvegarder le fichier audio ainsi obtenu.

8. Faire une copie de sauvegarder de la base de données mise à jour avec les résultats de la dernière personne interrogée.

Il est à noter que ce protocole était volontairement bridé à une seule conversation en même temps, car nous enregistrions les conversations les unes après les autres, mais en pratique, rien n'empêche le serveur vocal de supporter plusieurs appels simultanément.

2.3 LE QUESTIONNAIRE

Nous avons conçu un système de Questions/Réponses de manière générique, de sorte qu'il soit facilement modifiable pour tout autre questionnaire. Pour cela, les phrases à synthétiser ainsi que les grammaires vocales nécessaires pour que les utilisateurs expriment leurs réponses ne sont pas codés « en dur » dans le serveur vocal, mais plutôt, déployé, à la volée, en fonction de fichier texte, faciles à éditer et à modifier, comme le montre la Figure 1. On y voit les étiquettes grâce auxquelles les champs (*<field>* en VoiceXML) sont créés, et qui permettent d'effectuer des sauts d'une question à une autre, en fonction des réponses obtenues.

```
>presentation
Bonjour, je suis l'automate vocal du CUEEP. Je vais vous poser quelques questions afin d'assurer le suivi des anciens inscrits au cuèpe[8].:info_touche
>info_touche
Vous pourrez répondre vocalement, ou à l'aide des touches de votre téléphone à chacune des questions qui va vous être posée.:verification
>verification
Êtes-vous bien %prenom% %nom% ?
-oui:temps
-non:espoir
>temps
Avez-vous quelques minutes à m'accorder ?
-oui:info_navigation
-non:rappeler
>espoir
Pouvez-vous me passer %prenom% %nom% ?
-oui:verification
-non:erreur
[…]
>info_navigation
A tout moment, vous pourrez obtenir de l'aide en prononçant le mot aide, ou en appuyant sur la touche étoile. Pour faire répéter une question, dites répétez. Si vous voulez modifier la réponse que vous venez de donner vous pouvez dire annuler.:q1_statut
>q1_statut
Etes-vous en activité, à la recherche d'un emploi, en formation, ou en contrat de travail ?
-en activité:q2_salarie
-en recherche d'un emploi:q4_domaine
-en formation:q5_formation
-en contrat de travail:q12_formation_contrat
```

Fig. 1. Exemple de fichier permettant la génération automatique d'un fichier VoiceXML pour DHM sur serveur vocal

L'utilisateur interagit donc avec un automate qui lui fournit des répliques personnalisées de manière dynamique, en fonction des résultats obtenus au fur et à mesure de l'avancement du dialogue. Nous présentons ci-dessous les principaux éléments obtenus.

3 RÉSULTATS

Les résultats qui nous semblent les plus pertinents sont ici présentés sous la forme de deux catégories. Il s'agit d'une part d'un corpus de Questions/Réponses, et d'autre part du corpus de fichiers audio.

3.1 LE CORPUS QUESTIONS/ RÉPONSES SEC

Le serveur vocal utilisé pour le recueil du corpus SEC (Suivi des Etudiants du CUEEP) était le système Phonic, d'Idylic[9], supportant le langage VoiceXML version 1.0, avec une reconnaissance vocale de Philsoft de *Telisma* et une synthèse vocale *Tempo* d'*Elan Informatique*, et DTMF (touches du téléphone). Trois pré-tests ont été effectués afin de vérifier le bon fonctionnement du matériel et des logiciels. Cela portait notamment sur la génération automatique du fichier VoiceXML contenant les informations relatives à la personne à contacter, l'aboutement[10] téléphonique vers des téléphones fixes et mobiles, l'enregistrement audio des conversations Homme-Machine, et la sauvegarde des réponses obtenues dans la base de données.

[8] Cette forme phonétique a été utilisée car sinon, le mot CUEEP était prononcé « CUPE » par la machine.
[9] http://www.idylic.com/
[10] Dans les spécifications du langage VoiceXML, il est possible de paramétrer le type de transfert à l'aide de l'attribut *bridge* de la balise *transfer*. S'il s'agit du mode *blind*, l'aboutement s'effectue sur le réseau de l'opérateur, tandis que s'il s'agit du mode *bridge*, l'aboutement est réalisé localement, sur le serveur vocal interactif. De plus, si l'on aboute plus de deux lignes entre elles, on obtient une conférence téléphonique.

Le nombre de personnes à contacter dans le fichier était de 39. Le nombre de personnes effectivement contactées est de 23 (58,97 %). Sur les 16 autres contacts, 5 étaient absents à chaque tentative d'appel, 4 étaient de faux numéros (soit réattribués, soit inactifs), et 7 ont commencé le questionnaire mais ne l'ont pas terminé. La part des communications effectuées vers des téléphones fixes représente 47,83 % des appels (respectivement 52,17 % vers des téléphones portables).

L'enquête était donc destinée à obtenir de manière semi-automatique des données statistiques, comme par exemple, la situation professionnelle des personnes interrogées, au moment de l'appel. Les réponses attendues pour cet exemple de question, et pour lesquelles une grammaire vocale (et DTMF) avait été préparée, étaient les suivantes : *en activité*, *en contrat de travail*, *en formation*, *à la recherche d'un emploi*. La Figure 2, ci-après, synthétise les résultats automatiquement obtenus, grâce au questionnaire programmé sur le serveur vocal interactif, pour la question relative à la situation professionnelle des personnes interrogées.

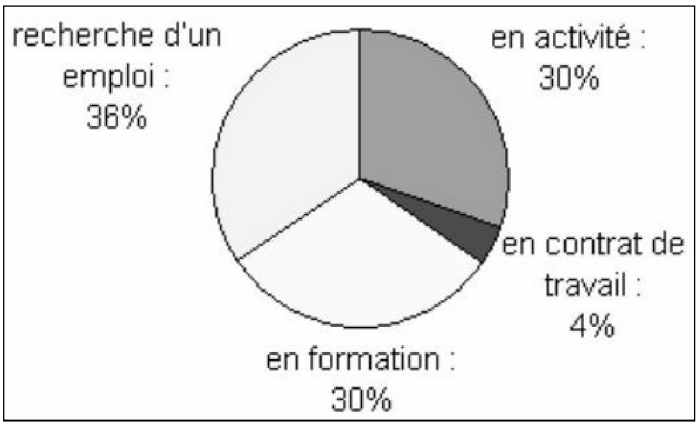

Fig. 2. Exemple de données obtenues grâce au questionnaire programmé sur le serveur vocal (ici, situation professionnelle des personnes interrogées)

L'âge des participants varie de 22 à 47 ans, avec une moyenne de 28 ans. Les autres résultats, qui ne font pas l'objet de cet article, et qui sont ici donnés à titre d'illustration, sont résumés sur la Figure 3 ci-après :

Type des activités : non salarié :1 vs salarié :6
Type des contrats : Sur le 6 salariés, 6 sont à durée indéterminé.
Domaine des activités : Pour les 16 personnes qui sont en activité, en contrat de travail ou à la recherche d'un emploi) : commercial : 5, formation : 2, santé : 3, social : 6.
Pour les 7 personnes en formation, les cours sont suivis en : école : 2 ; université : 5
Pour la seule personne en contrat de travail, les cours sont suivis en : école : 1
Pour les 5 personnes en formation en Université, les types de formation : littéraire : 2, technique et scientifique :3
Type de DAEU[11] obtenu : DAEU A : 20 ; DAEU B :3
Formation à distance : Non : 23 (100% en présentiel)
Objectif poursuivi en faisant cette formation : poursuite d'étude : 18, prétendre à un emploi : 1, satisfaction personnelle : 4.

Fig. 3. Quelques résultats propres à l'étude menée grâce au dialogue Homme-Machine vocal

La Figure 4 quant à elle, présente le nombre d'interventions vocales pour quelques questions du corpus. La rangée la plus éloignée donne le nombre d'intervention vocale au rang numéro 1, c'est-à-dire lorsque l'utilisateur a choisi ce mode pour répondre, lors de sa première intention.

[11] DAEU : diplôme d'accès aux études universitaires

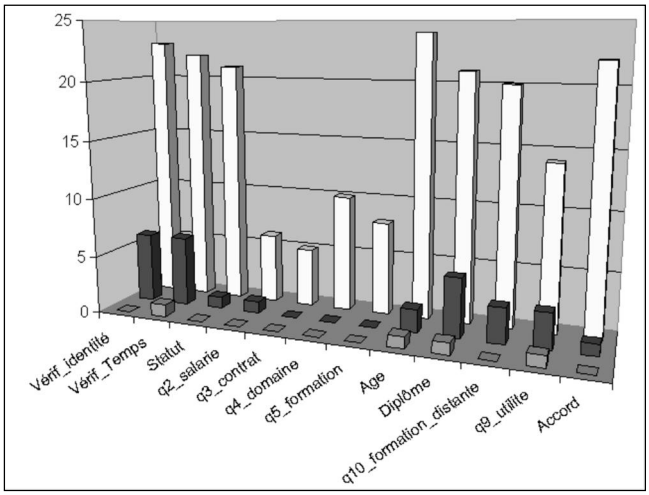

Fig. 4. Rangées V3, V2, V1, représentant les réponses vocales pour quelques questions posées par le SVI

La rangée intermédiaire représente le rang numéro 2, et la plus proche donne le rang numéro 3. Ainsi, pour la ligne 1 (étiquette verif_identité), 23 fois[12], les utilisateurs ont tenté de parler pour exprimer leur première réponse à cette question ; puis 6 fois lors d'un deuxième essai, toujours pour cette même question. On note que c'est pour donner leur âge que les utilisateurs ont le plus utilisé leur voix.

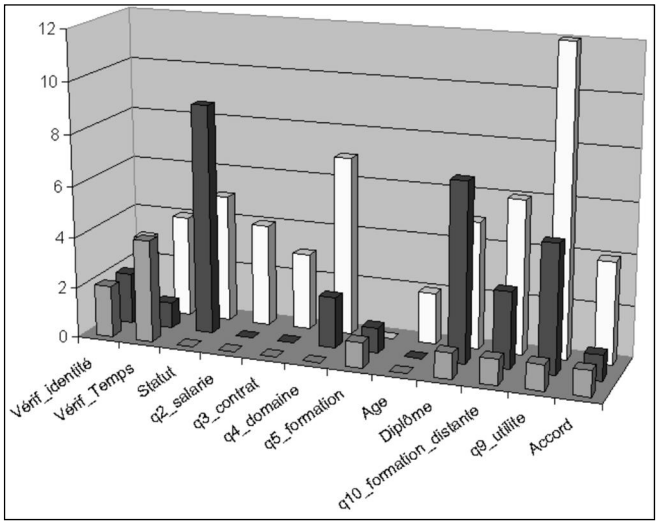

Fig. 5. Rangées D3 D2, D1, représentant les réponses par DTMF pour quelques questions posées par le SVI

Sur la Figure 5, on voit la répartition, pour les mêmes questions, mais en ce qui concerne le mode DTMF, cette fois-ci. On observe par exemple que c'est pour la question « Q9_utilite : Pourquoi avez-vous suivi cette formation ? satisfaction personnelle ? poursuite d'étude ? ou prétendre à un emploi ? » que les utilisateurs ont utilisé le plus leur clavier téléphonique.

La Figure 6, ci-après, résume les erreurs (rangée la plus éloignée), demande d'aide (rangée intermédiaire) et demande de répétition (rangée la plus proche). On voit donc que c'est en tentant de recueillir l'âge des utilisateurs que la machine a fait le plus d'erreurs, et aussi que les utilisateurs ont demandé le plus d'aide. C'est, en revanche, à propos du diplôme obtenu « DAEU A » ou « DAEU B » que les personnes interrogées ont demandé le plus souvent à la machine de répéter sa question.

[12] Le nombre d'observations est de 26 (et non pas 23), car une personne a recommencé deux fois le processus, avant de le valider, et une autre a recommencé une fois.

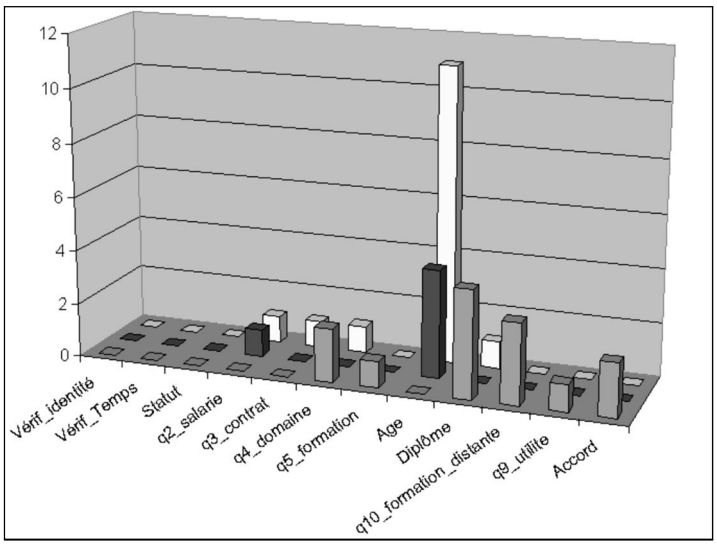

Fig. 6. Rangées Aide, Répéter et Erreur

3.2 LE CORPUS AUDIO SEC

Le corpus audio représente au total 4888 secondes d'enregistrement, soit 1h35 minutes. En moyenne chaque conversation dure 213 secondes (écart type de 90). Le dialogue le plus court dure 132 secondes, et le plus long dure 574 secondes. Ces durées ont été automatiquement calculées par l'automate qui estampillait le début et la fin de chaque conversation. Il s'agit ici des durées effectives des DHM, c'est-à-dire que l'on n'intègre pas dans ce calcul le laps de temps dans lequel l'expérimentateur explique le principe de fonctionnement à la personne appelée.

Il apparaît très nettement au vu des résultats d'interaction avec le serveur vocal, que l'hypothèse H1 que nous avions formulé était correcte, dans le cadre de cette étude. En effet, sur les 325 interactions, 228 (soit 70,15%) étaient orales, contre 97 par manipulation directe (DTMF).

Plus précisément, ces 228 interactions vocales ont été réalisées en première intention à 196 fois (étiquette notée V1 dans le corpus), en deuxième intention à 28 reprises (V2), et en troisième intention à 4 reprises (V3). Pour le DTMF, les valeurs D1, D2 et D3 sont respectivement de 55, 31 et 11.

Les résultats relatifs aux types de téléphones (11 téléphones fixes contre 12 téléphones mobiles dans l'étude), semblent aller dans le sens de l'hypothèse que nous avions formulé (H2) : il n'y a pas plus d'erreurs avec des téléphones mobiles qu'avec des téléphones fixes dans notre étude (respectivement 8 erreurs de compréhension, avec des téléphones fixes, corrigées après réécoute par l'expérimentateur, de manière asynchrone, contre 7 erreurs pour les portables).

En revanche, pour les 13 demandes d'aide, 12 émanent d'utilisateurs équipés des téléphones mobiles, contre 1 seule d'un téléphone fixe. Mais ce résultat n'est donné qu'à titre anecdotique, car rien ne permet, à ce stade, de prétendre que la demande d'aide est fortement liée au type de téléphone utilisé. Pour cela, nous devrons croiser plusieurs autres critères du corpus qui n'ont pas encore totalement été exploités.

Enfin, en ce qui concerne l'hypothèse H3, elle semble être correcte, puisque nous ne voyons pas de taux d'erreurs qui seraient plus accentuées avec l'une ou l'autre des voix de synthèse. Les taux d'erreurs sont proportionnels aux taux d'apparition des TTS respectives (les 14 utilisations de voix masculine contre 9 utilisations de voix féminine sont proportionnelles ont 11 erreurs avec des TTS masculine, et 7 avec des TTS féminine).

3.3 EXEMPLES D'ERREURS TIRÉES DU CORPUS

Voici quelques exemples, tirés du corpus SEC, que nous donnons pour illustrer les éléments que nous venons de citer, ci-dessus.

- Question : « Pourquoi avez-vous suivi cette formation ?[13] satisfaction personnelle ? poursuite d'étude ? ou prétendre à un emploi ? »

- Réponse : « Au début satisfaction personnelle, et ensuite …. »

La machine n'a pas compris cette phrase, car la grammaire vocale ne s'attendait pas à une telle amorce de la part de l'utilisateur. Sans le mécanisme de trace et d'écoute discrète que nous avons mis en œuvre, il n'aurait pas été possible, après coup, de se rendre compte d'où provenait l'erreur.

- Question : « Etes-vous en activité, à la recherche d'un emploi, en formation, ou en contrat de travail ? »

- Réponse : retraitée.

Cette réponse n'ayant pas été prévue par les commanditaires de l'étude, la machine n'a pas compris cette phrase. La même question a donc été reposée plusieurs fois à l'utilisateur, qui, après avoir insisté et changé de ton, a finalement a décidé de raccrocher, non sans avoir prononcé une dernière phrase de mécontentement : « oh, hein, ça va bien hein ».

- Question : « Etes-vous en activité, à la recherche d'un emploi, en formation, ou en contrat de travail ? »

- Réponse : « Oui ».

L'utilisateur a cru qu'on lui demandait s'il était dans l'une des situations évoquées, et n'a pas compris qu'il agissait d'énoncer la situation précise dans laquelle il se trouvait.

- Question : « Votre formation est-elle littéraire ou technique et scientifique ? »

- Réponse : « Non »

- Réponse : « Scientifique »

Ici, le découpage était d'une part « littéraire » et d'autre part « technique et scientifique ». L'utilisateur n'a pas su, à l'oreille, faire ce distinguo.

Ces quelques exemples illustrent bien le besoin de traces, d'instruments et d'outils dont les chercheurs ont besoin pour mener à bien leurs études scientifiques. Nous expliquons dans les lignes qui suivent notre approche pour proposer une solution originale à ce problème.

4 INSTRUMENTATION ET MÉCANISME DE TRACES POUR VOICEXML

A la lumière des résultats obtenus lors de cette première expérience, nous pouvions dire que le langage VoiceXML ne possédait pas, de manière interne, un mécanisme permettant de tracer les interactions avec les utilisateurs qui se connectaient sur le SVI. Jusqu'à la version 2.0 de VoiceXML, il n'était pas possible, à notre connaissance d'effectuer une trace réelle de ce qu'avait effectivement prononcé les utilisateurs au cours de leur dialogue avec le système. En revanche, il était possible de consulter la variable chargée de récupérer la valeur supposée correspondre à un élément de la grammaire vocale. Autrement dit, il n'était pas possible, jusqu'ici, d'enregistrer de manière automatique ce que l'utilisateur prononçait réellement lors des différents tours de parole.

Le processus que nous avions mis en œuvre afin d'enregistrer les conversations entre les utilisateurs et notre serveur vocal était externe au système lui-même et enregistrait également les autres bruits ambiants. Cette première étape a démontré que ce que disaient les utilisateurs n'était pas forcément ce que le système avait cru entendre. Typiquement, à la question « Quel est votre âge ? », il est arrivé que la machine enregistre la réponse « 33 » dans la base de données, alors que la véritable réponse prononcée par l'utilisateur était « 23 ». L'expérimentateur, en écoute discrète avait noté cette anomalie et a pu réécouter l'enregistrement sonore, plus tard, afin de conforter son opinion.

Depuis la version 2.1 du VoiceXML du W3C, il est techniquement possible d'enregistrer ce que prononce l'utilisateur lors d'une interaction vocale. Pour cela, il faut initialiser l'attribut *recordutterance* de la balise <*property*> à la valeur « *true* ». On peut alors obtenir, grâce à certaines variables d'application, les données suivantes :

[13] Même si la phrase n'est pas très correcte, syntaxiquement, nous y avons laissé plusieurs points d'interrogations afin d'obtenir une meilleure prosodie (ton montant pour une interrogative).

application.lastresult$.confidence
Le niveau de fiabilité de l'énoncé de cette interprétation dans l'intervalle 0.0-1.0. Une valeur de "0.0" indique une fiabilité minimale et une valeur de "1.0" une fiabilité maximale.

application.lastresult$.inputmode
Le mode selon lequel l'entrée d'utilisateur a été fournie : "dtmf" ou "voice".

application.lastresult$.recording
La donnée vocale correspondant à ce que l'utilisateur a dit.

application.lastresult$.recordingduration
La durée (en msec) de la dernière reconnaissance vocale.

application.lastresult$.recordingsize
La taille (en octets) de la dernière reconnaissance vocale.

application.lastresult$.utterance

La chaîne des mots bruts qui ont été reconnus pour cette interprétation.

Dans le cas d'une grammaire DTMF, cette variable contiendra la chaîne numérique reconnue. Nous avons utilisé cette spécificité dont dispose le serveur vocal de notre laboratoire[14] pour mettre un œuvre un mécanisme d'enregistrement global de toutes les traces d'interactions homme-machine possibles en VoiceXML (voix et clavier téléphonique). Cette instrumentation permet donc de collecter des traces qui reflètent l'usage d'une application. Ces informations sont estampillées et enregistrées dans une base de données. Nous avons développé un moyen d'accès à ces traces, pour qu'un expérimentateur, non informaticien, puisse analyser les données recueillies. A partir de cette interface, un « expert » du domaine étudié peut prendre connaissance de l'enregistrement vocal (fichier .wav) correspondant à la réponse d'un utilisateur et le comparer à ce que la machine a cru comprendre durant l'interaction.

Nous avons testé ce processus de traces avec une application multimodale de commerce électronique comportant une reconnaissance et une synthèse vocale, l'usage possible du clavier téléphonique DTMF, mais aussi des clics souris sur des hyperliens d'une page Web, la visualisation des images des produits présentés, etc.

La Figure 7 ci-après indique, en première ligne par exemple, que lorsque l'action consistait à choisir une taille de vêtement, la machine a cru reconnaître la réponse « 36 ». En cliquant sur le fichier .wav de cette même ligne, l'expert peut vérifier que l'utilisateur avait bien prononcé cette information, et le cas échéant rectifier l'information. Les statistiques de bonnes/mauvaises compréhension de la part de la machine sont ainsi mises à jour et permettent d'instrumentaliser les évaluations des interfaces générées.

Num	la_date	heure	action	utilisateur	trace_utilisateur
572	Tue16May	16h40min19s	choisir taille	36	utilisateur_Tue16May_16h40min19s_vox.wav
573	Tue16May	16h40min34s	choisir couleur	bleu	utilisateur_Tue16May_16h40min34s_vox.wav
574	Tue16May	16h40min53s	choisir référence	25	utilisateur_Tue16May_16h40min53s_vox.wav
575	Tue16May	16h41min05s	ajouter au panier	non	utilisateur_Tue16May_16h41min05s_vox.wav
576	Tue16May	16h44min12s	reference client	2	utilisateur_Tue16May_16h44min12s_vox.wav
577	Tue16May	16h44min30s	choisir produit	Robe Bleue	utilisateur_Tue16May_16h44min30s_vox.wav
578	Tue16May	16h44min40s	choisir rayon	Femme	utilisateur_Tue16May_16h44min40s_vox.wav

Fig. 7. Traces d'enregistrement vocal en VoiceXML 2.1

[14] En effet, le SVI Sibilo Voice de l'entreprise App-Line supporte partiellement la version 2.1 de VoiceXML.

Le mécanisme mis en œuvre pour cette instrumentalisation est schématisé sur la Figure 8 ci-dessous.

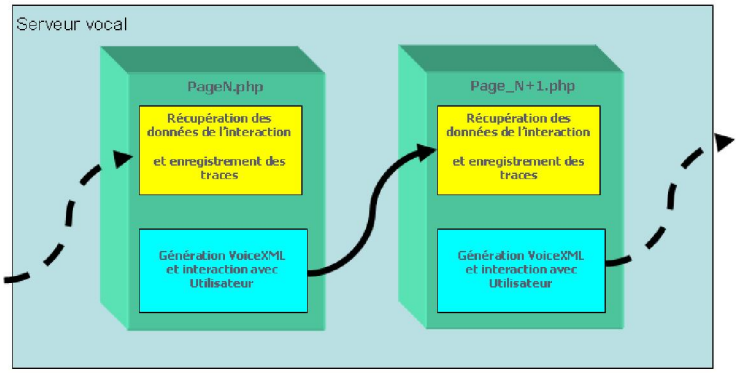

Fig. 8. Mécanisme pour recueillir des traces d'interactions sur SVI

En résumé, une page web dynamique récolte les traces du tour de parole précédent, puis sauvegarde ces informations dans une base de données ainsi que des fichiers audio, et enfin génère les fichiers VoiceXML pour l'interaction en cours.

5 LEÇONS À RETENIR POUR LA CONCEPTION DE DHM GRÂCE À VOICEXML

La conception et le développement d'une bonne interface Homme-Machine passe par diverses étapes. Nous en rappelons brièvement le cycle de vie. Il est tout d'abord nécessaire de passer par une phase d'analyse. Elle devra déterminer l'étendue de l'application, les besoins et les types d'utilisateurs identifiés, la valeur ajoutée que le service apportera à cette population d'usagers, etc. La réalisation passera par une phase de choix de la plate-forme VoiceXML, selon des critères de qualité des technologies vocales, des coûts, de la possibilité de suivre (en temps réel ou en différé) les activités des utilisateurs connectés, etc. Ensuite, les phases de développement, de tests et d'évaluation devront être menées à bien. Durant cette période, il est important de consulter régulièrement les fichiers de traces des interactions sur le serveur vocal (log files en anglais). Cela permet de vérifier le bon déroulement des différentes phases du dialogue, et l'on peut y déceler certaines anomalies ou problèmes techniques particuliers : on y découvrira, par exemple, qu'un fichier n'est pas réellement chargé car il se trouve déjà en mémoire cache de l'ordinateur. Les outils et mécanismes de traces précédemment décrits seront utiles non seulement lors des phases d'évaluations, mais également tout au long du cycle de développement d'applications monomodales (uniquement à l'oral par exemple) ou multimodales, pour lesquelles il existe très peu de moyens permettant de tracer les usages. Cela est d'autant plus vrai dans le cadre de campagne d'évalutions hors laboratoire, qui sont nécessaires pour des usages spécifiques dans le cadre de la mobilité, de l'informatique ambiante ou pervasive.

6 CONCLUSIONS ET PERSPECTIVES

Nous avons montré dans un premier temps qu'une tâche consistant à questionner une personne avec une liste de Questions/Réponses connues peut être avantageusement effectuée par un serveur vocal interactif supportant le langage VoiceXML. Au cours de notre étude préliminaire, nous avons recueilli un corpus de réponses, pour le commanditaire de l'étude (la région Nord Pas-de-Calais), mais également, des données permettant de confronter nos résultats à des hypothèses scientifiques. Il a été vérifié, qu'effectivement, l'interaction vocale est plus utilisée que la manipulation directe, dans cette étude, lorsque l'utilisateur en à la choix (H1), que le type de téléphone utilisé (fixe ou mobile) n'influence en rien les résultats obtenus (H2), ni même le type de synthèse vocale jouée, qu'elle soit masculine ou féminine (H3).

Mais nous avons surtout expliqué que la communauté scientifique manque significativement d'outils et d'instruments fiables permettant d'effectuer des traces d'interactions de nouvelles formes de communications multimodales. La deuxième étude présentée dans cet article a montré comment nous sommes passés de traces exogènes, avec enregistrements extérieurs au système à un mécanisme de traces endogènes, grâce notamment à l'usage de la version du langage standard VoiceXML 2.1. Cela a permis de récolter des traces provenant de différentes modalités d'interactions au sein d'une même application multimodale (parole, appui d'une touche du clavier téléphonique, clic souris sur un hyperlien dans une page web).

Pour rendre le corpus que nous avons succinctement présenté, véritablement exploitable par d'autres chercheurs, des travaux sont encore nécessaires. Il faudra anonymiser le corpus audio, l'annoter avec un outil comme Praat[15], puis permettre l'interrogation de la base de données sur des critères croisés : âge, sexe, type de téléphone (fixe ou mobile) des personnes interrogées, mais aussi par exemple le type de voix de la synthèse vocale utilisé (homme versus femme), la qualité audio de la conversation, la durée totale ou pour chaque question, l'heure de l'appel, etc.

Par ailleurs, nous travaillons actuellement, en collaboration avec l'entreprise App-Line[16] à l'amélioration des serveurs vocaux qui intègrent déjà certaines fonctionnalités du langage VoiceXML 2.1, comme l'enregistrement de ce que prononce l'utilisateur afin d'effectuer des traces de manière standard. Nous sommes en train de tester certaines balises (dites propriétaires, car ne faisant pas partie de la spécification VoiceXML 2.1 officielle) permettant de débuter et de stopper une trace automatique, et cela à tout moment de l'interaction avec le SVI. Cela peut se faire, soit grâce à une console de suivi en temps réel des conversations transitant sur le SVI (l'expert clique sur un bouton pour activer/stopper l'enregistrement vocal), soit de manière logicielle (une balise <object> en VoiceXML), soit encore par le biais de Web services supportant le protocole SOAP[17].

Enfin, nous continuons nos recherches, afin de mettre en place une solution complète de « push vocal », permettant de passer efficacement d'un système semi-automatique (dans lequel l'humain effectue encore l'amorce auprès de l'interlocuteur, en lui présentant la démarche et le principe d'utilisation), à un système totalement automatique, avec possibilités d'enregistrements de plusieurs conversations téléphoniques simultanément.

REMERCIEMENTS

Ces travaux sont, pour partie, le résultat de réflexions et de discussions avec Christian Ladesou, du Centre CUEEP de Villeneuve d'Ascq. D'autre part, ces études scientifiques sont partiellement financées le contrat de plan Etat Région Nord Pas de Calais, et le FEDER (Fonds Européen de Développement Régional).

[15] http://www.fon.hum.uva.nl/praat
[16] http://www.app-line.com
[17] SOAP : Simple Object Access Protocol

REFERENCES

[1] Anderson, E. A., Breitenbach, S., Burd, T., Chidambaram, N., Houle, P., D. Newsome, D, Tang, X., Zhu, X., *Early Adopter VoiceXML*, Wrox, 2001.

[2] Dettmer, R., "It's good to talk, speech technology, for on-line services access," *IEE Review*, Vol. 49, No. 6, June 2003, pp. 30-33.

[3] EMMA : *Extensible MultiModal Annotation markup language*. [Online] Available: http://www.w3.org/TR/2005/WD-emma-20050916/ (2013)

[4] Galibert O., Illouz G., Rosset S., *RITEL : dialogue homme-machine à domaine ouvert*, TALN 2005, Dourdan, 2005.

[5] GT ACA : *Groupe de Travail sur les Agents Conversationnels animés* [Online] Available: http://www.limsi.fr/aca/ (2013)

[6] Lamel, L., Rosset, S., Gauvain, J.L., Bennacef, S., Garnier-Rizet, M. et Prouts, B., "The LIMSI ARISE System," *Speech Communication*, 31(4):339-354, 2000.

[7] Leclet, D., Leprêtre, E., Peter, Y., Quénu-Joiron, C., Talon, B., Vantroys, T., "Améliorer un dispositif pédagogique par l'intégration de nouveaux canaux de communication," *EIAIH 2007*, Lausanne, Suisse.

[8] Lehuen J., "Un modèle de dialogue dynamique et générique intégrant l'acquisition de sa compétence. Le système COALA," *Thèse de doctorat, Université de Caen*, Juin 1997.

[9] Lemeunier T., "L'intentionnalité communicative dans le dialogue homme-machine en langue naturelle," *Thèse informatique, Le mans*, 2000.

[10] Luzzati D., "Recherches sur le dialogue homme-machine : modèles linguistiques et traitements automatiques," *Thèse de l'Université de la Sorbonne*, 1989.

[11] Oviatt, S. L. & Cohen, P. R., "Spoken language in interpreted telephone dialogues," *Computer Speech and Language*, 6 (3) 277-302, 1992.

[12] Rouillard J., "Hyperdialogue sur internet. Le système HALPIN," *thèse d'informatique de l'université Joseph Fourier, Grenobl*e, 2000.

[13] Rouillard J., "Hyperdialogue avec un agent animé sur le Web," *ERGO-IHM'2000*, Biarritz, 2000.

[14] Rouillard J., *VoiceXML. Le langage d'accès à Internet par téléphone*, éditions Vuibert, ISBN : 271174826X, 197 pages, Paris, 2004.

[15] Rouillard, J., Truillet P., *Enhanced VoiceXML*, HCI International 2005, Las Vegas, 2005.

[16] VoiceXML 1.0., *W3C Recommendation*. [Online] Available: http://www.w3.org/TR/voicexml10 (2013)

[17] VoiceXML 2.1, *Working Draft*. [Online] Available: http://www.w3c.org/TR/2004/WD-voicexml21-20040323 (2013)

[18] X+V : *XHTML+Voice Profile 1.0* [Online] Available: http://www.w3.org/TR/xhtml+voice/ (2013)

International Journal of Innovation and Applied Studies
ISSN 2028-9324 Vol. 3 No. 4 Aug. 2013, pp. 908-918

http://www.issr-journals.org/ijias/

La Performance des Fusions et Acquisitions bancaires : Le cas de la Banque Commerciale du Maroc et Wafabank

[The Performance of Bank Mergers and Acquisitions: The case of the Commercial Bank of Morocco and Wafabank]

Hicham MEGHOUAR[1] and Hicham SBAI[2]

[1]Ecole Nationale de Commerce et de Gestion - Settat (Maroc),
GREGOR - IAE de Paris, France

[2]Ecole Nationale de Commerce et de Gestion - El Jadida (Maroc),
CREOP - EA Université de Limoges, France

ABSTRACT: Measuring the effectiveness of bank mergers and acquisitions has been the subject of several studies mainly on Anglo-Saxon and European markets. The aims of this paper is to examine the performance of these operations realized on emerging markets and appreciate the creation of financial and strategic values of a bank merger, in this particular case, the merger between the Commercial Bank (BCM) and Wafabank who took place in Morocco on 2003. In this research, the method of event study, which measures stock performance in the short term, and the method of pairing, which assesses accounting performance, were used. The analysis of empirical results shows that at the announcement of the transaction a negative abnormal return for the acquirer and positive for the target firm. These first results are consistent with other empirical studies who emphasized the negative impact of mergers and acquisitions on shareholder wealth of the acquiring and positive impact on shareholder wealth of the target firm. Also, the financial ratio analysis shows an improvement in profitability and productivity of the combined entity in the medium term, which is consistent with research confirming that mergers lead to a better use of assets, and can benefit from operational synergies and efficiency gains.

KEYWORDS: Shareholder value created, Merger, Event method, Method of pairing, Profitability.

RESUME: La mesure de l'efficacité des fusions et acquisitions bancaires a fait l'objet de plusieurs études essentiellement sur les marchés anglo-saxon et européen. L'objectif de cet article est d'examiner la performance de ces opérations réalisées sur des marchés émergents et d'apprécier la création de valeur financière et stratégique d'un rapprochement bancaire, en l'occurrence la fusion entre la Banque Commerciale (BCM) et Wafabank qui a eu lieu au Maroc en 2003. Lors de cette recherche, la méthode de l'étude d'événement qui mesure la value financière à court terme, et la technique de pairage qui permet d'apprécier la performance comptable, ont été utilisées. L'analyse des résultats empiriques montre qu'à l'annonce de cette opération une rentabilité anormale négative pour l'acquéreur et positive pour la firme cible. Ces premiers résultats sont en conformité avec les autres études empiriques qui ont souligné un impact négatif des Fusions et Acquisitions sur la richesse des actionnaires de la firme acquéreuse et positif sur celle des actionnaires de la firme cible. Aussi, l'analyse des ratios financiers montre une amélioration de la profitabilité et de la productivité de l'entité regroupée ce qui corrobore avec les conclusions des recherches qui confirment que les fusions conduisent à une meilleure utilisation des actifs et permettent de bénéficier des synergies opérationnelles et des gains d'efficience.

MOTS-CLEFS: Création de valeur, Fusion, Méthode d'événement, Méthode de pairage, rentabilité.

Corresponding Author: Hicham MEGHOUAR (meghouar@gmail.com)

1 INTRODUCTION

Les fusions-acquisitions (noté ci-après F&A) constituent un mode de croissance qui permet aux entreprises de renforcer leur position concurrentielle, d'accéder à de nouveaux marchés, de s'internationaliser, d'acquérir de nouvelles compétences et de se diversifier [1]. Néanmoins, ce type d'opération est marqué par quelques difficultés. Ces opérations connaissent un taux d'échec très élevé, supérieur à 50% d'après les statistiques, quels que soient les indicateurs utilisés, boursiers ou opérationnels. Les plans stratégiques qui les commandent sont inégalement vérifiés. Ainsi, dès la fin du XIX° siècle, une contradiction a été relevée par Alfred Marshall : « *la course à la taille favorise a priori les situations oligopolistiques ; pourtant, l'augmentation de la taille des entreprises va de pair avec les besoins de la spécialisation qui pousse à créer de nouvelles entreprises* ».

Les opérations de F&A touchent tous les secteurs et se produisent le plus souvent par vagues en impliquant de nombreuses entreprises. Dans le secteur bancaire, la consolidation a été forte et rapide aux Etats-Unis puisque le nombre de banques est passé de près de 14400 au début des années 1980 ; à 11500 en 1992 et à 9200 au début de 1997. En Europe, la concentration bancaire a suivi la même dynamique : tout d'abord essentiellement sur une base nationale à partir de 1997, puis sur une base plus transfrontalière avec notamment la fusion en 2005 *d'Abbey National* avec la *SCH*, de *HVB* avec *Unicredito* ou l'acquisition en 2006 de la *Banca Nazionale del Lavoro* par *BNP Paribas*. Le nombre d'institutions de crédit a continué à diminuer en 2005, confirmant la tendance de consolidation du secteur observée depuis plusieurs années. Le mois de décembre 2005, on dénombrait 6.308 institutions de crédit dans la zone Euro (12 pays), soit 2,8% de moins qu'en 2004 et 12,5% de moins qu'en 2001. Au niveau de l'Europe des 25, 8.684 institutions de crédit ont été recensées à la fin 2005, soit une baisse de 1,7% par rapport à 2004 et 10,9% par rapport à 2001[1].

D'après la littérature en la matière, la majorité des travaux concernant les F&A bancaires peuvent être classées dans les catégories suivantes : (i) les études qui examinent les caractéristiques des banques impliquées dans les F&A, (ii) les recherches qui étudient les déterminants de la prime payée pour la cible, (iii) les travaux qui analysent les conséquences des F&A sur le rendement opérationnel, (iv) les études d'événement de la rentabilité anormale, autour de la date d'annonce, des banques qui ont fusionné, et (v) les conséquences des F&A bancaires sur les autres entreprises. Puisque cette recherche se focalise sur l'analyse de la performance d'une fusion bancaire, une revue de littérature des études empiriques qui ont examiné la performance des F&A bancaires sera présentée par la suite.

Le présent article prolonge ces travaux empiriques et vise un marché émergent en s'intéressant à la fusion de la Banque Commerciale du Maroc (noté ci-après BCM) et Wafabank. C'est une fusion qui a marqué l'actualité financière de la période dans la mesure où elle a permis à la nouvelle entité de grimper dans le classement des banques et d'occuper ainsi la première place au Maghreb et la 9éme en Afrique[2], il s'agit de la fusion la plus médiatisée dans ce pays d'où l'intérêt d'examiner la création de valeur de cette opération. Dans cette optique, deux méthodes, traditionnellement employées dans ce genre d'études, ont été utilisées, à savoir la méthode de l'étude d'événement qui mesure la valeur financière créée, et la méthode de pairage qui mesure la valeur stratégique. À notre connaissance, cette recherche est la première à examiner la valeur créée lors d'une opération de rapprochement au Maroc.

Le reste de cet article est organisé en trois sections. La première présente une revue de littérature des F&A bancaires. Une deuxième expose la méthodologie de recherche utilisée. Enfin, la dernière section est dédiée aux tests empiriques et à l'interprétation des résultats.

2 LES F&A BANCAIRES : UNE REVUE DE LITTERATURE

Qu'elles soient bancaires ou non, les F&A jouent un rôle primordial dans la restructuration du tissu économique. Il s'agit de l'une des modalités des opérations de prise de contrôle[3] et constituent de ce fait une solution pour renforcer la discipline des managers lorsque les mécanismes internes de gouvernance font défaillance. Le marché du contrôle des entreprises devient alors le mécanisme de gouvernance de dernier ressort lorsque les autres ne fonctionnent pas correctement et garantit, de ce fait, le bon fonctionnement du système économique et la bonne assignation des moyens disponibles [2]. Ainsi,

[1] Source: BCE, « EU banking structures ».
[2] D'après le classement effectué par le magazine « *Jeune Afrique ».*
[3] Voir schéma n°1 au niveau des annexes.

le secteur bancaire a été le témoin d'un vaste mouvement de F&A. Les justifications théoriques de ce processus ont été largement empruntées à la littérature économique du début du XIX° siècle, qui vise à identifier les déterminants de la performance des fusions, tout secteur confondu, et s'est par la suite élargie à l'étude des effets concurrentiels de ces opérations, dont le concept d'économies d'échelle et de gamme figure à la première place.

La vague de consolidation des années 1990 s'est caractérisée par sa dimension nationale. Elle fut encouragée par un contexte général de surcapacités bancaires et par la libéralisation intervenue à la fin des années 1980. Au début de la décennie, elle revêtait pour l'essentiel la forme de fusions-absorptions et a progressivement évolué vers des acquisitions impliquant des transferts de contrôle. Quant à la chronologie des consolidations domestiques, cette dernière varie au gré du calendrier législatif et réglementaire dans chaque pays. Elle s'est accélérée dès la fin des années 1980 au Royaume-Uni, avec la démutualisation des buildings societies, en Espagne (fusion en 1988 de *Banco de Bilbao* et *Banco de Vizcaya* (BBV), *Banco Santander* et *BCH* en 1999, *BBV* et *Argentaria* en 2000) et aux Pays-Bas (constitution d'*ABN AMRO* en 1991). Le mouvement a d'abord concerné le secteur mutualiste en France, entre 1989 et 1993, avant de s'étendre aux banques commerciales. En Italie, du fait d'une libéralisation plus tardive du secteur, la restructuration bancaire n'a véritablement pris son envol qu'à partir de la deuxième moitié des années 1990.

Avant de dresser un bilan des travaux empiriques consacrés à l'examen de la performance des F&A bancaires, les justifications théoriques de ces opérations sont, d'abord, présentées.

2.1 LES MOTIFS THÉORIQUES DES F&A BANCAIRES

La consolidation bancaire a fait l'objet d'une abondante littérature théorique. Plus rares sont, néanmoins, les études portant spécifiquement sur le caractère international du processus. L'analyse économique apporte traditionnellement deux justifications aux F&A bancaires. Celles-ci permettent, en théorie, de créer de la valeur actionnariale par l'obtention d'un gain en termes d'efficience ou par l'obtention d'un gain en termes de pouvoir de marché. L'idée générale est que la valeur du nouvel ensemble, issue de la fusion, excède la somme des valeurs respectives de chacune des deux entités préexistantes.

Les F&A, au niveau local et au sein d'une même activité, s'expliquent davantage par la création de valeur qui résulte de l'accroissement du pouvoir de marché. Ref. [3] conforte ceci et avance l'exemple de l'Union Européenne, où la plupart des opérations sont à caractère nationales et intra-sectoriel. Ainsi, les acteurs bancaires peuvent jouer sur deux types de prix, ceux de l'offre (banque-fournisseur) et ceux de la demande (banque-cliente). Dans le premier cas, la taille atteinte, via une fusion avec une autre institution, permettrait à la banque d'obtenir une part de marché dominante et par conséquent influencer le niveau des prix de ce marché ; soit à la baisse pour évincer du marché les établissements subsistants et/ou entrants, soit à la hausse en l'absence de concurrence effective. Dans le second cas, la taille obtenue va lui permettre de réduire ses coûts de refinancement grâce à plusieurs effets (effet de réputation dû à une pression de solidité du nouvel ensemble , effet de taille dans la mesure où la banque devient un objet incontournable de placement des marchés des capitaux , et effet de diversification dû aux sources de financement, la taille de la banque lui permet de bénéficier des meilleurs conditions par un arbitrage permanant entre les différents segments de marché).

Les F&A bancaires permettent d'obtenir des gains d'efficience par la réduction des coûts (synergies de coûts), l'accroissement des revenus (synergies de revenus), l'échange des meilleures pratiques (*best* practices), et la diversification des risques [4]. En effet, Les synergies de coûts résultent d'une meilleure organisation de la production bancaire, et de meilleures combinaisons des facteurs de production. L'objectif est de tirer profit des complémentarités en matière de coûts, d'économies d'échelle et d'économies de gamme. Ces synergies de coûts peuvent provenir de l'intégration des équipes et des plates-formes informatiques, de la mise en commun des back-offices et des services généraux, et du redimensionnement du réseau domestique et/ou international. Quant aux synergies de revenus, elles proviennent d'une meilleure combinaison des facteurs de production. Cependant, il faut y ajouter une meilleure organisation des activités, qui permet de tirer profit de la complémentarité des produits en termes de revenus. Les synergies de revenus peuvent provenir de l'harmonisation des gammes de produits, des complémentarités existantes entre les activités, de la généralisation de l'approche multi-distribution, dont l'objectif est bien l'adaptation des canaux de distribution aux différents segments de clientèles. Toutefois, les synergies de revenus sont bien plus difficiles à obtenir que les synergies de coûts, car elles ne dépendent pas seulement des décisions des dirigeants mais aussi du comportement des clients. À cet égard, l'étude [5] est parmi celles qui évaluent entre 5 et 10 % le nombre de clients qui sont susceptibles de quitter la banque après une fusion. Les gains d'efficience s'obtiennent par l'ajustement des quantités d'inputs et d'outputs en vue de réduire les coûts, accroître les revenus et/ou réduire les risques afin d'augmenter la valeur ajoutée. Les F&A peuvent également permettre l'obtention de gains d'efficience par la réorganisation des équipes (dirigeants et salariés) et/ou la généralisation des meilleures pratiques (best practices). On parle alors d'efficience-X au sens de [6]. Enfin, l'efficience peut aussi être améliorée, au-delà des seules économies d'échelle et de gamme, par une plus grande diversification des risques ; diversification fonctionnelle et/ou

géographique (puisque les cycles économiques des différents pays de l'Union Européenne ne semblent pas parfaitement corrélés, une bonne diversification géographique permettrait aux banques européennes de réduire significativement leur niveau de risque).

2.2 LA PERFORMANCE DES F&A BANCAIRES : UNE RECENSION EMPIRIQUE

Pour évaluer la performance des F&A, deux méthodes principales sont utilisées. La première est celle des études d'événement. La seconde utilise les données comptables, pour comparer la performance des entreprises avant et après l'union.

2.2.1 LES RENTABILITES ANORMALES DES F&A BANCAIRES

Plusieurs études, principalement aux États-Unis, ont utilisé les études d'événement afin de mesurer les effets des F&A bancaires sur les valeurs de marché. Certaines études ont examiné les rentabilités anormales de la banque « acquéreur » et de la « cible » séparément tandis que d'autres ont examiné le changement total de la richesse des actionnaires. La plupart des études empiriques a conclu, de façon unanime, que l'annonce d'une F&A bancaire crée de la valeur pour les actionnaires de la cible et nul pour l'ensemble. En revanche, les différentes études qui se sont intéressées à l'impact des F&A bancaires sur la richesse des actionnaires de l'entreprise acquéreuse ont présenté des résultats contradictoires. Plus précisément, [7], [8] et [9] montrent que les F&A bancaires reproduisent des gains pour les entreprises acquéreuses et à l'inverse, [10], [2], [11] et plus récemment [12] mettent en évidence des pertes. Le tableau 1, ci-après, résume ces travaux empiriques.

Tableau 1. Synthèse des rentabilités anormales à court terme lors des F&A bancaires

Auteurs	Période	Taille de l'échantillon	Fenêtre d'événement	RAC de l'acquéreur (%)	RAC de la cible (%)
Trifts et Scanlon (1987)	1982-1985	21	(-10,0)	-3,25**	21,37*
James et Wier (1987)	1972-1983	60	(-40,0)	1,77***	Na
Neely (1987)	1979-1985	26	(-10,0)	1,25	31,26***
Cornett et De (1991)	1982-1986	152	(-1,0)	0,55***	8,10***
Cornett et Tehranian (1992)	1982-1986	152	(-1,0)	-0,80	8,10***
Houston et Ryngaert (1994)	1985-1991	153	(-2,2)	-2,32***	14,39***
Houston et Ryngaert (1997)	1985-1992	184	(-2,2)	-2,40	20,40****
Toyne et Tripp (1998)	1991-1995	68	(-5,5)	-2,25**	14,77***
Becher (2000)	1980-1997	553	(-30,5)	-0,1	22,64**
DeLong (2001)	1988-1995	280	(-10,1)	-1,68***	16,61***
Hart et Apilado (2002)	1994-1997	28	(-5,5)	-0,41	6,02***
Caby et Descos (2007)	1997-2000	133	(-5,5)	-3,72***	6,77**
Bendeck et Waller (2007)	1980-1996	153	(-1,0)	-7,42**	11,89**
Al-Sharkas et Hassan (2010)	1980-2000	1077	(-10,10)	-0,88*	8,63***

*, **, *** significatif aux seuils de 10%, 5% et 1%.

2.2.2 LA PERFORMANCE COMPTABLE DES F&A BANCAIRES

Ref. [13] a examiné 39 études empiriques sur l'efficacité des F&A bancaires aux Etats-Unis, de 1980 à 1993, dont 19 utilisant des ratios financiers. En dépit des choix méthodologiques variés, la plupart des résultats converge vers un manque d'amélioration de la productivité ou de la profitabilité. La majorité des études vont dans le même sens ([14], [15], [16], [17]). En revanche, l'étude [18] analyse la performance opérationnelle de 30 fusions des firmes bancaires entre 1982 et 1987. Ils ont démontré une amélioration significative de la performance opérationnelle post-acquisition (0,87%). Ces auteurs ont également voulu déterminer la source de cette amélioration de la performance opérationnelle post-fusion. En effet, une hausse du flux de trésorerie d'exploitation est due selon ces auteurs à la capacité d'attirer les prêts et les dépôts, de la productivité des employées, et la croissance profitable des actifs. En conclusion, La plupart des études empiriques ne parviennent pas à trouver une relation positive entre les gains de la performance et l'activité des F&A.

3 METHODOLOGIE DE LA RECHERCHE ET SOURCES DE DONNEES

3.1 JUSTIFICATION DE L'ÉTUDE DE CAS

Pour atteindre le but de cette recherche, l'appréciation de la valeur créée lors de la fusion bancaire, l'étude de cas semblait la méthode de recherche la plus appropriée. Ref. [19] définit l'étude de cas comme stratégie de recherche empirique qui consiste à étudier un phénomène actuel dans son contexte réel, en utilisant plusieurs sources d'informations. Les deux éléments clé qui définissent l'étude de cas sont ainsi l'actualité du phénomène étudié (on parle de récit de vie lorsqu'on étudie un événement passé) et l'importance des éléments et nuances du contexte (sinon, il s'agit d'un sondage). Il devient donc intéressant de procéder par étude de cas lorsque l'on souhaite étudier un phénomène que l'on peut isoler ou reproduire en laboratoire et c'est ce qui fut privilège pour cette recherche.

Ainsi, dans le cadre d'une étude de cas, il est possible de fonctionner de deux façons différentes. Premièrement, l'étude d'un seul cas est possible, étude qui atteint un important niveau de profondeur et qui demande une étroite collaboration entre le chercheur et les individus impliqués dans l'entreprise visitée. Deuxièmement, il est possible d'étudier plusieurs cas différents. On appelle ce type de recherche une étude multi-sites ou multi-cas. Les études sont alors plus courtes et moins détaillées. Dans la présente recherche, l'étude d'un seul cas est privilégiée car notre objectif est de déceler et découvrir la nature de la valeur créée lors d'une opération de fusion en étudiant une seule opération en profondeur et mobilisant plusieurs données comptables et financières des entreprises concernées par l'opération.

3.2 LA MÉTHODE DE L'ÉTUDE D'ÉVÉNEMENT

Ref. [20], soutiennent que l'examen de la réaction des cours boursiers autour de la date d'annonce de la transaction est le meilleur moyen pour analyser la création ou la destruction de valeur générée par une opération de F&A. Cette méthodologie s'inspire des travaux de [21] qui s'appuient sur l'idée que le marché boursier réagit immédiatement à des annonces supposées affecter la rentabilité future de l'entreprise. Ces auteurs ont établi une relation linéaire entre le rendement d'équilibre d'un titre sur une période et le rendement moyen du marché.

La date d'annonce de l'opération est la date qui correspond à celle où l'offre du rapprochement est pour la première fois rendue publique par les autorités de bourse de Casablanca. L'étude d'événement est analysée sur une « fenêtre d'événement » et une « fenêtre d'estimation ». Dans le cadre de cette étude, la période d'événement choisie comprend les 10 jours précédents et suivants la date d'annonce d'acquisition et la période d'estimation, il n'y a pas de règle précise, il faut juste que cette dernière soit assez longue, afin que les paramètres estimés soient plus stables et décrivent au mieux le comportement des cours. La période d'estimation des *betas* que nous avons retenu de 200 jours compris entre -240 et - 40 jours.

Les rentabilités normales sont calculées à partir du modèle de marché, à l'instar de la plupart des études antérieures. Soit $R_{i,t}$ la rentabilité du titre i à la date t, on estime :

$$R_{i,t} = \alpha_i + \beta_i Rm_t + \varepsilon_{i,t}$$

Où Rm_t est la rentabilité de l'indice MASI[4]. Les paramètres α_i et β_i sont estimés à partir des moindres carrés ordinaires sur la fenêtre d'estimation. Les rentabilités anormales ($RA_{i,t}$) sont obtenues en calculant :

$$RA_{i,t} = R_{i,t} - \left(\hat{\alpha} + \hat{\beta}_i Rm_t\right)$$

[4] Le MASI (Moroccan All Shares Index) est le principal indice boursier de la bourse de Casablanca, il est composé de toutes les valeurs cotées sur la place casablancaise.

Après avoir constitué deux échantillons, le premier regroupe les données de Wafabank et le second celles de la BCM, et déterminé les rentabilités anormales (RA), nous avons cumulé ces RA pour chaque titre sur toute la période d'événement (RAC) : $RAC_t = \sum_{t=-10}^{+10} RA_t$

Au niveau de la dernière étape, les résultats obtenus ont été testés pour juger leur significativité. Le test de Student a été désigné afin de vérifier la significativité des rentabilités anormales. Comme ce travail porte sur un seul échantillon, et conformément à [25] et [26], l'estimation de *t* a été ajustée par l'auto- covariance des gains.

$$t = \frac{RAC}{ecarttpe_t} \qquad \text{Avec Écart type} = \sqrt{(T \times Var(RA_t) + 2(T-1)Co\,\mathrm{var}(RA_t, RA_{t-1}))}$$

Où T est égale à la différence entre le premier jour d'accumulation et le dernier jour plus 1. La variance et la covariance des deux entreprises ont été estimées sur une période de -220 à -20 jours avant la date d'événement.

3.3 LA MÉTHODE DE PAIRAGE

La méthode de pariage consiste à comparer les ratios financiers des entreprises concernées avant l'opération avec celles des mêmes entreprises après l'opération. L'objectif est de vérifier un tel impact de la fusion sur les ratios financiers. Elle consiste à comparer les changements des performances des groupes Wafabank et BCM avant la fusion avec celle de la société combinée Attijariwafa Bank après la fusion. Cette étude empirique adopte trois ans avant et trois ans après le regroupement c'est-à-dire une période de six ans $[-3ans,+3ans]$. Une période plus longue que trois ans après l'acquisition pourrait biaiser les résultats, puisque les entreprises sont impliquées dans d'autres événements. Conformément aux études précédentes, notamment [22], l'année d'acquisition (0) est exclue de l'analyse des performances car les coûts de transaction liés à l'opération du rapprochement seront reflétés dans les résultats d'exploitation de l'année de l'opération rendant la comparabilité avec d'autres années inadéquate.

D'après [13] et [18], sept ratios financiers ont été choisis pour analyser la productivité et la profitabilité. Le tableau 2, ci-après, expose les ratios utilisés comme indicateurs de productivité et de profitabilité dans cette recherche.

Tableau 2. Les critères de mesure de la performance

Ratios	Formules
Ratios de profitabilité	
ROA : Return On Assets ou Rentabilité des actifs	Résultat net / Actif total
ROE : Return On Equity ou Rentabilité des capitaux propres	Résultat net / Fonds propres
ROCE : Rentabilité économique	Résultat d'exploitation / Actif total
Ratios de productivité	
LTA : Loans to assets ou ratio d'endettement	Dettes totales / Actif total
SPE : Sales Per Employee ou productivité commerciale	Ventes réelles / Nombre d'employés
APE : Assets Per Employee ou productivité des actifs	Actif total / Nombre d'employés
IPE : Income Per Employee ou bénéfice par employé	Bénéfice net / Nombre d'employés

4 RÉSULTAT ET DISCUSSION

4.1 ANALYSE DE LA RENTABILITE ANORMALE

La figure 1 et 2, présentée ci-dessous, décrit la RAC pour l'entreprise acquéreuse et cible sur la fenêtre d'événement (-10 ; + 10). Pour l'acquéreur, ces RAC connaissent une baisse autour de la date d'annonce et demeurent négatives pendant la période post-annonce. Pour la cible, ces RAC connaissent à partir de 5 jours après la date d'annonce une forte croissance. L'analyse des rentabilités anormales pour l'acquéreur et la cible sur plusieurs fenêtres d'événement et des tests de significativité ont été conduits sur les différentes phases observées du processus de marché (tableau 3). La nature des

différentes réactions du marché à l'événement correspond à l'analyse par les investisseurs du contenu informationnel de chacune de ces phases.

Nous observons que les RAC pour Wafabank sont positives sur tous les intervalles à l'exception des deux fenêtres (0,0) et (-5,5). La RAC est positive et la plus élevé pendant 21 jours de l'événement (-10,10) avec 12,77%. Tandis qu'elle atteint le plus bas de la fenêtre (-5,-1) avec 0,26%. Nous pouvons comparer les résultats présentés dans le tableau 3 avec ceux rapportés dans les études précédentes (voir le tableau 1). Ce résultat rejoint celui obtenu par [12].

Pour BCM, les RAC sont négatives sauf pour la période post-acquisition (+6, +10) où elles sont positives et significatives. Il est à noter que la banque acquéreuse BCM montre une perte moins importante dans le cas des fenêtres d'événements courtes. Ces résultats sont cohérents avec certains des études empiriques dans le tableau 1. Par exemple, [2] trouve une RAC de -3,76% pour une fenêtre d'événement de 11 jours, la RAC constatée dans notre étude est comparable de -17,63%.

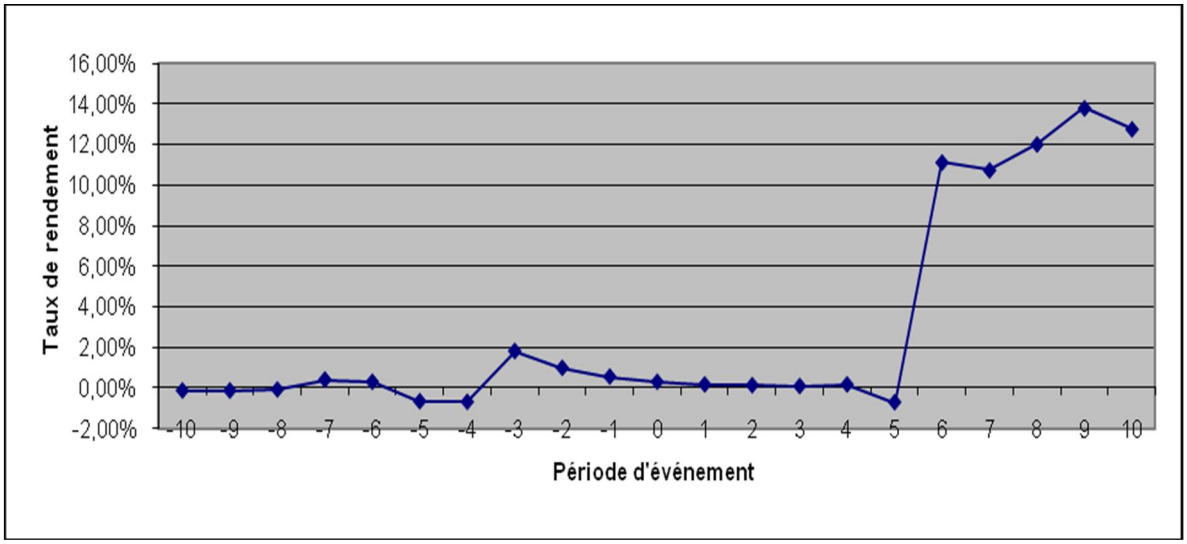

Fig. 1. Evolution des rentabilités anormales cumulées pour Wafabank pendant la période d'événement (-10,10 jours)

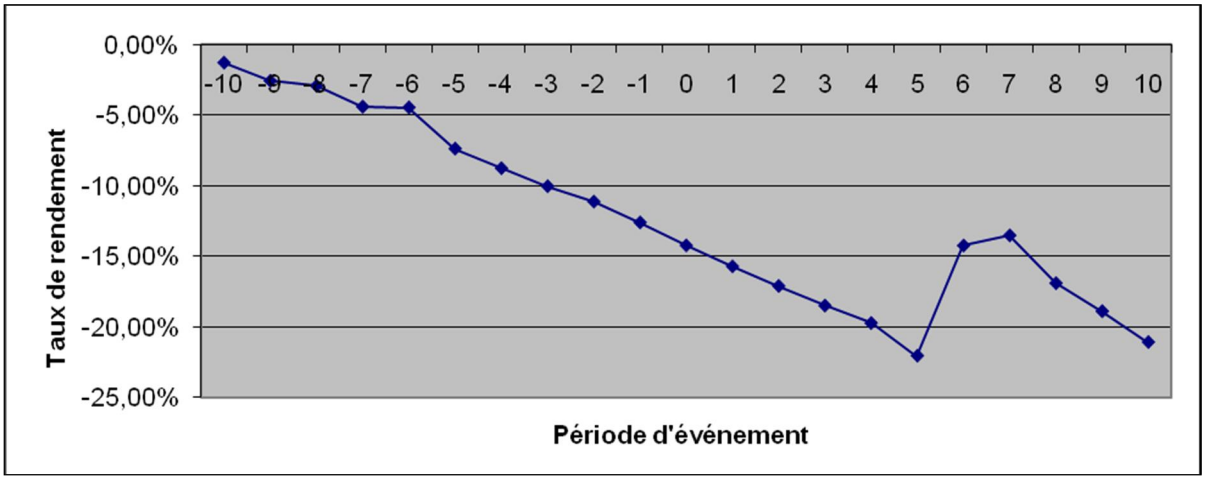

Fig. 2. Evolution des rentabilités anormales cumulées pour la BCM pendant la période d'événement (-10,10 jours)

Ces résultats indiquent que les actionnaires de la firme acquéreuse réalisent des rendements anormaux négatifs et significatifs tandis que ceux de la firme cible réalisent des gains significatifs.

Tableau 3. La Rentabilité anormale cumulée sur différentes fenêtres d'événement

	Fenêtre d'événement	RAC (BCM)	RAC (Wafabank)
Anticipation par le marché	(-10,-6)	-4,41%	0,29%
	(-5,-1)	-8,17%	0,26%
Réaction du marché à l'annonce	(0,0)	-1,63%	-0,26%
Zone de forte réaction	(-5, +5)	-17,63**%	-1,01%
Comportement du marché post-annonce	(+6, +10)	0,98*%	13,49**%
Total de la rentabilité anormale	(-10, +10)	-21,09**%	12,77**%

*, **, *** significatif aux seuils de 10%, 5% et 1%.

4.2 ANALYSE DE LA PERFORMANCE COMPTABLE

Le tableau 4 affiche les résultats montrant la variation des critères de comparaison.

Tableau 4. La variation de la productivité et de la performance opérationnelle de Wafabank et BCM

Ratios	Moyenne avant	Moyenne après	Médiane avant	Médiane après	Changement moyenne (après-avant)	% changement moyenne	Changement médiane (après-avant)	% changement médiane
Ratios de profitabilité								
ROE (Rentabilité des capitaux propres)	9,53	12	12,86	16,07	6,54	25,90	3,21	24,92
ROA (Rentabilité des actifs)	1,03	1,11	1,41	1,48	0,47	7,08	0,07	4,62
ROCE (Rentabilité économique)	1,34	1,59	1,41	1,69	0,35	19,29	0,27	19,43
Ratios de productivité								
SPE(Productivité commerciale)	1,30	2,59	1,31	2,41	1,29	99,1	1,10	84,58
IPE (Bénéfice par employé)	0,18	0,28	0,24	0,35	0,10	59,23	0,12	48,79
APE(Productivité des actifs)	17,47	35,46	16,98	33,45	17,98	102,94	16,47	97,04
DTA (Dette totale/ actif total)	64,76	67,83	63,40	68,84	3,62	5,64	5 ,44	8,59

4.2.1 RATIOS DE PROFITABILITÉ

Concernant la rentabilité économique, une variation de 19,29% a été enregistrée après le rapprochement. En effet, la croissance du chiffre d'affaires beaucoup plus importante que celle des charges d'exploitation, pendant les trois années suivant le regroupement, explique l'augmentation du résultat d'exploitation qui passe de 1,283 en 2004 à 2,333 Millions MAD en 2006. L'ensemble de ces éléments justifie l'amélioration de la rentabilité économique post-fusion. Ce premier résultat est cohérent avec l'optimisation des activités du groupe, issu de ce regroupement. Il s'agit d'une synergie de croissance qui a pour origine l'augmentation du chiffre d'affaires. S'agissant de la rentabilité financière (ou la rentabilité des capitaux propres), la variation est de l'ordre de 25,9% et s'explique par l'évolution du résultat net du groupe, qui passe de 200.730 en 2004 à 2.221.550 MAD en 2006. Ce taux important de rendement financier qui sert d'abord à financer des projets à VAN positive, rémunère largement les apporteurs de capitaux. Ce résultat permettrait aussi à l'entreprise d'attirer de nouveaux investisseurs. Enfin, pour la rentabilité des actifs, la variation est de l'ordre de 7,08%. Ce ratio donne une idée sur l'utilisation des actifs de l'entreprise par l'équipe dirigeante, afin de générer du bénéfice. D'après les résultats, le

regroupement des deux entités a permis une meilleure utilisation des actifs de l'ensemble. Il s'agit des gains d'efficience obtenus via la réorganisation des équipes (dirigeants et salariés), et une généralisation des meilleures pratiques ([6]).

Bien que ces résultats rejoignent ceux de [18], ils sont en contradiction avec la majorité des travaux empiriques portant sur le sujet ([14], [15], [16], [17]). Ces derniers ne trouvent pas une amélioration de la rentabilité après une fusion bancaire.

4.2.2 RATIOS DE PRODUCTIVITÉ

Parallèlement, les ratios de productivité affichent des taux de variation moyenne très importants en comparaison aux ratios de profitabilité. Il s'agit, premièrement, de la productivité commerciale et celle des actifs qui atteignent une variation de l'ordre de 99,1% et 102,94% successivement. En effet, l'amélioration du ratio de productivité commerciale, défini par le rapport entre les ventes réelles et le nombre d'employés, est justifiée par l'augmentation du volume du chiffre d'affaires que l'ensemble a réalisé grâce à la fusion (l'entreprise a dû augmenter ses prix ou/et ses quantités vendues). Cette amélioration s'inscrit toujours dans le cadre de l'optimisation des activités du groupe (synergie de croissance) grâce à la nouvelle taille critique et à ce nouveau pouvoir de marché acquis après la fusion. La variation positive du ratio de productivité des actifs, qui met en rapport l'actif total et le nombre d'employés, s'explique par l'importance de l'actif total des deux entités regroupées par rapport au nombre des employés. Le nouveau groupe restructuré crée plus de richesse grâce à l'opérationnalisation de ses actifs (synergies opérationnelles).

Le ratio du bénéfice par employé enregistre un taux de variation positif de l'ordre de 59,23% ce qui conduit à constater que la productivité des employés s'améliore après la fusion, une amélioration qui s'explique par la croissance importante du bénéfice net, due probablement à des synergies de coûts qui peuvent provenir par exemple de l'intégration des équipes et des plates-formes informatiques, de la mise en commun des back-offices et du re-dimensionnement du réseau domestique et/ou international. Enfin, concernant le taux de variation du ratio d'endettement, exprimé par le rapport entre la Dette totale et l'Actif total, il enregistre une variation de 5,64%. L'intégration des deux banques a permis au groupe de maximiser la capacité d'endettement et d'optimiser par la suite son coût du capital.

Ces résultats correspondent aux conclusions rapportées par [22] et [23], et qui confirment que les fusions conduisent à une meilleure utilisation des actifs, et à celles de [24] déduisant que ces opérations permettent de bénéficier des synergies opérationnelles et des gains d'efficience.

5 CONCLUSION

L'objectif de cette étude consiste à mesurer la création de valeur financière et stratégique à travers l'étude du rapprochement entre la Banque Commerciale du Maroc et Wafabank. Pour arriver à cette fin, une approche boursière et comptable permettant de mesurer la création de valeur a été mise en œuvre. Les résultats empiriques de cette recherche montrent qu'à l'annonce de cette opération une création de valeur pour l'entreprise cible et une destruction de valeur pour l'entreprise acquéreuse ont été enregistrées.

Ces résultats sont en conformité avec ceux de [10], [2], [11], et [12], qui ont souligné un impact négatif des F&A sur la richesse des actionnaires de la firme acquéreuse et positif sur celle des actionnaires de la firme cible. Ainsi, à moyen terme, il a été constaté une amélioration de la profitabilité et de la productivité de l'entité regroupée. Ces résultats rejoignent d'abord ceux de [18], qui ont noté une augmentation de la rentabilité lors des fusions bancaires, valident ensuite les conclusions rapportées par [23] et [22], sur le fait que les fusions conduisent à une meilleure utilisation des actifs, et corroborent enfin avec ceux de [24], qui ont déduit que les fusions permettent de bénéficier des synergies opérationnelles et des gains d'efficience.

Toutefois, il convient de signaler la portée limitée de nos résultats dans la mesure où un cas ne permet pas la généralisation statistique. Néanmoins, les études de cas contribuent à la compréhension en profondeur d'un phénomène contemporain. Cependant, ce genre d'études, à notre connaissance, est peu développé dans les études récentes notamment au Maroc. Les travaux récents se basent souvent sur la méthode d'événement pour mesurer la création de valeur à court et à long terme. Une étude portant sur un échantillon plus large serait intéressante dans la mesure où elle permettrait d'utiliser des tests statistiques sans recourir à la méthode d'événement.

REFERENCES

[1] Meier, O., Schier G., *Fusions, Acquisitions : Stratégie, Finance, Management*, 2ème édition, Dunod, 2003.

[2] J. Caby and C. Descos, "La performance des fusions bancaires européennes 1997-2000," *Cahier de recherche- GREGOR*, 2007.

[3] V.R. Vander, "The effect of mergers and acquisitions on the efficiency and profitability of EC credit institutions," *Journal of Banking and Finance*, n° 20(9), pp. 1531-1558, 1996.

[4] R. Ayadi, P. de Lima , and G. Pujals, "Les restructurations bancaires en Europe," *Revue de l'OFCE*, hors série, n°38 bis, pp. 325-382, 2002.

[5] Y. Burger, "European Banking consolidation: time out?," *Standard & Poor's,* October, 2001.

[6] H. Leibenstein, "Allocation efficiency and X-efficiency," *American Economic Review*, n° 56, pp. 392- 415, 1996.

[7] W.P. Neely, "Banking acquisitions: acquirer and target shareholder returns", *Financial Management*, vol. 16, pp. 66-74, 1987.

[8] C. James and P. Wier, "Returns to acquirers and competition in the acquisition market: the case of banking", *Journal Political Economy*, vol. 95, pp. 355–370, 1997.

[9] M.M. Cornett and S. De, "Medium of payment in corporate acquisitions: evidence from interstate bank mergers", *Journal of Money Credit and Bank*, vol. 23, pp. 767–776, 1991.

[10] J.W. Trifts and K.P. Scanlon, "Interstate Bank Mergers: the Early Evidence", *Journal of Financial Research,* vol. 10, pp. 350-311, 1987.

[11] Y.M. Bendeck and E.R. Waller, "Bank Acquisitions Announcements and Intra-Industry Effects," *Journal of Business & Economics Research*, vol. 5, n°7, pp. 15-22, 2007.

[12] A. Al-Sharkas and M. Hassan, "New Evidence on Shareholder Wealth Effects in Bank Mergers during 1980-2000", *Journal of Economics and Finance*, vol. 34 (3), pp. 326-348, 2010.

[13] S.A. Rhoades, "Efficiency Effects of Horizontal (In-Market) Bank Mergers," Journal *of Banking and Finance*, Vol. 17, n°2, pp. 411-422, 1993.

[14] S.J. Pilloff, "Performance Changes and Shareholders Wealth Creation Associated with Mergers of Publicly Traded Bank Institutions", *Journal of Money, Credit and Banking*, vol. 28, pp. 294-310, 1996.

[15] J.D. Akhavein, A.N. Berger, and D.B. Humphrey, "The Effects of Megamergers on Efficiency and Prices: Evidence from a Bank Profit Function," *Review of Industrial Organization*, vol. 12, n°1, pp. 95-139, 1997.

[16] S.L. Chamberlain, "The Effect of Bank Ownership Changes on Subsidiary-Level Earnings", in Y. Amihud, G. Miller (Eds), Bank Mergers and Acquisitions, Kluwer Academic Publisher, 1998.

[17] S. Fadzlan , A.M. Zulkhibri , and H. Razali , "Efficiency and Bank Merger in Singapore: A Joint Estimation of Non-Parametric, Parametric and Financial Ratios Analysis", MPRA Paper N°12129, 2007.

[18] M.M Cornett and H. Tehranian, "Changes in Corporate Performance Associated with Bank Acquisitions", *Journal of Financial Economics*, vol. 31, pp. 211-234, 1992.

[19] Yin R.K., "Case study research: design and methods," Rev. ed. Newbury Park, CA: Sage Publications, 1994.

[20] G. Andrade, M. Mitchell, and E. Stafford, "New Evidence and Perspectives on Mergers," *Journal of Economics Perspectives*, vol. 15, n°1, pp. 103-120, 2001.

[21] E.F. Fama, L. Fisher, M.C Jensen, and R.W Rool, "The Adjustment of Stock Prices to New Information," *International Economic Review*, vol. 10, pp. 1-21, 1969.

[22] P.H. Healy, K.G. Palepu, and R.S. Ruback, "Does Corporate Performance Improve after Mergers?," *Journal of Financial Economics*, vol. 31, pp. 35-175, 1992.

[23] A. Rappaport, "Corporate performance standards and shareholder value", The Journal of Business Strategy, 3(4): 28-38, 1983.

[24] A. Seth, "Value Creation in Acquisitions: A Reexamination of Performance Issues," Strategic Management Journal, Vol. 11, n°2, pp. 99-115, 1990.

[25] R.S. Ruback, "The Conoco Takeover and Stockholder Returns", *Sloan Management Review*, vol. 14, pp. 13-33, 1982.

[26] R. Bruner, "An Analysis of Value Destruction and Recovery in the Alliance and Proposed Mergers of Volvo and Renault," *Journal of Financial Economics*, vol. 51, pp. 125-166, 1999.

ANNEXES

Schéma 1. Modalités des opérations de prise de contrôle

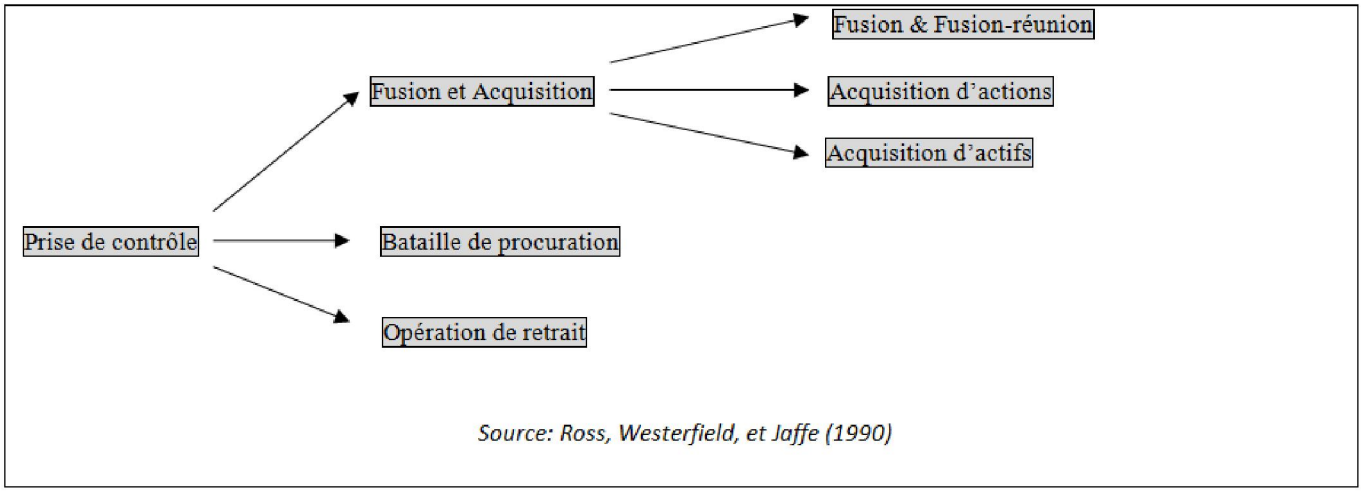

Tableau 5. Données financières et comptables des sociétés Wafabank, BCM et Attijariwafa Bank

Eléments (M=millions de dirhams)	BCM 2002	Wafabank 2002	BCM 2003	Wafabank 2003	Attijariwafa Bank 2005	Attijariwafa Bank 2006
Chiffre d'affaires M	3 754,08	3 225,08	3 609,24	3 392,92	9 384,69	11 949,00
Résultat d'exploitation (EBIT) M	NA	483,37	568,95	-145,91	2 454,36	3 645,62
Résultat net M	27,587	224,592	429,315	-393,515	1 635,97	2 021,55
Capitaux propres M	6 147,90	3 776,97	9 460,16	3 180,57	10 900,77	12 356,97
Dettes à long terme M	0,00	0,00	0,00	0,00	200,00	404,37
Dettes totales M	3 780,05	3 504,51	2 378,01	2 667,72	126 486,29	152 746,88
Total actif M	54 086,73	41 729,32	58 175,69	41 645,99	138 444,61	165 820,25
Effectif total au 31/12	2 453	2 695	2 453	2 695	4615	4 957
Nombre d'actions	13 250 000	6 457 637	13 685 137	6 457 637	19 299 596	19 299 596
Bénéfice net par action en dirhams	2,1	34,8	31,4	Ns	84,77	104,75

International Journal of Innovation and Applied Studies
ISSN 2028-9324 Vol. 3 No. 4 Aug. 2013, pp. 919-930

http://www.issr-journals.org/ijias/

Model for Technological Innovation Integration and New Product Development in High Tech Environments

Selma Regina Martins Oliveira and Jorge Lino

Department of Mechanical Engineering,
University of Porto,
Porto, Portugal

ABSTRACT: The products introduced to the market that make use of the technology developed require ensuring the integration between the technologies and the products developed, minimizing risks and maximizing results. This article aims to contribute to a new planning policy in the development of innovative products. To do so, it presents a new modeling proposal to integrate technological innovation and new product development (NPD) in high tech environments, carried out according to the following stages: Phase 1: Modeling of the information needs in PDP; Phase 2: Determining of technology integration dimensions to the product; Phase 3: Evaluation of performance of technology integration dimensions to the product. To demonstrate the feasibility and plausibility of the modeling, a study case was conducted in a high tech company in Brazil. The investigation was helped by the intervention of specialists with technical and scientific knowledge about the research object. In order to reduce the subjectivity in the obtained results, the methods of Categorical Judgment Law (CJL) of Thurstone from 1927, Artificial Neural Networks (ANN), the multicriteria Electre III methods, Compromise Programinng and Promethee II; Multivaried Analysis and the neurofuzzy technology were used. Few studies have investigated the Product-Integration Technology. It is hoped that this study will stimulate a broad debate on the issue and it is acknowledged that more studies are needed to build more robust results in the near future. The results were satisfactory, validating the present proposal.

KEYWORDS: Modeling proposal, Planning, Integration, Technological innovation, New product development, High tech environments.

1 INTRODUCTION

Recently, relevant changes have made organizational boundaries more fluid and dynamic in response to the rapid pace of knowledge diffusion [1]; [2]; [3], and innovation and international competition [4]. This helps to reconsider how to succeed with innovation [5]; [6]. Thus, innovative companies make use of their capabilities to appropriate the economic value generated from their knowledge and innovations [2]; [3]. Therefore, the supply of innovative products is presented as a quality standard in the race for pressing demands.

In this spectrum, the innovation process management becomes one of the greatest challenges. The literature refers to the product development process (PDP) and the technology development process (TDP) as the most relevant to the development of innovative products [7]. Thus, it is feasible that there is a concurrent and harmonic planning between these processes. For that, it is logical that the integration between these processes is successful, since the success of the innovation depends on the integration of them [7]. Because technology and product have different cycles, the development projects face problems related to the incorporation or commercialization of new technologies. The results are time and efforts underestimated to develop and use new technologies, besides developing Technologies without having a pre-determined product, with different maturity degrees, which implies in high costs, quality waste and inadequate deadlines.

Corresponding Author: Selma Regina Martins Oliveira (selmaregina@mail.uft.edu.br)

2 MODELING: STEPS AND IMPLEMENTATION

This article aims to contribute to a new planning policy in the development of innovative products. To do so, it presents a new modeling proposal to integrate technological innovation and new product development in high tech environments. The research was developed over the literature specialized and applied to a technologic base company in Brazil, in the field of nanotechnology, to confirm the modeling proposal and the theoretical excerpts. The research also had the intervention from specialists with knowledge about the investigated object, to confirm the modeling (structure and content).

At a second moment, the data (partners and owners) from the researched company were gathered to demonstrate the modeling. Next, the details from the modeling phases and stages were detailed. *Phase 1:* Modeling of the information needs in PDP; *Phase 2:* Determining of technology integration dimensions to the product*; Phase 3:* Evaluation of performance of technology integration dimensions to the product. Next, those procedures are detailed:

Phase1: Modeling of the Information Needs (technological base company)

This phase is structured according to the following stages and sub-stages: *stage 1* - definition of the characteristics of the products; *stage 2*: determination of the strategies of technological synchronization used by companies to the development of products; *stage 3* – Definition of the strategies of the innovation development and *stage 4*: Priorization of the information needs.

Stage 1: definition of the characteristics of the product: here are presented the product main characteristics.

Stage 2: determination of the strategies of the technological synchronization used by companies to manage the development of products. There are two strategies listed in the consulted literature: 1) simultaneous transference; 2) sequential transference.

Stage 3: Definition of the strategies of the innovation development. Two strategies were identified in the literature [13] consulted: bottom-up and top-down.

Stage 4: Priorization the needs of information the needs of information: This phase is structured in three stages: Sub-Stages 1) determination of the Critical Success Factors (CSF); 2) determination of the information areas (IAs); and 3) prioritization of the information needs starting from the crossing of CSF and the Areas of Information.

Sub-Stage 4.1: Determination of CSF: This phase is focused on determining the CSF, and is itself structured in two stages: (A) identification of CSF and (B) evaluation of CSF. (A) Identification: The identification of CSF is based on the combination of various methods: (a) environmental analysis (external variable: political, economical, legislation, technology and among others.); (b) analysis of the industry structure (users' needs, the evolution of the demand, users' satisfaction level, their preferences and needs; technological innovations); (c) meeting with specialists and decision makers; and (d) the study of literature. (B) CSF Evaluation:

After their identification, the CSF is evaluated in order to establish a ranking by relevance. Here the scale model of categorical judgments designed by [8] has been adopted. This model starts form mental behavior to explain the preference of a judge (individual) concerning a set of stimuli {O1, O2,…, On}. Thus, the evaluation of the CFS is systematized in the following steps: *Step 1:* determination of the frequencies by pairs of stimuli. *Step 2:* determination of the frequencies of ordinal categories. *Step 3:* calculation of the matrix [pij] of the relative frequencies accumulated. It is highlighted though that the results to be achieved in Step 3 reflect the probabilities of the intensity of the specialists' preferences regarding the stimuli, the Critical Factors of Success in this work. As a result, a hierarchical structure of CSF is obtained.

Sub-Stage 4.2:Determination of the Areas of Information

The CSF having already been defined, the information areas are delimited with respect to the different CSFs. After determining the CSF, the determination of the areas of information ensues. The goals of the areas of information define specifically what must be achieved by these areas to meet one or more objectives from the projects (business), contributing for the enhancement of the project performance as to quality, productivity and profitability.Thus, after their identification, the IAs is evaluated in order to establish a ranking by relevance. Here the scale model of categorical judgments designed by [8] has been adopted. As a result, a hierarchical structure of IAs is obtained.

Sub-stage 4.2.1: Determine the activities of the PDP In this sub-stage the main activities realized during the PDP are identified. The following activities performed according to the literature were identified [6]; [9], [10]; [11]: development of the concept of product, elaboration of the product syllabus, preparation of the production, launching and after-launching of the product. Determine strategies and product *portfolio*; elaboration and detailing of the project syllabus; determine technical and marketing merits of the project; realization of preliminary research to identify and analyze the market,

technology and business characteristics; Identify and evaluate the consumer's claim by market sector (market research); Define the architecture and requirements of the product; carry out product competitive benchmarking; define functionalities of the Math product; generate assessment criteria of the concept of the product and carry out tests of concept among others.

Sub-stage 4.2.2: Determine the TDP activities

In this sub-stage the main activities of TDP based on [6]; [9]; [12]; [10]; [11] are identified: (i) company strategic planning; (ii) determination of the technologic strategy; (iii) technology; (iv) consumer; (v) generation of ideas (vi) elaboration of project syllabus; (vii) future plans mapping; (viii) patent research; (vix) Identification of opportunities; (x) identification of the possibility of the idea in determined conditions through preliminary experiments; (xi) identification of the necessary resources and solutions for the identified failures; (xii) projection of platforms of products; (xiii) creation of QFD for technology (technological needs); among others. Soon after this procedure, the critical activities for integration are determined.

Sub-stage 4.2.3: Determination of the critical activities for integration

In this stage, the critical activities for integration of the technology to the product are defined. Integration must be understood as the set of activities or compatible practice between TDP and PDP [13], which aim at improving the application of knowledge to the products. Next, the IA global performances are evaluated according to the CSF.

Sub-Stage 4.3: Prioritization of the information needs starting from the crossing of CSF and the Areas of Information

Again, these information areas are ranked by application of the same Categorical Judgment Method of [8] and put into relation with the CSF. At this moment the following tools have been adopted: (a) Multi-objective utility – multi-attribute, in this case Compromise Programming ™, which represent mathematically the decision makers' preference structure in situations of uncertainty; (b) selective, taken on account for the situation, Promethee II ™ and (c) Electre III ™.

Phase 2: Determination of the dimensions of the integration of the technology to the product

In this stage the dimensions of the integration of the technology to the product are defined. [13] presents the following dimensions of the integration of the technology to the product: aspects, activities and time horizon. [14] considers other three dimnesions of the integration: Strategic and Operational synchronization, 2) Syllabus Transference, and 3) Transference Managemnet. Finally, [15] point out three basic elements for integration: 1) Synchronization; 2) Technology Equalization; 3) Technological Transference Management. [16] adopts the knowledge as the main dimension for the integration of the technology to the product. For this author, there will be integration IF the knowledge generated by the area of R&D is applied to a new product. In this work, the knowledge is the dimension to be considered for the integration. This dimension is detailed ahead. *Identification and Acquisition of Knowledge*

Initially, information topics which have been already identified will be elaborated, analyzed and evaluated in order to be understood by the decision makers during the formulation and the PDP and TDP. Following this, they will be reviewed and organized and validated by NPD and TDP specialists. Afterwards, relevant theories and concepts are determined. With respect to the acquisition procedures, the different procedures of the process of acquisition represents the acquisition of the necessary knowledge, abilities and experiences to create and maintain the essential experiences and areas of information selected and mapped out [17]; [18].

Acquiring the knowledge (from specialists) implies, according to [19], [20], the obtaining of information from specialists and/or from documented sources, classifying it in a declarative and procedural fashion, codifying it in a format used by the system and validating the consistence of the codified knowledge with the existent one in the system.

Therefore, at first, the way the conversion from information into knowledge [21] is dealt with, which is the information to be understood by and useful for the decision making in technological innovation integration and new product development. First the information is gathered. Then the combination and internalization is established by the explicit knowledge (information) so that it can be better understood and synthesized in order to be easily and quickly presented whenever possible (the information must be useful for the decision making and for that reason, it must be understood). In this work, we aim to elaborate the conversion of information into knowledge.

The conversion (transformation) takes place as follows: first, the comparison of how the information related to a given situation can be compared to other known situations is established; second, the implications brought about by the information for the decision making are analyzed and evaluated; third, the relation between new knowledge and that accumulated is established; fourth, what the decision makers expect from the information is checked. The conversion of information into knowledge is assisted by the information maps (elaborated in the previous phase by areas, through analysis

and evaluation of the information). We highlight that the information taken into account is both the ones externally and internally originated. The information from external origins has as a main goal to detect, beforehand, the long-term opportunities for the project. The internal information is important to establish the strategies, but it has to be of a broader scope than that used for operational management, because besides allowing the evaluation of the performance it also identifies its strengths and weaknesses.

Following from this, the proceedings for the acquisition of theoretical background and concepts are dealt with. Such proceedings begin with the areas of information, one by one, where the concept and the theory on which is based the performance of the actions (articulations) developed in those areas that allow to guarantee the feasibility of the new products development projects are identified. In other words, which knowledge and theory are required to be known in order to ensure the success of projects in the NPD in that area. Then, the analysis of surveys in institutions about the job market for these institutions takes place bearing in mind the demands of similar areas studied in this work. As for the offer, we intend to search for the level of knowledge required by the companies and other organizations in those areas, as well as what concerns technical improvement (means) for the professionals. This stage determines the concept of knowledge to be taken into account on the development of this work. So, for the operational goals of this work, we have adopted them as the "contextual information" and the theoretical framework and concepts.

Phase 3: Assessment of the performance of the integration of technology process to the product

In this phase the assessment of the performance of the integration of technology process to the product is done. This procedure is realized based on the neurofuzzy technology. The variables (knowledge) identified in the previous phase are input data for the neurofuzzy modeling (in this phase). Thus, this phase focuses on determining the optimal efficiency rate (OERP) of the high-tech industries'product development and technology integration using Neurofuzzy modeling. It is a process whose attributes usually possess high subjectivity characteristics, in which the experience of the decision maker is very significant. Thus within this spectrum there is the need for a tool that allows adding quantitative and qualitative variables that converge towards a single evaluation parameter [22]; [23]. This model combines the Neural Networks and Logic Fuzzy technology (neurofuzzy technology). Here this model supports the product development and technology integration using Neurofuzzy modeling of high-tech industries, as it allows to evaluate the desirable rate toward the acceptable performance of high-tech companies.

The model shown here uses the model of [22]. Based on the Neurofuzzy technology, the qualitative input data are grouped to determine the comparison parameters between the alternatives. The technique is structured by combining all attributes (qualitative and quantitative variables) in inference blocks (IB) that use fuzzy-based rules and linguistic expressions, so that the preference for each alternative priority decision of the optimal efficiency rate of the high-tech industries' product development and technology integration, in terms of benefits to the company, can be expressed by a range varying from 0 to 10. The model consists of qualitative and quantitative variables, based on information from the experts. The Neurofuzzy model is described below.

Architecture of the Neurofuzzy Network: In each network node, two or more elements are assembled in one single element, originating a new node. This new node is then added to other nodes, produced in parallel, which give rise to a new node. And so on, until the final node is attained. The neurofuzzy network architecture (NNA) is defined by the input variables in its first layer, always converging to their network nodes. Each node corresponds to a fuzzy rule base, designated as Inference Block (IB), in which the linguistic variables are computed by aggregation and composition in order to produce an inferred result, also in the linguistic variable form. Thus, the rules are defined in the IB of NNA. In summary, the input variables (IV) pass through the fuzzification process and through the inference block (IB), producing an output variable (OV), called the intermediate variable (IVa), if it does not correspond to the last IB on the network. This IV, then joins another IV, forming a set of new IVs, hence configurating a sequence on the last network. In the last layer, also composed of IV, it produces the output variable (OV) of the final NNA. The NNA architecture should be applied according to the number of specialists. These steps are detailed below.

Determination of Input Variables (IV): This section focuses on determining the qualitative and quantitative input variables (IV). These variables were extracted (15 variables) from the phase 2. (ranking of dimensions of knowledge). The linguistic terms assigned to each IV are: High, Medium and Low. Accordingly, phase 2 shows the IVs in the model, which are transformed into linguistic variables with their respective Degrees of Conviction or Certainty (DoC), with the assistance of twenty judges opining in the process. The degrees attributed by the judges are converted into linguistic expressions with their respective DoCs, based on *fuzzy* sets and IT rules (aggregation rules), next (composition rules).

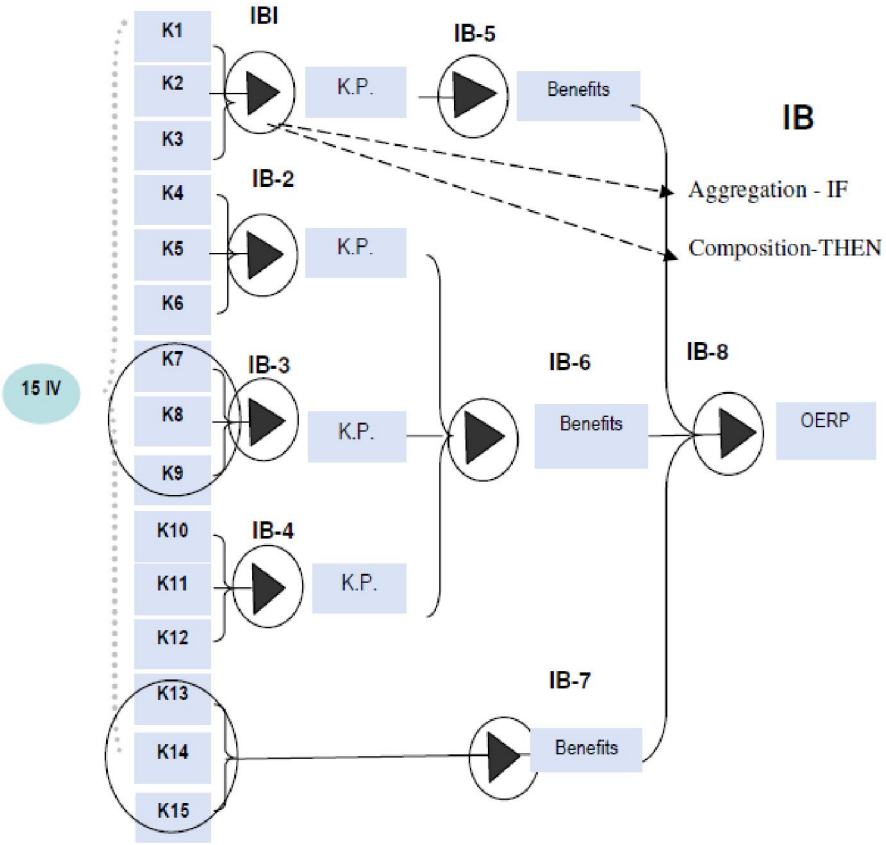

Fig. 1. Neurofuzzy Model

Determination of Intermediate Variables and Linguistic Terms: The qualitative input variables go through the inference fuzzy process, resulting in linguistic terms of intermediate variables (IVar). Thus, the linguistic terms assigned to IVar are: Low, Medium and High. The intermediate variables were obtained from: knowledge Performance. The architecture proposed is composed of eight expert fuzzy system configurations, four qualitative input variables that go through the fuzzy process and through the inference block, thus producing an output variable (OV), called intermediate variable (IVar).

Then, the IVars, which join the other IVar variables form a set of new IVars, thereby configuring a sequence until the last layer in the network. In the last layer of the network the output variable (OV) of the neurofuzzy Network is defined. This OV is then subjected to a defuzzification process to achieve the final result: Optimal Efficiency Rate (OERP) of product development and technology integration performance.of high-tech industries. In summary, the fuzzy inference occurs from the base-rules, generating the linguistic vector of the OV, obtained through the aggregation and composition steps. For example, when the experts' opinion was requested on the optimal efficiency rate for the product development and technology integration performance of company, the response was 8.0. Then the fuzzification (simulation) process was carried out, assigning LOW, MEDIUM and HIGH linguistic terms to the assessment degrees at a 1 to 10 scale. Degree 8, considered LOW by 0% of the experts, MEDIUM by 60% and HIGH by 40% of the experts. In summary, the expert's response enabled to determine the degree of certainty of the linguistic terms of each of the input variables using the fuzzy sets. .

The generic fuzzy sets were defined for all qualitative IVars, which always exhibit three levels of linguistic terms: a lower, a medium and a higher one. After converting all IVars into its corresponding linguistic variables with their respective DoC, the fuzzy inference blocks (IB), composed of IF-THEN rules, are operated based on the MAX-MIN operators, obtaining a linguistic value for each intermediate variable and output variable of the model, with the linguistic terms previously defined by the judges. With the input variables (features extracted from product development projects), the rules are generated. Every rule has an individual weighting factor, called Certainty Factor (CF), between 0 and 1, which indicates the degree of importance of each rule in the fuzzy rule-base. And the fuzzy inference occurs from the rule-base, generating the linguistic vector of OV, obtained through the aggregation and composition steps.

Determination of Output Variable – Optimal Efficiency Rate of product development and technology integration! Performance

The output variable (OV) of the neurofuzzy model proposed was called Optimal Efficiency Rate of *product development and technology integration* in high-tech company. The fuzzification process determines the pertinence functions for each input variable. If the input data values are accurate, results from measurements or observations, it is necessary to structure the fuzzy sets for the input variables, which is the fuzzification process. If the input variables are obtained in linguistic values, the fuzzification process is not necessary. A fuzzy set A in a universe X, is a set of ordered pairs represented by Equation 1.

$$A=\{(\mu_A(x),x)|x \in X\} \quad (1)$$

Where (x) is the pertinence function (or degree of pertinence) of x in A and is defined as the mapping of X in the closed interval [0.1], according to Equation 2 (Pedrycz and Gomide, 1998).

$$\mu_A(x):X\rightarrow [0.1] \quad (2)$$

Fuzzy Inference: The fuzzy inference rule-base consists of IF-THEN rules, which are responsible for aggregating the input variables and generating the output variables in linguistic terms, with their respective pertinence functions. According to [23], a weighting factor is assigned to each rule that reflects their importance in the rule-base. This coefficient is called Certainty Factor (CF), and can vary in range [0,1] and is multiplied by the result of the aggregation (IT part of inference). The fuzzy inference is structured by two components: (i) aggregation, i.e., computing the IF rules part; and (ii) composition, the THEN part of the rules. The Degree of Certainty (DoC) that determines the vectors resulting from the linguistic processes of aggregation and composition are defined with Equation 3.

$$DoC;:max[FC_1 . min\{GdC_{A11},GdC_{A12},...,GdC_{1n}\},...,FCn . min\{GdC_{An1},GdC_{An2},...,GdC_{Amn}\}| \quad (3)$$

Defuzzification: For the applications involving qualitative variables, as is the case in question, a numerical value is required as a result of the system, called defuzzification. Thus, after the fuzzy inference, fuzzification is necessary, i.e., transform linguistic values into numerical values, from their pertinence functions [23]. The IT Maximum Center method was popularized to determine an accurate value for the linguistic vector of OV. Based on this method, the degree of certainty of linguistic terms is defined as "weights" associated with each of these values. The exact value of commitment (VC) is determined by considering the weights with respect to the typical values (maximum values of the pertinence functions), according to Equation 4 presented below [22]; [23].

$$OV=\frac{\sum_{i=1}^{n} DoC_i . X_i}{\sum_{i=1}^{n} DoC_i . X_i} \quad (4)$$

Where i DoC represents the degrees of certainty of the linguistic terms of the final output variable and i X indicates the end of the typical values for the linguistic terms, which correspond to the maxima of fuzzy sets that define the final output variable. By way of demonstration, using assigned IT (average) hypothetical (Company) enters-IT into the calculation expression of TPCITj with GdCi of the following linguistic vector of the output variable, also hypothetical: LOW=0.35, MIDDLE=0.45, HIGH=0.20. The numerical value of OERP at a 0 to 1 scale corresponds to 0.8892, resulting from the arithmetic mean of the values resulting from the defuzzification of each of the simulated twenty judges. This value corresponds to an average value for OERP. With this result (optimal efficiency rate: 0.08892) produced for a better combination and interaction of knowledge (IV) of product development and technology integration that converged toward a single parameter, it is feasible to assert that this combination of knowledge (IV) activities of the firm at this time, can at least ensure the performance desired by the firm at that time. It is plausible that the company maintains at least this value (0.8892), which ensures the desired performance. It is also plausible to state that, to some degree, there is efficiency in the management of those planning technological innovation and product development in this category of industries high tech.

3 APPLICATION AND UNDERLYING ANALYSES

This section presents the verification procedures for the model. To demonstrate the feasibility and plausibility of the model, an implementation was based company in Brazil. Next, The detail of the steps.

Company structure and product characterization: The modeling was applied to a company of technological base in Brazil, in the nanotechnology Field. The data were gathered by consulting the partner-owners of the investigated company, through

a structured questionnaire. In this investigation, it was possible to know details of the company's PDP and TDP, in a way of verifying the practices conducted in the process of integration of the technology to the product. The research was based on a product (from the company) well succeeded in the national market, according to its innovation degree (for the market), having the OCDE (2005) reference as a basis. It is believed that the product passed through the 2 fundamental stages identified in the theoretic excerpts: the PDP and TDP. The organizational structure of the company is comprised of the following areas: R&D, commercial, administrative/financial, and by and administrative counseling. The company has been on the market for 8 years. The main object of the company is the development of products for application of tiles on different product surfaces, with multiple purposes, such as anti-germs, barriers against corrosion, among others that are possible through this kind of technology. Based on the proposal previously presented (section 2), the following CSF from the company were identified: Political/Legal; Economical and Financial; Market and Technical. The main IAs identified was: R&D; Commercial and Financial.

The process of development of the Technology: The technology of the studied product was developed in an approximately 2 years time. During its whole development, three partner owners from the company who are responsible for the P&D information, Commercial and Financial areas participated directly. The main PDT activities were as it follows: (i) carry out research through the literature, (ii) select and develop a superior concept of technology, define functionalities of the new technology (iii) optimize the technology from its critical parameters.

The product innovative technology in question was developed in a previous project, developed by the partner-owners, during a post-graduation course. Therefore, the activities were developed in labs of academic research, which enabled to obtain a structure of human resources involving teachers and physical resources comprising labs with the necessary support for the generation of the development of the technology. In this sense, the origin of this solution, which later would result in a business, had as a fundamental element the basic research. The owners established the company, therefore, with the technology in its early stage of development, a result from the post-graduation research. The first step was the realization of the research in the literature and in events to identify the trends in the market and in materials. Later, the group of research initiated the elaboration of the material, identifying the behavioral characteristics. Finally, tests in outsourced labs were conducted to get the certification of the technology developed. With that market opportunity, a patent was requested to secure the ownership [24].

The process of development of the product. Soon after the participation of the company in a fair of nanotechnology, the PDP was started. It was the moment in which there was the first commercial contact with a determined company that showed interest in the coverage of pieces of their products with the developed technology. The main PDP activities identified are as it follows: realization of the concept test; realization of the test and validation of the proposal of new product; realization of strength tests according to parameters; start the pilot production; launching of the product and realization of the effective production. Soon after the contact, the client company identified the pieces that were important to be covered in a way that it would aggregate value to the product. So, the pieces were submitted to applications and experiments with the new technology and the specific product to cover such types of parts was developed. To identify whether the technology met the needs of the client, such as appearance and bacterial property, tests in outsourced labs were conducted. After the results of test conclusions were released, the optimization of the application was started. In this stage, it was defined the structure of production for the application of the technology and improvement in the composition of materials [24]. It was produced a pilot lot so the client company could launch the product in an event within its sector. From the satisfactory results of product acceptance in the market, the large-scale production was started, which remains until the current moment of this study. The time between the first commercial contact and the delivery of the product with the applied technology was approximately one year, which half of this period was oriented to experiments and tests of application of the technology on the selected pieces.

The strategy of the development of the innovation adopted by the company for the development of the technology was bottom-up, or technology push, for on its beginning the development team, composed of three partner-owners, did not own a clear plan or idea to integrate this technology to the studied product. They did not even possess a more detailed vision about the possible consumer market or the focus of these markets. It was all about an academic research work that had only an informal perceptive identification, as they themselves called it, of the market opportunities. Initially the company did not have as the main target the studied product. In the beginning the idea was to develop a technology to cover the metal characterizing this strategy at first as top-down and later as a redirecting of its application, identifying market trends and the needs of applications of the technology in other products [24].

The strategy of technological synchronization adopted was the sequential transference of technology. At first, the technology was developed, then, the product. This was due to the fact that the technology was developed first to the market during the research in the post-graduation course of the partner-owners. Moreover, the company participated in the event

that led to the studied product in this work with the technology ready to be applied to the product. Yet not validated, but already in advanced stage of development. After some experiments were conducted with the selected pieces, it was verified the need of some adaptations in the technology [24]. At this moment, the existing synchronization between the processes becomes the simultaneous transference of technology, for during the adaptation of some chemical compositions of the technology; activities such as appearance and performance tests were also realized.

Besides, this case allowed to identify a time of 2 years, more than which the chance is smaller for the product project team and technology to share the results of the project. Thus, it is assumed that if the projects were realized with a time difference of 2 years maximum, they can be characterized as simultaneous synchronization. It is important to point out that through the identification of the strategy of synchronization the two-year time was noted as the necessary time for the company to validate and incorporate technology in a product so it can be commercialized. Once the activities of PDP and TDP and the critical activities were defined, the next step was to define the concept of technology to be adopted in this application. The concept adopted has basis in the knowledge. The literature defines technology as the knowledge applied to obtain a product (a practical result). Afterwards, iniciou-se the procedure of transference of technology (knowledge) to the product was started. On one hand, the knowledge/technologies demanded by the product (PDP). On the other hand, the knowledge offered by technology (TDP). As aforementioned, the integration of the technology to the product has basis on the proposal of [16], which has the knowledge as the main dimension of the integration of the technology to the product. The information area adopted in this application was R&D. The process of integration using the knowledge is shown as it follows.

The process of integration of the technology to the product: The concept adopted to knowledge are the theoretical bases and concepts and information of context. In this sense, the necessary knowledge to carry out the concept test was adopted; realization of test and validation of the proposal of a new product; realization of strength tests according to parameters; start of the pilot production; product launch and realization of the effective production, among others. The knowledge (technology) presented in tables 1 and 2 was preliminarily identified.

Table 1. Theoretical bases and concepts

Knowledge (Stmulis)	C1	C2	C3	C4	Total	Ranking
ENGE	-0,76471	0,430728	0,430728	0,76471	0,861456	**14º**
TI	-0,76471	-0,76471	0,430728	0,430728	-0,667964	**11º**
M.E.MQ	-1,22067	-1,22067	-1,22067	-0,43073	-4,09274	**2º**
GR	-1,22067	-1,22064	-0,13971	0,430728	-2,150292	**6º**
M.C.A.F.	-1,22067	-1,22067	-0,76471	-0,13971	-3,34576	**4º**
T.E.F.	-1,22067	-1,22067	-0,76471	0,76471	-2,44134	**5º**
CONT.	-1,22067	-1,22067	-0,13971	0,76471	-1,81634	**8º**
CUS	-1,22064	-0,13971	0,76471	1,220642	0,625002	**13º**
M.A.P.	-1,22067	-1,22067	-0,43073	1,220642	-1,651428	**9º**
T.P.	-1,22064	-0,13971	1,220642	0,13971	0,00017	**12º**
E.F.P.	-1,22067	-1,22067	-1,22067	-1,22067	-4,88268	**1º**
M.N.	-1,22067	-1,22067	-0,76471	0,76471	-2,44134	**5º**
R.D.P.	-1,22067	-1,22067	-0,43073	0,76471	-2,10736	**7º**
AD.	-1,22067	-1,22067	-1,22064	0,13971	-3,52227	**3º**
T.C.T.	-1,22067	-1,22064	-0,13971	1,220642	-1,360378	**10º**

Table 2. Contextual information

Knowledge (Stimulis)	C1	C2	C3	C4	Total	Ranking
E.F.	-1,22067	-1,22067	-1,22067	-1,22067	-4,88268	**1º**
E.T.	-1,22067	-1,22067	-1,22064	-0,13971	-3,80169	**3º**
P.T.	-1,22067	-1,22067	-1,22067	0,13971	-3,5223	**4º**
E.C.	-1,22067	-1,22067	-0,76471	0,13971	-3,06634	**5º**
G.R.	-1,22067	-1,22064	-0,43073	0,13971	-2,73233	**6º**
T.I.	-1,22064	-0,43073	0,430728	3,86499	2,644346	**12º**
E.F.	-1,22067	-1,22067	-0,76471	0,13971	-3,06634	**5º**
E.D.	-1,22067	-1,22064	-0,43073	0,76471	-2,10733	**8º**
I.E.F.	-1,22067	-0,76471	-0,13971	0,76471	-1,36038	**10º**
SU	-1,22067	-0,13971	-0,13971	1,220642	-0,27945	**11º**
S.F.	-1,22067	-1,22064	-0,43073	1,220642	-1,6514	**9º**
A.E.F	-1,22067	-1,22067	-0,76471	0,76471	-2,44134	**7º**
F.	-1,22067	-1,22067	-1,22067	-0,43073	-4,09274	**2º**

After being identified and acquired, the knowledge is evaluated, with the aid of the Method of Categorical Judgments of Thurstone (1927) and artificial neural network (ANN).

Evaluation for the method Categorical Judgments' Laws (1)

Stages The achievement method of the research results with the specialists of technological innovation, TDP and PDP, who revealed their preferences for pairs of stimulation (in the case, the objects of knowledge, and these submitted the ordinal categories C1 = 5º place, C2 = 3º place and C3 = 4º place). The evaluation of objects of knowledge (CJL) happened in three stages: In the stage (1), one determined the frequencies for pairs of stimulations, where Oi is equivalent to objects of knowledge and Oj the specialists. The data had been extracted from the preferences of the specialists in relation to objects of knowledge, attributing weights to the cognitive elements. After that (stage 2), the preferences of the specialists are determined in relation to the stimulations (knowledge/technology). The results were obtained by means of the ordinal frequencies from the results of the previous stage. Finally (stage 3), the accumulated relative frequencies were calculated first. The results obtained here reflect the probabilities of preferences intensity of the specialists in relation to the stimulations (theoretical bases and concepts). The result of the preferences, then, is presented in an upward order of importance (Tables 1 and 2).

Evaluation of Knowledge's Objects using the artificial neural network (ANN) (2)

The ANN is understood to simulate the behavior of the human brain through a number of interconnected neurons. A neuron executes weighed additions for the activations of the neurons representing nonlinear relations. The ANN has the capacity to recognize and to classify standards by means of processes of learning and training. The training of the net is the phase most important for the success of the applications in neural network. The topology of the net can better be determined of subjective form, from a principle that consists of adopting the lesser intermediate number of possible layer and neurons, without compromising the precision. Thus, in this application, the layer of the entrance data possess 15 neurons corresponding the 15 variable referring to objects of knowledge (technology). The intermediate layer possesses 7 neurons, and the exit layer possesses 1 corresponding neuron in a scale value determined for the ANN. The process of learning supervised based in the Back propagation algorithm applying software Easy NN determines the weights between the layers of entrance and intermediate, and between the intermediate and exit automatically. The training process was finished when the weights between the connections had allowed minimizing the error of learning. For this, it was necessary to identify which configuration that would present the best resulted varying the taxes of learning and moment. After diverse configurations to have been tested, the net of that presented better resulted with tax of an equal learning 0,37 and equal moment 0,88. The data had been divided in two groups, where to each period of training one third of the data is used for training of net and the remain is applied for verification of the results.

After some topologies of networks, and parameters, got the obtained network that showed better results was presented. The network was trained for the attainment of two result groups to compare the best-determined scale for the networks. In the first test the total of the judgment of the agents was adopted, however only in as test was gotten better scales, next of represented for method of the categorical judgments. With this, the last stage of the modeling in ANN consisted of testing the data of sequential entrance or random form, this process presented more satisfactory results. The reached results proved satisfactory, emphasizing the subjective importance of the scale methods to treat questions that involve high degree of

subjectivity and complexity. With regards to the topologies of the used networks, the results obtained some configurations of the ANN and compared with the CJT, it was observed that ANN 1, is the one that best approached the classification obtained for the CJT. Thus, even other topologies do not Tenaha been the best ones, it had been come however close in some objects of knowledge of the CJT. The results can be observed in Figure 2 that follows.

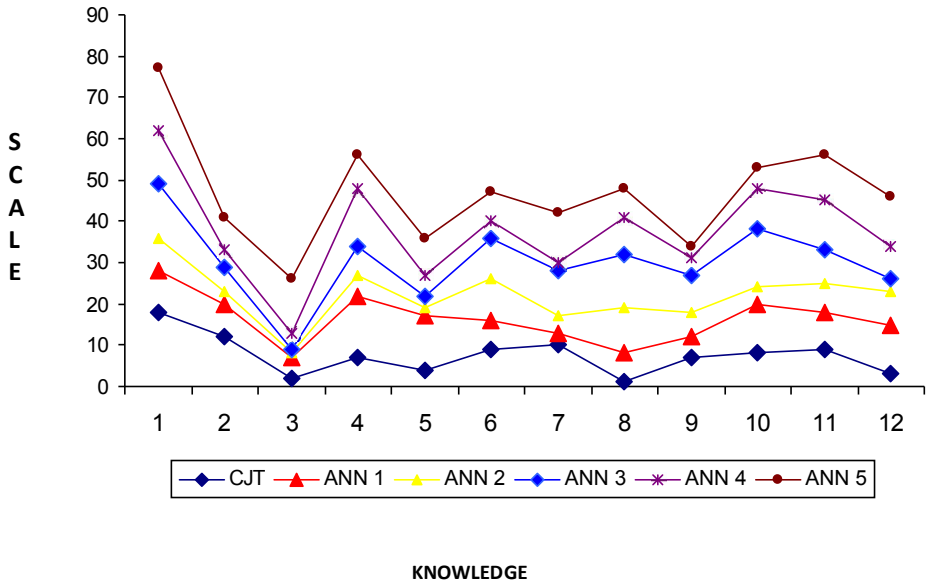

Fig. 2. Priority of Knowledge's Objects - ANN and CJT

The prioritized knowledge's objects for the tool proposals were for assessment of the performance of the integration of technology process to the product in high tech environments, Artificial Neural Networks (ANN), as well as Psychometric (CJL), was restricted only to the specialists' decisions in projects of raised subjectivity and complexity, needing other elements that consider the learning of new knowledge. However, it is interesting to highlight that the CJL method, as it considers a variable involving a high degree of subjective and complexity and because it works with probabilities in the intensity of preferences, considers the learning of new elements of knowledge. Thus, it can be said that for typology of application, as presented here, it is sufficiently indicated. Thus, even other topologies do not Tenaha been the best ones, it had been come however close in some objects of knowledge of the CJL. The integration of these variables in the *neurofuzzy* model results in a unique value which is the performance of the integration of the technology to the product. This enables to verify whether the procedure of integration was or not successful. The first 15 classified variables were used. The results showed a great efficiency rate of integration of the technology to the product equal to 0,89. This value corresponds to an average value for OERP. With this result (optimal efficiency rate: 0,89) produced for a better combination and interaction of knowledge dimensions (technologies) that converged toward a single parameter, it is feasible to assert that this combination of knowledge. It is also plausible to state that, to some degree, there is efficiency in the management of those NPD planning in this category of companies. To illustrate this, assuming that the study-object company demonstrate the following optimal efficiency rates (efficiency rate of integration of the technology to the product): T1 – 0.7833; T2-0.4442; T3-0.8974; T4-0.4983; AND- T5-0.4782 (Figure 3).

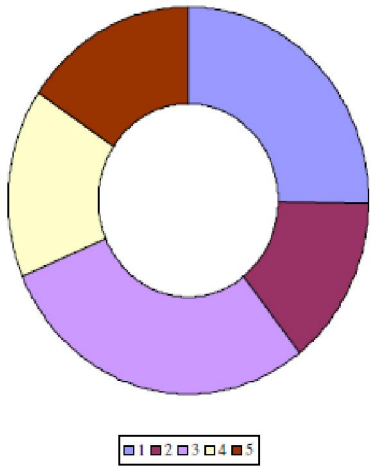

Fig. 3. Efficiency rate of integration of the technology to the product

The best performance of the integration of technology process to the product T3 (0,8974)

4 CONCLUSIONS AND IMPLICATIONS

This article aims to contribute to a new planning policy in the development of innovative products. To do so, it presents a new modeling proposal to integrate technological innovation and new product development in high tech environments. The modeling has as the central element the integration of technology to the product. The building started off from the modeling of the needs of information, with the definition of the characteristics of the product, of the strategies and the component activities of PDP and TDP, besides the priorities of information. Next, it was defined the knowledge as the dimension of the integration of the technology to the product, a proposal from [16]. Finally, the modeling to determine the performance of the process of integration of the technology to the product was developed. This procedure was conducted with the help of neurofuzzy technology. The performance of the integration was based on the knowledge (VE - input variables) of the neurofuzzy model. The performance is the result produced by the integration and convergence of the VEs to a unique value (output variable - VS), called performance rate of the integration of the technology to the product. The result enables to improve the planning policy to the development of new products, and set new strategies to the process of integration of technological innovations and the development of products.

The results obtained with the application of the proposed model show that this technology is adequate for supporting decision-making, due mainly to its low level of complexity and to its flexibility, that allows the input and output of variables. Through this method a more pragmatic and efficient guidance is sought, assisting the guidelines for long-term to integrate technological innovation and new product development in high tech environments, hence assuring this segment's competitiveness. Extensive and systematic procedures should be pursued that are capable of uniting the most diverse dimensions of planning of innovative products, surpassing the non-scientific practice often pervading some of the works. This proposal focuses on highlighting unexplored questions in this complex design. However, it evidently does not intend to be a "forced" methodology, but intends to render some contribution, even through independent course of actions.

By gathering the cognitive elements, it can be seen that this strategy requires a priority dynamics, which is dependent on the initial state of training, on the concrete characteristics of the projects and cognitive problems that emerge during the practice, always putting in view new contents. In the near future, we aim to demonstrate the suitability and feasibility of the proposed modeling framework, priority researches must be permanently and recurrently applied. Thus, this methodological support does not intend to be complete, but it is our intent to make it a generator of strategical elements for the development of new new products development projects. Of the findings of the state of the art and state of practice, it is reasonable to state that this research is vulnerable to criticism. This study includes limitations as specified below, which also helps to identify potential areas for future studies. A study was developed for Brazilian high tech company in a static context, which may represent a limiting factor. Therefore, it is recommended to reproduce and replicate the model in companies from other countries in order to confirm the results.

It is also recommended that the dimensions of the integration of the technology to the product should be extracted from the state of the art, but strongly confirmed by the state of practice, by the judgment of other experts (from other countries),

taking into account that values, beliefs, cultures and experiences are determinants in the assessment, which can overturn the effects on the results. It is also underscored that the methodologies and technical basis of this modeling should undergo evaluation by a multidisciplinary team of specialists permanently and periodically, hence proposing possible additions or adjustments to these methodologies. And also replace some of the technical implementations used herein by others, in order to provide a similar role to verify the robustness of the model. Nevertheless, the new products development will have to be anchored in efficient planning policies. One can argue that Brazil's high-tech industry still has a long way to go and also has tremendous growth potential. Hopefully Brazil can become a technological and competitive nation.

REFERENCES

[1] E. Abrahamson. "Managerial fad and fashion: the diffusion and rejection of innovations", *Academy of Management Review*, Vol. 16, pp. 586-612, 1991.

[2] Z. Griliches, "Patent Statistics as Economic Indicators: A Survey", *Journal of Economic Literature,* vol. 28, pp. 1661-1707, 1990.

[3] D.J. Teece, "Profiting from technological innovation", *Research Policy,* vol. 15, 6, pp. 285–305, 1986.

[4] F. Damanpour, "Organizational complexity and innovation: Developing and testing multiple contingency models". *Management Science,* vol. 42, 5, pp. 693-713, 1996.

[5] D.J. Teece, G. Pisano, A. Shuen, "Dynamic capabilities and strategic management", *Strategic Management Journal*, vol. 18, 7, pp 509-533, 1997.

[6] S. Wheelwright, K. Clark, *Revolutionising Product Development,* Free Press, New York, 1992.

[7] G. Johansson, et al., "Case studies on the application of interface dimensions in industrial innovation process," *Proceeding of the European Conference on Management of Technology (Euro MOT),* Birmingham, UK, vol. 2, 2006.

[8] L.L. Thurstone, A law of comparative judgment, Psychological *Review*, England, 1927.

[9] K. B. Clark, and T. Fujimoto, *Product development performance: strategy, organization and management in the world auto industry*, Boston: Harvard Business School Press, 1991.

[10] R.G. Cooper, "Managing technology development projects", *Research Technology Management,* vol. 49, 6, pp. 23-31, 2006.

[11] C.M. Creveling, J.L. Slutsky, and Antis, D., *Design for six sigma in technology & product development*, New Jersey: Prentice Hall, 2003.

[12] D. Clausing, *Total quality development: a step-by-step guide to world-class concurrent engineering.* New York: American Society of Mechanical Engineers, 1993.

[13] A. Drejer, "Integrating product and technology development", *International Journal of Technology Management,* vol. 24, 2/3, pp. 124-142, 2002.

[14] D. Nobelius, "Linking product development to applied research: transfer experiences from automotive company", *Technovation,* vol. 24, 4, pp. 321-334, 2004.

[15] W. Eldred, and M.E. McGrath, "Commercializing new technology", *Research Technology Management,* vol. 40, 1, pp. 41-47, 1997a.

[16] M. Iansiti, *Technology integration: making critical choices in a dynamic world,* Boston: Harvard Business School Press, 1998.

[17] C. Douligeris, and N. Tilipakis, "A knowledge management paradigm in the supply chain," *Int. Journal: EuroMed Journal of Business*, vol. 1, 1, pp. 66 – 83, 2006.

[18] C. Wu, "Knowledge creation in a supply chain", *Supply Chain Management: An International Journal*, vol. 13, 3, pp. 241-250, 2008.

[19] M. Buchanan, Nexus, Norton, New York, 2002.

[20] H. Eliufoo, "Knowledge creation in construction organisations: a case approach", *The Learning Organization,* vol. 15, 4, pp. 309- 325, 2008.

[21] R. T. Herschel, H. Nemati, and D. Steiger, "Tacit to explicit knowledge conversion: knowledge exchange protocols", *Journal of Knowledge Management*, vol. 5, 1, pp. 107-116, 2001.

[22] R. L. M. Oliveira, M.V. Q. Cury, "Modelo neuro-fuzzy para escolha modal no transporte de cargas," Tese of Doctoral Department Engeneering of Transportation, of Institute Militar of Engeneering, 2004.

[23] C. Von Altrock, *Fuzzy Logic and Neurofuzzy Applications in Business and Finance*, Prentice Hall, USA, 1997.

[24] J.S. Kurumoto, "Integração Tecnologia e Produto," Tese Doctoral Production Engeneering, University of São Paulo, 2009.

International Journal of Innovation and Applied Studies
ISSN 2028-9324 Vol. 3 No. 4 Aug. 2013, pp. 931-940

http://www.issr-journals.org/ijias/

Impact of Value Structure on Brand Engagement Depending on Degree of Self-Esteem of Adolescents

Blandína Šramová[1], Milan Džupina[2], and Olga Jurášková[3]

[1]Institute of Psychology and Speech Therapy Studies,
Faculty of Education,
Comenius University in Bratislava,
Moskovská 3,
811 08 Bratislava, Slovak Republic

[2]Department of Masmedia communications and advertisement,
Faculty of Arts,
Constantine the Philosopher University in Nitra,
Nitra, Slovak Republic

[3]Department of Marketing communications,
Faculty of Multimedia communications,
Tomas Bata University in Zlin,
Zlín, Czech Republic

ABSTRACT: This research demonstrates the relationship between the brand engagement, depending on the structure of values and level of self-esteem in adolescents. The research methods was used: Rosenberg´s Self-esteem Scale (Rosenberg, 1965), Portrait Values Questionnaire (Schwartz, 1992, 1994, 1999), Brand engagement (Sprott, Czellar, Spangenberg, 2009). The final outcomes showed differences, as well as a certain correlation between the values, which are attributed to adolescents, and engagement attributed to brand. Cultural values are identified as influential factors for the brand engagement perception of the importance of adolescents depending on their level of self-esteem. Research shows the importance of recognition of the values for understanding and foresight of relations between values and attitudes towards brands, which reflect both their behavior and their social experience. The result provides recommendations for marketing communication to easier identification of compatible and antagonistic values, which adolescents associate with a brand.

KEYWORDS: Brands Engagement, Portrait Values, Self-Esteem, Adolescents.

1 INTRODUCTION

One of important aspect influencing the buying behavior is the importance that the consumer attaches to brands. As the engagement of brands for the consumer is in close relationship with their relationship to it [1], marketers are trying to bring the brand as close as possible to consumers' personality in the form of brand personality and brand image. This serves to approximate a better understanding of consumer personality, its value preferences [2], as well as its degree of self-esteem [3]. There are a number of influences on consumers, consumer behavior is socially conditioned. Group influences, influences of social groups, particularly in adolescence, are particularly significant in these groups of products: products that are consumed publicly (e.g. alcohol, cigarettes), products which consumption the public notices (such as cosmetics); products, which are the subject in interviews (such as travel, movies). Important driver of consumer behavior are attitudes such as mental position towards a certain topic, which can positively influence the purchase of specific brands of products [4]. In case

Corresponding Author: Blandína Šramová (sramovab@fedu.uniba.sk)

the values of individual that co-create existing attitudes are consistent with the values represented by the mark, the assumption of a positive acceptance of the given product or service increases [5]. This factor is particularly significant in the process of consumer socialization during adolescence, when the adolescents try to express their personality through the brand while belonging to the certain social group, for what they are usually rewarded with favor by group members.

Values represent one of the major sources of human motivation, which gives a person meaning and direction of his efforts. They are present during the decision making process, they affect the mental processes of perception; survival and they are transformed into the ruling personalities. Values, as defined by Williams [6], refer to interests, desires, goals, needs and standards of preference. As in [7], there is eighteen terminal and eighteen instrumental values with varying percentages present for each individual, applicable depending on whether he speaks about terminal status of existence or about the ways that a person applies to achieve these objectives. He describes values as a general tendency to prefer certain states of reality to others. According to [8], values are one of the major components of culture (along with symbols, heroes and rituals) and they can be divided into two types: desirable, for instance those values relate to the wishes and preferences from a global perspective and desired, for instance wishes and preferences for a particular person according to his interests and needs.

One of the most widely used instruments to measure values is the range of values used by Schwartz [9]. According to Schwartz [9], values are standards that help person in ambiguous situations. They assist him in decision-making and subsequent separate proceedings.

In framing theory, [10, p. 21], stems from three basic requirements (individual biological needs coordination of social interaction, survival groups): (1) needs of individuals as biological organisms (abbreviated as "organisms"), (2) requisites of coordinated social interaction (abbreviated as "interaction") and, (3) requirements for the Smooth Functioning and survival of groups (abbreviated as "group"). Based on the theoretical concept a questionnaire, which describes 40 types of nature of the person (Portrait Values Questionnaire -PVQ) was developed. For the purposes of ESS (the European Social Survey) it was reduced to 21 entries, which was used in this research. The result is a structure consisting of ten universal cultural values (1^{st} order), which are grouped into four levels higher order (2^{nd} order). Values are displayed in the two-dimensional space fitted into the circular structure (Figure 1), which has two perpendicular axes illustrating conflict, or close relations between the ten core values. These axes are self-enhancement versus self-transcendence and openness to change versus conservatism. As in [9], values are interdependent, which means the closer in both directions around the ring they are, the more positive the relationship between them is and vice versa, the more remote they are, the more negative their relationship is.

Each of the ten basic values is characterized by describing its central motivational goal (e.g. [9], [12]):

1. **Benevolence**. Maintaining, improving the living conditions of people with whom one is in frequent personal contact (helping, honesty, forgiveness, loyalty, responsibility, spiritual life, true friendship, mature love, meaning of life)
2. **Universalism**. Comprehension, understanding, appreciation, tolerance and protection of the welfare of society and nature (generosity, wisdom, social justice, equality, peace, beauty, unity with nature, environmental protection, inner harmony).--
3. **Self-direction**. Independent thinking and decision making, creativity, research, independence (creativity, freedom, independence, curiosity, deciding on objectives, self- respect).
4. **Stimulation**. Excitement, life challenges, changes in life (courage, a varied life, an exciting life).
5. **Hedonism**. Sensuality and pleasure, enjoying life.
6. **Achievement**. Personal success demonstrated through competence adequate to social standards (success, ambition, ability, influence, intelligence).
7. **Power**. Social status and prestige, control or dominance over people and resources (social power, authority, wealth, protection of image in the public and recognition in society).
8. **Security**. Security, stability and harmony of society, as well as relationships with others and oneself (family security, national security, social order, cleanness, reciprocation of kindness, experiencing survival, health).
9. **Conformity**. Avoiding actions, inclinations and impulses, which could disrupt or harm others and violate social expectations or social norms, or cause offense (honesty, obedience, self-discipline, respect for parents and older).
10. **Tradition**. Respect, commitment and acceptance of ideas and attitudes that are the traditional cultures, and which are supplied and supported by region (humility, acceptance of one’s place in life, devotion, respect for tradition, moderation, impartiality).

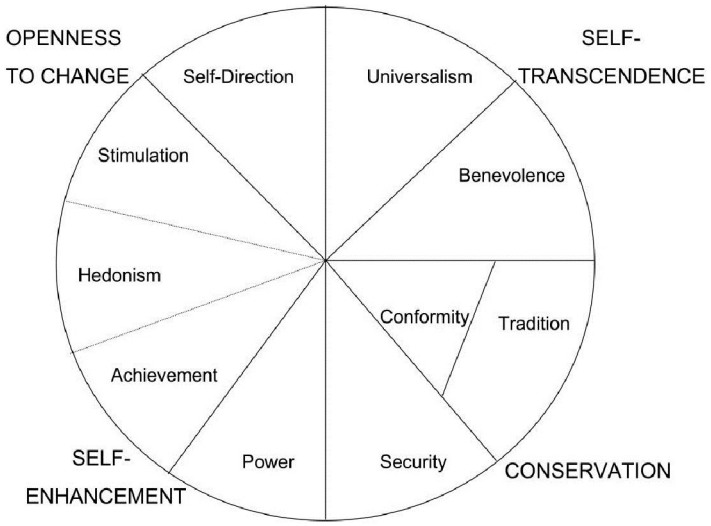

Fig. 1. Value structure (Schwartz,n.d.)

Self-esteem is one of important aspects of personality structure, which has been building over the life course. It is considered one of the components of self-concept resulting from the bio-psycho-socio-cultural factors. As in [13], self-esteem is the result of interpersonal and social comparisons of personality, under which the individual creates a positive or negative attitude toward himself. Positive self-esteem, as opposed to negative self-esteem, is reflected by increased confidence, satisfaction of an individual with oneself and other people's optimistic assessment. Several authors emphasize that the self-esteem is a mental representation of emotional relationship to oneself, which reflects the assessment, interpretation of the behavior of oneself as well as others (e.g. [14], [15]).

From the developmental point of view it is important to focus attention on the importance of self-esteem in adolescence, which is considered a sensitive period for the development of identity and of the related self-concept. It is in that given phase of development when self-esteem is vulnerable, heavily influenced by external socialization factors (family, media, peers, community, etc.), task of which is promoting a context of consistent and stable self-esteem. Existing relationships, the socially claimed and recognized values thus become a part of forming and stabilizing self-esteem.

Research studies dealing with measuring and explaining the self-esteem are trying to explain its social status of personality, interpersonal relationships, employment and so on (e.g. [16], [17]). Consumption in that period is also strongly focused on oneself, therefore by choosing products adolescents present defining of their identities [18], while the choice of brands depends on the brand personality, as well as its image.

Several tools were created to measure self-esteem, such as the Coopersmith Self Esteem Inventory (Coopersmith CSEI-1981), which measures attitudes toward oneself in general and in relation to peers, parents, school and personal interests. The other self-measuring instruments can be mentioned The Tennessee Self Concept Scale (TSCS) [19] and the Self Esteem Scale of the Jackson Personality Inventory (SEJPI) [20]. Rosenberg's Self-Esteem Scale, RSES is considered one of the most widely used scales (e.g. [17], [21]).

According to Rosenberg [13], self-esteem is one-dimensional and Scale (RSES) is designed on this principle, measuring global self-esteem, which means positive or negative attitudes to oneself as a whole. Several authors point to the multifactor structure of the self-esteem, which is measured by a given range (e.g. [22], [23], [24]). However, in the contribution the original concept is followed, which emphasizes one-dimensionality of self-esteem.

Several studies confirm a relationship of values with social experience of an individual (e.g. [25], [9]). Research findings show the importance of linking the brand with material values, but not with self-esteem, self-concept and life satisfaction [26]. On the other hand, there are findings that support greater efficiency of self-congruent promotional message in contrast to self-incongruent [27], [28], [29]. People with high self-esteem and confidence search more information on certain products [30], [31].

Adolescent period is the period in which the stabilization of the values that were influenced first by parents, later mainly by peers can be found [32]. Consumers prefer advertising themes that motivate them to purchase on the assumption that advertising and product are congruent with their self-scheme. People with low self-esteem are more affected by pressure from peers and by advertising in order to raise their self-esteem and stabilize self-concept (e.g. [33], [34]). Brands (mainly on

clothing) are one of the most decisive elements for the formation of adolescent identity and expression, while materialistic orientation is associated with lower mental well-being and with the distorted, unstable values relating to themselves [35].

Consumer behavior is put into relationship between the consumer and the brand with an emphasis on the dynamics of the relationship [36]. It will therefore be interesting to know what marketing strategies we need to accept to communicate brands, so that the communication with adolescents is targeted in relation to the preferences of values and self-esteem scale. Therefore, the aim is to determine to what extent attributing the significance to brand depends on adolescent´s degree of self-esteem. Due to our desired goal, research was based on theoretical concept of Schwartz.

Based on the mentioned above, the following hypothesis was set:

Hy: Assumption - the brand engagement will be different in adolescents with low a high degree of self-esteem depending on the structure of values.

2 METHOD

Portrait Values Questionnaire: The Schwartz values questionnaire (PVQ-Portrait Values Questionnaire) was used to measure the nature of represented values (developed by [10]). For purposes of the research, a questionnaire with 21 portraits of people, used by European Social Research, was exercised (European Social Survey, (e.g. [10], [38], [39]). The questionnaire consists of 21 characters of persons and the task of participants was to indicate at a 6-point asymmetric unipolar categorical scale (very much like me, like me, somewhat like me, a little like me, not like me, not like me at all) (Cronbach´s α=0.616), how much they resemble given portraits. Given portraits of people surveyed ten value orientations: power, achievement, hedonism, stimulation, self-determination, universalism, benevolence, tradition, conformity, security (the value of the first order). According to results of the factorial confirmatory analysis (e.g. [40], [39]) ten values were possible to combine into four levels higher, i.e. 2nd order (Table 1).

Table 1. Reliability coefficients for values of the first and second orders Portrait Values Questionnaire (PVQ)

Values- 1st order	Number of items	Cronbach's α	Values- 2nd order	Cronbach's α
Power	2	0.38	**Self- Enhancement**	0.79
Achievement	2	0.35		
Universalism	3	0.41	**Self-Transcendence**	0.70
Benevolence	2	0.39		
Hedonism	2	0.42	**Openness to change**	0.71
Stimulation	2	0.43		
Self-Direction	2	0.43		
Tradition	2	0.44	**Conversation**	0.77
Conformity	2	0.39		
Security	2	0.38		

The Rosenberg Self Esteem Scale [13] monitors global self-esteem (GSE) as one factor. The studies used the Czech version of this scale (the scale was validated by 14]. The Slovak version of the scale was validated by [23]. The questionnaire is composed of 10 items formulated as statements. The respondents assess their personal agreement with the statements on the Likert type scale ranging 4-item scale: 1. Strongly agree, 2. Agree, 3. Disagree, 4. Strongly disagree (Cronbach's α=0.81). Five items are formulated positively; the other five are formulated negatively. The scores of negative items were coded reversely.

Brand Engagement (BE). The engagement of brand was measured through a range of Brand Engagement [41], which combines linkage of engagement attached to the brand with personality self-concept. A questionnaire comprising of 32 items was used, which was adjusted after Principal Components Analysis to the one-dimensional 11-item questionnaire, explained 49.48% of total variance (eigenvalue = 9.63) (Cronbach's α = 0.93) (Table 2). Participants rated each item on a seven-point scales anchored by 1 (strongly disagree) to 7 (strongly agree).

Table 2. BE: Brand Engagement (Sprott, Czellar, Spangenberg, 2009, modified by the authors)

	Items	Component
1	My favorite brands feel like a part of me	0.72
2	I consider my favorite brands to be part of myself	0.76
3	The brands that I most prefer clearly indicate something about me	0.68
4	I often feel a personal connection between me and my brands	0.77
5	Part of me is defined by important brands in my life	0.72
6	I feel as If I have close personal connection with the brands I most like	0.76
7	I can identify with the important brands in my life	0.77
8	There are links between the brands that I prefer and how I view myself	0.71
9	My brands are more important indication of who I am	0.75
10	When a brand is important to me, it feels as if the brand defined who I am	0.65
11	You can learn a lot about me by looking at the important brands in my life	0.72

Operationalization of variables

The engagement of brands was measured by dependent variable with the help of Brand Engagement (BE) [41]. Independent variables were: the character of values measured with the help of the Portrait Values Questionnaire (PVQ) [10] and the rate of self-esteem (low, high), measured by Rosenberg's Self-Esteem Scale (RSES) [13]. The results were processed using SPSS 18.

Participants

Research set consisted of 745 adolescents studying at universities in Slovakia and the Czech Republic (N = 440 from Czech Republic and N = 305 from the Slovak Republic) at the age = 19.57 AM.

3 RESULTS

To determine differences of nature of values between the adolescents with low and high self-esteem, t-test (independent sample test) (Table 3) was used. First, participants were divided into the group with low level of self-esteem (N = 107) and the group with high level of self-esteem (N = 151) in the normal distribution of AM plus/minus 1sigma. Different representation of values among adolescents with low and high evaluation was showed in the assessment of values universalism (t =- 2.11, p = 0.035), conformity (t =- 2.67, p = 0.008) success (t =- 3.69, p = 0.000) (1^{st} order) and self-enhancement (t =- 2.38, p = 0.018) (2^{nd} order).

Table 3. Differences in value characteristics (t-test) in adolescents with low (N=107) and high (N=151) self-esteem (only scale with statistically significant difference is shown)

Values	Self-Esteem	Mean	Std. Deviation	t	p
Universalism	**low**	2.21	0.,67	**-2.11**	**0.035**
	high	2.39	0.67		
Conformity	**low**	3.38	1.37	**-2.67**	**0.008**
	high	3.81	1.20		
Achievement	**low**	1.98	0.75	**-3.69**	**0.000**
	high	2.41	1.02		
Self-Enhancement 2^{nd} order	**low**	2,50	0.76	**-2.38**	**0.018**
	high	2.77	1.00		

Identification with the values self-enhancement (represented by the success) is contained at a higher rate in participants with low self-esteem compared to adolescents with higher self-esteem, what might be interpreted as a need and also a desire to be successful and capable, to show off their skills and success. For participants with a high degree of self-esteem, there is less inclination to universalism (tolerance, understanding), conformity (obedience, strict compliance with the

standards), and success, which explains the greater self-assurance, confidence, openness, creativity and individualism (which means characteristics that are connected with high self-esteem).

The next step was the assessment the magnitude of influence of the individual scales of brand engagement and the clarification of the capacity of the present model using multiple regression analysis. The model included all range of first and second orders of the nature of values.

Table 4. Regression Analysis Reporting impact on value characteristics on Brands Engagement depending on degree of self-esteem (Hy)

Brands Engagement- 1st order	**R**	**R Square**	**Adjusted R Square**	**Std. Error of the Estimate**	**F**	**p**
Low self-esteem	0.810	0.656	0.621	0.87	18.50	0.000
High self-esteem	0.807	0.652	0.627	0.77	26.21	0.000
Brands Engagement- 2nd order	**R**	**R Square**	**Adjusted R Square**	**Std. Error of the Estimate**	**F**	**p**
Low self-esteem	0.774	0.599	0.584	0.91	38.51	0.000
High self-esteem	0.733	0.538	0.,525	0.87	42.46	0.000

Multiple correlation coefficient R shows that in adolescents with low self-esteem a strong relationship between brand engagement and the nature of the representation of values can be found, when we scale 65.6% variability in the nature of values (1st order) and 59.9% the variability of the nature of values (2nd order) (Table 4). Likewise, a strong relationship between surveyed items was showed also in adolescents with high evaluation. Scales of first order explained 65.2% variability of the nature of values and scales of 2nd order explained 53.8% of variability in the nature of values.

Since the test statistics F testing the hypothesis about the uselessness of all predictors showed that a given hypothesis at significance level of 0.001 can be rejected and it can be concluded that the nature of values and brand engagement at both levels are not independent in adolescents with low and high degree of self-esteem (table 4).

Table 5. Estimation of Regression Coefficients in adolescents with low self-esteem (N=107)

		Unstandardized Coefficients		**Standardized Coefficients**	**t**	**p**
		B	**Std. Error**	**Beta**		
Brands Engagement	*Constant*	6.80	0.65		10.50	0.000
	Universalism	0.77	0.30	**0.37**	2.60	**0.011**
	Benevolence	056	0.17	**0.29**	3.24	**0.002**
	Conformity	-0.23	0.10	**-0.22**	-2.35	**0.021**
	Tradition	-0.13	1.12	-0.09	-1.05	0.295
	Security	-0.17	0.15	-0.15	-1.13	0.260
	Power	-0.85	0.17	**-0.57**	-5.06	**0.000**
	Achievement	0.20	0.23	0.11	0.90	0.372
	Hedonism	-0.24	0.12	**-0.21**	-2.06	**0.043**
	Stimulation	-0.45	0.13	**-0.34**	-3.55	**0.001**
	Self-Direction	-0.39	0.17	**-0.16**	-2.29	**0.024**
2nd order		**Unstandardized Coefficients**		**Standardized Coefficients**	**t**	**p**
		B	**Std. Error**	**Beta**		
Brands Engagement	*Constant*	5.85	0.50		11.79	0.000
	Self-Transcendence	1.36	0.21	**0.59**	6.42	**0.000**
	Self- Enhancement	-0.89	0.13	**-0.48**	-6.78	**0.000**
	Conversation	-0.48	0.13	**-0.32**	-3.57	**0.001**
	Openness to change	5.85	0.50	**-0.33**	11.79	**0.000**

For the engagement of brands in adolescents with low self-esteem, a hypothesis about a zero regression coefficients can be rejected for predictors of axes self-transcendence (represented by scales of universalism and benevolence), protecting the status quo (represented by a range of conformity), self-enhancement (represented by a scale of power) and openness to change (represented by scales of hedonism, stimulation, self-determination) (Table 5).

Engagement attached to brands in adolescents with low self-esteem after the application of control of indirect effects, on the basis of scales of the 1st order the following can be predicted: universalism (ß = 0.37, p <0.05), benevolence (ß = 0.29, p <0.01), conformity (ß = 0.22 p <0.05), power (ß = 0.57, p <0.001), and hedonism (ß = 0:21, p <0.05). Stimulation (ß = 0:34, p <0.01), self-determination (ß = 0.16, p <0.05) and 2nd order scales: self-transcendence (ß = 0.59, p <0.001), self-enhancement (ß = 0.48, p <0.001), protection of status quo (ß = 0.32, p <0.01) and openness to change (ß = 0:33, p <0.001). The results therefore indicate that the engagement that is attached to brands in adolescents with low self-esteem contributes to higher self-transcendence, shared by universalism and benevolence. The engagement of brands in adolescents with low self-esteem also contributes to lower level of self-enhancement (determined by power - the highest predictor), protecting the status quo (conformism), as well as openness to change (driven by hedonism, stimulation and self-determination). If interest in the welfare of relatives and other people interested in conservation increase, the social status, prestige, protection of public image (power), enjoyment of life (hedonism), the excitement, challenges in life (stimulation) and independence in decision-making, action, thinking (self-determination) and cooperation with others decrease to avoid social rejection of an individual (conformity), then the engagements attributed to brands with low self-esteem among adolescents change. Therefore, if a given segment needs to be addressed, it is necessary to focus on communication with the inclination to brands with presentation not high level of identifying the interest in the welfare of other people, nature conservation, with reference to social status, prestige, conformity, independence of thought and joy of bringing about enjoyment of life.

Table 6. Estimation of Regression Coefficients Reliability in adolescents with high self-esteem (N=151)

		Unstandardized Coefficients		Standardized Coefficients	t	p
		B	**Std. Error**	**Beta**		
Brands Engagement	*Constant*	5.24	0.54		9.63	0.000
	Universalism	0.05	0.12	0.03	0.43	0.671
	Benevolence	0.34	0.10	**0.21**	3.54	**0.001**
	Conformity	-0.31	0.08	**-0.29**	-3.72	**0.000**
	Tradition	0.21	0.10	**0.19**	2.23	**0.027**
	Security	0.12	0.07	0.11	1.74	0.084
	Power	-0.45	0.09	**-0.41**	-5.00	**0.000**
	Achievement	-0.13	0.09	-0.11	-1.47	0.143
	Hedonism	-0.42	0.09	**-0.32**	-4.59	**0.000**
	Stimulation	0.10	0.09	0.08	1.09	0.278
	Self-Direction	-0.09	0.12	-0.05	-0.73	0.470
2nd order		**Unstandardized Coefficients**		**Standardized Coefficients**	**t**	**p**
		B	**Std. Error**	**Beta**		
Brands Engagement	*Constant*	4,.70	0.57		8.24	0.000
	Self-Transcendence	0.48	0.15	**0.22**	3.18	**0.002**
	Self- Enhancement	-0.73	0.09	**-0.57**	-8.08	**0.000**
	Conversation	0.05	0.10	0.03	0.45	0.651
	Openness to change	-0.18	0.14	-0.10	-1.25	0.213

Subprogram t-test for the factors of character of values tests the hypothesis that the given regression coefficient is zero (Table 6). For the engagement of brands thus for the segment of adolescents with high self-esteem the hypothesis of zero regression coefficients for predictors self-transcendence (represented by a scale of benevolence), self-enhancement (represented by scales of power and hedonism) and scales of conformity and tradition can be rejected.

Engagement attached to brands in adolescents with high self-esteem after the application of control of indirect effects, based on the scales of 1st order, the following can be predicted: benevolence (ß = 0:21, p <0.01), conformity (ß = 0.29, p

<0.001), tradition (ß = 0.19 p <0.05) power (ß = 0.41, p <0.001) and hedonism (ß = 0.32, p <0.001) and scales of 2 nd order: self-transcendence (ß = 0.22, p <0.01) and self-enhancement (ß = 0.57, p <0.001). As shown by the results, the strongest predictor is self-enhancement supported by a scale of power, which means if the dominant position associated with social status and prestige is reduced, engagements attributed to brands by adolescents changes. On the other hand, engagement attached to brands in adolescents with high self-esteem contributes to greater self-transcendence determined by benevolence, as well as to higher tradition and lower conformity and self-enhancement (especially hedonism and power). It is therefore necessary to bear in mind the necessity of strengthening the brand engagement in adolescents with high self-evaluation, so that in communication the level of responsibility, support, loyalty (benevolence), as well as respect for tradition is not increased; and the subordination of people with frequent social contact (for example parent, teacher, co-worker) (conformity), the emphasis on social status and prestige (power), as well as pleasure, joy of life (hedonism) is not reduced.

4 CONCLUSION

On the basis of preference of values it is easier to conclude compatible as well as antagonistic values, and thus marketing communication becomes more efficient and more focused.

Analysis of data observing dependence of attributing engagement to a brand on the rate of self-esteem of adolescents provides an indication that the investigation is justified. Engagement attached to brands in adolescents with low self-esteem can be predicted on the basis of more dimensions in comparison with adolescents with high self-esteem. The resulting findings can be applied not only in marketing but also in the educational practice, in building self-concept of adolescents. Adolescents with low self-esteem tend to attribute the engagement of brands in the direction of enhancing their social status, prestige, control and dominance over people and nature. They also see the brand in connection with the provision of enjoyment, independence, a certain level of activation and avoiding social rejection by close people. This is consistent with findings of other authors [42], [33]. In the direction of congruent communication of the brand with personality of adolescents with a low rating of evaluation is also important to take care and not to emphasize paying attention to the welfare and interest of other people.

For adolescents with high self-esteem it was shown that the more importance is attributed to values that are associated with self-enhancement with relation to social status and prestige together with an emphasis on enjoyment, the more the engagement of brands increases. People with high self-esteem and confidence care for each other on higher levels, which leads to greater consumption of products and services in order to feel great [43] and at the same time these people are also strongly motivated to purchase. On the other hand, the engagement of brand reduces demonstration of acceptance/commitment, cultural practices, and support of cooperative social relationships with people around oneself. Therefore, in the marketing communication with adolescents with high self-esteem the emphasis should be put on the authority, social power, prestige, openness, self-improvement, as well as on a certain degree of subordination of the interest of people who are in a frequent contact (e.g. parent, teacher, friend), but loyalty to friends, helping people around and rigid compliance of standards, patterns and traditions should not be emphasized.

REFERENCES

[1] H. Isakovich, "Consumer spending in a recession: How brands can capitalize on an economic downturn", 2009. [Online] Available: http://interbrand.com/images/papers/33_IP_Consumer_Spending _in_a_ Recession.pdf (2009).

[2] H. Kim, "Examination of Brand Personality and Brand Attitude within the Apparel Product Category," *Journal of Fashion Marketing and Management*, 4, pp. 243–252, 2000.

[3] B. Šramová, *Osobnosť v procese ontogenézy,* Bratislava: Melius, 2007.

[4] M. Fishbein, and I. Ajzen, *Belief, Attitude, Intention, and Behavior. An Introduction to Theory and Research*, Reading, MA: Addison–Wesley, 1975.

[5] J.C. Olson, and T. J. Reynolds, *Understanding Consumers´ Cognitive Structures: Implications for Advertising Strategy*. In: Percy, L., and Woodside, A., G. (Eds.), *Advertising Consumer Psychology*, MA: Lexington Books, pp. 77–90, 1983.

[6] R. M., Williams, *Changes and stability in values and value systems, a sociological perspective*. In: M. Rokeach (Eds.), *Understanding human values* NJ: The Free Press, pp. 15–46, 1979.

[7] M. Rokeach, *Understanding Human Values. Individual and Societal*, New York: The Free Press, 1979.

[8] G. Hofsede, *Cultures and Organizations Software of the Mind*, New York: NY: McGraw-Hill.

[9] S. H. Schwartz, "A Proposal for Measuring Value Orientations across Nations," Chapter 7 in the Questionnaire Development Package of the European Social Survey, 2003. [Online] Available: http://www.Europeansocialsurvey.org.,

[10] S. H. Schwartz, "Are There Universal Aspects in the Structure and Contents of Human Values?," *Journal of Social Issues*, 50, pp. 19-45, 1994.

[11] S. H. Schwartz, *Value orientations: measurement, antecedents and consequences across nations*. In: Jowell, R., Roberts, C., Fitzgerald, R., and Eva, G. (Eds.), Measuring attitudes cross-nationally. Lessons from the European Social Survey. London: *Sage Publications*, pp. 169–203, 2007.

[12] S. H. Schwartz, "Les valeurs de base de la personne: théorie, mesures et applications," *Revue française de sociologie*, 47, pp. 929–968, 2006.

[13] M. Rosenberg, *Society and the Adolescent Self-Image*, Princeton: Princeton University Press, 1965.

[14] M. Blatný and L. Osecká, "Rosenbergova škála sebehodnocení: Struktura globálního vztahu k sobě," *Československá psychologie*, 38, pp. 481–488, 1994.

[15] P. Macek, Sebesystém, vztah k vlastnímu Já. In: J. Výrost & I. Slaměník (Eds.), Sociální psychologie (2nd ed.). Praha: *Grada Publishing*, 2008.

[16] K. H. Trzesniewski, T. E. Moffitt, R. Poulton, M.B. Donnellan, R.W., Robins, and A., Caspi, "Low self esteem during adolescence predicts poor health, criminal behavior and limited economic prospects during adulthood," *Developmental Psychology*, 42, pp. 381–390, 2006.

[17] J. Šmídova, B. Hatlova, and J. Stochl, "Global Self Esteem in a Sample of Czech Seniors and Adolescents," *Acta Univ. Palacki. Olomuc.*, Gymn., 38, pp. 31–37, 2008.

[18] R. W. Belk, Possessions and the extended self, *Journal of Consumer Research*, 15, pp. 139–168, 1991.

[19] W. H. Fitts, *Tennessee Self Concept Scale, Manual*, Los Angeles: Western Psychological Services, 1991.

[20] I. L. Janis, and P. B. Field, *A behavioral assessment of persuasibility: Consistency of individual differences*. In C. I. Hovland and I. L. Janis (Eds.), *Personality and persuasibility* (29–54), New Haven, CT: Yale University Press, 1959.

[21] C. R. Martin, D. R. Thompson, and D. S. Chan, "An examination of the psychometric properties of the Rosenberg Self Esteem Scale (RSES) in Chinese acute coronary syndrome (ACS) patients," *Psychology Health and Medicine*, 11*,* pp. 507–521, 2006.

[22] M. Shevlin, B.P. Bunting, and CH. Sewis, "Confirmatory factor analysis of the Rosenberg self-esteem scale," *Psychological Reports*, 76, pp. 707–710, 1995.

[23] Ľ. Pilárik, *Analýza Rosenbergovej škály sebahodnotenia*. In: Poliaková, E., Šramová, B., Selvek, P. (Eds.). *Zdravie, morálka a sebahodnotenie adolescentov,* Nitra: UKF, 2004,

[24] M. Blatný, and A. Plháková, *Temperament, inteligence, sebepojetí*. Nové pohledy na tradiční témata psychologického výzkumu. Brno: Psychologický ústav Akademie věd ČR, Tišnov: Sdružení SCAN, 2003.

[25] R. Inglehart, *Modernization and postmodernization*. Princeton, NJ: Princeton University Press, 1997.

[26] D. Sprott, S. Czellar, and E. Spangenberg, "The Importance of a General Measure of Brand Engagement on Market Behavior: Development and Validation of a Scale," *Journal of Marketing Research*, 46, pp, 92–104, 2009.

[27] J. W. Hong, and G. M. Zinkhan, "Self-concept and advertising effectiveness. The influence of congruency, conspicuousness, and response mode," *Psychology & Marketing*, 12, pp. 53-77, 1995.

[28] C. Chang, "Ad–self-congruency effects: Self-enhancing cognitive and affective mechanisms," *Psychology & Marketing*, 22, pp. 887–910, 2005.

[29] H. Markus, *Self-schema and processing information about the self*. In: R. F. Baumeister (Ed.), The self in social psychology. Philadelphia: Psychology Press, 1999.

[30] S. Onkvisit, and J. J. Shaw, *Consumer behavior*, New York: Macmillan, 1994,
[31] W. B. Locander, and P. W. Hermann, "The effect of self-confidence and anxiety on information seeking in consumer risk reduction," *Journal of Marketing Research*, 16, pp. 268–274, 1979.
[32] M. Rokeach, *The nature of human values* (10th ed.). New York: *The Free Press*, 1973.
[33] G. M. Rose, D. M. Boush, and M. Friestad, "Self-esteem, susceptibility to interpersonal influence, and fashion attribute preference in early adolescents," *European Advances in Consumer Research*, 3, pp. 197–203, 1997.
[34] S. Shim, "Adolescent consumer decision-making styles: The consumer socialization perspective," *Psychology & Marketing*, 13, pp. 547–569, 1996.
[35] T. Kasser, and R. M., Ryan, "A dark side of the American dream: Correlates of financial success as a central life aspiration," *Journal of Personality and Social Psychology*, 65, pp. 410–422, 1993.
[36] S. Fournier, "Consumers and their brands: Developing relationship theory in consumer research," *Journal of Consumer Research,* 24, pp. 343–373, 1998.
[37] J. Ilgová, A. Ritomský, Hodnoty mladých Čechov a Slovákov – komparatívny empirický výskum, *Sociálne a politické analýzy*, 3, pp. 77–113, 2009.
[38] S. Schwartz, "A Theory of Cultural Values and Some Implications for Work," *Applied Psychology: An International Rewiew*, 48, pp. 23-47, 1999.
[39] S. Schwartz, (n.d.). A Proposal for Measuring Value Orientations across Nations. [Online] Available: http://www.europeansocialsurvey.org/index.php?option=com_docman&task=doc_view&gid=126&itemid=80
[40] B. Řeháková, Měření hodnotových orientací metodou hodnotových portrétu S. H. Schwartze. *Sociologický časopis*, 42, pp. 107–128, 2006.
[41] D. Sprott, S. Czellar, and E. Spangenberg, "The Importance of a General Measure of Brand Engagement on Market Behavior: Development and Validation of a Scale," *Journal of Marketing Research*, 46, pp. 92–104, 2009.
[42] T. Kasser, and R. M. Ryan," A dark side of the American dream: Correlates of financial success as a central life aspiration," *Journal of Personality and Social Psychology*, 65, pp. 410–422, 1993.
[43] N. Giges, Buying linked to self-esteem, *Advertising Age*, 68, April 13, 1987.

International Journal of Innovation and Applied Studies
ISSN 2028-9324 Vol. 3 No. 4 Aug. 2013, pp. 941-945

http://www.issr-journals.org/ijias/

Modeling photonic crystal fiber with low birefringence using fast multipole method

Yurii Bashkatov

Electronic Device Department,
National Technical University of Ukraine, Kiev Polytechnic Institute,
Kyiv, Ukraine

ABSTRACT: Currently fields of optics and photonics have urgent problem of fast and accurate simulation of photonic crystal fibers with different fillings. Although significant progress has been made from the time of first method founding, the rigorous analysis of light propagation remains problematic because of the large index contrast, the vectorial nature of the Maxwell equations and the complicated cross-sections of the hole geometries involved. This paper presents improved fast multipole method for low birefringence materials used in photonic crystal fiber core. Using this method, abruptly growth of modeling speed and accuracy is provided. Previously some research in the field of this method implementation in photonic crystal modeling have carried out, but suitable results for low birefringence fillings have not been reached yet. Implementation of this method for low birefringence fillings on photonic crystals is the main goal of this article. Modeling is implemented in Maple and show next results: monotonic decreasing of refraction index real part and linear character of refractive index imaginary part, attenuation has a plateau in bandwidth range and zero velocity group dispersion at 780 nm. Dissimilarity between numerical results and results presented in datasheet caused by nonideal cylindrical shape of air holes, but not by implemented theoretical method.

KEYWORDS: Photonic crystal, waveguide, simulation, numerical method, fiber optics.

1 INTRODUCTION

Photonic crystal fibers (PCF) are a new class of optical fibers using the properties of photonic crystals [1] – presence of specific energy regions photonic band gaps (PBG). In these regions no light can spread in any directions. Providing defect in fiber core leads to endlessly single mode propagation (Fig. 1). Filling core by low birefringence material makes nonlinear response of core material more predictable and has a wide usage in airspace applications.

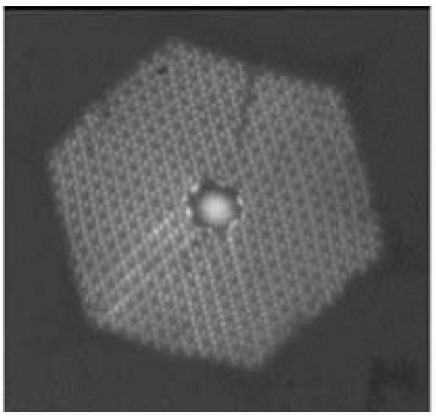

Fig. 1. Localization of electromagnetic field in photonic crystal fiber [2]

Corresponding Author: Yurii Bashkatov (yuriy.bashkatov@gmail.com)

Practical interest to optical waveguides and fibers gave rise necessity to develop methods for their study. Although significant progress has been made from the time of first method founding, the rigorous analysis of light propagation in PCF remains problematic because of the large index contrast, the vectorial nature of the Maxwell equations and the complicated cross-sections of the hole geometries involved [2]. Today there are several methods to calculate optical properties of PCF. We propose to use one of the analytical approaches for modeling PCF with low birefringence – fast multipole method (FMM) [3].

Usage of this method for simulation PCF properties was proposed by T. P. White and B. T. Kuhlmey [3]. W. Song, *et al.* [4] simulated the PCF with high birefringence by using multipole method, but using multipole method for modeling PCF with low birefringence have not implemented yet.

Using this method, we can get real and imaginary parts of the effective refractive index and propagation constant [3]. Using different multipole cutoff order to meet the varied diameter of air holes and wavelength ratio, we not only guarantee the calculation precision, but also speed up the calculation.

The goal of this article is building FMM for low birefringence materials in PCF core.

2 MATHEMATICAL INTRODUCTION OF PROPOSED METHOD

For the mode analysis of PCF, we assume the longitudinal axis is the z-axis, and that the structure of the PCF is defined by its cross-section in the xy-plane. Section of PCF is shown in Fig. 2.

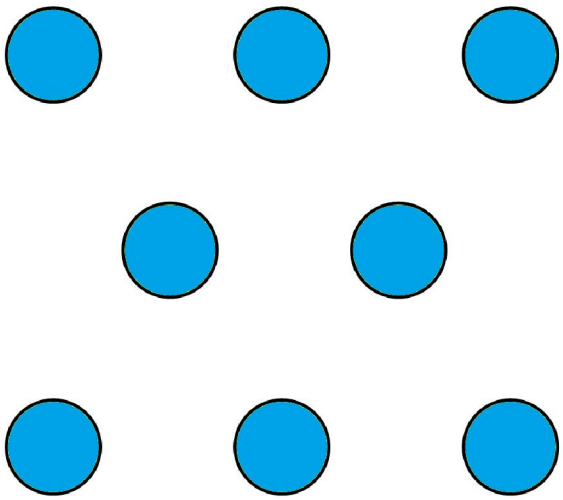

Fig. 2. Cross-section of modeled PCF

Propagation mode can be obtained as vectors of electric and magnetic field in *z* direction:

$$E(x,y,z,t) = E^{i(\beta z-\omega t)}\left(\frac{i\omega\mu}{k^2-\beta^2}\partial_y H_3^\beta + \frac{i\beta}{k^2-\beta^2}\times\partial_x E_3^\beta, \frac{-i\omega\mu}{k^2-\beta^2}\partial_x H_3^\beta + \frac{i\beta}{k^2-\beta^2}\partial_y E_3^\beta, E_3^\beta\right),$$

$$H(x,y,z,t) = H^{i(\beta z-\omega t)}\left(\frac{-i\omega n^2\varepsilon}{k^2-\beta^2}\partial_y E_3^\beta + \frac{i\beta}{k^2-\beta^2}\times\times\partial_x H_3^\beta, \frac{i\omega n^2\varepsilon}{k^2-\beta^2}\partial_x E_3^\beta + \frac{i\beta}{k^2-\beta^2}\partial_y H_3^\beta, H_3^\beta\right),$$

where ω is a frequency, β – propagation constant, ε, μ – electrical permittivity and magnetic permeability of free-space.

Assuming above mentioned and continuity of tangential components of the *E* and *H* fields we can summarize the eigenvalue problem which determines a mode with propagation constant β as follows:

$$\nabla^2 E + (k^2 - \beta^2)E = 0$$
$$\nabla^2 E + (k^2 - \beta^2)E = 0$$
$$[E] = 0$$
$$[H] = 0$$
$$\left[\frac{\beta}{k^2 - \beta^2}\frac{\partial H}{\partial t}\right] = -\left[\frac{k^2 / k_v}{k^2 - \beta^2}\frac{\partial E}{\partial n}\right]$$

Remember FMM approach shown in [3], edge of each hole in PCF structure is source of radiation inside and outside the hole. This is caused by division fundamental fields at the edge of hole boundary in two parts: transmitted through the boundary and reflected from the boundary [4].

Due to cylindrical geometry of the air holes, polar coordinates can be used to describe the fields inside and outside the holes:

$$E_z = \sum_{m=-\infty}^{\infty} a_m^{(l)} J_m(k_\perp^i r_l)\exp(im\phi_e)\exp(i\beta z)$$
$$E_z = \sum_{m=-\infty}^{\infty} (b_m^{(l)} J_m k_\perp^e r_l + c_m^{(l)} H_m^1 k_\perp^e r_l)\times\exp(im\phi_e)\exp(i\beta z)$$

$k_T = \sqrt{k_0^2 n_i^2 - \beta^2}$, $k_\perp = \sqrt{k_0^2 n_e^2 - \beta^2}$, refractive index of air n_i = 1, n_e is the refractive index of quartz material, k_0 is the wave vector in free space, r_l and J_m are coordinate of regional coordinate system $\vec{r}_l(r_l, \phi_l) = \vec{r} - \vec{c}_l$, c_l is the center of the air hole. The expression of magnetic field part *k* is similar to the electric field.

We can easily obtain $a_m^{(l)}$, $b_m^{(l)}$ and $c_m^{(l)}$ using boundary conditions of cylindrical inclusions. Calculating optical properties we choose proper cutoff value corresponding to the air hole diameter and the wavelength ratio *M*. Goal of this procedure is to optimize speed and precision of the calculation. The effective refractive index of the mode n_{eff} can be obtained by results of propagation constant β calculation.

Then, the imaginary part of the n_{eff} can be used to get the fiber confinement loss (the unit is dB/m):

$$L = \frac{40\pi}{\lambda \ln(10)} \mathrm{Im}(n_{eff}) \times 10^6$$

The unit of *L* is nanometer (nm), dispersion can be derived from the real part:

$$D = -\frac{\lambda d^2 \,\mathrm{Re}(n_{eff})}{dx^2}.$$

3 NUMERICAL RESULTS

To ensure the most accurate and actual results the parameters have been chosen one of the most well-known fiber Thorlabs HC-800B [5]: center wavelength: 820 nm, attenuation: <0.3 dB/m, bandwidth: 770 – 870 nm. The time and frequency discretization points are chosen to be 2^{10}, core diameter – 8 microns, fiber length – 1 m. Pump power 500 mW.

Light effectively coupled in PCF core. Localization of electromagnetic radiation in the fiber core is associated with a significant difference between the refractive index of core and effective refractive index of PCF coating. This corresponds to presence of defect mode in PBG.

Consider mentioned above about field localization, we can start calculation of dispersion and nonlinear properties. Simulating results for main mode and slight mode are shown on Fig. 3 and Fig. 4.

Monotonic decreasing of refraction index real part can be explained using Sellmeier law for quartz glass. Linear character of refractive index imaginary part correspond to low confinement loss (<4 mdB/km). To decrease these losses is necessary to increase number of holes in PCF. This will lead to increase nonlinearity of dispersion curve (greater efficiency of nonlinear processes).

Dispersion properties and attenuation (Fig. 5) can be compared with corresponding in datasheet [5]. Both figures show zero group velocity dispersion ZGVD near 780 nm. Group velocity dispersion have double zero points but in datasheet only one. This can be explained by interpolation mistake during numerical calculation. Dissimilarity between numerical results and results presented in datasheet caused by nonideal cylindrical shape of air holes, but not choosing and implementation of theoretical method. Attenuation in PCF has a plateau in bandwidth range. This confirm high field localization in PCF core and matches data in datasheet.

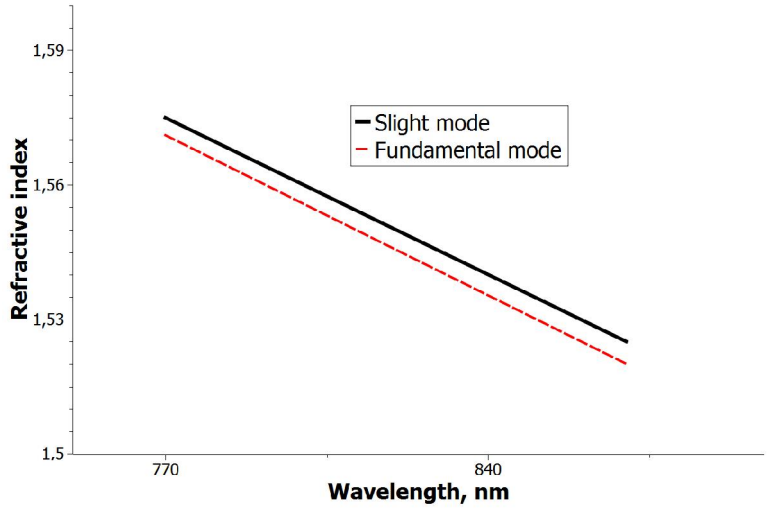

Fig. 3. Dispersion curves of low birefrigence PCF (real part of refractive index)

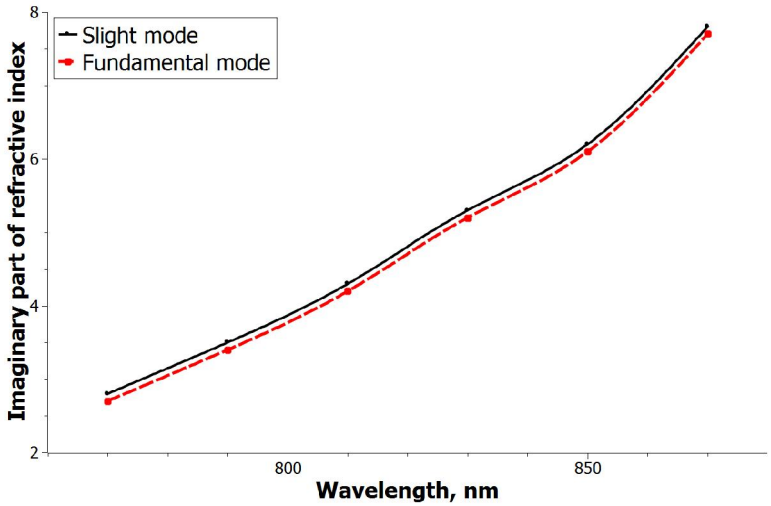

Fig. 4. Nonlinear curves of low birefringence PCF (imaginary part of refractive index)

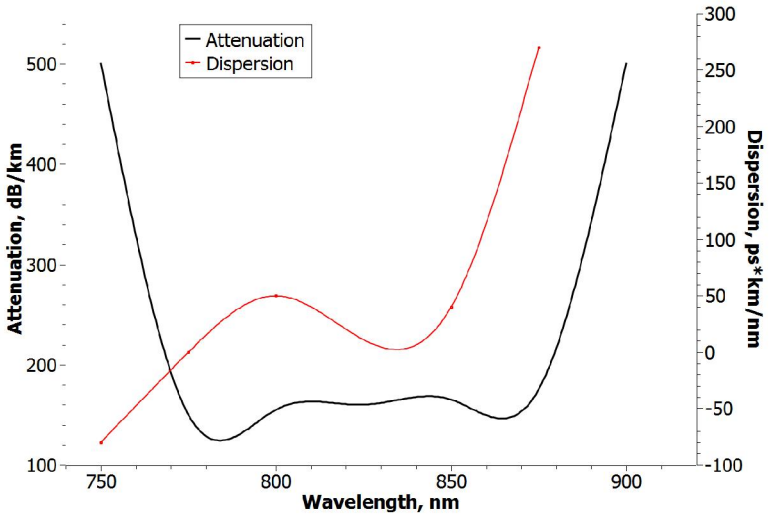

Fig. 5. Dispersion properties of hollow core PCF ant its attenuation [6]

4 CONCLUSIONS

Approach presented in paper provides fast and accurate simulation of PCF with low birefringence. Results can be used for modeling fiber devices in space applications. Linear character of refractive index imaginary part correspond to low confinement loss (<4 mdB/km). To decrease these losses is necessary to increase number of holes in PCF. This will lead to increase nonlinearity of dispersion curve (greater efficiency of nonlinear processes). Figures provided by modeling and data sheet show ZGVD near 780 nm. Dissimilarity between them caused by nonideal cylindrical shape of air holes, but not by used theoretical method.

ACKNOWLEDGMENT

Author acknowledges help of researchers of Institute of Physics NASU Department Quantum and Coherent Optics and Department of Radiation Processes.

REFERENCES

[1] L.A. Khromova, L.A. Melnikov, “Anisotropic photonic crystals: generalized plane wave method and dispersion symmetry properties,” *Optics Communications*, Vol. 281, No. 21, pp. 5458-5466, 2008.

[2] A B Fedotov, S O Konorov, O A Kolevatova, V I Beloglazov, N B Skibina, L A Mel'nikov, A V Shcherbakov, A M Zheltikov, “Waveguiding properties and the spectrum of modes of hollow-core photonic-crystal fibres”, *Quantum Electronics*, Vol. 33, No. 3, pp. 271–274, 2003.

[3] T. P White., R. C. McPhedran, L. C. Botten, “Calculations of air-guided modes in photonic crystal fibers using the multipole method”, *Optics Express*, Vol. 9, pp. 721- 732, 2001.

[4] W. Song, Y. Zhao, Y. Bao, S. Li, Z. Zhang and T. Xu, “Numerical simulation and analysis on mode property of photoniccrystal fiber with high birefringence by fast multipole method”, *PIERS Online*, Vol. 3, No. 6, pp. 836-841, 2007.

[5] ThorLabs HC-800B datasheet. [Online] Available: http://www.thorlabs.de/thorproduct.cfm?partnumber=HC-800B.

[6] Rajni Idiwal, Rekha Mehra, Manish Tiwari, “Photonic Crystal Fiber as Low Loss Dispersion Flattened Fiber and Ultra-Low Confinement Loss,” *International Journal of Emerging Technology and Advanced Engineering*, Vol. 1, Issue 2, pp. 48-53, 2011.

International Journal of Innovation and Applied Studies
ISSN 2028-9324 Vol. 3 No. 4 Aug. 2013, pp. 946-952

http://www.issr-journals.org/ijias/

Performance of Multiuser MIMO-OFDM downlink system with ZF-BF and MMSE-BF linear precoding

Mounir Esslaoui and Mohammed Essaaidi

Information and Telecommunication Systems Laboratory,
Faculty of Sciences, Abdelmalek Essaadi University,
Tetouan, Morocco

ABSTRACT: The forthcoming wireless communication networks, commonly referred to as fourth generation (4G) systems, are expected to support extremely high data rates as close as possible to the theoretical channel capacity while satisfying quality of service (QoS) constraints. The development of these systems must take into account the problem of limited radio resources and the harshness of wireless channel conditions. Two emerging technologies that are potential candidates for 4G wireless networks are multiuser multiple-input multiple-output (MU-MIMO) wireless systems and orthogonal frequency division multiplexing (OFDM). The MU-MIMO technique allows the spatial multiplexing gain at the base station to be obtained without the need for multiple antenna terminals, thereby allowing multiple users to receive data over the downlink simultaneously. The use of OFDM provides protection against intersymbol interference (ISI) and allows high data rates to be achieved. Linear precoding schemes for MU-MIMO wireless systems, e.g., zero forcing beamforming (ZF-BF) and minimum mean squared error beamforming (MMSE-BF), have been widely concerned for their high performance in single-carrier MU-MIMO networks where a base station attempts to communicate simultaneously with multiple users. In this paper, we evaluate and extend the ZF-BF and MMSE-BF schemes from single-carrier MU-MIMO to multicarrier MU-MIMO architecture based on OFDM, i.e., MU-MIMO-OFDM system, assuming the availability of channel state information (CSI) at the transmitter. Numerical results demonstrate that both introduced linear precoding strategies provide a higher sum-rate capacity improvement compared to a conventional MU-MIMO-OFDM system where the users are served on a time division multiple access (TDMA) basis.

KEYWORDS: Multiuser MIMO, OFDM, zero forcing, minimum mean squared error, beamforming, precoding.

1 INTRODUCTION

The main challenge of the forthcoming wireless communication systems, commonly referred to as fourth generation (4G) systems, is to satisfy the increasing demand for high data rates while satisfying quality of service (QoS) constraints. In particular, the use of multiple-input multiple-output (MIMO) wireless systems can improve the capacity by a factor dependent on the minimum number of transmit and receive antennas, if perfect channel state information (CSI) is available at the base station [1]. On other hand, orthogonal frequency division multiplexing (OFDM) is a popular method for high data rate wireless transmission. It is an effective technique to mitigate the effects of intersymbol interference (ISI) in frequency-selective channels by converting a frequency-selective channel into a parallel collection of frequency flat subchannels [2]. Combining MIMO antenna configurations with OFDM results in a powerful architecture, MIMO-OFDM, that is able to exploit spatial as well as frequency diversity and allow high data rates with large degrees of freedom available in the wireless environment [3].

Recently, multiuser MIMO (MU-MIMO) has been considered a key technology for system capacity improvement in modern wireless networks without the need for multiple antennas and expensive signal processing at user equipments. In contrast to single-user MIMO (SU-MIMO), where a base station can only communicates with a single user, MU-MIMO allows

Corresponding Author: Mounir Esslaoui (mounir.ess@gmail.com)

multiple mobile stations to be served simultaneously by means of space division multiple access (SDMA) [4]. Information theory reveals that if CSI is fully known at the transmitter, dirty paper coding (DPC) is the optimal transmit strategy for the MU-MIMO broadcast channel from a system capacity point of view [5]. However, deploying this technique in practice is hard to implement because of the high computational complexity it requires, especially when the number of users is large. Therefore, suboptimal linear precoding strategies such as zeroforcing beamforming (ZF-BF) [6], [7] and minimum mean square error beamforming (MMSE-BF) [8] have been investigated to provide the capacity gain promised by DPC while removing the multiuser interference among the simultaneously transmitted users.

In this paper, ZF-BF and MMSE-BF linear precoding schemes are evaluated and extended, in light of the available CSI at the transmitter, from single-carrier to multicarrier MU-MIMO systems where the users transmit strictly using OFDM (i.e., frequency is not used for multiple access). Simulations results have show that compared to a conventional MU-MMO-OFDM based time division multiple access (TDMA) strategy, where the BS transmits to the best user at each time slot, considerable sum-rate capacity improvement can be achieved by both proposed linear precoding techniques. The remainder of this paper is organized as follows. Section 2 presents the MU-MIMO-OFDM system model. Section 3 presents the proposed precoding schemes. Numerical results are shown in Section 4. Finally, Section 5 summarizes the main outcomes of the paper.

NOTATIONAL REMARK

Boldface letters denote matrix-vector quantities while non-bold letters are used for scalars. The operation $(.)^T$ and $(.)^H$ represent the transpose and the Hermitian transpose of a matrix, respectively. E(.) denotes the expectation operator, *Tr*(.) is the trace and C is the set of complex numbers. $\mathbf{I}$ is the identity matrix and $\|a\|$ denotes the Euclidean norm of a vector ***a***.

2 SYSTEM MODEL

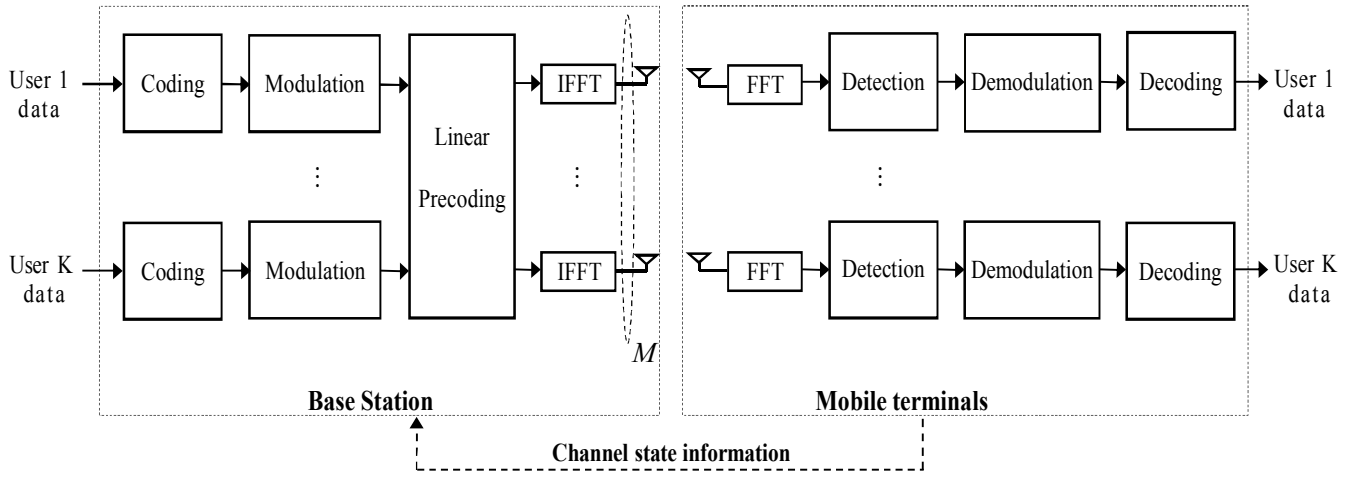

Fig. 1. Block diagram of MU-MIMO-OFDM downlink system with N_T transmit antennas and K single antenna mobile users

We consider the downlink of a single-cell MU-MIMO-OFDM system in which a single base station (BS) equipped with M transmit antennas communicates with $K \leq M$ mobile users, each equipped with a single receive antenna. The system operates in a total bandwidth W that is exploited by means of N_c OFDM subcarriers. The BS broadcasts to all K users simultaneously over all OFDM subcarriers. The system block diagram is depicted in Fig. 1. Let $s_{k,n}$ be the data symbol of user k over the n th subcarrier. The $M \times 1$ overall data vector of transmitted symbols from the BS antennas on subcarrier n for all K users is

$$\mathbf{x}_n = \left[s_{1,n} \; s_{2,n} \cdots s_{K,n} \right]^T . \tag{1}$$

Assuming perfect frequency synchronization between the transmitter and receiver and cyclic prefix duration exceeding the channel delay spread, the received signal, $y_{k,n}$, for user k on subcarrier n for an arbitrary OFDM symbol is given by

$$y_{k,n} = \mathbf{h}_{k,n}\mathbf{x}_n + \eta_{k,n}, \quad (2)$$

where $\mathbf{h}_{k,n} \in \mathrm{C}^{1xM}$ represents the channel gain response corresponding to user k over the subcarrier n and $\eta_{k,n}$ is a zero-mean additive white Gaussian noise (AWGN) sample with variance σ_η^2. The base station (BS) has full and instantaneous knowledge of the channel state information (CSI) of all K users. The transmitter is subject to an average power constraint P_T, i.e., $Tr(\mathsf{E}(\mathbf{x}_n\mathbf{x}_n^H)) \le P_T$, which implies that the total transmit power is not dependent on the number of transmit antennas.

The transmitter multiplies the data symbol, $s_{k,n}$, for each user k on each subcarrier n by a precoding vector $\mathbf{w}_{k,n} \in \mathrm{C}^{Mx1}$ so that the transmitted signal on each subcarrier n is a linear function hat can be written as

$$\mathbf{x}_n = \sum_{k=1}^{K} \sqrt{P_{k,n}}\,\mathbf{w}_{k,n} s_{k,n}, \quad (3)$$

where $P_{k,n}$ denotes the power allocated to the k th user on the n th subcarrier satisfying,

$$\sum_{n=1}^{N_C}\sum_{k=1}^{K} \left\|\mathbf{w}_{k,n}\right\|^2 P_{k,n} = P_T, \quad (4)$$

and thus, the resulting received signal for user k on subcarrier n may be rewritten as

$$y_{k,n} = \sum_{j=1}^{K} \mathbf{h}_{k,n}\mathbf{w}_{j,n}s_{j,n} + \eta_{j,n} \quad (5)$$

$$= \sqrt{P_{k,n}}\,\mathbf{h}_{k,n}\mathbf{w}_{k,n}s_{k,n} + \sum_{j=1, j\neq k}^{K} \sqrt{P_{j,n}}\,\mathbf{h}_{k,n}\mathbf{w}_{j,n}s_{j,n} + \eta_{k,n}, \quad (6)$$

where the second-term in (6) corresponds to the multi-user interference that represents the major impairment in this scenario. The challenge now is how to perform the precoding operation in order to eliminate all multiuser interference.

3 PRECODING TECHNIQUES FOR MU-MIMO-OFDM SYSTEMS

In MU-MIMO-OFDM downlink system, a BS communicates simultaneously with multiple receivers using the SDMA technique. To achieve this goal precoding strategies should be designed, in light of the available CSI, in order to increase system capacity and/or reduce the complexity of the receiver. In this section we present and evaluate linear precoding schemes using either ZF-BF and MMSE-BF. For comparison we also present a conventional MU-MIMO-OFDM based TDMA system where the base station transmits only to best user at a given time slot.

3.1 ZERO-FORCING BEAMFORMING

Let us define the $K \times M$ channel gain matrix and $M \times K$ precoding matrix, on subcarrier n, for all K users, respectively, as

$$\mathbf{H}_n = \left[\mathbf{h}_{1,n}^T\ \mathbf{h}_{2,n}^T \cdots \mathbf{h}_{K,n}^T\right]^T \quad (7)$$

$$\mathbf{W}_n = \left[\mathbf{w}_{1,n}\ \mathbf{w}_{2,n} \cdots \mathbf{w}_{K,n}\right]. \quad (8)$$

In Zero-Forcing Beamforming (ZF-BF) the precoder is designed to achieve the zero interference condition between the users,

$$\text{i.e.,} \begin{cases} \mathbf{h}_{k,n}\mathbf{w}_{j,n} = 0, \text{ for } j \neq k \\ \mathbf{h}_{k,n}\mathbf{w}_{j,n} = 1, \text{ for } j = k \end{cases}. \tag{9}$$

The ZF-BF precoding matrix for each subcarrier n is given by the pseudo-inverse of the channel gain matrix $\mathbf{H}_n$ [7], that is,

$$\mathbf{W}_n = \mathbf{H}_n^H \left(\mathbf{H}_n \mathbf{H}_n^H \right)^{-1}, \tag{10}$$

where the precoding vector $\mathbf{w}_{k,n}$ for each user k on subcarrier n is obtained by normalizing the k th column of $\mathbf{W}_n$. The achievable sum-rate capacity using ZF-BF over all subcarriers is expressed as,

$$R_{\text{ZF-BF}} = \frac{1}{N_c} \sum_{n=1}^{N_c} \sum_{k=1}^{K} \log_2 \left(1 + \frac{P_{k,n}}{\sigma_\eta^2} \gamma_{k,n} \right), \tag{11}$$

where $P_{k,n}$ denotes the power allocated to user k on subcarrier n. The optimal power allocation that achieves the maximum sum-rate capacity is given by the waterfilling algorithm [9].

3.2 Minimum Mean Squared Error Beamforming

The ZF-BF precoder completely eliminates multi-user interference at the expense of noise enhancement and thus the system can be treated as a group of parallel SU-MIMO communications at each subcarrier n. However, if some of the channels are in bad condition the system needs large power to compensate the bad channel condition. The minimum mean-square-error beamforming (MMSE-BF) precoder can reach a good tradeoff between noise and interference and is suitable to be used to overcome this problem. In presence of CSI at the transmitter, the MMSE-ZF precoder at each subcarrier n is given as follows:

$$\mathbf{W}_n = \mathbf{H}_n^H \left(\mathbf{H}_n \mathbf{H}_n^H + \beta \mathbf{I} \right)^{-1}, \tag{12}$$

where β is a regularization factor commonly chosen as $\beta = M\sigma_\eta^2 / P_T$ motivated by the results in [10] showing that, for single carrier systems, the performance of MMSE-BF is certainly significantly better at low-medium SNR and converges to that of ZF-BF at high SNR. However, MMSE-BF does not provide parallel channels and thus power allocation techniques cannot be performed in a straightforward manner.

The achievable sum-rate capacity using MMSE-BF over all subcarriers with equal power allocation is given by

$$R_{\text{MMSE-BF}} = \frac{1}{N_c} \sum_{n=1}^{N_c} \sum_{k=1}^{K} \log_2 \left(1 + \text{SINR}_{k,n} \right), \tag{13}$$

where $\text{SINR}_{k,n}$ represents the signal to interference plus noise ratio of user k on subcarrier n, and can be expressed as

$$\text{SINR}_{k,n} = \frac{\left| \mathbf{h}_{k,n}\mathbf{w}_{k,n} \right|^2}{\sum_{j=1, j\neq k}^{K} \left| \mathbf{h}_{k,n}\mathbf{w}_{j,n} \right|^2 + K\sigma_\eta^2 / P_T}. \tag{14}$$

3.3 Time Division Multiple Access

In a conventional MU-MIMO-OFDM network where user multiplexing takes place using TDMA techniques, the base station selects the best user at a time who will be allocated all the spectrum and power resources [11]. In this scenario it is easy to show that, once a user has been selected, the precoding operation on each subcarrier n is simply implemented by means of maximum ratio transmission (MRT) [12], that is,

$$\mathbf{x}_n = \sqrt{P_{k,n}}\,\mathbf{w}_{k,n} s_{k,n}, \tag{15}$$

where $\mathbf{w}_{k,n} = \mathbf{h}_{k,n}^H$. The maximum sum-rate capacity achieved by sending to the user with the largest channel norm is

$$R_{\text{TDMA}} = \max_{k\in\{1,\cdots,K\}} \frac{1}{N_c} \sum_{n=1}^{N_c} \log_2\left(1 + \frac{P_T}{\sigma_\eta^2}\left\|\mathbf{h}_{k,n}\right\|^2\right). \tag{16}$$

4 NUMERICAL RESULTS

In this section, we evaluate the performance of ZF-BF and MMSE-BF linear precoding schemes in MU-MIMO-OFDM scenarios, assuming the availability of CSI at transmitter, and compare them to conventional MU-MMO-OFDM based TDMA system. The simulations consider the use of parameters currently found in the latest WLAN standard IEEE 802.11n. The system has been configured to operate at 5.25GHz carrier frequency on a bandwidth of W=20MHz with N_c=64 OFDM subcarriers, where the subchannel gains are independent and identically distributed for each user. The channel profile used to generate the frequency-selective channel responses correspond to profiles B (residential) from channel models developed within the IEEE 802.11n standard [13]. The base station is assumed to communicate with a total of $K = M$ mobile users, each equipped with a single receive antenna.

Fig. 2 shows a performance comparison in terms of sum-rate capacity as a function of the average SNR for MMSE-BF, ZF-BF and the conventional TDMA network in a system with $M = 4$ transmit antennas and $K = M$ mobile users. As expected, it can be seen that the performance of MMSE-BF is certainly significantly better at low-medium SNR regime and converges to that of ZF-BF at high SNR regime. Moreover, the gain in sum-rate capacity gap between both linear precoding schemes and the conventional TDMA system exhibits a linear increase with SNR values reaching more that 10 bits/s/Hz for an SNR=30 dB.

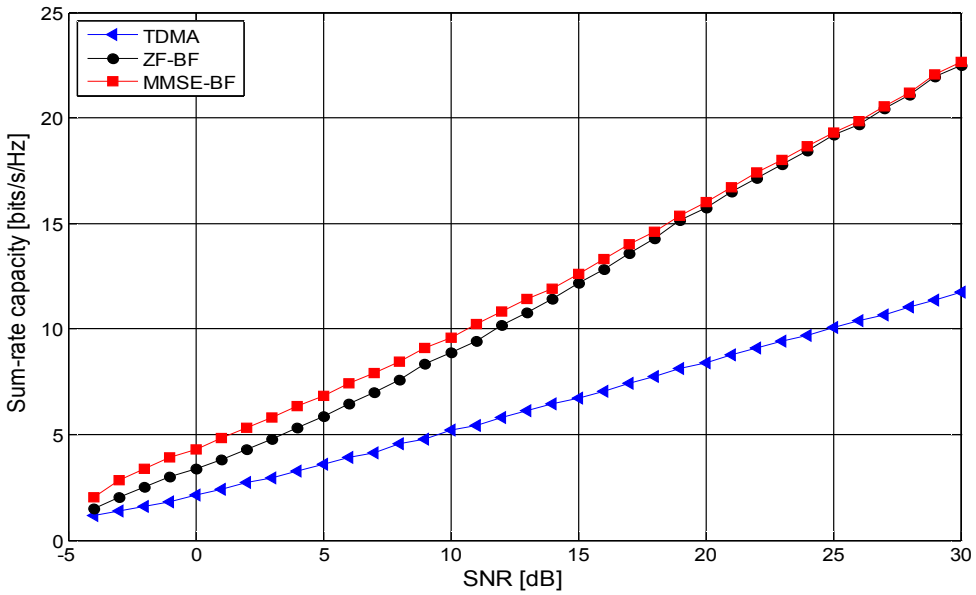

Fig. 2. Sum-rate capacity versus the average SNR. K = M = 4

In Fig. 3 we compare the sum-rate capacity versus the number of transmit antennas M for $K = M$ mobile terminals and an average SNR=10 dB. It can be observed that, increasing the number of transmit antennas M, i.e., increasing the number of simultaneously transmitting users K, has the detrimental effect of providing a linear sum-rate capacity growth for both linear precoding schemes, where the sum-rate capacity of MMSE-BF outperforms that of the ZF-BF. However, for the conventional case, where the best user is scheduled, the sum-rate capacity saturates at 7.7 bits/s/Hz. This can be explained by the fact that adding more transmit antennas does not improve the performance of the TDMA technique.

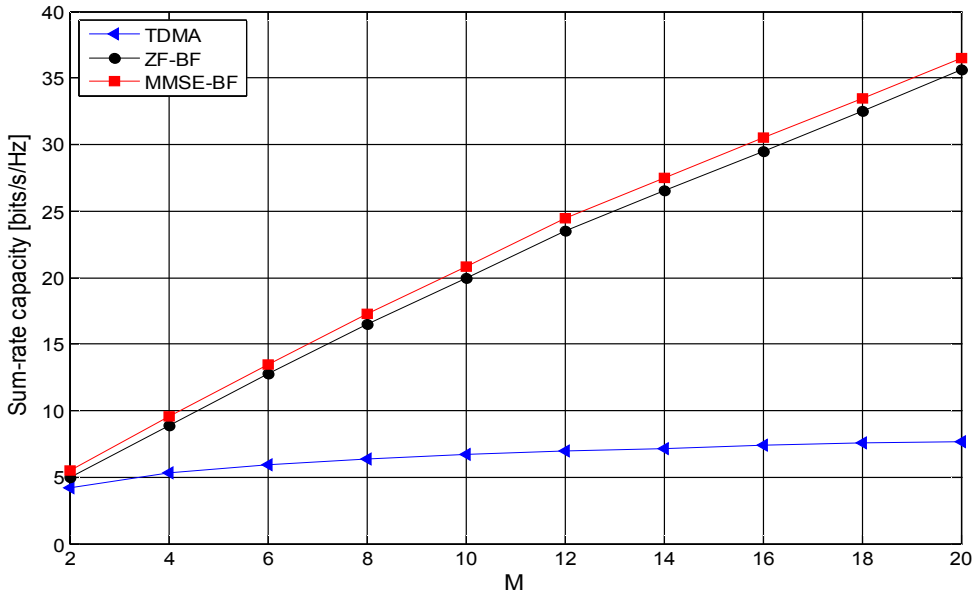

Fig. 3. Sum-rate capacity versus the number of transmit antennas M. K = M users, SNR=10 dB

5 CONCLUSION

In this paper, zeroforcing beamforming (ZF-BF) and minimum mean square error (MMSE-BF) linear precoding schemes have been analyzed and extended, from single-carrier MU-MIMO to a multicarrier MU-MIMO architecture based on OFDM. Simulation results have shown that, when channel state information (CSI) is available at the transmitter and for practical average SNR values, the performance of both proposed linear precoding techniques is significantly better than the conventional TDMA network and achieve a linear sum-rate growth with the number of transmit antennas. In addition, for a fixed number of transmit antennas at the base station, the performance of MMSE-BF is significantly better at low-medium SNR regime and converges to that of ZF-BF at high SNR regime.

ACKNOWLEDGMENT

The authors would like to thank the editor and the anonymous reviewers, whose careful consideration of the manuscript improved the presentation of the material.

REFERENCES

[1] E.Telatar, "Capacity of multi-antenna Gaussian channels," *Eur. Trans.Telecommun*., vol. 10, no. 6, pp. 585–595, Nov. 1999.

[2] R. van Nee and R. Prasad, *OFDM for wireless multimedia communications*. Artech House, 2000.

[3] A. J. Paulraj, D. A. Gore, R. U. Nabar, and H. Bolcskei, "An overview of MIMO communications a key to gigabit wireless," *Proceedings of the IEEE,* vol. 92, no. 2, pp. 198–218, 2004.

[4] D. Gesbert, M. Kountouris, R. Heath, C.-B. Chae, and T. Salzer, "Shifting the MIMO paradigm," *IEEE Sig. Proces. Mag*., vol. 24, no. 5, Sep. 2007.

[5] M. Costa, "Writing on dirty paper," *IEEE Trans. Info. Theory*, vol. 29,pp. 439–441, May. 1983.

[6] G. Caire and S. Shamai, "On the achievable throughput of a multiantenna Gaussian broadcast channel," *IEEE Trans. Inform.Theory*, vol. 49, no. 7, pp. 1691–1706, Jul. 2003.

[7] T. Yoo and A. Goldsmith, "On the optimality of multiantenna broadcast scheduling using zero-forcing beamforming," *IEEE Journal on Selected Areas in Communications*, vol. 24, no. 3, pp. 528–541, Mar. 2006.

[8] M. Joham, W. Utschick, and J. A. Utschick, "Linear transmit processing in MIMO communications systems," *IEEE Sig. Proces. Mag.*, vol. 53, no. 8, pp. 2700–2712, Aug. 2005.

[9] N. Jindal, W. Rhee, S. Vishwanath, S. A. Jafar, and A. Goldsmith, "Sum power iterative water-filling for multi-antenna gaussian broadcast channels," *IEEE Trans. on Information Theory*, vol. 51, no. 4, pp. 1570–1580, April 2005.

[10] C. B. Peel, B. M. Hochwald, and A. L. Swindlehurst, "A vector-perturbation technique for near-capacity multiantenna multiuser communication-part I: channel inversion and regularization," *IEEE Trans. Commun*., vol. 53, no. 1, pp. 195–202, Jan. 2005.
[11] D. Tse and P. Viswanath, Fundamentals of wireless communications. *Cambridge University Press*, 2005.
[12] P. Viswanath, D. Tse, and R. Laroia, "Opportunistic beamforming using dumb antennas," *IEEE Trans. on Inf. Theory*, vol. 48, no. 6, Jun. 2002.
[13] J. Kermoal, L. Schumacher, K. Pedersen, P. Mogensen, and F. Frederiksen, "A stochastic MIMO radio channel model with experimental validation," *IEEE JSAC*, vol. 20, no. 6, pp. 1211–1226, Aug 2002.

International Journal of Innovation and Applied Studies
ISSN 2028-9324 Vol. 3 No. 4 Aug. 2013, pp. 953-958

http://www.issr-journals.org/ijias/

Triple Band Hexagonal Meander-line Monopole Antenna for Wireless Applications

Manali Dongre, P.K. Singhal, Sonali Kushwah, and Tajeswita Gupta

Department of Electronics,
Madhav Institute of Technology and Science,
Gwalior-474005, M.P., India

ABSTRACT: In this paper, planar monopole antenna for wireless applications with triple band has been proposed. It simply consists of hexagonal meander-line structure and defected ground plane, which occupy a small PCB area of 50×60×1.676 mm^3. The proposed antenna has a measured impedance bandwidths of 1.689-1.781GHz, 2.49-2.71GHz and 2.75-2.98GHz which cover GSM1800 and 2.5WIMAX bands. The antenna has three distinct frequency bands centered at 1.74GHz, 2.63GHz and 2.93GHz. The radiation pattern and resonant frequency are mainly affected by meandered strip and a rectangular defected ground plane. The impedance bandwidth, current distribution, radiation patterns, gain and efficiency of the antenna are studied by computer simulation and measurement. The proposed antenna is fed by a coaxial probe through SMA connector.

KEYWORDS: Meander-line antenna, Planar monopole antenna, Small antenna, Triple band, Return loss.

1 INTRODUCTION

The emerging growth of modern wireless communication system has caused wide interests in designing wide band and multiband antennas; especially for wireless communication system and world interoperability for microwave access (WIMAX). It is well known fact that planar monopole antenna present really appealing physical features such as simple structure, small size, and low cost [1-2]. Meander-line antenna is one type of the microstrip antenna in which meandering the patch increases the path over which the surface current flows and that eventually results in lowering of the resonant frequency than the straight wire antenna of same dimensions [3-4]. The printed monopole antenna with the hexagonal meander-line structure has significant advantages. It is electrically small, Low profile antenna and has simple structure. Ground structure is realized by etching a defect in the ground plane of the planar circuits and antennas. This disturbs the shield current distribution in the ground plane and modifies transmission line parameters such as line capacitance and inductance [5-6]. In this letter a new hexagonal monopole antenna for the purpose of GSM1800 and WIMAX operations has been proposed. The antenna is originally designed as a meandered arm with defected ground plane and two parasitic meandered strips to generate the resonant responses [7]-[14]. This way, the antenna can achieve a triple band performance to simultaneously cover the most commonly used GSM1800 and WIMAX bands. The measured 10dB bandwidth are from 1.689-1.781GHz covering GSM1800 (1.710-1.785GHz) band and 2.49-2.71 GHz, 2.75-2.998 GHz band covering WIMAX MMDS (2.5-2.69GHZ, 2.7-2.9GHZ) bands respectively.

2 ANTENNA DESIGN

The geometry of the proposed hexagonal monopole antenna is presented in Fig. 1. The antenna consists of hexagonal meander line structure. The two parasitic strips are also embedded to the upper right and lower right of the hexagonal. In this novel design, the symmetric meandered monopole antenna is presented. Antenna was implemented on FR4 substrate with thickness of substrate h=1.6mm and permittivity of ε_r=4.3 and loss tangent δ=0.02 and ground of size 50×15.56mm^2.

Corresponding Author: Manali Dongre (manali.mits@gmail.com)

The total antenna dimension is 50×60×1.676mm^3. On the other side of the substrate, a conducting ground plane is placed. The proposed antenna is connected to a 50Ω Transmission line through SMA connector for signal Transmission. The design of the antenna is optimized using the CST MW Studio with the main dimensions listed in Table I. Fig. 2 shows the photograph of the fabricated antenna.

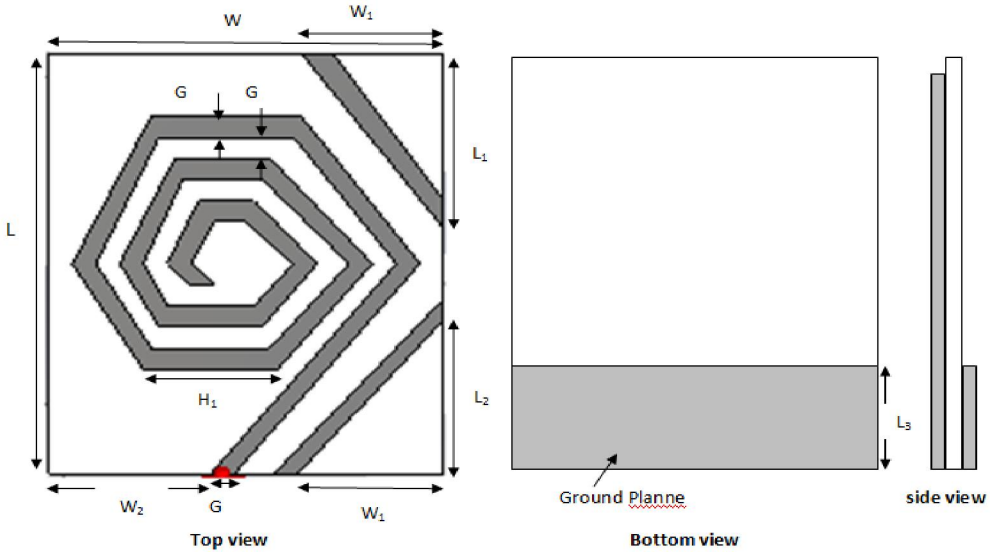

Fig. 1. Geometry of the proposed antenna

Table 1. Key dimensions of proposed antenna in millimeters

L	W	G	W_1	W_2	L_1	L_2	L_3	H_1
60	50	3	28.5	18.5	22	25	15.56	19

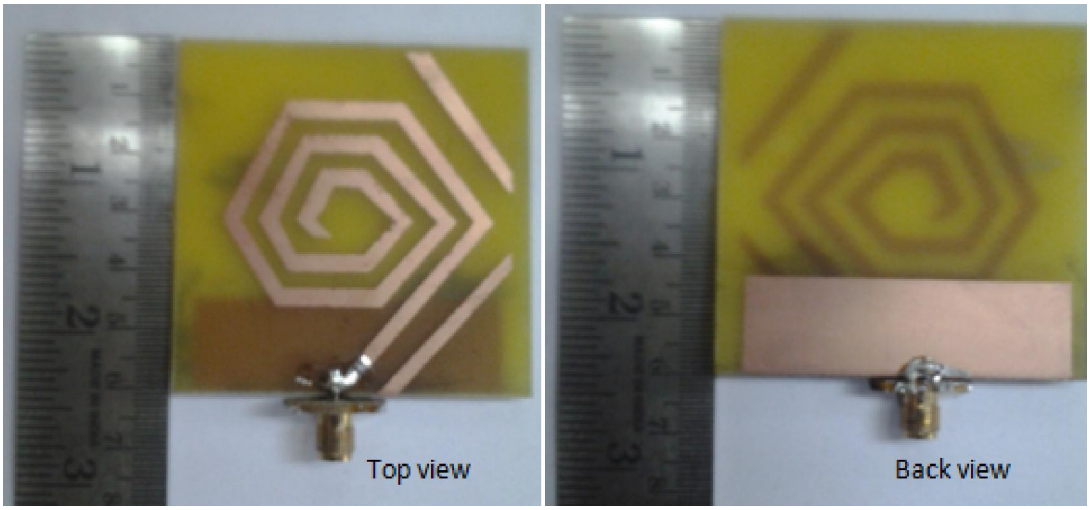

Fig. 2. Proto type of the antenna

3 RESULT AND DISCUSSIONS

In this section, the Hexagonal Meander-line Monopole antenna with various design parameters was simulated using CST Microwave Studio and experimental results of input impedance, radiation characteristics are presented and discussed here. With the insertion of Meander line structure in Monopole, results can be achieved easily. Fig. 3 shows the comparison between simulated and measured return loss of the proposed antenna. In the simulated design, the first band achieved is 1.702-1.811GHz covering GSM1800 (1.710-1.785GHZ), second band is 2.51-2.68GHz covering WIMAX (2.501-2.699) and third band is 2.71-3.01GHZ covering WIMAX MMDS (2.7-2.9GHZ). In the measured results, it is observed that first band achieved is 1.681-1.781GHz, second band is 2.49-2.71GHz and third band is 2.75-2.998GHz with return loss of -30dB, -31dB and -30.08dB respectively. From the Fig. 3 it is observed that simulation and experiment results both are same, showing good agreement between them. The reduction in the return loss ultimately improves the gain as well as the bandwidth of microstrip antenna.

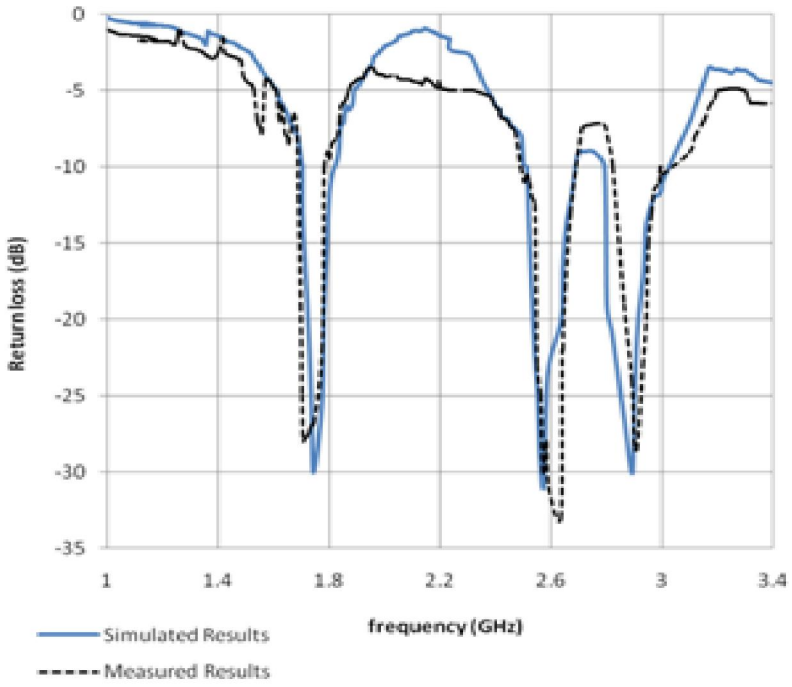

Fig. 3. Measured and Simulated Return loss

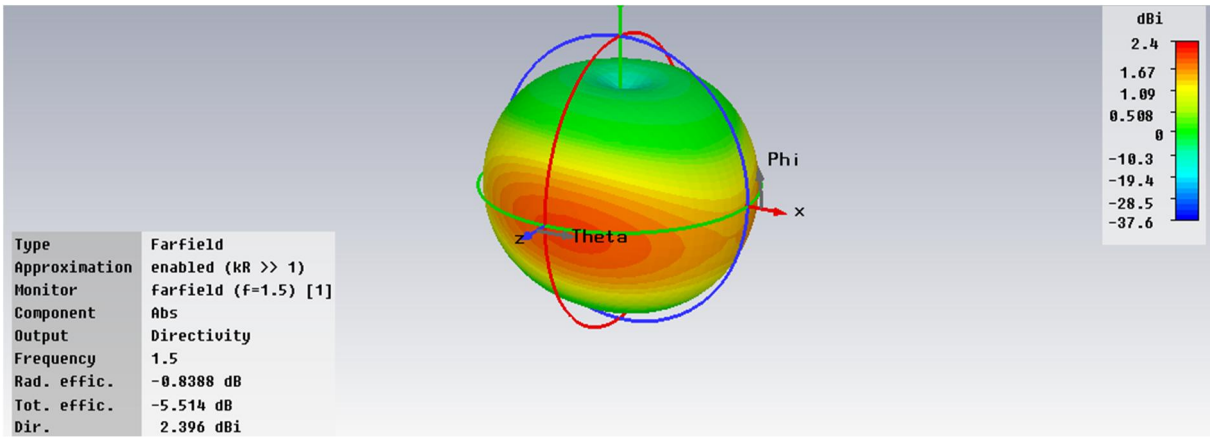

(a)

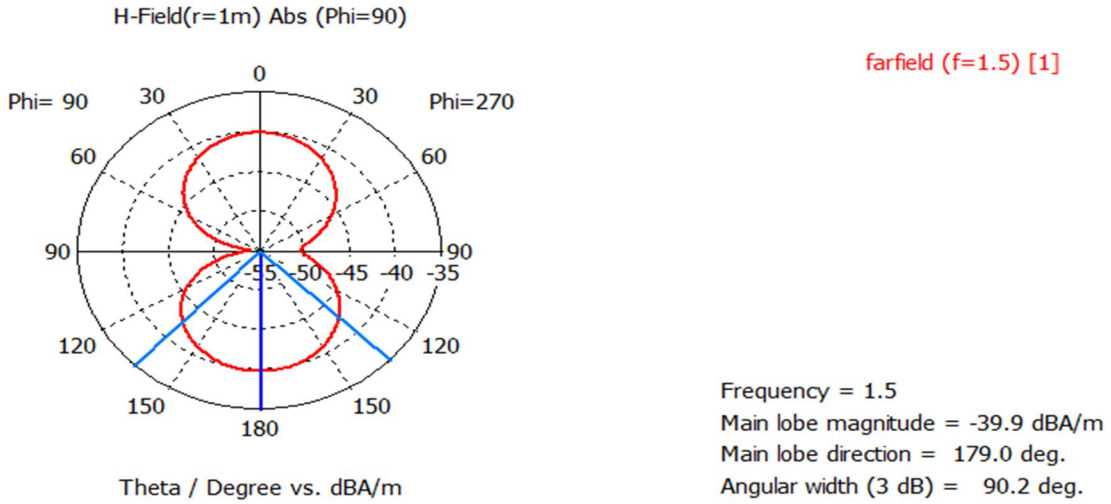

(b)

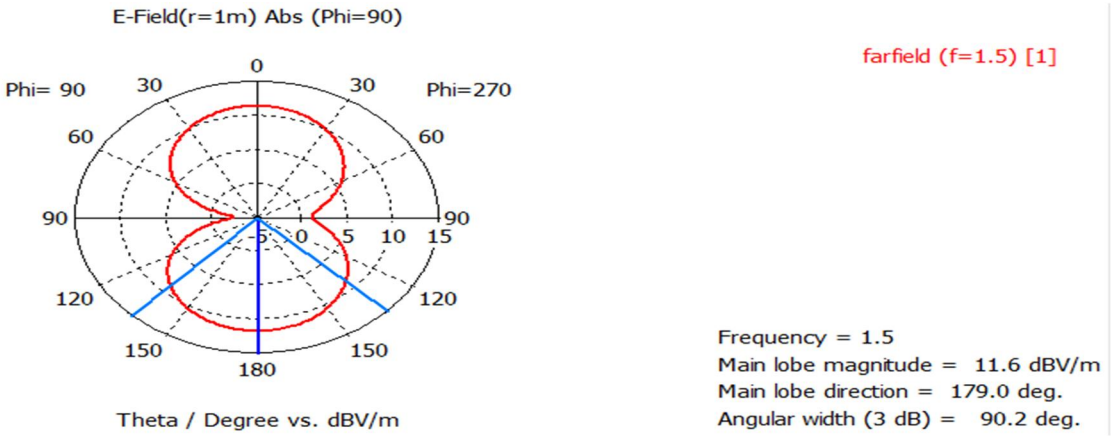

(c)

Fig. 4. (a) Radiation Characteristics Of Proposed Antenna (b) E-field Polar Plot (c) H-field polar plot

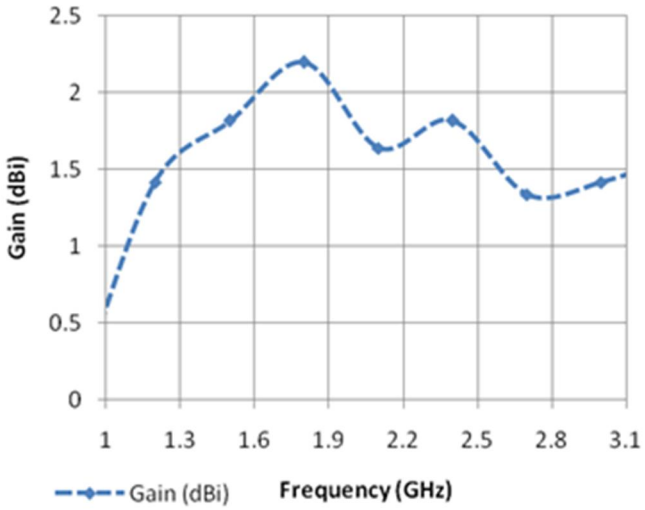

Fig. 5. Simulated Gain of proposed antenna

Simulated far field radiation pattern of the proposed antenna has been shown in Fig. 4(a) and Fig. 4(b) and 4(c) shows the E and H field polar plots of proposed antenna. Measured Gain of the antenna is shown in Fig. 5.

4 CONCLUSION

In this paper, design of printed Triple band Monopole Antenna with Meander line arms for wireless application is proposed. In this monopole antenna, Meander line structure is designed to generate a low frequency bands for GSM1800 and two more 2.5WIMAX bands. Simulation and measurement results have shown that the antenna has stable radiation pattern, high efficiency, and high gain in all the operating frequency bands.

REFERENCES

[1] M. Mehranpour, J. Nourinia, Ch. Ghobadi, and M. Ojaroudi, "Dual band-notched square monopole antenna for ultrawideband applications," *IEEE Antennas and Wireless Propagation letters*, Vol. 11, pp. 172-175, 2012.

[2] Hattan F. Abutarboush, H. Nasif, R. Nilavalan, S.W. Cheung, "Multiband and Wideband Monopole Antenna for GSM1900 and Other Wireless Applications," *IEEE Antennas and Wireless Propagation Letters*, Vol. 11, pp. 539-542, 2012.

[3] A. Jahanbakshi, Gh. Moradi, R. Sarraf Shirazi, "Design and Simulation Of different Types of Meander Line Antennas with Improved Efficiency," *PIERS proceedings*, Moscow, Russia, August 19-23, pp. 594-597, 2012.

[4] Asit K. panda, R. Suryanarayana, Abhishek Sahoo, Jayanta Nayak, Rabindra K. Mishra, "A Printed Monopole Antenna with Symmetric Meandered Arms For WLAN, WIMAX Applications," 2*011 international conference on communication systems and network Technologies*, pp. 224-227, 2011.

[5] C.A. Balanis, *Antenna Theory: analysis and design*, Third edition, John Wiley &sons Inc, 2005.

[6] Ayman A. R. Saad, Elsayed E.M.Khaled and Deena A. Salem, "Wideband Slotted Planar antenna With Defected Ground Structure," *PIERS Proceedings*, Suzhou, china, pp. 12-16, Sep 2011.

[7] F. Tseng, L. Huang, H. Hsu, "Microstrip-fed monopole antenna with a shorted parasitic element for wide band applications," *Progress in Electromagnetics Research Letters*, Vol. 7, pp. 115-125, 2009.

[8] Rabih Rahaoui and Mohammed Essaaidi, "Compact Cylindrical Dielectric Resonator Antenna excited by a Microstrip Feed Line," *International Journal of Innovation and Applied Studies*, vol. 2, no. 1, pp. 1–5, January 2013.

[9] Mohammed Younssi, Achraf Jaoujal, Yacoub Diallo, Ahmed El-Moussaoui, and Noura Aknin, "Study of a Microstrip Antenna with and Without Superstrate for Terahertz Frequency," *International Journal of Innovation and Applied Studies*, vol. 2, no. 4, pp. 369–371, April 2013.

[10] M. I. Hasan and M. A. Motin, "New slotting technique of making compact octagonal patch for four band applications," *International Journal of Innovation and Applied Studies*, vol. 3, no. 1, pp. 221–227, May 2013.

[11] Tajeswita Gupta and P. K. Singhal, "Ultra Wideband Slotted Microstrip Patch Antenna for Downlink and Uplink Satellite Application in C band," *International Journal of Innovation and Applied Studies*, vol. 3, no. 3, pp. 680–684, July 2013.

[12] Sonali Kushwah, P. K. Singhal, Manali Dongre, and Tajeswita Gupta, "A Minimized Triangular – Meander Line PIFA Antenna for DCS1800/WIMAX Applications," *International Journal of Innovation and Applied Studies*, vol. 3, no. 3, pp. 714–718, July 2013.

[13] Tajeswita Gupta, P. K. Singhal, and Vandana Vikas Thakre, "Modification in Formula of Resonating Frequency of Equilateral TMPA for Improved Accuracy and Analysis," *International Journal of Innovation and Applied Studies*, vol. 3, no. 3, pp. 727–731, July 2013.

[14] Anshul Agarwal, P. K. Singhal, Shailendra Singh Ojha, and Akhilesh Kumar Gupta, "Design of CPW-fed Printed Rectangular Monopole Antenna for Wideband Dual-Frequency Applications," *International Journal of Innovation and Applied Studies*, vol. 3, no. 3, pp. 758–764, July 2013.

International Journal of Innovation and Applied Studies
ISSN 2028-9324 Vol. 3 No. 4 Aug. 2013, pp. 959-966

http://www.issr-journals.org/ijias/

Characterization of Phosphate Solubilizing and Potassium Decomposing Strains and Study on their Effects on Tomato Cultivation

Tin Mar Lynn[1], Hlaing Swe Win[1], Ei Phyu Kyaw[1], Zaw Ko Latt[1], and San San Yu[2]

[1]Department of Biotechnology,
Mandalay Technological University,
Mandalay, Myanmar

[2]Molecular Life Science Research Center,
Jacobs University,
Bremen, Germany

ABSTRACT: Seven strains were collected for phosphate solubilizing and potassium decomposing activities from Microbiology Laboratory, Department of Biotechnology, Shweziwa Biofertilizer Plant. When phosphate solubilizing activity of selected strains was qualitatively determined, all strains except from B1 strain, gave clear zone formation on NBRIP media. But when quantitatively determined by spectrophotometric method, all strains solubilized insoluble tricalcium phosphate. Among seven strains, Ps strain gave the highest soluble phosphate concentration (386 ppm). Potassium decomposing activity was also determined for qualitatively and quantitatively. For qualitative determination, potassium decomposing activity was screened for clear zone formation on potassium decomposing media. Among seven strains, B1 and Y strains cannot give clear zone around their colonies. But when determined by AAS method, all strains can decompose potassium mica by giving soluble potassium concentration. Y strain gave the highest soluble potassium concentration (8.45 ppm). Phosphate solubilizing and potassium decomposing strains were combined differently for four treatments to study their effects on tomato cultivation. Chemical fertilizer was also applied to compare with selected strains. Among all treatments, T-4 showed better result on total yield although yields were not significantly different.

KEYWORDS: Phosphate solublizing, Potassium decomposing, NBRIP, AAS method, Tomato.

1 INTRODUCTION

Myanmar is the agricultural country and so business is mainly dependent an agriculture. Therefore, it is important to increase agricultural production and the improvement of soil is one of the most common strategies. The currently used agricultural inputs are mostly chemical. The poor farm management technique and improper use of agrochemical has a result in both soil quality and environmental degradation. In order to avoid these problems, application of biofertilizer is considered today to limit the use of mineral fertilizer and supports an effective tool for desert development under less polluted environment, decreasing agricultural costs, maximizing crop yield due to providing them with an available nutritive elements and growth promoting substances [1].

Biofertilizers are living microbial inoculants that are added to the soil to improve the plant growth and can be used as an alternative source of chemical fertilizer [2]. Use of soil microorganisms which can either fix atmosphere nitrogen, solubilizing phosphate, synthesis of growth promoting substances, will be environmentally begin approach for nutrient management and ecosystem function [3].

Nitrogen (N), Phosphorous (P) and Potassium (K) are major essential macronutrients for plant growth and development. Phosphorus is one major plant nutrients, second only to nitrogen in requirement. However, a greater part of soil phosphorus, approximately 95–99% is present in the form of insoluble phosphates and hence cannot be utilized by the plants. To

Corresponding Author: Tin Mar Lynn (light.lynn@gmail.com)

circumvent the P deficiency in soils, P fertilizers are applied. However, after application, a considerable amount of P is rapidly transformed into less available forms by forming a complex with Al or Fe in acid soils or Ca in calcareous soils [4] before plant roots had a chance to absorb it [5]. It has been reported that many soil fungi and bacteria can solubilize inorganic phosphates. The solubilization effect is generally due to the production of organic acid [6]. Last but not least, phosphate not only increase seed germination and early growth, it also can stimulates blooming, hastens maturity, enhance bud seed formation and aids in seed formation [7].

Potassium is one of the most important macronutrient for the growth and reproduction of the plants [8]. Potassium ions serve to activate certain enzymes especially those involved in photosynthesis, respiration and in starch and protein synthesis [9]. Moreover, opening and closure of stomatal guard cells or daily changes in the orientation of leaves are affected by potassium concentration [10]. Potassium is available in four forms in the soil which are K ions (K+) in the soil solution, as an exchangeable cation, tightly held on the surfaces of clay minerals and organic matter, tightly held or fixed by weathered micaceous minerals, and present in the lattice of certain K-containing primary minerals [11]. Inoculation with bacteria, which can improve P and K availability in soils by producing organic acids and other chemicals, stimulated growth and mineral uptake of plants ([12], [13]).

The aim of this research work was to increase the production of crop yields in order to improve farmers' profit by using biofertilizer in place of chemical fertilizer.

2 MATERIAL AND METHODS

2.1 STRAIN COLLECTION

Phosphate solubilizing and potassium decomposing strains were collected from Microbiology Laboratory, Department of Biotechnology, Shweziwa Biofertilizer Plant, Kyaukse District, Mandalay Region, Myanmar.

2.2 IDENTIFICATION OF SELECTED STRAINS

Selected strains were cultured on their respective media (Pikovaskaia's and potassium decomposing media) to study colonial morphology. Microscopic morphology of selected strains was examined by Gram's staining method. Biochemical characteristics of selected strains were also studied.

2.3 QUALITATIVE DETERMINATION OF PHOSPHATE SOLUBILIZING ACTIVITY

Selected strains were checked for phosphate solubilizing activity. All selected strains were inoculated in National Botanical Research Institute Phosphate (NBRIP) broth media, and incubated in water batch shaker at 37°C for three days. After incubation, the culture broth was centrifuged at 6000 rpm for 15 minutes and 50µl of supernatant was added to well that was punched on NBRIP media. The culture plates were incubated at 37°C. After incubation, clear zone formation around the well was recorded for every day.

2.4 QUANTITATIVE DETERMINATION OF PHOSPHATE SOLUBILIZING ACTIVITY

Selected strains were further evaluated for their phosphate solubilizing ability. Phosphate solubilization in Pikovaskaia's broth media was quantified in a flask (10 ml) and incubated in water batch shaker at 37°C for five days. Uninoculated medium served as control. After incubation, the culture broth was passed through the cation exchange resin and $(PO_4)^{3-}$ solution was reacted with color forming reagent (Sodium Molybdate and Hydrazium Sulphate). After blue color development, phosphate solubilizing activity was measured by UV-vis spectrophotometric method at 830 nm.

2.5 QUALITATIVE DETERMINATION OF POTASSIUM DECOMPOSING ACTIVITY

Potassium decomposing activities of selected strains was qualitatively screened on potassium decomposing media. Selected strains were firstly inoculated in potassium decomposing broth media and incubated in water batch shaker at 37°C until optimum growth. After getting optimum growth, the bacterial broth was centrifuged at 6000 rpm for 15 minutes and 50 µl of supernatant was added to well that was punched on media. After incubation, clear zone formation around well was recorded for potassium decomposing activity.

2.6 Qualitative Determination of Potassium Decomposing Activity

Selected strains were cultured as described in qualitative determination. After centrifugation, amount of soluble potassium in supernatant was measured by Atomic Absorption Spectrometry method (AAS).

2.7 Study on Co-existence Growth of Phosphate Solubilizing and Potassium Decomposing Strains

Co-existence growth of phosphate solubilizing and potassium decomposing strains was studied on Pikovaskaia's and Potassium Decomposing media by cross culturing of strains with each other. After incubation at 37°C, co-existence growth of strains was studied.

2.8 Preparation of Pellet Form Biofertilizer Using Selected Strains

For preparation of pellet form biofertilizer, P-solubilizing and K-decomposing strains were cultured in Pikovaskaia's and potassium decomposing broth media and incubated until optimum growth. When the bacterial broth culture was ready in use, the compost was crushed to obtain the finely powdered compost. The compost was mixed with zeolite and the bacterial broth culture was added to these mixtures. After mixing well, the mixture was placed into the pelletizing machine. While pelletizing, gypsum was used to coat the mixture of compost and zeolite. After pelletizing, the pellet form biofertilizer was dried in room temperature.

2.9 Study on Effect of Pellet Form Biofertilizer on Tomato Cultivation

Phosphate solubilizing and potassium decomposing strains were applied in tomato cultivation in pellet form biofertilizer to know their effects. Experiments were designed by randomized completely block design (RCBD). After three months of cultivation period, data analysis was taken and compared among treatments.

3 Results and Discussion

3.1 Strains Collection

Seven strains, two phosphate solubilizing, four potassium decomposing bacteria and one potassium decomposing yeast strain were collected.

3.2 Identification of Selected Strains

Four potassium decomposing and one phosphate solubilizing bacteria were gram-negative cocci and the other phosphate solubilizing bacteria was gram-positive in rod-shaped. Their biochemical characteristics were shown in Table 1. One collected yeast strain was Gram positive and its sugar assimilation and fermentation patterns were shown in Table 2. Antibiotic sensitivity patterns were shown in Table 3. According to colonial and microscopic morphology and biochemical characteristics, four potassium decomposing bacteria may be *Pseudomonas* spp. and the other phosphate solubilizing bacteria may be *Bacillus megaterium*.

Table 1. Microscopic Morphology and Biochemical Characteristics of Selected Strains

Biochemical Tests	Ps	B-1	Y	K-3	K-5	KA-2	KA-35
Gram's Reaction	- (cocci)	+ (rod)	+ (cocci)	- (cocci)	+ (cocci)	- (cocci)	- (cocci)
Motility	+	+	ND	+	+	+	+
Methyl Red	-	+	ND	+	+	+	+
Voges Prosakur	+	+	ND	-	+	+	+
Citrate Utilization	+	+	+	+	+	+	+
Starch Hydrolysis	-	-	+	-	-	+	-
Gelatin Agar	-	-	ND	-	-	-	-
Urease	-	-	ND	+	-	-	-
Indole	-	-	ND	-	-	-	-
Catalase	+	+	ND	+	+	+	+

Antibiotic sensitivity patterns were shown in Table 3. In antibiotic sensitivity pattern, Ps, K3 and A35 strains resistant to only Ampicillin, they were sensitive to other four antibiotics. But, all other strains were sensitive to all tested antibiotics.

Table 2. Sugar Assimilation and Fermentation Patterns of Yeast

Sugars	Assimilation Patterns	Fermentation Patterns
Glucose	+	+
D-xylose	+	+
Sucrose	+	+
Maltose	+	+
Lactose	-	-
Raffinose	+	+
Arabinose	-	-
Myo-Inositol	-	-

Table 3. Antibiotic Sensitivity Patterns of Selected Strains

Antibiotics	Ps	B 1	Y	K3	K5	KA2	A35
Ampicillin	R	S	S	R	S	S	R
Gentamycin	S	S	S	S	S	S	S
Kanamycin	S	S	S	S	S	S	S
Chloramphenicol	S	S	S	S	S	S	S
Tetracycline	S	S	S	S	S	S	S

R = Resistance S = Sensitive

3.3 Qualitative and Quantitative Determination of Phosphate Solubilizing Activity

According to plate screening for clear zone formation, all selected strains, except from B1, gave clear zone formation around the well. Index for clear zone formation of these strains was shown in Table 4. As they gave clear zone, it can be assumed that these strains have phosphate solubilizing activity. In clear zone formation, K3 strain gave the largest zone formation. During five days incubation, clear zone formation of all these strains was larger and larger.

After plate screening, Phosphate solubilizing activity of all selected strains was quantitatively determined by UV-vis spectrophotometric method at 830 nm using KH_2PO_4 as standard. Amount of solubilized phosphate of all selected strains were shown in Figure 1. Although K3 strain gave the largest clear zone in plate screening method after 5 day incubation (1.375 in Table-4), it showed the lowest amount of solubilized P in quantitative analysis (Fig-1). According to quantitative analysis, Ps strain was the best phosphate solubilizer by giving 386 ppm but the clear zone diameter of Ps was not the largest among all strains. Although B1 strain gave no clear zone formation on plate screening, soluble phosphate concentration of B1 could be quantitatively determined (306 ppm). So, it was known that clear zone diameter formation was not directly proportional to the amount of solubilized phosphate concentration. All these findings revealed that one should not rely only on qualitative method while isolating and screening the P solubilizing microorganisms. It is wise to supplement qualitative method with quantitative measurement of P solubilizing for getting more reliable inferences [14].

Similar results have been reported in ([15], [16], [17]). It has also been reported that many isolates which did not show any clear zone in qualitative method i.e. NBRIP medium- agar plate assay) solubilized insoluble inorganic phosphates in quantitative method ([18], [19], [16]). Thus, the plate screening method fails where the clear zone is inconspicuous or absent. This may be because of the varying diffusion rates of different organic acids secreted by an organism [20]. Contrary to qualitative method (indirect measurement) of phosphate solubilization by plate screening method, the quantitative analysis by UV-spectrophotometer in broth culture method resulted in reliable results [16].

Identification of individual isolates by colonial, microscopical and biochemical characteristics showed that these bacteria were different. But, these variations were not well depicted with phosphate solubilizing trait. Phosphate solubilizing activity

is determined by microbial biochemical ability to produce and release organic acids, which their carboxylic groups chelate the cations (mainly Ca) bound to phosphate converting them into soluble forms [21].

Table 4. P-solubilizing Activity of Selected Strains on NBRIP Media (in terms of Solubility Index)

Strains	Day 1	Day 2	Day 3	Day 4	Day 5
Ps	0.25	0.5	0.625	0.75	0.875
B 1	-	-	-	-	-
Y	0.125	0.25	0.375	0.5	0.625
K 3	0.875	1	1.125	1.125	1.375
K 5	0.25	0.375	0.5	0.625	0.75
KA 2	0.625	0.875	1.125	1.125	1.125
KA 35	0.25	0.5	0.75	0.75	1

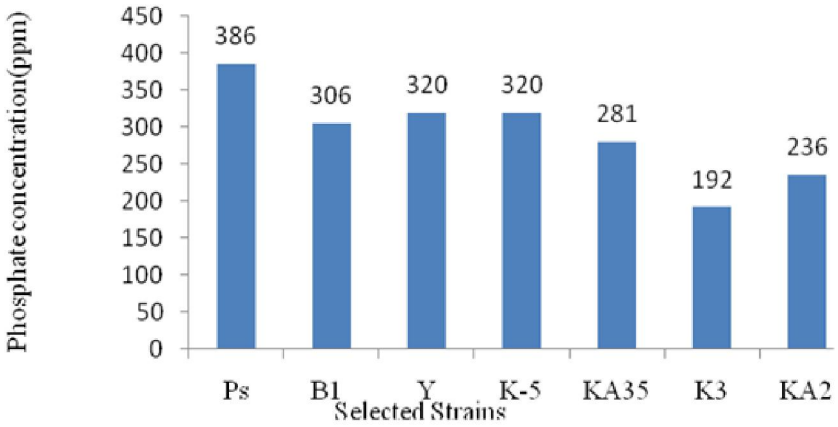

Fig. 1. P-concentration Solubilized by Selected Strains in Pikovaskia Broth after 5 Days Incubation by Spectrophotometric Method

Potassium decomposing activities of selected strains were firstly screened for clear zone formation on potassium decomposing media. The potassium solubility index of all selected strains was shown in Table 5. Like in P-solubilization by plate screening, clear zone formation of all strains, except from B1 and Y strains, was larger and larger until 5 days incubation. In qualitative determination, solubility index for all strains was almost the same. Quantitative measurement of potassium decomposing activity by AAS method was shown in Figure 2. Although B1 and Y strains cannot give clear zone formation when screened on media, they can solubilize potassium mica by giving 6.63 ppm and 8.45 ppm when measured by AAS method. In potassium decomposing activity, Y strain gave the highest amount of soluble potassium concentration and B1 strain was the second highest. Although Ps was the best strain in phosphate solubilizing activity, potassium decomposing activity was the lowest among all these strains. The ability of bacteria to release K largely depends on the nature of the mineral compounds [22]. The variability among the bacteria indicates the importance of exploration of different mineral potassium solubilizing bacteria and their solubilizing mechanisms.

Table 5. K-decomposing Activity of Selected Strains on K-decomposing Yeast Media (in terms of Solubility Index)

Strains	Day 1	Day 2	Day 3	Day 4	Day 5
Ps	0.75	0.875	0.875	1	1.125
B 1	-	-	-	-	-
Y	-	-	-	-	-
K 3	1	1.125	1.25	1.25	1.25
K 5	0.75	0.875	1	1	1.125
KA 2	0.625	0.75	0.875	1	1.125
KA 35	0.625	0.875	1.125	1.125	1.25

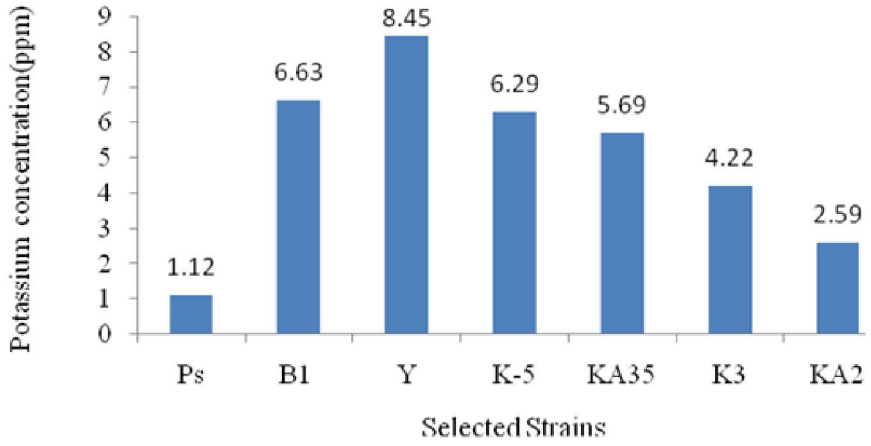

Fig. 2. K-decomposing Activity of Selected Strains by Atomic Absorption Spectrometry (AAS) Method

3.4 Study on Shelf-life of Pellet Form Biofertilizer

For convenience application, a carrier material is used as a vehicle for the microorganisms to be used as biofertilizer. Moreover, such materials may have a role in maintaining the viability (shelf-life) of the microorganisms prior to its release into the field as well as they also provide a suitable microenvironment for rapid growth of the organisms upon their release [23]. After formulating phosphate solubilizing and potassium decomposing strains as pellet form biofertilizer, microbial populations were checked for every month. It was shown in Table 6. Microbial populations were counted for 16 weeks. Among four different combinations, microbial population of all combinations was around 10^4 after 16 weeks. So, it was seen that there was no effect of combination on microbial population.

Table 6. Microbial Population in Formulated Biofertilizer

Treatment	0 week	2 week	4 week	6 week	8 week	10 week	12 week	14 week	16 week
Ps	$2.8x\ 10^7$	$1.08x10^8$	$2.4x10^7$	$4.4x10^6$	$1.2x10^6$	$6.8x10^5$	$7.3x10^4$	$5.2x10^4$	$3.6x10^4$
B 1	$4.8x10^8$	$1.0x10^8$	$2.0x10^7$	$5.2x10^6$	$7.6x10^5$	$6.0x10^5$	$6.0x10^4$	$4.8x10^4$	$2.4x10^4$
Y	$6.8x10^7$	$7.6x10^7$	$3.2x10^7$	$4.4x10^6$	$1.2x10^6$	$7.6x10^5$	$4.6x10^4$	$1.2x10^4$	$1.2x10^4$
K 3	$1.68x10^7$	$8.4x10^7$	$8.2x10^6$	$8.0x10^6$	$3.2x10^6$	$1.2x10^6$	$6.0x10^4$	$2.4x10^4$	$2.4x10^4$

3.5 Study on Effect of Pellet Form biofertilizer on Tomato Cultivation

With four different combinations of phosphate solubilizing and potassium decomposing strains, their effects were studied on tomato cultivation. Water was used as negative control and combination of compost, gypsum and zeolite served as positive control. And only chemical fertilizer was used as Treatment 1. So, there were five treatments.

According to data analysis, all of these treatments had no differently resulted on height of tomato plants, number of branches, and fruits per plant (data not shown). But, T4 gave the better results on total yields of tomato plants at 126 days after sowing. Yields of tomatoes from all treatments were shown in Table 7 and Fig. 3. All treatments gave the better results when compared with negative control, but when compared with positive control, total yield of T1 and T5 were lower than positive control. Although there was no significance difference on total yield and yield per plant among all treatments, T4 was suitable for biofertilizer formulation according to this study. The results are in agreement with [3] who recorded increase in yield significantly in maize crop and also improve soil properties such as organic content due to co-inoculation of KSB and PSB. The results are also comparable with [24], whose studied the increase rice grain yield in a field experiment due to effect of silicate solubilizing bacteria recorded 5218 kg ha grain yield than control 4419 kg per ha.

Table 7. Treatment System for Tomato Cultivation and Yield of Tomatoes after 120 DAS

Treatments	Formulation	Total Yield (Kg)	Yield Per Plant (Kg)
Negative Control	Water	36.602	1.22±0.28
Positive Control (PC)	Compost, Gypsum, Zeolite	34.66	1.16±0.18
Treatment 1	Chemical Fertilizer	35.47	1.18±0.28
Treatment 2	PC+Ps+B1+Y+K5	37.89	1.19±0.19
Treatment 3	PC+Ps+B1+Y+K5+KA35	37.62	1.25±0.3
Treatment 4	PC+ Ps+B1+Y+K5+KA35+K3	48.95	1.63±0.14
Treatment 5	PC+ Ps+B1+Y+K5+KA35+K3+KA2	35.82	1.19±0.1

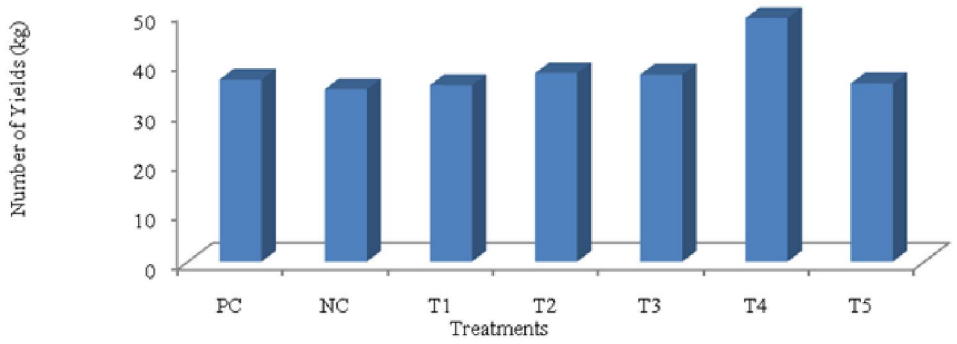

Fig. 3. Total yields of tomatoes at 126 days after sowing

Among seven strains, K-3 showed largest clear zone formation but Ps gave the highest solubilized phosphate amount when quantitatively determined. For potassium decomposing activity, A35 and K3 were the best for clear zone formation. But, yeast strain was the best K-decomposer with the highest concentration of soluble potassium (8.45 ppm). These seven strains were formulated as pellet form biofertilizer with different combinations for field trial observation. Among five treatments, T-4 was the best for yields of tomatoes when compared with other treatments. Use of these bacteria and yeast strain as bioinoculants will increase the available phosphate and potassium in soil and promote plant growth.

4 CONCLUSION

Among seven strains, K-3 showed largest clear zone formation but Ps gave the highest solubilized phosphate amount when quantitatively determined. For potassium decomposing activity, A35 and K3 were the best for clear zone formation. But yeast strain was the best K-decomposer with the highest concentration of soluble potassium (8.45 ppm). These seven strains were formulated as pellet form biofertilizer with different combinations for field trial observation. Among five treatments, T-4 was the best for yields of tomatoes when compared with other treatments. Use of these bacteria and yeast strain as bio-inoculants will increase the available P and K in soil, helps to minimize the chemical fertilizer application, reduces environmental pollution and promotes sustainable agriculture.

ACKNOWLEDGMENT

This research work was kindly supported by Department of Biotechnolgy, Mandalay Techological University, Myanmar. The authors would like to thank Dr. Mya Mya Oo, Rector, Mandalay Technological University and His Excellency U Thaung, Minister, Ministry of Science and Technology, Myanmar.

REFERENCES

[1] El-Ghany Abd, Bouthaina F, "Effect of some soil microorganisms on soil properties and wheat production under North Sinai Conditions," *Journal of Applied sciences Research*, 4(5):559-579, 2010.

[2] Ivanova Evelina, "Alginate based micro-capsule as inoculants carriers for production of nitrogen fixing biofertilizer," Department of Food Process Engineering, National High School of food Technology, France, 2005.

[3] Wu, S.C, and ZH Cao, zg Li, K, C Cheung and M.H Wag, "Effect of biofertilizer containing N-fixer, P and K solubilizers and AM fungi on maize growth: A green house trail," *Geoderma*, 125: 155-166, 2005.

[4] Lindsay, W.L., P.L.G. Vlek and S.H. Chien, "Phosphate Minerals. In: Minerals in Soil Enviroment," Dixon, J.B. and S.B. Weed, (Ed.). Soil Science Society of America Madison, USA, pp: 1089, 1989.

[5] Vikram, A, "Efficacy of phosphate solubilizing bacteria isolated from vertisols on growth and yield parameters of sorghum," *Res. J. Microbiol*., 2: 550-559, 2007.

[6] Kucey, R.M.N., Phosphate-solubilizing bacteria and fungi in various cultivated and Virgin Alberta soils. *Canadian Journal of Soil Science* 63: 671-678, 1983.

[7] Tucker, M.R., "Essential Plant Nutrients: Their Presence in North Carolina Soils & Role in Plant Nutrition," North Caroline: NCDA & CS bulletin, Agronomic Division, pp. 45-61, 2001.

[8] Budr, M. A., "Efficiency of K-feldspar combined with organic materials and silicate Dissolving Bacteria on Tomato Yield," *Journal of Applied sciences Research*, 2(12): 1191-1198, 2006.

[9] Hopkins, W., "Introduction to Plant Physiology," John Wiley and Sons, INS. New York. pp. 414-415, 1995.

[10] Shehata, M.M. and El-Khawas, S.A., "Effect of two biofertilizers on growth parameters, yield characters, nitrogenous components, nucleic acid contents, minerals, oil content, protein profiles and DNA banding pattern of sunflower (Helianthus annus L. cv. Vedock) yield," *Pakistan Journal of Biological Sciences* 6 (14): 1257-1268, 2003.

[11] Ahmad Azinuddin Bin Zakaria, "Growth optimization of potassium solubilizing bacteria isolated from biofertilizer," Faculty of Chemical & Natural Resources Engineering, University Malaysia Pahang, May 2009.

[12] Girgis, M.G.Z., H.M.A. Khalil and M.S. Sharaf, "*In vitro* evaluation of rock phosphate and potassium solubilizing potential of some *Bacillus* Strains," *Aust. J. Basic Applied Sci*., 2: 68-81, 2008.

[13] Garcia, L., A. Prob anza, B. Ramos, J. Barriuso and F.J. Gutierrez Manero, "Effects of inoculation with plant growth promoting rhizobacteria (PGPRS) and *Sinorhizobium fredii* on biological nitrogen fixation, nodulation and growth of Glycine max cv. Osumi," *Plant and Soil*, 267: 143-153, 2004.

[14] Baig, K.S., Arshad, M., Zahir, Z.A. and Cheema, M.A., "Comparative efficacy of qualitative and quantitative methods for rock phosphate solubilization with phosphate solubilizing rhizobacteria," *Soil & Environ*. 29(1): 82 – 86, 2010.

[15] Gupta, R., R. Singal, A. Shankar, R.C. Kuhad and R.K. Saxena, "A modified plate assay for screening phosphate solubilizing microorganisms," *Journal of Genetics and Applied Microbiology*, 40: 255-260, 1994.

[16] Nautiyal, C.S., "An efficient microbiological growth medium for screening phosphate solubilizing microorganisms," *FEMS Microbiology Letters* 170: 265–270, 1999.

[17] Nautiyal, C.S., S. Bhadauria, P. Kumar, H. Lal, R. Mondal and D. Verma., "Stress induced phosphate solubilization in bacteria isolated from alkaline soils," *FEMS Microbiology Letters* 182: 291-296, 2000.

[18] Louw, H.A. and D.M. Webley, "A study of soil bacteria dissolving certain phosphate fertilizers and related compounds," *Journal of Applied Bacteriology* 22: 227-233, 1959.

[19] Leyval, C. and J. Barthelin, "Interactions between *Laccaria laccata, Agrobacterium radiobacter* and beech roots: influence on P, K, Mg and Fe mobilization from mineral and plant growth," *Plant and Soil* 17: 103-110, 1989.

[20] Johnston, H.W., "The solubilization of phosphate: the action of various organic compounds on dicalcium and tricalcium phosphate," *New Zealand Journal of Science and Technology* 33: 436-444. 270, 1952.

[21] Kpomblekou, K. and Tabatabai, M.A., "Effect of organic acids on release of phosphorus from phosphate rocks," *Soil Sci*. 158, 442–453, 1994.

[22] Yakhontova,. K., Andreev, P. I., Ivanova, M. Y. and Nesterovich, L.G., "Bacterial decomposition of smecite minerals," *Doklady AkademiiNauk, SSR*, 296 : 203-206, 1987.

[23] Satinder K. B., Saurabh J.S. and Emna C, "Shelf-life of Biofertilizers: An Accord between Formulations and Genetics, Biofertilizers & Biopesticides," *J Biofertil & Biopestici*, 3:5, 2012.
[Online] Available: http://dx.doi.org/10.4172/2155-6202.1000e109 (2012)

[24] Balasubramaniam, P. and Subramanian, S. (2006). Assement of soil test based potassium requirement for low land rice in udic haplustalf under the influence of silicon fertilization, Tamil Nadu Agric., Kumulur, Truchirapalli, pp. 621-712.

International Journal of Innovation and Applied Studies
ISSN 2028-9324 Vol. 3 No. 4 Aug. 2013, pp. 967-978

http://www.issr-journals.org/ijias/

Mixed Convection Flow and Heat Transfer Behavior inside a Vented Enclosure in the Presence of Heat Generating Obstacle

M. U. Ahammad[1-3], M. M. Rahman[2], and M. L. Rahman[3]

[1]Department of Mathematics, Dhaka University of Engineering and Technology (DUET), Gazipur-1700, Bangladesh

[2]Department of Mathematics, Bangladesh University of Engineering and Technology (BUET), Dhaka-1000, Bangladesh

[3]Department of Mathematics, Rajshahi University, Rajshahi-6205, Bangladesh

ABSTRACT: A numerical investigation has been carried out for an MHD mixed convection problem to realize the influence of solid fluid thermal conductivity ratio as well as diameter of the centered obstacle on the flow and thermal fields in a ventilated cavity. The basis of the current paper is the numerical solutions of the Navier-Stokes equation along with the energy equation, wherein Galerkin weighted residual finite element technique is adopted with the help of Newton–Raphson iterative algorithm. The computation is performed for a wide range of relevant parameters such as thermal conductivity ratio between solid and fluid K (0.2 – 50), diameter of the inner block D (0.1 – 0.7) and Richardson number Ri (0.1 – 10). The streamlines and isotherms have been used for the visualization of the fluid flow structure and thermal field characteristics. Moreover, the findings of this analysis are also displayed by the average Nusselt number on the heated surface and average fluid temperature in the cavity. The study concludes that a small sized block and a lower value of thermal conductivity ratio is more effective for heat transfer phenomenon of the enclosure.

KEYWORDS: Heat transfer, heat generation, mixed convection, solid block, vented enclosure.

1 INTRODUCTION

Combined free and forced convection flow and heat transfer in an enclosure has many significant engineering, technological and natural applications. This includes nuclear reactors, heat rejection systems, heat exchangers, solar energy storage, refrigeration devices, lubrication technologies and cooling of electronic systems.

Many numerical and experimental studies have been performed on the mixed convection in the cavity. Costa and Raimundo [1] analyzed the problem of steady mixed convection in a square enclosure with a rotating circular cylinder where the enclosure was considered differentially heated. The effect of mixed convection in a partially divided rectangular enclosure was carried out by Hsu and How [2]. Manca et al. [3] experimentally performed mixed convection for the assisting forced flow configuration in a channel with an open cavity. They reported that for a large Reynolds number (Re = 1000), two nearly distinct fluid motions such as parallel forced flow in the channel and recirculation flow inside the cavity were found. Raji and Hasnaoui [4] analyzed the mixed convection in ventilated cavities for opposing and assisting flows. In their work, the horizontal top wall and the vertical left wall were arranged with equal heat fluxes. Gau and Sharif [5] investigated combined forced and free convection in rectangular cavities with various aspect ratios considering moving isothermal side walls and a constant-flux heat source on the bottom wall. Mixed convection flow inside a ventilated cavity along with a centered heat conducting horizontal circular cylinder was presented by Billah et al. [6]. A numerical study was carried out by Shuja et al. [7]

Corresponding Author: M. U. Ahammad (main3737@gmail.com)

for mixed convection in a square cavity due to heat generating rectangular body effect of outlet port positions. Rahman et al. [9] studied mixed convection in a rectangular cavity having a heat-conducting horizontal circular cylinder using finite element technique For a wide range of Rayleigh number ($10^3 \leq Ra \leq 10^6$), Kumar and Dalal [10] conducted natural convection in an enclosure with a heated square cylinder. They focused that the uniform wall temperature heating is significantly unlike from the uniform wall heat flux heating. Rahman et al. [11] performed mixed convection in a ventilated square cavity with heat conducting solid circular cylinder placed horizontally. Chamkha [12] studied unsteady laminar mixed convection problem assuming the effect of magnetic field of electrically conducting and heat generating or absorbing fluid in a vertical lid-driven cavity. The fluid flow behavior of combined convection in lid-driven cavity containing a circular body was computed by Oztop et al. [13]. Oh et al. [14] performed a numerical analysis on the natural convection in a vertical square cavity keeping a temperature difference across the enclosure with a heat generating conducting body. The authors reported the variation of streamlines, isotherms and average Nusselt number for each Rayleigh number at the hot and cold walls with respect to temperature difference ratios. Prandtl number's effect on hydromagnetic mixed convection in a double-lid driven cavity confining a heat-generating obstacle have been investigated by Rahman et al. [15]. Ahammad et al [16] studied the performance of different inlet and outlet locations on the flow and heat transfer for the MHD mixed convection problem in a ventilated cavity containing a heat generating square block and they were established that flow and thermal fields have strong dependence on the position of inlet and outlet openings. Heat transfer characteristics of horizontal cylinder cooling under single impinging water jet was presented by Abo El-Nasr et al [17]. Veera Suneela Rani et al [18] performed the radiation effects on convective heat and mass transfer flow in a rectangular cavity. The combine influence of radiation and dissipation on the convective heat and mass transfer flow of a viscous fluid through a porous medium in a rectangular cavity using Darcy model was analyzed in their study.

In this paper, we focus attention on the flow and heat transfer characteristics inside a vented enclosure heated bottom wall in the presence of heat generating centered solid block for a two-dimensional steady laminar mixed convection problem.

2 GEOMETRY OF THE PROBLEM

The geometry of the present study is illustrated in Fig. 1. in which a Cartesian co-ordinate system is used with origin at the lower left corner of the working domain. It consists of a square enclosure of length L having a centered heat generating square solid block. The bottom wall of the cavity is subjected to hot with temperature T_h while the other sidewalls are kept insulated. The solid body with diameter d and a thermal conductivity of k_s generates uniform heat Q_0 per unit volume. The inflow opening is placed on the left bottom corner of the cavity while the outflow opening is on the right top corner as shown in the schematic and the size of each opening is $w = 0.1L$. A uniform magnetic field of strength B_0 is enforced in the horizontal direction on the right adiabatic wall. The incoming flow through the inlet is assumed at a uniform velocity u_i, ambient temperature T_i whereas the outgoing flow by the exit port is assumed to have zero diffusion flux for all variables and all solid boundaries are supposed to be rigid no-slip walls.

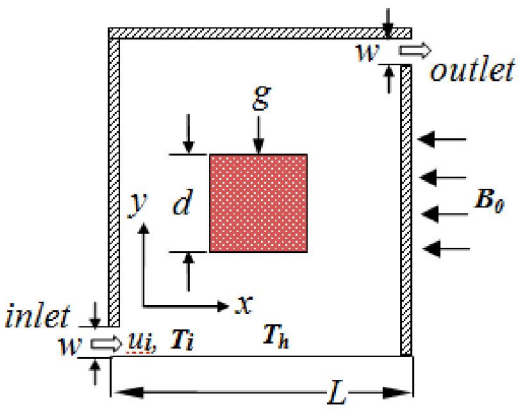

Fig. 1. Computational system

3 MATHEMATICAL MODELING AND SOLUTION PROCESS

The working fluid within the enclosure is supposed to be incompressible, Newtonian, two-dimensional, steady and laminar with all the fluid properties assumed as constant except for density variation. The radiation effect is negligible and the viscous dissipation is absent for the considered fluid. The governing equations for the problem under Boussinesq approximation can be described in vector forms as below:

$$\underline{\nabla}.\ \underline{q} = 0 \tag{1}$$

$$\left(\underline{q}.\underline{\nabla}\right)\underline{q} = -\frac{1}{\rho}\underline{\nabla}\, p + \upsilon\, \nabla^2\ \underline{q} + \underline{F} \tag{2}$$

$$\left(\underline{q}.\underline{\nabla}\right)T = \alpha\, \nabla^2\ T \tag{3}$$

$$\left(\underline{q}.\underline{\nabla}\right)T_s + \frac{\rho c_p}{k_s} Q_0 = 0 \tag{4}$$

where it is taken that $F_x = 0$ and $F_y = g\beta\left(T - T_i\right) - \dfrac{\sigma {B_0}^2 v}{\rho}$

where $\underline{q}$ is the velocity vector, $\underline{F}$ is the body force, T and T_s denotes the temperature of the fluid and solid block, ν and α are the kinematics viscosity and the thermal diffusivity respectively; p is the pressure, ρ is the density, c_p is the specific heat at constant pressure k_s is the thermal conductivity of the solid block and Q_0 is the uniform constant heat flux.

The above equations are made dimensionless by introducing the following non-dimensional variables

$$X = \frac{x}{L},\ Y = \frac{y}{L},\ U = \frac{u}{u_i},\ V = \frac{v}{u_i},\ P = \frac{p}{\rho\, {u_i}^2}, \theta = \frac{\left(T - T_i\right)}{\left(T_h - T_i\right)},\ \theta_s = \frac{\left(T_s - T_i\right)}{\left(T_h - T_i\right)}$$

Taking into account the aforesaid assumptions on the equations (1-4), the non-dimensional equations for the problem are given as follows:

$$\frac{\partial U}{\partial X} + \frac{\partial V}{\partial Y} = 0 \tag{5}$$

$$U\frac{\partial U}{\partial X} + V\frac{\partial U}{\partial Y} = -\frac{\partial P}{\partial X} + \frac{1}{Re}\left(\frac{\partial^2 U}{\partial X^2} + \frac{\partial^2 U}{\partial Y^2}\right) \tag{6}$$

$$U\frac{\partial V}{\partial X} + V\frac{\partial V}{\partial Y} = -\frac{\partial P}{\partial Y} + \frac{1}{Re}\left(\frac{\partial^2 V}{\partial X^2} + \frac{\partial^2 V}{\partial Y^2}\right) + \frac{Ra}{Re^2 Pr}\theta - \frac{Ha^2}{Re}V \tag{7}$$

$$U\frac{\partial \theta}{\partial X} + V\frac{\partial \theta}{\partial Y} = \frac{1}{Re\, Pr}\left(\frac{\partial^2 \theta}{\partial X^2} + \frac{\partial^2 \theta}{\partial Y^2}\right) \tag{8}$$

For solid obstacle the energy equation

$$\left(\frac{\partial^2 \theta_s}{\partial X^2} + \frac{\partial^2 \theta_s}{\partial Y^2}\right) + \frac{RePr}{K} Q = 0 \tag{9}$$

The dimensionless parameters appeared in the equations (6) - (9) are defined as follows

$$Re = u_i L/\upsilon,\ Ra = g\ \beta\ \Delta T\ L^3/\upsilon\alpha,\ Pr = \upsilon/\alpha,\ Ri = Gr/Re^2,\ Ha = B_0 L\sqrt{\sigma/\mu},$$

$$Q = \frac{Q_0 L^2}{k_s \Delta T}\ and\ K = k_s/k$$

where, *Re*, *Ra*, *Pr*, *Ri*, *Ha*, *Q*, and *K* stand for Reynolds number, Rayleigh number, Prandtl number, Richardson number, Hartmann number, heat generating parameter and solid fluid thermal conductivity ratio respectively. Also, $\Delta T = T_h - T_i\ and\ \alpha = k/\rho c_p$ are respectively the temperature difference and thermal diffusivity of the fluid.

The appropriate non-dimensional boundary conditions for the present problem are:

$U = 1$, $V = 0$, $\vartheta = 0$ at the inlet.

Convective boundary condition (CBC), $P = 0$ at the exit.

$\vartheta = 1$ at the heated bottom wall.

$U = 0, V = 0, \frac{\partial \theta}{\partial N} = 0$ at all the adiabatic walls.

$\left(\frac{\partial \theta}{\partial N}\right)_{fluid} = K\left(\frac{\partial \theta_s}{\partial N}\right)_{solid}$ at the fluid- solid interfaces.

The average Nusselt number *Nu* at the hot surface is given by

$$Nu_{av} = -\int_0^1 (\partial\theta/\partial Y) dX$$

where as the bulk average fluid temperature inside the enclosure is

$\theta_{av} = \int \theta \, d\overline{V} / \overline{V}$, the volume of the enclosure is $\overline{V}$.

The Galerkin weighted residual finite element scheme is used for the studied problem to solve the governing equations numerically. In this method, the continuum area of interest is discretized into finite element meshes, which are composed of irregular triangular elements. The coupled equations (5)-(9) are transformed into a system of integral equations using Galerkin weighted residual technique to reduce the continuum domain into discrete triangular domains. Then by imposition of boundary conditions the so obtained nonlinear algebraic equations are modified into a set of linear algebraic equations applying Newton-Raphson iteration technique. Last of all with the aid of triangular factorization method these linear equations are solved.

Grid Refinement Test and Code Validation

The details of grid refinement test and code validation for mixed convection problem with heat generating square block located at the center has been discussed in Ahammad et al. [16] and so is not repeated here.

4 RESULTS AND DISCUSSION

A numerical study is conducted herein to investigate the mixed convective two-dimensional laminar fluid flow along with thermal field characteristics considering the effect of thermal conductivity ratio *K* between solid and fluid as well as diameter *D* of the solid block. Governing parameters in this problem are the Reynolds number, Prandtl number, Hartmann number, and Richardson number. The value of Richardson number which is taken in the present work is 0.1, 1.0 and 10 to make simple the comparison process. Streamlines, isothermal lines, average Nusselt number at the hot wall and average fluid temperature inside the enclosure are used for the explanation of fluid flow and heat transfer manner.

Effect of Thermal Conductivity Ratio

Fig. 2. presents the streamlines for different values of *K* for the convective regimes of *Ri* (0.1, 1, 10) while *Re* = 100, *Ha* =10.0, and *Pr* = 0.71 are kept fixed. At *Ri* = 0.1 and *K* = 0.2 it is observed that the mainstreams capture almost the cavity and a counter-clockwise rotating cell develops just above the inlet openings. This is the reason that outer fresh and colder fluids which enters the cavity cannot come into intimate mixing with the inner hotter fluids. There is no disparity in the streamlines for the rest higher values of *K*. In the mixed convection domain (*Ri* = 1) for *K* = 0.2 it follows that the size of lower vortex increases and the top-left cornered open lines squeezes, as a result another anti- clockwise vortex appears occupying that region. But it can be noticed that with the increasing of thermal conductivity ratio the upper vortex reduces in size. A drastic change in flow lines is found at the higher value of *Ri* = 10. The main flow is found merely the right side of the obstacle and an extremely large vortex is created starting just above the inlet that spreads up to the top wall of the enclosure confining the obstacle.

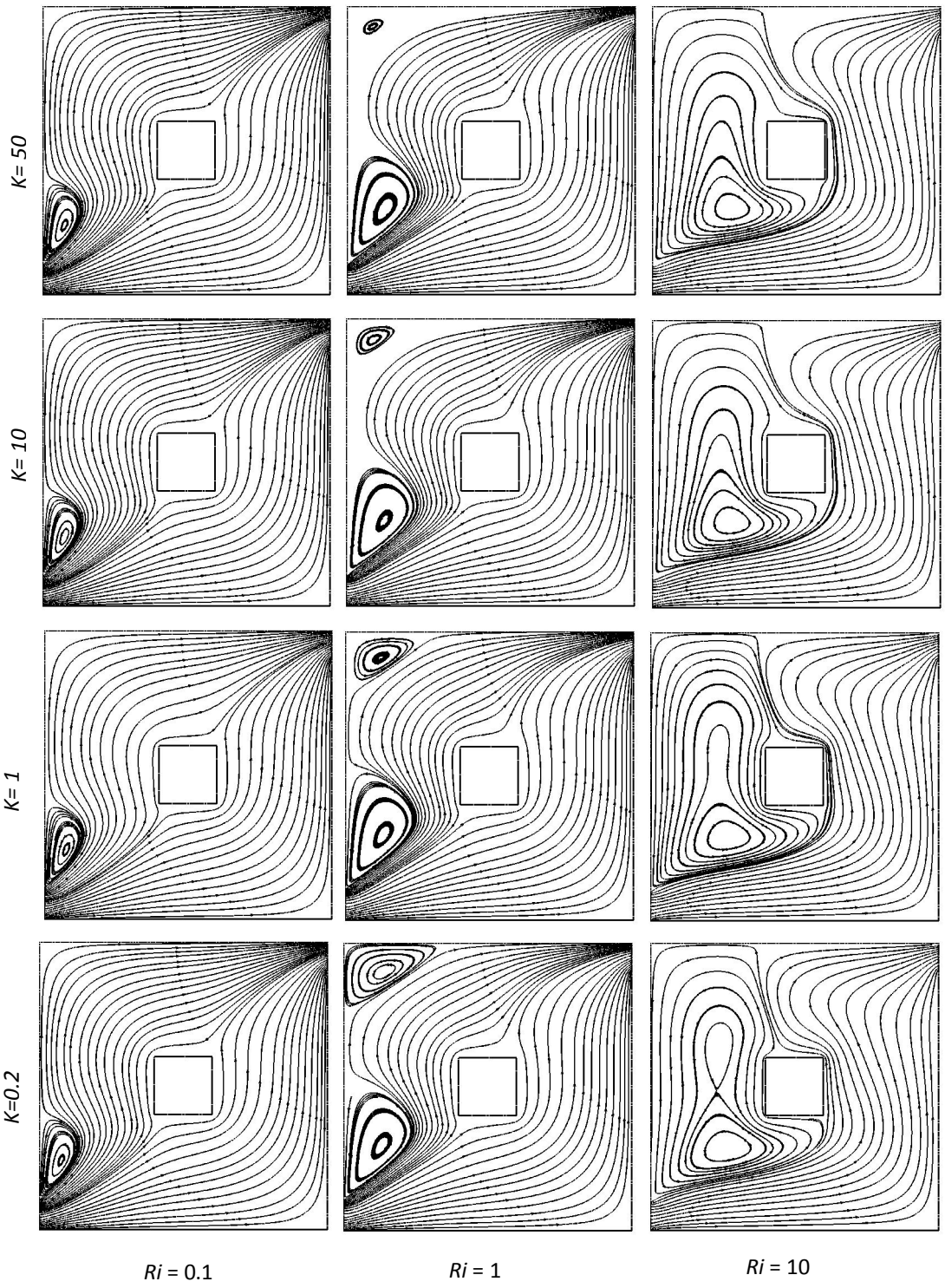

Fig. 2. Streamlines in a square ventilated cavity at different values of K, while Re = 100, Ha = 10, Pr = 0.71 and Ri = 0.1, 1.0, 10.

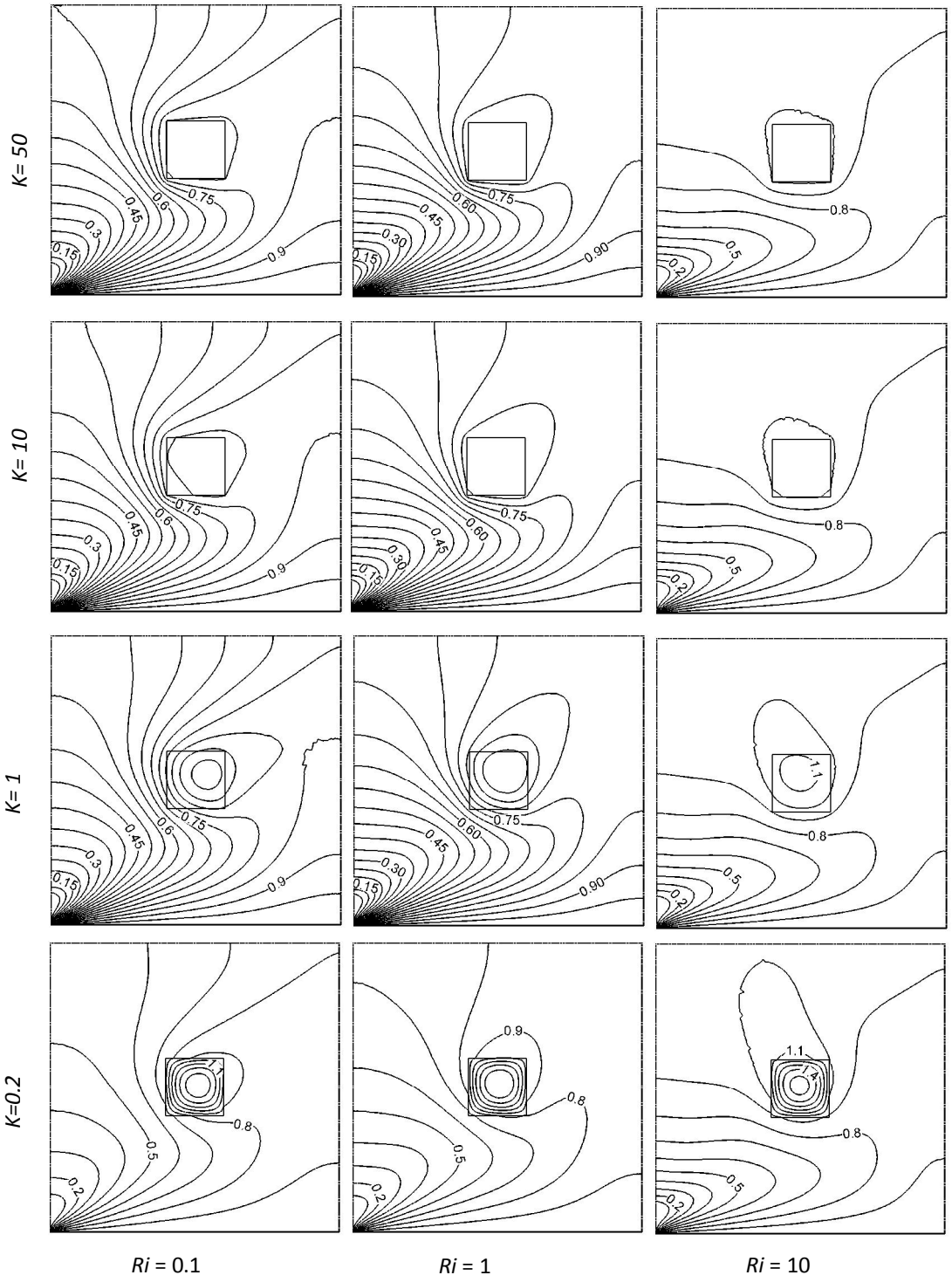

Fig. 3. Isotherms in a square ventilated cavity at different values of K, while Re = 100, Ha = 10, Pr = 0.71 and Ri = 0.1, 1.0, 10.

The corresponding isothermal lines for the chosen values of K in the range $0.1 \leq Ri \leq 10$ are displayed in Fig. 3. In the forced convection dominated region, highest circular thermal lines are distributed inside the centered solid block for the lowest value of K = 0.2. As the value of K increases from 0.2 to 1 it is noticed that the isotherms are dispersed all over the cavity and the compactness of heat lines inside the block reduces. It can be summarized that with increasing the value of K isothermal lines move out gradually from the solid obstacle and as a result it disappears at K = 50. With the comparison of Ri = 0.1, a minor change including right-top cornered plume shaped heat line is found in the patterns of isotherms at Ri = 1. For the free convection dominated region the behavior of temperature distribution changes markedly. The majority of isothermal lines are distributed below the heat generating block and plume shaped isotherm alters it direction from the right-top corner to left-top corner.

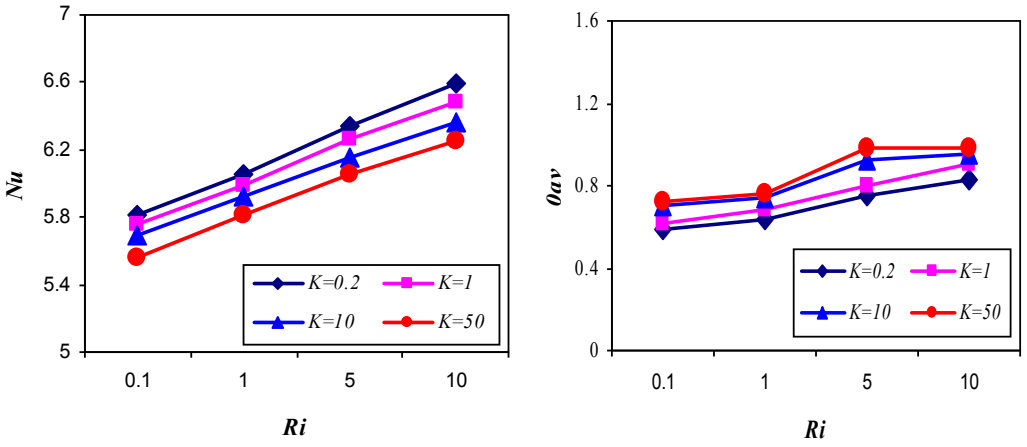

Fig. 4. Effect of thermal conductivity ratio K on average Nusselt number and average fluid temperature in the cavity while Re = 100, Pr = 0.71, Ha = 10, and 0.1≤ Ri≤10

In order to investigate the effect of thermal conductivity ratio K at solid fluid interface on heat transfer manner, average Nusselt number Nu at the bottom heated surface and average fluid temperature ϑ_{av} in the cavity are shown in Fig. 4. From this it can be observed that average Nusselt number enhances sharply as the value of K decreases and Ri increases. Therefore the rate of heat transfer is found optimum for the smallest value of K. On the other hand, ϑ_{av} increases for the rising value K and minimum average temperature is occurred when K = 0.2. Also for the lower values of K (0.2, 1) it is apparent that ϑ_{av} raises with the increasing value of all Ri but ϑ_{av} is seen about stationary in the domain $0.1 \leq Ri \leq 1$ and $5 \leq Ri \leq 10$ while it grows up in the area $1 \leq Ri \leq 5$ in the case of upper values K= 10 and K= 50.

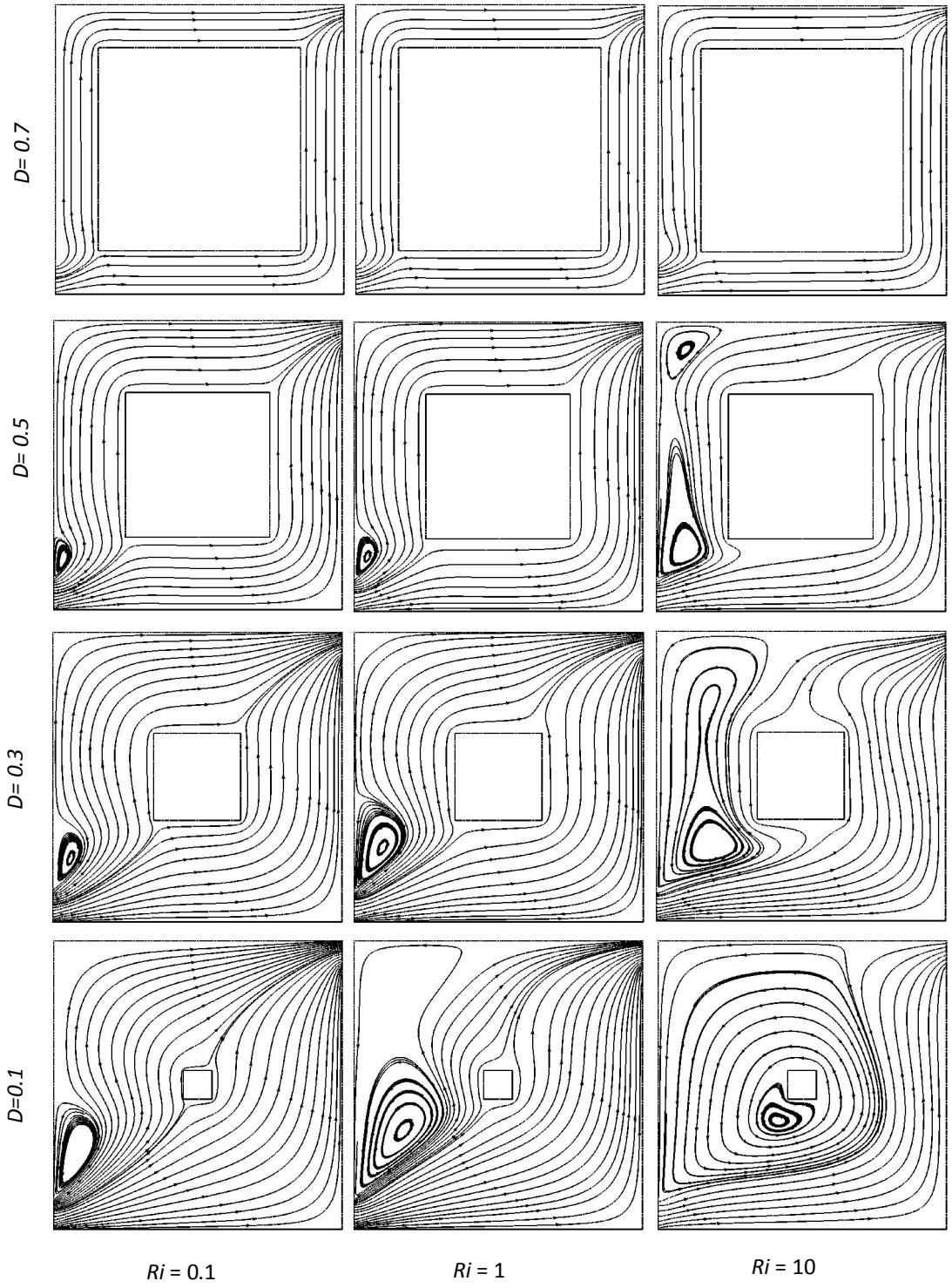

Fig. 5. Streamlines in a square ventilated cavity at different values of D, while Re = 100, Ha = 10, Pr = 0.71 and Ri = 0.1, 1.0, 10

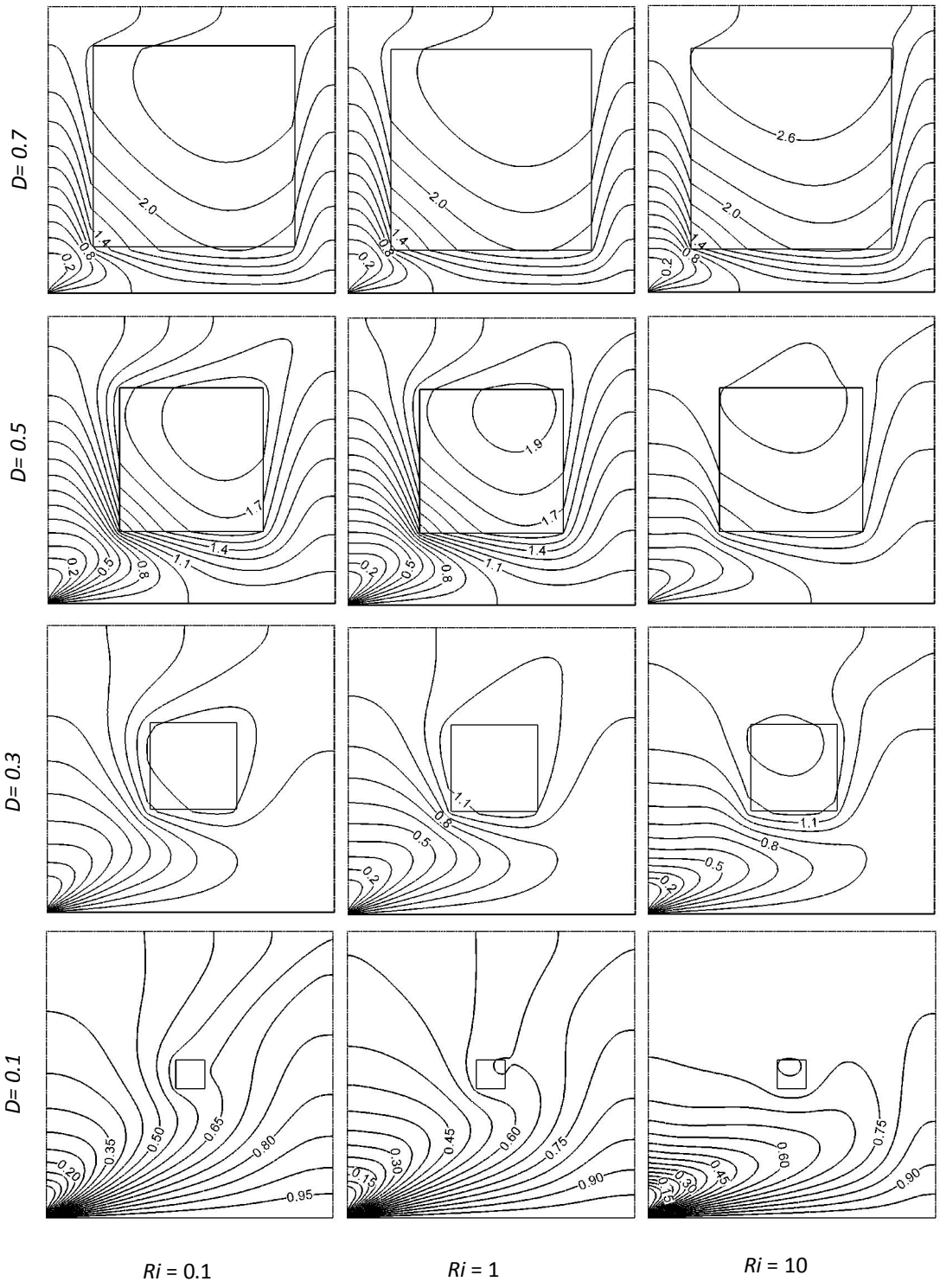

Fig. 6. Isotherms in a square ventilated cavity at different values of D, while Re = 100, Ha = 10, Pr = 0.71 and Ri = 0.1, 1.0, 10

Effect of Diameter of the Solid Block

The streamlines for different block size are depicts in Fig. 5. in the range of Richardson number 0.1 ≤ *Ri* ≤10. At *Ri* = 0.1 and *D* = 0.1 the major streams stretched diagonally from the inlet to the exit opening and a recirculation cell is created just above the inlet of the cavity as expected. As the value of *D* increases the vortex becomes smaller and consequently it diminishes at the largest value of *D* = 0.7 due to the space availability in the cavity. Besides, streamlines are found to be nearly flat and vertical between the cavity and centered solid block for larger values of *D* (= 0.5, 0.7). In the pure mixed convection case (*Ri* = 1) the vortex expands rapidly at *D* = 0.1 and this recirculation cell sharply reduces and finally disappears for the maximum blocked size (*D* = 0.7) with the similar flow structures as seen at *Ri* = 0.1. One can easily be observed that for *D* = 0.1 the intensity of the vortex in the cavity increases too much and it captures the obstacle in the case of higher value of *Ri* = 10, this is happened since buoyancy effect increases. For *D* = 0.3 the counter-clockwise vortex shrinks from the right side and it vacates the block. A bi-cellular recirculation cell is created at *D* = 0.5 and it becomes narrow regarding *D* = 0.1 and *D* = 0.3. There is no change in flow patterns for *D* = 0.7 with the comparison of *Ri* = 0.1 and *Ri* = 1.

Fig. 6. illustrates the temperature distribution inside the vented enclosure for the four chosen value of block diameter *D*. For all the convective regimes of Richardson number *Ri* (=0.1, 1, 10) it is noticed that at *D* = 0.1 isotherms are concentrated near the inlet and a thermal boundary layer is formed in the vicinity of the bottom hot wall. The heat lines are scattered in the whole domain for the lower values of *Ri* (=0.1, 1) while for *D* = 0.1 these are seems to be curved below the heat generating block at *Ri* = 10. For higher values of *D* the heat lines are almost similar in all the selected range of Richardson number.

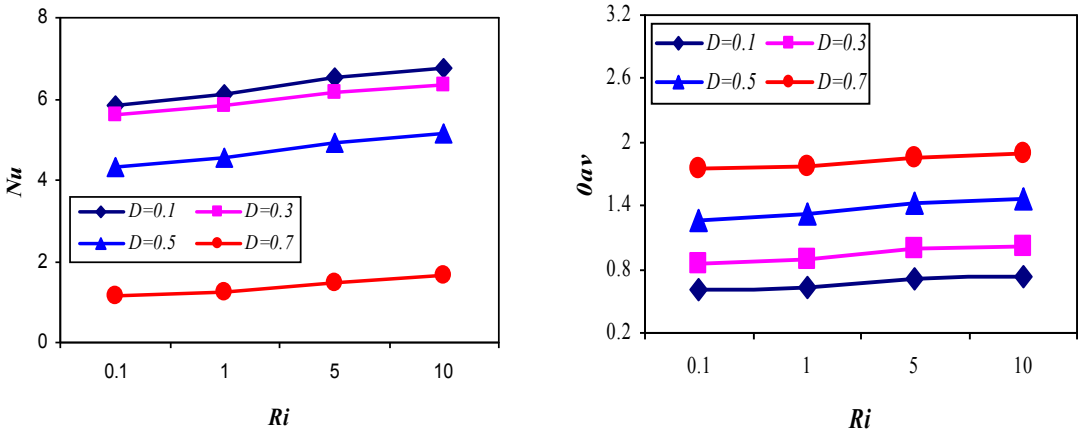

Fig. 7. Effect of solid block diameter D on average Nusselt number and average fluid temperature in the cavity while Re = 100, Pr = 0.71 Ha = 10 and 0.1≤ Ri≤10

5 CONCLUSION

Combined convection thermal along with flow field is analyzed numerically in a heat generating obstacle located in the ventilated enclosure. The considered pertinent parameters in this analysis are solid fluid thermal conductivity ratio and diameter of the obstacle with three convective regimes of Richardson number (0.1, 1, 10). The main conclusions that are drawn from the present article are as follows. (*i*) The highest heat transfer is recorded for the lowest value of *K* and it increases with increasing *Ri*. (*ii*) Lower thermal conductivity ratio shows the minimum average fluid temperature in the cavity. (*iii*) A small size of obstacle gives the maximum average Nusselt number. (*iv*) Average fluid temperature in the cavity is about independent of *Ri* and it is lowest for the smaller value of *D*.

REFERENCES

[1] V. A. F. Costa and A. M. Raimundo, "Steady mixed convection in a differentially heated square enclosure with an active rotating circular cylinder," *International Journal of Heat and Mass Transfer,* vol. 53, pp. 1208–1219, 2010.

[2] T.H. Hsu and S.P. How, "Mixed convection in a partially divided rectangular enclosure," *Numerical Heat Transfer, Part A*, vol. 31, pp. 655-683, 1997.

[3] O. Manca, S. Nardini, and K. Vafai, "Experimental investigation of mixed convection in a channel with an open cavity," *Numerical Heat Transfer, Part A*, vol. 19, pp. 53-68, 2006.

[4] A. Raji and M. Hasnaoui, "Mixed convection heat transfer in ventilated cavities with opposing and assisting flows," *International Journal Computer-Aided Engineering. Software,* vol. 17, no. 5, pp. 556–572, 2000.

[5] G. Gau and M. A. R. Sharif, "Mixed convection in rectangular cavities at various aspect ratios with moving isothermal side walls and constant flux heat source on the bottom wall," *International Journal Thermal Science*, vol. 43, pp. 465–475, 2004.

[6] M. M. Billah, M. M. Rahman, and M. A. Uddin, "Mixed convection inside a ventilated cavity along with a centered heat conducting horizontal circular cylinder," *Engineering e-Transaction*, vol. 6, no. 1, pp. 62–69, 2011.

[7] S. Z. Shuja, B. S. Yilbas, and M.O. Iqbal, "Mixed convection in a square cavity due to heat generating rectangular body effect of cavity exit port locations," *International Journal of Numerical Methods for Heat and Fluid flow*, vol. 10, no. 8, pp. 824–841, 2000.

[8] J.N. Reddy, An Introduction to Finite Element Analysis, *McGraw-Hill*, New-York, 1993.

[9] M. M. Rahman, M. A. Alim, and M. A.H. Mamun, "Finite element analysis of mixed convection in a rectangular cavity with a heat-conducting horizontal circular cylinder," *Non-linear analysis: Modeling and Control,* vol. 14, no. 2, pp. 217-247, 2009.

[10] A. Kumar De and A. Dalal, "A numerical study of natural convection around a square, horizontal, heated cylinder placed in an enclosure," *International journal Heat Mass Transfer*, vol. 49, pp. 4608-4623, 2006.

[11] M. M. Rahman, M. Elias, and M. A. Alim, "Mixed convection flow in a rectangular ventilated cavity with a heat conducting square cylinder at the center," *Journal of Engineering and Applied Sciences*, vol. 4, no.5, pp. 20-29, 2009.

[12] A. J. Chamkha, "Hydro magnetic combined convection flow in a vertical lid- driven cavity with internal heat generation or absorption," *Numerical Heat Transfer Part A*, vol. 41, pp. 529-546, 2002.

[13] H. F. Oztop, Z. Zhao, and B. Yu, "Fluid flow due to combined convection in lid-driven enclosure having a circular body," *International journal Heat and Fluid Flow*, vol. 30, pp. 886–901, 2009.

[14] J. Y. Oh, M. Y. Ha, and K. C. Kim, "Numerical study of heat transfer and flow of natural convection in an enclosure with a heat generating conducting body," *Numerical Heat Transfer, Part A*, vol. 31, pp. 289-304, 1997.

[15] M. M. Rahman, R. Nasrin, and M. M. Billah, "Effect of Prandtl number on hydromagnetic mixed convection in a double-lid driven cavity with a heat-generating obstacle," *Engineering e-Transaction*, vol. 5, no. 2, pp. 90–96, 2010.

[16] M.U. Ahammad, M.M. Rahman, and M.L. Rahman, "Effect of inlet and outlet position in a ventilated cavity with a heat generating square block," *Engineering e-Transaction*, vol. 7, no. 2, pp. 107–115, 2012.

[17] M. M. Abo El-Nasr, M. A. Abidou, and H. A. Hussein, "Heat transfer characteristics of horizontal cylinder cooling under single impinging water jet," *International Journal of Applied Sciences and Engineering Research*, vol. 1, no. 2, pp. 287–301, 2012.

[18] A. Veera Suneela Rani, Dr. V. Sugunamma, and N. Sandeep, "Radiation effects on convective heat and mass transfer flow in a rectangular cavity," *International Journal of Innovation and Applied Studies*, vol. 1, no. 1, pp. 118-152, 2012.

APPENDIX I. NOMENCLATURE

B_0	magnetic induction (Wb/m^2)
g	gravitational acceleration (ms^{-2})
Gr	Grashof number
h	convective heat transfer coefficient ($Wm^{-2}K^{-1}$)
Ha	Hartmann number
k	thermal conductivity of fluid ($Wm^{-1}K^{-1}$)
k_s	thermal conductivity of solid ($Wm^{-1}K^{-1}$)
K	solid fluid thermal conductivity ratio
L	length of the cavity (m)
Nu	Nusselt number
n	dimensional distances either x or y direction acting normal to the surface
N	non-dimensional distances either X or Y direction acting normal to the surface
p	dimensional pressure (Nm^{-2})
P	dimensionless pressure
Pr	Prandtl number
Ra	Rayleigh number
Re	Reynolds number
Ri	Richardson number
Q	non-dimensional heat-generating parameter
Q_0	uniform heat flux
T	dimensional temperature (K)
ΔT	dimensional temperature difference (K)
u, v	dimensional velocity components (ms^{-1})
U, V	dimensionless velocity components
$\overline{V}$	cavity volume (m^3)
w	height of the opening (m)
x, y	Cartesian co-ordinates (m)
X, Y	dimensionless Cartesian coordinates
Greek symbols	
α	thermal diffusivity (m^2s^{-1})
β	thermal expansion coefficient (K^{-1})
ν	kinematic viscosity (m^2s^{-1})
θ	non dimensional temperature
ρ	density of the fluid (kgm^{-3})
Subscripts	
av	average
h	heated wall
i	inlet state

International Journal of Innovation and Applied Studies
ISSN 2028-9324 Vol. 3 No. 4 Aug. 2013, pp. 979-986

http://www.issr-journals.org/ijias/

Enhancement of Cellulolytic Nitrogen Fixing Activity of *Alcaligenes* sp. by MNNG Mutagenesis

Zaw Ko Latt[1], San San Yu[2], and Tin Mar Lynn[1]

[1]Department of Biotechnology,
Mandalay Technological University,
Mandalay, Myanmar

[2]Molecular Life Science Research Center,
Jacobs University,
Bremen, Germany

ABSTRACT: For effective degradation of agricultural residues into more useful forms, cellulolytic nitrogen fixing bacteria were isolated from soil samples of central region of Myanmar. Among 32 isolated strains, six best isolates (three strains of *Azomonas agilis*, two strains of *Azotobacter chroococcum*, and one strain of *Alcaligenes* sp.) were selected. Best strains were selected by their nitrogen fixing activities. Nitrogen fixing bacteria cannot excrete significant amount of ammonia into their environment. To improve cellulolytic nitrogen fixing activities, *Alcaligenes* sp. among six isolates was muatgenized with chemical mutagen, MNNG. From treatment of *Alcaligenes* sp. with three concentrations of MNNG (7.5 ppm, 10 ppm and 12.5 ppm), six potential mutant colonies were obtained. After screening of nitrogen fixing activities of wild type and mutagenized strains, four out of six mutant strains excreted higher amount of ammonium concentration than wild type strain. Although wild type strain of *Alcaligenes* sp. excreted 46.64 ppm of ammonium concentration, 101.35 ppm of ammonium concentration was excreted by mutant strain (M2-F) of *Alcaligenes* sp. According to results obtained, 10 ppm of MNNG was more effective for obtaining better mutant strain for nitrogen fixing activity. Although nitrogen fixing activities of mutant strains were increased, cellulolytic activities were decreased than those of wild type strain. Reducing sugar concentrations produced by all mutant strains were decreased using cellulose and CMC as substrates than wild type strain.

KEYWORDS: Agricultural residues, cellulose, nitrogen fixation, MNNG mutagen, *Alcaligenes* sp.

1 INTRODUCTION

Agricultural residues are produced in plentiful every year. Approximately one kg of residues is produced for each kilograms of grains harvested [1]. The annual crop of corn, wheat, and soybean produce about 16, 10 and 10 billion ton of residues respectively and most of this material is left in the field after grain harvest. In some developing countries, these residues are used as a major source of cattle feed. In developed countries, these agricultural residues are not allowed to use as cattle feed because of the presence of various pesticide, herbicide, and insecticide residues. Utilization of biomass resources such as starchy and cellulosic materials of plant origin for production of energy and chemicals by microorganisms has attracted considerable interest in recent years ([2, 3]). Cellulose is the most abundant renewable resource on the earth (100 million dry tons per year). It is the primary products of photosynthesis in the environment [4]. This study was aimed for effective conversion of these residues into more useful forms by microorganisms.

There are many nitrogen fixing bacteria that possess cellulose activities, such as *Sinorhizobium fredii* [5,6], *Bacillus spharricus* [7], *Bacillus circulans* [8], *Paenibacillus azotofixans* [9], *Gluconacetobacter* [10], *Azospirillum* [11]. Although there are many reports about cellulolytic nitrogen fixing activities of other bacteria, there are few reports about *Alcaligenes* sp. for

Corresponding Author: Zaw Ko Latt (zaw.zk23@gmail.com)

studying of these activities. So, this research work leaded to study the cellulolytic nitrogen fixing activities of *Alcaligenes* sp. and to enhance these activities by MNNG mutagenesis.

Alcaligenes is a genus of Gram-negative, aerobic, rod-shaped bacteria. The species are motile with one or more peritrichous flagella. *Alcaligenes* species have been used for the industrial production of non-standard amino acids; *A. eutrophus* also produces the biopolymer polyhydroxybutyrate (PHB).They are rods, coccal rods, or cocci sized at about 0.5-1.0 x 0.5-2.6. They are obligately aerobic, but some can undergo anaerobic respiration if nitrate is present. They tend to be colorless. They typically occur in the soil and water, and some live in the intestinal tract of vertebrates. Samples from blood, urine, feces, discharge from ears, spinal fluid and wounds have produced this type of bacteria [12]. The diazotrophic *Alcaligenes faecalis* is capable of entering rice roots [13].

Use of nitrogen fertilizer is of great importance in rice production, as nitrogen is the major factor limiting growth under most conditions [14]. Since agriculture is expected to move toward environmentally sustainable methods [15], much attention has been paid to natural methods of biological nitrogen fixation. Several diazotrophic bacteria, including *Klebsiella oxytoca*, *Enterobacter cloacae* [16], *Alcaligenes* [13], and *Azospirillum* [17], have been isolated from the rhizosphere of wetland rice.

Free living diazotrophs fix dinitrogen sufficient for their own needs and do not generally excrete significant amounts of ammonia into their environment. In nitrogen fixing bacteria, nitrogen fixation is controlled at the transcriptional level by the regulatory proteins encoded by Nif A. Nif L inhibits Nif A function in response to ammonium, high oxygen concentration and reduced energy charge. To inhibit nif transcription, Nif L binds to Nif A, and normal regulation occurs only when the proteins are present in approximately stoichiometric amounts [18]. For these problems, nitrogen fixing bacteria cannot excrete significant amounts of ammonium into their environment. So, it is necessary to produce significant amounts of ammonia into their environment for production of N-rich biofertilizers using these bacteria and effective conversion of agricultural residues into more useful forms.

After isolation and detection of cellulolytic nitrogen fixing activity of isolated *Alcaligenes* sp., cellulolytic nitrogen fixing activities of this strain was enhanced by MNNG mutagenesis.

2 MATERIALS AND METHODS

2.1 MATERIALS

The Visocolor Alpha Ammonia Detection Kit was obtained from Macherey-Nagel (Duren, Germany). All other compounds used were of the highest quality available from Kanto Chemical (Tokyo, Japan), Nacalai Tesque (Kyoto, Japan), and Wako Pure Chemical Industries (Osaka, Japan).

2.1.1 SOIL SAMPLING

Soil samples were collected from rhizosphere of rice and under decayed rice straw around Patheingyi Township, Mandalay Region, Myanmar.

2.1.2 CULTURE MEDIA

Cellulolytic nitrogen fixing bacteria were isolated on Cellulose Nitrogen Free Mineral Medium (C-NFMM) by serial dilution method. The C-NFMM contained (g/L): KH_2PO_4 1.0, $CaCl_2$ 1.0, $MgSO_4.7H_2O$ 0.25, NaCl 0.5, $FeSO_4.7H_2O$ 0.01, $MnSO_4.H_2O$ 0.01, Na_2MoO_4 0.01, Cellulose powder 7.0, Agar 20.0.

2.2 METHODS

2.2.1 ISOLATION OF CELLULOYTIC NITROGEN FIXING BACTERIA

Cellulose Nitrogen Free Mineral Medium (C-NFMM) was used to isolate cellulolytic nitrogen fixing bacteria and carbon source was cellulose (7 g/L). Solid medium was produced by adding 2% agar.

2.2.2 SCREENING OF NITROGEN FIXING ACTIVITY

Nitrogen fixing activities of isolated strains were tested by growing the strains on Glucose Nitrogen Free Mineral Medium (G-NFMM) and C-NFMM plates substituted with Bromothymol Blue (BTB) as an indicator. The strains that change the color of the BTB containing media to blue were marked as nitrogen fixers, suggesting excretion of ammonia.

2.2.3 DETECTION OF EXCRETED AMMONIA CONCENTRATION

Excreted ammonium concentration by isolated strains was estimated using the Viscolor Alpha Ammonium Detection Kit (Macherey-Nagel). Single colony of isolated strains were inoculated in G-NFMM or C-NFMM broth and incubated for one week. After one week incubation, culture broth was centrifuged at room temperature (RT) and supernatant (1 ml) was transferred into a test tube. Two drops of NH_4-1 were added to the sample and mixed well, after which one-fifth of a spoonful of NH_4-2 was added. After mixing well, the sample was left at RT for 5 min. One drop of NH_4-3 was added, mixed well and left at RT for 5 min. The color development of supernatants was observed and the ammonium concentration was recorded by comparing with the color chart from the Viscolor Alpha Ammonium Detection Kit [19].

Ammonium concentration was also estimated by constructing standard curve of ammonium sulphate solution reacted with the same reagent using UV-vis spectrophotometer.

2.2.4 SCREENING OF CELLULOLYTIC ACTIVITY OF ISOLATED STRAINS

Cellulolytic activity of isolated strains were studied by growing the single colony of strains on C-NFMM or Sodium Carboxylmethyl Cellulose-NFMM (CMC-NFMM) plates and then the plates were incubated at 37°C for one week to allow for the excretion of cellulase. After incubation, cellulolytic activity was detected by flooding the agar media with an aqueous solution of Congo red solution (0.1% w/v) for 10 min. After then, the solution was poured off, and the plates were washed with 1M NaCl solution for two or three times. The formation of clear zones around bacterial colonies indicated cellulose degradation.

2.2.5 QUANTITATIVE DETERMINATION OF CELLULOLYTIC ACTIVITY

Cellulolytic activities of isolated strains were also detected quantitatively by the 3,5-dinitrosalicylic acid (DNS) method [20]. The bacterial strains were preliminary inoculated in C-NFMM broth and the culture broth was incubated at 37°C in water bath shaker. After incubation, culture broth was centrifuged and supernatant (1 ml) was transferred into a test tube. Cellulose as substrate was added into supernatant and it was allowed to react. After reaction time, cellulase activity was measured by DNS method.

2.2.6 IDENTIFICATION OF ISOLATED STRAINS

Isolates were identified through its morphological and some biochemical characteristics according to Bergey' Mnaual of Systematic Bacteriology [21] and 16s rDNA sequencing. Sequencing reactions were performed using the Big Dye Terminator Cycle Sequencing Kit (v.3.1) and the results were analysed in a GA 33130 sequencer. Nucleotide sequences were analysed using BLAST on the NCBI BLAST and Greengenes.IBI.gov.

2.2.7 ENHANCEMENT OF NITROGEN FIXING ACTIVITY BY N-METHYL-N-NITRO-N-NITOSOGUANIDINE (MNNG) MUTAGENESIS

MNNG mutagenesis was performed by [22, 23].The wild type bacterial strain grown in G-NFMM broth at 37°C for 24 hr was harvested after centrifugation and washed twice with phosphate buffer. The cells were resuspended in phosphate buffer and various concentrations of MNNG (7.5 ppm, 10 ppm, 12.5 ppm) were added. And then, it was allowed to react for 30 min and 1 hr. After reaction time, the cells were centrifuged again and washed with phosphate buffer for two to three times. The treated cells were resuspended in NFMM broth and diluted serially. After dilution, 20 µl of sample was spread on G-NFMM plates containing BTB. The culture plates were incubated at 37°C for one week and the development of mutant colonies was observed by changing the color of BTB containing plates.

3 RESULTS AND DISCUSSION

3.1 ISOLATION OF CELLULOYTIC NITROGEN FIXING BACTERIA

32 strains were isolated on C-NFMM media from collected soil samples. As these all strains were isolated from various soil samples, their growth rates and colonial morphology were different.

3.2 SCREENING OF NITROGEN FIXING ACTIVITY

All isolates were screened for their nitrogen fixing activities, but six isolates showed a color change in BTB containing media from dark green to blue. Although other isolates did not change the color of media, they may have nitrogen fixing activities. Nitrogen activity of *Azotobacter beijerinckii* and *Lysobacter enzymogenes* DMS 2043^T and rhizospheric bacterial isolates were screened by changing the color of BTB containing nitrogen free media, and these strains showed a color change in BTB containing media, suggesting excretion of ammonia [19], [24].

3.3 DETECTION OF EXCRETED AMMONIUM CONCENTRATION

On detection by Viscolor Alpha Ammonia Detection Kit, six isolates that showed a color change on plate screening also showed the highest color development after one week incubation, assuming that these six isolates excreted above 3 ppm of ammonium concentration when compared with the color chart. Although these isolated strains showed nitrogen fixing activity by giving color development during one week incubation, the highest color development was given after one week incubation. Free-living diazotrophs fix dinitrogen sufficient for their own needs and do not generally excrete significiant amounts of ammonium into their environment: fixed nitrogen is released after death and lysis of bacteria [25]. Among best nitrogen fixers, *Alcaligenes* sp. was selected for further study.

3.4 SCREENING OF CELLULOLYTIC ACTIVITY OF ISOLATED STRAINS

All isolates grew well on C-NFMM and CMC-NFMM plates and gave clear zones around their colonies when detected by pouring Congo red solution. But, the best strains for cellulolytic activity could not be selected by observing clear zone formation. So, six isolates that gave highest ammonium concentration were also selected for quantitative determination.

3.5 QUANTITATIVE DETERMINATION OF CELLULOLYTIC ACTIVITY BY DNS METHOD

By using Cellulose and CMS as substrates, reducing sugar concentrations in terms of cellulose activity were measured by DNS method. Table 1 showed the reducing sugar concentrations produced by six isolates. Reducing sugar concentration converted from cellulose and CMC substrates by six isolates were not obviously different among them.

Table 1. Reducing Sugar Concentration Produced by Six Selected Strains Using Cellulose and CMC as Substrates by DNS Method

Strains	Reducing sugar concentration (mg/ 0.5 ml) (using cellulose substrate)	Reducing sugar concentration (mg/ 0.5 ml) (using CMC substrate)
M-1	0.429	0.493
M-2	0.590	0.456
M-3	0.402	0.461
M-4	0.498	0.439
M-5	0.525	0.439
M-6	0.413	0.300

3.6 IDENTIFICATION OF SELECTED SIX STRAINS

Some biochemical characteristics of six isolates were studied according to Bergey's Manual of Systematic Bacteriology. From this study, selected six strains could not be identified by studying these characteristics. But according to 16s rDNA sequencing analysis, M-1, M-3 and M-4 were *Azomonas agilis*, M-2 was *Alcaligenes* sp. and M-5 and M-6 were *Azotobacter chroococcum*. Table 2 showed some biochemical characteristics of *Alcaligenes* sp.

3.7 STRAIN IMPROVEMENT BY MNNG MUTAGENESIS

Wild type *Alcaligenes* sp. was subjected to successive mutagenic treatment using MNNG. After mutagenic treatment, no better mutant colonies for ammonium excretion were obtained from three treatments of 30 min. So, reaction time was increased to 1 hr. Six potential mutant colonies were obtained from three treatments based on colour change of medium around their colonies. Figure 1 showed the colour change of the BTB containing media from the growth of wild type and selected mutant colonies of *Alcaligenes* sp. Survival rates decreased when MNNG concentration was increased. Reference [26] said that survival rates decreased with increasing MNNG concentration from studying of Ultraviolet irradiation and MNNG mutagenesis of *Acetobacter* species for enhanced cellulose production.

Table 2. Some Biochemical Characteristics of Alcaligenes sp. (M-2)

Biochemical Tests	*Alcaligenes* sp.
Motility	+
TSI	+
Nitrate reduction	+
Citrate utilization	+
Indole test	+
Methyl red	+
Voges proskauer	-
Catalase	+
Starch hydrolysis	+
Gelatin agar test	+

Table 3 showed survival rates of *Alcaligenes* sp. from three treatments of MNNG for 30 min and 1 hr. Among six selected potential mutant colonies, four colonies excreted higher ammonium concentration than wild type strain. Table 4 showed the excreted ammonium concentration of wild type and mutant strains of *Alcaligenes* sp. Among six selected potential mutant strains, two strains excreted lower amount of ammonium concentration than wild type strain. Mutant strains (M-2E and M-2F) excreted highest amount of ammonium concentration.

In this study, it was found that 10 ppm MNNG concentration for 1 hr reaction time was suitable for obtaining better mutant nitrogen fixing bacteria. According to higher ammonium excretion by selected potential mutant colonies of *Alcaligenes* sp., it was assumed that mutant strains of *Alcaligenes* sp. for higher ammonium excretion were obtained by MNNG mutagenesis. Although various methods of mutation were tested on *Azotobacter beijerinckii*, including UV radiation and chemical mutagenesis using N-methyl-N'-nitro-N-nitrosoguanidine (MNNG) and ethylmethane sulphonate (EMS), no ammonia-excreting mutants were isolated, even using the mating approach [27]. This may have been due to the production by *A. beijerinckii* of polysaccharide that surrounds the cell [28], rendering mutation problematic. However, mutant strain (MV376) of *A.vinelandii* was successfully produced, secreting significiant quantities of ammonium during diazotrophic growth [25]. Figure 2 showed that color development of six potential mutant and wild type *Alcaligenes* sp. for excreted ammonium concentration from detection by Viscolor Alpha Ammonium Detection Kit.

Table 3. Concentration of MNNG, Reaction Time and Survival Rates of Alcaligenes sp. (M-2) for Mutagenesis

Strain	MNNG Concentration (ppm)	Reaction Time	Survival Rate	Nitrogen Fixing Activity
M-2	7.5	30 min	0.688%	< wild type
M-2	10	30 min	0.45%	= wild type
M-2	12.5	30 min	0.15%	< wild type
M-2	7.5	1 hr	0.83%	> wild type
M-2	10	1 hr	0.53%	> wild type
M-2	12.5	1 hr	0.43%	< wild type

Table 4. Comparison of Excreted Ammonium Concentration of Wild Type and Mutant Alcaligenes sp. (M-2)

Strain	MNNG Concentration (ppm)	Ammonium Concentration (ppm) by Spectrophotometric Method
M-2 (wild type)	Without treatment	46.64
M-2A	7.5	9.66
M-2B	7.5	57.52
M-2C	7.5	69.85
M-2D	7.5	43.37
M-2E	10	71.98
M-2F	10	101.35

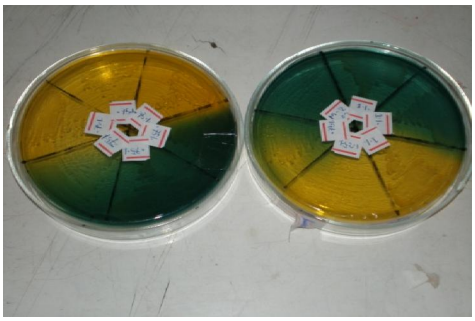

Fig. 1. Screening of Nitrogen Fixing Activities of Six Potential Mutant Colonies and Wild Type Alcaligenes sp.

Fig. 2. Screening of Nitrogen Fixing Activities of Six Potential Mutant Colonies and Wild Type Alcaligenes sp.

3.8 CELLULOLYTIC ACTIVITY OF WILD TYPE AND MUTANTS *ALCALIGENES* SP .

Two mutant strains (M-2E and M-2F) were studied for their cellulase activities by comparing with wild type strain. Table 5 showed reducing sugar concentration produced by wild type and mutant *Alcaligenes* sp. Although these two mutant strains excreted higher amount of ammonium concentration than wild type, their cellulase activities were lower than wild type. Although the aim of this study is to enhance cellulolytic nitrogen fixing activities of *Alcaligenes* sp., the resulted mutant strains did not possess higher cellulase activities than wild type. So to get better strain for dual activities, it may need to study using various MNNG concentrations, various reaction times for mutagenesis and reaction time for cellulase activity, pH of medium and various incubation temperatures.

Mutagenesis by UV and MNNG caused changes in cellulose production or secretion. However, enhanced cellulose production of *Acetobacter* species by UV irradiation and MNNG mutagenesis [26] enhanced cellulose production of *Cellulomonas* sp. TSU-03 by UV mutagenesis and MNNG mutagenesis [23] improvement of cellulase production of fungal strains using repeated and sequential mutagenesis were studied. They reported that mutant strains possessed more cellulase activities than their parental strains. In this study, mutant strains of *Alcaligenes* sp. were selected based on ammonium excretion, not mainly on cellulolytic activity. So, as mutant strain selection was based on only nitrogen fixing activity, cellulolytic activity of mutant strains was not better than wild type strain.

Table 5. Comparison of Reducing Sugar Concentration of Wild Type and Mutant Alcaligenes sp. (M-2)

Alcaligenes sp.	Reducing Sugar Concentration (mg/0.5ml) (cellulose as substrate)	Reducing Sugar Concentration (mg/0.5 ml) (CMC as substrate)
M-2 (Wild type)	0.590	0.456
M-2E	0.504	0.386
M-2F	0.402	0.370

4 CONCLUSION

Although six best nitrogen fixing isolates were selected from 32 isolates, only one *Alcaligenes* sp. was obtained. Isolated *Alcaligenes* sp. possessed cellulolytic and nitrogen fixing activities. Attempts were made to enhance cellulolytic nitrogen fixing activities of this strain by MNNG mutagenesis. According to this study, although nitrogen fixing activity of *Alcaligenes* sp. was higher after treatment with 10 ppm of MNNG for 1h, cellulase activity was decreased than wild type strain. But, resulted mutant strains still possessed dual activities.

ACKNOWLEDGMENT

The author would like to thank H.E. U Thaung, Ministry of Science and Technology, Myanmar for permission to do this research work at the Department of Biotechnology, Technological University (Kyaukse), Myanmar. The author also thanks to Prof: Dr. Mya Mya Oo, Rector, Yangon Technological University, Myanmar and Dr. Ei Phyu Kyaw for their kind supporting and suggestions.

REFERENCES

[1] Fahey, G. C, Bourquin, L.D., Titgemeyer, E.C. and Atwell, "Post-harvest Treatment of Fibrous Feedstuffs to Improve their Nutritional Value," *Paper presented at the International Symposium on Forage Cell Wall Structure and Digestibility*, Madison, Wisconsin, May 20-26, 1991.

[2] Mielenz, J.R., "Ethanol Production from Biomass: Technology and Commercialization Status," *Current Opinion in Microbiology*, 4: 324-329, 2001.

[3] Vasey, R.B. and K.A. Powell, "Single Cell Protein," *Biotechnology and genetic engineering review*, 2: 285-311, 1984.

[4] Jarvis M, "Cellulose stacks up," *Nature*, 426: 611-612, 2003.

[5] Chenet, P.J., T.C. Wei, Y.T. Chang and L.P. Lin, "Purification and Characterization of Carboxymethyl Cellulase from *Sinorhizobium fredii*," *Bot. Bull. Acad. Sin*., 45: 111-118, 2004.

[6] Mateos, P.F., J.I. Jimenez-Zurdo, J. Chen, A.S. Squartini, S.K. Haack, E. Martinez-Molina, D.H. Hubbell and F.B. Dazzo, "Cell-associated Pectinolytic and Cellulolytic Enzymes in *Rhizobium leguminosarum*," *Biovar trifolii*, 58: 1816-1822, 1992.

[7] Singh, J., N. Batra and R.C. Sobti, "Purification and Characterization of Alkaline Cellulose Produced by a Novel Isolate, *Bacillus sphaericus* JS1.J." *Ind. Microbiol. Biotechnol*., 31: 51-59. 2004.

[8] Baird, D.S., D.A. Johnson and V.L. Seligy, "Molecular Cloning, Expression and Characterization of Endo-1,4-glucanase Genes from *Bacillus polymyxa* and *Bacillus circulans*." *J. Bacteriol*., 172: 1576-1586, 1990.

[9] Rosado, A.S., F.S. de Azevedo, D.W. da Cruz, J.D. van Elsas and l. Seldin, "Phenotypic and Genetic Diversity of *Paenibacillus azotofixans* Strains Isolated from the Rhizolpane or Rhizosphere Soil of Different Grasses," *J. App. Microbiol*., 84: 216-226, 1998.

[10] Emtiazi, G., Z. Etemadifar and M. Tavassoli, "A Novel Nitrogen-fixing Cellulytic Bacterium Associated with Root of Corn is a Candidate for Production of Single Cell Protein," *Biomass. Bioenergy*, 25: 423-426, 2003.

[11] Steenhoudt O, Vanderleyden J, "*Azospirillum*, a Free-living Nitrogen-fixing Bacterium Closely Associated with Grasses: Genetic, Biochemical and Ecological Aspects," *FEMS Microbiol Rev*, 24 (4): 487-506, October, 2000.

[12] Holt, John G., "Determinative Bacteriology; 9th edition," *Maryland: Williams & Wilkins*. p. 75, 1994. ISBN 0-683-00603-7.

[13] You C and Zhou F, "Non-nodular Endorhizospheric Nitrogen Fixation in Wetland Rice," *Can. J. Microbiol*. 35, 403-408, 1989.

[14] Dong, Z., Heydrich, M., Bernard, K. and McCully, M.E., "Further Evidence that the N_2-fixing Endophytic Bacterium from the Intercellular Spaces of Sugarcane Stems is *Acetobacter diazotrophicus*," *Applied and Environmental Microbiology.* 61:1843–1846, 1995.

[15] Sturz A. V., Christie B. R. and Nowak J. "Bacterial Endophytes: Potential Role in Developing Sustainable Systems of Crop Production*," Crit. Rev. Plant Sci.* 19:1–30, 2000.

[16] Fujie T., Huang Y. D., Higashitani A., Nishimura Y., Iyama S., Hirota Y., Yoneyama Y and Dixon R. A., "Effect of Inoculation with *Klebsiella oxytoca* and *Enterobacter cloacae* on Dinitrogen Fixation by Rice-bacteria Associations," *Plant Soil* 103:221–226, 1987.

[17] Baldani V. L. D and Dobereiner J., "Host-plant Specificity in the Infection of Cereals with *Azospirillum* spp," *Soil Biol. Biochem.* 12:433–439, 1980.

[18] Brewin, B., Woodley, P. and Drummond, M. "The Basis of Ammonium Release in nifL Mutants of *Azotobacter vinelandii*," *Journal of Bacteriology*, 181: 7356–7362, 1999.

[19] Iwata Kenichi, San San Yu, Nik Noor Azlin binti Azlan and Toshio Omori, "Ammonia Accumulation of Novel Nitrogen-Fixing Bacteria," *Biotechnology - Molecular Studies and Novel Applications for Improved Quality of Human Life*, Prof. Reda Sammour (Ed.), ISBN: 978-953-51-0151-2, InTech, 2012.
[Online] Available: http:// www.intechopen.com/books/biotechnology-molecular-studies-and-novel-applications-for-improvedquality-of-human-life/ammonia-accumulation-of-novel-nitrogen-fixing-bacteria (2012)

[20] Miller GL, "Use of Dinitrosalicylic Acid Reagent for Determination of Reducing Sugars," *Anal. Chem*., 31:426-428, 1959.

[21] Williams, S. T., Sharpe, M. E., and Holt, J. G. "Bergy's Manual of Systematic Bacteriology", Vol. 4, *Williams & Wilkins*, Baltimore, Md., 1989.

[22] Adelberg, E.A., M. Mandel and G.C.C. Chen, "Optimal Conditions for Mutagenesis by N-methyl-N'-nitro-N-nitrosoguanidine in *Escherichia coli* K12," *Biochem. Biophys. Res. Commun*, 18:788-795, 1965.

[23] Sangkharak K., Vangsirikul P., and Janthachat S., "Strain Improvement and Optimization for Enhanced Production of Cellulase in Cellulomonas sp. TSU-03," *African Journal of Microbiology Research*, Vol. 6(5), pp. 1079-1084, 9 February, 2012.

[24] Gothwal R.K., Nigam V. K., Mohan M. K., Sasmal D., Ghosh P., "Screening of Nitrogen Fixers from Rhizospheric Bacterial Isolates Associated with Important Desert Plants," *Applied Ecology and Environmental Research*, 6(2): 101-109, 2008.

[25] Bali, A., Blanco, G., Hill, S. and Kennedy, C., "Excretion of Ammonium by a nifL Mutant of *Azotobacter vinelandii* Fixing Nitrogen," *Applied and Environmental Microbiology,* 58: 1711–1718, 1992.

[26] Siripong P., Chuleekorn S. and Duangporn P., "Enhanced Cellulose Production by Ultraviolet (UV) Irradiation and N-methyl-N'-nitro-N-nitrosoguanidine (NTG) Mutagenesis of an *Acetobacter* Species Isolate," *African Journal of Biotechnology*, Vol. 11(6): 1433-1442, 19 January, 2012.

[27] Owen, D. J. & Ward, A. C., "Transfer of Transposable Drug-resistance Elements Tn5, Tn7, and Tn76 to *Azotobacter beijerinckii*: Use of Plasmid RP4: Tn76 as a Suicide Vector," *Plasmid*, 14: 162–166, 1985.

[28] Danilova, V., Botvinko, I. V. and Egorov, N. S, "Production of Extracellular Polysaccharides by *Azotobacter beijerinckii*," Mikrobiologiya, 61(6), 950–955, 1992.

International Journal of Innovation and Applied Studies
ISSN 2028-9324 Vol. 3 No. 4 Aug. 2013, pp. 987-994

http://www.issr-journals.org/ijias/

Design of an H-shaped Microstrip Patch Antenna for Bluetooth Applications

Alak Majumder

Department of ECE,
National Institute of Technology,
Agartala, Tripura, India

ABSTRACT: In this paper, a design of small sized, low profile patch antenna is proposed for BLUETOOTH applications at 2.4GHz frequency with coaxial feeding technique. The patch is H-shaped and different parameters like return loss, VSWR, gain along two directions, radiation pattern in 2-D and 3-D, axial ratio, E and H Field Distributions, Current Distributions are simulated using Ansoft HFSS. The measured parameters satisfy required limits hence making the proposed antenna suitable for BLUETOOTH applications in 2.4GHz band.

KEYWORDS: Patch antenna, Radiation pattern, Return loss, Coaxial fed, Bluetooth.

1 INTRODUCTION

The BLUETOOTH technology provides short range of wireless connections between electronic devices like computers, mobile phones and many others thereby exchanging voice, data and video. The rapid increase in communication standards has led to great demand for antennas with low real estate, low profile and size, low cost of fabrication and ease of integration with feeding network. Microstrip patch antennas are widely used because they are of light weight, compact, easy to integrate and cost effective. However, the serious problem of patch antennas is their narrow bandwidth due to surface wave losses and large size of patch for better performance.

Various techniques like using Frequency Selective Surface[13]-[14], Employing stacked configuration[6], using thicker profile for folded shorted patch antennas[8], use of thicker substrate[10], slot antennas ike U-slot patch antennas together with shorted patch[4], double U-slot patch antenna[5], L-slot patch antenna[8], annular slot antenna[9], double C patch antenna[3], E-shaped patch antenna[2], and feeding techniques like L-probe feed[7], circular coaxial probe feed[1], proximity coupled feed are used to enhance bandwidth of Microstrip patch antenna. The size of feeding patch and thickness of dielectric should be taken care. The techniques to reduce the size of the patch like use of short circuited element [15]-[16], high dielectric constant material [17], slots [10], and resistive loading [19] have been proposed.

But, the choice of slot antenna [20] introduced the drawback of narrow bandwidth and poor circular polarization performance and complex laser cutting of solar cells is required to achieve desired shape during fabrication. Monopole [12], printed monopole [21]-[26], dipole [11] antennas improve the bandwidth to a greater extent. But, monopole antennas are of large size and difficult to build and integrate. Printed monopole antennas also have numerous advantages like low profile, small size, and easy integration but has disadvantage of low broad impedance bandwidth and low omnidirectional radiation pattern. The dipole antennas have large input impedance. So, an impedance matching transformer or balun coil at feed point is required which increases the size of antenna [27]-[33].

In this paper, a compact size patch antenna is proposed with dielectric substrate as FR4 with $\varepsilon r=4.4$ and dimensions are based on resonant frequency. Various attempts are made to adjust the dimensions of the patch to improve the parameters like return loss, VSWR, gain along Θ, $\emptyset$ directions, radiation pattern in 2-D and 3-D, axial ratio, E and H Field Distributions, Current Distributions using HFSS which is a high performance full wave EM field simulator for arbitrary 3D volumetric passive device modelling that takes advantage of the familiar Microsoft Windows graphical user interface. It integrates simulation,

Corresponding Author: Alak Majumder (majumder.alak@gmail.com)

visualization, solid modelling, and automation in an easy to learn environment where solutions to your 3D EM problems are quickly and accurate obtained. Ansoft HFSS employs the Finite Element Method (FEM), adaptive meshing, and brilliant graphics to give you unparalleled performance and insight to all of the 3D EM problems.

2 DESIGN CONSIDERATION

The design specifications for the proposed antenna are: The proposed structure of the antenna is shown in Fig (1). The antenna is simulated on an FR4 substrate with a dielectric constant of 4.4 and a loss tangent of 0.02. The thickness of the substrate is 6.7 mm. The size of the antenna is 80* 80 mm^2, which is suitable for most Bluetooth devices. Rectangle shaped patches are cut at middle to form H-shaped patch antenna and width of each arm is 25mm.

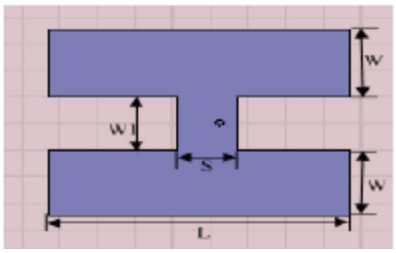

Fig. 1. Geometry of Patch Antenna

A patch can also be fed with a probe through ground plane. The probe position can be inset for matching the patch impedance with the input impedance. This insetting minimizes probe radiation. The ease of insetting and low radiations is advantages of probe feeding as compared to microstrip line feeding. The dimensions of H shaped patch shown in Fig (1) are L=80mm, W=20mm,S=16mm, W1=20mm. These are designed at operating frequency 2.4 GHz.

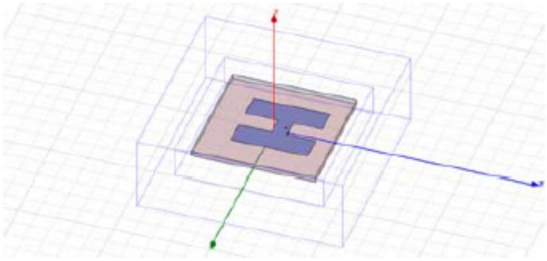

Fig. 2. Ansoft – HFSS Generated Antenna Model

Figure 2 shows the proposed antenna on FR4 Substrate using Ansoft-HFSS.

3 SIMULATION RESULTS

3.1 RETURN LOSSES

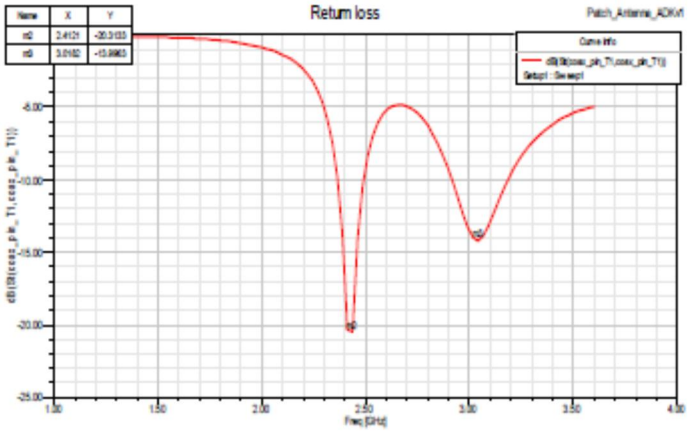

Fig. 3. Return Loss

Figure (3) shows the return loss Curve for the proposed antenna at 2.4 GHz. A return loss of 22.90dB is obtained at desired frequency.

3.2 2D GAIN & 3D GAIN TOTALS

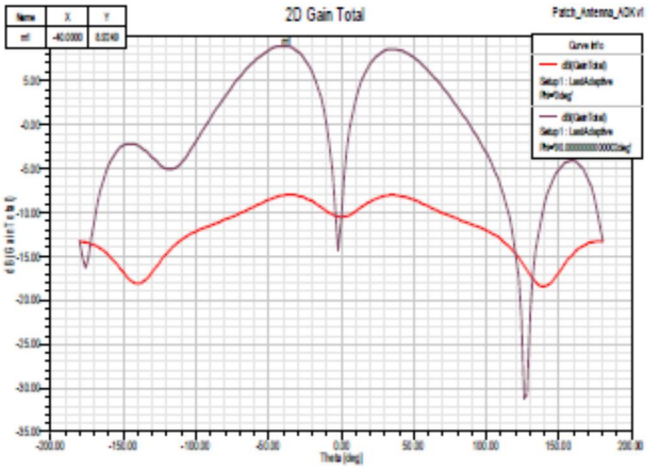

Fig. 4. 2D Gain Total

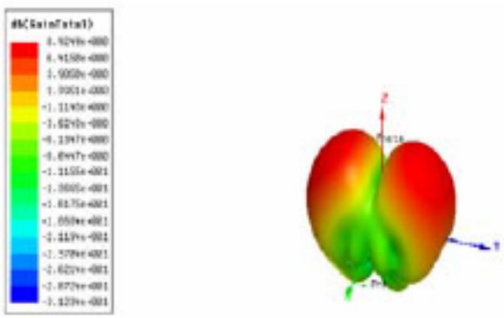

Fig. 5. 3D Gain Total

Figure (4-5) shows the antenna gain in 2D &3D patterns. The gain of proposed antenna at 2.4GHz is obtained as 8.9367dB. The gain above 6dB is acceptable.

3.3 VSWR

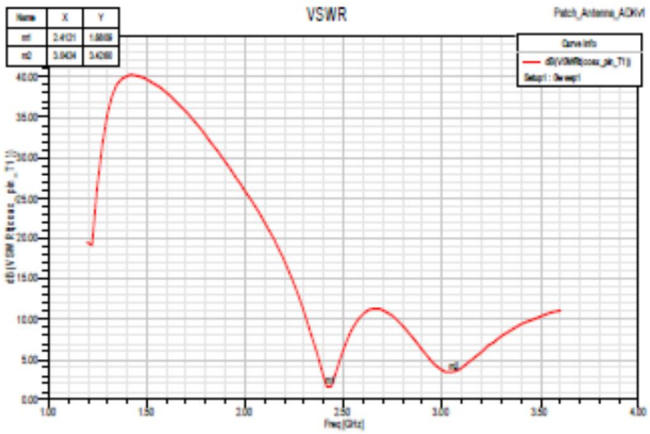

Fig. 6. VSWR

The VSWR for the proposed antenna is less than the 2dB. The obtained value is 1.5089 from Fig 6.

3.4 RADIATION PATTERNS

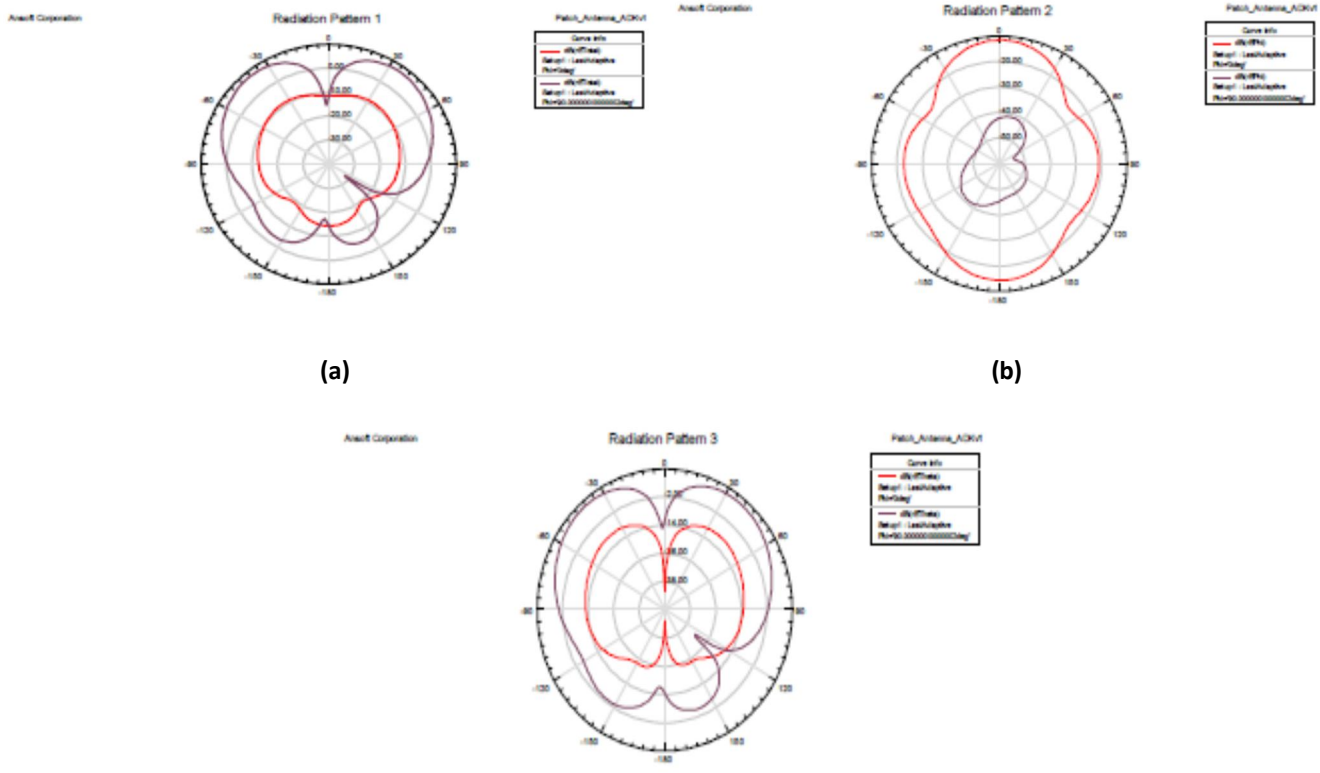

(a) **(b)**

(C)

Fig. 7. (a) Gain in Total; (b) Gain Along Phi; (c) Gain Along Theta

Since a Micro strip patch antenna radiates normal to its patch surface, the elevation pattern for ϕ = 0 and ϕ = 90 degrees would be important. The radiation pattern for proposed microstrip patch antenna for gain-Total, phi and theta at 0deg and 90deg is presented in figure 7(a), 7(b) and 7(c).

3.5 AXIAL RATIO

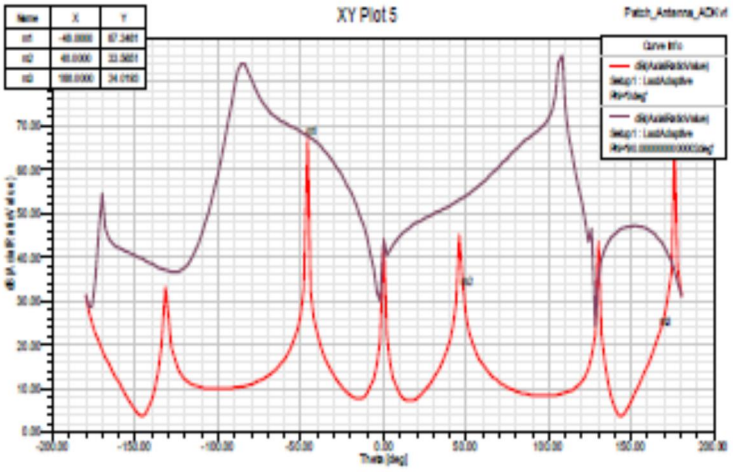

Fig. 8. Axial Ratio

Axial ratio which is the ratio of the major axis to the minor axis of the polarization ellipse where the resulting pattern is an oscillating pattern is obtained as in Fig 8.

3.6 FIELD DISTRIBUTIONS

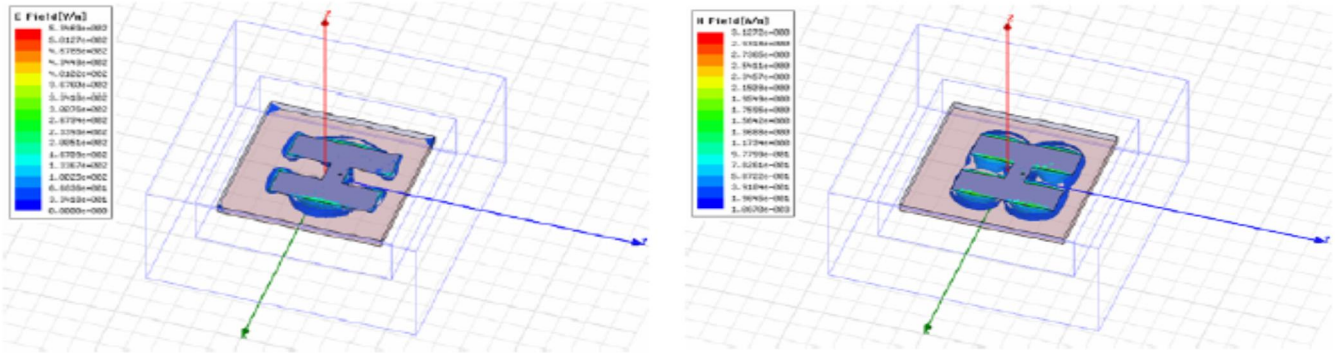

(a) (b)

Fig. 9. (a) E – Field Distribution; (b) H – Field Distribution

The effect produced by an electric charge that exerts a force on charged objects is the E-Field and its distribution in the patch is as shown in Fig 9(a). The measured intensity of a magnetic field in the patch is shown in Fig 9(b).

3.7 CURRENT DISTRIBUTION

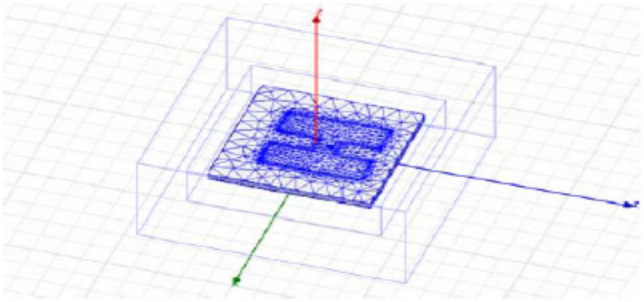

Fig. 10. Mess Pattern

The triangles show the current distribution. Here the numbers of triangles inside the patch are more than those on the substrate i.e. the current distribution in the patch is more when compared to that inside the substrate in Fig10.

3.8 FIELD VECTORS

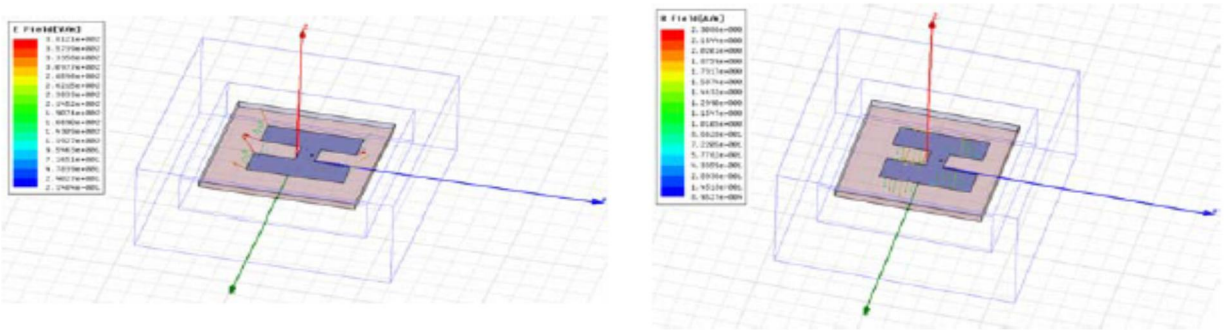

(a) (b)

Fig. 11. (a) E – Field Vector; (b) H – Field Vector

The E-Field Vector and H-Field vectors of proposed patch antenna are obtained as shown in Fig 11(a) and 11(b).

4 CONCLUSION

Finally, the optimum dimension of circular polarized patch antenna on FR4 substrate for BLUETOOTH applications has been investigated. The performance properties are analysed for the optimized dimensions and the proposed antenna works well at the required 2.4GHz BLUETOOTH frequency band.

ACKNOWLEDGEMENT

The author likes to express his thanks to the department of ECE and his friend Mr. Joydeb Singha for their support and encouragement during this work.

REFERENCES

[1] M A Matin, M.P Saha, H. M. Hasan “Design of Broadband Patch Antenna for WiMAX and WLAN,” IC*MMT 2010 Proceedings*, pp. 1-3.

[2] F. Yang, X. X. Zhang, X. Ye, and Y. Rahmat-Samii, “Wide-band Eshaped patch antennas for wireless communications,” *IEEE Trans. Antennas Propag*., vol. 49, no. 7, pp. 1094–1100, Jul. 2001.

[3] M. Sanad, "Double C-patch antennas having different aperture shapes," in *Proc. IEEE AP-S Symp*., Newport Beach, CA, Jun. 1995, pp. 2116–2119.

[4] Shackelford, A.K., Lee, K.F., and Luk, K.M., "Design of small-size wideband width microstrip-patch antennas", *IEEE Antennas Propag. Mag.*, 2003, AP-45, (1), pp. 75–83.

[5] H. F. AbuTarboush, H. S. Al-Raweshidy, and R. Nilavalan, "Triple band double U-slots patch antenna for WiMAx mobile applications," in *Proc. Of APCC, Tokyo*, Feb. 2008, pp. 1-3.

[6] Waterhouse, R.B., "Broadband stacked shorted patch", *Electron. Lett*., 1999, 35, (2), pp. 98–100.

[7] Guo, Y.X., Luk, K.M., and Lee, K.F., "L-probe proximity-fed shortcircuited patch antennas", *Electron. Lett.*, 1999, 35, (24), pp. 2069–2070.

[8] K.L. Lau and K.M. Luk, "Wideband folded L-slot shorted-patch Antenna," *Electronics Letters,* 29th September 2005, Vol. 41, No. 20.

[9] Madhur Deo Upadhayay, A. Basu, S.K. Koul and Mahesh P. Abegaonkar, "Dual Port ASA for Frequency Switchable Active Antenna," *IEEE*, pp. 2722-2725, 2009.

[10] R. Chair, K.F. Lee, K.M. Luk, "Bandwidth and cross polarisation characteristics of quarter wave shorted patch antenna," *microwave and op. technol. Latt*, vol. 22 no. 2, pp. 101-103, 1999.

[11] N. Zhang, P. Li, B. Liu, X.W. Shi and Y.J. Wang, "Dual-band and low cross-polarisation printed dipole antenna with L-slot and tapered structure for WLAN applications," *Electronics Letters*, 17th March 2011 Vol. 47, No. 6.

[12] Xue-jie Liaa, Hang-chun Yang, and Na Han, "An Improved Dual Band-Notched UWB Antenna with a Parasitic Strip and a Defected Ground Plane," *2010 International Symposium on Intelligent Signal Processing and Communication Systems (ISPACS 2010),* December 6-8, 2010.

[13] Hsing-Yi Chen and Yu Tao, "Performance Improvement of a U-Slot Patch Antenna Using a Dual-Band Frequency Selective Surface with Modified Jerusalem Cross Elements," *IEEE Transactions on Antennas and Propagation*, vol. 59, no. 9, pp. 3482-3486, September 2011.

[14] Hsing-Yi Chen and Yu Tao, "Antenna Gain and Bandwidth Enhancement Using Frequency Selective Surface with Double Rectangular Ring Elements," *IEEE Trans. on Antenna Propagation and EM Theory*, pp. 271-274, December 2010.

[15] S. Pinhas and S. Shtrikman, "Comparison between computed and measured bandwidth of quarter-wave microstrip radiators," *IEEE Trans. Antennas Propag.,* vol. 36, no. 11, pp. 1615–1616, 1988.

[16] R. Waterhouse, "Small microstrip patch antenna," *Electron. Lett.*, vol. 31, no. 8, pp. 604–605, 1995.

[17] J. R. Games, A. J. Schuler, and R. F. Binham, "Reduction of antenna dimensions by dielectric loading," *Electron. Lett.*, vol. 10, pp. 263–265, 1974.

[18] K. L. Wong and K. P. Yang, "Compact dualfrequency microstrip antenna with a pair of bent slots," *Electron. Lett.*, vol. 34, no. 3, pp. 225–226, 1998.

[19] K. L. Wong and Y. F. Lin, "Small broadband rectangular microstrip antenna with chip-resistor loading," *Electron. Lett.*, vol. 33, no. 19, pp. 1593–1594, 1997.

[20] Shynu S.V, Maria J. Roo Ons, Max J. Ammann, Sarah McCormack, Brian Norton, "Dual Band a-Si:H Solar-Slot Antenna for 2.4/5.2GHz WLAN Applications," *IEEE Trans.*, pp.408-410, March 2009.

[21] Ke-Ren Chen, Chow-Yen-Desmond Sim, and Jeen-Sheen Row, "A Compact Monopole Antenna for Super Wideband Applications," *Ieee Antennas and Wireless Propagation Letters*, Vol. 10, 2011, pp. 488-491.

[22] N.D. Trang, D.H. Lee and H.C. Park, "Compact printed CPW-fed monopole ultra-wideband antenna with triple subband notched characteristics," *Electronics Letters*, 19th August 2010, Vol. 46, No. 17.

[23] L. Y. Cai, G. Zeng, H. C. Yang, "Compact Triple band Antenna for Bluetooth/WiMAX/WLAN Applications," *Proceedings of International Symposium on Signals, Systems and Electronics* (ISSSE2010), 2010.

[24] Zhi-Qiang Li, Chang-Li Ruan "a small integrated Bluetooth and UWB antennas with WLAN band notched characteristics", *Proceedings of International Symposium on Signals, Systems and Electronics* (ISSSE2010), 2010.

[25] Mohamed H. Al Sharkawy, "Miniaturized Wideband Slotted Monopole Antenna for WLAN Applications," Middle East Conference on Antennas and Propagation (MECAP), Cairo, Egypt, October 2010.

[26] L.Y. Cai, Y. Li, G. Zeng and H.C. Yang, "Compact wideband antenna with double-fed structure having band notched characteristics", *Electronics Letters*, 11th November 2010, Vol. 46, No. 23.

[27] Rabih Rahaoui and Mohammed Essaaidi, "Compact Cylindrical Dielectric Resonator Antenna excited by a Microstrip Feed Line," *International Journal of Innovation and Applied Studies*, vol. 2, no. 1, pp. 1–5, January 2013.

[28] Mohammed Younssi, Achraf Jaoujal, Yacoub Diallo, Ahmed El-Moussaoui, and Noura Aknin, "Study of a Microstrip Antenna with and Without Superstrate for Terahertz Frequency," *International Journal of Innovation and Applied Studies*, vol. 2, no. 4, pp. 369–371, April 2013.

[29] M. I. Hasan and M. A. Motin, "New slotting technique of making compact octagonal patch for four band applications," *International Journal of Innovation and Applied Studies*, vol. 3, no. 1, pp. 221–227, May 2013.

[30] Tajeswita Gupta and P. K. Singhal, "Ultra Wideband Slotted Microstrip Patch Antenna for Downlink and Uplink Satellite Application in C band," *International Journal of Innovation and Applied Studies*, vol. 3, no. 3, pp. 680–684, July 2013.

[31] Sonali Kushwah, P. K. Singhal, Manali Dongre, and Tajeswita Gupta, "A Minimized Triangular – Meander Line PIFA Antenna for DCS1800/WIMAX Applications," *International Journal of Innovation and Applied Studies*, vol. 3, no. 3, pp. 714–718, July 2013.

[32] Tajeswita Gupta, P. K. Singhal, and Vandana Vikas Thakre, "Modification in Formula of Resonating Frequency of Equilateral TMPA for Improved Accuracy and Analysis," *International Journal of Innovation and Applied Studies*, vol. 3, no. 3, pp. 727–731, July 2013.

[33] Anshul Agarwal, P. K. Singhal, Shailendra Singh Ojha, and Akhilesh Kumar Gupta, "Design of CPW-fed Printed Rectangular Monopole Antenna for Wideband Dual-Frequency Applications," *International Journal of Innovation and Applied Studies*, vol. 3, no. 3, pp. 758–764, July 2013.

International Journal of Innovation and Applied Studies
ISSN 2028-9324 Vol. 3 No. 4 Aug. 2013, pp. 995-998

http://www.issr-journals.org/ijias/

Electrophysiology Activity of the Photoreceptors Using Photopic Adapted Full-Field Electroretinogram in Young Malay Adults

Ai-Hong Chen, Saiful Azlan Rosli, and Muhamad-Syukri Mohamad Rafiuddin

Optometry, Faculty of Health Sciences, Universiti Teknologi MARA (UiTM),
Selangor, Malaysia

ABSTRACT: The full-field electroretinogram (ffERG) was used as an electrophysiological test of retinal function. The electrophysiology activity of the photoreceptors in the retina was investigated using photopic adapted full-field electroretinogram (ffERG) in a sample of Malay ethnic (Melayu), (mean 21.72 ± 0.88 years old). About 10 minutes room illumination of photopic adaptation was used, single flashes of 3 cd.s.m-2 presented until 4 similar artifact free ERG waveforms, and 30 Hz flickers ERG was averaged based on 15 sweeps of 250 milliseconds (ms) duration, which based on the International Society of Clinical Electrophysiology of Vision (ISCEV) 2008 ERG Standard. The mean, standard deviation and median of amplitude (μV) of cone a-wave (-30.73 ± 12.49, -29.22) and cone b-wave (119.26 ± 37.76, 119.45), and the latency time (ms) of cone a-wave (14.30 ± 1.15, 14.50) and cone b-wave (30.02 ± 0.98, 30.00), 30 Hz peak amplitude (97.12 ± 28.63, 86.51), and latency time for peak (26.27 ± 1.77, 26.00) and trough (13.13 ± 2.10, 13.00) respectively were shown in descriptive data. The normal value of young Malay adults as the baseline data for Malay population and comparable to other population around the world is important for ffERG practical.

KEYWORDS: Full-field Electroretinogram, Electrophysiology, retinal function, room illumination, cone adapted.

1 INTRODUCTION

Electrophysiology function of the retina was widely tested using the full-field electroretinography (ffERG), which should be standardized and comparable throughout the world [1]. The ffERG was used in detecting various retinal problems affecting the photoreceptors such as Rod-Cone Dystrophies, the Retinal Pigment Epithelium (RPE) disease likes Retinitis Pigmentosa and other retinal layers.

Base on the standard protocol from International Society of Clinical Electrophysiology of Vision (ISCEV) 2008, the two most common investigations used to find out the functional values of the photoreceptors; scotopic ffERG (dark-adapted ffERG) and photopic ffERG (light-adapted ffERG). This investigation was performed by having the subject on light adapted in room illumination for at least 10 minutes. Meanwhile, the dark-adapted ffERG was used to investigate the rod photoreceptors as they were activated during scotopic condition [2].

Even though these factors had been investigated extensively, the majority of the tests were performed on either Caucasian population in Americas or Europe while the Asian populations mainly from the ethnic group of Japanese, Chinese or Persian. Currently, there are limited studies using ERG whether ffERG or mfERG on the Austronesian people in particular young Malay (*Melayu*) population.

Malay or *Melayu,* which primarily inhabits the Malay Peninsula including Malaysia, was originating from an ethnic group of Austronesian peoples (as its main ethnic group comprising of 50.4% of the population). The current Malays were the descendants of Iron Age people from the Chams of Mainland Southeast Asia, who migrated to the peninsular and islands of Southeast Asia around 300 BC, called Deutero Malays [3]. Deutero Malays were the relatives of Proto Malays that are now known as Aboriginal People (*Orang Asli*) in Malaysia. The Proto Malays were also of Austronesian origin that was thought to

Corresponding Author: Ai-Hong Chen (aihong0707@yahoo.com)

have migrated to the Malay Archipelago between 2500 and 1500 BC, earlier than Deutero Malays. However, Proto Malays were forced to migrate deeper into the hill and further upriver due to the Deutero Malays influences, which settled on coastal and downstream areas [4]. In corresponded to the East Asian such as Chinese, Japanese and Korean, the Human Genome Organization (HUGO), who investigated the human genome and do the genome mapping across the world, had postulated that the South East Asian civilizations including Malays are possibly much older than the East Asian civilizations. This finding suggested that East Asian population originated from the South East Asian population [5][6].

The function of the photoreceptors cells in a sample of Malay population using ffERG was reported in this study. The functions were represented by the values produced by the ffERG and this had direct connection to retinal cells activities in this sample population. Population variation on electrophysiology respond also suggested in the study done by Al Abdlseaed et al. and Fulton et al. [7] [8].

2 RESEARCH METHOD

All data collection was carried out at the Advanced Electrophysiology for Vision Laboratory (AEVo Lab), Optometry Clinic, Universiti Teknologi MARA (UiTM), Malaysia. Thirty-two subjects with the age range of 18 – 24 years old were recruited. The ethnicity of the subjects was confirmed by checking their national identity card under the race and ethnic section. The ethical consideration of this research had been approved by the institution of the researcher, and followed the tenet of the Helsinki Declaration.

Prior to the investigation using the ffERG, subjective refraction, funduscopy, slit lamp examination, color vision testing, binocular vision testing and intra-ocular pressure measurement were measured. Subjects with color vision defects, binocular vision problems like strabismus, ocular diseases including history of retinal and corneal disorders were excluded, to avoid complication during dilation due to high intra-ocular pressure. Subjects were included with the refractive error less than ±6.00 D, who represented low to moderate degree of ametropia, had Best Corrected Visual Acuity (BCVA) of 6/6, normal color vision and normal binocular vision.

After full dilation, the subject was light adapted in room illumination for 10 minutes. After light adaptation, the pupil size of the subjects was measured with conventional pupillary size ruler, before performing photopic ffERG. Photopic ffERG protocols included single flashes of 3 $cd.s.m^{-2}$ that were presented until 4 similar artifact-free ERG waveforms were obtained and averaged (the Cone ERG). And later on, 30 Hz flickers ERG was averaged based on 15 sweeps of 250 milliseconds (ms) duration (the 30 Hz Flicker ERG).

The ffERG subject preparation and protocols for photopic stimulation followed the ISCEV Standard 2008 set by the International Society for Clinical Electrophysiology of Vision (ISCEV) [2].

3 RESULTS

The mean, standard deviation and median for cone a-wave amplitude, cone a-wave latency time, cone b-wave amplitude and cone b-wave latency time for photopic ffERG were presented in Figure 1. For the light adapted 30 Hz flicker, the amplitude of peak (μV) in mean, standard deviation and median were 97.12 ± 28.63 and 86.51 respectively, while the latency time (ms) for peak and trough in mean, standard deviation and median were 26.27 ± 1.77 and 26.00, 13.13 ± 2.10 and 13.00 respectively.

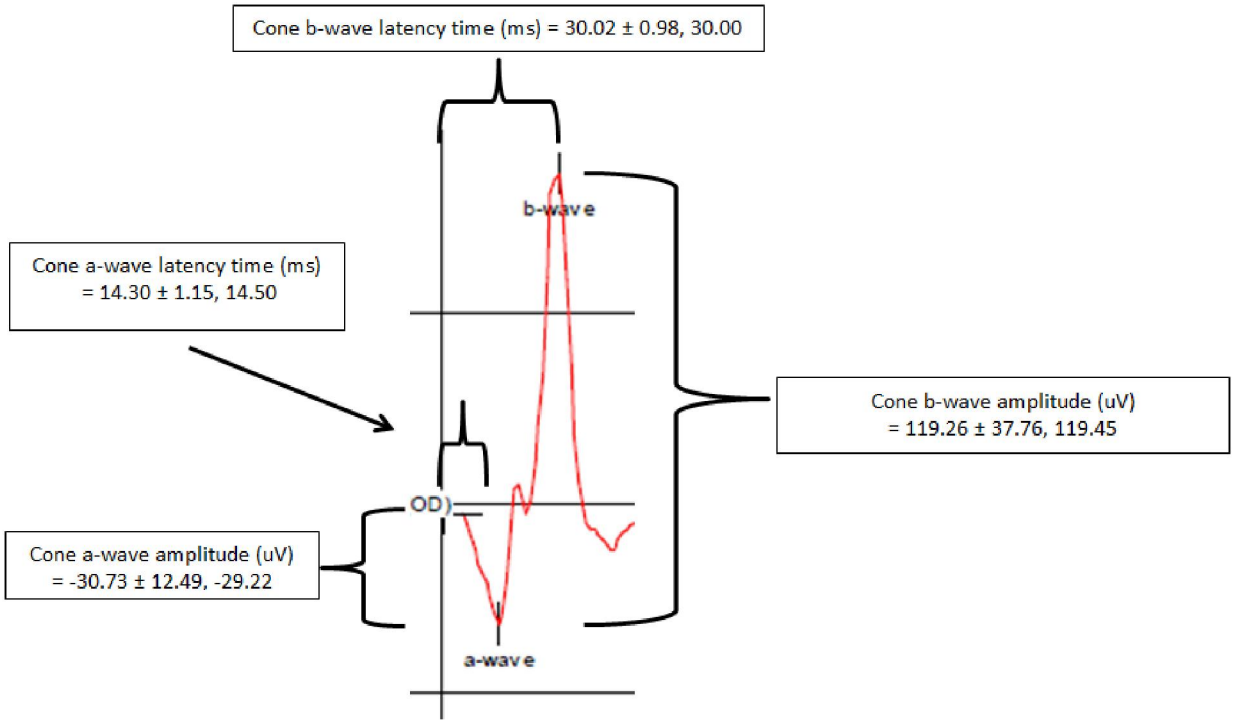

Fig. 1. Summary of mean, standard deviation (SD) and median for photopic adapted cone responses (indication: mean ± SD, median)

The comparison of a-wave amplitude and implicit time, b-wave amplitude and implicit time for photopic condition between our study and other population was summarized in Table 1. Comparing the findings from UK, Canada and USA, there was a large difference on the a-wave amplitude, where negative value rather than positive value was recorded in our population. The minimum value also recorded for amplitude of b-wave in our population. The different locations revealed different value especially on median amplitude of a-wave and b-wave in comparison to our study. The lowest value on median amplitude and almost the same pattern on median latency time of a-wave and b-wave were recorded in our study.

Table 1. Comparison the photopic adapted on different population [7] [8]

Study	(Al Abdlseaed, McTaggart, Ramage, Hamilton, & McCulloch, 2010)		(Fulton, Hansen, & Westall, 2003)		Saiful A.R, Muhamad-Syukri MR, & Chen A.H., 2013
Population	Blue-eyed Caucasians	Brown-eyed Asians	Boston adults	Toronto adults	Young Malays Adult
Location	Glasgow Caledonian University, UK		Boston, USA	Toronto, Canada	Klang Valley, Malaysia
ffERG Parameter Mean (95 CI)					
a-wave amp (lV)	39 (34 to 46)	52 (47 to 58)	N/A	N/A	-30.73 (-35.1 to -26.4)
a-wave lat (ms)	14.6 (14.2 to 15)	14 (14 to 14)			14.30 (13.9 to 14.7)
b-wave amp (lV)	133 (115 to 153)	209 (179 to 245)			119.26 (106.2 to 132.3)
b-wave lat (ms)	29.7 (29.4 to 30.1)	29.1 (28.6 to 29.7)			30.02 (29.7 to 30.4)
ffERG Parameter Median					
a-wave amp (lV)	N/A	N/A	92	42	29.22
a-wave lat (ms)			15	14	14.5
b-wave amp (lV)			137	164	119.45
b-wave lat (ms)			28	29	30

N/A = not available

4 DISCUSSION

Our finding on ffERG will serve as a preliminary guide for ERG measurement in clinical setting for young Malay adults as well as a guide for main comprehensive normative data collection in future. The values were considered important, as this is the first study that produced such values for this population. Comparing the five different populations, the lowest values were recorded in our population. Most probably due to 'internal factor' rather than the technical factor such as age, race, pupil size, axial length, diurnal variation, geographical environment, the genetic contribution, the physical of the retina in different population and the quality of electrical potential produced by the retinal cells [9]. In addition to that, the ffERG values also reflected the conditions and wellbeing of the retinal cells. Values of the electrical potential from the retina produced by the retinal cells had direct relationship to the functions of the cells as specific as the biochemical reaction involved in creating the signals.

5 CONCLUSION & RECOMMENDATION

A normative data is recommended for Malay population. The ffERG values for Malay Malaysian can be used as additional information to detect abnormalities in the electrophysiology practice besides using data from other population.

ACKNOWLEDGEMENTS

This study supported by Fundamental Research Grant Scheme (FRGS) (600-RMI/ST/FRGS 5/3/Fst 45/2011) and Exploratory Research Grant Scheme (ERGS) (600-RMI/ERGS 5/3 59/2011) from Minister of Higher Education Malaysia, and UiTM for the facilities. This work is in collaboration with Associate Professor Dr. Stuart Coupland, from University of Ottawa, Canada.

REFERENCES

[1] M. Marmor, G. Arden, S. Nilsson, and E. Zrenner, "Standard for clinical electroretinography: International standardization committee," *Archives of Ophthalmology*, vol. 107, no. 6, 1989.
[2] M. Marmor, A. Fulton, G. Holder, Y. Miyaki, M. Brigell, and M. Bach, "ISCEV Standard for full-field clinical electroretinography (2008 update)," *Doc Ophthalmol.*, vol. 118, no. 1, pp. 69-77, 2009.
[3] A. Collins, *Security and Southeast Asia: domestic, regional, and global issues*. Institute of Southeast Asian Studies, 2003.
[4] N. J. Ryan, *A history of Malaysia and Singapore*. Oxford University Press, 1976, p. 322.
[5] HUGO, "Mapping Human Genetic Diversity in Asia," vol. 326, no. 5959, pp. 1541-5, 2009. doi: 10.1126/science.1177074
[6] BBC News, "Genetic 'map' of Asia's diversity," no. November, 2009.
[7] A. Al Abdlseaed, Y. McTaggart, T. Ramage, R. Hamilton, and D. L. McCulloch, "Light- and dark-adapted electroretinograms (ERGs) and ocular pigmentation: comparison of brown- and blue-eyed cohorts.," *Documenta ophthalmologica. Advances in ophthalmology*, vol. 121, no. 2, pp. 135–46, Oct. 2010.
[8] A. B. Fulton, R. M. Hansen, and C. a Westall, "Development of ERG responses: the ISCEV rod, maximal and cone responses in normal subjects.," *Documenta ophthalmologica. Advances in ophthalmology*, vol. 107, no. 3, pp. 235–41, Nov. 2003.
[9] R. Karanjia, M. W. Hove, and S. G. Coupland, *Electroretinograms and Normative Data*. In: Gregor Belusic, *Electroretinogram*s, InTech, 2007. DOI: 10.5772/23387

International Journal of Innovation and Applied Studies
ISSN 2028-9324 Vol. 3 No. 4 Aug. 2013, pp. 999-1005

http://www.issr-journals.org/ijias/

Determinants of Capital Structure in Nigeria

Oladele John AKINYOMI and Adebayo OLAGUNJU

Financial Studies Department,
Redeemer University,
Mowe, Ogun State, Nigeria

ABSTRACT: Capital structure represents one of the most discussed concepts in financial management. Capital structure refers to how a company finances its operations whether through shareholders equity-fund or debt or a combination of both. Various internal and external factors contribute to the choice of these sources of fund. The external factors include factors such as tax policy, capital market conditions and tax policy, among others. Meanwhile, the internal factors are those that relate to individual firm characteristics. This study examines the determinants of capital structure in Nigeria using the descriptive research design. The population comprised of the eighty-six manufacturing firms that are listed in the Nigerian Stock Exchange. The sample firms were selected using the simple random sampling method. Secondary data obtained from the annual accounts of 24 randomly selected manufacturing firms for 10 years period culminating in 240 firm-year observations. The results of the regression analysis revealed that leverage (a measure of capital structure) has a negative relationship with firm size and tax on one hand and a positive relationship with tangibility of assets, profitability and growth on the other hand. However, only with tangibility of assets and firm size that significant relationship is established. It is recommended for future researchers to carry out similar studies in multiple sectors.

KEYWORDS: Capital Structure, Leverage, Tangibility, Firm Growth, Manufacturing.

1 INTRODUCTION

One of the most repeatedly discussed subjects in financial management is that of organizations' capital structure [1]. A company's capital structure refers to how a company finances its operations whether through shareholders equity fund or debt or a combination of both [2]. It usually comprise of all the sources of finance a company is utilizing to finance its operations. Usually, capital structure is made up of ordinary share capital, preference share capital, and debt capital among others.

Literature revealed that various external and internal factors affect the capital structure of corporate organizations [1]. The external factors include factors such as tax policy, capital market conditions and tax policy, among others. Meanwhile, the internal factors are those that relate to individual firm characteristics. Capital structure theories have identified a wide range of internal factors potentially influencing capital structure choice [3]. Reference [1] identified some of these internal factors to include: firm size, profitability, assets tangibility, taxation, firm growth rate, and liquidity. However, [3] observed that the factors affecting capital structure vary from one country to the other due to variation in the level social, environmental, economic, technological and cultural development. As a result of this, finding from studies in one country cannot be reasonably generalized to other countries, thus calling for country specific studies.

1.1 STATEMENT OF THE PROBLEM

One of the tough challenges that organizations face is the choice of capital structure. Gill, Biger, Pai and Bhutani (2009) observed that the determinants of capital structure have been debated for several years and still remain one of the most significant unsettled issues in the field of corporate finance. Reference [6] reported that several studies have been conducted

Corresponding Author: Oladele John AKINYOMI (delejohn21@yahoo.com)

on the determinants of corporate capital structure over the years. However, most of these studies were conducted in the advanced market economies such as USA and the UK, only limited studies have been carried out in emerging economies [7]. Moreover, the results of these prior studies have been inconclusive, controversial and open to further investigation [6]. In Nigeria in particular, only limited studies have been carried out on the determinants of capital structure in the manufacturing industry thus [8] recommended further studies. Therefore this study sets out to bridge this gap in knowledge by examining the determinants of capital structure in Nigeria.

1.2 OBJECTIVES OF THE STUDY

The main objective of this study is to ascertain the determining factors of capital structure of firms in Nigeria. Furthermore, the following are the specific objectives of this study:

1. To determine the influence of firm size on capital structure in Nigeria.
2. To investigate the influence of tangibility of assets on capital structure in Nigeria.
3. To examine the influence of profitability on capital structure in Nigeria.
4. To explore the influence of taxation on capital structure in Nigeria.
5. To examine the influence of growth on capital structure in Nigeria.

1.2.1 RESEARCH QUESTIONS

The following research questions have been raised on order to achieve the objectives of this study:

1. What is the influence of firm size on capital structure in Nigeria?
2. What is the influence of tangibility of assets on capital structure in Nigeria?
3. What is the influence of profitability on capital structure in Nigeria?
4. What is the influence of taxation on capital structure in Nigeria?
5. What is the influence of growth on capital structure in Nigeria?

1.2.2 RESEARCH HYPOTHESES

The following hypotheses have been formulated to determine whether or not the relationship between the dependent and each of the independent variables is significant.

Ho_i: There is no significant relationship between firm size and capital structure in Nigeria.

Ho_{ii}: There is no significant relationship between tangibility of assets and capital structure in Nigeria.

Ho_{iii}: There is no significant relationship between profitability and capital structure in Nigeria.

Ho_{iv}: There is no significant relationship between taxation and capital structure in Nigeria.

Ho_v: There is no significant relationship between growth and capital structure in Nigeria.

2 LITERATURE REVIEW

Several theories of capital structure have been highlighted in the literature. In their review of some theories of capital structure, [9] identified: MM theory, agency theory, trade-off theory, signaling theory, pecking order theory and free cash flow theory. Never the less, this study is anchored on the pecking-order and trade-off theories.

Reference [10] conducted a study on the determinants of capital structure in Pakistan. Secondary data from audited annual reports were obtained from the textile, chemical, fuel and energy sectors of the economy. Using leverage as the dependent variable while size, non-debt tax shield, growth, earnings volatility, profitability and tangibility of assets as the independent variables; the study employed correlation and regression analysis. The results revealed a negative relationship between earnings volatility, growth of firm, profitability and leverage on one hand, meanwhile a positive relationship was established between firm size, non-tax shield, tangibility of assets and leverage on the other hand.

Reference [11] investigated capital structure determinants in the United States service industry. Collateralized assets, profitability, non-debt tax shield, firm size, income tax, growth of firm were regressed against leverage. The results of the study revealed a negative relationship between profitability and leverage on one hand while a positive relationship was reported between effective income tax rate and leverage on the other hand. Meanwhile, no significant relationship was observed between non-debt tax shield, firm size, growth opportunity and leverage.

Reference [12] investigated the determinants of capital structure in 48 selected profit-making manufacturing firms in India. Data for the study were obtained from annual accounts of 2006 to 2010 period. The analysis was carried out using multiple regression models. The results of the study confirmed pecking order hypothesis, the leverage was found to be negatively related to profitability. Asset tangibility was found to be positively related to leverage. In contrast with theory, the tax rate was found to be negatively related to leverage.

Reference [13] examined the determinants of capital structure of 81 randomly selected Thai companies. Secondary data were obtained from the audited annual accounts of the selected firms from 6 industries during 2004-2008 periods. The analysis was carried out using correlation and regression analysis. After controlling for industry, the results revealed a significant relationship with the level of profitability, size, and tangibility. Negative relationship was observed with profitability and debt ratio; showing that companies with high profitability issue less debt. Positive relationship was observed with size and debt ratio; exhibiting that large companies issue high level of debt. Finally, a negative relationship was observed with tangibility and debt ratio; demonstrating that companies with high proportion of fixed assets to total assets issue less debt.

Reference [14] explored the factors that affect capital structure of manufacturing firms in Pakistani firms. The study set out to examine whether the capital structure models derived from developed economies provide persuasive explanations for capital structure decisions in the selected Pakistani firms. The investigation was conducted using panel data procedures for a sample of 160 firms listed on the Karachi Stock Exchange during 2003-2007. The results revealed that there is a negative relationship between debt ratio (as the dependent variable) and profitability, liquidity, earnings volatility, and tangibility (as independent variables); while firm size has a positive relationship with debt ratio. There was no significant relationship identified between the dependent variable of debt ratio and the independent variables of non-debt tax shields and growth opportunities. The study concluded that capital structure models derived from advanced economies does provide some help in understanding the financing behaviour of firms in Pakistan.

Reference [15] investigated the determinants of capital structure in Pakistan with focus on the cement industry. The study was based on 5 years financial data of the selected firms obtained from the State Bank of Pakistan publications. The sample comprise of 16 selected firms resulting into 80 firm-years which were subjected to panel data analysis. The independent variables of the study included tangibility of assets, firm size, growth of firm, and profitability; meanwhile leverage represented the dependent variable. The result of the regression analysis revealed a negative relationship with size and profitability on one hand, and positive relationship with tangibility and growth.

In Malaysia, [16] surveyed the determinants of capital structure among small and medium scale enterprises in Malaysia with data obtained from 50 award-winning enterprises from 1998 to 2010. The data analysis was carried out using regression analysis. Seven factors of: profitability, size, tangibility of assets, growth of firm, age of firm, non-debt tax shield and liquidity were considered in the analysis. The results of the study revealed in overall that three out of seven selected firm's characteristics (liquidity, tangibility of assets and non-debts tax shield) were found to have statistically significant relationship with firm's capital structure. Furthermore, all the three variables of liquidity, tangibility of assets and non-debts tax shield were also found to have ability in explaining variations in the firm's capital structure.

Reference [8] investigated the determinants of capital structure in Nigeria using panel data. Secondary data were obtained from 66 firms listed on the Nigerian stock Exchange during the period 1999-2007. The study analyzed six potential determinants of capital structure namely size, profitability, growth, tangibility, business environment and liquidity. Using regression analysis, the study reported a negative relationship between leverage (dependent variable) and each of growth, profitability, and tangibility of assets. However, a positive relationship was reported between leverage (dependent variable) and each of firm size and liquidity.

Reference [17] explored the determinants of capital structure of 88 public-listed companies in China. Six main factors of profitability, growth opportunities, size, asset structure, cost of financial distress, and tax shield were investigated. The data were subjected to correlation and regression analysis. The results of the study revealed a negative relationship with profitability, growth opportunity, and firm's size; meanwhile a positive relationship was found with tangibility. The study further disclosed that firm-specific factors when correlated with leverage has shown that neither the tradeoff model nor the

Pecking order hypothesis derived from the developed economies has strong explanatory power in elucidating the capital structure preference of firms in China.

Reference [18] explored the determinants of capital structure among 33 listed and non-listed companies during the period 2003-2007 in Ghana. Six factors of profitability, assets' tangibility, size of firm, business risk, growth and tax were examined. Multiple regression analysis of pooled-cross sectional and time-series observations was employed in the analysis. The results revealed that leverage has a positive relationship with profitability, assets tangibility, size, business risk on one hand; but a negative relationship was observed with growth and tax on the other hand.

Reference [19] studied the determinants of capital structure in Jordan. Secondary data were obtained from the annual reports of 30 companies that were listed in the Amman Stock Exchange between the period of 2001 and 2005. Five factors comprising of company size, tangibility of fixed assets, profitability, long-term debt to total assets, and short-term debt to total assets were examined. Using correlation and regression analysis, the results of the study revealed a positive relationship with company size, tangibility, long-term debt, and short-term debt, while a negative relationship was reported with profitability.

3 MATERIALS AND METHODS

This study employs descriptive survey research design in investigating the determinants of capital structure in Nigeria. The population comprised of the eighty-six manufacturing firms that are listed in the Nigerian Stock Exchange, out of which a sample size of twenty-four was obtained. The audited annual reports of twenty-four randomly selected manufacturing firms for ten year-period of 2003-2012 were used for the study; this amounts to 240 firm-year observations. The data were analyzed using correlation coefficient and regression analysis. The regression model is as follows:

$LEV = b_0 + b_1SIZE + b_2TANG + b_3PROFIT + b_4TAX + b_5GROWTH + \varepsilon$

Where:

LEV is measured as total liabilities divided by total assets.

SIZE measured by log of sales.

TANG measured as average total fixed assets divided by total assets.

PROFIT measured as operating income divided by total assets (ROA).

TAX measured by the ratio of tax paid to PBT

GROWTH measured as a percent change in sales.

4 RESULTS AND DISCUSSIONS

The results of the analysis are presented in this section with the discussion of findings. The analysis begins with a range of descriptive statistics on the dependent variable and the independent variables with minimum, maximum, mean and standard deviation presented in table 1. From the table, the mean leverage of this industry is 0.57571, profitability accounted for 0.22664, size 7.81224, tangibility 0.62924, tax 0.3997 and growth 0.23997. The standard deviation of leverage is 0.074041, profitability 0.085698, size 0.485305, tangibility 0.070879, tax 0.020892 and growth 0.180937. The result of minimum value ranges from 0.027 to 6.489 while that of maximum value ranges from 0.376 to 8.403.

Table 1. Descriptive Statistics

	N	Minimum	Maximum	Mean	Std. Deviation
LEV	240	.325	.691	.57571	.074041
ROA	240	.027	.393	.22664	.085698
SIZE	240	6.489	8.403	7.81224	.485305
TANG	240	.507	.776	.62924	.070879
TAX	240	.276	.376	.32027	.020892
GROWTH	240	.077	.961	.23997	.180937
Valid N (listwise)	240				

Source: Output of data analysis by author

The results of the correlation reveal that firm's size and tax have negative relationship with leverage, meanwhile each of: profitability, tangibility of assets and growth has positive relationship with leverage. However, only with tangibility of assets and tax that significant relationship is established. Furthermore, a significant relationship is established between tangibility of assets and size, tax and size, tangibility of assets and tax, tangibility of assets and growth, and finally between tax and growth.

Table 2. Summary of Pearson Product Moment Correlations

	LEV	ROA	SIZE	TANG	TAX	GROWTH
LEV	1					
ROA	.008	1				
SIZE	-.005	.083	1			
TANG	.132*	.108	.806**	1		
TAX	-.200**	.087	.228**	.212**	1	
GROWTH	.031	-.028	-.078	-.212**	-.404**	1

*. Correlation is significant at the 0.05 level (2-tailed). **. Correlation is significant at the 0.01 level (2-tailed).

Table 3 below is a summary of the regression model used in this study. It reveals R^2 value of 0.10 meaning that only 10% of the variation in leverage can be explained by the degree of GROWTH, ROA, SIZE, TAX, and TANG.

Table 3. Model Summary[b]

Model	R	R Square	Adjusted R Square	Std. Error of the Estimate	Change Statistics					Durbin-Watson
					R Square Change	F Change	df1	df2	Sig. F Change	
1	.316[a]	.100	.081	.070982	.100	5.208	5	234	.000	2.371

Table 4 below further presents the coefficients of the models used in the study. The coefficient for size variable is -0.044 and shows a negative relationship between size and leverage. The coefficient for tax is -0.779 which shows that there is a negative relationship between tax and Leverage. The coefficient for growth variable is 0.0003 and shows a positive relationship with leverage of the firm. The coefficient for tangibility variable is 0.428 and shows a positive relationship with Leverage. The coefficient for ROA variable is 0.006 and shows a positive relationship with the Leverage. The overall model is statistically significant.

Table 4. Coefficients

Model		Unstandardized Coefficients		Standardized Coefficients	T	Sig.
		B	Std. Error	Beta		
1	(Constant)	.894	.103		8.705	.000
	ROA	.006	.054	.007	.115	.908
	SIZE	-.044	.016	-.286	-2.650	.009
	TANG	.428	.114	.410	3.770	.000
	TAX	-.779	.247	-.220	-3.151	.002
	GROWTH	.003	.029	.008	.109	.913

a. Predictors: (Constant), GROWTH, ROA, SIZE, TAX, TANG. b. Dependent Variable: LEV

Table 5. ANOVA

Model		Sum of Squares	Df	Mean Square	F	Sig.
1	**Regression**	.131	5	.026	5.208	.000[a]
	Residual	1.179	234	.005		
	Total	1.310	239			

a. Predictors: (Constant), GROWTH, ROA, SIZE, TAX, TANG. b. Dependent Variable: LEV

The results revealed that there is a positive relationship between Growth and Leverage in the selected firms, which suggests that internally generated funds are sufficient for the firms to meet their growing need, so they will use less debt. This result is consistent with that of [15]. However, the result contradicts those of [8], [17], [18]. This suggests that growing firms among the selected companies prefer to use funds from debt to finance growth. The growth variable with P value 0.031 is insignificant (at 0.05 level), thus we accept the null hypothesis and conclude that there is no significant relationship between growth of firm and capital structure in Nigeria.

The results also revealed that tangibility is positively related with leverage, which is also found by [19], [12], [10]. This suggests that the firms in this sector of the Nigerian economy having a large amount of fixed asset use more debt. The hypothesis of positive relationship of Tangibility with Leverage is accepted. Nevertheless, the results of this study contradict that of [8] who reported a negative relationship between tangibility of assets and leverage. The tangibility variable with P value 0.132 is significant (at 0.05 level), thus we reject the null hypothesis and conclude that there is significant relationship between tangibility of assets and capital structure in Nigeria.

Furthermore, the results revealed that there is a positive relationship between Profitability and leverage which supports the results of [18]. The results suggest that firms which are more profitable use more debt. On the other hand, the result contradicts that of [5], [12], [13], [10]. The profitability variable with P value 0.008 is insignificant (at 0.05 level), thus we accept the null hypothesis and conclude that there is no significant relationship between profitability and capital structure in Nigeria.

Additionally, the results revealed that there is a negative relationship between Size and leverage, which confirms the results of [17], [15]. However, the result contradicts that of [19], [18], [10]. The size variable with P value 0.005 is insignificant (at 0.05 level), thus we accept the null hypothesis and conclude that there is no significant relationship between size and capital structure in Nigeria.

Finally, a negative relationship between tax and Leverage is established in this study in line with the findings of [12], [18]. The result contradicts that of [11] who reported a positive relationship between tax and leverage. The tax variable with P value -0.200 is significant (at 0.05 level), thus we reject the null hypothesis and conclude that there is significant relationship between tax and capital structure in Nigeria.

5 CONCLUSION

This study examines the determinants of capital structure in the Nigerian manufacturing firms. Data were obtained from 24 selected manufacturing firms with a total 240 observations. The results of the analysis revealed that leverage (a measure of capital structure) has a negative relationship with firm size and tax on one hand and a positive relationship with tangibility of assets, profitability and growth on the other hand. However, only with tangibility of assets and firm size that significant relationship is established. Therefore, this study concludes as follows: (i) that there is no significant relationship between size, profitability, growth of firms and capital structure in Nigeria; (ii) that there is significant relationship between tangibility of assets, tax and capital structure in Nigeria.

This study focuses on the manufacturing sector of the Nigerian economy. It is suggested for future researchers to conduct their studies with data from multiple sectors and compare the results among the sectors. This may provide evidence on the influence of industry on capital structure determinants.

REFERENCES

[1] P. Pinkova, "Determinants of capital structure: evidence from the Czech automotive Industry," *Acta Universitatis Agriculturae Et Silviculturae Mendelianae Brunensis*, Vol. 60, no. 7, pp. 217-224, 2012.

[2] O. Akinsulire, *Financial management, 5th edition*. Lagos: El-Toda Ventures, 2008.

[3] K. Mazur, "The determinants of capital structure choice: Evidence from Polish companies," *International Atlantic Economic Society*, Vol. 13, pp. 495-514, 2007.

[4] M. Psillaki and N. Daskalakis, "Are the determinants of capital structure country or firm specific?," *Small Business Economics*, Vol. 33, pp. 319–333, 2009.

[5] A. Gill, N. Biger, C. Pai and S. Bhutani, "The determinants of capital structure in the service industry: Evidence from United States," *The Open Business Journal,* Vol. 2*,* pp. 48-53, 2009.

[6] G. Morri and C. Beretta, "The capital structure determinants of REITs: Is it a peculiar industry?," *Journal of European Real Estate Research,* Vol. 1, pp. 6-57, 2008.

[7] S. G. H. Huang and F. M. Song, "The determinants of capital structure: Evidence from China," *Working Paper Series*, No. 1042, 2002.

[8] O. Akinlo, "Determinants of capital structure: Evidence from Nigerian panel data," *African Economic and Business Review,* Vol. 9, No. 1, pp. 1-16, 2011.

[9] S. A. Owolabi and U. E. Inyang, "International pragmatic review and assessment of capital structure determinants," *Kuwait Chapter of Arabian Journal of Business and Management Review*, Vol. 2, No. 6, pp. 82-96, 2013

[10] S. Kiran, "Determinants of capital structure: A comparative analysis of textile, chemical and fuel and energy sectors of Pakistan (2001-2006)," *International Review of Management and Business Research*, Vol. 2, No. 1, pp. 37-47, 2013.

[11] A. Gill, N. Biger, C. Pai and S. Bhutani, "The determinants of capital structure in the service industry: evidence from United States," *The Open Business journal, 2*, 48-53, 2009.

[12] C. S. Mishra, "Determinants of capital structure: A study of manufacturing sector PSUs in India," *International Conference on Financial Management and Economics IPEDR,* Vol. 11, pp. 247-252, *IACSIT Press, Singapore,* 2011.

[13] B. Wanrapee, "Capital structure determinants of Thai listed companies," *The Clute International Academic Conference,* New Orleans Louisiana, 2009. [Online] Available: http://conferences.cluteonline.com/index.php/IAC/2011NO/schedConf/presentations?searchInitial=B&track=11 (2009)

[14] N. A. Sheikh and Z. Wang, "Determinants of capital structure: An empirical study of firms in manufacturing industry of Pakistan," *Managerial Finance,* Vol. 37, No. 2, pp. 117 – 133, 2011.

[15] Y. B. Tariq and S. T. Hijazi, "Determinants of capital structure: A case for the Pakistani cement industry," *The Lahore Journal of Economics,* Vol. 11, No. 1, pp. 63-80, 2006.

[16] S. M. Zabri, "The determinants of capital structure among SMES in Malaysia," *Proceedings, International Conference of Technology Management, Business and Entrepreneurship 2012* (ICTMBE2012), Renaissance Hotel, Melaka, Malaysia 18-19 Dec, 2012.

[17] J. J. Chen, "Determinants of capital structure of Chinese-listed companies," *Journal of Business Research,* Vol. 57, pp. 1341-1351, 2004.

[18] P. K. Oppong-Boakye, K. O. Appiah and J. K. Afolabi, "Determinants of capital structure: Evidence from Ghanaian firms," *Research Journal of Finance and Accounting,* Vol. 4, No. 4, pp. 44-54, 2013.

[19] H. A. Khrawish and A. H. A. Khraiwesh, "The determinants of capital structure: Evidence from Jordanian industrial companies," *JKAU: Economics and Administration,* Vol. 24, No. 1, pp. 173-196, 2010.

International Journal of Innovation and Applied Studies
ISSN 2028-9324 Vol. 3 No. 4 Aug. 2013, pp. 1006-1014

http://www.issr-journals.org/ijias/

Bandwidth Extension of Constant-Q Bandpass Filter using Bandwidth Extension Techniques

Megha Chitranshi[1], Sudha Radhika[1], and Anand Mishra[2]

[1]Department of Electronics and Communication Engg.,
Jaypee University of Engineering and Technology,
Raghogarh, Guna(M.P.)-473226, India

[2]Department of Control System,
Nagaji Institute of Technology and Management,
Gwalior (M.P.)-474001, India

ABSTRACT: CMOS spiral inductors suffer from a number of drawbacks including a low Q factor, a low self- resonant frequency, and a small and non-tunable inductance and require a large chip area. On the other hand active inductor offers many unique advantages over their spiral counterparts including small chip area, large and tunable inductance and high quality factor. These active inductors have been used successfully in many applications such as in radio frequency (RF) front end integrated circuits, filters, and phase shifter and oscillator circuits. The effectiveness of these active inductors is however affected by a number of limitation including small dynamic range, a high noise level and high power consumption. High speed applications such as preamplifier of data transceiver require large bandwidth hence there is a need for technique that achieve larger bandwidth without increased power consumption and design complexity. In this paper, bandwidth extension techniques are used to extend the bandwidth of the bandpass filter. Active inductors are used in the designing of the bandpass filter. A swing independent quality factor, called constant-Q active inductor is used as an active element in the designing of the bandpass filter. Bandpass filter is implemented on both 0.5 µm and 0.35 µm CMOS process. Comparisons are made between resistive compensation technique and inductive series peaking technique. Simulation results shows that the bandwidth is improved by 72%.The operating frequency is also increases from 122.995 MHz to 194.276 MHz at 0.5 µm technology and operating frequency increases from 163.641 MHz to 259.189 MHz at 0.35 µm technology.

KEYWORDS: Bandpass filter, bandwidth extension, constant-Q active inductor, inductive series peaking, resistive compensation.

1 INTRODUCTION

In recent years, the demand of the wireless communication systems has led the IC design trend to low cost, low power, and high integration. An analog RF filter is an essential block in wireless receivers. Implementing on-chip high-Q IF/RF bandpass responses for band channel-selection filtering or image frequency rejection filtering is a very demanding problem, due to the extremely powerful specifications in terms of accuracy, stability, and dynamic range at very high operating frequencies. Typically, this requires the use of high quality spiral inductors with auxiliary active circuitry for compensation of inductor losses and achieving the necessary tuning ability.

Many circuits in literature are based on RLC realization using passive inductors [1]. Much architecture for active has been proposed [2], [3], [4]. Active inductors are realized by using the classical gyrator- C topology. Gyrators realized operational transconductors feature transconductance that can be adjusted with applied bias, thereby allowing for whose values can be adjusted, or “tuned”, electronically. Basic CMOS active inductor is described in section II. Various

Corresponding Author: Megha Chitranshi (chitranshi.megha@gmail.com)

approaches for designing of bandpass filter using active inductor have been proposed [5], [6], [7], [8], [9]. Designing of bandpass filter using active inductor is described in section III.

Passive filtering (e.g. shunt and series peaking) has been used since the 1930s to extend amplifier bandwidth; it uses inductors to trade off bandwidth versus peaking in the magnitude response. Bandwidth extension techniques based on passive filtering as proposed in [10], [11], [12] is described in section IV.

In this paper, Inductive series peaking technique suggested in [12] is used for bandwidth enhancement of current mirror, is applied for bandwidth enhancement of active inductor. Comparisons are made between resistive compensation technique and inductive series peaking technique. Bandpass filter is implemented in both 0.5µm and 0.35 µm CMOS process.

2 ACTIVE INDUCTOR

Active inductors are realized by using the classical gyrator- C topology. The gyrator is a two port network that is designed to transform load impedance into input impedance where the input impedance is proportional to the inverse of the load impedance. Gyrator network can be used to transform a load capacitance into an inductance. When two transconductors are connected back to back, they form gyrator-C active inductor. Where one port of the gyrator is terminated with a capacitive load and the other port exhibits an inductive characteristic.

2.1 BASIC CMOS ACTIVE INDUCTOR

Figure 1 shows the Wu current reuse active inductor as proposed in [5], which in comparison to other topologies could use biasing current more efficiently. A common gate configuration of the positive transconductor along with a common source configuration of the negative transconductor creates the NMOS version of the active inductor.

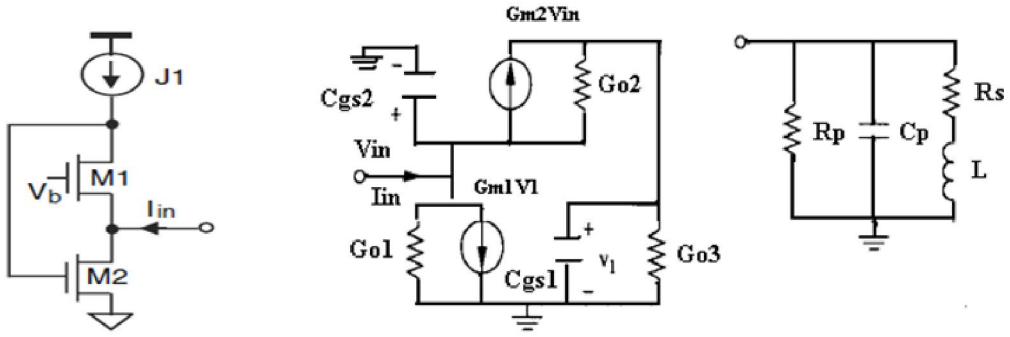

Fig. 1. Wu current reuse active inductor and its equivalent Small signal model and RLC circuit

Figure 1 shows the small signal equivalent circuit of the active inductor. Neglecting gate drain capacitance we have

$$C_p = C_{gs2} \tag{1.1}$$

$$R_p = \frac{1}{G_{o1}} \parallel \frac{1}{G_{m2}} \cong \frac{1}{G_{m2}} \tag{1.2}$$

$$R_S = \frac{G_{o1}}{G_{m1}G_{m2}} \tag{1.3}$$

$$L = \frac{C_{gs2}}{G_{m1}G_{m2}} \tag{1.4}$$

$$\omega_0 = \sqrt{\frac{G_{m1}G_{m2}}{C_{gs1}C_{gs2}}} = \omega_{t1}\omega_{t2} \tag{1.5}$$

$$Q \cong \sqrt{\frac{G_{m1}C_{gs2}}{G_{m2}C_{gs1}}} = \sqrt{\frac{\omega_{t1}}{\omega_{t2}}} \tag{1.6}$$

From above equations we can see that the inductance L, the parasitic series resistance R_S, and parasitic parallel resistance R_P all are functions of G_{m1} and G_{m2}, which are determined by the channel current of M1 and M2.The channel current of M2 is greatly affected by the input current I_{in}, especially when I_{in} is large. As a result both the inductance and quality factor of the active inductor are strong functions of the swing of the input current.

2.2 CONSTANT -Q CMOS ACTIVE INDUCTOR

Constant-Q CMOS active inductor consist Wu's active inductor and a current feedback network. In the applications, where the quality factor of the active inductor varies largely, such as LC-tank oscillators, the inductance, parasitic resistances, and quality factor of the active inductors all vary with signal swing.CMOS active inductor with nearly constant quality factor, called constant-Q active inductor is used as proposed in [13].

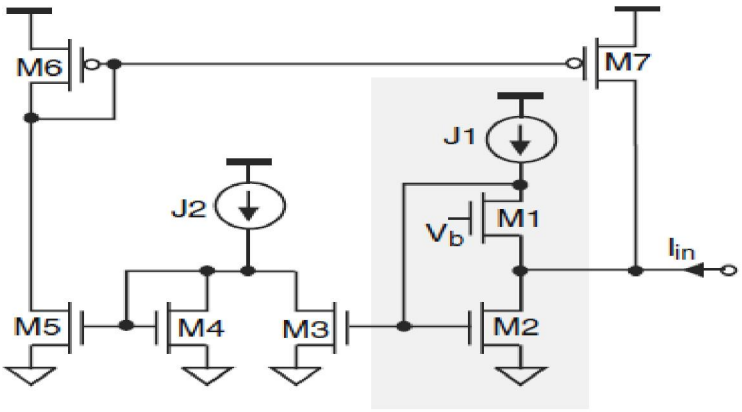

Fig. 2. Constant-Q CMOS active inductor

The transistors M2-M3, M4-M5, and M6-M7 form a current mirror pair having current gain k1, k2 and k3 respectively.J2 is set at maximum input current swing $i_{in,max}$.

3 FILTER ARCHITECTURE

A simple way of implementing a bandpass filter with the active inductor proposed in [9] is shown in Figure 3. The input transconductor Gm, realized by Min, converts the input voltage Vin to a current that is applied to the active inductor. The output voltage is taken at the inductor port. A source follower output buffer is included to drive the resistive loads and to prevent a load resistor and capacitor from reducing the resonant frequency and quality factor of the filter. The parasitic capacitors of the input Gm and the output buffer can be included in C1.

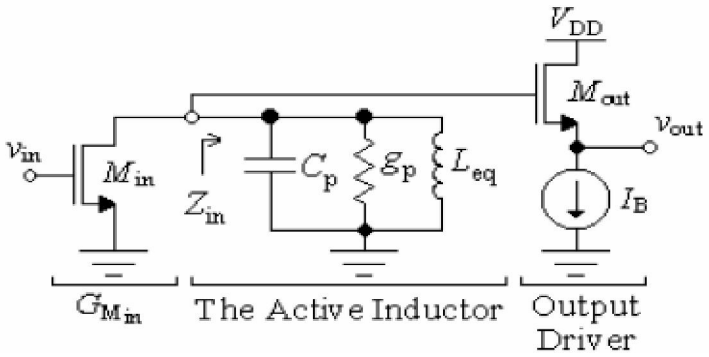

Fig. 3. Block diagram of the bandpass filter based on active inductor

4 BANDWIDTH EXTENSION TECHNIQUES

4.1 RESISTIVE COMPENSATION TECHNIQUE

Resistive compensation technique as proposed in [10] enhances the bandwidth of current mirrors without distorting the DC characteristics of the original circuits. In this a resistor is introduces between the gates of the input and output transistor of the basic current amplifier to introduce a zero in the system which cancels the dominant pole and increases the bandwidth.

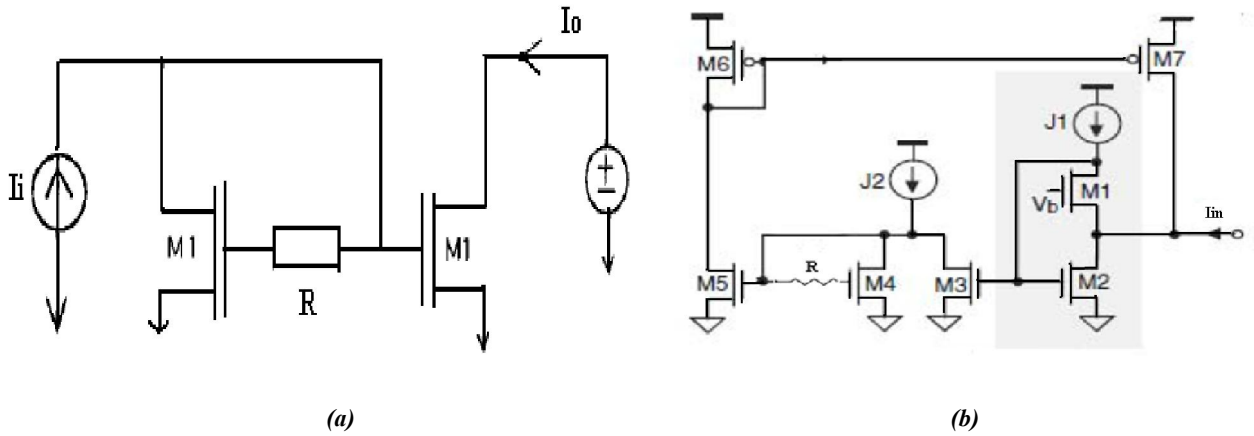

(a) *(b)*

Fig. 4. (a) Simple current mirror (b) Constant-Q active inductor bandpass filter with resistive compensation

However, the resistor eventually delays the response but also introduces a zero which cancels that delay. The addition of the zero makes the system faster and more oscillatory as the zero moves in the negative axis toward the origin. When R = $1/G_{m1}$ and $C_{gs1}= C_{gs2}$, zero cancels one of the poles, yielding a first order system with a frequency response determined by $\omega_0= G_{m1}/C_{gs2}$, which is twice the frequency of the uncompensated current mirror.

Figure3 (b) shows the constant Q active inductor with resistive compensation technique as proposed in [14]. Without compensation resistor the input impedance of the constant Q active inductor is given as

$$Z_{in} = \frac{\frac{s}{C_1}}{s^2+s\frac{G_{m1}}{C_1}+\frac{G_{m1}G_{m2}}{C_1C_2}} \tag{1.7}$$

By introducing a compensation resistor between the gates in one of the current mirror pair M4-M5, one zero two pole system is transposed into four zero five pole system.

$$Z_{in} = \frac{s^2(g+sC_3)/C_1C_3C_5}{s^4+s^3\left(\frac{g}{C_5}+\frac{G_{m1}}{C_1}\right)+s^2\left(\frac{G_{m1}g}{C_1C_5}+\frac{G_{m2}G_{m1}}{C_1C_2}\right)+ s\left(\frac{G_{m2}G_{m1}g}{C_1C_2C_5}+\frac{G_{m1}G_{m4}g}{C_1C_3C_5}\right)+\frac{G_{m1}G_{m2}G_{m4}g}{C_1C_2C_3C_5}} \tag{1.8}$$

At $g = s/C_5$ one pole and zero gets cancelled. Maximum bandwidth is achieved when zero cancels a pole.

Figure 5 shows the frequency curve of the constant Q active inductor bandpass filter at 0.5 µm technology. The frequency of the Constant Q active inductor bandpass filter is 122.995 MHz with a bandwidth of 21 MHz

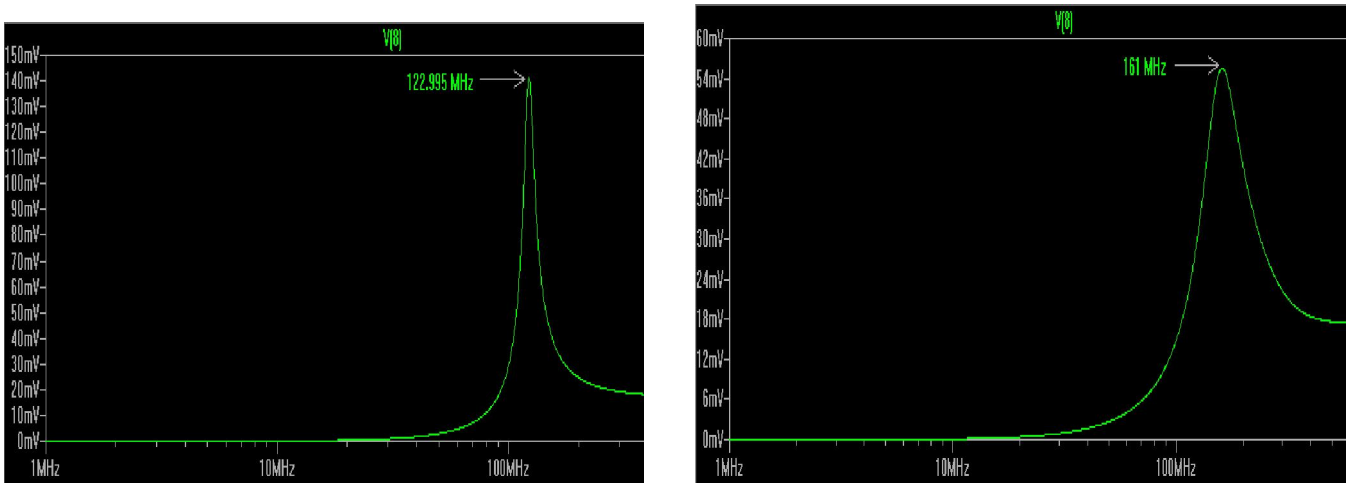

(a) *(b)*

Fig. 5. (a) Frequency curve of constant Q active inductor bandpass filter with frequency 122.995 MHz and bandwidth is 21 MHz (b) Frequency curve of constant Q active inductor bandpass filter with resistive compensation with frequency 161 MHz and bandwidth is 69.61 MHz

After resistive compensation bandwidth of the constant Q active inductor bandpass filter is increased from 21 MHz to 69.61 MHz and frequency is also increased from 122.995 MHz to 161 MHz. The frequency curve of constant Q bandpass filter with resistive compensation is shown in Figure5 (b).

4.2 INDUCTIVE SERIES PEAKING TECHNIQUE

Inductive series peaking technique as proposed in [12], improves the bandwidth by utilizing the resonance characteristics of LC network. Because the dominant pole of CMOS current mode circuits is attributed to the gate source capacitances of the input and output transistors, a compensation inductor can be placed between the gates of the input and output transistors, and in series with C_{gs2} as shown in Figure 6.

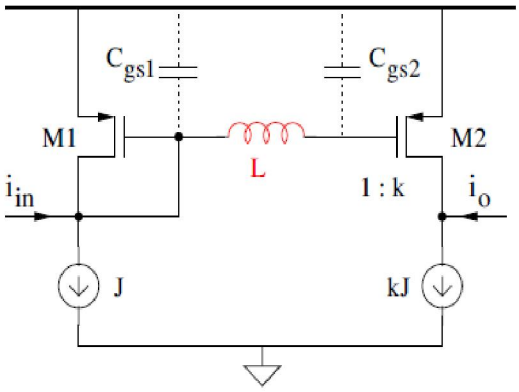

Fig. 6. Current mirror amplifier with series peaking inductor

The characteristics of the amplifier depend upon the value of the peaking inductor [18], as detailed in Table 1. To maximize the bandwidth and avoid ringing in time domain, the peaking inductor is sized based on the criterion of the critical damping, where $L = C_{gs2} / 4G^2_{m1}$, and the circuit has the bandwidth of $\omega 0 = 2G_{m1} / C_{gs2}$

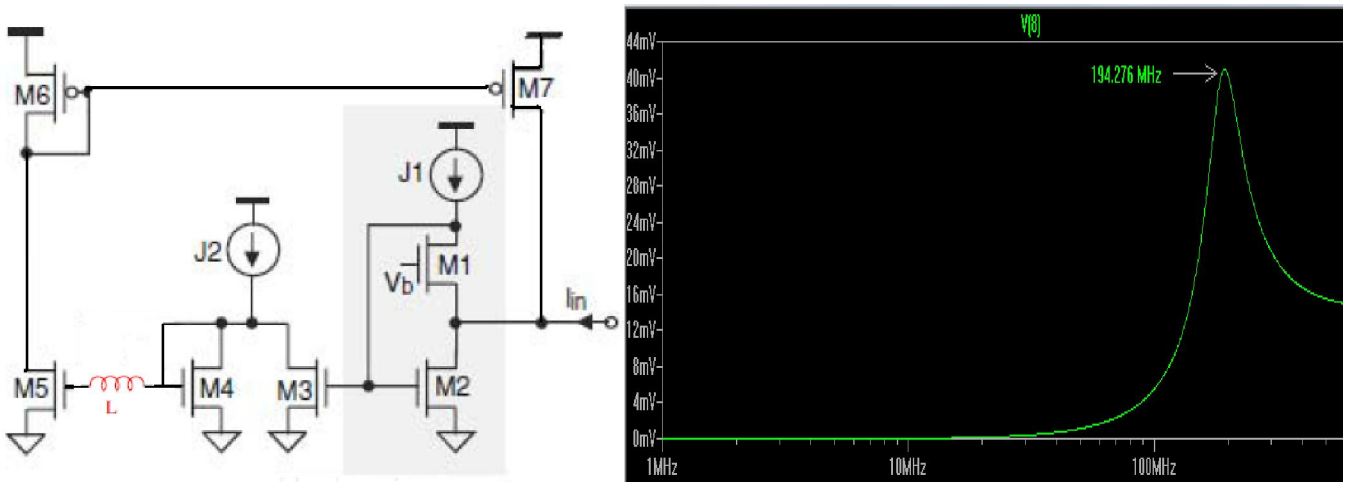

(a) *(b)*

Fig. 7. (a) Modified constant Q bandpass filter with inductive series peaking (b) frequency response curve with frequency 194.276 MHz and bandwidth is 74.395 MHz

When constant-Q active inductor bandpass filter with inductive series peaking is simulated on 0.5 µm technology, then frequency is increased from 122.995 MHz to 194.276 MHz and bandwidth is increased from 21 MHz to 74.395 MHz. Figure 7(b) shows the frequency curve of constant-Q bandpass filter with inductive peaking.

Now constant- Q active inductor bandpass filter is simulated on 0.35 µm technology. Frequency curves of bandpass filter with and without bandwidth extension are shown in section V.

Table 1. Damping characteristics

L	Poles	Damping characteristics	Responses
$L < C_{gs2}/4G^2_{m1}$	Two distinct negative real poles	Over-damped	Small bandwidth Large rise time No ringing
$L = C_{gs2}/4G^2_{m1}$	Two identical negative real poles	Critically damped	Large bandwidth Small rise time No ringing
$L > C_{gs2}/4G^2_{m1}$	Complex conjugate poles with negative real part	Under-damped	Large bandwidth Small rise time Ringing

5 SIMULATIONS ON 0.35 µM TECHNOLOGY

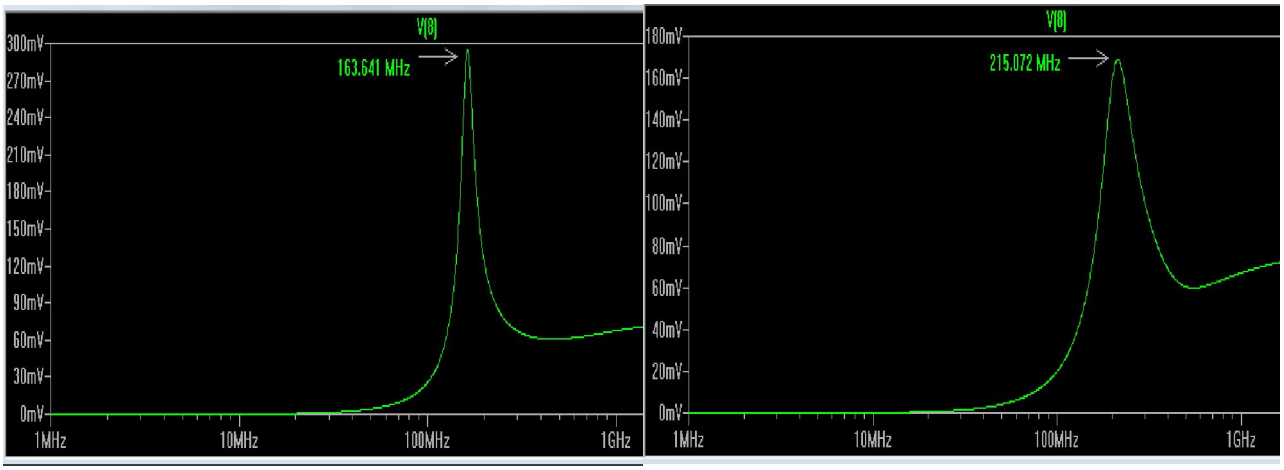

(a) *(b)*

Fig. 8. (a) Frequency curve of constant-Q active inductor bandpass filter with frequency is 163.641 MHz and bandwidth is 26 MHz
(b) Frequency curve of constant-Q bandpass filter with resistive compensation: frequency 215.072 MHz and bandwidth is 89 MHz

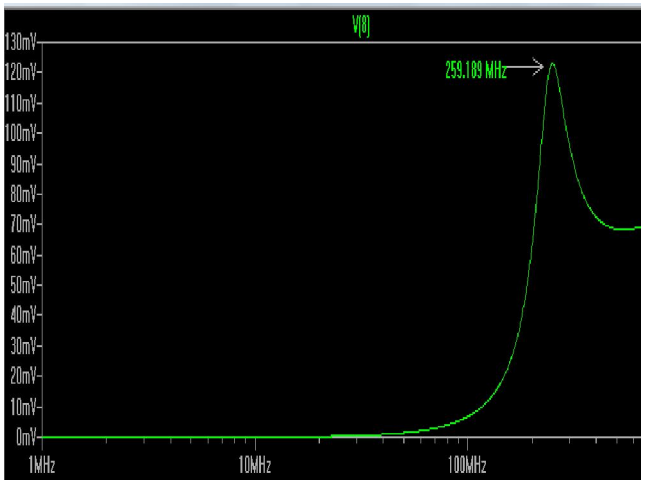

Fig. 9. Frequency curve of constant-Q active inductor bandpass filter with inductive series peaking: frequency is 259.189 MHz and bandwidth is 94 MHz

6 SIMULATION RESULTS

Simulation is done on 0.5 µm and 0.35 µm technology. With inductive series peaking technique bandpass filter has maximum bandwidth 74.395 MHz with frequency 194.276 MHz at 0.5 µm technology. With resistive compensation technique bandpass filter has frequency 161 MHz and bandwidth is 69.61 MHz. Simulation results of bandpass filter at 0.35 µm technology are better than the 0.5 µm technology. With inductive series peaking, frequency of the bandpass filter is 259.189 MHz with 94 MHz bandwidth bandwidth. With resistive compensation technique, frequency is 215.072 MHz with bandwidth 89 MHz.

Table 2. Comparison of bandwidth extension techniques

Parameters	Without extension technique at 0.5 µm [14]	Resistive compensation at 0.5µm[14]	Inductive series peaking at 0.5µm	Without extension technique at 0.35µm	Resistive compensation at 0.35 µm	Inductive series peaking at 0.35µm
Frequency	122.462 MHz	148.59 MHz	194.276 MHz	163.641 MHz	215.072 MHz	259.189 MHz
Bandwidth	16 MHz	60 MHz	74.395 MHz	26 MHz	89 MHz	94 MHz

7 CONCLUSION

Constant Q active inductor bandpass filter with and without bandwidth extension techniques are described. Bandpass filter is simulated on both 0.5 µm and 0.35 µm technology. From simulation results we can say that inductive series peaking is best for bandwidth extension in bandpass filter. With the help of bandwidth extension techniques, bandwidth of the bandpass filter is extended more than thrice of the bandwidth of the bandpass filter without any extension technique.

REFERENCES

[1] M. Ismail, R. Wassenaar, and W. Morrison, "A high speed continuous- time bandpass VHF filter in MOS technology," *Proc. IEEE Int. Symp. on Circuits and Systems*, pp. 1761-1764, 1991.

[2] Wu, Y., Ismail, M., Olsson, H., "A novel CMOS fully differential inductorless RF bandpass filter," In Proceedings of the *IEEE ISCAS*, Vol. 4, pp. 149–152, Geneva, 2000.

[3] U. Yodprasit and J. Ngarmnil, "Q-enhanced technique for RF CMOS active inductor," In *Proc. IEEE Int'l Symp. Circuits Syst.* vol. 5, pp. 589-592, Geneva, 2000.

[4] Karsilayan and R. Schaumann, "A high-frequency high-Q CMOS active inductor with DC bias control," *Proc. 43rd IEEE Midwest Symp. on Circuits and system*, pp. 486-489, 2000.

[5] Wu, Y., Ismail, M., Olsson, H., "Inductorless CMOS RF bandpass filter," *Electron. Lett.,* vol. 37, pp. 1027–1028, 2001.

[6] Wu, Y., Ismail, M., Olsson, H., "CMOS VHF/RF CCO based on active inductors," *IEE Electronic Letters*, 37(8), pp. 472–473. 2001.

[7] Wu, Y., Ismail, M., Olsson, H., "RF bandpass filter design based on CMOS active inductors," *IEEE transactions on circuits and systems*, 50(12), pp. 942–949, 2003.

[8] Wu, Y., Ismail, M., Olsson, H., "CMOS active inductor and its application in RF bandpass filter," *IEEE Radio frequency integrated circuits' symposium*, 2004.

[9] H. Xiao and R. Schaumann, "A radio-frequency CMOS active inductor and its application in designing high Q filters," In *Proc. IEEE Int'l Symp. Circuits Syst*., pp. 197-200, 2004.

[10] T. Voo and C. Toumazou, "High speed current mirror resistive compensation technique," *IEE Electronics Letters*, 31(4), pp. 248-250, 1995.

[11] Sudip Shekhar, Jeffery S. Walling, and David J. Allstot, "Bandwidth extension techniques for CMOS amplifiers," *IEEE journal of solid state circuits*, Vol. 41, No. 11, pp. 2424-2433, Nov. 2006.

[12] B. Sun, F. Yuan, and A. Opal, "Inductive-peaking in wideband CMOS Current amplifiers," *proceedings of the IEEE ISCAS*, Vol. 4, pp. 285-288, 2004.

[13] A. Tang, F. Yuan, and E. Law, "A new constant-Q CMOS active inductor with applications to low-noise oscillators," Analog integrated circuits and signal processing, Vol. 58, pp. 77-80, 2009.

[14] A. Neekhra and M. Gupta, "Bandwidth extension of a constant Q active," *conference on computer and communication technology*, pp. 311-313, 2010.

[15] H. Xiao and R. Schaumann, "A low-voltage low-power CMOS 5-GHz oscillator based on active inductors," *IEEE International Conference on Electronics, Circuits and Systems*, vol. 1, pp. 231-234, 2002.

[16] Barthelemy, H., and Rahajandraibe, W., "NMOS transistors based Karsilayan & Schaumann gyrator: Lowpass and bandpass filter applications," *IEEE Midwest symposium on circuits and systems*, 2000.

[17] T. Voo and C. Toumazou, "Precision temperature stabilized tunable CMOS current mirror for filter applications," *IEE Electronics Letters,* 32(2), pp. 105-106, 1996.

[18] B. Sun and F. Yuan, "A new inductor series- peaking technique for bandwidth enhancement of CMOS current-mode circuits," *Analog integrated circuits and signal processing*, Vol. 37, pp. 259-264, 2003.
[19] S. Rooznow and V. Sohani, "Integrated bandpass filter designed for 13.56 MHz RFID reader," *Journal of applied science and research*, 8(2), pp. 1018-1025, 2012.
[20] F. Yuan, *CMOS Active Inductors and Transformers: Principle, Implementation, and Applications*, Springer, New York, ISBN: 978-0-387-76477-1, 2008.

International Journal of Innovation and Applied Studies
ISSN 2028-9324 Vol. 3 No. 4 Aug. 2013, pp. 1015-1024

http://www.issr-journals.org/ijias/

Theorems of Forming and Summing of Natural Numbers and Their Application

Manaye Getu Tsige

Department of Agricultural Engineering,
School of Engineering, Adama science and Technology University,
Adama, Ethiopia

ABSTRACT: This paper presents the way to form other set of natural numbers from a given set of natural numbers and formulae to determine the sum of resulting numbers. The other set of natural numbers can be formed either by arranging a given natural numbers in specific order that is by using the principles of permutation rule or by using the principle of product rule provided that a given set of natural numbers should contain equal number of digits. The major areas of study to carry out this particular research work are probability rule, counting principles like permutation rule and product rule, and geometric series. Paper contains some essential theorems that help to arrive at main findings. The objective of this paper is to contribute additional knowledge to the Mathematical and Statistical science. The research results are two fundamental theorems and their applications in Mathematics, Statistics and other expected field of study. They are used to analyze complex numerical data computation and to create a password for a given numerical data with its importance to protect information flow management within a socio economic organization. The findings are foot step for the other related findings and applications that will be presented in the future. The future expected formulas or equations help to solve some difficult scientific and socio economic problems and also to derive approximation formula.

KEYWORDS: natural numbers, probability rule, product rule, permutation rule, geometric series.

1 INTRODUCTION

It is very elementary and obvious that digits are used to form numbers. In this paper any given set of natural numbers are used to form other set of natural numbers either by arranging numbers in specific order(by using the principle of permutation rule) or by using the principle of product rule provided that a given set of natural numbers should contain equal number of digits. The possible areas of study to carry out this particular research work are counting principles (product and permutation rules), probability rule and geometric series.

1.1 PRODUCT RULE

References [1], [2], [3], [4] and [5] suggest that if the sequence of *n* events in which the first one has k_1 possibilities and the second events has k_2 possibilities and then third has k_3, and forth, the total number of possibilities of the sequence will be:

$$k_1 * k_2 * k_3 \ldots . k_n$$

1.2 PERMUTATION RULE

The arrangement of *n* objects in specific order using *r* objects at time is called a permutation of *n* objects talking r objects at time [6]-[7].

Corresponding Author: Manaye Getu Tsige (getumanaye100@gmail.com)

$$nPr = \frac{n!}{(n-r)!}$$

1.3 GEOMETRIC SERIES

It is the sum of terms of geometric sequence. If the ratio between successive terms of sequence is constant, then the sequence is geometric progression [8].

Let $a_1,\ a_2,\ a_3, \ldots a_n$ is geometric sequence

$$\frac{a_2}{a_1} = \frac{a_3}{a_2} = \cdots \frac{a_n}{a_{n-1}} = r$$

The n[th] terms of the geometric sequence is given by

$$a_n = a_1 r^{n-1}$$

The sum of finite geometric series is given by [9]-[10]

$$\sum_{n=1}^{M} a_1 r^{n-1} = a_1 \frac{1-r^M}{1-r}$$

1.4 CLASSICAL DEFINITION OF PROBABILITY

Suppose we have an experiment and its sample space has finitely many elements, each of which is equally likely to occur. Then for an event E, the probability of E, denoted by $P(E)$, is defined by [11], [12], [13]

$$P(E) = \frac{number\ of\ element\ in\ E}{number\ of\ element\ in\ S}$$

1.5 PROBABILITY RULE

The sum of the probabilities of outcome in the sample space is one [14].

2 MATERIALS AND METHODS

2.1 STEPS TO ARRIVE AT TWO FUNDAMENTAL THEOREMS

Use $\boldsymbol{M}$ numbers of dissimilar digits (natural numbers) and form different $\boldsymbol{X}$ digits natural numbers by arranging digits in specific order (by using the principle of permutation rule) and by using the principle of product rule. Use permutation rule and Product rule to count $\boldsymbol{X}$ digits numbers, they are $\frac{\boldsymbol{M}!}{(\boldsymbol{M}-\boldsymbol{X})!}$ and $\boldsymbol{M^X}$ respectively. Study the distribution of digit $\boldsymbol{d_i}$ at a given $\boldsymbol{Z}$ places of $\boldsymbol{X}$ digits numbers, the probability of digit $\boldsymbol{d_i}$ will to be appear at a given $\boldsymbol{Z}$ places (for instance, at unit places of $\boldsymbol{X}$ digits numbers) is calculated by using the classical definition of probability.

$$P(d_i) = \frac{n(d_i)}{n(x)} \quad (1)$$

Where $n(\boldsymbol{d_i}) =$ number of digit $\boldsymbol{d_i}$ at a given $\boldsymbol{Z}$ places

$n(\boldsymbol{x}) =$ number of all $\boldsymbol{X}$ digits numbers

If $\boldsymbol{X}$ digits numbers are formed by using the principle of product rule, then

$$n(x) = M^X$$

Substitute it into equation (1)

$$P(d_i) = \frac{n(d_i)}{M^X} \quad (2)$$

Let digit and its respective probability is $\boldsymbol{d_1}, \boldsymbol{d_2}, \ldots \boldsymbol{d_M}$ and $\boldsymbol{P(d_1)}, \boldsymbol{P(d_2)}, \ldots \boldsymbol{P(d_M)}$ respectively. It is Mathematical fact that each digit has equal chance to be appear at a given $\boldsymbol{Z}$ places. If digit $\boldsymbol{d_i}$ is any digit from a given digits, therefore:

$$P(d_1) = P(d_2) = \cdots = P(d_M) = P(d_i) \quad (3)$$

Since the sum of the probabilities of outcome in the sample space is one, then

$$P(d_1) + P(d_2) + \cdots + P(d_M) = 1 \quad (4)$$

Substitute equation (3) into (4)

$$P(d_i) + P(d_i) + \cdots + P(d_i) = 1$$

Since the number of digits is equal to $\boldsymbol{M}$, then

$$M * P(d_i) = 1 \quad (5)$$

Substitute equation (2) into (5)

$$M * \frac{n(d_i)}{M^X} = 1$$

$$n(d_i) = \frac{M^X}{M} = M^{X-1} \quad (6)$$

Similarly, if $\boldsymbol{X}$ digits numbers are formed by arranging numbers in specific order (by using the principles of permutation rule), then $n(d_i)$ can be calculated by

$$n(d_i) = \frac{(M-1)!}{(M-X)!} \quad (7)$$

Defined notation: In similar way as digits, use $\boldsymbol{M}$ numbers of dissimilar $\boldsymbol{T}$ digits natural numbers and form different $\boldsymbol{N}$ digits natural numbers by arranging $\boldsymbol{T}$ digits numbers in specific order(by using the principle of permutation rule) and by using the principle of product rule.

If $\boldsymbol{G}$ is the numbers of $\boldsymbol{T}$ digits numbers that makeup one $\boldsymbol{N}$ digits number, then it is determined by

$$G = \frac{N}{T}$$

Equations (6) and (7) hold true if when digits are used to form numbers. If $\boldsymbol{T}$ digits numbers are replaced in the place of digits and they are used to form numbers, and then equations (8) and (9) can be derived in similar way as equations (6) and (7). They are used to determine the number of similar $\boldsymbol{T}$ digits numbers provided that it traces the similar meaning as above.

If $\boldsymbol{N}$ digits numbers are counted using the product rule, then

$$n(T_i) = M^{G-1} \quad (8)$$

If $\boldsymbol{N}$ digits numbers are counted using the permutation rule, then

$$n(T_i) = \frac{(M-1)!}{(M-G)!} \quad (9)$$

Where T_i is the any $\boldsymbol{T}$ digits number from a given set of $\boldsymbol{T}$ digits numbers.

State equations (8) and (9) as theorem of counting:

2.1.1 THEOREM OF COUNTING

If $\boldsymbol{M}$ numbers of $\boldsymbol{T}$ digits natural numbers are used to form $\boldsymbol{N}$ digits natural numbers by arranging $\boldsymbol{T}$ digits natural numbers in specific order (by using the principle of permutation rule) and by using the principle of product rule, then the number of similar $\boldsymbol{T}$ digits numbers ($\boldsymbol{T_i}$) at the same order places of $\boldsymbol{N}$ digits numbers is equal to $\frac{(\boldsymbol{M-1})!}{(\boldsymbol{M-G})!}$ and $\boldsymbol{M^{G-1}}$ respectively.

2.1.2 THEOREM OF SUBSTITUTING

If different $\boldsymbol{N}$ digits natural numbers are formed by arranging $\boldsymbol{T}$ digits natural numbers in specific order (by using the principle of permutation rule) and by using the principle of product rule, then the sum of $\boldsymbol{N}$ digits numbers is equal to the sum of each number obtained by replacing all $\boldsymbol{T}$ digits numbers that are at lowers order place by a $\boldsymbol{T}$ digits number ($\boldsymbol{T_i}$) that is at higher order place of each $\boldsymbol{N}$ digits number.

This theorem is proofed to be true since all $\boldsymbol{T}$ digits numbers have equal chance to hold any order place of $\boldsymbol{N}$ digits numbers. Suppose digits 3 and 6 are used to form two digits numbers ($N = 2$) by using the principle of product rule. Those two digits numbers are 33, 36, 63 and 66.

Table 1. Theorem of substituting

Before substituting	After substituting
36	33
63	66
33	33
66	66

From table 1

$36 \longrightarrow 33 = 3 * \underline{11}$ given that $N = 2$

$63 \longrightarrow 66 = 6 * \underline{11}$ given that $N = 2$

$33 \longrightarrow 33 = 3 * \underline{11}$ given that $N = 2$

$66 \longrightarrow 66 = 6 * \underline{11}$ given that $N = 2$

$36 + 63 + 33 + 66 = 33 + 66 + 33 + 66 = 2(3 + 6) * \underline{11}$

2.1.3 STEPS CONTINUING FROM THEOREM OF SUBSTITUTION

Focus on underlined right side product. For the sake of study, consider one among $\boldsymbol{N}$ digits numbers since the right side product is the same for the same set of $\boldsymbol{N}$ digits numbers. The right side product varies as function of $\boldsymbol{N}$ and $\boldsymbol{T}$.

If when digits are used to form $\boldsymbol{N}$ digits numbers (let 3, 5 and 8)

$3 \longrightarrow 3 = 3 * \underline{1}$ given that $N = 1$

$35 \longrightarrow 33 = 3 * \underline{11}$ given that $N = 2$

$358 \longrightarrow 333 = 3 * \underline{111}$ given that $N = 3$

- - - -

If when two digits numbers are used to form $\boldsymbol{N}$ digits numbers (Let 36, 54 and 89)

$36 \longrightarrow 36 = 36 * \underline{1}$ given that $N = 2$

$3654 \longrightarrow 3636 = 36 * \underline{101}$ given that $N = 4$

$365489 \longrightarrow 363636 = 36 * \underline{10101}$ given that $N = 6$

- - - -

If when three digits numbers are used to form $\boldsymbol{N}$ digits numbers (Let 361, 542 and 893)

$361 \longrightarrow 361 = 361 * \underline{1}$ given that $N = 3$

$361542 \longrightarrow 361361 = 361 * \underline{1001}$ given that $N = 6$

$361542893 \longrightarrow 361361361 = 361 * \underline{1001001}$ given that $N = 9$

- - - -

In general, if $\boldsymbol{N}$ digits numbers are formed from digits, two digits numbers, three digits numbers or any $\boldsymbol{T}$ digits numbers, then the corresponding underlined right side products are:

Digits($T = 1$) : $1, 11, 111, 1111, \ldots$.

Two digits numbers($T = 2$) : $1, 101, 10101, 1010101, \ldots$.

Three digits numbers($T = 3$): $1, 1001, 1001001, \ldots$.

T digits numbers($T = T$): $1,\ 10^T + 1,\ 10^{2T} + 10^T + 1, \ldots \sum_{i=1}^{G} 10^{T(i-1)}$

$\sum_{i=1}^{G} 10^{T(i-1)}$ is the finite sum of the geometric series with common ratio $r = 10^T$ and first term=1

The finite sum of Geometric series is determined by

$\sum_{i=1}^{G} 10^{T(i-1)} = \frac{1-r^G}{1-r}$

$\sum_{i=1}^{G} (10^T)^{i-1} = \frac{1-10^{GT}}{1-10^T} = \frac{10^{GT}-1}{10^T-1}$ (10)

The target problem is to derive formulae in order to determine the sum of $\boldsymbol{N}$ digits numbers.

Let $T_1,\ T_2,\ T_3, \ldots \ldots T_M$ are $\boldsymbol{T}$ digits natural numbers and $N_1,\ N_2,\ N_3 \ldots \ldots N_j$ are $\boldsymbol{N}$ digits natural numbers.

Each $\boldsymbol{N}$ digits number can be expressed by $\boldsymbol{T}$ digits numbers, For instance, consider the following numbers.

$N_1 = 10^{N-T} * T_1 + 10^{N-2T} * T_2 + 10^{N-3T} * T_3 + \cdots + T_M$

$N_2 = 10^{N-T} * T_4 + 10^{N-2T} * T_3 + 10^{N-3T} * T_6 + \cdots + T_M$

$N_3 = 10^{N-T} * T_M + 10^{N-2T} * T_3 + 10^{N-3T} * T_4 + \cdots + T_1$

. . .

$N_j = 10^{N-T} * T_4 + 10^{N-2T} * T_3 + 10^{N-3T} * T_2 + \cdots + T_{M-1}$

Apply theorem of substituting: $N_1 + N_2 + N_3 + \cdots + N_j = Y_1 + Y_2 + Y_3 + \cdots + Y_j$

$Y_1 = 10^{N-T} * T_1 + 10^{N-2T} * T_1 + 10^{N-3T} * T_1 + \cdots + T_1 = T_1(10^{N-T} + 10^{N-2T} + 10^{N-3T} + \cdots + 1)$

$Y_2 = 10^{N-T} * T_4 + 10^{N-2T} * T_4 + 10^{N-3T} * T_4 + \cdots + T_4 = T_4(10^{N-T} + 10^{N-2T} + 10^{N-3T} + \cdots + 1)$

$Y_3 = 10^{N-T} * T_M + 10^{N-2T} * T_M + 10^{N-3T} * T_M + \cdots + T_M = T_M(10^{N-T} + 10^{N-2T} + 10^{N-3T} + \cdots + 1)$

- - - -

$Y_j = 10^{N-T} * T_4 + 10^{N-2T} * T_4 + 10^{N-3T} * T_4 + \cdots + T_4 = T_4(10^{N-T} + 10^{N-2T} + 10^{N-3T} + \cdots + 1)$

Consider common expression of $Y_1,\ Y_2,\ Y_3$ .....Y_j

$(10^{N-T} + 10^{N-2T} + 10^{N-3T} + \cdots + 1)$ (11)

Consider Theorem of counting for the numbers formed by using the principle of product rule.

$n(T_1) = n(T_2) = n(T_3) = \cdots = n(T_M) = M^{G-1}$ (12)

Since (11) and (12) are common factors. Therefore, the sum of $\boldsymbol{N}$ digits numbers is given by

$N_1 + N_2 + N_3 + \cdots + N_j = M^{G-1}(10^{N-T} + 10^{N-2T} + 10^{N-3T} + \cdots + 1) \sum_{i=1}^{M} T_i$ (13)

Equation (14) holds true

$10^{N-T} + 10^{N-2T} + 10^{N-3T} + \cdots + 1 = \sum_{i=1}^{G} 10^{N-iT}$ (14)

$G = \frac{N}{T}$

Substitute equation (14) into (13)

$N_1 + N_2 + N_3 + \cdots + N_j = M^{G-1}(\sum_{i=1}^{G} 10^{N-iT}) \sum_{i=1}^{M} T_i$ (15)

Equation (16) holds true provided that $\boldsymbol{N}$ is the function of $\boldsymbol{T}$

$\sum_{i=1}^{G} 10^{N-iT} = \sum_{i=1}^{G} (10^T)^{i-1}$ (16)

Substitute equation (10) into (16)

$\sum_{i=1}^{G} 10^{N-iT} = \frac{10^{GT}-1}{10^T-1}$ (17)

Substitute equation (17) into (15)

$$N_1 + N_2 + N_3 + \cdots + N_j = M^{G-1}\left(\frac{10^{GT}-1}{10^{T}-1}\right)\sum_{i=1}^{M} T_i \quad (18)$$

Let $S(M,G,T,S) = N_1 + N_2 + N_3 + \cdots + N_j$

$$S = \sum_{i=1}^{M} T_i \quad (19)$$

$$S(M,G,T,S) = M^{G-1}\left(\frac{10^{GT}-1}{10^{T}-1}\right)S \quad (20)$$

Next consider theorem of counting for $\boldsymbol{N}$ digits numbers that are formed by arranging $\boldsymbol{T}$ digits numbers in specific order.

$$n(T_1) = n(T_2) = n(T_3) = \cdots = n(T_M) = \frac{(M-1)!}{(M-G)!} \quad (21)$$

Since all other step is the same as above, therefore

$$R(M,G,T,S) = \frac{(M-1)!}{(M-G)!}\left(\frac{10^{GT}-1}{10^{T}-1}\right)S \quad (22)$$

G = number of $\boldsymbol{T}$ digits natural numbers that makeup $\boldsymbol{N}$ digits natural number

$G\varepsilon\{1,2,3,4,\ldots\}$

$T = 1 \Rightarrow N = G$

$T = 2 \Rightarrow N = 2G$

$T = 3 \Rightarrow N = 3G$

- - -

$T = T \Rightarrow N = TG$

$$G = \frac{N}{T} \quad (23)$$

From possible set of digits $\{0,1,2,\ldots 9\}$, there are maximum ten different alternatives to select digit from the possible set to use it at unit,… 10^{r-1} place value of $\boldsymbol{T}$ digits natural numbers and maximum of nine different ways to use it at 10^{r} place value of $\boldsymbol{T}$ digits natural numbers.

Table 2. Place values versus different ways

Place value	10^{r}	10^{r-1}	10^{r-2}	…….	10	1
Different ways	9	10	10	…….	10	10

Maximum number of different ways= $9 * 10 * 10 * \ldots * 10 = 9 * 10^{r}$
Therefore, there are $9 * 10^{r}$ different ways to form $\boldsymbol{T}$ digits natural numbers from digits.
Draw relationship between $\boldsymbol{r}$ and $\boldsymbol{T}$ considering that $9 * 10^{r}$

$r = 0 \Rightarrow T = 1$

$r = 1 \Rightarrow T = 2$

$r = 2 \Rightarrow T = 3$

- - -

$r = r \Rightarrow T = r + 1$

$$r = T - 1 \quad (24)$$

Substitute equation (24) into $9 * 10^{r}$

Therefore, there are $9 * 10^{T-1}$ numbers of dissimilar $\boldsymbol{T}$ digits natural numbers. In other word, it can be expressed by the following inequality.

$$1 \leq M \leq 9 * 10^{T-1} \quad (25)$$

Consider equation (22)

$R(M,G,T,S) = \frac{(M-1)!}{(M-G)!}\left(\frac{10^{GT}-1}{10^{T}-1}\right)S$ provided that $M - G \geq 0$ since $0! = 1$

$M - G \geq 0 \Rightarrow M \geq G$

Therefore, for this case

$G \leq M \leq 9 * 10^{T-1}$ (26)

3 RESULTS AND DISCUSSION

3.1 TWO FUNDAMENTAL THEOREMS

State equations (20) and (22) as theorem of all summing possible and under restriction summing respectively by incorporating equations (19) and (23) with both equations and also incorporate equation (25) and (26) with (20) and (22) respectively.

3.1.1 THEOREM OF ALL SUMMING POSSIBLE

If $\boldsymbol{M}$ numbers of dissimilar $\boldsymbol{T}$ digits natural numbers are used to form different $\boldsymbol{N}$ digits natural numbers by using the principle of product rule, then the sum of $\boldsymbol{N}$ digits natural numbers is determined by

$$S(M,G,T,S) = M^{G-1}\left(\frac{10^{GT}-1}{10^{T}-1}\right)S$$

Where $S(M,G,T,S) =$ the sum of $\boldsymbol{N}$ digits natural numbers

$$S = \sum_{i=1}^{M} T_i$$

$$G = \frac{N}{T}$$

3.1.2 THEOREM OF UNDER RESTRICTION SUMMING

If $\boldsymbol{M}$ numbers of dissimilar $\boldsymbol{T}$ digits natural numbers are used to form different $\boldsymbol{N}$ digits natural numbers by arranging $\boldsymbol{T}$ digits natural numbers in specific order, then the sum of $\boldsymbol{N}$ digits natural numbers is determined by

$$R(M,G,T,S) = \frac{(M-1)!}{(M-G)!}\left(\frac{10^{GT}-1}{10^{T}-1}\right)S$$

Where $R(M,G,T,S) =$ the sum of $\boldsymbol{N}$ digits natural numbers

$$S = \sum_{i=1}^{M} T_i$$

$$G = \frac{N}{T}$$

Example1. Numbers 22, 24 and 67 are used to form different four digits natural numbers by applying the principle of product rule. What is the sum of four digits numbers?

First list down four digits numbers by following arrow diagram below

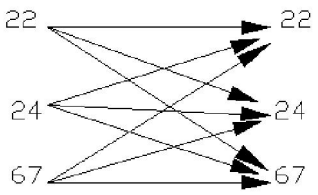

Those four digits numbers are: 2222, 2224,2267,2422,2424,2467,6722,6724 and 6767

The sum of four digits numbers= $S(M,G,T,S)$

Two digits numbers used to form numbers($T=2$)

Three 'two digits numbers' used to form numbers($M=3$)

Formed numbers are four digits numbers ($N=4$)

$G=\frac{N}{T}=\frac{4}{2}=2$

$S=\sum_{i=1}^{M}T_i=T_1+T_2+T_3+\cdots+T_M$

$T_1=22,\ T_2=24,\ T_3=67$

$S=\sum_{i=1}^{3}T_i=T_1+T_2+T_3=22+24+67=113$

$S(M,G,T,S)=M^{G-1}\left(\frac{10^{GT}-1}{10^{T}-1}\right)S$

$S(3,2,2,113)=3^{2-1}\left(\frac{10^{2*2}-1}{10^{2}-1}\right)*113=34239$

Therefore, $2222+\ 2224+2267+2422+2424+2467+6722+6724+\ 6767=\ 34239$

Example2. What is the sum of four digits natural numbers that are formed by arranging two digits natural numbers in specific order (by using the principle of permutation rule) in example1 above?

In this case, those four digits natural numbers are: 2224, 2267,2422,2467,6722 and 6724

$R(M,G,T,S)=\frac{(M-1)!}{(M-G)!}\left(\frac{10^{GT}-1}{10^{T}-1}\right)S$

$R(3,2,2,113)=\frac{(3-1)!}{(3-2)!}\left(\frac{10^{4}-1}{10^{2}-1}\right)*113=22826$

Therefore, $2224+\ 2267+2422+2467+6722+\ 6724=22826$

4 APPLICATIONS

4.1 MATHEMATICS AND STATISTICS

The operation of two fundamental theorems (adding, summing, multiply and dividing one formula by other) is helpful for numerical data analysis. It provide easy way for the complicated numerical data analysis (average, sum, recover and omit numerical data for wise use of time and space available).

4.2 PASSWORD WITH INCREASING CHANCE OF CONFUSION

Theorems act as temporary passwords so then the immediate access of data on paper can be protected by increasing chance of confusion. The values for variables M,G,T and S are given since then it is possible to find the sum without listing down numerical data records by using only variables M,G,T and S. To know individual numerical data record the values of $\boldsymbol{T_i}$ should be given. The value of $\boldsymbol{T_i}$ is hidden and protected by passwords $S(M,G,T,S)$ and $R(M,G,T,S)$. It is also possible to find the probable value of $\boldsymbol{T_1}$ but one cannot tell which value exactly it is. As value of $\boldsymbol{S}$ increases, the chance of confusion increases for $\boldsymbol{T_1}$. Hereinafter, $\boldsymbol{S}$ is called numerical data locking number and referencing number since it contains information to handle data in short form and to recover data from password respectively. Password is supposed to be advantageous for information flow management within a socio economic organization.

Example3. Protect the following numerical data on this page from immediate access.

Table 3. Account data record

List of bank account	Amount of account
B	33
C	39
D	93
E	99

Let $S(M,G,T,S) = 33 + 39 + 93 + 99 = 264$

Consider theorem of all summing possible

$S(M,G,T,S) = M^{G-1}\left(\frac{10^{GT}-1}{10^{T}-1}\right)S$

The value for variables M, T and N is determined by referring the numerical data given.

$N = 2,\ T = 1,\ M = 2$

$G = \frac{N}{T} = \frac{2}{1} = 2$

$S(2,2,1,S) = 2^{2-1}\left(\frac{10^{2*1}-1}{10-1}\right)S = 264$

$22S = 264$

$S = \frac{264}{22} = 12$

Therefore, password is $S(2,2,1,12)$. It tells sum result but it does not tell about individual data record. To know individual data records the value of T_1 and T_2 should be known. $S = T_1 + T_2 = 12$, there is the probability to find different pairs of digits having sum 12. For instance, if $T_1 = 4$, then $T_2 = 8$, if $T_1 = 7$, then $T_2 = 5$, if $T_1 = 3$, then $T_2 = 9$ etc. This increases the chance of confusion for non-data user. Therefore, numerical data given above can be protected from immediate access by using password $S(2,2,1,12)$ because the values for variables $T_1 = 3$ and $T_2 = 9$ are in the user memory.

5 CONCLUSION

In general, the future implication of this paper is that it provides foot step to derive other related findings and applications that will be presented in the future. These have advantage to solve some difficult scientific and socio economic problems and to derive approximation formula.

ACKNOWLEDGMENT

Above all I thank God for all things happen. Next I would like to bring heartfelt thanks to Dr. Yewelsow, Dr. Ayele Taye, Dr. Nigatu, Mr. Abraham Tulu, Mohammed Nuri, Assegid Chernet , Bishaw Taddele and Applied Mathematics department committee members-2008 from Hawassa University for their big support, comment and encouragement from very beginning. I thank Dr. Brahanu from Addis Ababa University for his excellent encouragement and comment and I thank all my family especially Getu Tsige and Muluwork Admase. My thanks also goes to Hayleyesus Kamso, Alemu Amelo, Tesfahun Hatya, Getahun Heramo, Mickias Girma, Melaku Teshome, Lissanwork Tilahun and Manuhe Mircana.

REFERENCE

[1] Triola, M.F., *Elementary Statistics*, Pearson Education, Boston, USA, 2012.
[2] Walpole, R.E., Myers, R.H., Myers, S.L., and Keying Ye, *Probability and Statistics for Engineers and Scientists*, Pearson education, Boston, USA, 2012.
[3] Weiss, N., *Introductory Statistics*, Pearson education, Boston, USA, 2008.
[4] Koshy, T., *Discrete Mathematics with Applications*, Academic Press/Elsevier, 2005.
[5] Rosen, K.H, *Discrete Mathematics and its Applications*, Mc Graw-Hill companies, Inc., China, 1998.
[6] Allan G. Bluman, *Elementary Statistics*, McGraw-Hill Education, ISBN 0071154310, 1997.
[7] Riley, K.F, Hobsonand, M.P., and Bence, S.J, ''Mathematical Methods for Physics and Engineering,'' *Press syndicate of the University of Combridge*, 975 p., 2005.

[8] Solomon, R.C., *Advanced level Mathematics*, London: DP publications, 1992.
[9] Larson, R., and Hosteller, R.P., *Algebra and Trigonometry*, Houghton Mifflin Company, 2001.
[10] Stewart, J., *Calculus Concepts and Contexts*, Gary W. Ostedt publisher, 2001.
[11] Pal, N., and Sarkar, S., *Statistics Concepts and applications*, Prentice-Hall of India private limited, New Delhi, India, 2005.
[12] Gupta, C.B., and Gupta, V., *An introduction to Statistical Methods*, VIkas publishing enterprise PVT LTD, 2004.
[13] Harrison, M., and Wadsworth, Jr., *Hand book of Statistical Methods for Engineers and Scientists*, Mc Graw-Hill, 1990.
[14] Kreyszig, E., *Advanced Engineering Mathematics*, John Wiley and Sons, Inc., USA, 2006.

International Journal of Innovation and Applied Studies
ISSN 2028-9324 Vol. 3 No. 4 Aug. 2013, pp. 1025-1032

http://www.issr-journals.org/ijias/

Scalable TDB based RSUs deployment in VANETs

Ramneek Kaur and Ravreet Kaur

Department of Computer Science,
Guru Nanak Dev University,
Amritsar, Punjab, India

ABSTRACT: Vehicular ad hoc networks (VANETs) are the flaming topic of research. VANET comprises of moving vehicles communicating with each other. VANETs involve three types of communication: vehicle to vehicle (V2V), vehicle to roadside (V2R) or vehicle to infrastructure (V2I) communication. VANETs consist of some vital components: RSU, OBU and Trusted Authority. Among them Roadside units (RSUs) are one of the fundamental components of Vehicular ad hoc network (VANET). Roadside Units (RSUs) are placed across the road for infrastructure communication. But the deployment cost of RSUs is very high, so to deploy more and more number of RSUs across roads is quite expensive. Thus, there is a need to optimally place a limited number of RSUs in a given region or road in order to achieve maximum performance. In this paper, we present a solution to this problem using parallel processing. A so-called scalable TDB based RSUs deployment algorithm with a goal of minimizing the parallel time taken to place roadside units in a given area and to attain high efficiency and cover maximum area has been presented. The performance of the proposed algorithm and optimization strategy is assessed by evaluating different parameters like efficiency, power consumption, serial elapsed time, parallel elapsed time, speedup and overheads incurred in running the algorithm in parallel.

KEYWORDS: VANETs, RSUs, Scalable TDB, Efficient, Deployment, Speedup, Overhead, Scalability.

1 INTRODUCTION

Vehicular networks are being used for a plethora of applications including enabling automotive safety. Intelligent transportation systems can also leverage these vehicular networks to enable applications such as traffic congestion prediction, mitigation and dissemination [1]. Vehicular Networks deploy the concept of continuously varying vehicular motion. The nodes or vehicles in VANETS can move around with no boundaries on their direction and speed. Vehicular adhoc network (VANET) involves vehicle to vehicle (V2V), vehicle to roadside (V2R) or vehicle to infrastructure (V2I) communication [2], [6]. VANET generally consists of On Board Unit (OBU) and Roadside Units (RSUs). OBUs enables short-range wireless ad hoc network to be formed between vehicles. Each vehicle comprises of hardware unit for determining correct location information using GPS. Roadside Units (RSUs) are placed across the road for infrastructure communication [6]. The number of RSU to be used depends upon the communication protocol. However due to the high cost of deployment of RSUs, it is desirable to cover maximum area with minimum cost.

Corresponding Author: Ramneek Kaur (ramneek4025@gmail.com)

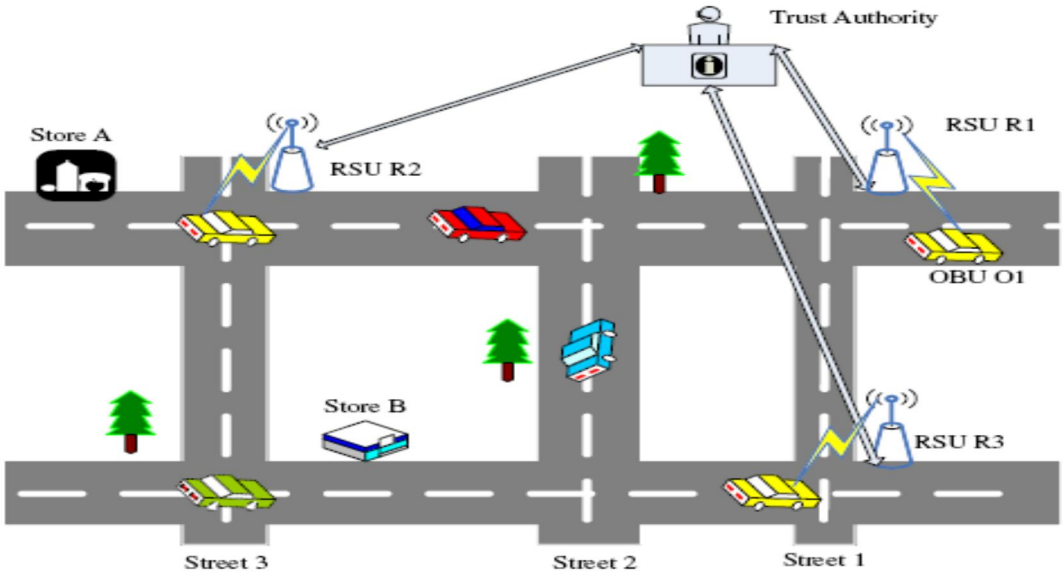

Fig. 1. System Model

VANET provide assistance to vehicle drivers for communication and coordination among themselves in order to avoid any critical situation through Vehicle to Vehicle communication [2] e.g. road side accidents, traffic jams, speed control, free passage of emergency vehicles and unseen obstacles etc. Besides safety applications VANET also provide comfort applications to the road users. Due to the dynamic nature of nodes in VANET the routing of data packets is much complex. Several factors like the type of the road, daytime, weather, traffic density and even the driver himself affect the movements of vehicles on a road. Hence, the network topology change frequently, and the routing protocol used has to adapt itself to these instantaneous changes continuously [2].

2 SYSTEM MODEL

As illustrated in Fig. 1, a typical VANET consists of three entities in city scenarios: the top TA, the fixed RSUs along the road side, and the mobile OBUs equipped on the running vehicles [6].

2.1 TA

TA is in charge of the registration of the RSUs and OBUs. TA can reveal the real OBU identity of a safety message and publishes the CRL periodically to the RSUs. Moreover, TA can be a road authority, such as the government. It has the basic information about streets and traffic statistics, and proposes the RSUs deployment plan according to the tradeoff between the requirements of most OBUs and the investment budget.

2.2 RSU

RSUs are erected at intersections for the considerations of power and management. RSUs use the same communication technology and the deployment cost is constant at any intersections. RSUs connect with TA by wired links, and act as certificate proxies of TA. An RSU can issue short-time certificates for the OBUs with valid membership.

2.3 OBU

Each OBU has a long-term unique identity. OBUs mainly communicate with each other for sharing local traffic information, and with the RSUs for updating the short time certificates. Digital maps are available for the OBUs. It provides the street-level map, the communication coverage of RSUs and the traffic statistics such as vehicle speed on roads, and traffic signal schedule at intersections.

3 RELATED WORK

Earlier works in optimal placement in VANET [6] include:

Y. Liang et. al in [1] has proposed a novel optimization framework for Roadside Unit (RSU) deployment and configuration in a vehicular network. Their objective is to minimize the total cost to deploy and maintain the network of RSU's. A user specified constraint on the minimum coverage provided by the RSU is also considered. The efficiency and scalability of the optimization procedure for large scale problems are also studied.

Sun et al. optimize the location of RSUs such that vehicle can reach an RSU within some timing constraint, given by sum of driving time and an overhead time (for adjusting the route), to update short term certificates. The optimization scheme may require vehicles to change their route which may have effects on local traffic condition. We do not have any route changing condition; we optimally place the RSUs considering the vehicles current routes only.

Lee et al. [4] seek optimal placement of RSUs to improve connectivity. Each intersection is considered as a potential RSU location. These potential locations are then ordered based on number of vehicle-reports received within communication range of each RSU. The placement scheme only considers taxi location reports and does not consider speed or density of all vehicles.

Li et al. [5] consider the optimal placement of gateways, which connect RSUs (access points - AP) to the Internet, while minimizing the average number of hops from APs to gateways. They consider pervasive APs such that every vehicle is connected to an AP. They do not consider vehicle speed, density or movement patterns.

Lochert et al. [7] use genetic algorithm for optimal placement of RSUs for a VANET traffic information system. The optimal placement is to minimize travel for some fixed landmarks and may not be useful for travel between any two points in an area.

Zhao et al. [8] optimize placement of Thowboxes, standalone units that act as relays, to improve contact and data-rate/throughput within context of a delay tolerant network. They aim at improving V2V communication and not the V2I communication.

Fiore et al. [9] optimally place RSUs (Access Points -AP) in an urban environment to improve cooperative download of data among vehicles. They aim at placing the APs at point where maximum vehicles cross each other, this helps in relaying the data from AP to a downloading vehicle via other vehicles.

Trullols et al. [10] optimally deploy RSUs (Dissemination Points – DPs) in an urban area to maximize the number of vehicles that contact the DPs.

Malandrino et al. [11] optimally deploy the RSUs (APs) to maximize the system throughput. They consider both the V2I (or I2V) and V2V communications for optimal placement of APs. Vehicle trajectory information (time and location) forms basis of this optimization which may not be available in many cases.

Zheng et al. [12] optimally deploy APs to improve contact opportunity; defined in terms of time for which a user remains in contact with an AP. These optimizations aims at transfer of data from RSUs to vehicles whereas, our optimization aims at transfer of data from vehicles to RSUs with an area coverage constraint. Also, we do not consider V2V communication in our optimization problem.

4 PARALLEL PROCESSING

Parallel processing is an efficient approach to meet the computational constraints of a large number of the current and emerging applications. Parallel processing is an efficient form of information processing which emphasizes the exploitation of concurrent events in the computing process. Parallel processing demands concurrent execution of many programs in the computer. It is in contrast to sequential processing. It is a cost-effective means to improve system performance through concurrent activities in the computer. So, we have used this approach to deploy RSUs efficiently. The main steps adopted during implementing the process are as:

- Application Specification : RSUs deployment in VANETs is chosen as application
- Subtask Decomposition: Fork and Join Construct is used to divide the problem into subtasks.
- Scheduling: Scheduling is done using Scalable Task Duplication Based RSU Deployment Algorithm (given later on).
- Programming: Writing executable program both in serial and in parallel.

5 PROBLEM STATEMENT

This paper deals with utilizing the fork and join algorithms in VANETs, for efficiently deploying RSUs in given area or road. As shown in literature survey the cost of the RSUs are too high so we are not able to deploy more and more RSUs to cover the given road, so need of the hour is to deploy them optimistically, such that the minimum number of RSUs can cover maximum range. But we have found that optimistic deployment of RSUs takes too much time i.e. serial time. So in order to reduce the amount of time required doing the same, we have proposed a new strategy of RSUs deployment which will use fork and join algorithms using TDB in such a way, so that it will result in the reduction of execution time. The overall objective is to deploy RSUs in the minimum time, to cover more and more area and to improve efficiency.

Throughout the paper emphases is on the parallel algorithm in VANETs, so no other VANET problems are considered in this research work**.** The proposed algorithm is also scalable. It gives better results till 45 no. of RSUs**.**

6 PROPOSED METHODOLOGY

Scheduling and allocation is a highly important issue since an inappropriate scheduling of tasks can fail to exploit the true potential of the system and can offset the gain from parallelization [12]. The objective of scheduling is to minimize the completion time of parallel application by properly allocating the tasks to the processors.

In this paper task duplication based scheduling is applied for optimizing the placement of roadside units. The task duplication scheduling provides greater efficiency and minimum make span time as compared to other scheduling techniques. The main idea behind the task duplication based scheduling is utilizing processor idle time to duplicate predecessor tasks [13]. This can avoid the transfer of data from a predecessor to a successor thus reducing the communication cost, network overhead and potentially reduce the start times of waiting task Task duplication scheduling provides better results than the serial placement of roadside units.

The new '**Scalable TDB based RSU deployment'** algorithm has been proposed. The scalability of the algorithm can be increased up to 50 number of RSUs. This algorithm works by using fork and join technique. The fork divides the job into equal parts and on each part the algorithm is applied simultaneously. The flag bit is assigned to each processor the when which will get free first will set its flag bit and the coming process will be allocated to that processor.

Following steps are included in the proposed algorithm:

Step I: Define the number of RSUs, the dimensions of the vanet area or road and initially place the first seed. Rest of the seeds will be placed randomly accordingly.
Step II: Deploy network considering parameters in step I.
Step III: Apply Task Duplication Based Scheduling Parallel algorithm using fork method. Fork will divide the job into equal parts on the basis of the number of matlab clients in the matlabpool.
Step IV: Apply optimistic RSUs deployment algorithm on each set separately. The solutions thus obtained will be joined.
Step V: If the result thus obtained is not optimal then repeat from stepIII, until the optimistic deployment is achieved.
Step VI: Evaluate parallel parameters and compare the results.
Step VII: End.

The above algorithm is developed and designed in matlab. The experimental results are obtained by running the proposed algorithm on matlab. Matlab provides an interactive software package. It has inbuilt toolboxes which we have used in calculating results. The variance in the results is achieved by running the algorithm serially and in parallel for deploying the RSUs. Serial and Parallel deployment of RSUs is compared using some metrics. Some of them are:

1. **Sequential Time:** This gives the serial elapsed time experienced by a particular job when run on a given system. It is denoted by $T_{s.}$

2. **Parallel Elapsed Time:** It is the time required to run the program on an n-processor parallel computer. It is denoted by $T_{p.}$

3. **Speed up:** Speedup is the ratio between sequential execution time and parallel execution time where the sequential time execution time is sum of total computation time of each task and parallel time execution is the scheduling length on limited number of processors.

$$S_P = (\sum^{n}_{i=1} T_i) / T_p$$

4. **Efficiency**: The efficiency of a parallel program is a measure of processor utilization.

$$EFF = S_P / N_P$$

S_P : Speed up and N_P: Number of processors

5. **Power consumption**: It gives the total power consumed by the unit. It can be calculated by adding up the power of each individual unit.

$$Pc = \sum (\text{power consumed by each unit})$$

6. **Overheads**: It gives the overhead incurred in running the algorithm in parallel on multiple clients.

$$O = \text{parallel time} / (\text{serial time/no. of processors or clients})$$

7 Results and Discussion

We have carried out the experimental work in Matlab technology. Various parameters have been evaluated by taking different values of road side units, side dimensions and random seed placement. Comparisons on the basis of serial elapsed time, parallel elapsed time, speed up and efficiency has been done. The results are as:

7.1 Results and analysis of Road Side Units

Figure below shows the variance of serial elapsed time and parallel elapsed time with the increase in number of road side units.

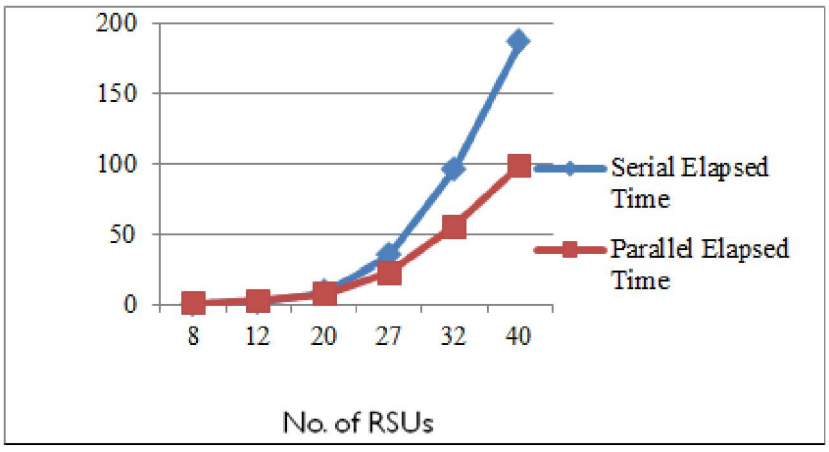

Fig. 2. Plot showing no. of RSUs and serial and parallel time

Fig. 2 shows that the serial elapsed time increases significantly with increase in the number of road side units. Initially for 8 and 12 rsus the serial elapsed time is more than the parallel elapsed time. After 20 rsus the serial elapsed time is much more than the parallel elapsed time.

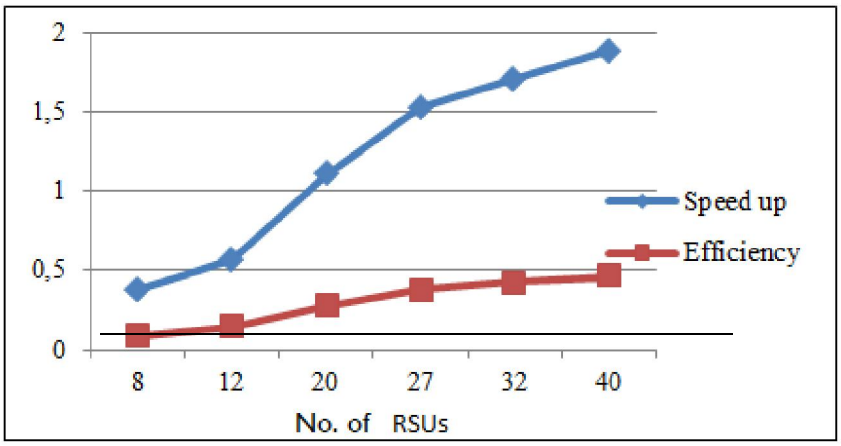

Fig. 3. Plot showing no. of RSUs and speedup and efficiency

The above plot shows the variation of speedup and efficiency with increase in number of RSUs.

The speedup increases significantly with increase in number of RSUs. But increase in efficiency is small.

7.2 RESULTS AND ANALYSIS OF SIDE DIMENSIONS

The figure4 shows the variation of serial time and parallel time against the changing side dimensions. It describes that what will be the effect of changing side dimensions on the serial elapsed time and parallel elapsed time.

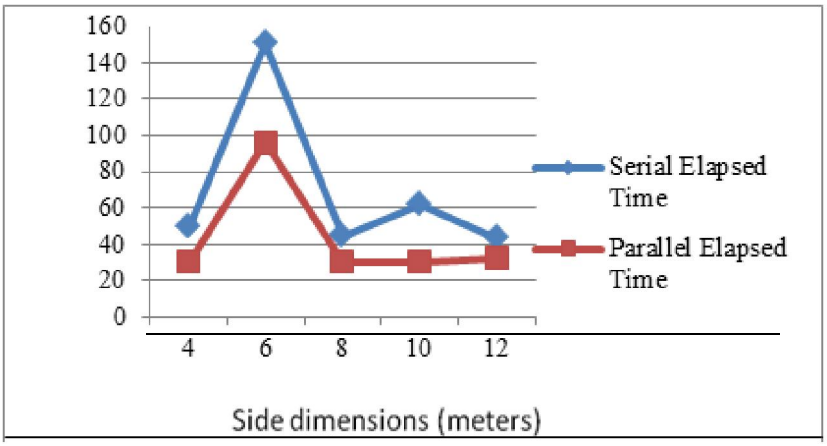

Fig. 4. Plot showing variance in serial and parallel time

The results of figure 4 shows that with increase in side dimension serial elapsed time increase to certain limit and then vary irregularly. As in fig. we can see that serial elapsed time increases up to 6 meters side and after that at 8meters dimension it falls and at 10 meters it again rises but a little.

Similarly parallel time increases but not much as compared to serial time and then falls and become almost constant. It concludes that you can get better parallel results by increasing side dimensions up to a certain limit.

Figure 5 shows the measure of speedup and efficiency against the increasing side dimension. The fig5 is showing that the speedup upto a certain limit decreases with increase in side dimensions after that it rises and again falls to a certain fixed value. The decrease in speedup shows that increase in side dimension up to a certain limit gives less parallel RSU deployment time. The efficiency is almost constant. It shows small fluctuations with increase in side dimensions.

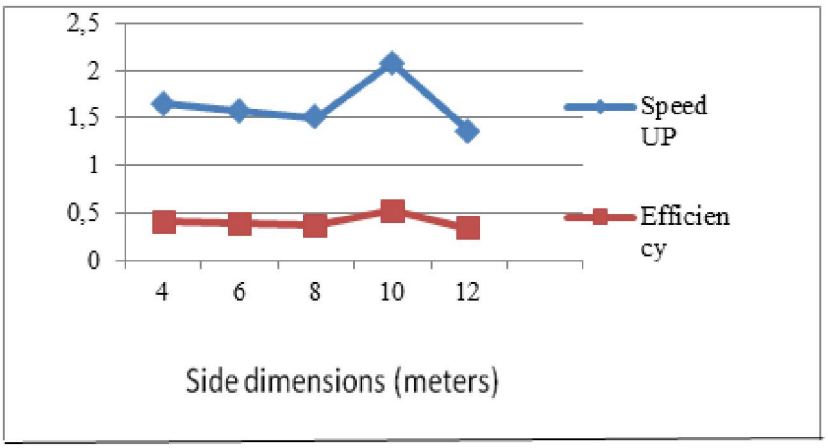

Fig. 5. Plot showing speedup and efficiency against changing dimensions

8 CONCLUSION AND FUTURE WORK

The main contribution of this paper have been the proposal of an approach for optimizing the placement of networked roadside infrastructure—supporting units—based on 'Scalable TDB based RSUs deployment' algorithm. The maximization of the network coverage and minimization of cost are considered as conflicting objectives to be achieved. It is shown that the task duplication scheduling provides greater efficiency and minimum make span time. The main idea behind the task duplication based scheduling is utilizing processor idle time to duplicate predecessor tasks. This paper gives related analysis for the optimistic deployment of RSUs. The results show that all the parameters vary with the change in the number of roadside units and side dimensions. With the increase in number of RSUs the increase in parallel elapsed time is less as compared to the large increase in serial elapsed time. Thus the proposed algorithm has great implication for large number of RSUs. The speedup and efficiency also increases with scalability in RSUs. The increase in side dimensions is favorable upto certain limit after that there will be only minor fluctuations with further increase in side dimensions.

In the near future research work can be extended in making this approach more suitable for realistic world. In this paper more emphasis is on parallel processing. But there are great number of issues in VANETs e.g. road side accidents, traffic jams, speed control, free passage of emergency vehicles and unseen obstacles and several other factors like the type of the road, daytime, weather, traffic density etc. which can be addressed to in future.

REFERENCES

[1] Y. Liang, H. Liu, and D. Rajan, "Optimal Placement and Configuration of Roadside Units in Vehicular Networks", *Proceedings of VTC Spring 2012*.

[2] Anup Dhamgaye and Nekita Chavhan, "Survey on security challenges in VANETS", *International journal of computer science and network*, Vol. 2, No. 1, pp. 88-96, 2013.

[3] Y. Sun, X. Lin, R. Lu, X. Shen, and J. Su, "Roadside Units Deployment for Efficient Short-time Certificate Updating in VANETs", *IEEE ICC proceedings*, 2010.

[4] J. Lee and C. Kim, "A roadside unit placement scheme for Vehicular Telematics networks", *AST*, 2010.

[5] P. Li, X. Huang, Y. Fang, and P. Lin, "Optimal placement of gateways in Vehicular Networks", *in IEEE Transactions on Vehicular Technology 2007*, Vol. 56, No. 6, pp. 3421-3430, 2007.

[6] Baber Aslam, Faisal Amjad, and Cliff C. Zou, "Optimal Roadside Units Placement in Urban Areas for Vehicular Networks", *University of Central Florida*, 2011.

[7] C. Lochert, B. Scheuermann, C. Wewetzer, A. Luebke, and M. Mauve, "Data aggregation and roadside unit placement for a VANET traffic information system", *ACM*, 15 Sept, 2008

[8] W. Zhao, Y. Chen, M. Ammar, M. Corner, B. Levine, and E. Zegura, "Capacity enhancement using Throw boxes in DTNs", *MASS* 2006.

[9] M. Fiore and J. Barcelo-Ordinas, "Cooperative download in urban vehicular networks," *MASS* 2009.

[10] O. Trullols, M. Fiore, C. Casetti, C.F. Chiasserini, and J.M. Barceló Ordinas, "Planning roadside infrastructure for information dissemination in intelligent transportation systems", *Computer Communications*, Vol. 33, No. 4, pp. 432-442, March 2010.

[11] F. Malandrino, C. Casetti, C. Chiasserini, and M. Fiore, "Content downloading in vehicular networks: What really matters," *INFOCOM*, 2011.
[12] Z. Zheng, Z. Lu, P. Sinha, and S. Kumar, "Maximizing the Contact Opportunity for Vehicular Internet Access," *INFOCOM*, 2010.
[13] Y.-K. Kwok and I. Ahmad, "Benchmarking the task graph scheduling algorithms," *IPPS/SPDP*, 1999.

International Journal of Innovation and Applied Studies
ISSN 2028-9324 Vol. 3 No. 4 Aug. 2013, pp. 1033-1044

http://www.issr-journals.org/ijias/

Design and Simulation of Edge-Coupled Stripline Band Pass Filter for U band

Pawan Shakdwipee

M.Tech (Pursuing), Arya College of Engineering & IT,
Jaipur, Rajasthan, India

ABSTRACT: In this paper, a band pass filter structure using Ansoft designer software and Matlab software simulation tool are presented. The filter is operated at U Band range in higher order 50 GHz edge-coupled Stripline band pass filter for different microwave application. For the proposed work we consider simulation using Roger R03203 substrate with dielectric constant of 3.02, Conductor Thickness 0.035 mm and Substrate Height 0.787 mm. This filter is design at a center frequency of 50 GHz with 8 GHz bandwidth. Simulation results show that the filter operation is optimum & best in this range and results show good performance and agree well with the high frequency EM full wave simulation. In this paper, band pass filter development with the assistance of the Richards-Kuroda Transformation method, is used. Moreover, measured S parameters denote the center frequency is also strongly influenced by the variation of Roger's material's dielectric constants. By analyzing the characteristics at center frequency of the filter, both theoretical and simulated data are accumulated for broadening application filed. The band pass filter exhibits advantages of small size and high reliability compared to conventional planar filter structure, which makes the band pass filter suitable for U Band communicational application. This filter shows attractive characteristics for BPF applications.

KEYWORDS: Stripline, Dielectric substrate, Chebyshev band pass filter, U band spectrum, Band pass filter.

1 INTRODUCTION

In this paper design and simulation of an edge-coupled bandpass filter realized in stripline technology is presented. The presented process includes the estimation of filter parameters using analytical formulas, the simulation of ideal and stripline transmission line models in a circuit simulator. Stripline circuit uses a flat strip of metal which is sandwiched between two parallel ground planes. The insulating material of the substrate forms a dielectric.

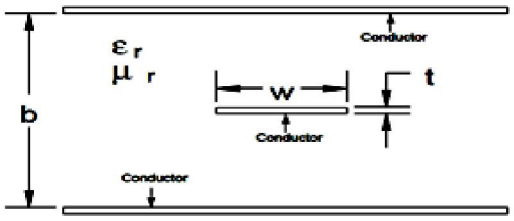

Fig. 1. Model used by Designer for edge-coupled Stripline Band pass filter

These transmission lines are compact edge-coupled stripline is used instead of microstrip line as because stripline does not suffer from dispersion losses and its propagation mode is TEM mode. Hence it is the preferred structured for coupled-line filters. Stripline is much harder fabricate than microstrip, and because of the second ground plane, the strip widths are much narrower for a given impedance and board thickness than for microstrip line [1],[2]-[3].

Corresponding Author: Pawan Shakdwipee (pawan21_uda@yahoo.in)

We describe the design and simulation of a stripline bandpass filter with Chebyshev filter response [4]. The process of designing the filter includes the usage of formulations, MATLAB software use as an equation solver and Ansoft Designer v2.2 as the circuit simulator [7].A bandpass filter is an important component must be found in the transmitter or receiver. Bandpass filter is a passive component which is able to select signals inside a specific bandwidth at a certain center frequency and reject signals in another frequency region, especially in frequency regions, which have the potential to interfere the information signals[6]-[11]. In designing the bandpass filter, we are faced the questions, what is the maximal loss inside the pass region, and the minimal attenuation in the reject/stop regions, and how the filter characteristics must look like in transition regions[10]. The development of the frequency bands in microwave filter, play an important role in many microwave applications. Through an investigation into and a subsequent implementation of filter theory, U band (40-60 GHz) range filters design is developed in this report [8],[9]-[10]. Filters are an essential part of communication and radar systems and are key items in the performance and cost of such systems [14], especially in the increasingly congested spectrum. A frequency range from 10 GHz to 66 GHz is planned as part of network standardization for point-to-point connections.

2 RESEARCH METHODOLOGY

2.1 DESIGN AND SIMULATION OF CHEBYSHEV BAND PASS FILTER

The BPF circuit is simulated with Ansoft Designer Student Version 2.2 Software in order to predict the performance of the filter. Few parameters in the circuit are analyzed and have a good relationship to microwave theory. An optimization process has been introduced along the simulation procedure focusing on the filter dimension in order to improve the response of the filter. Refer to the filter tables given in D.M Pozar and G. L. Matther [5] to find the following coefficients for a third order Chebyshev filter. Normalized element values for 0.5 dB ripple low-pass chebyshev filter given in was $g_0 = 1$, $g_1 = 1.5963$, $g_2 = 10967$, $g_3 = 1.5963$, $g_4 = 1.000$ for simulated third order filter. The band pass filter is realized as a cascade of n+1 coupled line sections as shown in table 1.

Table 1. Specifications of Edge-Coupled Stripline Band Pass Filter for U band Application

Specifications of Dielectric Material From ROGERS Corporation. RT/duroid® 3203 microwave laminates are PTFE Ceramic Reinforced Woven Glass composites designed for electronic and microwave circuit applications requiring a high dielectric constant. Dielectric Material Used Rogers R03203 from Rogers High frequency Material.		
1).	Input and Output Impedance:	Z = 50 Ohms
2).	Pass band ripple of	S_{21}: 0.5 dB
3).	Filter Order:	n = 3
4).	Pass band Centre Frequency: 50 GHz for U band	
5).	Ripple Bandwidth:	8 GHz
6).	Substrate:	Rogers R03203
7).	Conductor Thickness:	0.035 mm
8).	Dielectric Constant:	3.02
9).	Loss Tangent:	0.0016
10).	Substrate Height:	.787 mm

The sections are numbered from left to right. The source is connected at the left and the load is connected to the right. The filter could be reversed without affecting the response [2]. The results of Z_{oo} and Z_{oe}, are shown in table 3, are almost identical to that of the n=3 order approach, except an additional coupling section is used to represent the increased order. This similar result of ideal filter design is evidence that, according to the formulation, a n=3 order filter should be sufficient and get perfect simulated result. The filter design wizard (FDW) in Ansoft Designer was again utilized to formulate the lengths and widths of the physical circuit from given input of filter design and material properties. Rogers R03203 was again chosen as the dielectric, but the center frequency was chosen in U band at 50 GHz.

Table 2. Element values for equal ripple band-pass filter prototypes (g_0 = 1, ω_c = 1, n = 1 to 10 and 0.5 dB ripple)[5]

	0.5 dB Ripple										
n	g_1	g_2	g_3	g_4	g_5	g_6	g_7	g_8	g_9	g_{10}	g_{11}
1	0.6986	1.0000									
2	1.4029	0.7071	1.9841								
3	1.5963	1.0967	1.5963	1.0000							
4	1.6703	1.1926	2.3661	0.8419	1.9841						
5	1.7058	1.2296	2.5408	1.2296	1.7058	1.0000					
6	1.7254	1.2479	2.6064	1.3137	2.4758	0.8696	1.9841				
7	1.7372	1.2583	2.6381	1.3444	2.6381	1.2583	1.7372	1.000			
8	1.7451	1.2647	2.6564	1.3590	2.6964	1.3389	2.5093	0.8796	1.9841		
9	1.7504	1.2690	2.6678	1.3673	2.7239	1.3673	2.6678	1.2690	1.7504	1.0000	
10	1.7543	1.2721	2.6754	1.3725	2.7392	1.3806	2.7231	1.3485	2.5239	0.8842	1.984

2.2 CHOICE OF FILTER TYPE AND ORDER

A good band pass filter has minimal signal loss in its pass band, as well as a narrow pass band with as much out of band attenuation as possible. Chebychev filters have narrower pass band response in trade for more ripples in the pass band section. Higher order filters can have a narrower shape factor but will be physically larger in shape. The filter order will be chosen to achieve the desired bandwidth while minimizing the physical size of the filter. The filter specification goals for return loss (scatter parameter S_{11}) are >40 dB and for insertion loss (scatter parameter S_{21}) <10dB. Simulations showed a filter order of n=3 will achieve this goal. The required order for a filter meeting the given specifications is calculated below.

$$n = \frac{\cosh^{-1}\sqrt{\frac{10^{\frac{L_T}{10}}-1}{K-1}}}{\cosh^{-1}(\frac{f}{fc})} \tag{1}$$

$$n = \frac{\cosh^{-1}\sqrt{\frac{10^{\frac{L_T}{10}}-1}{K-1}}}{\cosh^{-1}(\frac{f}{fc})} = \frac{\cosh^{-1}\sqrt{\frac{10^{\frac{10}{10}}-1}{10^{5}-1}}}{\cosh^{-1}(1.4)} = \frac{\cosh^{-1}\sqrt{73.759}}{\cosh^{-1}(1.4)} = \frac{2.840}{0.8670} = 3.27 \tag{2}$$

Where L_T is the minimum attenuation at frequency f_t, and **K = 10^(L_{ar}/10),** with L_{ar} being the maximum ripple in dB allowed in the pass band. The order of the filter is a measure of the minimum number of elements to be included in the filter to realize the required amount of ripple in the pass band and attenuation at a frequency outside of the pass band. Additional elements may be included in the filter which will further improve the filter response at the cost of size and increased design time.

The following equations are used to calculate the order for edge coupled band pass filter values. Using Fig. 2 we get the value of [f_t / fc =1.4].

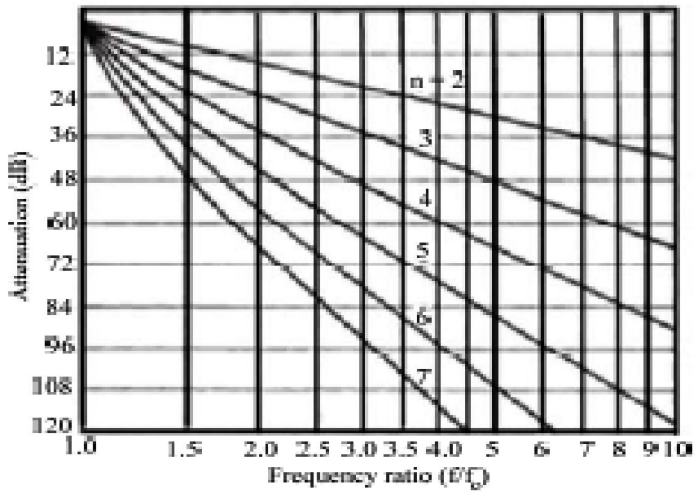

Fig. 2. Characteristics for a Chebyshev filter with 0.5dB ripple [9]

2.3 FIND THE LOW PASS PROTOTYPE

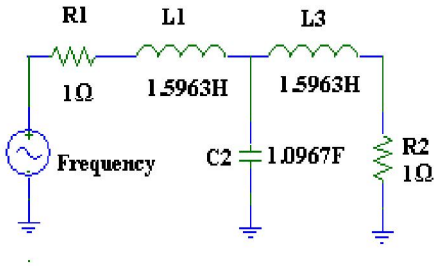

Fig. 3. Third order low pass prototype [8]

After getting the low pass filter prototype values, then it's transformed into band pass filter design. The transformation from low pass to band pass all shunt element of the low pass prototype circuit becomes parallel-resonant circuit, and all series elements become series-resonant circuit in Fig. 4.

2.4 TRANSFORMING THE LOW PASS INTO BAND PASS CONFIGURATION

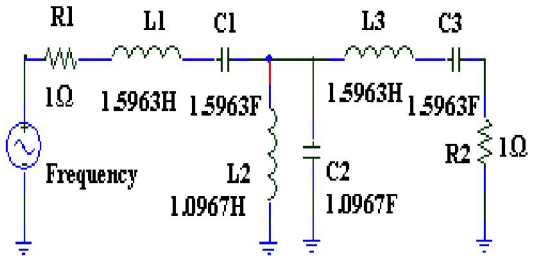

Fig. 4. Transformation third order low pass prototype to band pass prototype [8]

The transformed the filter is then frequency-scaled and impedance-scaled using the following formulas [11]

$$L_S = \left(\frac{1}{FBW \times \omega_0}\right) Z_0 \times g \quad (3)$$

$$C_S = \left(\frac{FBW}{\omega_0}\right)\frac{1}{Z_0 \times g} \quad (4)$$

$$C_P = \left(\frac{1}{FBW \times \omega_0}\right)\frac{g}{Z_0} \quad (5)$$

$$L_P = \left(\frac{FBW}{\omega_0}\right)\frac{Z_0}{g} \quad (6)$$

2.5 SCALING THE BAND PASS CONFIGURATION IN BOTH IMPEDANCE AND FREQUENCY

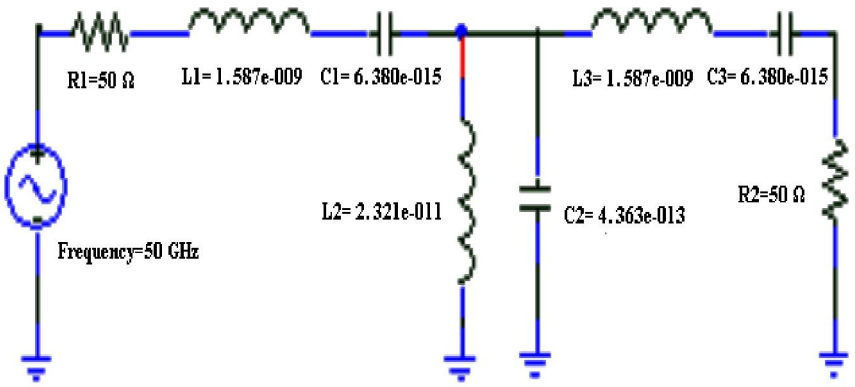

Fig. 5. Band pass prototype for designed at center frequency 50GHz

2.6 EVEN AND ODD MODES IN A COUPLED TRANSMISSION LINE

Calculation of Odd and Even Resistances to design the stripline filter, an approximate calculation is made based on the design equations [16]-[18]. The no of stages (n) = 3. The characteristic impedance Z_0 is typically 50 Ohms. The unitary bandwidth BW is given by

Where $FBW = \frac{(\omega_2 - \omega_1)}{\omega_0}$ is the fractional

$$FBW = \frac{(54 \times 10^9 - 46 \times 10^9)}{50 \times 10^9} \approx .16 \quad (7)$$

$$\frac{J_{01}}{Y_0} = \sqrt{\frac{\pi}{2}\frac{FBW}{g_0 g_1}} \quad (8)$$

$$\frac{J_{j,j+1}}{Y_0} = \frac{\pi FBW}{2}\frac{1}{\sqrt{g_j g_{j+1}}} \quad \text{For j=1 to n-1} \quad (9)$$

$$\frac{J_{n,n+1}}{Y_0} = \sqrt{\frac{\pi}{2}\frac{FBW}{g_n g_{n+1}}} \quad (10)$$

Where g_0, $g_{1...}$ g_n are the element of a ladder-type low-pass prototype with a Normalized cutoff Ωc = 1, and FBW is the fractional bandwidth of band-pass filter. $J_{j,j+1}$ are the characteristic admittances of J-inverters and Y_0 is the characteristic admittance of the terminating lines. The equation above will be used in end-coupled line filter because the both types of filter can have the same low-pass network representation. However, the implementation will be different [15].

To realize the *J*-inverters obtained above, the even- and odd-mode characteristic impedances of the coupled strip line band pass filter are determined by

$$(Z_{0e})_{j,j+1} = \frac{1}{Y_0}\left[1 + \frac{J_{j,j+1}}{Y_0} + \left(\frac{J_{j,j+1}}{Y_0}\right)^2\right] \quad \text{for j=0 to n} \quad (11)$$

$$(Z_{0o})_{j,j+1} = \frac{1}{Y_0}[1 - \frac{J_{j,j+1}}{Y_0} + (\frac{J_{j,j+1}}{Y_0})^2] \qquad \text{for j=0 to n} \qquad (12)$$

Table 3. Circuit design parameters (impedance value from FDW and calculated impedance value) of the 3rd Order, parallel-coupled strip line band pass filter

j	$J_{j,j+1}/ Y_0$	$(Z_{oe})_{j,j+1}$ (Ω) (Derived Results)	$(Z_{oo})_{j,j+1}$ (Ω) (Derived Results)	$(Z_{oe})_{j,j+1}$ (Ω) (Simulated results)	$(Z_{oo})_{j,j+1}$ (Ω) (Simulated results)
0	0.3968	77.71	38.03	78.45	37.95
1	0.1900	61.30	42.30	61.85	42.06
2	0.1900	61.30	42.30	61.85	42.06
3	0.3968	77.71	38.03	78.45	37.95

2.7 Effective Dielectric Constant And Length Measurement

2.7.1 For W=.4311mm (Standard value)

$$\varepsilon_{re} = \frac{\varepsilon_r + 1}{2} + \frac{\varepsilon_r - 1}{2}\frac{1}{\sqrt{1 + \frac{12h}{W}}} \qquad = 2.22106 \text{ mm} \qquad (13)$$

Thus the required length, $\ell = \frac{\lambda_g}{4} = \frac{c}{4f\sqrt{\varepsilon_{re}}}$ =1.0064 mm

(14)

The length of the resonator requires for third order coupled line filter will have four, quarter wavelength segments. So final filter length is:

L= (n+1) × l = (3+1) ×.1.0064=4.0256 mm (15)

2.7.2 For W=.3911 (Calculate value by simulation)

$$\varepsilon_{re} = \frac{\varepsilon_r + 1}{2} + \frac{\varepsilon_r - 1}{2}\frac{1}{\sqrt{1 + \frac{12h}{W}}} \qquad = 2.211408 \text{ mm} \qquad (16)$$

Thus the required length, $\ell = \frac{\lambda_g}{4} = \frac{c}{4f\sqrt{\varepsilon_{re}}}$ =1.0086 mm (17)

The length of the resonator requires for third order coupled line filter will have four, quarter wavelength segments. So final filter length is:

L= (n+1) × l = (3+1) ×1.0086=4.0347 mm (18)

3 Simulated Result and Discussion

In this section we discuss and compare the results obtained from Ansoft Designer/Nexxim SV2.2 Simulation Software and Matlab software. The frequency sweep for the linear simulation of the Advanced numerical models were performed from 40 to 60 GHz in 0.1 GHz steps.

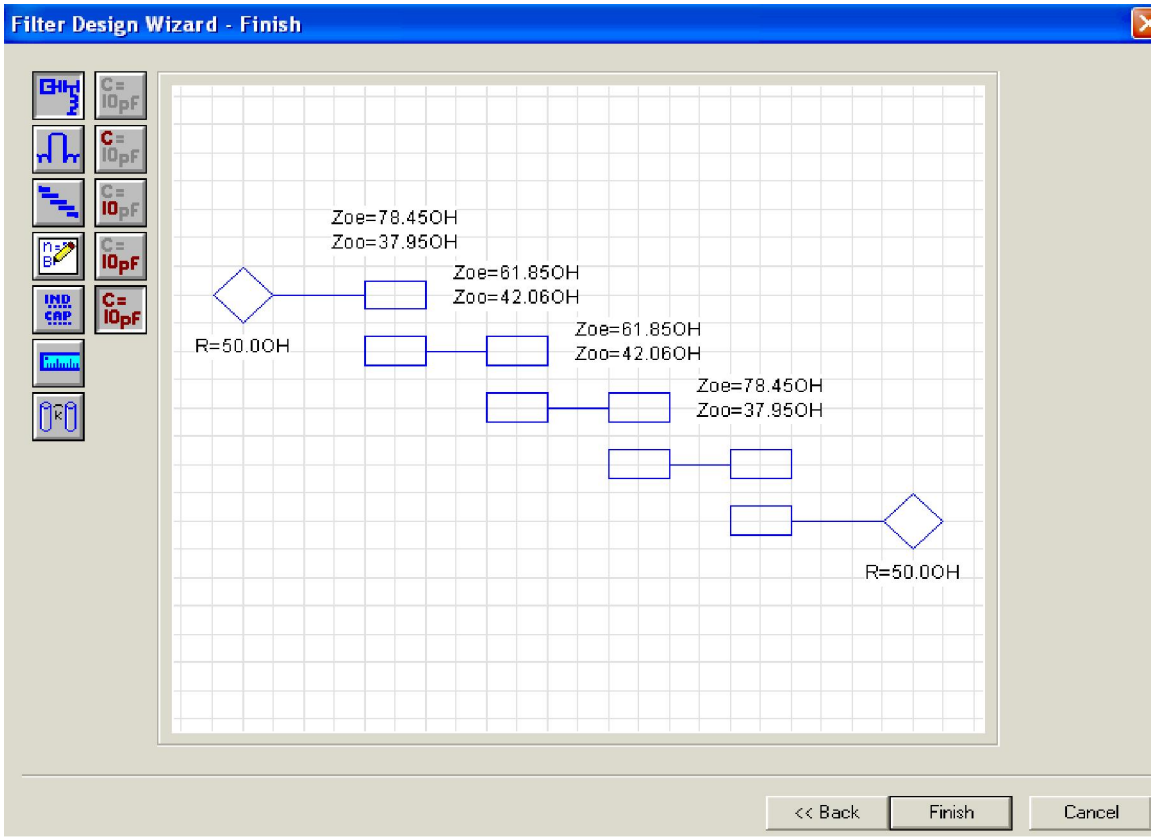

Fig. 6. Software Result of Odd and Even Impedances of 3rd order Edge-coupled Stripline Band pass Filter

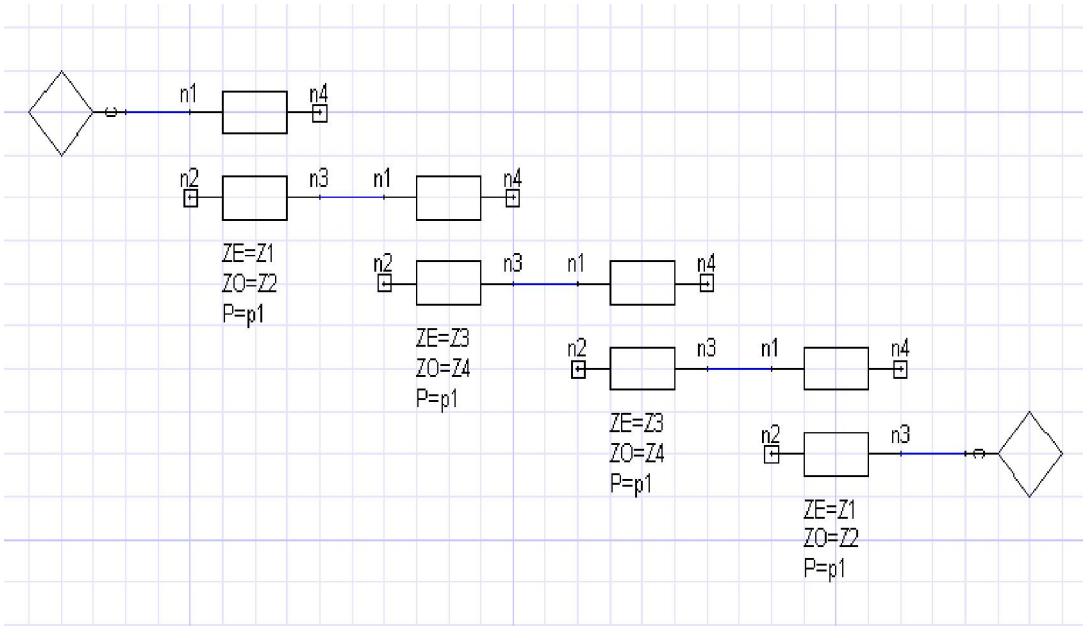

Fig. 7. Electrical Model of 3rd order Edge-coupled Stripline Band pass Filter ideal transmission lines

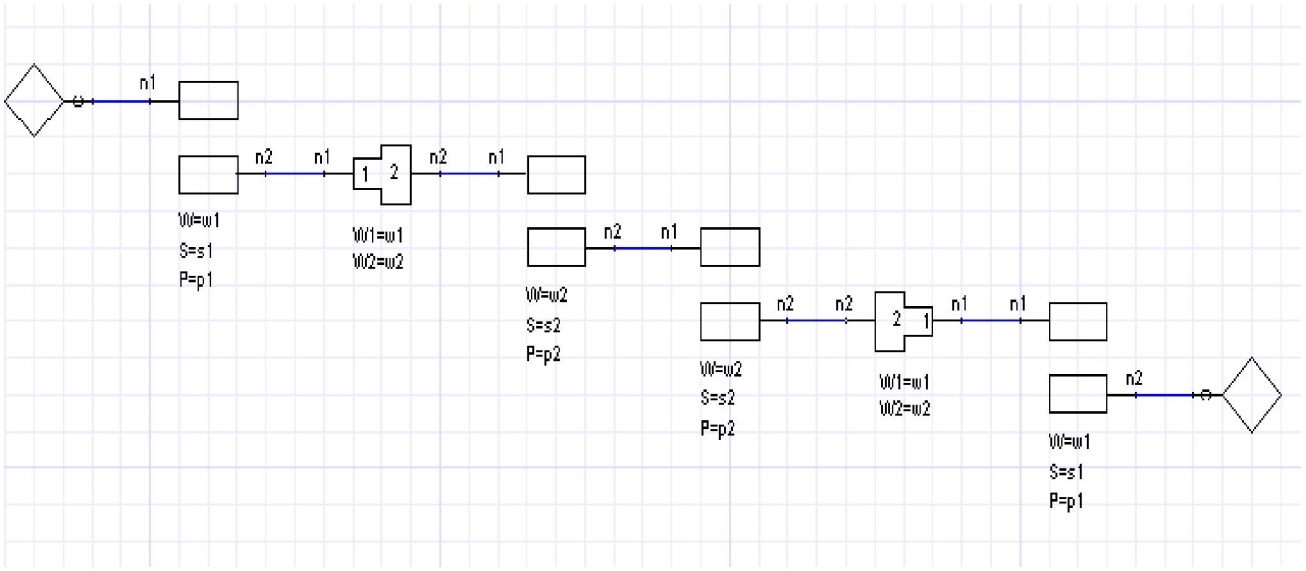

Fig. 8. Tuned Chebyshev bandpass filter made from Physical Model of 3rd order Edge-coupled Stripline Band pass Filter

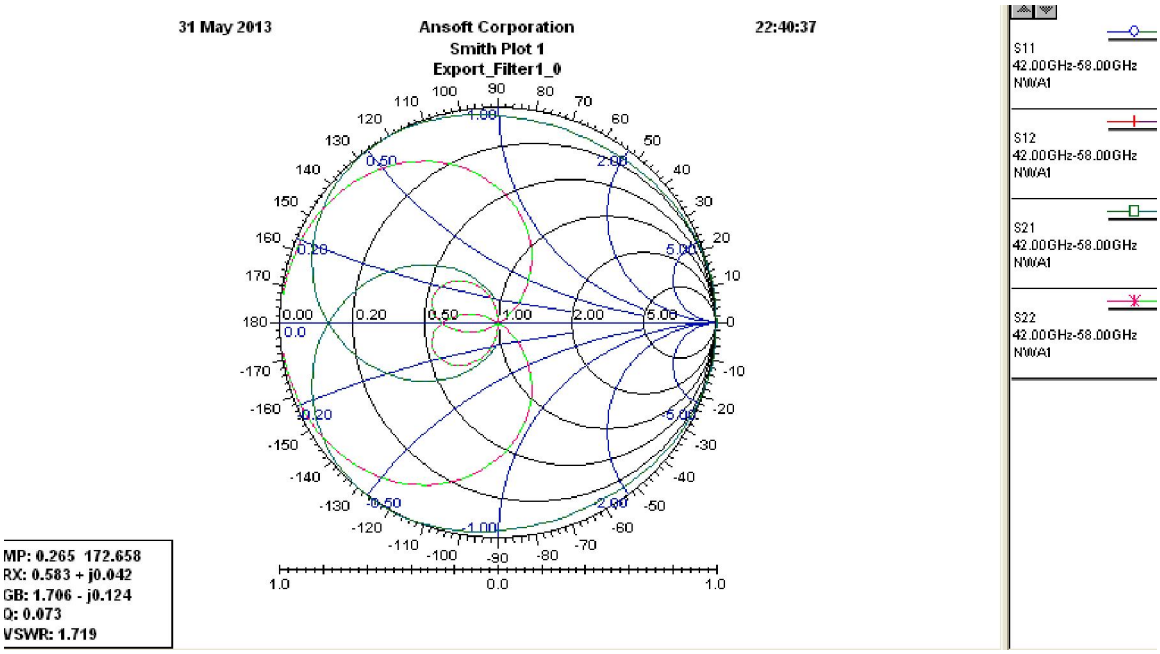

Fig. 9. Simulated Smith Chart impedance Result of 3rd order Edge-coupled Stripline Band pass Filter

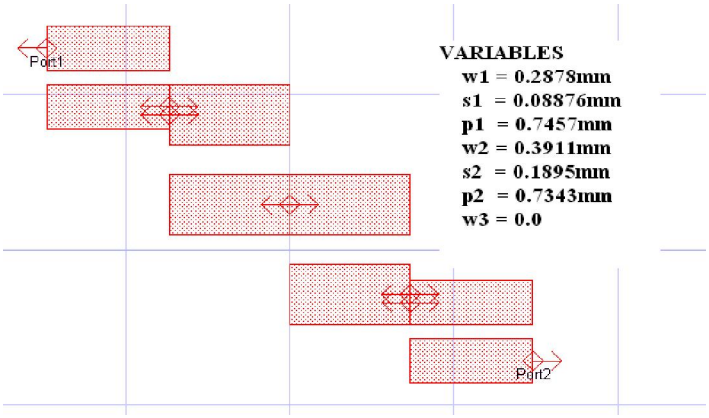

Fig. 10. Detail dimensions of the Simulated Layout Model Result of 3rd order Edge-coupled Stripline Band pass Filter

We can determine the width of parallel-coupled striplines **w** and the distance between them **s**. A pair of parallel-coupled striplines with certain width and separation distance will deliver a pair of characteristic impedances, the even mode and the odd mode ones. In layout Fig. 10 shows simulated layout model result of 3rd order edge-coupled stripline band pass filter and Fig 6 show the parallel-coupled band pass filter configuration the graph for stripline in separation is small the even mode impedance is high, and the odd mode impedance is small. In order to achieve the impedance pair (Z_{oe}) = 77.71 Ω, and (Z_{oo}) = 38.03 Ω, we built a table 3 and which match the values of the impedance pair.

According to layout Fig. 10, we get w1=0.2878mm and s1=0.0887mm respectively. The length of the resonator required is l_1=1.0086mm, which must be geometrically reduced in order to take into account the fringe effects due to open end. The same data will be also used another for the fourth resonator.

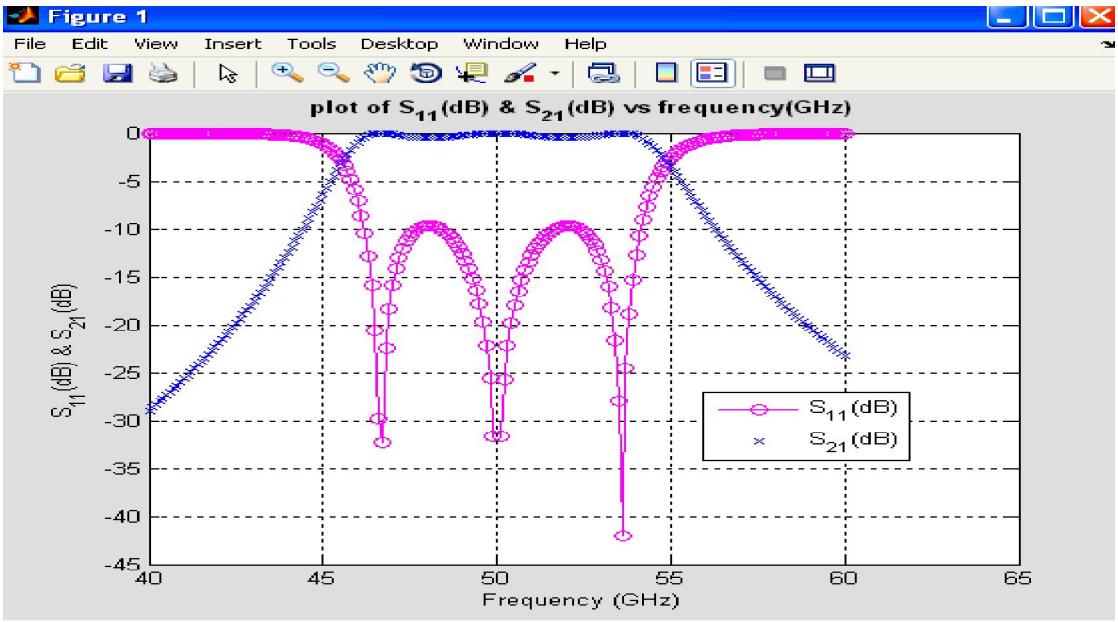

Fig. 11. Simulated result By MATLAB Simulated Tool of 3rd order Edge-coupled Stripline Band pass Filter

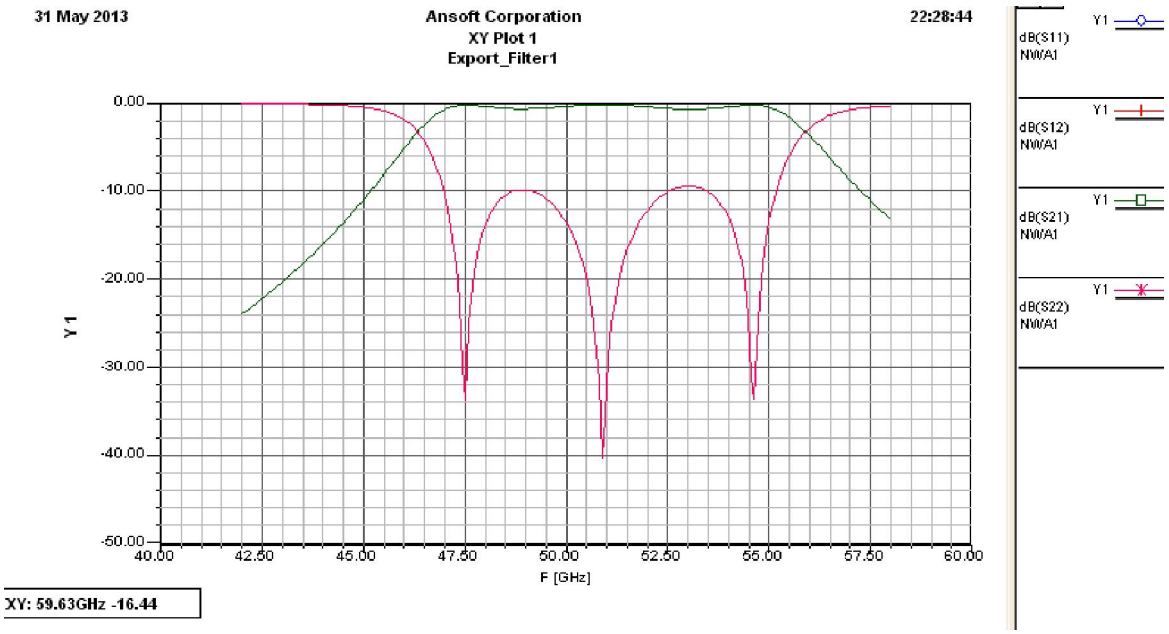

Fig. 12. Simulated Insertion Loss and Return Loss Result for physical model of 3rd order Edge-coupled Stripline Band pass Filter

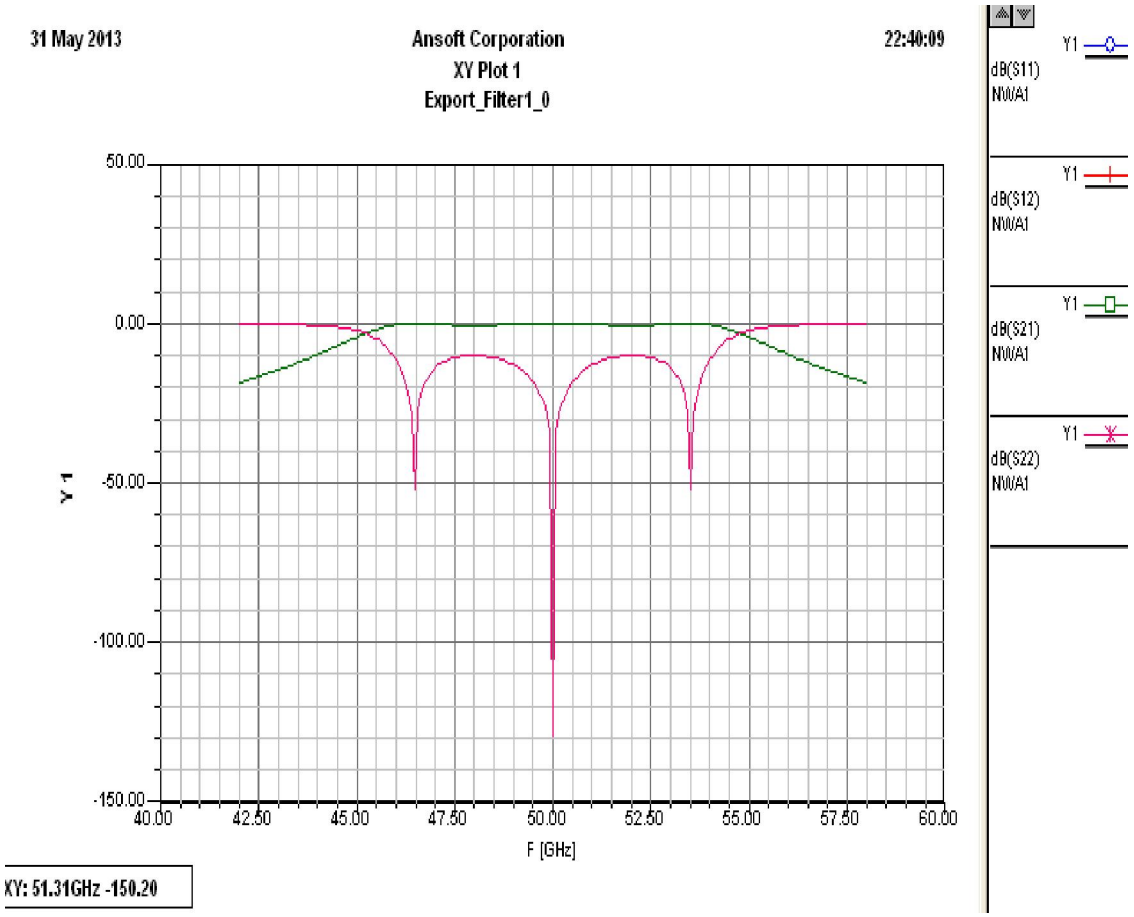

Fig. 13. Simulated Insertion Loss and Return Loss Result for electrical model of 3rd order Edge-coupled Stripline Band pass Filter

The result of such a procedure is shown in Fig. 11, Fig. 12 & Fig. 13 Comparisons were made between the Ansoft simulation and the Matlab results for the designs. As predicted, the simulation in Ansoft Designer the pass band center frequency by about 50 GHz. This is the focus of continued optimizations in designer, in an attempt to have results predict S_{11} to be less than -10dB throughout our pass band. For a lossless filter, with an insertion loss having a maximum ripple of .5dB, the return loss must be 40dB or higher.

The overall performance of edge-coupled strip line band-pass filter can often be judged by its simulated insertion loss and return loss result response. All simulated results are nearly identical with the calculated results and also they are good agreement to the design specifications. Design an edge-coupled strip line band-pass filter centered at 50 GHz with a 8 GHz bandwidth based on Chebyshev approximation. The filter is based on the preceding formulation, MATLAB programs [11]-[12]and Ansoft Designer design entitled edge-coupled strip line band-pass filter has been developed. Simulation results the authors agree that the errors are not overly extensive and the presented process may be considered a success.

Modeled performance is shown in Fig. 12-13 Simulated Insertion Loss and Return Loss Result of 3rd order Stripline Edge coupled Band pass Filter. EM analysis results from Ansoft Designer, which indicates that the response satisfies the design criteria [13]. These plots show the passband, stopband, return loss results of the Ansoft Designer simulation, along with shown in Fig. 9 a Smith chart plot of input/output impedance. These plots show that the Ansoft Designer model meets the filter's design criteria. The simulated insertion loss is less than 0.5 dB in pass band. Also the response is flat and uniform over the entire pass-band. In addition, reflection coefficient is 0.00001 which is nearly equal to 0 and a perfect match exists. Therefore, the designed filter shows attractive characteristics for BPF applications.

4 CONCLUSION

This technique was implement for an efficient method to design microwave filters with modern simulation software, using standard techniques of many microwave designed has been reviewed. The mathematical analysis was done for each design and verified by written a MATLAB code. The effects due to conductor and dielectric losses were ignored in the code. Ansoft Designer v2.2 was used to accurately arrive at the final design. Comparisons were made between the Ansoft Designer simulation and the designs involving MATLAB code section. All simulated results are nearly with the calculated results with best agreement to the design specifications. This paper describes a procedure for designing edge coupled strip line band pass filter. Experimental implementation of this work involves the Roger R03203 substrate with dielectric constant of 3.02 dielectric characterizations at microwave frequencies. Third-order stripline edge-coupled band pass filter is used in order to realize these objectives. The filter is simulated with Ansoft Designer 2.2 software and MATLAB to predict the performance of filter.

The simulated insertion loss is less than 0.5 dB in the desired passband and the simulated return loss is almost greater than 50 dB at center frequency. Design an edge-coupled bandpass filter centered at 50 GHz with a 8 GHz bandwidth based on Chebyshev approximation. As predicted, the simulation in Ansoft designer the passband center frequency by about 50 GHz. This is the focus of continued optimizations in Designer, in an attempt to have results predict S_{11} to be less than -10dB throughout our passband. For a lossless filter, with an insertion loss having a maximum ripple of .5dB, the return loss must be 40dB or higher. Simulation results the authors agree that the errors are not overly extensive and the presented process may be considered a successfully use for microwave in U band at 50 GHz for microwave application.

REFERENCES

[1] Michael S. Flanner, "Microwave filter design: Coupled line filter," *California State University, Chico project by Spring* 2011.

[2] R.E. Collin, *Foundations for microwave engineering*, 2nd edition, McGraw-Hill, 1992.

[3] F.F. Kuo, *Network analysis and synthesis*, 2nd edition, John-Wiley & Sons, 1966.

[4] Bhushan R. Vidhale, M.M. Khanapurkar, "Design of Low Cost and Efficient Strip Line Band Pass Filter for Bluetooth Application," *IJERA*, Vol. 2, No. 4, pp. 2340-2345, July-August 2012.

[5] D.M. Pozar, *Microwave engineering*, 2nd edition, John-Wiley & Sons, 1998.

[6] Rhodes, J. D.,*Theory of Electrical Filters*, Willey, New York, ISBN: 0-471-71806-8, 1976.

[7] Pawan Shakdwipee, Kirti Vyas, Naveen Shakdwipee, "Design and simulation of microstrip edge coupled band pass filter for gps application," *International Journal of Electrical Electronics and Mechnical Control*, Vol. 1, No. 1, November 2012.

[8] Hnin Yu Wai, Zaw Min Naing, Kyaw Soe Lwin, and Hla Myo Tun, "Design and Simulation of Edge-coupled Stripline Band Pass Filter for Ka Band Application," *International Conference on Trends in Electrical, Electronics and Power Engineering (ICTEEP'2012),* Singapore, July 15-16, 2012.

[9] R. R. Mansour, "High-Q tunable dielectric resonator filters," IEEE Microwave Magazine, vol. 10, no. 6, pp. 84-98, Oct. 2009.
[10] VB Atanassov, MG Balan, SJ Haimov, GP Kulemin, MA Michalev, L.H Mladenov, Y.A. Pedenko, VB Razskazovsky, AK Savchenko, and VL Vasilev, "Experimental study of nonstationary X-and Q-band radar backscattering from the sea surface," *Radar and Signal Processing, IEE Proceedings F*, vol. 137, no. 2, pp. 118–124, 1990. DOI: 10.1049/ip-f-2.1990.0017.
[11] J.W Robbin, *Matrix Algebra: Using Minimal Matlab*, A K Peters, Wellesley, MA, 1995.
[12] Brian R. Hunt, Ronald L. Lipsman, Jonathan M. Rosenberg, Kevin R. Coombes, John E. Osborn, and Garrett J. Stuck, *A Guide to MATLAB for Beginners and Experienced Users*, Cambridge University, 2001.
[13] Gunthard Kraus, *Ansoft Designer SV 2.0*, Elektronikschule Tettnang, 2005.
[14] J. A. Ruiz-Cruz, C. Wang, and K. A. Zaki, "Advances in microwave filter design techniques," *Microwave Journal*, vol. 51, no. 11, pp. 26–44, Nov. 2008.
[15] Mudrik Alaydrus, "Designing Microstrip Bandpass Filter at 3.2 GHz," *International Journal on Electrical Engineering and Informatics*, Vol. 2, No. 2, pp. 71-83, 2010.
[16] R. J. Wenzel, "Exact theory of interdigital bandpass filters and related coupled structures," *IEEE Trans. Microwave Theory Tech*., vol. 13, no. 9, pp. 559 -575, 1965.
[17] D. F. Williams and S. E. Schwarz, "Design and Performance of Coplanar Waveguide Bandpass Filters," *IEEE Transactions on Microwave Theory and Techniques*, vol. MTT-31, No. 7, July 1983.
[18] Riddle, "High performance parallel coupled microstrip filters," in *IEEE MTT-S Int Micrwave Symp. Dig*., pp. 427-430, May 1988.

AUTHOR'S PROFILE

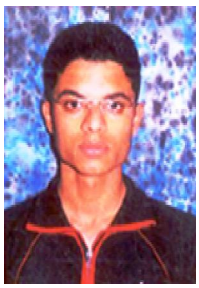

Pawan Shakdwipee received the Electronic & Communication engineering degree from Geetanjali Institute technical Studies Udaipur ,2009 (HONOURS) and M.Tech (pursuing) from Arya College Of engineering & IT Jaipur ,RTU Kota University, India 2013. His research interests include Microwave Engineering, Antenna Design, signal processing for communications, and adaptive signal processing. He has published 7 national papers and 16 international papers/journal and 1 text book for VHDL.

International Journal of Innovation and Applied Studies
ISSN 2028-9324 Vol. 3 No. 4 Aug. 2013, pp. 1045-1052

http://www.issr-journals.org/ijias/

Experimental and modeling study of sulfur dioxide oxidation in packed-bed tubular reactor

Hanen NOURI and Abdelmottaleb OUEDERNI

Laboratory of Engineering Process and Industrial System (LR GPSI),
National School of Engineers of Gabes (ENIG),
University of Gabes (UG),
Omar Ibn Elkhattab Street, 6029 Gabes, Tunisia

ABSTRACT: The conversion of sulfur dioxide into sulfur trioxide is a reaction which interests not only the industry of sulfuric acid production but also the processes of pollution control of certain gas effluents containing SO_2. This exothermic reaction needs a very good control of temperature, that's why it is led in the industry in a multistage converter with intermediate heat exchangers. Microreactors represent a good alternative for such reaction due to their intensification of mass and heat transfer and enhancement of temperature control. In this study, this reaction was conducted in a stainless steel tubular (4mm ID) packed bed reactor using particles of vanadium pentoxide as catalyst at atmospheric pressure. Experiments were performed with different inlet SO_2 concentration in 3-9% range and reaction temperature between 685-833K. We noticed that the conversion decreases with the amount of SO_2 and increases with the temperature until an optimum, above this value the conversion drop according to the shape of the equilibrium curve. Controlling rate mechanism is studied by varying temperature. Pseudohomogeneous perfect plug flow is used to describe this small tubular reactor. Numerical simulations with MATLAB were performed to validate the experimental results. Good agreement between the model predictions and the experimental results is achieved. Fluid flow description inside the packed bed reactor was performed by using the free fluid and porous media flow model. This model was solved by the commercial software COMSOL Multiphysics. Velocity profile inside the reactor is theoretically obtained.

KEYWORDS: Sulfur dioxide, pentoxide vanadium, catalysis, kinetic model, heterogeneous reactor, hydrodynamic simulation.

1 INTRODUCTION

Sulfuric acid is one of the most important chemicals in the world. It is produced via the contact process in a gas phase catalytic oxidation reaction. In this process, a gas mixture containing sulfur dioxide and air is passed over a catalyst, which oxidizes SO_2 to SO_3 [1]. Only two types of catalysts gained widespread commercial acceptance. These are platinum and vanadium pentoxide. Today, the dominating catalyst is vanadium pentoxide due to its lower cost and greater availability [1]. This catalyst consists of 4-9 wt% vanadium pentoxide V_2O_5, being the active component, together with alkali metals as promoters [2]. The oxidation of SO_2 is an exothermic reaction with fast reaction kinetics and high reaction enthalpy (-99 kJ/mol). Due to the negative reaction enthalpy the equilibrium conversion decreases with rising temperature. However, with rising temperature the reaction rate increases but the equilibrium is shifted towards lower SO_3 concentration. So, an effective control of the temperature is very important. That is why, recent studies have been oriented to use microstructured reactor to conduct such exothermic reaction due to its outstanding heat transfer performance [1].

In fact, micro-structured reactors represent a new approach of processes development that has attracted the attention of many researchers in several engineering processes. Microreactors, as the name implies, involve reaction chamber whose dimensions are typically in the range of micrometers with volumetric capacity in the range of micro liters [3]. The possibility of reduction in dimensions with small volumes of reaction zone would allow locally application of high temperature or

Corresponding Author: Hanen NOURI (hanennouri@gmail.com)

concentration with significant ease of process control and thermal management. The main advantage of microstructured reactors is their high surface to volume ratio in the range of 10000-50000 m^2/m^3 compared to more classic chemical reactors [4]. This ratio enhances mass and heat transfer and thus an improvement in the conversion ratio. Heat transfer is also increased since the heat transfer coefficient is inversely proportional to the diameter of the channel; its value for microstructured reactors is around 10kW / (m^2.K), far higher than classical known reactors. The energy and economic gains are significant because the high heat transfer allows using of the full potential of catalysts during highly endothermic or exothermic reactions and avoiding hot-spots formation. In addition, the small inventories of reactants and products lead to inherent safety during the reactor operation. It has been reported that microstructured reactors run safely under conditions, which lay in the explosion regime. Small reactor dimensions facilitate the use of distributed production units at the place of consumption. This avoids the transport and storage of dangerous materials [5]. For these reasons, Pfeifer et al.[6] demonstrated the basic principle of producing SO_3 with pure oxygen in a one pass process without stepwise cooling or quenching. The goal is to reach a sufficiently high SO_3 concentration in a microstructured reactor being part of a compact plant installed on site.

It is proposed in our laboratory to take advantage of this new type of structures in the context of development of chemical reactors. That's why a micro channeled reactor is being developed but before using it we suggest to study the kinetic reaction and the influence of operating conditions in a tubular packed bed reactor. So, the aim of this work is to conduct the conversion of sulfur dioxide to sulfur trioxide in a tubular low diameter packed bed reactor with different SO_2 inlet content and reaction temperatures. Numerical simulations with MATLAB were performed to validate the experimental results and a detailed model solved by COMSOL Multiphysics to describe the fluid flow in the reactor.

2 EXPERIMENTAL

To highlight the effects of miniaturization, a simple packed bed tubular reactor was used. The reactor is a stainless steel tube of 4 mm inner diameter and 100 mm in length. The catalyst used in this study is the vanadium pentoxide commercial catalyst. The catalyst has a low total surface area determined with liquid nitrogen adsorption according to Brunauer ,Emmetand Teller(S_{BET}) about 4 m^2/g and estimated very reduced total pore volume $4.2.10^{-3}$cc/g. The catalyst was crushed sieved and particles of sizes of 500µm were introduced into the reactor. Microreactor is filled with approximately 400 mg of catalyst in most runs. The reactor was positioned in controlled temperature electric furnace capable of reaching 1000 °C. Type K thermocouple was fitted in the catalyst bed to measure the catalyst temperature inside the reactor. Pure nitrogen, oxygen and sulfur dioxide were metered by mass flow controller type Brooks, mixed in a micro mixer and preheated until the temperature of activation of catalyst before passing in the reactor. The reaction product was analyzed by iodometric method.

The conversion of SO_2 was studied in the temperature range of 685-833K and the inlet gas of sulfur dioxide content was varied from 3 to 9% volumetric. The nitrogen flow rate was varied in such a way that the total flow rate at the inlet was the same in all the runs.

3 MODELLING

In order to validate the experimental results and to evaluate the performance of the micro packed bed reactor, a simple model was used assuming a pseudohomogeneous plug flow reactor with an inlet flow F_{A0} and a mass of catalyst W.The mass balance equation was solved using MATLAB.

$$\frac{dX}{dW} = \frac{-r_A}{F_{A0}} \quad (1)$$

In order to ensure plug flow conditions, absence of back mixing, and absence of channeling, certain criteria reported by Froment and Bischoff (1990)[7] were respected. These criteria are: (1) ratio of catalyst bed height to catalyst particle size (Lr/dp)≥ 50, and (2) ratio of internal diameter of the reactor to the catalyst particle size (d/dp)≥10. In this work, we used Lr/dp and d/dp of 100 and 8 respectively.

For the rate expression, we used the modified equation of Calderbank [7] based on the Langmuir-Hinshelwood concept and on the observation that the reaction between the adsorbed SO_2 and oxygen from the gas phase is the rate controlling step.

$$r = \frac{K_1 P_{O2} P_{SO2} (1 - \frac{P_{SO3}}{P_{SO2}\sqrt{P_{O2}} K_P})}{22{,}414(1 + K_2 P_{SO2} + K_3 P_{SO3})^2} \quad (2)$$

where : r: kmol SO_2/kg cat hr

and temperature influence on constants expressed by:

$$K_1 = \exp(12{,}160 - \frac{5473}{T})$$

$$K_2 = \exp(-9{,}953 + \frac{8619}{T})$$

$$K_3 = \exp(-71{,}745 + \frac{52596}{T})$$

$$K_P = \exp(-10{,}68 + \frac{11300}{T})$$

On the other hand, it is essential to study the hydrodynamics behavior and the flow in the catalytic bed. That is why a numerical simulation with the commercial software COMSOL Multiphysics 4.1 had been performed for the tubular packed bed reactor. The model couples the free fluid and porous media flow through the Navier-Stokes equations and Brinkman's extension of Darcy's law [8] . The stationary Navier-Stokes equations describe the fluid flow in the free-flow regions:

$$\nabla .\left[-\eta (\nabla u + (\nabla u)^T + PI \,] = -\rho (u.\nabla) u \right] \quad (3)$$

$$\nabla .u = 0 \quad (4)$$

In the porous bed, we used the Brinkman equations:

$$\nabla .[-\frac{\eta}{\varepsilon_p}(\nabla u + (\nabla u)^T + PI \,] = -\frac{\eta}{\kappa} u \quad (5)$$

$$\nabla .u = 0 \quad (6)$$

In the above equations, η denotes the viscosity of the fluid (NS/m^2), ε_p is the bed porosity (dimensionless), u the velocity (m/s), ρ the density (kg/m^3), P the pressure (Pa), and κ the permeability (m^2).

A constant velocity profile is assumed at the inlet boundaries:

$$u = u_{in} \quad (7)$$

The boundary condition for the Navier-Stokes equations at the outlet reads

t.u=0 (8)

p=0 (9)

where t is any tangential vector to the boundary.

4 RESULTS AND DISCUSSION

4.1 EXPERIMENTAL RESULTS

The temperature is a key operating parameter in this gas heterogeneous catalyst reactor. In this condition, kinetics are generally limited by heat and mass transfers, it is thus imperative to take into account the parameter temperature, to adjust and control it according to the studied reaction way. A series of experiments was undertaken to four inlet concentration of SO_2 :3%, 5%, 7% and 9% (v/v) and for a total volume flow rate of 20ml/s.

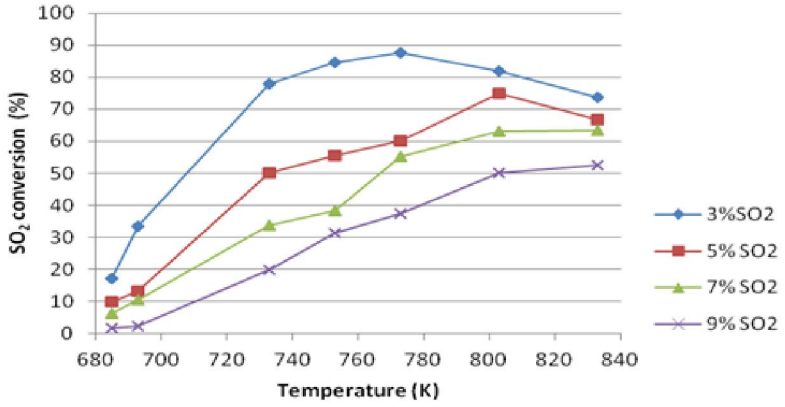

Fig. 1. Influence of temperature on conversion rate for various inlet SO_2 contents

It can be seen from figure1 that SO_2 conversion decreases with the SO_2 inlet content and that the increase in the temperature from 683 K to 773 K allows an improvement of conversion into SO_3 up to a value almost of 90% for a content of sulfur dioxide of 3%. Above this value, the effect of the temperature becomes harmful and induced a drop in conversion rate. This result is well expected since the thermodynamics of this reaction which shows that the SO_2 conversion rate is increasing up to a precise value of the temperature from which it decrease according to the shape of the equilibrium curve. This is well explained by Figure 2 that represent the conversion of SO_2 as a function of temperature for different reaction rates. The dashed line represent the Optimal Temperature Progression. It is the path that can achieve the highest conversion with the minimum volume reactor.

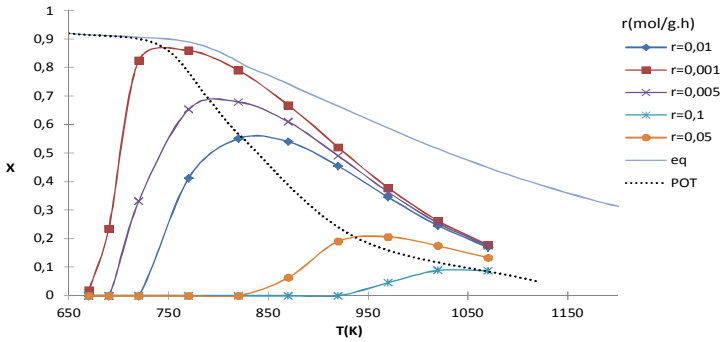

Fig. 2. Conversion of SO_2 versus temperature at various reaction rates

The variation of the observed rate versus reaction temperature for different SO_2 inlet content is reported in figure 3. The benefit effect of temperature on the reaction rate is well shown. But there is an inflexion point at a temperature of 773 K. This point divided the reaction domain in two zones. Below 773k, the inlet SO_2 content had no effect on the reaction rate and it had a significant effect above this value. To highlight this result, we represented in figure 4 the variation of logarithm of the observed rate $Ln(r_{obs})$ as function of the inverse of reaction temperature. It is very clear that the catalytic process is controlled by two different process owing temperature range: diffusional and chemical control regimes.

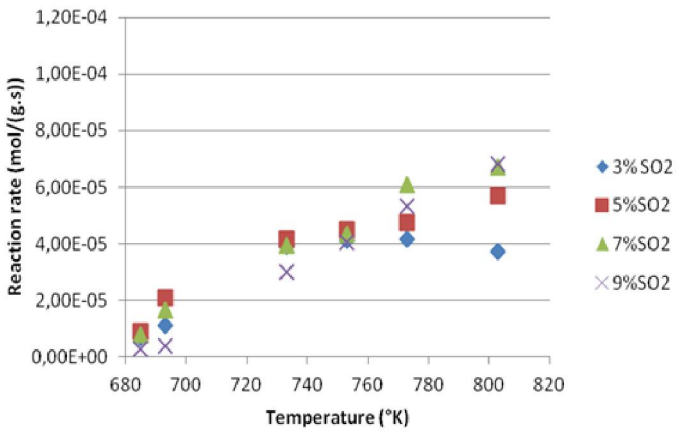

Fig. 3. Reaction rate versus temperature for different SO_2

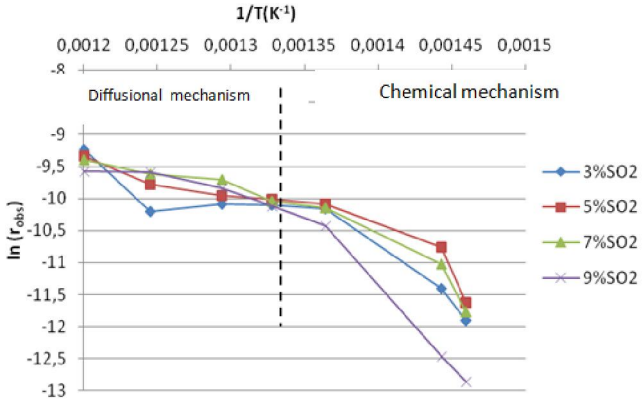

Fig. 4. $Ln(r_{obs})$ versus 1/T content

In order to calculate the kinetic parameters of the reaction rate, we used the domain of chemical control since in this domain the observed kinetic and intrinsic reaction parameters are the same. Table1 present the calculated activated energy and the frequency factor of the reaction determined by Arrhenius law.

Table 1. Activated Energies and kinetic Arrhenius constants for different SO_2 content

$\%SO_2$	Ea(J/mol)	A(mol/(g.s.atm))
3	$1.14\ 10^5$	$1.34\ 10^4$
5	$1.26\ 10^5$	$7.92\ 10^4$
7	$1.45\ 10^5$	$1.68\ 10^6$
9	$2.13\ 10^5$	$8.13\ 10^{10}$

4.2 NUMERICAL STUDY

The numerical resolution of the system of the equations achieve a theoretical model which describes the conversion of sulfur dioxide in a catalytic bed with vanadium pentoxide. This model is a tool that allows simulation of the reactor performances on the same operating conditions as the experiment. The table 2 summarizes the results of the simulation at the outlet of the reactor and compares them with the experimental results. We note that there is a good agreement between the numerical and experimental results, the relative error (e %) calculated didn't exceed 20% in all experiments except for the content of 9% SO_2. This difference can be explained by the analysis method used which requires many precautions.

Table 2. Comparison between experimental and simulated results

SO2 %	3			5			7			9		
T(°K)	X_{exp}(%)	X_{th}(%)	e(%)	X_{exp}(%)	X_{th}(%)	e(%)	X_{exp}(%)	X_{th}(%)	e(%)	X_{exp}(%)	X_{th}(%)	e(%)
685	17,14	21,11	18,81	9,972	10,63	6,19	6,2	6,21	0,16	1,639	3,92	58,19
693	33,33	32,22	3,45	13,33	16,16	17,51	10,34	9,29	11,30	2,44	5,79	57,86
733	77,91	82,65	5,74	50	53,59	6,70	33,82	33,89	0,21	20	22,33	10,43
753	84,74	88,41	4,15	55,56	66,44	16,38	38,46	46,59	17,45	31,43	33,06	4,93
773	87,72	89,12	1,57	60	73,94	18,85	55,26	56,37	1,97	37,5	42,77	12,32
803	81,93	85,47	4,14	75	77,57	3,31	63	64,64	2,54	50	52,68	5,09
833	73,68	78,75	6,44	66,66	74,32	10,31	63,41	66,09	4,06	82,5	56,68	45,55

We reported in figure 5 and 6 the variation of the SO_2 conversion ratio along the catalytic bed for different reaction temperature and inlet flows. We note a good enhancement of conversion from 32% at 693K to 82% at 733K, this is explained by the activation of catalyst at this temperature. For temperature below 803K the conversion decreased according to the equilibrium curve.

In figure 6, we tested the effect of the total inlet flow. We can see that in spite of the small residence time in the reactor, the decrease of the inlet flow enhance the conversion ratio. A flow rate of 5 ml/s could achieve a conversion ratio of 90% in the first 10 mm of the packed bed.

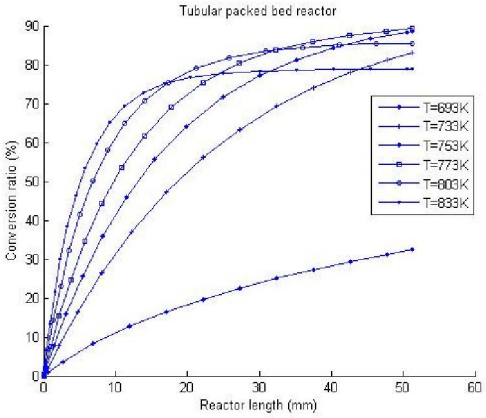

Fig. 5. Conversion of SO_2 along the packed bed (3%SO_2, Q=20ml/s)

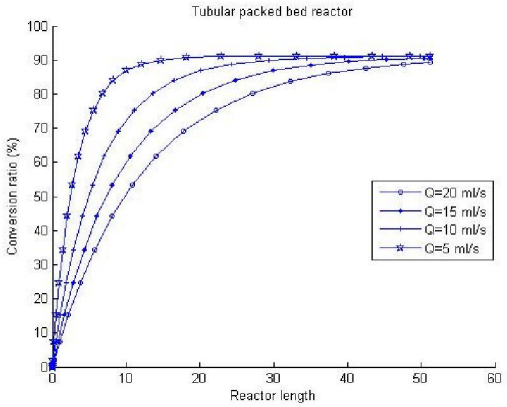

Fig. 6. Effect of flow rate on the conversion of SO_2 along the packed bed (3%SO_2, T=773K)

The effect of the flow on the conversion rate of this reaction can be explained by a limitation by mass transfer. To confirm this idea we calculated criterion available in literature to determine the effects interparticle and intraparticle mass transport limitation could have on the rate of reaction.

To determine whether film mass transfer resistance has any effect on the rate of reaction, the ratio of observed rate to the rate if film resistance controls was examined. Equation (10) illustrates this criterion:

$$\frac{observed\ \ rate}{rate\ if\ film\ resist\ ance\ controls} = \frac{-r_{A,obs}}{C_{Ab}k_c}\frac{d_p}{6} \tag{10}$$

r_{Aobs} is the observed rate of reaction, d_p is the particle diameter, C_{Ab} is the bulk concentration and k_c is the mass transfer coefficient obtained to be 0.57 m/s from the correlation of Theones Kramers [9].

The estimated value for the equation (10) was $6.966.10^{-10}$. The result indicates that the observed rate is very much less than the limiting film mass transfer rate. Thus the resistance to film mass transfer should not influence the rate of reaction [10]. Mears'criterion [9] is often considered a more rigorous criterion for determining the onset of mass transfer limitation in the film. Therefore, we decided to apply this criterion to determine if there was any mass transfer limitation during the collection of the kinetic data. This correlation is given in

$$\frac{r_{obs}\rho_b R_c n}{k_c C_a} < 0.15 \tag{11}$$

The value of this equation is $1.3.10^{-6}$. Therefore, it can be concluded that there was no mass transport limitation in the film.

The internal pore mass transfer resistance was calculated using Weisz-Prater criterion as given by:

$$C_{wp,ipd} = \frac{-r_{A,obs}\rho_c R_C^2}{D_{eff}C_{AS}} \tag{12}$$

Where $C_{wp,ipd}$ is the Weisz-Prater criterion for internal pore diffusion, ρ_c the pellet density, R_c catalyst radius, D_{eff} is the effective mass diffusivity obtained from Deff=($D_{AB}\varepsilon/\zeta$) [9] where D_{AB} is the bulk diffusivity of compound A in B, ε is the void fraction(=0.4), ζ is the tortuosity factor taken as 8[9] and C_{As} is the concentration at the pellet surface assumed to be equal to the bulk concentration as suggested by Levenspiel [10].

The estimated value for $C_{wp,ipd}$ was $6.26.10^{-5}$. This value is much less than 1. Thus this result indicates that the concentration on the catalyst surface is more or less the same as the concentration within its pores. So there is no internal pore diffusion limitations. We must mention that these effects were investigated at a temperature of 733 K, the low amount of SO_2 (3%) and an observed rate of $3.89.10^{-5}$ mol/(g.s).

4.3 FLOW MODELING

For the hydrodynamic study, The model presents the coupling of free and porous media flow in fixed bed reactors. Due to the symmetry only half of the reactor has to be considered. The flow within the reactor is laminar. COMSOL 4.1 solved the three dimensional Navier-Stokes equations for the flow through the reactor.

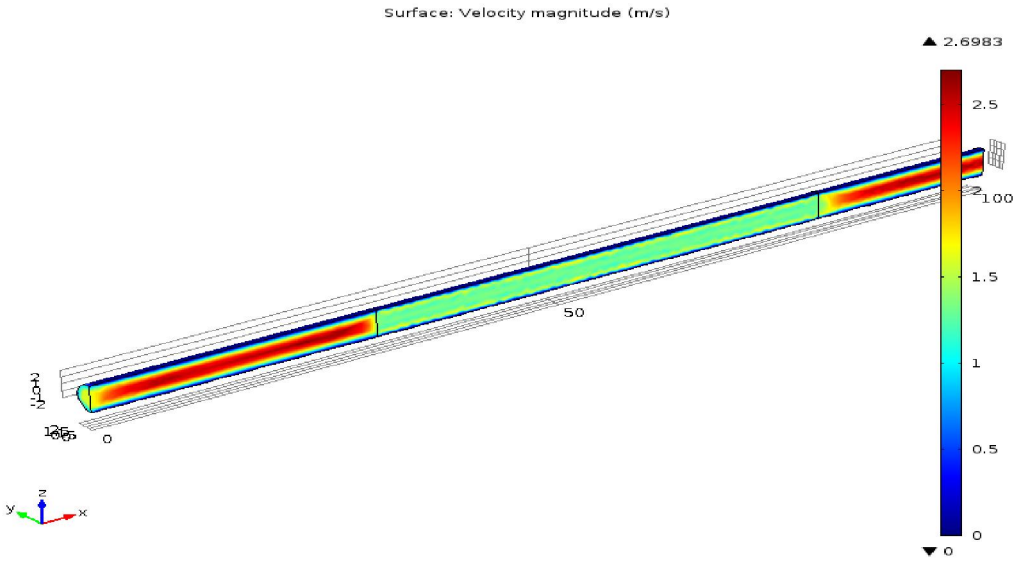

Fig. 7. Magnitude of the velocity field in the free and porous reactor domains

Figure 7 shows the velocity profile of inert gas inside the packed bed reactor for a total gas flow of 20 ml/s. Due to the non-slip conditions, the velocity profile close to the wall becomes zero by definition, obtaining a maximum value in the middle of the free part of the reactor. In the catalyst bed, the velocity decreases until almost the half. The Figure 8 below shows the variation of the number of Reynolds Re across the tubular reactor. Re is about 7 in the catalytic bed assuring a laminar flow.

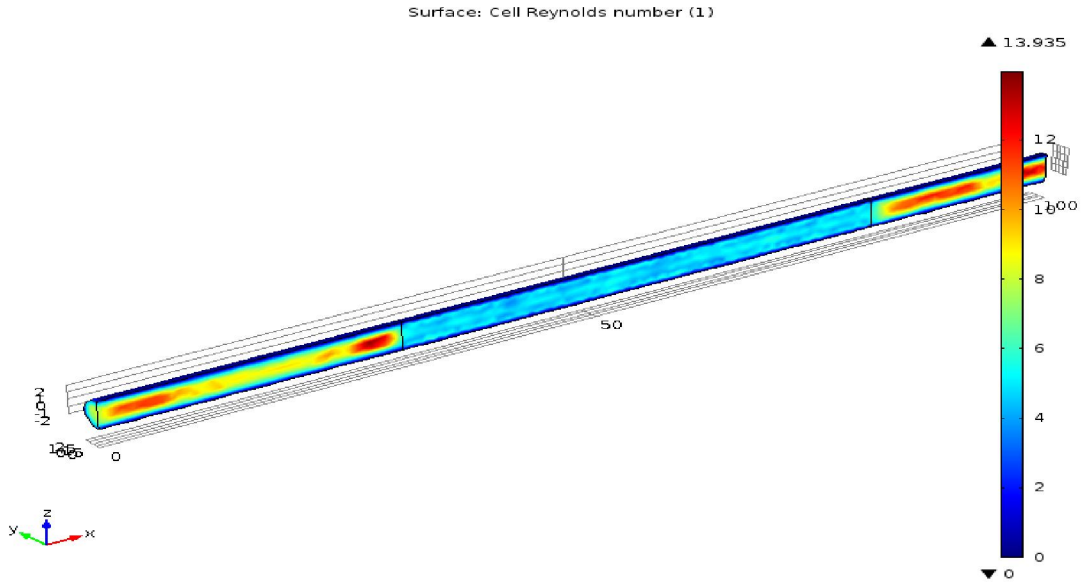

Fig. 8. The Reynolds Number across the reactor

5 CONCLUSION

This work is interested in the oxidation of sulfur dioxide in a tubular packed bed reactor. This reaction had been performed for different sulfur dioxide content and temperature reaction in the range of 685-833 K. The catalyst used was commercial vanadium pentoxide with particles's diameter of 500µm. Experimental data show that the conversion ratio of SO_2 decrease with the inlet content of sulfur dioxide and increase with reaction temperature until an optimum equal to 773K, above this value the conversion is limited by the equilibrium curve. Numerical simulations with MATLAB were performed to validate the experimental results and a detailed model solved by COMSOL Multiphysics to describe the fluid flow in the reactor. Good agreement between the model predictions and the experimental results is achieved.

REFERENCES

[1] W. Benzinger, A. Wenka, and R. Dittmeyer, "Kinetic modelling of SO_2 oxidation with Pt in a microstructured reactor", *Applied Catalysis A: General 397*, pp. 209-217, 2011.
[2] P. Pfeifer, T. Zscherpe, K. Haas-Santo, R. Dittmeyer, "Investigations on a Pt/TiO_2 catalyst coating for oxidation of SO_2 in a microstructured reactor for operation with forced decreasing temperature profile", *Applied Catalysis A: General*, 2010.
[3] Kolb G., Hessel V., "Microstructured reactors for gas phase reactions", *Chemical Engineering Journal*, 98, 2004.
[4] Gokhale S., Tayal R., Jayaraman V., Kulkarni B., "Microchannel Reactors: Applications and Use in Process Development," *International journal of Chemical Reactor Engineering,* 3, 2005.
[5] Renken A. and Kiwi-Minsker L., "Microstructured reactors for catalytic reactions," *Catalysis today*, 110, 2005.
[6] P. Pfeifer, K. Haas-Santo, J. Thormann, K. Schubert, *Chim. Oggi,* 25 (2), 42-46, 2007.
[7] Froment F; Bichoff B. , *Chemical reactor analysis and design*, Second edition, Wiley New York, 494, 2002.
[8] COMSOL Multiphysics 4.1 User's Guide, 2010.
[9] Fogler, H.S., *Element of Chemical Reaction Engineering*, third edition, Prentice-Hall, Englewood Cliffs, NJ., 1999.
[10] Levenspiel, O., *Chemical Reaction Engineering*, Third edition, Wiley New York, 1999.

International Journal of Innovation and Applied Studies
ISSN 2028-9324 Vol. 3 No. 4 Aug. 2013, pp. 1053-1065

http://www.issr-journals.org/ijias/

Une approche d'identification moléculaire des souches d'actinomycètes productrices d'activités antimicrobiennes par séquençage de l'ADNr 16S

[A molecular approach to the identification of actinomycetes producing antimicrobial activities strains by sequencing of the 16S rDNA]

Elarbi BOUSSABER[1], Sidi Brahim Salem EL IDRISSI[1-2], Issam MEFTAH KADMIRI[1-3], Lahoucine HILALI[1], and Abderraouf HILALI[1]

[1]Laboratoire d'Agroalimentaire et Santé
Université Hassan 1er, Faculté des Sciences et Techniques, Settat, Maroc

[2]Laboratoire de polymères, rayonnement et environnement
Université Ibn Tofail, Faculté des Sciences, Kenitra, Maroc

[3]Unité de biotechnologie
Moroccan Foundation for Advanced Science, Innovation and Research,
Rabat, Maroc

ABSTRACT: This work is a part of research of rare Actinomycetal bacteria producing antimicrobial substances that may be used in agricultural, food and pharmaceutical fields. Among the 77 strains of actinomycetes isolated from different types of Moroccan ecosystems, 25 were selected according to their biological activity for molecular identification by sequencing the 16S rDNA fragment. After DNA extraction from isolates, amplification of 16S rDNA fragments by PCR technique (Polymerase Chain Reaction), sequencing of the amplified fragments and comparison of characteristic sequences obtained with the contents of a database and phylogenetic studies using special programs were used to develop phylogenetic trees of the twenty-five isolates. The results Analysis showed the taxonomic affiliation of all isolates to the genus Streptomyces and assign each of them to one or more species. This shows the abundance of this kind in relation to others in the studied ecosystems. While the absence of other types of actinomycetes can be explained either by the absence of these genera in these ecosystems, or by the isolation techniques used, or by the fact that microbial population in the sample is non-culturable. Thus, in the last case, the confirmation of the presence of other types in these ecosystems could be performed by amplification of the 16S rDNA PCR from DNA mixture obtained directly from samples.

KEYWORDS: Molecular identification, sequencing, rDNA, phylogenetic trees, *Streptomyces*.

RESUME: Ce travail se situe dans un cadre de recherche des bactéries actinomycétales rares productrices des substances antimicrobiennes susceptibles d'être utilisées dans des domaines agricoles, alimentaires ou pharmaceutiques. Parmi les 77 souches d'actinomycètes isolées de différents types d'écosystèmes marocains, 25 ont été sélectionnées selon leurs activités biologiques pour une identification moléculaire par séquençage du fragment d'ADNr 16S. Après l'extraction d'ADN à partir des isolats, l'amplification des fragments d'ADNr 16S par la technique de la PCR (Polymerase Chain Reaction), le séquençage des fragments amplifiés et la comparaison des séquences caractéristiques obtenues avec le contenu d'une base de données, des études phylogéniques utilisant des programmes spéciaux ont permis d'élaborer les arbres phylogéniques des vingt-cinq isolats. L'analyse des résultats obtenus a montré l'appartenance taxonomique de tous les isolats au genre *Streptomyces* et a permis d'assigner chacun d'eux à une ou plusieurs espèces. Cela montre l'abondance de ce genre par rapport aux autres dans les écosystèmes étudiés. Alors que, l'absence des autres genres d'actinomycètes pourrait être expliquée, soit par l'absence de ces genres dans ces écosystèmes , soit par les techniques d'isolement utilisées, ou bien par le fait que la population

Corresponding Author: Elarbi Boussaber (larbi_boussaber@yahoo.fr)

microbienne dans les échantillons est non cultivable. Ainsi, dans ce dernier cas, la confirmation de la présence des autres genres dans ces écosystèmes pourrait être effectuée par l'amplification de l'ADNr 16S par PCR à partir du mélange d'ADN obtenu directement d'échantillons.

MOTS-CLEFS: Identification moléculaire, Séquençage, ADNr, Arbres phylogénétiques, *Streptomyces*.

1 INTRODUCTION

Les méthodes classiques d'identification bactérienne basées sur la détermination des caractères culturaux, physiologiques et métaboliques ont montré leurs limites, en particulier, pour la détection des micro-organismes non cultivables [1]. Elles n'ont conduit qu'à la description d'une très faible partie de la diversité microbienne. La taxonomie moléculaire a été mise en place à partir des années 80 et consiste à l'application des méthodes d'analyses génétiques et moléculaires, notamment la détermination du pourcentage en GC [2], l'hybridation ADN-ADN [3] et le séquençage de l'ARN ribosomique 16S [4], [5], [6]. Ces techniques ont permis de tracer toute la phylogénie des bactéries notamment, celle des actinomycètes.

Le gène ADNr 16S qui code pour l'ARNr 16S (ARN ribosomique 16S) est l'un des gènes les mieux conservés parmi les organismes procaryotes (Eubactéries et Archaea). Il a été choisi comme marqueur phylogénétique en constituant une base de comparaison efficace et fiable pour pouvoir à la fois comparer et différencier les bactéries entre elles. En effet, L'ADNr 16S :

- Comporte des séquences internes très conservées qui permettent de sélectionner des amorces universelles pour l'amplification de l'ADNr 16S de la majorité des bactéries existantes ;
- Comporte des séquences internes variables qui, une fois analysées, permettent de distinguer les espèces de bactéries entre elles et de les classer en fonction de leur phylogénie ;
- Est d'une taille suffisamment courte (~1500 pb) pour être analysé rapidement.

La corrélation des pourcentages d'identité entre séquences d'ADNr 16S et des pourcentages de réassociation ADN/ADN a montré que les séquences d'ADNr 16S ayant des similarités inférieures à 97 %, ne correspondaient jamais à des pourcentages de réassociation ADN/ADN supérieurs à 60 % [7]. Par conséquent, les séquences qui partagent moins de 97 % de similarité correspondent à des espèces différentes.

Cette technique a largement contribué dans la classification et l'identification des bactéries actinomycétales [8]. Grâce au séquençage de l'ARN 16S, certains genres bactériens non mycéliens ont été inclus dans l'ordre des *Actinomycétales*, tandis que d'autres en ont été exclus [9], [10].

Aujourd'hui, plus d'une centaine de milliers de séquences d'ARNr 16S ou du gène ADNr 16S sont mises à la disposition des scientifiques et des chercheurs sur le réseau internet, dans des bases de données généralistes comme Genbank (http ://www.ncbi.nlm.nih.gov/), ou des bases de données spécialisées comme le ribosomal database project (RDP) (http://rdp.cme.msu.edu) à l'Université du Michigan aux États-Unis ou the European ribosomal RNA database à l'Université de Gand en Belgique (http://www.psb.ugent.be/rRNA/index.html).

Dans ce travail, on s'est fixé comme objectif principal l'identification, par l'amplification et le séquençage de l'ADNr 16S, des bactéries actinomycétales isolées d'environnements marocains variés et productrices d'activités antimicrobiennes intéressantes.

2 MATÉRIEL ET MÉTHODES

Parmi les 77 souches d'actinomycètes isolées au Laboratoire d'agroalimentaire et santé de la Faculté des Sciences et Techniques de Settat, 25 ont fait l'objet d'une identification moléculaire par le séquençage de l'ADNr 16S. Ces souches ont été choisies et regroupées selon leurs activités antimicrobiennes (tableau 1) [11].

Les travaux de la présente étude ont été réalisés au laboratoire de séquençage, Unité d'Appui Technique à la Recherche Scientifique (UATRS) au Centre National pour la Recherche Scientifique et Technique(CNRST), Rabat, MAROC.

Tableau 1. Isolats d'actinomycètes sélectionnés pour l'identification moléculaire

N°	Isolat	Origine
1	SP2	Sol de décharge de poterie
2	SP6	
3	SP13'	
4	SDJ1'	Sol de décharge
5	SEU1	Sol irrigué par des eaux usées
6	BEU1	Boue d'eau usée
7	BEU2	
8	EBB	Eaux de barrage
9	EC3	Ecorce de *Casuarina sp.*
10	EA2	Ecorce *Atriplex nummularia*
11	SPO1	Sol phosphaté d'Oued-Zem
13	SPO6	
12	EUS2	Eaux usées
14	SFr1'	Sol de forêt
15	SFr4'	
16	SR1'	Substrat attaché aux rochets
17	Act1	Rhizosphères de conifère
18	Act2r	
19	Act3	Rhizosphères de conifère
20	Rhc1	
21	Rhc-ac1'	
22	Rhc-ac2'	
23	Rhc-ac3'	
24	Rhc-ac10'	
25	Rhc-ac4'	

2.1 EXTRACTION DE L'ADN À PARTIR DES SOUCHES D'ACTINOMYCÈTES

L'extraction de l'ADN est effectuée à partir des cultures d'actinomycètes de 48 heures en milieu liquide. Les cultures des vingt-cinq souches étudiées sont centrifugées à 10000 g pendant 30 secondes. Le culot est lavé avec 0,5 mL de Tris-EDTA à pH égal à 8. Deux centrifugations successives à 10000 g pendant 30 secondes sont réalisées. Après élimination du surnageant, l'extraction de l'ADN est réalisée selon le protocole du kit « GenElute Bacterial Genomic DNA kit » de SIGMA.

Le dosage de la concentration de l'ADN extrait à partir des vingt-cinq échantillons a été réalisé par le Nanodrop 8000.

2.2 REACTION DE POLYMERISATION EN CHAINE (PCR)

2.2.1 AMPLIFICATION DU FRAGMENT D'ADN RIBOSOMIQUE 16S

L'amplification de l'ADN in vitro est effectuée par la technique de la PCR (Polymerase Chain Reaction) qui permet d'obtenir un très grand nombre de copies d'une séquence d'ADN. La séquence choisie dans cette étude est le gène ribosomal 16S (1500 paires de bases).

Les gènes codant l'ARN ribosomal 16S des souches sont amplifiées par l'utilisation des amorces (ou primers) suivantes :

- Fd1 (5'-AGAGTTTGATCCTGGCTCAG-3') ;
- Rp2 (5'-AAGGAGGTGATCCAGCC-3').

L'amplification est réalisée dans un thermocycleur de type « Verity » d'Applied Biosystems. Le tableau 2 donne la composition du milieu de réaction PCR. L'opération débute par une dénaturation initiale à 96°C pendant 4 min, ensuite 35 cycles comportant 10 secondes de dénaturation à 96°C, 40 secondes d'hybridation à 52°C, 2 min d'élongation à 72 °C et enfin terminée par une élongation finale à 72°C pendant 4 min.

Tableau 2. Mélange réactionnel et quantité de réactifs utilisés pour une réaction PCR

Réactifs (Tampon et Taq platinium d'Invitrogen)	Quantités en (µl) pour un tube
Tampon 10x	2.5
dNTP 10 mM	2
Amorces Fd1 (100 µM)	0.125
Amorce Rp2 (100 µM)	0.125
MgCL2 (50 mM)	0.75
Taq DNA polymerase 5 U/µl	0.2
H2O	14.3
ADN (30 ng/µl)	5

2.2.2 PURIFICATION DES PRODUITS DE PCR

La purification des produits de PCR a pour but d'enlever les amorces et les nucléotides (dNTPS) non utilisés durant la réaction de PCR. Elle est réalisée selon le protocole du Kit « ExoSAP-IT » qui consiste, d'abord, à mélanger dans des plaques de réaction « MicroAmp optical 96 », 5 µL du produit de la réaction de PCR et 2 µL de l'ExoSAP-IT, pour un volume final de 7 µL. Ensuite, incuber la plaque de réaction à 37°C pendant 15 min dans le thermocycleur pour dégrader les amorces et les nucléotides libres. Enfin, incuber la plaque de réaction à 80°C pendant 15 min pour inactiver l'ExoSAP-IT. Le produit de PCR est, donc, prêt à l'analyse pour le séquençage.

Après amplification, les échantillons sont analysés par éléctrophorèse dans un gel d'agarose à 1 % en présence d'un marqueur de poids moléculaire 100 paires de bases. Après migration, le gel est examiné sous lumière ultraviolette pour repérer les bandes amplifiées. Les photos ont été visualisées par le système de photo documentation « G Box ».

2.3 SEQUENÇAGE

La méthode de séquençage utilisée est celle automatisée en utilisant un séquenceur automatique capable de réaliser à la fois les réactions ainsi que la détermination de la séquence nucléotidique du fragment d'ADN étudié.

Dans ce travail, on a utilisé le séquenceur automatique ABI 3130 Genetic Analyser (séquenceur 16 capillaires de la société Applied Biosystems). La méthode utilisée est celle de Sanger [12] se basant sur la technologie des ddNTPs (Société Applied Biosystems). Les réactions de séquences ont été réalisées dans des plaques PCR de 96 puits en utilisant le kit de séquençage (Big Dye Terminator version 3.1 ou version 1.1 cycle sequencing –Applied Biosystems).

2.4 ANALYSE DES SEQUENCES NUCLEOTIDIQUES

Les résultats du séquençage des fragments d'ADNr amplifiés ont été obtenus sous forme d'électrophorégrammes bruts. Ces derniers ont été visualisés par le logiciel SequenceScanner (Applied Biosystems) et analysés par le logiciel Chromas lite 2.1. Les alignements du couple des séquences sens/antisens sont effectués par le logiciel DNAMAN pour définir la séquence consensus. Les séquences obtenues sont comparées à des séquences homologues contenues dans la banque informatique internationale de données dénommée « GenBank » à l'aide de Blast (Basic Local Alignment Search Tool) [13] dans le site web de Genbank « http ://blast.ncbi.nlm.nih.gov/Blast.cgi » afin de déterminer leur affiliation phylogénétique. Les résultats sont exprimés en pourcentage de similarité de la souche à identifier avec les espèces les plus proches, et sous forme d'arbres phylogénétiques qui montrent la position taxonomique de chaque isolat.

3 RESULTATS ET DISCUSSION

3.1 EXTRACTION ET AMPLIFICATION DU GENE DE L'ADN RIBOSOMIQUE 16S

Après extraction de l'ADN à partir des souches d'actinomycètes isolées et dosage par Nanodrop d'ADN extrait, la pureté est particulièrement analysée. La figure 1 donne les concentrations des vingt-cinq échantillons étudiés. La pureté de l'ADN est considérée comme étant correcte. En effet, la densité optique 260/280 est supérieure à 0,8 et la densité optique 230/280 est supérieure à 2 pour la majorité des échantillons.

Les fragments d'ADNr 16S ont été, ensuite, amplifiés par PCR universelle. Après l'électrophorèse des produits de la PCR, le gel d'agarose est photographié sur table UV, les bandes d'ADN ont bien migré dans la région 1500 paires de bases (Figure 2).

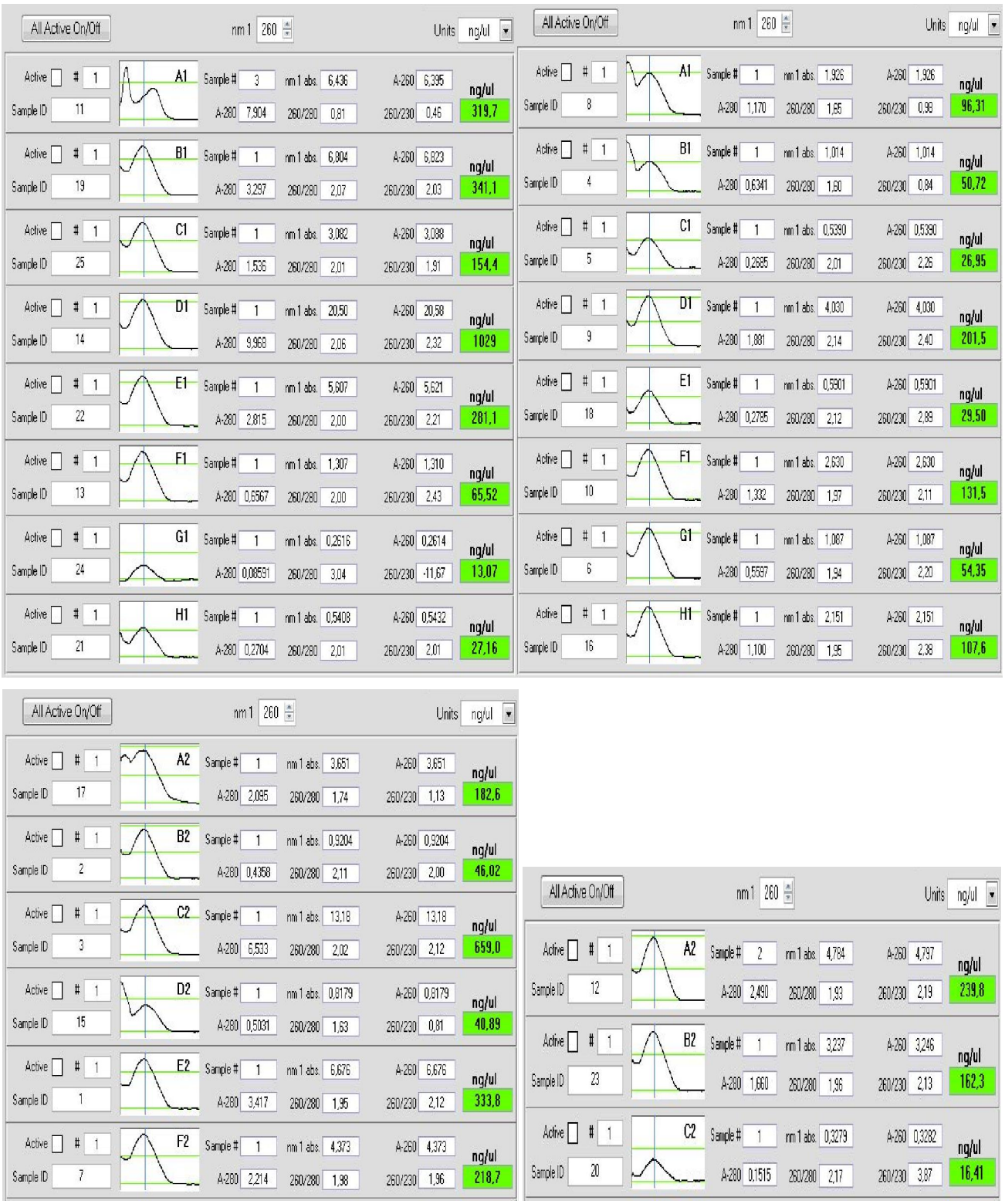

Fig. 1. Résultats du dosage d'ADN extrait par Nanodrope

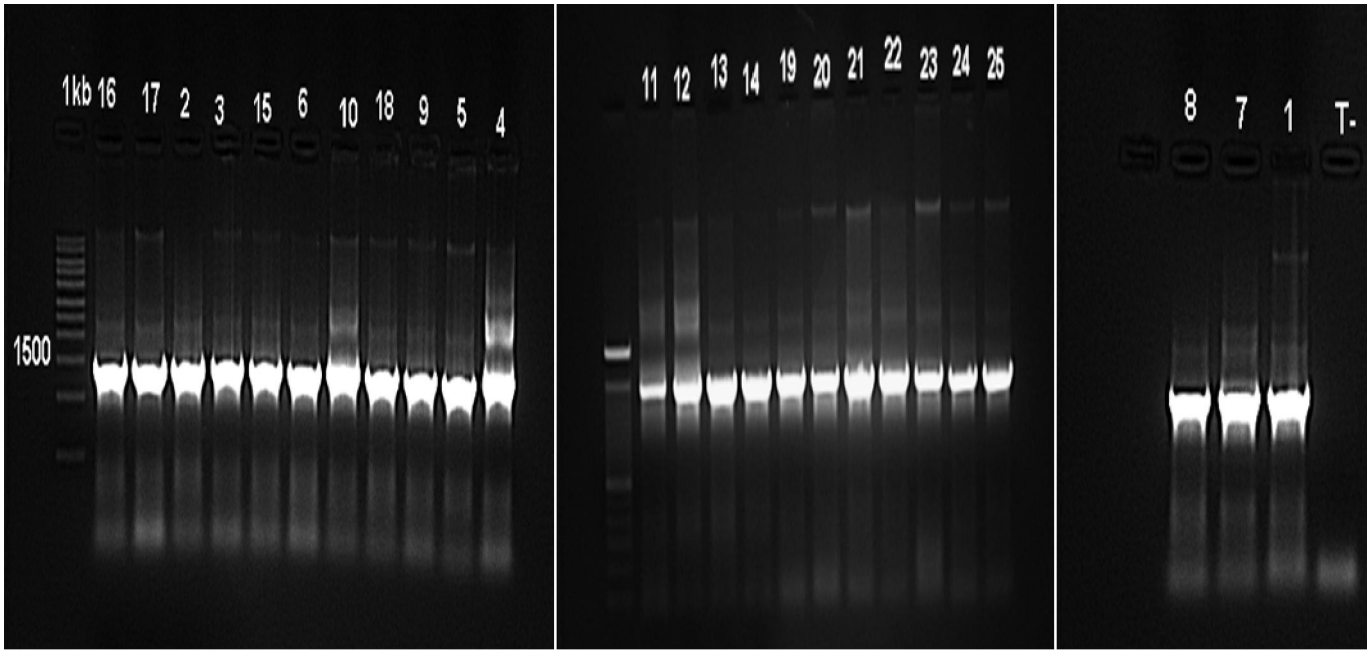

Fig. 2. Résultats de l'électrophorèse des produits de la PCR des vingt-cinq souches étudiées

3.2 SEQUENÇAGE DES FRAGMENTS D'ADN RIBOSOMIQUE 16S

Le séquençage des fragments obtenus, sous forme d'électrophorégrammes, permet d'accéder à la diversité des actinomycètes présents dans les échantillons étudiés.

Les électrophorégrammes obtenus par le logiciel SequenceScanner (Applied Biosystems), relatifs aux vingt-cinq souches d'actinomycètes, ont été analysés par le logiciel Chromas lite 2.1 pour déterminer les séquences nucléotidiques de chaque échantillon.

3.3 ALIGNEMENT ET COMPARAISON DES SEQUENCES OBTENUES AVEC CELLES CONTENUES DANS LA BANQUE DE DONNEES « GENBANK »

Les couples des séquences sens/antisens, ainsi obtenues, sont alignés par le logiciel DNAMAN pour définir les séquences consensus. Ces dernières sont comparées à des séquences disponibles au niveau de la banque informatique internationale (GenBank). Les résultats sont exprimés en pourcentage de similarité de la souche à identifier avec les espèces les plus proches.

L'alignement des séquences nucléotidiques avec celles de la banque de données montrent que les 25 souches d'actinomycètes isolées sont classées dans le phylum des *Actinobacteria*, la classe V des *Actinobacteridae* et l'ordre I des *Actinomycetales* et toutes font partie au genre *Streptomyces.*

Chaque isolat présente une similitude avec plusieurs espèces de la banque de donnée « Genbank ». Pour affilier chacun des isolats à l'une des espèces les plus proches, une analyse phylogénétique est donc nécessaire.

3.4 ANALYSE PHYLOGENETIQUE

Les arbres phylogénétiques représentent les relations phylogénétiques entre les séquences nouvellement obtenues et des séquences de référence dans les banques de données. Ils ont été construits par la méthode des distances Neighbor-Joining par le programme Blast. C'est une méthode de distance basée sur le nombre moyen de substitutions nucléotidiques entre des séquences prises deux à deux. Elle permet de trouver les paires de séquences les plus voisines qui minimisent la somme des longueurs des branches de chaque étape de regroupement.

Les figures 3, 4, 5 et 6 représentent les différents types d'arbres qui ont été élaborés pour déterminer l'appartenance taxonomique aux espèces les plus similaires à l'isolat SP13'. Ce dernier est pris comme exemple afin de montrer la démarche suivie pour trouver les espèces très similaires aux vingt-cinq souches d'actinomycètes concernées.

La figure 3 montre l'affiliation de cet isolat au groupe des bactéries Gram positives dont le coefficient de Chargaff (G+C %), est élevé. Chez les actinomycètes, ce coefficient est supérieur à 55 %, généralement compris entre 60 et 75 % [14]. Cela confirme l'appartenance de l'isolat SP13' aux bactéries actinomycétales.

Dix-sept espèces appartenant au genre Streptomyces présentent des séquences très similaires à l'isolat SP13' (figure 3, 4). Le pourcentage de similarité varie entre 97 % et 98 % (tableau 3). Les arbres phylogénétiques élaborés sous forme triangulaire (figure 5) et radiale (figure 6), où les nœuds sont écartés les uns des autres pour une meilleure présentation, montrent que *Streptomyces crystallinus* NBRC 15401 est l'espèce la plus apparentée à la souche SP13'.

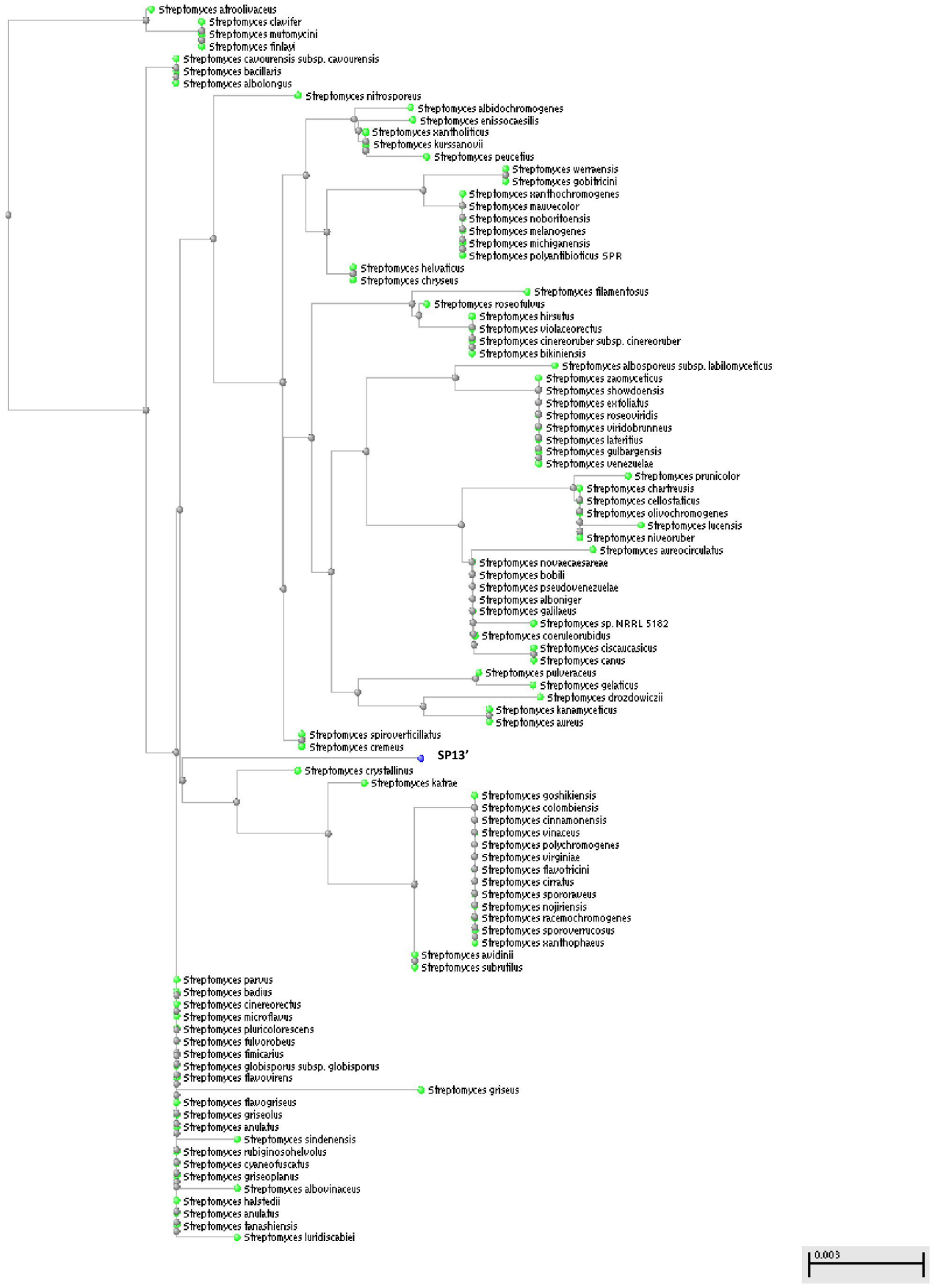

Fig. 3. Arbre phylogénétique basé sur les gènes codant l'ARNr 16S montrant la position de l'isolat SP13'

Tableau 3. Espèces proches de l'isolat SP13' et leur degré de similarité

Espèces proches	Degré de similarité	Accession
***Streptomyces crystallinus* NBRC 15401**	98 %	NR_041177.1
***Streptomyces avidinii* NBRC 13429**	98 %	NR_041132.1
***Streptomyces subrutilus* DSM 40445**	98 %	NR_026203.1
***Streptomyces sporoverrucosus* NRRL B-16379**	98 %	NR_043837.1
***Streptomyces goshikiensis* NRRL B-5428**	98 %	NR_044147.1
***Streptomyces colombiensis* NRRL B-1990**	98 %	NR_043494.1
***Streptomyces cinnamonensis* NBRC 15873**	98 %	NR_041194.1
***Streptomyces vinaceus* NBRC 13425**	98 %	NR_041131.1
***Streptomyces polychromogenes* NBRC 13072**	98 %	NR_041109.1
***Streptomyces virginiae* NBRC 12827**	98 %	NR_041078.1
***Streptomyces flavotricini* NRRL B-5419**	98 %	NR_043380.1
***Streptomyces cirratus* NRRL B-3250**	98 %	NR_043356.1
***Streptomyces spororaveus* LMG 20313**	98 %	NR_042306.1
***Streptomyces nojiriensis* LMG 20094**	98 %	NR_042303.1
***Streptomyces racemochromogenes* NRRL B-5430**	97 %	NR_043499.1
***Streptomyces katrae* NBRC 13447**	97 %	NR_041136.1
***Streptomyces xanthophaeus* NRRL B-5414**	97 %	NR_043848.1

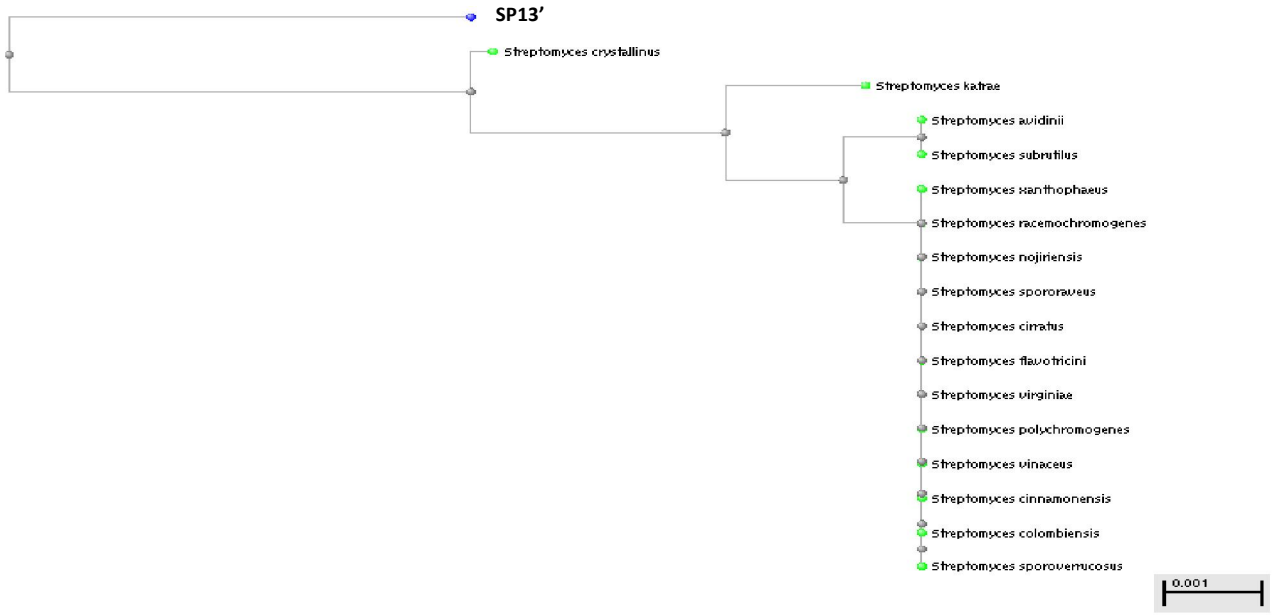

Fig. 4. Arbre phylogénétique basé sur les gènes codant l'ARNr 16S montrant l'affiliation de SP13'

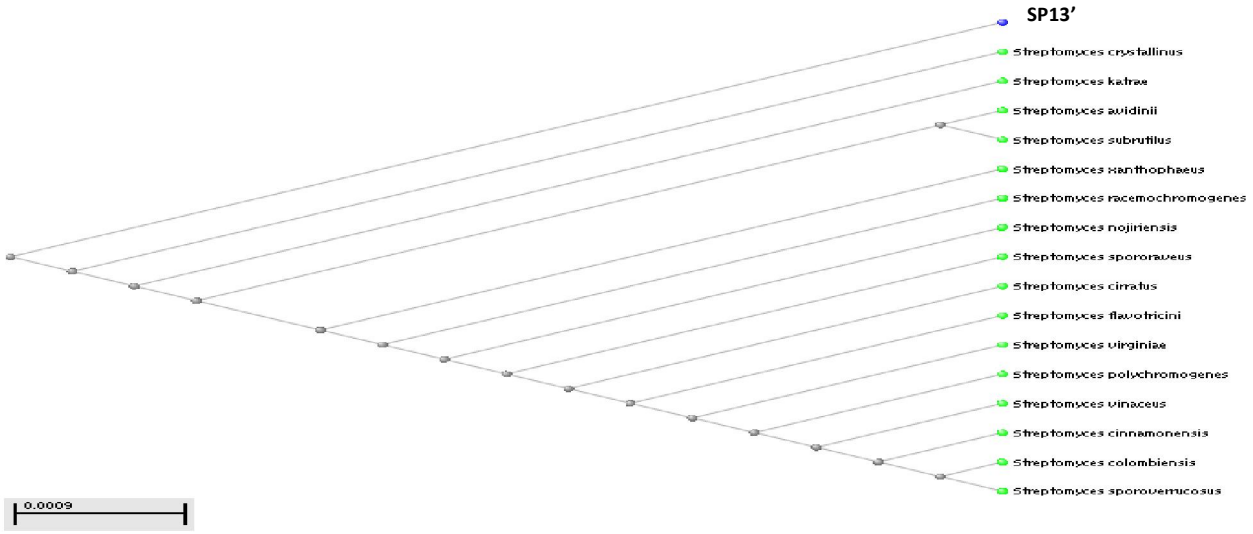

Fig. 5. Arbre phylogénétique sous forme triangulaire basé sur les gènes codant l'ARNr 16S montrant l'affiliation de SP13'

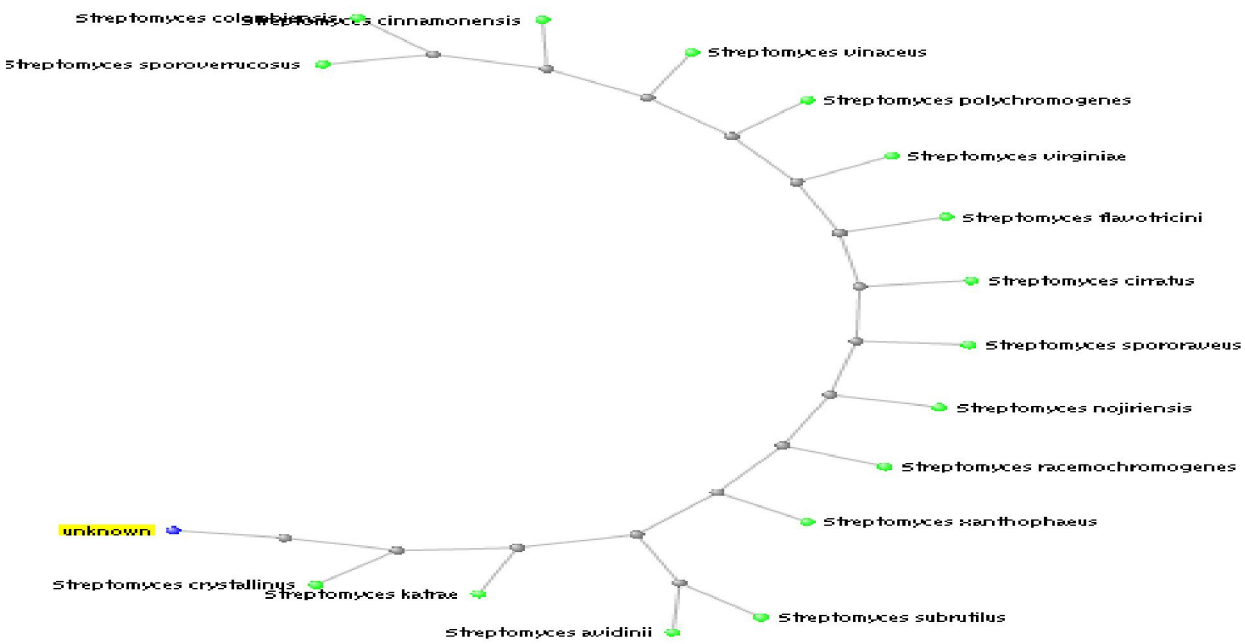

Fig. 6. Arbre phylogénétique sous forme radiale basé sur les gènes codant l'ARNr 16S montrant l'affiliation de la souche SP13'

Le même travail a été effectué pour les vingt-quatre autres souches. Les résultats obtenus sont rassemblés dans le tableau 4. Chaque isolat présente une forte similitude avec une ou plusieurs espèces. 19 (76 %) isolats présentent des pourcentages de similarité supérieurs ou égal à 97 %, 5 (20 %) présentent des pourcentages de similarité compris entre 90 et 96 % et c'est seulement 1 (0,4 %) qui présente une similarité de 74 %.

Lorsqu'il existe moins de 97 % de similarité entre les séquences des ADNr 16S de deux souches, ces souches appartiennent à des espèces différentes [7]. Par contre, si le pourcentage de similarité est égal ou supérieur à 97 %, l'affiliation taxonomique à une unique espèce ou à deux espèces différentes nécessite la mise en œuvre d'autres techniques, telle que celle se basant sur les hybridations ADN-ADN.

Tableau 4. Espèces proches des vingt-cinq souches d'actinomycètes étudiées et leurs degrés de similitude

Isolat	Espèces proches	Degré de Similarité	N° d'accession
SP2	*Streptomyces parvus* NRRL B-1455	99 %	NR_043833.1
	Streptomyces badius NRRL B-2567	99 %	NR_043350.1
SP6	*Streptomyces cavourensis* subsp. *Cavourensis* NRRL 2740	98 %	NR_043851.1
SP13'	*Streptomyces crystallinus* NBRC 15401	98 %	NR_041177.1
SDJ1'	*Streptomyces alanosinicus* NBRC 13493	74 %	NR_041148.1
SEU1'	*Streptomyces melanogenes* NBRC 12890	97 %	NR_041089.1
BEU1	*Streptomyces globisporus* subsp. *Globisporus* NRRL B-2872	97 %	NR_044145.1
BEU2	*Streptomyces cellulosae* NRRL B-2889	98 %	NR_043815.1
EBB	*Streptomyces flavovirens* NRRL B-2685	97 %	NR_043487.1
EC3	*Streptomyces badius* NRRL B-2567	98 %	NR_043350.1
EA2	*Streptomyces iakyrus* NBRC 13401	93 %	NR_041231.1
SPO1	*Streptomyces viridodiastaticus* IFO 13106	95 %	NR_043367.1
EUS2	*Streptomyces griseus* KACC 20084	92 %	NR_042791.1
SPO6	*Streptomyces cinnabarinus* NBRC 13028	91 %	NR_041097.1
SFr1'	*Streptomyces melanogenes* NBRC 12890	98 %	NR_041089.1
SFr4'	*Streptomyces rectiviolaceus* NRRL B-16374	98 %	NR_043502.1
SR1'	*Streptomyces badius* NRRL B-2567	98 %	NR_043350.1
Act1	*Streptomyces coeruleorubidus* NBRC 12761	98 %	NR_041217.1
Act2r	*Streptomyces peucetius* JCM 9920	98 %	NR_024763.1
Act3	*Streptomyces badius* NRRL B-2567	98 %	NR_043350.1
Rhc1	*Streptomyces crystallinus* NBRC 15401	98 %	NR_041177.1
Rhc-ac1'	*Streptomyces griseoflavus* LMG 19344	97 %	NR_042291.1
Rhc-ac2'	*Streptomyces sampsonii* ATCC 25495	96 %	NR_025870.1
Rhc-ac3'	*Streptomyces humiferus* DSM 43030	98 %	NR_025250.1
Rhc-ac10'	*Streptomyces ciscaucasicus* NBRC 12872	97 %	NR_041085.1
	Streptomyces canus NRRL B-1989	97 %	NR_043347.1
	Streptomyces plumbiresistens CCNWHX 13-160	97 %	NR_044518.1
Rhc-ac4'	*Streptomyces sp.* 40003	98 %	NR_042760.1
	Streptomyces tendae ATCC 19812	98 %	NR_025871.1

4 CONCLUSION

Après amplification par PCR de l'ADNr 16S des isolats et comparaison des séquences obtenues avec celles des espèces d'actinomycètes disponibles au niveau des bases de données (GenBank) en utilisant le programme Blast, les 25 souches étudiées ont été assimilées au genre *Streptomyces* avec des pourcentages d'homologies allant de 74 % à 99 %. Ces résultats confirment donc l'abondance des *Streptomyces* par rapport aux autres dans les écosystèmes étudiés. L'absence des autres genres d'actinomycètes pourrait être expliquée soit par l'absence de ces genres dans les écosystèmes étudiés, soit à cause des techniques d'isolement utilisées. En plus, seulement 0,001 à 15 % de la population microbienne présente dans les différents écosystèmes serait cultivable [15]. La confirmation de la présence des autres genres dans ces écosystèmes pourrait être effectuée par amplification du gène codant pour l'ARNr 16S par PCR à partir du mélange d'ADN obtenu directement d'échantillons [16]. En effet, la caractérisation d'un organisme en terme de phylotype ne nécessite qu'une séquence génétique et non pas une cellule fonctionnelle. Ce qui pourrait permettre la détection de microorganismes inaccessibles en culture.

Les techniques moléculaires, principalement celles basées sur l'analyse des séquences d'ADNr 16S, permettent, donc, la mise en évidence de la diversité phylogénétique dans les différents types d'écosystèmes.

Des études antérieures ont montré que ces souches d'actinomycètes (S*treptomyces)* présentent une activité antimicrobienne intéressante. Mais, pour certains auteurs, les métabolites bioactifs d'intérêts pharmaceutiques isolés à partir des S*treptomyces* ont été largement exploités. Ils suggèrent qu'il faudrait s'orienter vers la recherche et l'isolement des bactérie actinomycétales autres que les *Streptomyces* afin de découvrir des substances bioactives nouvelles [17], [18], [19], [20], [21],[22], [23]. Par contre, les travaux d'autres chercheurs qui se sont lancés dans des screening de toute la flore actinomycétale sans écarter les *Streptomyces,* ont montré que les *Streptomyces* constituent encore une ressource d'antibiotiques et de diverses substances pharmaceutiques très intéressantes [24], [25], [6].

REFERENCES

[1] Douga Catherine, Joel Dore, Abdelghani Sghir, "La diversité insoupçonnée du monde microbien," *MEDECINE/SCIENCES,* vol. 21, pp. 290-296, 2005.

[2] Chargaff, E. and Vischer E., "The composition of the desoxypentose nucleic acids of thymus and spleen," *J. Biol. Chem.,* vol. 177, pp. 405–416, 1949.

[3] Labeda D. P., "DNA-DNA hybridization in the systematics of *Streptomyces*," *Gene.,* Vol. 115, pp. 249-253, 1992.

[4] Jeffrey, L. S. H., "Isolation, characterization and identification of actinomycetes from agriculture soils at Semongok, Sarawak," *African Journal of Biotechnology,* Vol. 7, n°. 20, pp. 3697-3702, October, 2008.

[5] Afifi M.M., H. M. Atta, A.A. Elshanawany, U.M. Abdoul-raouf and A.M. El-Adly, "Biosynthesis of Hygromycin-B Antibiotic by Streptomyces crystallinus AZ151 Isolated from Assuit, Egypt," *Bacteriol. J.*, vol. 2, pp. 46-65, 2012.

[6] Boughachiche Faiza, "Étude de molécules antibiotiques secrétées par des souches appartenant au genre Streptomyces, isolées de Sebkha," Thèse *de doctorat, Université Mentouri- Constantine., Faculté des Sciences de la Nature et de la Vie*, Algérie, 164p, 2012.

[7] Stackebrandt E., and Goebel B. M., "Taxonomic note: a place for DNA-DNA reassociation and 16S rRNA sequences analysis in the present species definition in bacteriology," *Int. J. Syst. Bacteriol*., vol. 44, pp. 846-849, 1994.

[8] Laurent F.J., Provost F., Boiron P., "Rapid identification of clinically relevant *Nocardia species* to genus level by 16S rRNA gene PCR," *J. Clin. Microbiol*., vol. 37, pp. 99-102, 1999.

[9] Kim B. S., Lonsdale J., Seong C.N., et Goodfellow M., "*Streptacidiphilus* gen. nov., acidophilic actinomycetes with wall chemotype I and emendation of the family *Streptomycetaceae*," *Ant. V Leeuwenhoek.,* vol. 83, pp. 107-116, 2003.

[10] Labeda D. P., Goodfellow M., Brown R., Ward A. C., Lanoot B., Vanncanneyt M., Swings J. et al., "Phylogenetic study of the species within the family *Streptomycetaceae*," *Antonie van Leeuwenhoek*, vol. 101, pp. 73-104, 2012.

[11] Boussaber Elarbi, "Isolement et identification des souches d'actinomycètes productrices de substances antimicrobiennes à partir de différents types d'écosystèmes marocains," *Thèse de doctorat, Université Hassan 1er, FST Settat, Maroc*, 232p, 2013.

[12] Sanger F., Nicklen S. et Coulson A.R., "DNA sequencing with chain terminating inhibitors," *Proc Nat Acad Sci USA*, Vol. 74, pp. 5463-5467, 1997.

[13] Altschul S. F., Madden T. L., Schaffer A. A., Zhang J., Zhang Z., Miller W., Lipman D. J. Gapped, "BLAST and PSI-BLAST: a new generation of protein database search programs," *Nucleic Acids Res.,* vol. 25, pp. 3389-3402, 1997.

[14] Chun J., Youn H.-D., Yim Y.-I., Lee H., Kim M. Y., Hah Y.C., Kang S.O., "*Streptomyces seoulensis sp.,*" *Nov. Int. J. syst. Bact*., vol. 47, pp. 492-498, 1997.

[15] Amann R. I., Ludwig W. and Schleifer K.-H., "Phylogenetic identification and in situ detection of individual microbial cells without cultivation," *Microbiol. Rev*., vol. 59, pp. 143-169, 1995.

[16] Meftah k. I., Boussaber E., Amahdar L., Abboussi O., Amghar S., Hilali L. et Hilali A., "An improved extraction procedure of DNA from the "El Halassa" phosphate deposit (Khouibga, Morocco)," *Engineering Science and Technology Int. J. (ESTIJ),* vol. 2, n°. 6, pp. 1002-1008, 2012.

[17] SHEARER MC, "Methods for the isolation of non-*streptomycetes actinomycetes*," *J. Ind. Microbiol.,* vol. 28, pp. 91-8, 1997.

[18] Ouhdouch, Y., Barakate, M., Finace, C., "Actinomycetes from Maroccan Habitats: Screening for antifungal activites," *Eur. J. soil Biol*., vol. 37, pp. 1-6, 2001.

[19] LAMARI L., ZITOUNI A., "New dithiolopyrrolone antibiotics from *Saccharothrix sp*. SA 233. I. Taxonomy, fermentation, isolation and biological activities," *J. Antibiot*. Vol. 55, pp. 696-701, 2002.

[20] Zakharova O S OS, G M GM Zenova, and D G DG Zviagintsev, "Selective isolation of actinomycetes of the genus Actinomadura from soil," *Mikrobiologiia,* vol. 72, n°. 1, pp. 126-30, 2003.

[21] Zitouni A, Boudjella.H, Lamari L, Badji.B, Mathieu.F, Lebrihi A, Sabaou. N., "*Nocardiopsis* and *Saccharothrix* genera in saharan soils in Algeria: Isolation, biological activities and partial characterization of antibiotics," *Res. Microbio*., Vol. 42, pp. 1-10, 2005.

[22] Hilali L., "Isolement et sélection de souches d'actinomycètes productrices de substances antifongiques de structure non-polyénique. Production, extraction, purification de métabolite active et étude taxonomique," *Thèse de doctorat : Université Hassan II- Faculté des sciences (Maroc)*, 177p, 2006.

[23] Marinelli F., "Antibiotics and *Streptomyces*: the futur and antibiotic discovery," *Microbiol. Today*, vol. 2, pp. 20-23, 2009.

[24] BORAMORA A., ATTILI A., ARENGHI F., "A novel chimera : "the trancated hemoglobin-antibiotic monooxygenase" from *Streptomyces avermitilis*," *Gene*, vol. 393, pp. 52-61, 2007.

[25] Smaoui S., "Purification et caractérisation de biomolecules à partir de microrganismes nouvellement isolés et identifiés," *Thèse de Doctorat en Génie de Procédés et Environnement, Université de Toulouse, France*, 251p, 2010.

International Journal of Innovation and Applied Studies
ISSN 2028-9324 Vol. 3 No. 4 Aug. 2013, pp. 1066-1071

http://www.issr-journals.org/ijias/

Studies of Uranium Recovery from Tunisian Wet Process Phosphoric Acid

Naima Khleifia[1], Ahmed Hannachi[1], and Noureddine Abbes[2]

[1]Chemical-Process Engineering Department,
National Engineering School of Gabes, University of Gabes,
Gabes, Tunisia

[2]Research Direction of Tunisian Chemical Group,
Gabes, Tunisia

ABSTRACT: The growing worldwide energy demand associated with several inter related complex environmental as well as economical issues are driving the increase of the share of uranium in energy mix. Subsequently, over the last few years, the interest for uranium extraction and recovery from unconventional resources has gained considerable importance. Phosphate rock has been the most suitable alternative source for the uranium recovery because of its uranium content. Solvent extraction has been found to be a successful process for uranium separation from phosphoric acid. The synergistic solvent mixture of Di-2-EthylHexyl Phosphoric Acid (DEHPA) and TriOctyl Phosphine Oxid (TOPO) diluted in kerosene has been the favored because of its high efficiency and selectivity for uranium extraction. In the present work, uranium extraction from Tunisian Wet Process Phosphoric Acid (WPA) using DEHPA in combination with synergistic reagent TOPO is presented. An experimental study was conducted in order to optimize the operating parameters affecting uranium recovery from phosphoric acid. The effect of temperature, solvent ratio, acid concentration and extractants concentrations were considered. The experiments were performed at a laboratory scale with batch extractions. Overall extraction yields are reported in this work. High uranium extraction yields exceeding 95% were obtained in all extraction steps but one where the yield was 92%. The overall recovery yield was 81%.

KEYWORDS: Uranium, industrial phosphoric acid, recovery, solvent extraction, yield.

1 INTRODUCTION

Nuclear power is expected to be an important part of the worldwide energy mix for the next 50 years. This in turn will make it necessary to develop alternatives and economically feasible technologies for the uranium production from sources other than uranium ore [1]. Many countries with limited energy resources, has invested substantial efforts in the study of uranium separation from non conventional resources such as coal, natural waters, including seawater and phosphate ores. These routes are technically feasible, economically attractive and potentially important because they may allow access to vast uranium resources [2].

Phosphate rocks have been the most suitable alternative source for uranium recovery. The concentration of uranium in phosphate rocks changes from one deposit to another, ranging from 50 to 200 ppm. It represents a significant potential source of uranium as large amounts of phosphate rock are processed [3]-[4]. Table 1, shows the uranium concentrations in phosphate rocks in various parts of the world.

Over the last few years, extensive studies on uranium recovery from wet-process phosphoric acid have been carried out. Various methods were used for uranium recovery from phosphoric acid. The most common are: solvent extraction, precipitation and ionic exchange [5]-[8]. Solvent extraction has been found to be the most successful process for industrial recovery of uranium from phosphoric acid [8]-[9].

Corresponding Author: Naima Khleifia (naima_khleifia@yahoo.fr)

Several solvent extraction processes have been developed [10]-[16]. Of the various extraction solvents reported in the literature, only three have a commercial interest:

- Octyl pyrophosphoric acid (OPPA)
- Octyl phenyl acid phosphate (OPAP)
- Synergistic solvent mixture of di-2-ethylhexyl phosphoric acid (DEHPA) and trioctyl phosphine oxide (TOPO).

While the first solvents are capable of extraction tetravalent uranium, the last extracts hexavalent uranium. Processes based on the latter are the most successful. Several plants adopting the DEHPA-TOPO solvent were constructed in many countries [17]-[19].

Exhaustive experimental studies were conducted in the literature on the uranium recovery from phosphoric acid employing different synergistic extractant mixtures. However, most reported studies were focused on uranium recovery from synthetic phosphoric acid solutions. Uranium extraction studies from real solutions are very scarce.

In the present paper, the uranium extraction process from Tunisian Wet Process Phosphoric Acid (WPA) using DEHPA in combination with synergistic reagent TOPO was considered. An experimental study has been carried out to optimize the main operating parameters affecting the uranium recovery from phosphoric acid. The considered variables are: temperature, solvent ratio, acid concentration and extractants concentrations. In this work, only extraction yields for each process extraction steps are reported.

Table 1. Uranium content of selected world phosphate rocks

Country	Uranium (ppm)
Tunisia	45 – 140
Algeria	25-100
Australia	80 – 92
Egypt	40 – 120
Jordan	46
Morocco	70 – 80
Saudia Arabia	25 – 185
Senegal	64 – 70
Syria	75
Tanzania	390
Togo	77 – 110
USA	41 – 200

2 URANIUM RESERVES IN TUNISIAN PHOSPHATE ORES

In Tunisia, the phosphate ores represent the most important source of uranium. They are extracted from four main locations in the Gafsa region in the southern part of the country: Metlaoui, Moulares, Redeyef and Mdhilla. Since the discovery of phosphate deposits in 1896, phosphate production is controlled and operated by Gafsa Phosphate Company (CPG). CPG currently processes annually an average of 8 million tons of commercial phosphates. Table 2 shows an average chemical composition and uranium content of the main exploited phosphate ores in Tunisia. The average uranium content in Gafsa basin phosphate ores is above 50 ppm. Phosphate reserves in these deposits are estimated to several hundreds of million tons. Consequently, the corresponding uranium amount in the phosphate reserves can be evaluated at 50 000 tons. Tunisia possesses other large phosphate deposits with reserves matching those of the Gafsa basin. They are located in Sraa-ouertane region in the north western part of Tunisia. Up to date, these reserves having an average uranium content of 100-140 ppm are not exploited.

Table 2. Typical chemical composition of the main exploited phosphate ores in Tunisia

Elément chimique	Metlaoui	Mdhilla	Moulares
P_2O_5 (%)	28,8	28,2	29,8
Fe (%)	0,18	0,10	0,18
Mg (%)	0,29	0,51	0,42
Al (%)	0,37	0,21	0,32
Cr (ppm)	115,0	84,0	139,0
Zn (ppm)	318,0	107,0	406,0
Cd (ppm)	37,0	20,0	50,0
Cu (ppm)	9,0	5,0	13,0
Ni (ppm)	12,0	7,0	23,0
Mn (ppm)	20,0	22,0	23,0
V (ppm)	32,0	31,0	53,0
U (ppm)	57,0	49,0	68,0

Nearly 80% of the extracted phosphate is processed into WPA and mineral fertilizers in the Tunisian Chemical Group (GCT). Tunisia is ranked among the top producers of phosphoric acid and fertilizers. Because of the huge quantities of processed phosphate ores in Tunisia, the corresponding uranium quantities are large. For instance, considering the presently processed phosphate quantities in GCT, the total amount of uranium at stake mounts to approximately 360 tons/year. This alone represents potentially a large resource of uranium when extracted economically as a by-product of the WPA production process.

In Tunisia, the WPA is produced by a chemical reaction of the phosphate rock with sulfuric acid according to the dihydrate process. This process involves the solubilization of most heavy metals and radionucleides contained in the raw material (Cd, U, Ni, Pb, Zn, Cr, Cu, etc.). A typical detailed analysis of Tunisian WPA is given in table 3.

Table 3. Typical analysis of Tunisian WPA

P_2O_5 (wt.%)	U (ppm)	Fe (ppm)	Mg (ppm)	Cd (ppm)	Al (ppm)	Cr (ppm)	V (ppm)	F (%)	SO_4^{2-} (%)
25	37	1500	2900	14	1860	160	38	0.82	0.91

3 MATERIALS AND METHODS

In order to economically obtain uranium from the WPA, recovery process should be investigated in detail. Therefore, experimental work has been conducted on a laboratory scale to select and optimize the operating parameters of each process step. To reach this aim, the experimental design method was used to study the effect of each parameter separately and their interactions. The main variables that can affect uranium recovery process were included: temperature, solvent ratio, phosphoric acid concentration, and extractants concentrations.

The WPA used in this study, of 25% wt. P_2O_5 content, was provided by the GCT. Its average chemical composition is shown in Table 3. Uranium extraction process flowsheet is shown in figure 1. The phosphoric acid has an initial ElectroMotive Force (EMF) of approximately 400 mV. Prior to extraction, the acid was treated with activated carbon for removal of soluble organic matter. The treated acid was oxidized with hydrogen peroxide till an adequately high EMF was obtained in order to convert all of uranium into the hexavalent state. The uranium rich pretreated phosphoric acid is extracted with DEHPA-TOPO system dissolved in kerosene. The extraction step is followed by a reductive stripping using phosphoric acid containing ferrous ions. In each of the previous operations, uranium gets concentrated in the main stream. The uranium content is further increased by performing a second extraction cycle. The uranium loaded acid, then feeds a second extraction step using the same solvent. Uranium is stripped from the organic solvent by an ammonium carbonate solution.

The DEHPA and TOPO used were of a purity exceeding 96%. The commercial grade kerosene was used as diluent after acid washing followed by alkaline solution neutralization and alkaline stripping with water. Extraction experiments were

carried out in covered beakers with a magnetic stirring and temperature control. The aqueous and organic phases were mixed and allowed to separate for 15 minutes. The uranium concentration in the aqueous phase was determined using a Jobain Yvon ICP 2000 spectrometer. The uranium content of the organic phase was calculated by mass balance.

4 RESULTS AND DISCUSSION

4.1 FIRST CYCLE OF URANIUM RECOVERY PROCESS

4.1.1 URANIUM OXIDATION

Hydrogen peroxide (H_2O_2) 30% wt. was employed as oxidizing agent in order to convert uranium into the hexavalent state. The electromotive force EMF was used as an indicator for the oxidation degree of uranium in the acid. To ensure that uranium was at its highest valence, the oxidant was added until the uppermost EMF value was reached. The effects of WPA concentration and temperature were examined to find the best operating conditions of this operation. Results showed that the temperature has a significant effect on contact time needed and subsequently on the hydrogen peroxide amount required for oxidation.

4.1.2 URANIUM EXTRACTION BY DEHPA-TOPO

The pretreated phosphoric acid with sufficient high EMF value is extracted with DEHPA-TOPO system. The study examined the effect of various factors on uranium extraction yield. Experiments were conducted at several levels of acid concentration, temperature, solvent rate and DEHPA-TOPO molar ratio according to a factorial design. The experimental domain was chosen in order to obtain the effect of each parameter on extraction performances. The results showed that the phosphoric acid concentration has a significant negative effect on the uranium extraction. However, the other parameters have slight effects on the extraction performance. The uranium extraction yield reached over 92% in the best operating conditions.

4.1.3 URANIUM REDUCTION

In the recovery process, uranium was stripped from the loaded DEHPA-TOPO solvent in the first cycle by reduced phosphoric acid. Iron was used as reducing agent. It was initially activated by sulfuric acid in order to enhance its reactivity and reduction capacity. The effect of the parameters affecting the reduction step was separately investigated. The operating parameters considered in the study were: contact time, temperature, phosphoric acid concentration and the amount of iron powder needed for the reduction. The electromotive force EMF was used as an indicator for the reduction degree of uranium.

The experimental study was intended to assess the best operating conditions for the reduction of U(Vl).The results showed that the reduction depends on the temperature, the iron acid initial content and the amount of added iron.

4.1.4 STRIPPING OF URANIUM FROM LOADED ORGANIC SOLVENT

The reduced acid was used to strip uranium from the organic extract exiting the extraction operation. The aim was to find the best operating conditions for the upper most uranium concentration in WPA. This study investigated the main operating parameters affecting the stripping operation. These were: phosphoric acid concentration, temperature and solvent rate. A factorial design was used. In the experimental study, results showed that uranium in the stripping acid could be 20 times, as much concentrated as the initial WPA.

4.2 SECOND CYCLE OF THE URANIUM RECOVERY PROCESS

4.2.1 URANIUM EXTRACTION

The uranium rich acid exiting the first cycle was diluted and oxidized before undergoing a second extraction with the same solvent. This operation was optimized following a similar procedure as for the first cycle. Results showed that the uranium extraction yield could reach 94%.

4.2.2 SOLVENT PURIFICATION

4.2.2.1 WASHING OF ORGANIC SOLVENT

The extract exiting the extraction step was then washed with distilled water. This treatment was intended to eliminate the traces of P_2O_5 in the extract. Washing experiments were conducted at several levels of washing rate. Results showed that the elimination rate of P_2O_5 increased with rising washing rate.

4.2.2.2 SEPARATION OF IRON FROM ORGANIC SOLVENT

Among the various impurities in the solvent, iron is one of the most detrimental to the quality of uranium oxide (U_3O_8). Often, iron is stripped using oxalic acid solutions. This stripping step was studied to find the best operating conditions: oxalic acid concentration and solvent rate. The experiments were conducted according to a factorial design. Under optimized operating parameters, 95% of iron can be stripped from organic solvent with uranium loss not exceeding 0.2%.

4.2.3 URANIUM STRIPPING BY AMMONIUM CARBONATE SOLUTION

The purified extract was then treated to extract uranium with an aqueous solution. The uranium stripping is mainly affected by the following factors: temperature, ammonium carbonate solution concentration and solvent rate. A factorial design was used to determine the best experimental operating conditions for the stripping operation. Results showed that all parameters had a significant effect on the extraction yield. At the best operating conditions, the average uranium extraction yield was 99%.

5 CONCLUSIONS

In this paper, an experimental work on uranium recovery process from the Tunisian WPA was reported. The DEHPA-TOPO dissolved in kerosene was used for uranium extraction step. The best operating conditions, for each uranium recovery process step, were selected according adequate experimental designs. Experiments were performed at a laboratory scale. In batch tests, under optimized operating conditions, a high uranium extraction yield was obtained. For three steps in the extraction process, out of four, the yields exceeded 95%. However, for the first extraction step, the yield was approximately 92%. The uranium rich solvent before exiting the second cycle was treated for purification purposes allowing to eliminate 95% of iron. The overall uranium extraction yield was 81%. The extraction yield could be further increased if continuous counter current extractions operations were performed.

ACKNOWLEDGMENT

The authors thank the Tunisian Chemical Group for continuing support of this research.

REFERENCES

[1] Analysis of Uranium Supply to 2050, International Atomic Energy Agency, 2001.
[2] R. Magdi and K. Mohammed, "Uranium fuel as byproduct fertilizer production", *INREC 10*, Jordan, 21-24, 2010.
[3] M. Walters, T. Baroody and W. Berry, "Technologies for uranium recovery from Phosphoric Acid", *AIChE Central Florida Section, Clearwater Convention*, 2008.
[4] The recovery of uranium from phosphoric acid, *IAEA-TECDOC-533.*
[5] K. Weterings and J. Janssen, "Recovery of uranium, vanadium, yttrium and rare earths from phosphoric acid by a precipitation method", *Hydrometallurgy,* 15, pp 173-190, 1985.
[6] N. T. EL-hazek, M. S. EL Sayed, "Direct uranium extraction from dihydrate and hemi-dihydrate wet process phosphoric acids by liquid emulsion membrane", *Journal of Radioanalytical and Nuclear Chemistry*, Vol. 257, No. 2, pp. 347-352, 2003.
[7] Z. Ketzinel, Y. Volkman, "Récupération d'uranium d'un acide phosphorique de voie humide par échange d'ions liquide-solide", *Brevet européen*, N°843009341, 1988.
[8] Singh H, "Uranium recovery from phosphoric acid, Rare Earth Development Section", *Bhabha Atomic Research Centre.*
[9] F. J. Hurst, "Uranium from phosphoric acid*", ORNL*, Tennessee 37830, pp. 15-17, 1983.

[10] S. Harvinderpal, S.L. Mishra, M. Anitha, A.B. Giriyalker, R. Vijayalakshmi, and M.K. Kotekar, "Uranium extraction from partially neutralised and diluted phosphoric acid using a synergistic organophosphorous solvent mixture", *Hydrometallurgy,* 70, pp. 197–203, 2003.

[11] M. Krea, K. Hussein, "Liquid–liquid extraction of uranium and lanthanides from phosphoric acid using a synergistic DOPPA–TOPO mixture", *Hydrometallurgy,* 58, pp. 215-225, 2000.

[12] S. Girgin, N. Acarkan, A.S. Ali, "The uranium(VI) extraction mechanism of DEHPA-TOPO from a wet process phosphoric acid", *Journal of Radioanalytical and Nuclear Chemistry*, 251, pp. 263–271, 2002.

[13] S.K. Singh, P.S. Dhami, S.C. Tripathi, A. Dakshinamoorthy, "Studies on the recovery of uranium from phosphoric acid medium using synergistic mixture of (2-Ethyl hexyl) P hosphonic acid, mono (2-ethyl hexyl) ester (PC88A) and Tri-n-butyl phosphate (TBP)", *Hydrometallurgy* 95, pp. 170-174, 2009.

[14] S. Harvinderpal, S.L. Mishra, R. Vijayalakshmi, "Uranium recovery from phosphoric acid by solvent extraction using a synergistic mixture of di-nonyl phenyl phosphoric acid and tri-n-butyl phosphate", *Hydrometallurgy*, 73, pp. 63–70 2004.

[15] S. Harvinderpal, R. Vijayalakshmi, S.L. Mishra, C.K. Gupta, "Studies on uranium extraction from phosphoric acid using di-nonyl phenyl phosphoric acid-based synergistic mixtures", *Hydrometallurg,* 59, pp. 69-76, 2001.

[16] D.A. Wesley, R.M Donna, F.B. Charles, "Effects of organic and aqueous phase composition on uranium extraction from phosphoric acid with Octylphenyl Acid Phosphate", *Ind. Eng. Chem. Process Des. Dev*, 27, pp. 301-308, 1982.

[17] F.J. Hurst, D.J. Crouse, "By-product recovery of uranium from wet process phosphoric acid", *Proceeding of Int. Symp. Am. Chem. Soc.,* 1981.

[18] P. Gasôs and A. Moral, "The D2T process of uranium recovery from phosphoric acid: A process model*", Proceedings of a technical committee meeting,* Vienna, pp. 26-29, 1983.

[19] F.J. Hurst et D.J. Crouse, "Recovery of uranium from Di(2-Ethylhexyl) Phosphoric acid (DAPEX) Extractant with ammonium carbonate", *ORNL-2952*.

International Journal of Innovation and Applied Studies
ISSN 2028-9324 Vol. 3 No. 4 Aug. 2013, pp. 1072-1078

http://www.issr-journals.org/ijias/

Selecting Appropriate Quayside Equipment for Grain Unloading Using TOPSIS and Entropy Shannon Methods

Hassan Jafari

Marine Transportation Department,
Faculty of Maritime Economics and Management,
Khoramshahr marine science and Technology University,
Khoramshahr, Iran

ABSTRACT: Now day selection of optimum quay Sid equipment for loading and discharging the dry bulk cargo can maximize the overall efficiency of Terminal. For this end the current applied study was implemented by the aim to choose the best equipment for discharging dry bulk cargoes in BIK Grain terminal using TOPSIS and Shannon entropy method in three phases. In the 1st phase, the most important decision-making criteria for choosing the most appropriate equipment were identified by using experts' interview and investigating the previous researches and holding brain storm meetings with the Grain Terminal's experts. Then in the 2nd phase, the weight of every identified criteria using Shannon entropy method, Was determined. The abstained result from Shannon entropy method indicates that service facility criterion with the scale of 0.06 has earned the maximum and operator cost criterion with the scale of 0.034 obtained the least. In the 3rd phase, using scale 1-9 of each equipment regarding shall be scored based on the criteria and according to the obtained scores for each equipment of the decision- making matrix of the TOPSIS method was established and finally, with respect to the weight of each earned criteria, the equipment shall be scored in the 2nd phase and the most optimum shall be selected. The final results from TOPSIS method indicates that unloader with (C_i=0.91346) enjoys the 1st and the vacuum with (C_i=0.26382) the 2nd and grab with (C_i=0.00000) ranks.

KEYWORDS: Grain Terminal, Discharging and loading operation, selection, dry bulk cargo, quay Sid equipment, AHP, TOPSIS.

1 INTRODUCTION

The optimum equipment for loading and discharging can maximize HR sources, facilities and convenience scientifically, cost reduction, also providing services in the current conditions in a progressive way. Thus, the aim of providing equipment is to accelerate loading and discharging processes of goods in the ports [1]. Acceleration in loading and discharging operations not only provides in time delivery throughout the world, but it also prevents vessels' too much waiting in the quay [2]. Therefore, proper selection of equipment shall increase exploitation to a large extent. In choosing jetty's bulk –discharging equipment, lots of things are involved which are all studied in the research and eventually, three types of jetty equipment are compared based on this standard and TOPSIS method and that the optimum is chosen. Bulk carrier is those types of cargos that is not packed and shipped. These cargoes have different types including liquid and solid, small- big or powder like. Generally, for loading and discharging bulk cargos, special equipment is used. Clearly, one can divide bulk cargos in dry and liquid type [3].

Dry bulk cargos are illustrated as follows:

- Granular dry-bulk cargo such as wheat, barley, corn, soya, rice, sugar.
- Dry bulk cargo as mineral or factorial like different types of clay and aluminum and concrete powder.
- Lump of earth dry bulk materials such as different mineral stone and metal types that are carried in big volumes.

Corresponding Author: Hassan Jafari (hassanport53@yahoo.com)

Liquid bulk materials also include those types of liquid raw productions that are carried by special vessels. Liquid bulk materials are divided into four types:

- Petroleum
- Refined productions of oil
- Liquid bulk food
- Gaseous liquefied materials

In transporting all bulk materials, the recommended notes relative to juxtapose and marine transportation should be observed. A dry bulk terminal, normally, can load/ discharge a bulk-carrier with the speed 10000-20000 per day. For better access to higher productivity, all loading and discharging equipment are made for special purpose. The most important impacts of the most proper equipment choice for discharging dry-bulk cargos in ports are as follows [4]:

- Increasing efficiency and speed of port operations
- Time saving
- Decrease in expenditure
- Decrease the waiting time in the quay
- Port terminal capacity and their optimization with the least waiting time in port and maximum usage of quay equipment has been estimated.

Discharging methods for dry cargo from ship: Regarding using loading and discharging equipment of bulk carriers, the technical specifications of each part of the mechanical system should be clear for the terminal beforehand; because the so called specifications have wide impact on the performance of the mentioned system. E.g. if the discharging of bulk cargo take place by a special grab, the discharging tonnage will depend on elements such as volume capacity of the grab, special weight and the nature of the cargo, speed of the grab, conveyor belt's speed, brake's system, skills of the system's operators, bilge and valves of the vessel, vessel's width and the plant's arm. Thus, about the system's capacity concerning discharging of dry bulk cargo from the ship, one cannot present any figures whilst vessel's specifications and the related terminal are given [5].

Discharging by Grab: In this way which is still the same in the past 50 years, the bulk cargo is moved by a mobile arm attached to a grab along the jetty on a railway which is taken from the ship's stevedore and then transferred into a hopper with a base situated on the jetty. Then, the bulk cargo is taken from under the hopper onto the conveyor belt and to the depot point or the silos. The discharging capacity of this method (by grab) is variable between 1000-500 ton per hour and subject to different elements including the average loading capacity, no. of the maneuvers per hour, the speed by which a grab is closed, movement speed of the carne carrying the grab, width, depth and the shape of the vessel's stevedore and finally the skill of the operational personnel. To increase efficiency in this method they have tried that the taken portion average weight be more in comparison to the grab. Previously, this proportion was around one but with the new wave of grabs, this amount has doubled. The dry bulk cargo that in discharging them this method is used are as Iron ore, coal, bauxite, alumina, phosphorous, other non- major bulk commodities like sugar, fertilizer, for coal industry and grain by a mobile smaller crane equipped by a grab [6].

Discharging by compressed air system: For different types of dry cargo that have special weight and low adhesion such as grain through compressed air system for discharging is used. This equipment functions as vacuum, suction and pressure. Vacuum method in collecting bulk cargo from several places and deliver them in one place uses vacuum and pressure methods to do so. Compression methods create dust and environmentally are drastic. Before erecting terminals, an economical and technical comparison between air compression and mechanical method should be taken. The capacity of the small mobile discharging unit on average is said to be 50 tons per hour, this is while the same amount for the different installed types on the gate cranes is 200 tons per hour. In some ports like Rotterdam of Netherlands the discharging compressed air system with the capacity of 1500-200 tons per hour is used. This system with special design for discharging ships has the capacity of between 100-150 thousand tons [6]. Other ways of discharging are available in Iran that is not of common use which is as follows:

- Vertical conveyor belt
- The bucket left system
- Vessels equipped with discharging machine

2 RESEARCH METHODOLOGY

The current research is practical and from its essence and method aspects is said to be descriptive and is a branch of field work and as the title of the research indicates it aims at choosing the most appropriate equipment for discharging dry bulk cargo in BIK suing TOPSIS and Shannon Entropy methods. In this regard achieving the goals is implemented within 3 stages.

In the 1st phase, the most important decision making criteria for selecting the most proper choice for discharging dry bulk cargo from ship at the jetty shall be identified by using interview with experts, investigating previous researches and holding brainstorm sessions with the Grain Terminal Persian Gulf's experts.

In the 2nd phase, the identified decision making criteria in the 1st phase for the most appropriate choice in discharging dry bulk cargo from ship at the jetty shall be weighted using Shannon Entropy method.

In the 3rd phase, using scale 1-9 of each equipment regarding shall be scored based on the criteria and according to the obtained scores for each equipment of the decision- making matrix of the TOPSIS method was established and finally, with respect to the weight of each earned criteria, the equipment shall be scored in the 2nd phase and the most optimum shall be selected.

2.1 TOPSIS

TOPSIS method was introduced for the first time by Yoon and Hwang and was appraised by surveyors and different operators. TOPSIS is a decision making technique [7]. It is a goal based approach for finding the alternative that is closest to the ideal solution. In this method, options are graded based on ideal solution similarity [8]. If an option is more similar to an ideal solution, it has a higher grade [9]. Ideal solution is a solution that is the best from any aspect that does not exist practically and we try to approximate it. Basically, for measuring similarity of alternative (or option) to ideal level and non-ideal, we consider distance of that alternative from ideal and non-ideal solution [10]. The steps of TOPSIS method are as follow [11]:

First step: Construct the normalized decision matrix. This step converts the various attribute dimensions into non dimensional attributes. An element rij of the normalized decision matrix R is calculated as follows: (x_{ij} is the value of ith alternative in jth criteria),

$$r_{ij} = \frac{x_{ij}}{\sum_{i=1}^{m} x_{ij}^2} \tag{1}$$

Second step: Obtain a weighted normalized decision matrix, where w_j is the weight of jth criteria.

$$\Sigma \mathrm{wj} = 1,\ \mathrm{W} = \{\mathrm{w}_1, \mathrm{w}_2, \dots \mathrm{w}_\mathrm{n}\}.$$

$$\mathrm{R} = \begin{bmatrix} \mathrm{r}_{11} & \dots & \mathrm{r}_{1\mathrm{n}} \\ \vdots & \dots & \vdots \\ \mathrm{r}_{\mathrm{m}1} & \dots & \mathrm{r}_{\mathrm{mn}} \end{bmatrix}$$

Third step: Determine the positive ideal solution (V^+) and negative ideal solution (V^-).

$$\mathrm{V}^+ = \left\{ \left(\max_{\mathrm{i}} \mathrm{v}_{\mathrm{ij}} | \mathrm{j} \in \mathrm{j}_1 \right), \left(\min_{\mathrm{i}} \mathrm{v}_{\mathrm{ij}} | \mathrm{j} \in \mathrm{j}_2 \right) | \ \mathrm{i} = 1,2, \dots, \mathrm{m} \right\} \tag{2}$$

$$\mathrm{V}^- = \left\{ \left(\min_{\mathrm{i}} \mathrm{v}_{\mathrm{ij}} | \mathrm{j} \in \mathrm{j}_1 \right), \left(\max_{\mathrm{i}} \mathrm{v}_{\mathrm{ij}} | \mathrm{j} \in \mathrm{j}_2 \right) | \ \mathrm{i} = 1,2, \dots, \mathrm{m} \right\} \tag{3}$$

V^+ and V^- are the best and the worst weighted normalized values for all alternatives according to jth criterion, respectively. j_1 is the set of benefit attributes while j_2 is the set of cost attributes [12]-[13]-[14].

Fourth step: In this step the Euclidean distance of each alternative from the overall ideal and negative ideal solution is determined, respectively, as follows:

$$d_i^+ = \sqrt{\sum_{j=1}^{n} (v_{ij}\ v_{ij}^+)^2}\ , \qquad i = 1,2, \dots, m \tag{4}$$

$$d_i^- = \sqrt{\sum_{j=1}^{n} (v_{ij}\ v_{ij}^+)^2}\ , \qquad i = 1,2, \dots, m \tag{5}$$

Fifth step: Calculate the relative closeness to the ideal solution.

$$c_i^* = \frac{s_i}{(s_i^+ + s_i)}\ , 0 < c_i^+ < 1, \qquad i = 1,2, \dots, m \tag{6}$$

$$C_i^* = 1 \text{ if } A_i = A^+$$

$$C_i^* = 0 \text{ if } A_i = A \tag{7}$$

Sixth step: Rank the alternatives in descending order of C_i^* or select alternatives with maximum value of C_i^*.

2.2 SHANNON ENTROPY AND OBJECTIVE WEIGHTS

Shannon and Weaver proposed the entropy concept, which is a measure of uncertainty in information formulated in terms of probability theory. Since the entropy concept is well suited for measuring the relative contrast intensities of criteria to represent the average intrinsic information transmitted to the decision maker, conveniently it would be a proper option for our purpose. Shannon developed measure H that satisfied the following properties for all pi within the estimated joint probability distribution P [14]-[15]:

It is proved that the only function that satisfied these properties is:

$$H_{shannon} = -\sum_i p_i \log(p_i) \tag{8}$$

Shannon's concept is capable of being deployed as a weighting calculation method, through the following steps:

Step 1: Normalize the evaluation index as:

$$p_{ij} = \frac{x_{ij}}{\sum_j x_{ij}} \tag{9}$$

Step 2: Calculate entropy measure of every index using the following equation:

$$e_J = -K \sum_{i=1}^{m} P_{ij}\ 1n\ (P_{ij}) \tag{10}$$

$$\text{Where } K = (1n(m))^{-1} \tag{11}$$

Step 3: Define the divergence through:

$$div_j = 1 - e_j \tag{12}$$

The more the div_j is the more important the criterion jth

Step 4: Obtain the normalized weights of indexes as:

$$p_{ij} = \frac{div_j}{\sum_j div_j} \tag{13}$$

3 RESULTS

First phase: To choose the most appropriate option for discharging the dry bulk cargo from the vessel at the jetty, there are 3 decision making criteria which are studied:

Operational criteria: paying attention to characteristics and technical specifications of the equipment used in the ports and the extent of their consistency with the port manager's demands is considered one of the strategies to improve the performance of the ports. The most important decision making operational sub-criteria concerning choosing the most appropriate equipment for discharging the dry bulk carriers are as the followings:

- Operation time: the total time needed for discharging cargoes
- Operation space: a space needed for rotating and performing the operation by equipment
- Unloading capacity: the load that a plant is able to discharge through one phase
- Accessories: the main equipment to join operations

Economic criteria: there's no doubt that the limitations and economic elements are among the most important decision making criteria for ports' strategies. The most important sub-criteria for studying the best discharging instrument for dry bulk cargo are as below:

- Cost of equipment purchase: sub-criteria of equipment purchase depend on factors such as order time, place of purchase and seller, equipment specification and market situation.
- HR and operators' expenses: presence of an expert operator is one of the requirement of using machineries in an optimum way at the bulk terminals
- Maintenance and repair of machineries: sub-criterion for machineries depends on use of equipment and handling the plants and the type of fuel.
- Depreciation cost of equipment: depreciation costs and decreasing no. of equipment is one of the constant challenges facing the industrial managers. Incorrect assessment of these costs, definitely; shall lead plants non-profit (inefficiency).
- Leases: in case the equipment purchase for ports has no economic justification, the ports officials shall decide on rental of equipment.

Logistics criteria: the most important logistics standards that can be considered for selecting the best equipment for discharging dry bulk are as follows:

- Continuous development: getting feedback from each operation and identifying the weak points and amending them for the subsequent operations for operations development and more efficiency
- Service features: all presented services that are necessary for operation's process.
- Berth's infrastructure improvement: includes all conditions, facilities and basic requirements that ought to be there at the berth.

Table 1. Decision making criteria for choosing the most appropriate bulk cargo discharging equipment from the vessel

Criterion	Code	Criterion	Code
Loading Capacity	(L)	Cost Of Equipment	(PC)
Accessories	(F)	Operator's Cost	(OC)
Ease Of Implementation	(E)	Maintenance Cost	(MC)
Operational Space	(OY)	Leases	(LC)
Continuous Development	(QC)	Depreciation Cost	(DC)
Service Facilities	(S)	Operational Cost	(OPC)
Berth's Foundations	(B)		

2nd phase: At this stage the scale for each criterion is identified in the previous phase using SHANON entropy method, the results of this stage are shown in table 2.

Table 2. The weight of decision making criteria abstained from SHANON entropy method

Criteria	(PC)	(E)	(B)	(LC)	(MC)	(QC)	(OY)	(F)	(DC)	(OC)	(S)	(L)	(OPC)
Scale	0.05	0.041	0.047	0.45	0.041	0.05	0.049	0.044	0.044	0.034	0.06	0.047	0.043

3rd phase: At this stage using scale 1-9 per equipment with regard to the criteria, they shall be ranked and based on the obtained grants, the TOPSIS method has been made as per equipment and is described in the following table. Regarding each criterion' obtained weight in the 2nd phase, the mentioned equipment was assessed and the most optimum shall be identified. The 1st step is that the decision making matrix is made based on one of the reasons and using 1equition of this matrix was normalized as it is illustrated in table 3.

Table 3. Decision making matrix

Criteria	(PC)	(E)	(B)	(LC)	(MC)	(QC)	(OY)	(F)	(DC)	(OC)	(S)	(L)	(OPC)
unloader	5	4	3	6	7	6	5	6	8	5	8	8	5
suction	6	5	4	7	6	9	8	7	7	7	9	8	6
grab	4	4	3	6	5	5	4	5	7	4	6	7	4

Table 4. Normalization Matrix

Criteria	(PC)	(E)	(B)	(LC)	(MC)	(QC)	(OY)	(F)	(DC)	(OC)	(S)	(L)	(OPC)
unloader	0.57	0.53	0.51	0.55	0.67	0.50	0.49	0.57	0.63	0.53	0.59	0.60	0.57
suction	0.68	0.66	0.69	0.64	0.57	0.76	0.78	0.67	0.55	0.74	0.67	0.60	0.68
grab	0.46	0.53	0.51	0.55	0.48	0.42	0.39	0.48	0.55	0.42	0.45	0.53	0.46
Weights	0.05	0.04	0.05	0.45	0.04	0.05	0.05	0.04	0.04	0.03	0.06	0.05	0.04

At the 3rd step, in this step by using equations number 2 and 3, we nominate ideal positive and negative solution as Table 5.

Table 5. Positive and Negative solutions

Criteria	(PC)	(E)	(B)	(LC)	(MC)	(QC)	(OY)	(F)	(DC)	(OC)	(S)	(L)	(OPC)
Ideal	0.03419	0.02715	0.03224	0.28636	0.02736	0.03776	0.03826	0.02937	0.02766	0.02509	0.04014	0.02826	0.02940
Basal	0.02279	0.02172	0.02418	0.24545	0.01955	0.02098	0.01913	0.02098	0.02420	0.01434	0.02676	0.02473	0.01960

And then the Euclidean distance of each alternative from the overall ideal and negative ideal solution is determined. Finally according to relative closeness to the ideal solution the identified measures have been prioritized. Results are represented on table 6.

Table 6. Final result of TOPSIS method

	di+	di+	ci	rank
unloader	0.04772	0.01710	0.26382	2
suction	0.00522	0.05508	0.91346	1
grab	0.05561	0.00000	0.00000	3

4 CONCLUSION

The abstained result from SHANON entropy method indicates that service facility criterion with the scale of 0.06 has earned the maximum and operator cost criterion with the scale of 0.034 obtained the least. At the 3rd stage, all equipment shall be classified using 1-9 criterion and according to the obtained grants, TOPSIS method was made for every decision making equipment matrix. Finally, with regard to each criteria' obtained scale in the 2nd phase, the mentioned equipment were classified and the most optimum shall be identified. The final gained results through TOPSIS show that in the order of unloader with $((C_i = 0.91346)$ the 1st rank the vacuum with $(C_i = 0.26382)$ the 2nd rank and grab with $(C_i = 0.00000)$the 3rd rank. Thus it can be understood that the most optimum and appropriate berth equipment is the vacuum and also the unloader which holds the 2nd rank. Considering using the above mentioned equipment, important effects on efficiency and terminal's operation, saving time, lowering costs and waiting time of vessels at BIK's quay shall eventuated.

REFERENCES

[1] Jafari, H., "*Increase the efficiency Rate of container loading and unloading in the BIK, using Six Sigma method*," Bachelor Thesis, School of Economics and maritime management, Khorramshahr University of Marine Science and Technology, 2012.

[2] Saeidi, N., Jafari, H., Khosheghbal, B., and AliAlaei, M., "Managing the Causes of Delay in General Cargo Handling Operation", *Journal of Basic and Applied Scientific Research*, vol. 3, no. 4, pp. 419-424, 2013.

[3] Yousefi, H., Jafari, H., Rash, K., Khosheghbal, B., and Dadkhah, A., "Evaluation of Causes of Delay in Container Handling Operation at Lebanese Container Ports (Case Study Beirut Container Terminal)", *International Journal of Accounting and Financial Management*, Vol. 5, December 2012.

[4] Jafari, H., "Identification and Prioritization of Causes of Halt and Lag in Container Handling Operation", *International Journal of Basic Sciences and Applied Research*, vol. 2, no. 3, pp. 345-353, 2013.

[5] Jafari, H., "Increase the Efficiency Rate of Container Loading and Unloading Using Six Sigma Method", *International Research Journal of Applied and Basic Sciences*, vol. 4, no. 6, pp. 1438-1447, 2013.

[6] Jafari, H., Noshadi, E. and khosheghbal, B. "Ranking Ports Based on Competitive Indicators by Using ORESTE Method", *International Research Journal of Applied and Basic Sciences*, vol. 4, no. 6, pp. 1492-1498, 2013.

[7] Hwang, C. and Yoon, K. "Multiple Attribute Decision Making Methods and Application", Berlin Heidelberg, Springer, pp. 13–25, 1981.

[8] Kabassi, K. and Virvou, M., "A technique for preference ordering for advice generation in an intelligent help system, Systems", IEEE International Conference on Man and Cybernetics, vol. 4, pp. 3338-3342, 2004.

[9] Kelemenis, A., and Askounis, D., "A new TOPSIS-based multi-criteria approach to personnel selection", Expert Systems with Applications, vol. 37, no. 7, pp. 4999-5008, 2010.

[10] M. Zeleny, *Multiple Criteria Decision Making*, McGraw-Hill, New York, 1982.

[11] Shih, H. S., Shyur, H. J., and Lee, E. S., "An extension of TOPSIS for group decision making", Mathematical and Computer Modelling, vol. 45, no. 7, pp. 801-813, 2007.

[12] Kelemenis, A., and alberta, D., "multi-criteria approach to personnel selection", Expert Systems with Applications, vol. 37, no. 7, pp. 4999-5008, 2010.

[13] Lin, M. C., Wang, C. C., Chen, M. S., and Chang, C. A., "Using AHP and TOPSIS approaches in customer-driven product design process," Computers in Industry, vol. 59, no. 1, pp. 17-31, 2008.

[14] Shanian, A., and Savadogo, O., "TOPSIS multiple-criteria decision support analysis for material selection of metallic bipolar plates for polymer electrolyte fuel cell", Journal of Power Sources, vol. 159, no. 2, pp. 1095-1104, 2006.

[15] Shih, H. S., Shyur, H. J., and Lee, E. S. "An extension of TOPSIS for group decision making", Mathematical and Computer Modeling, vol. 45, no. 7, pp. 801-813, 2007.

International Journal of Innovation and Applied Studies
ISSN 2028-9324 Vol. 3 No. 4 Aug. 2013, pp. 1079-1085

http://www.issr-journals.org/ijias/

Study of Neutron and Gamma Radiation Protective Shield

Eskandar Asadi Amirabadi[1], Marzieh Salimi[2], Nima Ghal-Eh[2], Gholam Reza Etaati[3], and Hossien Asadi[4]

[1]Department of Physics,
Payam-e-Noor University,
Tehran, Iran

[2]School of Physics,
Damghan University,
Damghan, Iran

[3]Energy Engineering and Physics Department,
Amir Kabir University of Technology,
Tehran, Iran

[4]Department of Physics,
Damghan Branch, Islamic Azad University,
Damghan, Iran

ABSTRACT: Due to the development of nuclear technology and use of these technologies in various fields of industry, medicine, research and etc, protection against radioactive rays is one of the most important topics in this field .The purpose of this is to reduce the dose rate from radioactive sources. The sources in terms of components are emitted various types of nuclear radiation with different energies. These radiations are involving of alpha particles, beta, and neutron and gamma radiation. Given that alpha and beta particles can be fully absorbed by the shield, the main issue in the debate protection radioactive rays is stopping of gamma rays and neutrons. Accordingly in shield design usually two types of radiation should be considered. First, X-rays and gamma rays, which have great influence, and by the mass of any suitable material, can be more efficiently attenuate the higher the density, the better the potential attenuation effect against gamma rays and the required shielding thickness decreases. The second type of radiation is neutrons. Often a combination of three materials is desirable that include heavy metals, light metals, and neutron-absorbing material to omit the slow neutrons through adsorption to the neutron shield. There are different materials that can be used to shielding against radioactive rays. The main materials that are used in protection include: water, lead, graphite, iron, compounds that contains B, concrete, and polyethylene. Accordingly, the main objective of this paper is evaluating the kind of shield against gamma and neutrons rays.

KEYWORDS: Neutrons, Gamma rays, Protective shield, Gamma absorbing, Radioactive sources.

1 INTRODUCTION

Due to the development of nuclear technology and using this technology in various fields of industry, medicine, research, etc, protection against radioactive radiation is the most important aspect in this context in order to minimizing the radiation rate of radioactive sources. The sources in terms of components are emitted different types of radiation with different energies. These radiations are involving of alpha particles, beta, and neutron and gamma radiation. Radioactive rays protection is a physical barrier that is placed between the radioactive ionization source and the object or purpose of the protection to reduce the amount of radiation exposure in the safeguard place. In order to protect of nuclear radiation maybe

Corresponding Author: Eskandar Asadi Amirabadi (asadi_54@yahoo.com)

a variety of materials such as lead, iron, graphite, water, polyethylene or concrete are used. Among these materials, Concrete is one of the best and most widely used materials for manufacture of Gamma and neutron radiation shield, because in addition to having the proper Structural properties of the material, there are variety choice of the materials used to build it, that lead to manufacture of concrete with different densities and different combinations. . Ease of fabrication, low cost for the construction and maintenance of concrete are another advantage. In fixed installations and large nuclear power plants, Such as power plants, medical centers and nuclear particle accelerators of concrete are used to protect against nuclear radiation. Given that alpha and beta particles can be fully absorbed by the shield, the main issue in the debate of protecting of radioactive rays, is stopping of gamma rays and neutrons ,because with increasing thickness of the absorbent material can only be reduced gamma rays and neutrons. Accordingly in shielding design usually two types of radiation should be considered. First X-rays and gamma rays, which have great influence and by using the mass of any suitable material they can be more efficiently attenuation good. Most materials can attenuate gamma-ray and photon energy in effect of Compton scattering. Attenuation of operating efficiency, which is roughly proportional to the mass of the material, is exposed in radiation path. Since the photon attenuation function is not affected by the type of material, so different materials with the same mass, has virtually identical ability to protect against X-rays and gamma rays .The higher the density of the shielding material, the ability to better attenuation effect against gamma rays and reduces the thickness of required shielding. Therefore, in cases where there is limited space, we can use the heavy concrete instead of ordinary concrete to reduce thickness of required shield largely. The second type of radiation is neutrons. Designing an effective neutron shield is very complex. A good shielding for neutrons should contain a heavy material such as iron, barium or elements with higher atomic number. These heavy elements reduce fast neutrons through inelastic collisions. Light elements is desirable to reduce the moderately fast speeds of neutrons through inelastic. In this context, the presence of hydrogen is very effective because its mass is about the mass of the neutron. Finally, removal of the slow neutrons through the absorption operation is necessary. Hydrogen is effective at absorbing neutrons, but with absorption of neutrons by hydrogen- gamma rays with the energy 2/2 million electron volts (secondary gamma) are produced, these radiations due to the high permeability of the material will increase the thickness of the shield [5], [1].

Among the neutron absorber material, boron element not only contains high neutron absorption, but after absorbing neutrons produces secondary gamma rays with energies 378/0 of millions of electron volts, which have a lower permeability (compared to secondary gamma radiation of neutron absorption in other shielding materials). For this reason, materials containing boron are used often in neutron shields. It should always be considered in the protection discussion that a material efficiency in protection is determined by the effectiveness of it in attenuation per unit thickness .view of this, that the weight and volume of maintenance are surrounding a radioactive system ,Approximately increases with third exponent of the shield thickness and dependent on other factors such as increasing the total cost (both in material and in cases where the amount of savings), Particularly is easy to understand the important of using protection with excellent efficiency. Accordingly, the main objective of this article is choosing the best protection for mixed fields of neutrons and gamma rays.

2 TYPES OF NUCLEAR RADIATION

Alpha radiation, beta and gamma rays and neutrons are the most particles that may be emitted in nuclear reactions. Alpha particle is a helium nucleus that consisting of two neutrons and two protons. It is based on two positive charges and as the particle is relatively large, has a little bit of range in target material so easy to stop. For example, it stops an ordinary sheet of paper of alpha particles that is emitted from a radioactive element. Beta particle is high-energy electrons that are thrown out of the nucleus. It is believed that a neutron at the nucleus is changed into a proton and an electron and an electron is thrown out with considerable kinetic energy. Because beta particle is much smaller than the alpha and contains only one negative charge that permeability of it in the material is more than alpha. Permeability depends on the energy of the beta, but to stop a beta particle with an average energy, aluminum plates of thickness less than six - seven millimeters is sufficient. Gamma ray is High-energy photons; the nuclear gamma-ray emission is just very rare. What usually happens is that when a nucleus emitting alpha or beta particles maybe radiation one or more photons of gamma. Because gamma photons have no electric charge and mass so the permeability of it is much higher than beta particles. Permeability of gamma photons in the material depends on its energy. To stop gamma photons with average energy is needed elements with mass numbers up to several centimeters in thickness such as pieces of lead. Gamma radiation can directly or indirectly impact on the body and can cause serious risks both internal and external. Gamma irradiation plant is found in machine containing radioactive material around each nuclear power and in most plant the workers exposed to radiation, Thus, in plants everywhere which there is the possibility of gamma-ray radiation ,the proper shields are embedded into alignment that to reduce radiation to a safe level [3].

3 GAMMA PHOTONS COLLIDE WITH MATTER

How gamma rays dealing with the matter are different in compared with alpha and beta particles. So that the alpha and beta can be absorbed in substance completely so they have certain range, but gamma-rays cannot be absorbed completely, But with increasing thickness of the absorbent material can only reduce the radiation intensity. Since gamma rays have no mass and charge the Probability of collision or in other words cross sections dealing with the matter is much lower in contrast to alpha and beta particles. Therefore, the influence of gamma radiation, are much more penetrating power than alpha and beta particles and it is to some extent to which high-energy photons can penetrate the material without loss of energy from several centimeters to few meters . The initial collision of a photon with material occurs in orbital electrons. During the collision, Part of the photon energy is converted into kinetic energy of fast electrons and other part is removed from material as scattered radiation. Express electrons in its path, causing ionization, excitation of atoms and breaking of molecular bonds. It may some of the express electrons in dealing with material can cause brake beams. The beam and the scattered photons with matter can be treated with material as having the primary photons. Gamma rays or X-rays collide with matter is in several different ways. As one of the most important encounters of gamma with material are photoelectric effect, Compton scattering, Thomson scattering and ion production. Photoelectric effect: on the phenomenon of photoelectric effect, a photon includes energy deal with an atom [2]. The result of this collision is sala, following the collision with the electrons that come out of atoms are called photoelectrons.

4 PHOTOELECTRONS WITH KINETIC ENERGY

Leaves atom in this regard, Eb, is the binding energy of the orbital. However, when the electrons are replaced by electrons from higher orbits one or more photons are emitted from the atom. On the photoelectric effect, the probability of photon collision with electrons that are closest to the nucleus is higher. If gamma rays have enough energy, in 80% of cases with electrons of K orbit collide. The collision of electron orbits in M, L and N is also possible. Based on the photoelectric effect, the photon absorption coefficient that known as the photoelectric coefficient strongly dependent on the photon energy and absorber atomic number (Z). Although there is not the simple correlation that expressed coefficient of the photocurrent variation with respect to all of the energy levels, however, we can use the following approximate relation for the photoelectric coefficient [6].

In this regard, changes in n and m can be expressed as follows:

In the above equation, based on the Mev and a is equal with

9-10×1.25

From this relationship can be derived that the heavy material is capable of absorbing photons of low energy as well and this has led to this lead is used as the best protection against low energy gamma rays. Compton scattering: the phenomenon of Compton scattering, photons may deal with any of the orbital electrons. In fact, this phenomenon can be assumed that the elastic collision is carried out between a photon with and a free electron at rest energy. From a practical standpoint, if the photon energy is MeV1 R 0, the orbit electrons in comparison with photon energy are assumed release. In phenomenon Compton, unlike photoelectric effect transferring all the energy of the photon to released electron is not possible, because that according to The principle of conservation of energy and angular momentum it requires that after the electron left the atom, continuing the movement with the speed of light is impossible. Thus, the Compton scattering process, only part of the photon energy is converted to the free electron kinetic energy [7].

Probability of collision between a photon and a free electron in the Compton effect is anticipated by using the equations that proved by Nyshyn and Klasn proved. Based on this equation, the probability of a photon collision with orbital electrons regardless of the binding energy of nuclear are equal. In other words, the coefficient of Compton scattering, depends solely on the number of electrons in the absorption material and, therefore, is independent of the atomic number of the absorber material. The Compton scattering coefficient decreases with increasing photon energy, but the rate of decline compared with the photoelectric effect, is much slower. In general, it is very important that the probabilities of Compton collision at energies which have declined the photoelectric absorption coefficient are more important [9], [12].

Thomson scattering: In this phenomenon, photons with energy collision with a free electron and with no loss of energy, only to be deflected from its original path. Pair production: when a photon passes near the nucleus of an atom, it disappears and instead a positron and an electron are created. Therefore, this phenomenon is called pair production. Therefore, because the phenomenon occurs, it is necessary that at least the energy of the photon be equal with mass energy of an electron and a positron in the rest. Contrast phenomena photoelectric and Compton, pair production cross section is increased by increasing the photon energy. Also, due primarily to the phenomenon of pair production occurs naturally

influenced by atomic absorption with increasing atomic number, the probability of pair production increases. Attenuation coefficient of the photons collide with matter, each process photoelectric Compton scattering, Thomson scattering and pair production may occur, but one process can only happen in every encounter, whereas in multiple interactions may occur in the whole process. It is evident that the probability of each of these processes is proportional to the surface area. In any case, the probability of a photon collision is equal to the total cross section of the process. Neutron-proton mass is nearly equal mass but no charge [11]. Therefore, unlike charged particles neutrons are not able to loss their energy during a series of closely ionizations. Moreover, the neutron was not component of the electromagnetic wave and based on this will not have collision with absorbent electron. After the neutrons penetrate into matter, continue their path to collision with the nucleus of an atom generally, this is the kind of elastic scattering and inelastic or absorption. Neutrons collision probability (cross-section) are not only material, but also strongly depends on the neutron energy. So, it is performed collisions of neutrons with matter to be discussed with respect to energy of this particle. The neutron energy is divided into the following groups:

A – Fast neutrons: they have the addition of 1/0 millions of electron volts of energy. In this energy range, the neutron collision is mainly dispersion and absorption cross section of the material is much lower than scattering cross section.

B - Thermal neutrons: that the energy of them are an electron volt or less (Often 025/0 eV). These neurons, like gas molecules cuffed in thermal equilibrium with its environment and finally absorbed or in short duration (minutes) are analyzed to the proton.

C – Neutrons that their energy is located between fast neutrons and thermal neutrons, to these neurons are given different topics such as medium, slow and near thermal neutrons. In this energy range, neutron can create varied reactions.

5 ATTENUATION AND ABSORPTION OF NEUTRONS

Attenuation of neutron in a material that occurs by the absorption and scattering phenomena is as the exponential function: In which is the microscopic cross sections of neutron collides with the nucleus of an atom per cm, N the number of absorbent atoms on cm3 and X is adsorbent material thickness in terms of cm. Fast neutrons, usually during Elastic collisions with surrounding atoms, rapidly lose their energy and change into thermal neutrons or near heat. As the neutron loss energy, the probability of its absorption is increased by the absorbent material core. In the case of many-core, neutron absorption cross section with low energy is proportional to the neutron velocity inversely. Scattering of neutrons: neutron collision with a nucleus can be elastic or inelastic collision. In an elastic collision, the maximum neutron loses its energy during a collision with a hydrogen nucleus. In general, elastic scattering is the most likely type of collisions between fast neutrons and light absorbing materials. During an inelastic collision, part of kinetic energy of the neutrons has been transferred to the hit nucleus, effect arousing the nuclear. Aroused nucleus then emitted the extra energy as gamma rays [5].

6 BIOLOGICAL EFFECTS OF RADIATION

Radiation emitted from radioactive materials or which are produced in radiation generating devices, in collision with the human body put extra energy, that this energy, has deleterious effects on living body tissue. Physical radiation effects are different in partial and temporary disruption of some physical exercise and also some serious consequences such as shortening life expectancy, decreased body resistance against diseases, reduced reproductive output cataract and leukemia and other cancers and damage to a developing fetus. Extent of the damage is a function of radiation dose and is different about different people. Local exposure (to a small area of the body) basically affects only the exposed tissues, but the whole body irradiation cause the general reaction of the body. It is possible that the light shine on it from outside or from within the body. External dose can be limited by reduceing the exposure time, distance from the radiation source, and finally protection. Generally emission of alpha particles and emitted beta slow energy particles are not dangerous from outside to the body, they are not usually dangerous, but if the particles are absorbed into the body, their energy is transferring to the sensitive tissues of a living organism during short distance. If energetic particles shine from outside on the body can enter a huge dose to the skin. X-rays and gamma rays have high permeability and can affect the entire body from the inside and outside [7].

7 PROTECTION AGAINST RADIATION

In summary, two important factors in the proper radiation protection are: distance, shielding or absorbent material that in this regard a brief study of the topic will be discussed. Distance from the source: the distance makes us this sure that the person is not exposed unnecessary radiation source .For example, while distribution of radioactive material in the laboratory, we should not use the fingers, but must use tools such as pliers, scissors or tweezers. This is kind of protection method using

the distance. With increasing distance from the source of radiation, the beam decreases. The relationship is inverse-square law, which states that track radiation is proportional to the inverse square of the distance from an exposure point source. By simple calculations we found that imagine of this point is wrong that rapid transport of radioactive material by hand (in a very short time) to the more time which is consuming their transform by the help of long-handled tools (to keep away of the body)which significantly this will reduce radiation dose. It should be noted that when calculating the radiation we must considered together the attenuated inverse square rule and the exponential attenuation of absorbent barrier.

Protecting: One of the most important ways to protect against nuclear radiation is using suitable protective material between the radiation source and human or environmental protection. Materials used in nuclear reactors protection must have the property of making neutrons slow and can make gamma rays in order to attenuation. To slow the neutrons that are used usually from the layers of graphite, beryllium and water and for the attenuation of gamma rays are used heavy metals and concrete. In addition to that concrete is capable to attenuation the gamma radiation is very important at slowing and absorbing neutrons of thermal neutrons. Hence concrete with high availability, low cost and its effects suppressive properties are of great use in protecting, especially in the outer shield [7].

Protecting materials: Making an appropriate and effective shielding against neutrons and gamma of a nuclear facility requires proper selection of materials and thickness. Choosing the right material for making protective shield interconnected optimality analysis are the weight, volume and cost considerations such as these. It is possible that these considerations affect the choice of materials and consequently affect on the final design. However, cannot usually design protection that to ensure the entire above range. Usually, for practical purposes, one of the above cases is considered as main goals and the other goals are settings in order to be optimal. Most important characteristic of a material protection is its ability in attenuation of neutron and gamma radiation. In general, lighter materials have higher ability in attenuation of neutrons and heavy materials have higher ability in attenuation of gamma rays. The use of only one material is impossible for shielding source of gamma and neutron. Meanwhile, heavy materials often activated by absorbing neutron and irradiation secondary gamma that should be considered in shielding design. In practice an appropriate protection forms from the combination of different layers of hevy and light materials to control neutron, gamma and secondary gamma. Different materials are that can be used for protecting against radioactive rays. The main materials that are used in protecting include: water, lead, graphite, iron, boron, concrete, and polyethylene. However, experience has proven that the use of appropriate concrete has a lot of advantages compared to other materials. Boron (usually in addition to other materials such as polyethylene and concrete) has many applications in protecting. The use of this is due to primarily higher neutron absorption cross sections. Particularly this particle interesting is because of its dominant reaction that results in complete inhibition of neutrons and does not produce any secondary particles with high penetration [3].

8 WATER AS THE SHIELDING

Water due to the high hydrogen content and the availability and cheap is useful shield for neutrons. However, due to the low atomic number of the constituent nuclear of water are not acceptable against the gamma rays. There are Issues over the use of water as the shielding that is hard case for storage, corrosion problem, purified, corrosion problem and removing stiffness. Another problem of using water as a shield against neutron sources (reactors are widely used around the blue shield) is neutron absorption in oxygen and producing of excited.

Lead as shielding: Lead is the most common substance for the attenuation of gamma rays. Lead's blocks with relatively high prices can provide good attenuation of gamma rays. The power of gamma rays Attenuation in the lead back to its proper density and high atomic number. Pieces of Lead Because of the softness and flexible are suitable for filling pore in the doors and fittings. Lead is not satisfactory and cannot creat acceptable neutron attenuation in neutron field. Lead by absorbing the neutron is emitting 7.4 Mev that cause it to worse the neutron properties. The impurities in commercial sorbs can have activation gamma with full energy.

Graphite as shielding: Graphite is good retarders for neutron and in the types of reactors used as retarders. Neutron absorption cross section is low in graphite and hence (as the possibility of the comfortable production of highly pure) problem of secondary Gama is largely absent. Like Water graphite is not proper attenuation for gamma. Graphite has good thermal properties which can also be involved in its use as a shield. Iron as shield, iron in the form of steel has widely used in the shielding against radioactive sources. In addition to the shield in front of radiation iron is also used as a heat shield. Of course, iron in effect of absorption of neutrons is emitted Gammas impart maximum MeV10 energy. Iron contains attenuation effect somewhere between carbon as low and tungsten as high against gamma. Isotopes readily activated with absorbing of thermal neutrons and isotope with half-life of the - 59 days and Gama with 1.5 MEV energy is producing.

Concrete as a barrier: Most commonly employed shield in different sectors of the nuclear is shield of concrete. It is cheap and has features that are used as building materials. Concrete is known and this case facilitates its making and using. Because concrete is a mixture of several different materials (in any combination may be highly variable) its composition is not constant. Even two of the same type of concrete with depending on the materials have used very different in composition. So when referring to concrete as shielding material, the material used in its composition should be told correctly. Generally concrete are divided to batch "ordinary" and "heavy". Common concrete density was2/2 up to 2/4 gr / cc and the most common substances has found in it is oxygen and depending on the material used for heavy making concrete is silicon or calcium (or both). Usually granite, sandstone or limestone is used for this purpose. The heavy concrete with a density of 3 to 6 gr / cc as heavy concrete iron ore, barite (barium sulfate), steel balls, steel punch or other additives are used.

Typically, the concrete is as mix of cement, water (water in which the matter is considered too heavy concrete) and the reinforcement of concrete .As stated, by vary of the reinforcement material can be prepared by various concrete types. Various additives to improve the attenuation of neutrons or gamma rays, or increasing the hydrogen content of concrete can be used to better mental health [10].

9 CONCLUSIONS

By the study of nuclear radiation such as alpha, beta, gamma and neutron we conclude that, by given that alpha and beta particles can be fully absorbed by the shield, the main issue in the debate of radioactive rays shielding is stopping of gamma rays and neutrons. Accordingly, in designing of the shield, usually two types of neutron and gamma radiation should be considered. With examining of with these two types of radiation and processing of the prevention of these radiation with different materials can be examined types of shield against these radiations. Protective material between the source of radiation and humans must have the slowing property of neutrons and be able to attenuate gamma radiation. Making protective and affective shield against neutron and the gamma of a nuclear facility requires choosing the right material and considering the required thickness for them. Choosing right materials for making shield are interconnected with optimality analysis of the weight, volume and cost and considerations such as these. It is possible that these considerations affect the choice of materials and consequently on the final design. However, usually we cannot design shield that to satisfy all cases highly and will be optimal from all sides. Usually, for practical purposes, one of these cases is considered as main goals and other purposes besides it are being regulated to the optimum. Most fundamental characteristic of a sconce or protection material is its ability in attenuating of gamma and neutron radiation. Accordingly types of protection can be designed. Design a shield against nuclear sources requires highly accurate dose and effective intensity of nuclear radiation in the total generated dose is in the out of shield. Often the computational methods used to obtain this information. All calculation methods can be evaluated in two ways certainty and probabilistic methods. Simple equations for describing the behavior of functions in certain ways (such as flux or neutron radiation) are introduced and the coefficients are determined by methods. In short, semi-empirical methods based on predetermined rules of radiation change are determined in protection. Accordingly, we can be summarized shielding design methods in a more accurate classification in the following three categories [9]:

- Experimental methods
- Methods for solving the transport equation
- Monte Carlo methods

Monte Carlo method is the statistical simulation of the parameters of probabilistic nature. Nature is the examining quantitative in statically protection of issues that means quantitatives such as flux is determines by the average performance of very large number of neutrons. Based on this it is expected that by Using statistical methods can be calculated common amounts such as flux and rates of dose and this is the basis of Monte Carlo method. The ultimate goal of the Monte Carlo method is determining the neutron flux, the rate of varies reaction, dose rate and also identifying the critical state of the system. Issues considered in the Monte Carlo method (in the field of reactor physics) can be classified in two categories: constant source issues and critical issues. Our next article (if God willing) will investigate the problems of constant source (or guards problems) [8].

REFERENCES

[1] Aprsht, W., "identification of structural materials in nuclear technology", r*efugees, H, printing, Tehran, Tehran University Institute for Publishing and Print*, 2009.

[2] ACI Committee 211, "Standard Practice for Selecting Proportions for Normal, Heavy weight, and Mass Concrete", Appendix 4, *American Concrete Institute*, 2002.

[3] ACI Committee 304, "Heavyweight concrete, Measuring, Mixing, transporting, and, Placing (ACI 304.3R-96)", Detroit, *American Concrete Institute*, 1996.

[4] Akkurt, I, et al., "Radiation shielding of concretes containing differed aggregates", *Cement and Concrete Composites*, Vol. 28, no. 2, 2006.

[5] American Society for Testing and Materials, "Annual Book of ASTh Standards, Significance of tests and properties of concrete an concrete making materials," *United States, ASTM special Technical Publication*, Vol. 04.01, 04.02, 2007.

[6] Bashter, I. I., "Calculation of radiation attenuation coefficients for shielding concretes", *Annals of Nuclear Energy*, Vol. 24, no. 17, pp. 1389-1401, 1997.

[7] Basyigit, C. et al., "The effect of freezing-thawing (FT) cycles on the radiation shielding properties of concretes", *Building and Environment*, Vol. 41, no. 8, pp. 1070-1073, 2009.

[8] Chilton, A. B., Shultis., J.K., and Few, R. E., "Principles of Radiation Shielding", *Prentice-Hall, Englewood Cliffs, NJ 07632*, 1984.

[9] RG Jaeger, *Engineering Compendium on Radiation Shielding*, Springer-Verlag, New York, USA, 1968.

[10] Sakr, K, et al., "Effect of high temperature or fire on heavy weight concrete properties", *Cement and Concrete Research*, Vol. 35, no. 3, pp. 590-596, 2005.

[11] Suzuki, A, et al., "Trace Elements with Large Activation Cross Section in Concrete Materials in Japan", *Journal of Nuclear Science and Technology*, Vol. 38, No. 7, pp. 542-550, 2001.

International Journal of Innovation and Applied Studies
ISSN 2028-9324 Vol. 3 No. 4 Aug. 2013, pp. 1086-1093

http://www.issr-journals.org/ijias/

Calculation of Corrosion in Oil and Gas Refinery with EOR Method

Amir Samimi[1], Ali Bagheri[2], Sepanta Dokhani[1], Sepehr Azizkhani[1], and Ehsan Godini[1]

[1]Department of Chemical Engineering,
Shahreza Branch, Islamic Azad University,
Shahreza, Iran

[2]Department of Engineering,
Saveh Branch, Islamic Azad University,
Saveh, Iran

ABSTRACT: EOR method evaluation is performing for petroleum gravity, stone type, and tank humectant and tank localities conditions for liquid injection. If the frame is humectant, petroleum exit will perform whenever the pressure is more than threshold; this is controllable by the height of tank block. Experiments and experimental data for recovery capillary absorption are according to data in 1950. Brownscoble & Dyse (1952) studied the ability of water absorption in the sandstone lands. The studies have been done on the tube lines, land and the metal workforces that are related to the oil and gas industries, shows that in most cases, weld lines and edge of a sharp regions has been influencing on location of corrosion and eroding of effective thickness of coating film. In this study we studied EOR methods for dense oil recovery from mold in the breakage tanks. Analyze and comparison of recovery with capillarity of salty water, polymeric solution and hot water on different sample of rocks showed high recovery of dense row oil in the EOR methods, and it is more detected in the diluted row oil. Oil (diluted) can recover by water injection in the sand stone condition and with chemical matter and thermal methods. Hot water recovery is more rapid and higher than chemical recovery.

KEYWORDS: EOR, Petroleum, Water, Oil, Gas Industries, Chemical recovery.

1 INTRODUCTION

EOR method evaluation is performing for petroleum gravity, stone type, and tank humectant and tank localities conditions for liquid injection. If the frame is humectant, petroleum exit will perform whenever the pressure is more than threshold; this is controllable by the height of tank block. Experiments and experimental data for recovery capillary absorption are according to data in 1950. Brownscoble & Dyse (1952) studied the ability of water absorption in the sandstone lands. It will discuss about technical and economic condition, in the next year, it was performed by many of universities of United States in laboratory. Caspian sea is one of the good case for water injection and row petroleum recovery by capillary absorption, that is because of carbon in the tank`s stone. Row petroleum viscosity, is one of the limitation factor in the tank recovery. High viscosity in the petroleum leads to low recovery. In this article, it was performed many experiments on different stones by dense row petroleum and for comparison between dense petroleum and diluted petroleum on sand stones and lime stones. Whenever diluted and dense petroleum are comparing, lower final recovery of dense petroleum is because of its high incipient factor temperature and low humectant of tank is for coupling of water and dense petroleum. In any case, recovery is usually dependent to the petroleum viscosity. So, first is rapid production and Second point is increasing of find recovery. In this condition, it is evaluating the interaction between water phase and hemi cylindrical frame, and as we observe, recovery velocity and final recovery of dense petroleum is limited. The high cost of corrosion, the corrosion engineer's concern and its reduction in oil, gas and petrochemical countries is essential, about 10 percent of the cost of producing a barrel of crude oil now costs related to the corrosion industry. Corrosion rates in the world

Corresponding Author: Amir Samimi (amirsamimi1161@gmail.com)

costs 42 to 80 cents a barrel for crude oil is produced, Specific climatic conditions, history of the country's refineries and oil production, the main factors affecting the cost of corrosion in oil country.IJIAS hopes that Researchers, Graduate students, Developers, Professionals and others would make use of this journal publication for the development of the scientific research. Accepted papers are available freely with online full-text content upon receiving the final versions, and will be indexed at major academic databases. There is no submission or publication fee [2]-[4].

2 CHEMICAL MATTERS LEAD TO EOR

Polymer: Before these experiments, polymeric solution injection as aqueous phase was performed for tank petroleum recovery in the laboratorial condition, for diluted, petroleum. The only case about polymeric solution injection that leads to the high recovery was in the river basin in Vioming (2000).In this study, for both sandstone and limestone, the polymeric matter was as an aqueous phase. The results were shown in the figure 4a, about injection on dense petroleum with sandstone. One of the limitation factors in this method is: it is necessary to use very dense polymeric, for high viscous petroleum, clay increases the surface absorption of polymer will have good results, when the polymer injection begins before increasing the relation between water to petroleum. Polymeric solution injection leads to increasing of recovery velocity. But final recovery is not affected by adding polymeric solution. Fluids characters are noted in table Pay attention that polymer injection leads to decrease of IFT. Everyone can see polymeric solution effects on dense petroleum recovery for limestone. Dense petroleum reaction is the same as limestone, without taking into that polymeric matter injected to the dense petroleum. When limestone and sandstone diluted petroleum are comparing with each other, evaluating of absorption effect become more logical. It expected that, because of higher surface absorption of polymeric matter on limestone than sandstone, recovery results decrease. Stripe coat is a coating film of color which is applied before and after a full coating on the edge or weld lines of metal skeleton. This kind of coating is applied in order to create an appropriate structure and enough resistance against corrosion in these regions. Therefore SC has more protection for the edge of the coverage or weld line. It is applied before preparation of surface or before a full coating. Technical knowledge is relevant to community of protective coatings that has the following recommendations about SC {color usage, the shape of painted area and keeping of color of steels. [1]

- It should involve around the edges at least 2cm.
- To prevent from peeling of Primer during the actions, it should reach to touch dry {it should be dry enough and non-sticky} and then use Primer {so this time should not be too long because it cause to regions without Primer become corrode.}
- Maybe SC use once after Primer action, especially if much time is needed to dry.
- SC is more effective on surfaces that are reduced of sharpness by grinding. [5]

Most SC is used for all edges, vertebrates and the weld because liquid colors move and flow in these parts; this phenomenon is the result of tension of surface and contraction of color film during drying. If this event happens, the color film will become thinner at location or close of edges. When color destroys in the regions of vertebrates, screws and welds can lead to crisis. Because these factors cause the continuity of skeleton become destroy. Overall SC has 2important advantages: the first one cause to cover small defects and differences of surface such as: porosity of welds, the second one: If enough time gave to SC for drying, it would have prevented from flowing of last coating on the edges and causes more problem for them. Colors with high percentage of solid toward colors with low percentage of solid are less apt to be thin in the edge of the regions because overall, colors with high solid have more curing time and against Viscosity are higher and have less tension on the surface. [16]

However SC is used for sharp regions and the edges which maybe have not suitable thickness for coating. We should remember that the first advantage of SC is reducing the thickness of coating. We can use SC for all the coating layers. Excess colors increase the residual tension of film of coating that leads to gap or become membranous. Operator of color and expert at first maybe choose the best method by quality of control. It is able to inject gases into the pit as a gas phase. Gas phase is usually as a phase that leads to high recovery of pit, whenever, we have gas oil gravity drainage, that because of different gravity between fluids in the breaking point of mold and in the mold. This process will decrease the recovery than other mechanism, especially about dense oil, and it can lead to high recovery by heat and mixed gases injection. Many studied had performed on oil recovery from pit by mixed gases. They use Nitrogen gas for breaking tank because of it is available and cheap. If the mixed condition exits, it can increase the oil recovery of the tank. Methane is another gas that is used for this purpose. Morel et al. observed that oil recovery by methane is twice of nitrogen. Lately, Lenormand et al., purposed transfer subsidiary for diffusion between tank and breakage, in these studies diluted oil is used as a typical from in the oil tank. CO_2 injection is one of the most available ways about non-hydro carbonic gases that release industry about natural gas injection for grazing, CO_2 gas can exits diluted and medium components from oil, and if the pressure is high, it can exits oil from the

tank by more mixing, so the viscosity become lower and oil turgid. This method is very valuable for dense oil with varicose type of solvents. In the current study, an experiment for increasing the recovery of pit by saluted gases was performed. So, part of this study is experimental. It is important to note that, availability to mixed methane and nitrogen with dense oil is so difficult, and we can use another solvent for that, and it is not economical, but it is successful way for technical aspect. Whenever, there is low humectant and permeability, the only substitute for heating method in the carbonate tank or tanks with dense oil is, saluted gas injection (CO_2), and the oil recovery increase. CO_2 limitations are: very low viscosity for CO_2, leads to low control on movement, so quick separation become difficult and other problems and limitation. [21]

Nitrogen or combustion gas means: high injection of nitrogen, or other gases into the tank that it can mix with each other according to the pressure and it`s components. This method is used for diluted oil recovery that is able to absorbed added gas into the tank. This condition is low methane and at least 5000 feet depth that leads to resistant of rock tank on high pressure of injection, and it wouldn`t break. When nitrogen injects into the tank, we will have mixture phase, that`s because of light component evaporation. It forms a mixture or solution phase, by its movement from injection phase to the tank. Continuous injection leads to oil mass movement into the production pits. It is able to use water injection, alternatively, for higher recovery and high buoyancy index for oil. Nitrogen advantage that is, it doesn`t have corrosive effect. Because of its price that is cheap, we will have more injection. Nitrogen injection is usually after the carbonic. Gas or mixed hydro carbons. This method`s limitations are: mixing will performed in the diluted oil and high pressure, so it`s necessary to be more depth, slope excavation is suitable for decreasing unsuitable movement, that`s because it allows gravity to control movement.

In the EOR project: remains oil determinations in the tank, necessary mechanisms for better exploitation and in-use equipment are important factors, Generally, if the purpose is to exit tank oil completely, it`s important to pay attention to the final recovery, but if the purpose is high production, it`s important to focus on the increasing recovery velocity methods, than final recovery. The best candidates for this strategy are low recovery factors (dense oil carbonates). Final recovery and its velocity are practical factors of recovery in this article. Following the experimental methods is not suitable for total expense analyze. That`s because of I statics nature of this method, but in reality, continuous injection in the abuse phase is possible. Understanding the injection velocity and it`s density is one way for determining method`s expense and chemical matter that`s necessary for injection and final recovery. It`s necessary to perform exact experiments in laboratories for determining Fluid`s amount for final recovery. [16] This fact determines how the method is effective, and finally it leads to determine project expense. Beaver et al. performed exact analyze for determining exploitation amount of chemical matters injection in to the homogeneous samples, they performed various experiments according to the absorption and salty water effects and analyzing different ways for chemical injection, for determining the best way. Results were useful in the same forms (breaking systems), but there`s no report about chemical injection into the breakage tanks, until now. Useful numerical and experimental studies were performed for fluid flow in the breakage environments. Expenses analyze for water injection, are an important factor because of low expense for its injection, and were performed studies about numerical dramatis tic to determine optimistic velocity of vapor injection for different tanks, according to breakage and days. Both two studies showed that, injection velocity is depending on tank type and penetration and its thermal capacity. In these studies, chemical absorption (especially for carbonate rocks), critical density (for chemical matters or gas injection), or thermal degree (hot water) were taken into consideration for optimize process.

2.1 TEST CONDITIONS

Aqueous solution used in the laboratory , Actual water samples from the production fluid and gas field in Iran and Water samples from the injection well-chosen that the owner refused to wear the wellhead facilities Corrosion studies of the corrosion rate of fluid can be precisely manufactured and also reduce the corrosion rate in the psychological effects are still. The PH of the solution should be study. Generally it is better not to be blown in the air, unless a solution is needed. If a solution is needed to allow air to be blown to the surface oxygen to the deal, where the reactions take place reducing the oxygen and cause corrosion on the surface, to eliminate air in solution can be use the azot without oxygen, nitrogen and argon. In this experiment, nitrogen out of air from the cylinder must be at least half an hour before the test. Volume of solution should be high enough to reduce the corrosive materials in the experiment and the high accumulation of corrosion products in place to avoid. In these experiments, the solution volume is 500 mL of TB laboratory,(± 1°C) temperature must be controlled carefully and Room temperature is 25°C is usually, The temperature should be fixed in the test chamber to create a thermal gradient changes the solubility and the ability to prevent the potential changes. The effect of fluid velocity on the corrosion of a metal sample was used to pump And the appointment of the place was very small laboratory cell output and soluble cell surface can be kept constant laboratory For this purpose, a bypass path from the output of the pump inlet to the pump tank and a path of pump output to the input cell is built The heat pump is used to prevent burning at a low capacity pump, and maybe taken. With both the control flow path taken Equipment required for the fluid flow can be seen in the movie, too. [19]

3 FACTORS IN THE CORROSION OF GAS WELLS

Temperature: Effect of fluid temperature corrosion in oil and gas industry in similar chemical environments, Corrosion rate is increased at higher reaction temperature corrosion so often that every 20 degrees Fahrenheit (C_{11}) increasing temperature, the corrosion rate is doubled. Corrosion of steel in corrosive CO_2 gas in the vicinity there are three temperature diets: [22]

A) Low temperature and non-protective iron carbonate C_{60} and the corrosion rate is a function of CO_2 partial pressure.

B) Between temperature and C_{150}-C_{60} almost protective iron carbonate layer is formed and the corrosion rate reaches an acceptable value. [23]

C) C_{150} Mgntayt top layer is formed which completely cover and it is also resistant to high velocities and extreme turbulence and is only sensitive to chloride ions. The combination of these three types of diet excluding salt water, the fluid velocity and the ratio of partial pressure of CO_2 to H_2S gas on the corrosion rate, these factors should also be entered in the protective layer. [24]

Pressure: High pressure gas wells in the gas solubility in liquid corrosive effects. Gas pressure can reach psi 12000. Partial pressure of corrosive gases is an important point. The amounts of corrosion of a well produced by CO_2 are as follows:

- Partial pressure of CO_2 is less than 7 psi: non-corrosive environment.
- Partial pressure of CO_2 between 7-30 psi: corrosive environments.
- Partial pressure of CO_2 is 30 psi: highly corrosive environments. [27]

The role of Fluid in the Corrosion: Experience shows that the wells have corrosion problems when Water cut in the total amount of fluid in them is more than 85 percent. Of course it has plenty of exceptions. Fluid emulsion of water in the fluid conductivity and efficiency as a conductor affects. Mode of the large amount of water wells (without emulsion) produce more corrosive than water wells with Less water cut and more emulsions . Many studies have been conducted to determine the corrosive fluid within the well. Brad Bern 20 different wells of the contract and amounts of water and acidic gas CO_2 produced as the variables considered. He found that the amount of water is more productive; the amount of CO_2 is more soluble in the vicinity of the wall and creates more corrosion.

Fluid Velocity: Fluid velocity in the fluid regime and the regime's fundamental role in determining the type of fluid are corrosive and performance inhibitors. Experiments have shown that a diet supplemented fluid and field tests are equal, Mechanism and the corrosion rate was similar in both conditions. Regardless of diet, fluids, in order to evaluate the effect of corrosion rate in the temperature range considered three, The corrosion of CO_2 at low temperature (less than C_{20}) has a range of corrosion depends on the hydrolysis rate of CO_2 And is independent of the speed . Range 20 to 60°C. The rate of corrosion is very little because the phase of the reaction is CO_2. But in high temperature conditions (above C_{150}) that Mgntayt layer is formed. The wear rate of the m / s 15 is also more corrosion product layer without being damaged. Unless there are factors such as chloride ions, so if the temperature is well over C_{150} and chloride ions there is no corrosion of any kind, unless the flow rate of is 15 m/s, but if the temperature is lower than C_{150} is just a well with corrosion. But if there is a well producing at high water, all wells will be affected by corrosion.

Fluid Composition: As mentioned before, the combination of salt water and dissolved solids in terms of the protective layer is effective. Chlorine in water is not corrosive and destructive only in the carbonate layer and the corrosion rate is increased. The presence of condensate in turn will prevent corrosion, even some of the condensate containing natural inhibitors to prevent corrosion, but not local.

Corrosive Gases: CO_2 and H_2S gases, corrosive agents in the oil and gas wells are considered, however, each of these gases alone can protect the right circumstances can produce. For example, hydrogen sulfide gas at high temperature C_{100} product of pyrite (FeS_2) is completely stable, which protects the metal surface. When these two gases are combined effects of corrosion leave the complex, Mr. Dunlop has an opinion on this situation, if the ratio is less than 500 CO_2 to H_2S, sulfide layer is formed. Haslrv Astgman believes in higher temperature conditions, this number (500) is larger, when the partial pressure of CO_2 partial pressure of H_2S is more than 2000. Hydrogen sulfide can't damage to iron carbonate layer.

Corrosion Control Methods: Check for corrosion protection of pipes and walls of gas wells can be used the following methods:

A) Creating a durable plastic coating inside the tube
B) The use of corrosion resistant alloys
C) The use of non-metallic materials

D) The stabilizer PH
E) Corrosion inhibitor injection

3.1 POLYOLEFIN COATINGS

Poly olefin coatings include polyethylene or poly propylene that has mechanical strength; fairly low pride and high resistance to carrion. The big problems of these coatings are less adhesion of them to steel pipes. For solve the problem has recommended to use three layer coating system including epoxy lining, middle layer, improved copolymer polyolefin and surface coating is polyolefin. In this systems cohesion and resistance to cathodic disbanding by epoxy lining and penetration to water and oxygen, mechanical properties and chemical resistance has supply by polyolefin larger. Epoxy lining by spindle and middle coatings and polyolefin surface coatings has apply on pipes by extrusion methods. Low resistance against penetration sharp edge of stones and rooks especially in high temperature, mad crackup due to soil stress and low thermal resistance, has made some restrictions to using from polyethylene coating.

While high stroke resistance in extensive range of temperature and resistance against penetration of sharp edge of stones and rocks even in temperature more than 100C, has spread largely using from there layer systems on base of polypropylene. Polyurethane is a thermoses polymer with various applications. Using form this polymer has spread for military applications by Otto Bayer in 1930. In one general look polyurethane is product of iso Syanate and polyol with each other, So that: Iso + polyol = polyurethane.

Term of "100% Solid" Used for Coatings that in them has been any Solvent for dissolve, carrying or reduce amount of coating resins. In addition to, Resins that usually are liquid, after implementation (use) completely change to Solid. Contrary to common coatings Such as epoxies that just limit number of them has been usable for coating, polyurethane coatings have large output from types and shapes; (forms).Tem (Statement) of polyurethane coating is general. Tem, because already contains all things, from wood Seal to building floor and underground tanks coatings. Nowadays, various type of polyurethane has used in money applications. Flexible polyurethane foams has used for make bed, pillow and car Seat. Hard foams has used for insulation of freezers, refrigerators and roofs. Many Sport Shoes manufactures, has used impact resistance and elastic polyurethane in make shoes surface. In automobile industry, parts such as dashboard and bumper cuttings has mad by polyurethane. In addition to, polyurethane coatings also has used as bridges, seals, surface or tanks lining. Tem "100% Solid" make a little short Range of all kind of polyurethane Bust yet there are hundred different types of iso syanate and polyol that by them has produced much polyurethane in this range. Another factor that could limit polyurethane by it is type of used iso syanate in them. The most common isomers that used in polyurethane production are aromatic. Polyurethane that make by aromatics, have economic profit, and doing their work well, But when put against sun light, become as chalky and dark. Corrosion feature and other physic features of aromatics a system has not affected by sunlight. But if required, are used these coatings in applications that their appearance are important, and cover surface of them should be coatings. Automobile colors named as dominate sample of this type of polyurethane.

3.2 POLYURETHANE COATINGS PROPERTIES

There are many reasons for tendency to using 100% solid polyurethane coating for pipeline coating.

First of that, using this material has excellent results and this material are famous. Due to harmless, this material are more adjustment than anti-corrosion traditional coatings with environment secondly, due to quick rate of cooking this material, could be put coating pipes under holiday pores test and buried. Third, this material has ability to cook in low temperature, this subject is impossible in other coatings at last, due to this coatings for application are not need to exothrimicity, and they are applied in any thickness or length and diameter of pipe. Response nature of Iso syanate and polyol for polyurethane production is exothermic. Due to this reason, the reaction itself provides needed heat. At last this coatings could be applied in any environment temperature, until apply this coatings unlit 40C' temperature under zero without using extra heat, is not impossible. In spite of properties that mention, 100% solid polyurethane has other good properties, such as: [32]

1- Without pothole
2- High hardness and impact resistance
3- Good flexibility
4- Strong adhesion to metal surface
5- Be resist against steam penetration
6- Separable resistance due to climate factors
7- Chemical resistance

The polyurethane coatings can be classification according to type and their additive quantity. But this additives, usually is added to reduce extra price. Also, should be attention additives that reduce price, will be reduce quality. Adding 10 to 20 percent filling material (especially tar) has effective impact on price reduction, but the impact on coating qualities is small. Increase 40 percent or more will reduce price intensively, but will reduce coating properties so much. The common usable filling in 100% solid polyurethane, are tar materials. In this state, usually is use raw oil, asphalt or tar pitch, although should be attention tar pitch is carcinogen. [31], [34], [35], [24], [22], [14]

The existence of much amount of sulfate in swedge cause to produce H_2S, as result, in state that speed of Swedes movement in pipes are low (level region) , produced sulfuric acid, and due to it , internal coatings pipes destroyed severely. Experience presented that iron case pipes without internal coatings, in this condition has corrode less than 3 years. In analysis has done in Virginia water and swedge research center, samples of cast – iron pipes with 100% solid polyurethane internal coatings has put in Acid souphric 20% and evaluate internal surface resistance. This analysis has present high resistance of this coating. From 1988 until now, about 610 kilometer from internal coatings of pipes with 12 to 48 inch diameter has used in virginal swage network, and covered by 100% solid polyurethane and this usage has increase process. Covered swedge pipes, has not found any problem during work and operation (application) method of this coatings are very ideal.100% solid polyurethane coating, is non- toxin and has effect on smell or taste of drinking water and is not pollute it.

For this reason, it used widely as internal coatings of water drinking pipes and has cover intemal coating of water drinking tanks. With adding antibacterial factors to 100% solid polyurethane could be achieve coating that prevent from bacterial growth in the water. Also with adding special compound to 100% solid polyurethane, achieved coating that has high chemical resistance and used for internal coatings of chemical transaction pipes.

4 CONCLUSION

In this study we studied EOR methods for dense oil recovery from mold in the breakage tanks. Analyze and comparison of recovery with capillarity of salty water, polymeric solution and hot water on different sample of rocks showed high recovery of dense row oil in the EOR methods, and it is more detected in the diluted row oil. Oil (diluted) can recover by water injection in the sand stone condition and with chemical matter and thermal methods. Hot water recovery is more rapid and higher than chemical recovery. For higher recovery of sand stone, hot water has higher and more rapid recovery than gas injection, polymeric matter can increase recovery velocity, but finally its recovery is as the same as salty water. Because of thermal breakage, hot water has the most rapid recovery of dense row oil for oil-wet carbonate. So, it`s possible to use hot water injection instead of mixed gas injection. To final exploiting, hot water degree and process optimize is technical and economical. Berea sand stone and Indiana lime stone were used as rock samples. They were cut in 2.5cm diameter and 7.5cm length from blocks and they have medium value in porosity and penetration is 17% and 8.5cm for lime stone. Each sample was examined once to avoid error. Experiments were performed in the statistical condition with oil injection, in the 100% saturated condition, and recovery than time, until when there is no oil from sample.

In addition to suitable (proper) properties, not be toxin and harmless, more adjustment with environment in comparison with traditional cold coatings , high speed of cooking and in result quick use ability and cooking low temperature of these coatings and lack of need to exothrimicity has cause. [37]

100% Solid polyurethane coatings has account as ideal choice for covering (coating).Has mentioned in thermal cases such as, transitational water tanks, external surface of urban pipes, internal surface of swedge pipes, internal surface of carrying limy and abrasive solution, mobile concrete coating and upper ground pipes coating. [35]

According to very suitable (proper) properties and qualities of 100% Solid polyurethane coatings could have used these coatings widely in covering to equipments inside the country, for example used in pipeline. High electrical, strength and cohesion resistance and also resistance to crack developing such as important specification of suitable coating for external pipes of gas and oil transition pipes and tar, fusion bounded epoxy and polyamine coatings are as the most common coatings that used. In spite of dominate specifications of polypropylenes coatings in comparison with other coatings choose type of coating, number layers and their thickness, are severity under effect of installment environment condition of and oil transition pipes. [14]

Polarization Resistance: Corrosion rate of various experiments by the use of inhibitors was tested and In each experiment, the corrosion rate was different Indicating that this is The effect of change static to turbulent, concentration polarization is reduced and corrosion is increased and the speed of the electrolyte can be beneficial, because the inhibitor to reach the metal surface and the inhibitor can act more effectively.

1) With increasing concentrations of inhibitors by testing the electrochemical corrosion rate can be achieved and see the reducing. However, in practice the optimum injection rate and corrosion inhibitor with respect to the issue of reasonable economic gain. [8]

2) The effect of velocity on corrosion rate at low speeds is a dual On the other hand reduces the corrosion inhibitor material to the metal surface is due to reach more and on the other hand The concentration polarization is reduced, because the solution will be homogeneous and the corrosion rate increases and most of the reduction material reaching to the surface. When the solution is turbulence, because of the washing solution can be increased and the corrosion abrasion is increased too. [5]

3) Using various electrochemical tests reached the conclusion that the Potantio dynamic test in comparison with other tests gets more useful information about Corrosion.

4) With Comparison about Galvano acetate and Potantio acetate can be said: Routine does not find in the case of metals such as current density is determined for each potential, it is indicative Corrosion rate, Potantio acetate method offers current in each potential is more useful than Galvano acetate method.

REFERENCES

[1] A, Samimi and S, Zarinabadi, "An Analysis of Polyethylene Coating Corrosion in Oil and Gas Pipelines," *Journal of American science*, U.S.A., 2011.

[2] A, Samimi and S, Zarinabadi, "Scrutiny Water Penetration in Three-layer Polyethylene Coverage," *Journal of American science, U.S.A*., 2011.

[3] A, Samimi and S, Zarinabadi, "Reduction of greenhouse gases emission and effect on environment," *Australian journal of basic and applied science,* 752-756, 2011.

[4] A, Samimi and S, Zarinabadi, "Problems of hydrate formation in oil and gas pipes deal," *Australian journal of basic and applied science,* 2011.

[5] A, Samimi and S, Zarinabadi, Marouf, M, "Modeling and Simulation for Olefin Production in A Kabir Petrochemical," *Proceedings of the World Congress on Engineering and Computer Science 2010*, WCECS, San Francisco, USA, 2010.

[6] A, Samimi and S, Zarinabadi, "Application Polyurethane as Coating in Oil and Gas Pipelines", *International Journal of science and investigations,* France, pp. 43-45, 2012.

[7] A, Samimi and S, Zarinabadi, M, Samimi, "Solar Energy Application on Environmental Protection", *International Journal of science and investigations,* France, 2012.

[8] A, Samimi, B, Almasinia, E, Nazem, R, Rezaei, Hedayati and M, Afkhami, "Investigating MIDEA Corrosion Treatment on Carbonic Simple Steel in Amin Unit of Isfahan Refinery", *International Journal of science and investigations*, France.

[9] A, Samimi, "Investigation Results of Properties of Stripe Coatings in Oil and Gas Pipelines", *International Journal of science and investigations,* France, 2012.

[10] A, Samimi," Studying Corrosion Electrochemical Mechanism in Tube Line and Gas Wells", *International Journal of science and investigations, France*, 2012.

[11] A, Samimi, "Preventing Hydrate Formation in Gas Transporting Pipe Lines with Synthetic Inhibitors", *International Journal of science and investigations, France*, pp. 48-50, 2012.

[12] M, Samimi and A, Samimi, "Non-Climatically Factors Causing Weather Changes", *International Journal of science and investigations, France*, pp. 35-31, 2012.

[13] A, Samimi, S, Zarinabadi and M, Setoudeh, "Experimental Study of Factors Affecting Corrosion in Gas Wells Using Potantio Acetate and Galvan Acetate Tests," *International Journal of science and investigations,* France, pp. 13-16, 2012.

[14] A, Samimi, S, Zarinabadi, M, Setoudeh and A, Safavian, "Review Applications to Prevent Corrosion Reducing Gas Pipe Line", *International Journal of Basic and Applied science,* Indonesia, pp. 423-428, 2012.

[15] A, Samimi, S, Zarinabadi and M, Setoudeh,"Safety and Inspection for Preventing Fouling in Oil Exchangers," *International Journal of Basic and Applied science,* Indonesia, 2012.

[16] A, Samimi and S, Zarinabadi, "The Comparison of Increasing Method for Petroleum Pits Output (Fluids Dynamic)," *International Journal of Basic and Applied science*, pp. 435-439, 2012.

[17] A, Samimi and M, Afkhami, "Check Solution Corrosive a–MEDA on 316 & 304 Stainless Steel in Hydrogen Unit", *International Journal of Basic and Applied science*, pp. 594-604, 2012.

[18] A, Samimi, "Review Applications to Prevent Corrosion Reducing Gas Pipe Line", *International Journal of Basic and Applied science,* Indonesia, pp. 423-428, 2012.

[19] A, Samimi, "Causes of Increased Corrosion in Oil and Gas Pipelines in the Middle East", *International Journal of Basic and Applied science,* Indonesia, pp. 572-577, 2012.

[20] A, Samimi, S, Dokhani, N, Neshat, B, Almasinia and M, Setoudeh, "The Application and New Mechanism of Universal Produce the 3-Layer Polyethylene Coating," *International Journal of Advanced Scientific and Technical Research* (IJAST), India, 2012.

[21] A, Samimi, "Normal Paraffin Production Process of Kerosene in Oil Refinery Company", *International Journal of Innovation and Applied Studies,* ISSN 2028-9324, Vol. 1, Dec. 2012.

[22] A, Samimi, "Offer a New Model to Prevent Formation of Hydrate in Gas Pipeline in Gas Refinery", *International Journal of Innovation and Applied Studies,* ISSN 2028-9324, 2012.

[23] A, Samimi, "Study an Analysis and Suggest New Mechanism of 3 Layer Polyethylene Coating Corrosion Cooling Water Pipeline in Oil Refinery in Iran", *International Journal of Innovation and Applied Studies*, ISSN 2028-9324, Vol. 1, No. 2, Dec. 2012.

[24] A, Samimi, "Use of Polyurethane Coating to Prevent Corrosion in Oil and Gas Pipelines Transfer", *International Journal of Innovation and Applied Studies,* ISSN 2028-9324, 2012.

[25] M, Samimi and A, Samimi, "Explotion of Resources Management in Iran", *International Journal of Innovation and Applied Studies*, ISSN 2028-9324, Vol. 1, No. 2, Dec. 2012.

[26] A, Samimi and S, Zarinabadi, "Investigation of Corrosion of the Pipeline Using TOEFLT in Iran Refinery", *International Journal of Innovation and Applied Studies,* ISSN 2028-9324, Dec. 2012.

[27] M, Setoudeh, A, Samimi, S, Zarinabadi, B, Almasinia, E, Nazem, R, Rezaei and A, hedayati, "Experimental Study of Factors Affecting Corrosion in Gas Wells Using Potantio Acetate and Galvan Acetate Tests", *International Journal of science and investigations*, 2012.

[28] A, Samimi and S, Zarinabadi, "Scrutiny Water Penetration in Three-layer Polyethylene Coverage," *International Congress of Chemical and Process Engineering, CHISA 2010, and 15 Conference on Process Integration, Modelling and Optimisation for Energy Saving and Pollution,* 2010.

[29] A, Samimi and S, Zarinabadi, "Application Solid Polyurethane as Coating in Oil and Gas Pipelines," *International Congress of Chemical and Process Engineering , CHISA 2012, and 16 Conference on Process Integration, Modelling and ptimisation for Energy Saving and Pollution,* 2012.

[30] A, Samimi and S, Zarinabadi, "Investigation Results of Properties of Stripe Coatings in Oil and Gas Pipelines," *International Congress of Chemical and Process Engineering , and 16 Conference on Process Integration, Modelling and ptimisation for Energy Saving and Pollution,* Check, 2012.

[31] A, Samimi, "Investigating Corrosion Electrochemical Mechanism in Tuble Lines and Gas Shaft", *American Journal of Research Communication (AJRC),* U.S.A, 2013.

[32] R, Rezaei and A, Samimi, "Effects of Phosphorus and Nitrate in Wastewater Shahinshahr City Use for Oil Refinery", *International Journal of Innovation and Applied Studies*, 2012.

[33] A, Samimi and A, Bagheri, "Studying and Investigation Corrosion in Tube Line and Gas Wells in Oil and Gas Refinery", *International Journal of Chemistry*; (IJC), Austria, pp. 27-38, 2013.

[34] A, Samimi, "Preservation Ways and Energy Consumption in Oil Refinery", *International Journal of Chemistry*; (IJC), Austria, pp. 41-47, 2013.

[35] A, Samimi, A, Bagheri, "Investigation of Corrosion in Oil and Gas Pipelines in Southwestern Iran", *World of Sciences Journal*; (WSJ), Austria, pp. 114-127, 2013.

[36] A, Samimi, A, Bagheri, "Investigating Corrosion Treatment on Carbonic Steel in Amin Unit with TOEFEL Polarization", *World of Sciences Journal*; (WSJ), Austria, pp. 128-141, 2013.

[37] A, Samimi, "Micro-Organisms of Cooling Tower Problems and How to Manage them", *International Journal of Basic and Applied science*, Indonesia, pp. 705-715, 2013.

International Journal of Innovation and Applied Studies
ISSN 2028-9324 Vol. 3 No. 4 Aug. 2013, pp. 1094-1100

http://www.issr-journals.org/ijias/

Design of Rectangular Microstrip Antenna with Metamaterial for Increased Bandwidth

B R Koushik and B Ajeya

Department of Electronics and Communication,
Canara Engineering College,
Bantwal, Mangalore, Karnataka, India

ABSTRACT: In this paper a Rectangular Patch Antenna is specifically designed and analysed using metamaterial concepts. Based on an ordinary patch antenna, it has a double C shaped resonant structure embedded in the centre of the substrate of the Rectangular Patch Antenna. The resonant structure has a strong electric response in a certain frequency of interest, and can be used to construct metamaterials with negative permittivity. It is found the great impact on the antenna performance to modify the dimension to 57% of a conventional patch antenna. This antenna has strong radiation in the 45° to the horizontal direction for some specific Broadcast applications within the sub-resonant band, and can construct a dual frequencies antenna under certain conditions. Numerical results verify that the novel antenna performance is satisfactory.

KEYWORDS: Patch Antenna, Metamaterial, Double C-Shaped Structure, Feeding Point, Return Loss.

1 INTRODUCTION

Rectangular microstrip patch antennas, due to their inherent capabilities such as low cost, low weight, and low profile, are widely used in the applications of the wireless communication. However, their transverse dimensions cannot be made arbitrarily small, since the resonance frequency of the rectangular microstrip antennas at a given frequency when its linear transverse dimension is of the order of half wavelength [1]. Over the years, indeed, several techniques have been proposed in order to squeeze the resonant dimensions of patch radiators and enhancement in gain of the antenna, while maintaining their other radiation features [2]. The conventional approach to miniaturizing an antenna is to set the radiator on a high dielectric substrate. Obviously, there are two drawbacks to this [3]. one problems are the electromagnetic field remains highly concentrated around the high permittivity region, and another one is the characteristic impedance in a high permittivity medium is rather low, which creates difficulties in the impedance matching. The use of the metamaterials is properly to improve some basic antenna features (impedance matching, gain, bandwidth, efficiency, front-to-back ratio, etc.), which has represented a novel way of overcoming the limitations shown by some of the well-known techniques for reducing the antenna size [4]. Several examples of compact radiators have been recently proposed.

The metamaterials are artificially structures, and the electromagnetic properties of the materials provided are not encountered in nature [5]. Double negative metamaterials (dng) and single negative metamaterials (sng) have been designed and fabricated [6-7].

In this paper novel rectangular resonator structures with the metamaterials are first analysed and the modes for the sub-wavelength resonance of the rectangular microstrip antenna are excited. Then, a subwavelength structure of the rectangular microstrip patch antenna loaded with the rectangular double c shaped resonator is considered and analysed. Numerical results are shown that the novel antenna has a subwavelength resonance, and reduce the geometry size efficiently. Also the enhancement in gain and bandwidth of an antenna is also observed.

Corresponding Author: B R Koushik (koushikbr19@gmail.com)

2 RECTANGULAR MICROSTRIP ANTENNA

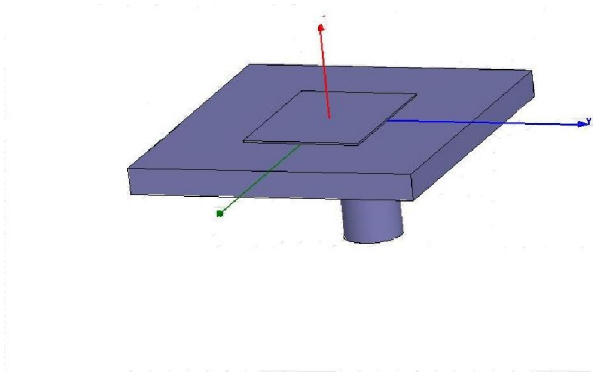

Fig. 1. Rectangular Patch Antenna

The Rectangular patch antenna is having a dimension of 8.49 X 6.171 X 0.1 mm (Fig.1) The dielectric substrate used is FR4 of thickness 1.5 mm, with dielectric constant 4.4. The resonating frequency considered is 10.2 GHz. The Co-axial feeding is applied to an antenna.

3 METAMATERIAL STRUCTURE

After the first metamaterials were fabricated in 2000 by Smith D.R. and his group [5], scientists have proposed many structures to form metamaterials. But most of the structures are based on the split ring resonators (SRRs) and the PEC bars or their transfigurations. In Ref. [8], a substrate with embedded capacitive loaded strips (CLSs) and SRRs has been proposed. Moreover, a double H-shaped resonator for an isotropic ENG metamaterial and a rectangular ELC resonator structure have presented and discussed [9-17].

In our model, a new rectangular double C shaped structure resonator (DCR) with the ENG metamaterial has been formed a SRRs shown in Fig.1. The parameters in the structure are chosen the FR-4 substrate thickness as 0.203 mm with 4.8 dielectric constant, and a metal clad 0.017 mm. Finally, the length and width are chosen as 5mm and 2mm, respectively for the rectangular substrate, and the gap between the PEC strips and the width of the PEC strips are all chosen as 0.1mm shown in Fig.1.

The patch is printed on centre of a thin substrate of FR4 with dielectric constant 4.4 with dimensions of 20 X 10 X 2 mm3, and the patch has dimensions of 8 X 5mm2. A coaxial probe is fed to the patch antenna with characteristic impedance Z0=50Ω, the feed point is at (-1.2, 0.8) as shown in Fig.3 and Fig. 4.

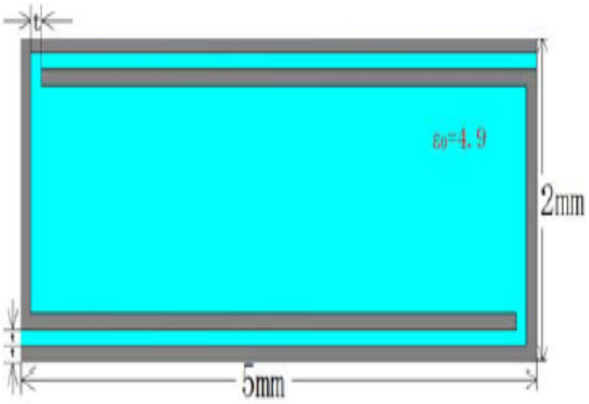

Fig. 2. Geometry of the rectangular double C shaped structure resonator (DCR)

The DCR is loaded in the centre of structure with its strip against the probe. Fig.5 is the distribution of the S parameters of the new patch antenna. It is found that the microstrip patch antenna loaded with DCR structure has two resonant frequencies with f1 = 5.1800 GHz and f2 = 10.2625 GHz because of the insertion of the DCR structure into the substrate of

the antenna, with a return loss of -16.6074 dB and -30.3188 dB Respectively (Fig.5). The designed antenna satisfies the required VSWR over these frequency ranges (Fig.7).

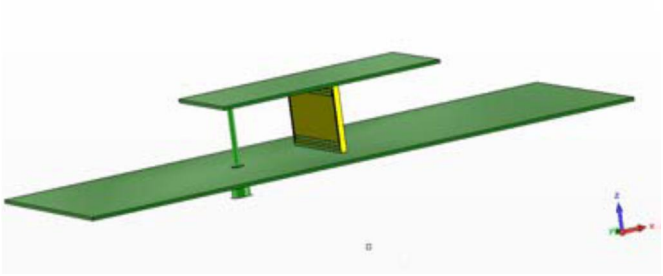

(a)

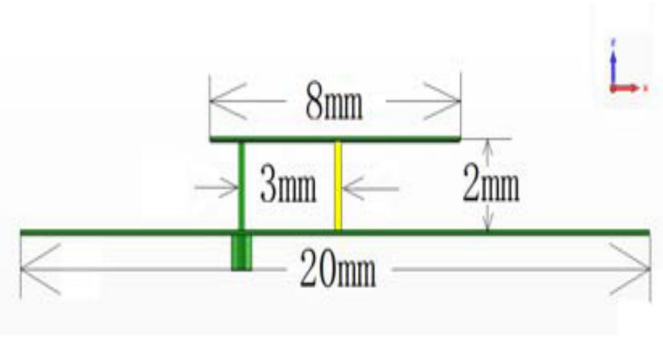

(b)

Fig. 3. Sketch of the rectangular patch antenna with the DCR resonator structure, (a) 3D view; (b) xz-plane view

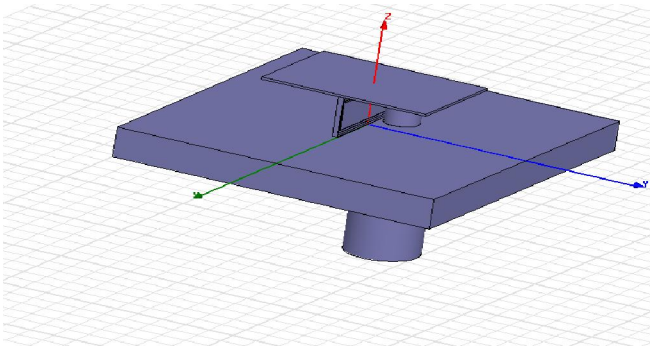

Fig. 4. Rectangular Microstrip antenna with Metamaterial structure

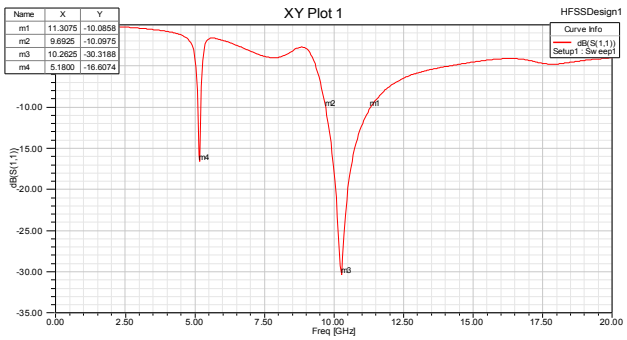

Fig. 5. Return loss of an antenna with Metamaterial structure

The higher resonant frequency is excited by the patch, and the subwavelength resonant is considered as exciting by the DCR structure. Under the subwavelength resonance, the effective permittivity of the DCR medium is expected to be negative value. The -10dB bandwidth, which is defined standard for engineering applications, is 615.5MHz and 1180MHz respectively. Further, the linear gain of first resonant frequency is 4.89 dB, and the antenna efficiency is 89 percent, which is better than a traditional patch antenna. It is also found from the pattern that this antenna has strong radiation in the 45° to the horizontal direction at the sub-wavelength frequency because the wave propagation along the patch has been effected by the left-hand transmission characteristics of the DCR structure. The new patch character has potential in the antenna designs and applications.

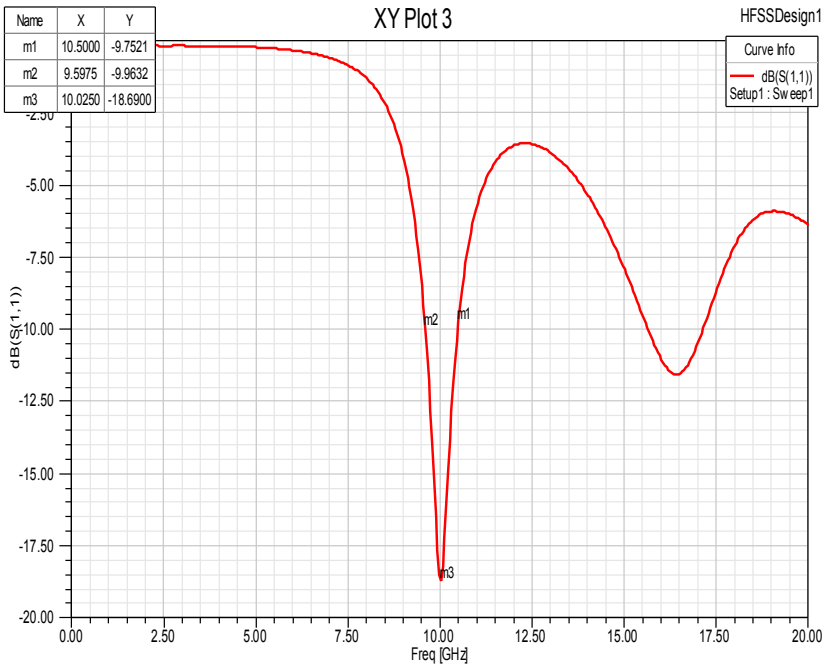

Fig. 6. Return loss of an antenna without metamaterial structure

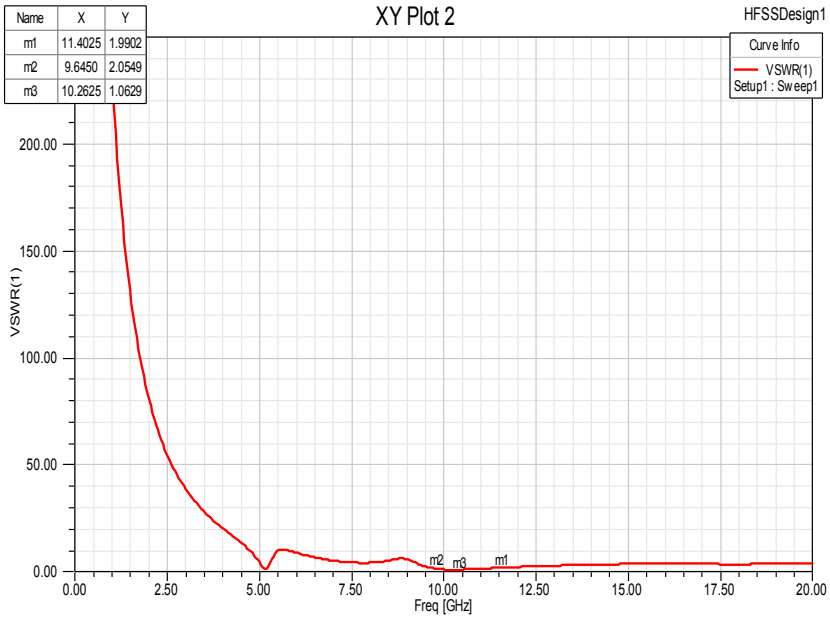

Fig. 7. VSWR of an antenna with Metamaterial structure

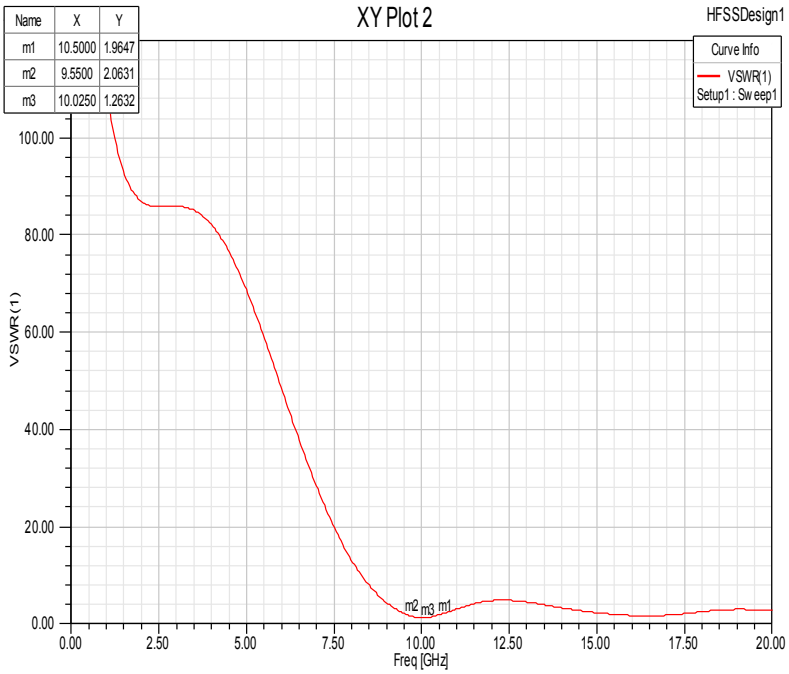

Fig. 8. VSWR of an antenna without Metamaterial structure

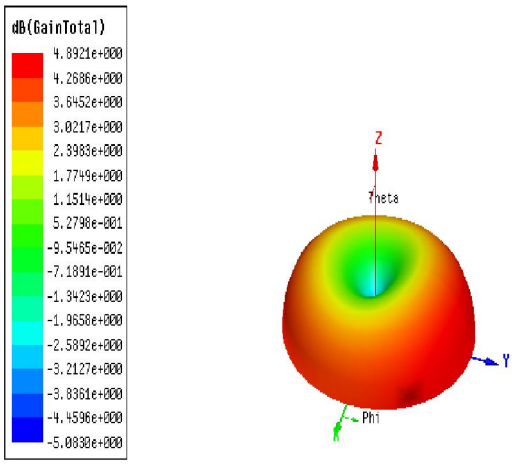

Fig. 9. Gain of an antenna with Metamaterial structure

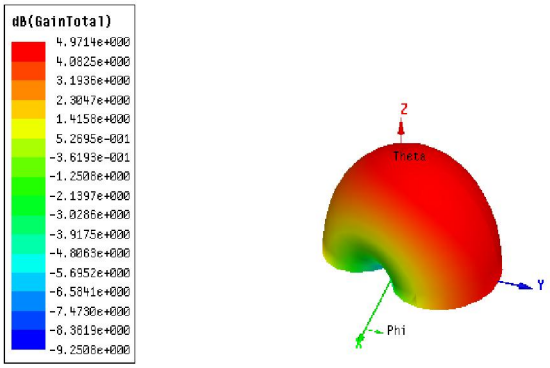

Fig. 10. Gain of an antenna without Metamaterial structure

4 CONCLUSION

A miniature metamaterial microstrip patch antenna has been designed and analyzed in this paper. The working frequency of the rectangular microstrip antenna has significantly descended 57% and increased bandwidth of 0.6 GHz to that of the conventional microstrip antenna, and this antenna has strong radiation near the horizontal direction at the subwavelength frequency. The antenna can be used for dual resonant frequencies and Broadcast communication.

ACKNOWLEDGEMENT

We wish to acknowledge the support given by Principal, Canara Engineering College, Bantwal for carrying out present research work and HOD of Electronics And Communication Engineering for constant encouragement.

REFERENCES

[1] Andrea Alù, Filiberto Bilotto, N. Engheta, and Lucio Vegni, "Subwavelength, compact, resonant patch antennas loaded with metamaterials," *IEEE Trans. Antennas Propag*., vol. 55, pp. 13–25, 2007.

[2] S.S. Zhong and J.H. Cui, "Compact circularly polarized microstrip antenna with magnetic substrate," in *Proc. IEEE AP-S Int. Symp., San Antonio, TX,* vol. 1, pp. 793–796, Jun. 2002.

[3] D. Psychoudakis, Y.H. Koh, J.L. Volakis, and J.H. Halloran, "Design method for aperture-coupled microstrip patch antennas on textured dielectric substrates," *IEEE Trans. Antennas Propag*., vol. 52, no. 10, pp. 2763 – 2766, Oct. 2004.

[4] J.S Lim, C.B. Kim, J.S. Jang etc "Design of a subwavelength patch antenna using metamaterials," *Microwave Conference, EuMC 2008, 38th European*, pp. 547-550, Amsterdam, 2008.

[5] V.G. Veselago, "The electrodynamics of substances with simultaneously negative values of ε and μ," *Sov. Phys. Uspekhi,* vol. 10, no. 4, pp. 509-514, Jan-Feb. 1968.

[6] D.R. Smith, W. J. Padilla, D.C. Vier, S.C. Nemat-Nasser and S. Schultz, "Composite Medium with Simultaneously Negative Permeability and Permittivity," *Physical Review Letters*, vol. 84, no. 18, pp.4184-4187, May 2000.

[7] J.B. Pendry, A. J. Holden, D.J. Robbins and W.J. Stewart, "Magnetism from Conductors and Enhanced Nonlinear Phenomena*," IEEE Trans. on MTT*, vol. 47, pp. 2075-2084, 1999.

[8] R. W. Ziolkowski, "Design, fabrication, and testing of double negative metamaterials," *IEEE Trans. on Antennas and Propag*., vol. 51, no. 7, pp. 1516-1529, July 2003.

[9] J. Machac, M. Rytir, P. Protiva, and J. Zehetner, "A double H-shaped resonator for an isotropic ENG metamaterial," *Microwave Conference, EuMC 2008, 38th European*, pp. 547-550, Amsterdam, 2008.

[10] D. Schuring, J.J. Mock, and D.R. Smith, "Electric-field coupled resonators for negative permittivity metamaterials," *Applied physics letters*, vol. 88, Issue: 4, pp. 041109-041109 -3, 2006.

[11] Rabih Rahaoui and Mohammed Essaaidi, "Compact Cylindrical Dielectric Resonator Antenna excited by a Microstrip Feed Line," *International Journal of Innovation and Applied Studies*, vol. 2, no. 1, pp. 1–5, January 2013.

[12] Mohammed Younssi, Achraf Jaoujal, Yacoub Diallo, Ahmed El-Moussaoui, and Noura Aknin, "Study of a Microstrip Antenna with and Without Superstrate for Terahertz Frequency," *International Journal of Innovation and Applied Studies*, vol. 2, no. 4, pp. 369–371, April 2013.

[13] M. I. Hasan and M. A. Motin, "New slotting technique of making compact octagonal patch for four band applications," *International Journal of Innovation and Applied Studies*, vol. 3, no. 1, pp. 221–227, May 2013.

[14] Tajeswita Gupta and P. K. Singhal, "Ultra Wideband Slotted Microstrip Patch Antenna for Downlink and Uplink Satellite Application in C band," *International Journal of Innovation and Applied Studies*, vol. 3, no. 3, pp. 680–684, July 2013.

[15] Sonali Kushwah, P. K. Singhal, Manali Dongre, and Tajeswita Gupta, "A Minimized Triangular – Meander Line PIFA Antenna for DCS1800/WIMAX Applications," *International Journal of Innovation and Applied Studies*, vol. 3, no. 3, pp. 714–718, July 2013.

[16] Tajeswita Gupta, P. K. Singhal, and Vandana Vikas Thakre, "Modification in Formula of Resonating Frequency of Equilateral TMPA for Improved Accuracy and Analysis," *International Journal of Innovation and Applied Studies*, vol. 3, no. 3, pp. 727–731, July 2013.

[17] Anshul Agarwal, P. K. Singhal, Shailendra Singh Ojha, and Akhilesh Kumar Gupta, "Design of CPW-fed Printed Rectangular Monopole Antenna for Wideband Dual-Frequency Applications," *International Journal of Innovation and Applied Studies*, vol. 3, no. 3, pp. 758–764, July 2013.

International Journal of Innovation and Applied Studies
ISSN 2028-9324 Vol. 3 No. 4 Aug. 2013, pp. 1101-1109

http://www.issr-journals.org/ijias/

Use of Non-Conventional Fillers on Asphalt-Concrete Mixture

M. N. Rahman and M. A. Sobhan

Department of Civil Engineering,
Rajshahi University of Engineering and Technology,
Rajshahi-6204, Bangladesh

ABSTRACT: Stone dust and cement are usually used as filler in asphalt-concrete mixture in Bangladesh. This study has made to prepare asphalt-concrete mixtures using non-conventional fillers which are locally available. Bangladesh is a developing country, where cost is the main concern for any type of constructions. From this point of view, the prime aim of this investigation has been set out to examine the effect of non-conventional filler such as non-plastic sand, brick dust and ash as a filler replacement on the performance of asphalt-concrete mixture and to compare the characteristics of asphalt-concrete mixtures with conventional ones according to the test procedure specified by AASHTO. From the experimental data, it is observed that the value of Marshall Stability is comparatively higher by using non-plastic sand than other non-conventional filler materials. It is also observed that brick dust and ash requires higher asphalt content because of their higher absorption capabilities. The retained strength of the asphalt-concrete mixture using non-plastic sand, brick chips and ash are approximately 89%, 87% and 84% respectively which satisfies the limiting value 75%. Based on this experimental program, it is verified that inclusion of non-conventional filler can be efficiently used in asphalt-concrete mixture as a filler replacement from the viewpoint of stability, deformation and voids characteristics.

KEYWORDS: Asphalt-Concrete mixture, deformation, non-conventional filler, stability, retained strength.

1 INTRODUCTION

Asphalt concrete is a mixture of binder, aggregate and air in different relative amount that set up the substantial properties of the mix. The superiority and stability of asphalt mixtures are influenced by several features together with gradation of aggregates and type and amount of filler materials. Filler acts as one of the major constituents in asphalt-concrete mixture. Fillers not only fill voids in the coarse and fine aggregates but also affect the aging characteristics of the mix. Generally, the aggregate materials those are finer than 75 µm in size is referred to as filler. Filler is defined as consisting of finely divided mineral matter, such as rock dust, slag dust, hydrated lime, hydraulic binder, fly ash, loess, or other suitable mineral matter [1]. In an asphalt-concrete mixture the filler, whether artificial or natural, may stiffen the asphalt-concrete, extend the asphalt cement and affect the workability and compaction characteristics of the mix [2]. Filler imparts a considerable importance on the properties of asphalt-concrete mixture. The amount of filler influences the optimum asphalt content [3]. The workability during the operation of mixing and compaction of asphalt-concrete mixture a consequential property of asphalt-filler mastic also affected by filler materials [4]. The addition of mineral filler increases the resilient modulus of an asphalt-concrete mixture [5]. On the other hand, a disproportionate amount of filler may weaken the mixture by raising the amount of asphalt [6].

Different types and quantity of filler have an effect on the performance of asphalt-concrete mixture [7]. Filler provides better resistance to micro cracking so that it can increase the fatigue life of asphalt-concrete mixture [8]. Structural characteristics of asphalt-concrete mixture are improved by using hydrated lime and phosphogvypsum as filler material [9]. Significant improvement in fatigue life of the asphalt-concrete mixtures can be obtained by using fly ash from oil shale [10]. Waste cement dust as filler on the asphalt-concrete mixture enhances the mechanical properties of the mix, and the laboratory results indicate that the cement dust can totally replace limestone powder in the asphalt paving mixture [11].

Corresponding Author: M. N. Rahman (mnrahmanruet@gmail.com)

Four types of industrial by-product wastes filler namely, limestone as reference filler, ceramic waste dust, coal fly ash, and steel slag dust increases the stiffness and fatigue life of Stone Mastic Asphalt (SMA) Mixtures [12]. Hydrated lime is more effective in stiffening binders than limestone fillers [8]. The temperature susceptibility and durability of the asphalt binder and asphalt-concrete mixture can be improved by using filler materials ([13]-[14]). Using fly ash as filler on asphalt-concrete mixture provides better resistance against low temperature cracking and fatigue cracking [15]. Various conventional materials such as cement, lime, granite powder are normally used as filler in asphalt-concrete mixtures in Bangladesh. Cement, lime and granite powder are expensive and are used for other purposes more effectively. With the economic point of view, the present investigation has been taken in order to study the performance of asphalt-concrete mixtures with non-conventional filler such as, non-plastic sand, brick dust and ash and to compare with the conventional filler materials.

2 MATERIALS AND METHODS

In this study the asphalt-concrete mixture composed of aggregates and binder. Aggregates are divided into three categories namely, coarse aggregate, fine aggregate and filler according to their individual size. Aggregates have to bear load stresses occurring on the roads and have to defend against wear due to the abrasive action of traffic. Binder content in mix ensure proper bond together with durable pavement under suitable compaction. Thus the properties of mineral aggregates and binder are of considerable impact of proper asphalt-concrete mix design.

2.1 COARSE AGGREGATE AND FINE AGGREGATE

In the laboratory test program, crushed stone chips which are smaller than 25 mm and larger than 2.36 mm in size were regarded as coarse aggregate and the coarser sand smaller than 2.36 mm and larger than 75 µm in size were used as fine aggregate [16]. The coarse aggregate and fine aggregate were collected from Panchagarh, Bangladesh and Padma River, Rajshahi, Bangladesh respectively. Properties of coarse aggregate and fine aggregate are shown in Table 1 which were determined according to the test procedures specified by AASHTO.

Table 1. Properties of coarse aggregate and fine aggregate

Properties	Coarse aggregate	Fine aggregate
Dense unit wt. (Kg/m^3)	1670	1570
Loose unit wt. (Kg/m^3)	1535	1440
Bulk specific gravity	2.846	2.461
Apparent specific gravity	2.949	2.637
Water absorption, %	0.9	2.720
Loss angles abrasion value, %	12	…
Aggregate impact value, %	6	…
Aggregate crushing value, %	12	…

2.2 FILLER

Three types of non-conventional filler, non-plastic sand, brick chips and ash which is finer than 75 µm in size are used in this investigation. The properties of this non-conventional filler along with two types of conventional filler stone dust and cement were ascertained according to the test procedure specified by AASHTO and test results are given in Table 2.

Table 2. Properties of mineral filler

Properties	Filler material				
	Stone dust	Cement	Non-plastic sand	Brick dust	Ash
Dense unit wt. (Kg/m^3)	1520	750	1200	1320	476
Loose unit wt. (Kg/m^3)	1270	1020	1000	1050	370
Apparent specific gravity	2.630	2.722	2.438	2.333	1.765

2.3 ASPHALT BINDER

Asphalt binder having a wide range of consistency from fluid to hard and brittle for flexible pavement construction. The asphalt was of 80/100 penetration grade asphalt cement used in this study which was purchased from local distributors. Properties of asphalt used in this investigation shown in Table 3 which were performed according to the procedures specified by the AASHTO.

Table 3. Properties asphalt binder

Test	AASHTO designation	Test value
Penetration, (1/10th mm)	T49	98
Specific gravity	T229	1.002
Ductility (cm)	T51	107.5
Solubility, %	T44	99.75
Softening point, ^{o}C	T53	46.5
Loss on heating, %	T47	1.8
Flash point, ^{o}C	T48	293

2.4 MIX TYPES AND AGGREGATE GRADATION

One of the main objectives of this research is to make a comparative study of the asphalt-concrete mixture with different types of filler material. Five types of mixture were studied and these were designated as A, B, C, D and E which contain stone dust, cement, non-plastic sand, brick dust and ash respectively. Coarse aggregate, fine aggregate and binder were remaining same for all types of mixture.

The changing the proportions of fine and coarse aggregates with the same nominal maximum aggregate size did not affect the permanent deformation significantly [8] and there is no significant difference between the rutting resistance of coarse and fine graded Super pave mixtures [6]. But it can be seen that the mix becomes finer for the given gradation size, the asphalt content increases [17]. On the other hand, excessively small maximum sizes of the particles cause instability and excessively large maximum size particles may result in poor workability and segregation [18]. The asphalt-concrete mixture with medium graded aggregate size provides better resistance to rutting than asphalt-concrete mixture with coarse graded aggregate size [19]. In the continuously graded asphalt mixture, the aggregate blend is designed to be evenly graded from coarse to fine so as to arrive at a dense mix with a controlled void content, hence producing a stable and durable paving. Aggregate gradation used in this study shown in Figure 1.

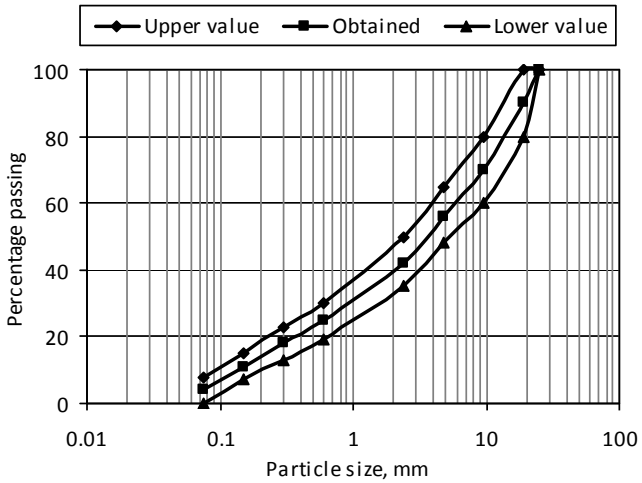

Fig. 1. Gradation of aggregate

2.5 Design and Tests of Asphalt-Concrete Mixture Using Marshall Test Method

In order to study the effect of different filler materials on asphalt-concrete mixture, specimen from Mix A, Mix B and Mix C, Mix D and Mix E were prepared with 5.0%, 5.5%, 6.0%, 6.5% and 7.0% Asphalt content (AC). Marshall test specimens were prepared using different types of mix separately according to the selected aggregate grading. Marshall test specimens of 101.6 mm diameter and 63.5 mm thick were prepared for medium traffic which requires 50 blows in each side of the specimens as per AASHTO T245-82 by varying asphalt content. The bulk specific gravity of compacted specimens was determined according to the test procedure specified by ASTM 2726. After determination of the bulk specific gravity, the specimens were then subjected to Marshall stability and flow test as per AASHTO T245-82. The cylindrical specimens were then compressed on the lateral surface at a constant rate of 2 in/min. (50.8 mm/min.) until the maximum load (failure) is reached. The load resistance and the corresponding flow value were recorded. Voids analysis was made for each series of test specimens after the completion of the stability and flow tests. Then the optimum Asphalt content (OAC) was determined according to the following Equation 1.

$$\text{OAC} = \frac{\text{AC at maximum stability} + \text{AC at maximum unit weight} + \text{AC at 4\% air voids}}{3} \quad (1)$$

3 Test Results and Discussion

3.1 Volumetric Properties of the Mixture

The type of mineral filler in an asphalt-concrete mixture significantly influences the volumetric properties [4]. To determine the effect of non-conventional filler materials on volumetric properties of the mixtures, the properties were investigated at different amount of asphalt content separately shown in Figures 2, 3, 4 and 5. The laboratory test result shows that the bulk density of the mixture with the inclusion of non-plastic sand gives higher value than other non-conventional fillers. On the other hand, the total voids in the mix (VTM) and voids in mineral aggregate (VMA) is higher when brick dust is used as filler in asphalt-concrete mixture. Using of ash in the asphalt-concrete mixture gives higher value of voids filled with asphalt (VFA).

Brick dust and ash has a relatively higher surface area so that they absorb more asphalt than non-plastic sand. Non-plastic sands gives higher bulk density but not so higher than conventional fillers. The value of VFA by using non-conventional filler remains within the range by using conventional fillers.

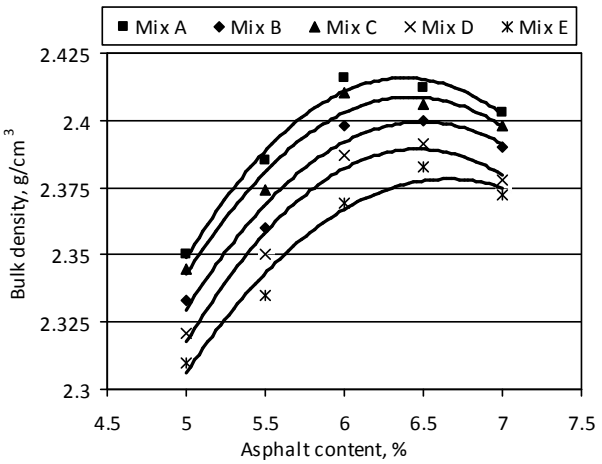

Fig. 2. Bulk density of asphalt-concrete with different filler materials

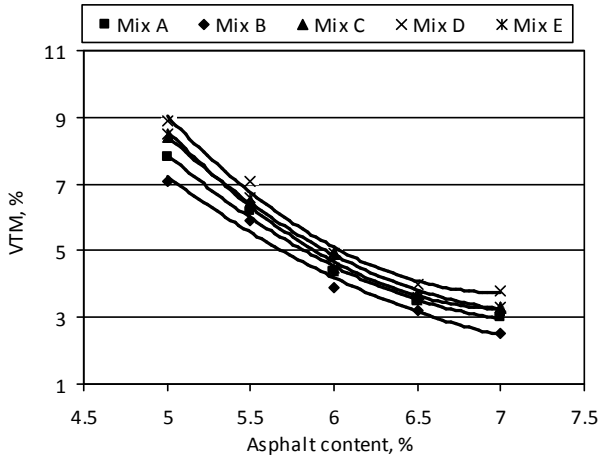

Fig. 3. Voids in total mix of asphalt-concrete with different filler materials

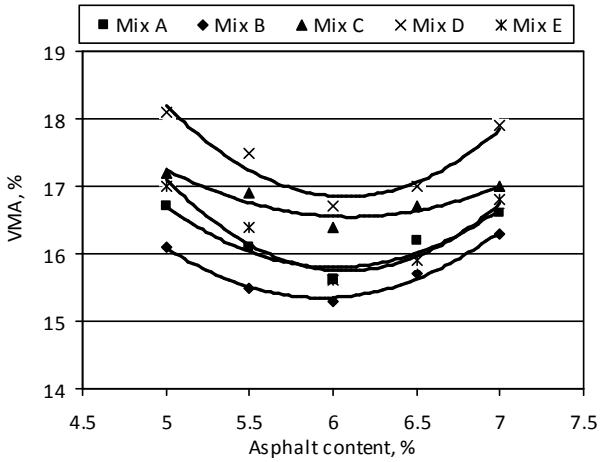

Fig. 4. Voids in mineral aggregate of asphalt-concrete with different filler materials

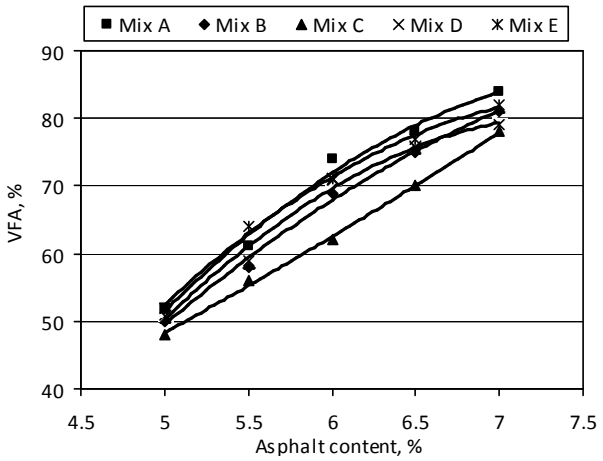

Fig. 5. Voids filled with asphalt of asphalt-concrete with different filler materials

3.2 MARSHALL STABILITY AND FLOW VALUE

The use of non-conventional filler has immense influence on Marshall stability and flow value of the asphalt-concrete mixture which shown in Figure 6 and Figure 7. In the experimental program, non-plastic sand shows higher stability than brick dust and ash. But all types of non-conventional filler possess stability which is higher than the specific value recommended by the Asphalt Institute. It can be seen that the flow value of the asphalt-concrete mixture by using ash gives higher value than non-plastic sand and brick dust. The average flow value is approximately same as the cement dust by using brick dust in the asphalt-concrete mixture.

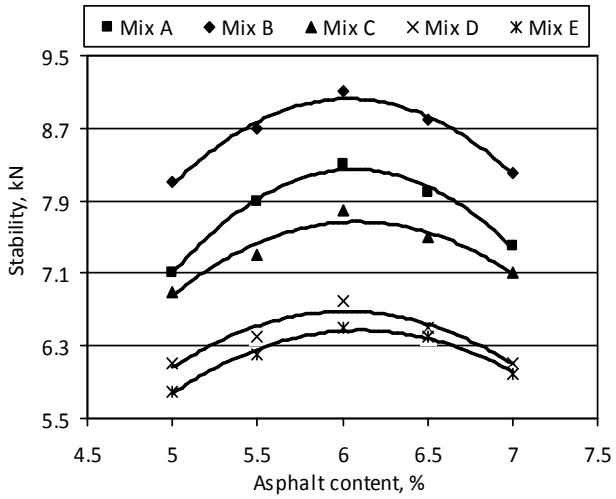

Fig. 6. Marshall stability of asphalt-concrete with different filler materials

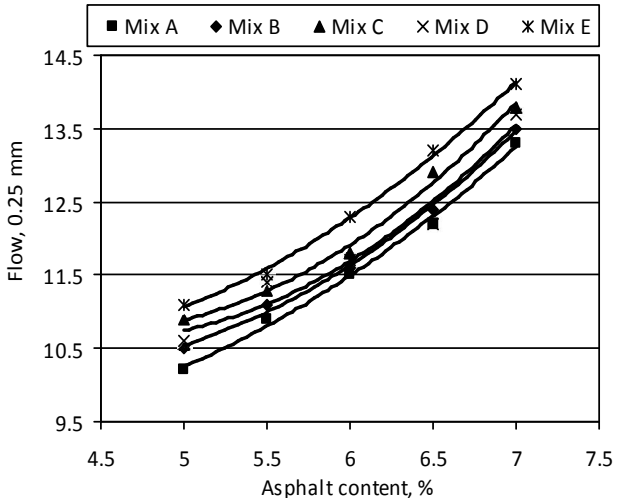

Fig. 7. Flow value of asphalt-concrete with different filler materials

3.3 OPTIMUM ASPHALT CONTENT

Optimum asphalt content is appreciably affected by the mineral aggregates, binder and mix design. In this investigation optimum asphalt content significantly affected by different types of filler materials. Optimum asphalt content is strongly affected by the amount of asphalt absorption in the mixture. Ash absorbs higher asphalt than other non-conventional filler like non-plastic sand and brick dust that's why it requires higher asphalt content. Optimum asphalt content by using non-plastic sand is very much closer to conventional filler materials. The optimum asphalt content by using conventional and non-conventional filler materials are shown in Figure 8. At optimum asphalt content the Marshall characteristics of the asphalt-concrete mixture using different types of mineral fillers are tabulated in the Table 4.

Table 4. Marshall characteristics of Asphalt-concrete mixture at optimum asphalt content

Properties	Mix Type				
	A	B	C	D	E
OAC (%)	6.2	6.1	6.3	6.5	6.6
Unit weight (Kg/m^3)	2415	2405	2398	2390	2379
Stability (kN)	8.2	9.0	7.7	6.5	6.3
Flow (0.25 mm)	11.8	11.8	12.4	12.2	13.1
VTM (%)	4.1	4.0	4.4	4.1	3.6
VMA (%)	15.8	15.4	16.6	17.7	16.1
VFA (%)	75	69	67	75	79

3.4 MARSHALL STIFFNESS

The ratio between Marshall stability and corresponding flow value at optimum asphalt content is termed as Marshall stiffness which represents the combination of stability and flow in a single value. Marshall stiffness gives a sign about the resistance of asphalt mixture to plastic flow resulted from loading [20]. Higher values of Marshall stiffness are an indication of considerable resistance to permanent deformation of the asphalt-concrete mixtures which will be used in pavement construction. Non-plastic sand and brick dust give almost the same value of Marshall stiffness on the other hand ash provide lower value. In this investigation, it is seen that non-plastic sand provides higher resistance to plastic flow of the mixtures than the other non-conventional filler materials. Marshall stiffness of different types of filler materials at optimum asphalt content are shown in Figure 9.

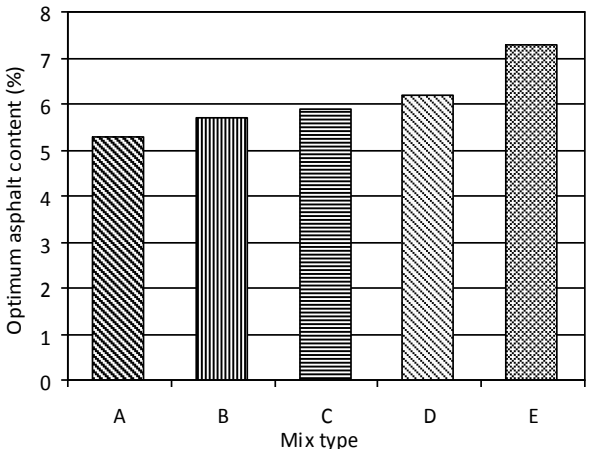

Fig. 8. Optimum asphalt content of asphalt-concrete with different filler materials

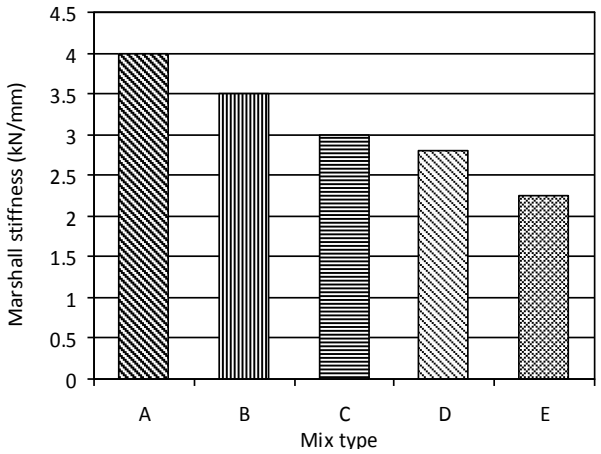

Fig. 9. Marshall stiffness of asphalt-concrete with different filler materials

3.5 MOISTURE SUSCEPTIBILITY OF THE MIXTURES

Water is the worst enemy of the asphalt-concrete mixtures. The premature failure of a flexible pavement may be caused by the presence of water [21]. To determine the moisture susceptibility of the mixtures, retained stability (RS) test were performed according to AASHTO T 283. RS is expressed as the ratio of average Marshall stability of the specimens which were immersed in water at 60 ºC for 2h to the average Marshall stability of the specimens which were immersed in water at 60 ºC for 30 minutes [4]. RS for different types of filler materials is shown in Table 5 and effect of soaking periods on an asphalt - concrete mixture for various filler materials is shown in Figure 10. In this investigation it can be seen that the non-conventional filler materials exhibit lower value than conventional filler materials. But all the values of the RS for both conventional and non-conventional filler satisfy the Indian Criterion of RS which is 75%.

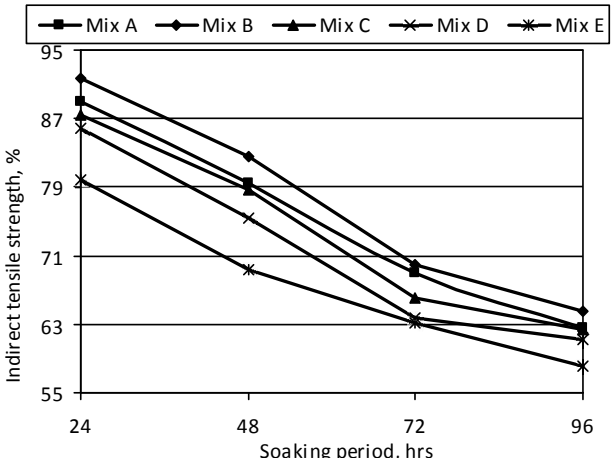

Fig. 10. RS of different filler materials at different soaking periods

Table 5. Retained stability of Asphalt-concrete mixture for different types of filler materials

Material Types	Retained Stability (%)
Stone dust	96.98
Cement	95.39
Non-plastic sand	88.92
Brick dust	87.22
Ash	83.59

4 CONCLUSION

Investigation was made to determine the volumetric properties and deformation characteristics of the asphalt-concrete mixture using different types of non-conventional filler materials. This investigation revealed that different types of filler exhibit significant progresses of the mixture. Volumetric properties of the mixture using non-conventional filler is not similar as the conventional fillers but it can be said that, the volumetric properties of the mixture using non-conventional filler is within the recommended range. Stability and deformation characteristics of the mixture using non-conventional filler are not so higher than the conventional filler but it can be seen from the experimental data that those values are well above the limiting values.

The main drawbacks of these non-conventional filler materials that, they require more asphalt than conventional filler that means they have higher optimum asphalt content compared to the conventional filler. But from the availability and economic (which is related to transportation cost) points of view, it can be said that non-conventional filler materials which have higher resistance to permanent deformation and premature failure, is a feasible option in the construction of flexible pavement.

REFERENCES

[1] American Society for Testing and Materials (ASTM), *Road and Paving Materials; Vehicle Pavement System*, *Annual Book of ASTM Standards*, Section 4, Volume 04.03, 2003.

[2] D. A. Anderson, J. P. Tarris and D. Brock, "Dust collector fines and their influence on mixture design," in *Proc of the Association of Asphalt Paving technologists*, 51, 1982, pp. 363–374.

[3] J. M. I. Hyyppa, *The influence of quality of mineral aggregates upon the optimum binder content of asphalt concrete pavement determined by Hveem's Cke method*, Julkaisu / Valtion teknillinen tutkimuslaitos, 88, 1964.

[4] A. Zulkati, W. Diew and D. Delai, "Effects of Fillers on Properties of Asphalt-Concrete Mixture," *J. Transp. Eng.*, vol. 138, no. 7, pp. 902–910, 2012.

[5] A. A. Tayebali, G. A. Malpass and N. P. Khosla, "Effect of mineral filler type and amount on design and performance of asphalt concrete mixtures," *Transp. Res. Rec.*, vol. 1609, no. 1, pp. 36–43, 1998.

[6] P. S. Kandhal, and J. Parker, *Aggregate tests related to asphalt concrete performance in pavements*, NCHRP Rep. 405, Transportation Research Board, National Research Council, Washington, D.C. 1998.

[7] A. M. Sharrour and G. B. Saloukeh, *Effect of quality and quantity of locally produced filler (passing sieve no. 200) on asphaltic mixtures in Dubai. Effect of aggregates and mineral fillers on asphalt mixtures performance*, ASTM STP 1147, Richard C. Meininger, Ed., American Society for Testing and Material, Philadelphia, 1992.

[8] Kim, Little and Song, "Mechanistic evaluation of mineral fillers on fatigue resistance and fundamental material characteristics," *TRB Annual Meeting,* Paper no. 03-3454, 2003.

[9] S. T. Sudhakaran, R. S. Chandran and M. Satyakumar, "Study on structural characteristics of bituminous mix with added hydrated lime and phosphogvypsum," *International Journal of Emerging trends and Engineering and Development*, vol. 2, no.4, pp. 73-83, 2011.

[10] I. Asi and A. Assaad, "Effect of Jordanian oil shale fly ash on asphalt mixes," *J. Mater. Civ. Eng.*, vol. 17, no. 5, pp. 553–559, 2005.

[11] H. Y. Ahmed and Othman, "Effect of using waste cement dust as mineral filler on the mechanical properties of hot mix asphalt," *Assoc. Univ. Bull Environ Res*, vol. 9, no. 1, pp. 51-59, 2006.

[12] R. Muniandy and E. Aburkaba, "The effect of type and particle size of industrial wastes filler on Indirect Tensile Stiffness and Fatigue performance of Stone Mastic Asphalt Mixtures," *Australian Journal of Basic and Applied Sciences*, vol. 5, no. 11, pp. 297-308, 2011.

[13] H. U. Bahia, H. Zhai, K. Bonnetti and S. Kose, "Non-linear viscoelastic and fatigue properties of asphalt binders," *J. Asso. Asphalt Paving Technol*., vol. 68, pp. 1–34, 1999.

[14] S. Wu, J. Zhu, J. Zhong and D. Wang, "Experimental investigation on related properties of asphalt mastic containing recycled brick powder," *Constr. Build. Mater.,* vol. 25, no. 6, pp. 2883–2887, 2011.

[15] P. Kumar, H. C. Mehndiratta, and V. Singh, "Use of fly ash in bituminous layer of pavement," *Indian Highways*, New Delhi, India, pp. 41–50, 2008.

[16] Asphalt Institute, *Mix Design Methods for Asphalt Concrete and Other Hot-Mix Types*, Manual Series No. 2, (MS-2), 1984.

[17] J. M. Matthews and C. L. Monismith, *The Effect of Aggregate Gradation on the Creep response of Asphalt Mixtures and Pavement Rutting Estimates, Effect of Aggregates and Mineral Fillers On asphalt Mixtures Performance*, ASTM STP 1147, Richard C. Meininger, Ed., American Society for Testing and Material, Philadelphia, 1992.

[18] G. P. Bouchard, *Effects of Aggregate Absorption and Crush Percentage on Bituminous Concrete, Effect of Aggregates and Mineral Fillers On asphalt Mixtures Performance*, ASTM STP 1147, Richard C. Meininger, Ed., American Society for Testing and Material, Philadelphia, 1992.

[19] Y.R Kim, N. Kim and N. P. Khosla, *Effects of Aggregate Type and Gradation on Fatigue and Permanent Deformation of Asphalt Concrete, Effect of Aggregates and Mineral Fillers On asphalt Mixtures Performance*, ASTM STP 1147, Richard C. Meininger, Ed., American Society for Testing and Material, Philadelphia, 1992.

[20] D. Whiteoak, *The Shell Bitumen Handbook*, Thomas Telford, London, UK, 1991.

[21] V. Sharma, S. Chandra and R. Choudhary, "Characterization of Fly Ash Bituminous Concrete Mixes," *Journal of Materials in Civil Engineering*, Vol. 22, no. 12, December 1, 2010.

International Journal of Innovation and Applied Studies
ISSN 2028-9324 Vol. 3 No. 4 Aug. 2013, pp. 1110-1115

http://www.issr-journals.org/ijias/

Design of S-Band Frequency Synthesizer for Microwave Applications

S. Shurender[1], K. Srividhya[1], V. Mantharachalam[2], K. Suresh[2], and M. Umma Habiba[1]

[1]Department of Electronics and Communication Engineering,
Anna University, Sri Venkateswara College of Engineering,
Sriperumbudur, Chennai, India

[2]RFTD, SAMEER,
Tharamani, Chennai, India

ABSTRACT: A phase locked loop based indirect frequency synthesizer is designed for S-band frequency. A Phase locked loop is designed and the phase noise response and transient response of the designed PLL is simulated for 2100MHz frequency. The phase noise response of total PLL and its individual components are obtained. A 3rd order low pass passive loop filter is used and by varying the loop bandwidth and phase margin the trade-off between lock time and phase noise is observed and an optimum value of loop bandwidth and phase margin is chosen such that its phase noise contribution is less. The designed phase locked loop has a low phase noise value of -112.4dBc/Hz at 100 kHz offset frequency and has a fast lock time of 119.5 us. The time taken by the designed frequency synthesizer to lock to 10 Hz frequency error and 1° phase error under transient conditions is found to be 149 us and 116 us respectively. The RMS phase jitter obtained for the designed phase locked loop is 0.3° rms. The phase locked loop is designed and simulated using ADIsimPLL tool. The phase locked loop design aims at achieving low phase noise, reduced lock time and high reliability for S-band applications.

KEYWORDS: Phase locked loop, integer-N PLL, loop filter, phase noise, lock time.

1 INTRODUCTION

Frequency synthesizers are key component in any communication systems from satellite receivers to mobile phones. PLL based indirect frequency synthesizers are used as local oscillators for producing stable high frequency output in wireless communication systems. Direct frequency synthesizers have high speed, low noise but because of their complex size and high power consumption in this paper we use indirect synthesis technique. The indirect synthesis technique which generates the output frequency by utilizing a feedback system is less complex and produces low phase noise and low spurs.

In this paper, an S-band PLL frequency synthesizer at 2.1 GHz is designed. To predict the phase noise contributions a phase locked loop is designed and simulated. The design is simulated for different loop bandwidth and phase margin. The resultant phase noise and lock time are analyzed and an optimum value of loop bandwidth and phase margin is chosen to obtain better phase noise performance and fast locking.

A PLL is a circuit that causes a particular system to track with another one. More precisely, a PLL is a circuit synchronizing an output signal (generated by an oscillator) with a reference or input signal in frequency as well as in phase. In the synchronized—often called "locked"—state, the phase error between the oscillator's output signal and the reference signal is zero, or it remains constant [4]. The basic block diagram of a PLL system is given in Fig. 1

Corresponding Author: S. Shurender (shurender@gmail.com)

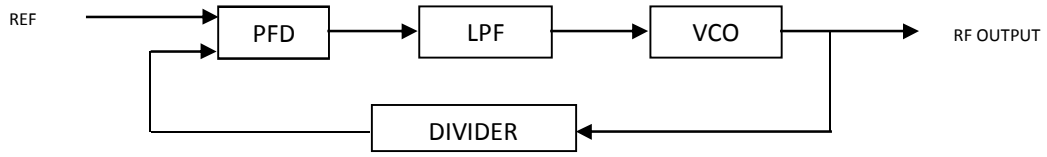

Fig. 1. PLL Block Diagram

The frequency synthesizer is designed using ANALOG DEVICES- ADF4351 integrated synthesizer with VCO. The ADF4351 allows implementation of fractional-N or integer-N phase-locked loop (PLL) frequency synthesizers when used with an external loop filter and external reference frequency. The ADF4351has an integrated voltage controlled oscillator (VCO) with a fundamental output frequency ranging from 2200MHz to 4400MHz. The device operates with a power supply ranging from 3.0 V to 3.6 V. Control of all on-chip registers is through a simple 3-wire interface [5].

The RF VCO frequency (RFOUT) equation is [5]

$$RF_{OUT} = f_{PFD} \times (INT + (FRAC/MOD)) \quad (1)$$

Where, RF_{OUT} is the output frequency of the voltage controlled oscillator (VCO), INT is the preset divide ratio of the binary 16-bit counter (23 to 65,535 for the 4/5 prescaler; 75 to 65,535 for the 8/9 prescaler), FRAC is the numerator of the fractional division (0 to MOD − 1), MOD is the preset fractional modulus (2 to 4095).

2 3RD ORDER LOOP FILTER DESIGN AND OPTIMIZATION

Passive loop filters are used widely in the frequency synthesizers for converting the current pulses output of charge pump into error voltage for tuning the voltage controlled oscillator. A 3rd order loop filter is used for designing the frequency synthesizer. The topology of the 3rd order loop filter used in the design of the PLL is given in Fig. 2

Having low phase noise in communication systems will improve the data transmission and having a fast lock time will decrease the power consumption. Hence the system should have an optimum phase noise performance and fast lock time.

The capacitor C1 is added, because it reduces the spurs level significantly. Also the components R3 and C3 can optionally be added in order to further the reference spur level [2].

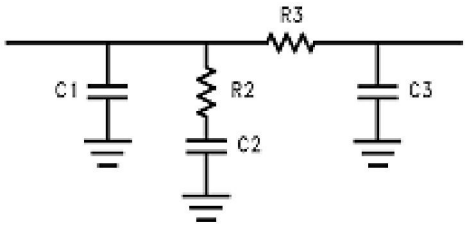

Fig. 2. Passive low pass loop filter

2.1 LOOP BANDWIDTH OPTIMIZATION

Using Narrow loop bandwidths will remove unwanted spurious signals from the synthesizer output, but it also increases the lock time. Using a wider loop bandwidth reduces lock times but leads to increased spurious signals inside the loop bandwidth. The PLL design is simulated for various loop bandwidths and the obtained phase noise and lock time are analyzed.

Table 1. Simulated Phase Noise and Lock Time for various Loop Bandwidth

Loop Bandwidth(kHz)	Phase noise(dBc/Hz)	Lock time(us)
10	-116.0	672
15	-115.5	370
20	-114.8	245
25	-113.7	186
30	-112.4	149
35	-111.1	130
40	-109.8	113
45	-108.5	109
50	-107.3	99.7
55	-106.3	92.5
60	-105.4	86.5
65	-104.6	81.4

From the values in table 1 it can be seen that as the loop bandwidth increases the lock time decreases but phase noise increases. Hence an optimum value of 30 kHz loop bandwidth is chosen.

2.2 PHASE MARGIN OPTIMIZATION

The phase margin denotes how far the PLL system is from instability. Typical value of phase margin ranges from 40^0 to 70^0. Increasing the phase margin increases the phase noise and reduces the lock time.

Table 2. Simulated Phase Noise and Lock Time for various Phase Margin

Loop Bandwidth(kHz)	Phase noise(dBc/Hz)	Lock time(us)
35	-113.2	199
40	-112.8	167
45	-112.4	149
50	-112.0	190

From the table 2 it can be seen that increasing the phase margin reduces the lock time. But after 45^0 phase margin the lock time increases. Hence an optimum value of 45^0 phase margin is chosen.

The following parameters are used for designing the loop filter:

- I_{CP}= 5.0 mA
- K_V = 40 MHz/V
- F_{PFD} = 10 MHz
- Loop bandwidth: 30 kHz
- Phase margin: 45^0

3 PLL DESIGN AND SIMULATION USING ADISIMPLL

The Phase locked loop is designed using ANALOG DEVICES PLL chip ADF4351 for an operating frequency of 2100 MHz with designed 3rd order loop filter and a reference frequency of 10 MHz using ADIsimPLL software. The schematic of designed PLL is given in the Fig. 3

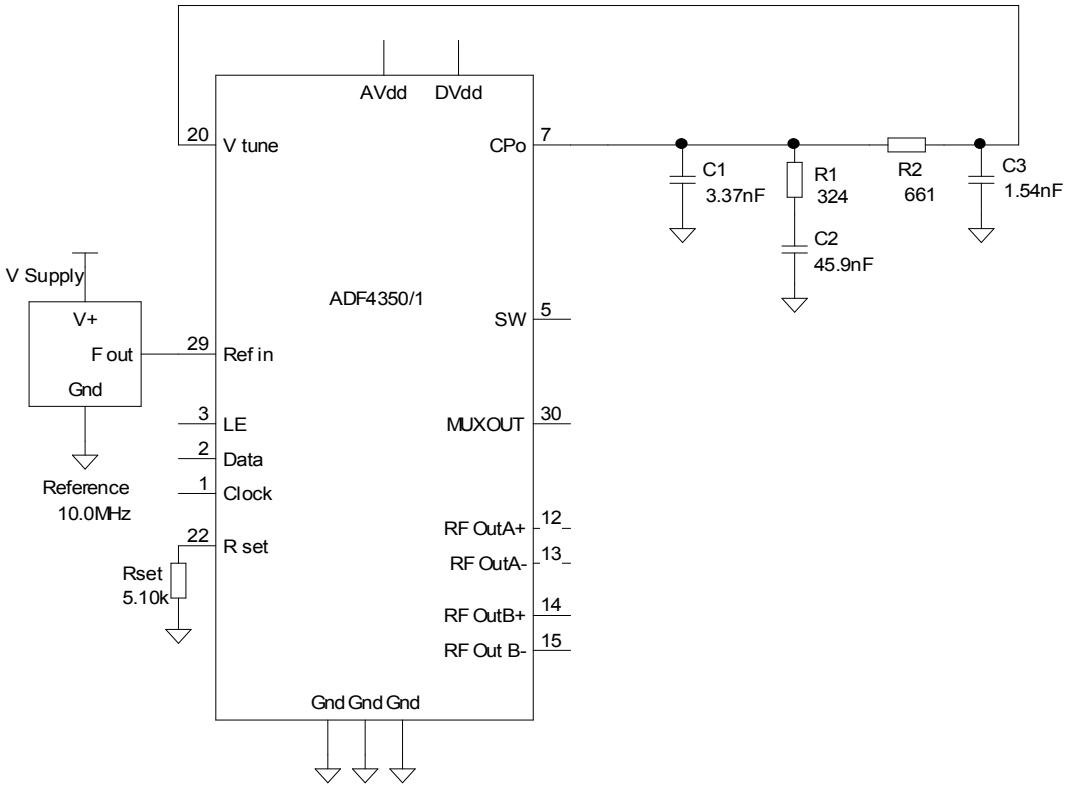

Fig. 3. PLL Schematic using ADIsimPLL

The phase locked loop design is simulated and the simulation results for 2100MHz operating frequency with a comparison frequency of 10 MHz are obtained. Total phase noise of the PLL and also phase noise curves of various individual components like loop filter, VCO and PLL chip are given in the fig. 3.

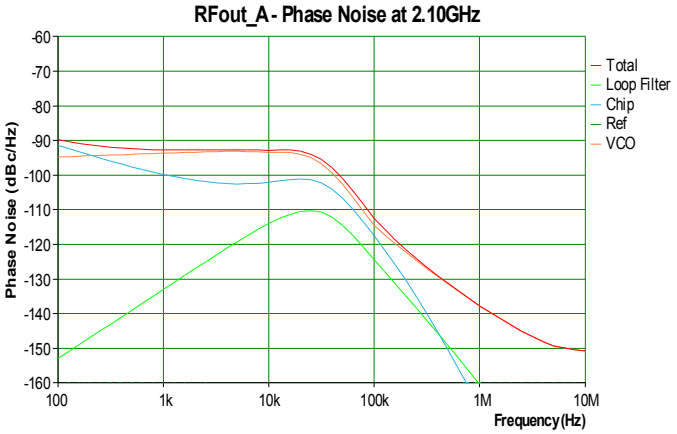

Fig. 4. Phase Noise of Total System and Individual Components

The table 3 shows the total phase noise of the PLL and also phase noise curves of various individual components like loop filter, VCO and PLL chip for various offset frequencies. The phase noise obtained at 100k offset frequency is -112.4dBc/Hz.

Table 3. Phase Noise Results

Frequency Offset(kHz)	Total	VCO	Chip	Filter
100	-89.70	-94.73	-91.34	-153.0
1.00k	-92.69	-93.64	-99.76	-133.0
10.0k	-92.89	-93.49	-102.1	-114.0
100k	-112.4	-114.5	-117.5	-124.3
1.00M	-137.7	-137.7	-167.4	-160.5

The output frequency of the PLL is shown in fig. 4. The time taken by the frequency synthesizer to lock to 2.1GHz frequency is 119.52us. This lock time is optimum for the PLL synthesizer to be used in wireless communication system applications.

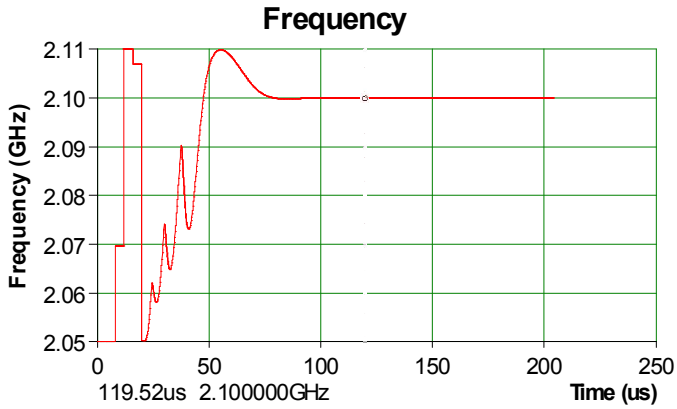

Fig. 5. PLL Output Frequency

The output phase error of the PLL system is given in fig.6. This plot shows the output phase error at the output of PLL during transient conditions. It can be seen that the Time to lock to 1.0 deg phase error is 116us.

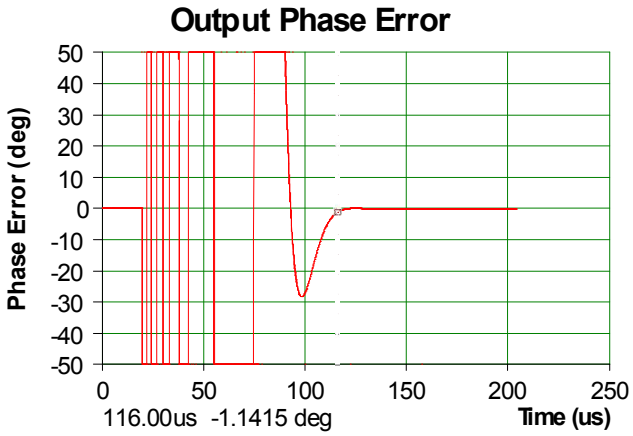

Fig. 6. PLL Output Phase Error

The output frequency error of PLL during transient condition is given in fig.7. The time to lock to 10 Hz frequency error is 149us.

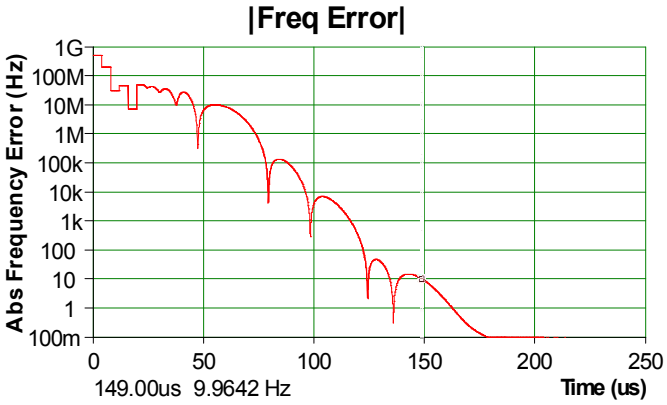

Fig. 7. PLL Output Frequency Error

The system maximum phase error specification for GSM receivers/transmitters (Rx/Tx) is 5° rms [1]. The RMS phase jitter obtained for the simulated phase locked loop is 0.3^0 rms.

4 CONCLUSION

This paper presents a design of S-band frequency synthesizer for microwave application. An optimum value of loop bandwidth and phase margin is obtained by simulating the phase locked loop for various values of loop bandwidth and phase margin and analyzing the resultant lock time and phase noise. A 3^{rd} order passive loop filter with 30 kHz bandwidth and 45^0 phase margin is used in designing the frequency synthesizer. The phase locked loop is designed and simulated by ANALOG DEVICES PLL chip ADF4351. This design has reduced phase noise and lock time for use in wireless communication systems.

REFERENCES

[1] Adrian Fox, “Ask the Applications Engineer- PLL Synthesizers,” *Analog Dialogue*, vol. 36, no. 3, pp. 1-4, 2002.
[2] D. Banerjee, *PLL Performance, Simulation and Design*, Dog Ear Publishing, 4^{th} Edition, 2006.
[3] Mike Curtin and Paul O'Brien y, “Phase Locked Loop for High- Frequency Receivers and Transmitters”, *Analog Dialogue*, vol. 33, no. 7, pp. 1-5, 1999.
[4] R. E. Best, *Phase-Locked Loops Design, Simulations and Applications*, McGraw Hill, 6th Edition, 2007.
[5] Analog Devices Inc., *Wideband Synthesizer with Integrated VCO ADF4351 Datasheet*, 2012.

International Journal of Innovation and Applied Studies
ISSN 2028-9324 Vol. 3 No. 4 Aug. 2013, pp. 1116-1124

http://www.issr-journals.org/ijias/

Etude cinétique et thermodynamique d'adsorption de Composés phénoliques sur un matériau mesoporeux hybride organique-inorganique

[Kinetics and thermodynamics adsorption of phenolic compounds on organic-inorganic hybrid mesoporous material]

Mourad Makhlouf[1], Rachida Hamacha[1], Frédéric Villièras[2], and Abdelkader Bengueddach[1]

[1]Laboratoire de Chimie des Matériaux,
Université d'Oran, BP 1524, 31100 Oran, Algérie

[2]Laboratoire d'Environnement et Minéralurgie,
Université de Lorraine – CNRS-INSU, ENSG BP40, 54501
Vandoeuvre-lès-Nancy, France

ABSTRACT: The objective of this work is thus to study the kinetics, thermodynamics and adsorption isotherms of two phenolic compounds phenol (PhOH) and P-hydroxy benzoic acid (4AHB) on a mesoporous material type MCM- 48 functionalized with an organosilane type trimethylchlorosilane (TMCS) (MCM-48-G). At first, the study of the kinetics, thermodynamics and adsorption isotherms of phenolic compounds in each single solution was performed. In a second step, a similar study was performed on a mixture of these two molecules. Several kinetic models (pseudo-first order, pseudo-second order) were used to determine the kinetic parameters of adsorption. Several adsorption models (Langmuir, Freundlich) were also used to determine the thermodynamic parameters of adsorption isotherms. The effect of three-dimensional pores of MCM-48 and comparison of adsorption of PhOH and 4AHB was examined. It was found that MCM-48-G to a significant adsorption capacity for PhOH and 4AHB, this may be related to the hydrophobicity created by the organic function of TMCS in the MCM-48-G.The results of adsorption and PhOH 4AHB were analyzed using the Freundlich and Langmuir models. It was observed that the adsorption of 4AHB was higher than PhOH. Thermodynamics of adsorption showed that the values obtained for our sample confirm well the interactions with phenol and 4AHB are physical in nature. The adsorption of pollutants on our MCM-48 (G) is a spontaneous and exothermic process.

KEYWORDS: Adsorption, kinetics, isotherm, mesoporous materials, Phenol, P-hydroxy benzoïque acid.

RESUME: L'objectif de ces travaux est ainsi d'étudier la cinétique, la thermodynamique et les isothermes d'adsorption de deux composés phénoliques le phénol (PhOH) et l'acide P-hydroxy benzoïque (4AHB) sur un matériau mesoporeux de type MCM-48 fonctionnalisée par un organosilane de type Trimethylchlorosilane (TMCS) (MCM-48-G). Dans un premier temps, l'étude de la cinétique, la thermodynamique et les isothermes d'adsorption de chacun des composés phénoliques en mono solution a été réalisée. Dans un second temps, une étude similaire a été effectuée sur un mélange de ces deux molécules. Plusieurs modèles cinétiques (pseudo-premier ordre, pseudo-second ordre) ont été utilisés afin de déterminer les paramètres cinétiques d'adsorption. Plusieurs modèles d'adsorption (Langmuir, Freundlich) ont également été utilisés afin de déterminer les paramètres thermodynamiques des isothermes d'adsorption. L'effet de pores tridimensionnels du MCM-48 et la comparaison d'adsorption du PhOH et 4AHB a été examiné. Il a été trouvé que MCM-48-G à une grande capacité adsorption significative pour PhOH et 4AHB; ceci peut être lié à l' hydrophobicité créé par la fonction organique du TMCS dans le MCM-48-G. Les résultats d'adsorption pour PhOH et 4AHB ont été analysés en utilisant les modèles Freundlich et Langmuir. Il a été observé que l'adsorption du 4AHB était plus haute que PhOH. La thermodynamique d'adsorption a montré

Corresponding Author: Mourad Makhlouf (makhlouf.amia@gmail.com)

que les valeurs obtenues pour notre échantillon confirment bien que les interactions avec le phénol et 4AHB sont de nature physique. L'adsorption de nos polluants sur la MCM-48 (G) est un processus spontané et exothermique.

MOTS-CLEFS: Adsorption, cinétique, isotherme, matériaux mesoporeux, TMCS, Phénol, acide P-hydroxy benzoïque.

1 INTRODUCTION

Depuis 1992, date de leur découverte, de nouveaux matériaux mésoporeux (appelés MTS), comparables aux zéolithes (catalyseurs importants en pétrochimie), suscitent l'intérêt de très nombreux laboratoires. Ces matériaux, pour la plupart des silicates ou des aluminosilicates, possèdent une grande surface spécifique et une porosité parfaitement contrôlée. Ils se distinguent des zéolithes par des pores nettement plus gros (de 1,8 à 10 nm contre 1,3 nm au maximum pour les zéolithes) .Ces matériaux offrent ainsi la possibilité d'élargir, à des molécules volumineuses, le domaine de la catalyse hétérogène ou de la séparation, de servir de nanoréacteurs, de vérifier des théories physiques telles que les modèles d'adsorption, le confinement quantique… [1]. Les MTS (Mésoporeux aux Tensioactifs Structurants, ou Micelle-Templated Silica) sont des silicates ou des aluminosilicates formés par assemblage coopératif d'une phase minérale autour d'une phase organique de micelles de tensioactifs. Les MTS sont formées par condensation de silice autour de composés organiques tensio-actifs qui seront ensuite éliminés pour laisser la place à des pores, qui pourront être le siège de réactions chimiques ou physiques contrôlées. Le processus de formation est complexe. Les phases obtenues peuvent être, selon les cas, lamellaires, hexagonales ou cubiques [2]. Il est aussi possible de greffer, par liaison covalente, des fonctions organiques à l'intérieur des pores, cette fonctionnalisation à pour but d'obtenir une surface plus hydrophobe sans changer la structure du matériau, et pour améliorer l'activité, la sélectivité, et la stabilité dans un grand nombre de réactions et de processus catalytiques de sorption[3]. Ces matériaux ont été en particulier été testés pour des applications optiques et pour l'absorption des composés organiques volatils. Certains composés organiques, le plus souvent aromatiques de type phénols, présents dans ces effluents industriels ne peuvent pas être traités par les stations d'épuration conventionnelles car leur toxicité perturbe le traitement par voie biologique. Ce travail s'inscrit dans la première étape de synthétiser et fonctionnaliser un matériau de type MCM-48, et de les testé dans une application environnementale qui consiste a l'étude de l'adsorption compétitive de ces composés aromatiques, le phénol et l'acide p-hydroxy benzoïque.

2 PRÉPARATION D'ÉCHANTILLON

Notre échantillon utilisé et de type MCM-48, il est synthétisé à partir de la composition stoechiométrique décrite par Shen et al. [4] : 1 SiO_2 ; 0,65 CTABr ; 0,5 NaOH ; 60 H_2O. Ce matériau est formé par condensation de silice de type tétraéthylorthosilicate (TEOS), autour de composés organiques tensio-actifs le bromure de cétyltriméthylammonium (CTABr) qui sera ensuite éliminé pour laisser la place à des pores, qui pourront être le siège de réactions chimiques ou physiques contrôlées.

3 GREFFAGE DU TRIMÉTHYLCHLOROSILANE (TMCS) PAR POST-SYNTHÈSE

Pour obtenir une surface plus hydrophobe sans changer la structure du matériau, nous avons adopté la silylation avec le Triméthylchlorosilane (TMCS) qui est ainsi attaché en covalence au groupe silanol de la surface du matériau (Figure I). La réaction de silylation est donnée ci-dessus :

$$\text{Si-OH} + \text{Cl} - \text{Si}(\text{CH}_3)_3 \longrightarrow \text{Si-O-Si}(\text{CH}_3)_3 + \text{HCl}$$

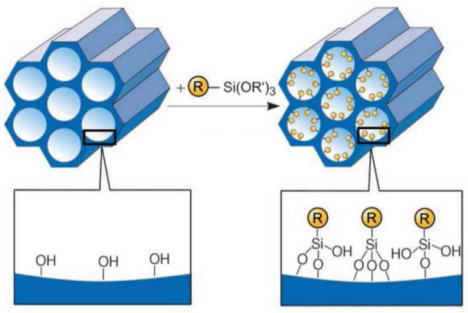

Fig. 1. Greffage post synthétique de fonctions organo/siliciques sur une phase mésoporeuse silicique à l'aide d'un groupement $(R'O)_3SiR$ (R et R', fonctions organiques) [5]

3.1 MODE OPÉRATOIRE DE GREFFAGE PAR LE (TMCS)

Pour le greffage de notre matériau nous avons suivi le protocole de silylation décrit par X.S. Zhao [6] qui est composé des étapes suivantes :

3.2 PRÉTRAITEMENT THERMIQUE

Après avoir synthétisé le matériau, on procède au prétraitement thermique de 2 g de matériau pendant 3 h .Ce prétraitement permet surtout d'éliminer une partie de l'eau qui est liée par liaison d'hydrogène aux groupements silanols superficiels. Tout ceci est réalisable à la seule condition du choix de la température dite température optimale de déshydratation 723 K.

3.3 SILYLATION

La réaction de silylation est effectuée en agitant les matériaux siliciques avec une solution de TMCS dans le toluène (1g : 50ml) à 343K pendant 3 h.

3.4 RINÇAGE ET SÉCHAGE

Apres la réaction de silylation le matériau obtenu est rincé avec deux solvants le toluène puis l'acétone, dans le but d'éliminer tous les produits qui existent sur la surface et qui n'ont pas été greffé. Enfin, la poudre est séchée à 323 K.

4 CARACTÉRISATION PHYSICO-CHIMIQUE

4.1 CARACTÉRISATION PAR DIFFRACTION DES RAYONS X SUR POUDRES

Le diffractogramme du matériau synthétisé est présenté (figure 2). L'allure indique des réflexions qui s'indexent facilement dans une maille cubique tridimensionnelle des pores (groupe de symétrie (Ia3d)). Il indique l'apparition d'un pic intense attribué à la réflexion (211) et d'un pic de plus faible intensité dû à la réflexion (220), de même que deux pics distincts mais d'intensité assez faible correspondant aux réflexions (420) et (332).

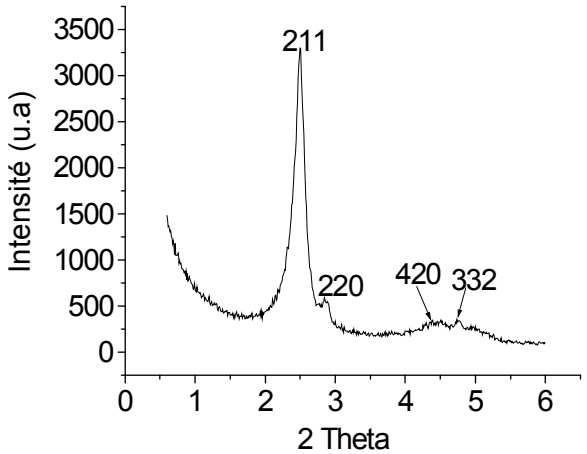

Fig. 2. Diffractogramme RX de MCM-48

4.2 CARACTERISATION PAR ADSORPTION-DESORPTION D'AZOTE A 77 K (ANALYSE BET)

La courbe d'adsorption-désorption de N2 dans la MCM-48 (figure 3) est superposable. L'adsorption des molécules d'azote se fait aux mêmes pressions relatives que la désorption.

Pour des basses pressions, l'isotherme d'adsorption se traduit par l'apparition d'un film d'azote liquide à la surface des pores pour former les mono-multicouches. Une variation de l'isotherme entre 0.2 et 0.4 en p/p0 indique un phénomène de condensation capillaire dans les pores et un plateau final avec une faible inclinaison à des pressions relatives élevées, correspondant à l'adsorption sur la surface externe.

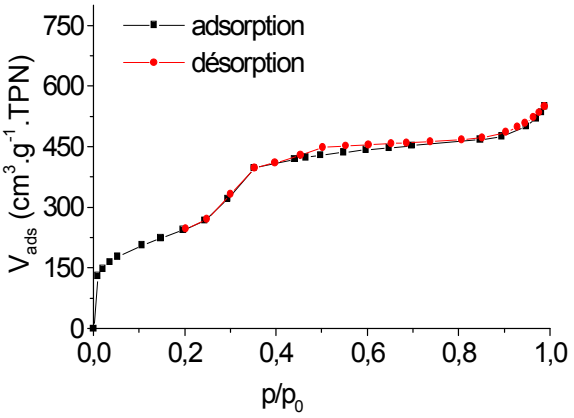

Fig. 3. N_2 sorption MCM-48

Tableau 1. Propriétés texturales

	a_0 (Å)	S (BET) (m^2g^{-1})	V méso (cm^3g^{-1})	Dp (Å)	Ep (Å)
MCM-48	86.51	925	0,65	33.30	9.82

5 ADSORPTION COMPÉTITIVE ACIDE P-HYDROXYBENZOÏQUE-PHÉNOL EN PHASE AQUEUSE

L'adsorption d'un seul constituant (phénol ou 4AHB) a représenté la première étape de notre travail. La suite de cette étude est consacrée à l'adsorption du mélange initial équimolaire binaire de ces deux composés phénoliques.

La démarche adoptée est la même que pour l'étude des constituants seuls : suivi des dynamiques d'adsorption des deux constituants à température ambiante pour déterminer le temps d'équilibre, établissement des isothermes d'adsorption à température ambiante.

5.1 ESTIMATION DU TEMPS D'ÉQUILIBRE POUR UN MÉLANGE ÉQUIMOLAIRE D'ACIDE 4-HYDROXYBENZOÏQUE ET DE PHÉNOL SUR MCM-48 GREFFÉ À TEMPÉRATURE AMBIANTE

Les dynamiques d'adsorption du phénol et du 4AHB obtenues en compétition pour un mélange équimolaire (C0, 4AHB = 0 ,8 g/L, C0, phénol = 0,8 g/L) mettent en évidence des différences de comportements amplifiées par rapport aux produits purs .la présentation de la dynamique d'adsorption des mélanges équimolaires 4AHB – phénol et celles de chaque adsorbat seul est représenté dans (Figure 4).

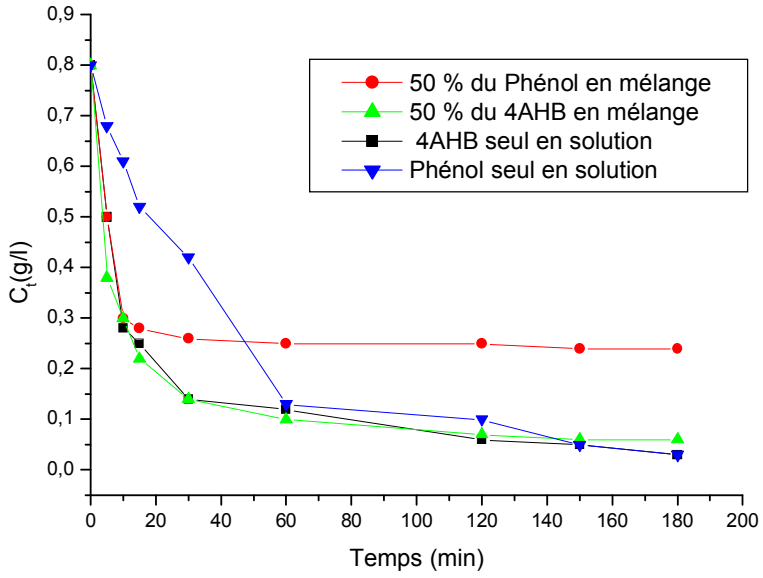

Fig. 4. Comparaison de l'adsorption d'un mélange équimolaire 4AHB – phénol avec celles du 4AHB et du phénol, seuls en solution

L'équilibre est atteint beaucoup plus rapidement pour le phénol (moins de 30 minutes contre 60 minutes en phénol pur) que pour le 4AHB (plus de 120 minutes).

A l'équilibre, il reste en solution plus de phénol que de 4AHB (0,25/0,05) : en compétition dans un mélange équimolaire, le 4AHB s'adsorbe très préférentiellement.

5.2 ISOTHERMES D'ADSORPTION DES POLLUANTS EN PROPORTIONS ÉQUIMOLAIRES

La (figure 5) qui représente l'évolution de la quantité adsorbée en fonction du temps permet de comparer les isothermes d'adsorption d'un mélange équimolaire (phénol + 4AHB) sur MCM-48 greffée. Les cinétiques d'adsorption des deux polluants présentent les mêmes allures caractérisées par une forte adsorption du (phénol + 4AHB) sur MCM-48(G) dès les premières minutes de contact, suivie d'une augmentation lente jusqu'à atteindre un état d'équilibre.

La cinétique d'adsorption rapide pendant les premières minutes de réaction, peut être interprétée par le fait qu'en début d'adsorption, le nombre des sites actifs disponibles à la surface du matériau adsorbant, est beaucoup plus important que celui des sites restant après un certain temps [7,8].

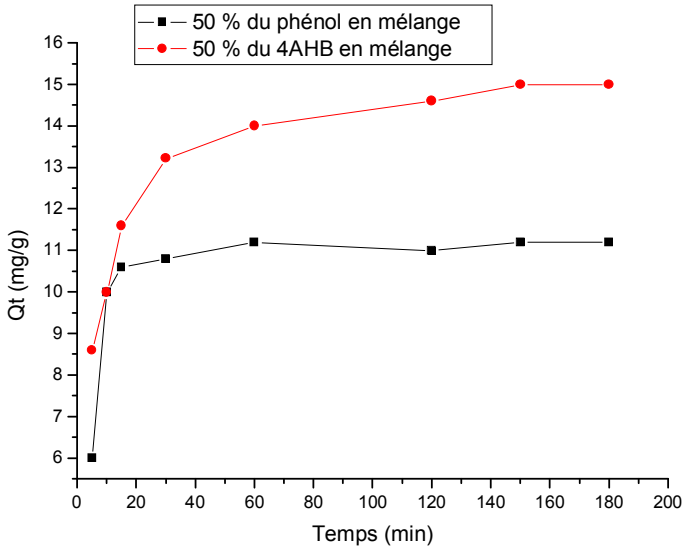

Fig. 5. Cinétiques d'adsorption du phénol et du 4AHB en mélange équimolaire ($V_{solution}$ = 0.01L, MMCM-48 (G) = 0,05 g)

Ensuite, plus la concentration augmente, plus l'adsorption du 4AHB prend le pas sur celle du phénol : la quantité de phénol adsorbée diminue (presque saturé). Sur un même site d'adsorption, quand le phénol et le 4AHB sont en compétition, c'est le 4AHB qui s'adsorbe préférentiellement.

L'adsorption préférentielle du 4AHB s'explique principalement par la différence de solubilité des deux molécules.

Le 4AHB est environ 19 fois moins soluble dans l'eau que le phénol. En accord avec la littérature, ce phénomène est particulièrement marqué aux fortes concentrations près des limites de solubilité de l'espèce la moins soluble, le 4AHB [9]. Le caractère attracteur d'électrons du groupement -COOH augmente la force des interactions entre la surface du MCM-48 (G) et le noyau aromatique.

Il est intéressant de noter que des différences relativement faibles sur les capacités maximales d'adsorption du phénol et du 4AHB, seuls en solution ne traduisent pas la très forte différence d'adsorption en compétition. C'est plutôt le paramètre KL, la constante d'adsorption (0.044 pour le 4AHB et 0.036 pour le phénol), qui traduit l'affinité d'une espèce pour l'adsorbant.

5.3 CINÉTIQUES D'ADSORPTION DES POLLUANTS EN PROPORTIONS ÉQUIMOLAIRES

La constante de vitesse d'adsorption du premier ordre est déduite à partir du modèle établi par Lagergren [10]. Dans le souci d'approcher le plus possible le mécanisme réactionnel réel, Ho et Mc Kay [11] ont opté plutôt pour un modèle cinétique d'ordre 2. Ces modèles mathématiques ont été choisis d'une part pour sa simplicité et d'autre part par son application dans le domaine d'adsorption des composés organiques sur les différents adsorbants.

Pour le premier ordre : la constante de vitesse k est donnée par la relation suivante :

$$\mathbf{Ln\ (qe-qt)/qe=-Kt}$$

Pour le pseudo second ordre, la constante de vitesse K' est donnée par la relation suivante :

$$\mathbf{t/qt=1/2K'qe2+t/qe}$$

Avec : qe : Quantité d'adsorbat à l'équilibre par gramme d'adsorbant (mg/g), t : le temps de contact (min), k et K': Constantes de vitesse d'adsorption respectivement pour le premier ordre (min-1), le pseudo second ordre (g min/mg).

Les constantes de vitesse d'adsorption des polluants sur la MCM-48(G) pour le premier et le pseudo second ordre sont déterminées graphiquement (figures 6 et 7). Pour chaque polluant, nous avons calculé les constantes de vitesses pour le premier et pseudo second ordre à partir des droites obtenues.

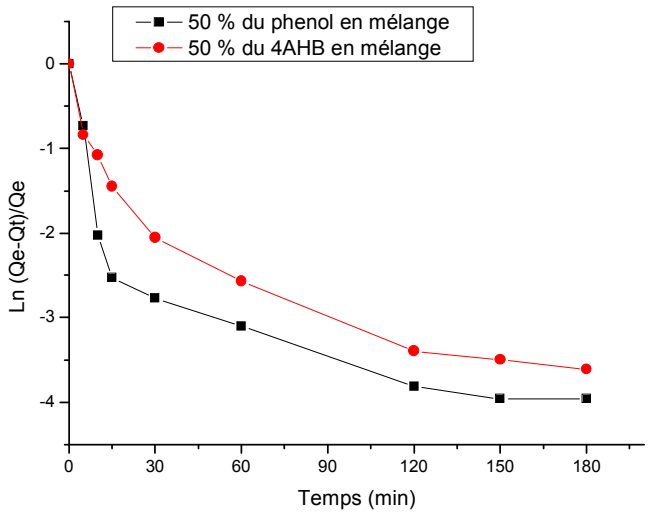

Fig. 6. Détermination des constantes de vitesse du premier ordre de l'adsorption du (phénol + 4AHB) par la MCM-48(G)

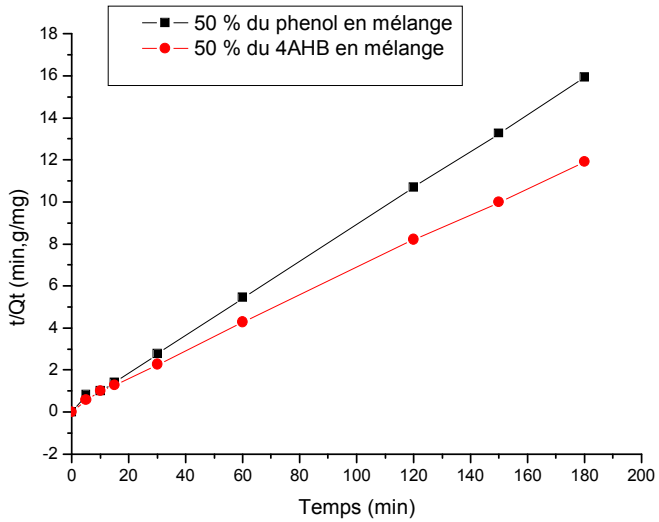

Fig. 7. Détermination des constantes de vitesse du pseudo second ordre de l'adsorption du (phénol + 4AHB) par la MCM-48(G)

Tableau 2. Constantes de vitesse de l'adsorption du phénol

Constantes de vitesse du premier ordre		*Constantes de vitesse du pseudo second ordre*		
K(min^{-1})	**R^2**	**K'(min^{-1}.g/mg))**	**R^2**	**Qe (mg/g)**
1.469	0.408	0.02	0.998	12.5

Tableau 3. Constantes de vitesse de l'adsorption du 4AHB

Constantes de vitesse du premier ordre		*Constantes de vitesse du pseudo second ordre*		
K(min^{-1})	***R^2***	***K'(min^{-1}.g/mg)***	***R^2***	***Qe (mg/g)***
0.016	0.687	0.008	0.999	15.384

D'après les résultats obtenus indiqués sur les Tableaux 5 et 6 nous remarquons que le modèle de pseudo second ordre est plus adapté pour déterminer l'ordre des cinétiques d'adsorption des deux polluants par la MCM-48(G). En effet, un bon coefficient de corrélation (R^2 = 0.998 pour le phénol et R^2 = 0.999 pour le 4AHB).

La MCM-48(G) utilisé dans ce travail a montré une nette efficacité dans la diminution de la pollution des eaux. Les expériences ont montré que les deux polluants étudiés s'adsorbent sur la MCM-48 greffé par le TMCS. Les cinétiques d'adsorption du phénol et Acide 4-hydroxybenzoïque (4AHB) sur la MCM-48 greffé sont toutes les deux de type pseudo second ordre.

6 THERMODYNAMIQUE D'ADSORPTION

L'adsorption des atomes d'un gaz ou d'un liquide va avoir pour conséquence de diminuer l'énergie de surface du matériau. Les expériences d'adsorption du phénol et acide p-hydroxybenzoïque ont été menées en régime statique.

Il est possible de déterminer la chaleur d'adsorption ΔHads par la relation suivante :

$$\ln Kad = -\Delta Hads / RT + \ln K0$$

Où Kad est la constante d'adsorption à l'équilibre avec **Kc =Ce/(Ci-Ce)**, R la constante des gaz parfaits (valeur usuelle **R = 8,314 J.mol-1.K^{-1}**) et T est la température absolue.

La variation globale d'énergie libre ΔGads et entropie d'adsorption ΔSads qui en résultent peut se calculer selon les équations suivantes :

$$\Delta Gads = RT\ln Kads \; ; \; \Delta Sads = (\Delta Hads - \Delta Gads)/T.$$

La chaleur d'adsorption Qads est définie comme étant l'opposée de la variation d'enthalpie

ΔHads soit : Qads = - ΔHads

Les donnes expérimentales sont regroupées dans le tableau 4.

Tableau 4. Résultats expérimentaux de la Thermodynamique d'adsorption du Phénol et 4AHB

	T (K)	ΔH (KJ/mol)	ΔG (KJ/mol)	ΔS (J/mol K)
Phénol	298	-11,95	-5,57	-21,34
	308		-5,22	-21,78
	318		-5,15	-21,32
4AHB	298	-15,91	-6,98	-29,96
	308		-6,50	-30,55
	318		-6,39	-29,93

Les taux d'adsorption obtenus montrent que la quantité adsorbée est limitée par la porosité. Ces résultats montrent à la fois l'influence de la nature géométrique des matériaux mésoporeux (cubique et hexagonale) et l'hydrophobicité de la surface de ces derniers.

Les expériences d'adsorption du phénol et 4AHB montrent que la MCM-48 (G) greffé par TMCS est un bon adsorbant à 25°C.

Les isothermes d'adsorption montrent que l'adsorption des deux constituants augmente avec l'augmentation de la concentration à l'équilibre.

Il est bon de rappeler que, la structure cubique facilite la diffusion des molécules et leur piégeage dans les cavités. Le greffage des organosilanes par la méthode post-synthèse sur ces matériaux, est un assemblage d'une partie inorganique (silice) et une partie organique

(TMCS) ce qui augmente l'hydrophobicité de cette surface, donc sa capacité a adsorbé les molécules organiques.

L'adsorption obéit à la fois aux isothermes de Langmuir et aux isothermes de Freundlich. Dans notre cas l'adsorption est une adsorption non-spécifique caractérisée par une faible valeur de la chaleur d'adsorption de l'ordre de -11,93kJ/mol pour le phénol et de -15,91kJ/mol pour le 4AHB. Les valeurs obtenues pour notre échantillon confirment bien que les interactions avec le phénol et 4AHB sont de nature physique. L'adsorption de nos polluants sur la MCM-48 (G) est un processus

spontané et exothermique. Les faibles valeurs de la chaleur d'adsorption confirment bien que les interactions entre ces polluants et le matériau sont de nature physique.

7 CONCLUSION

L'adsorption du phénol et de l'acide 4-hydroxybenzoïque sur le matériau mesoporeux de type MCM-48 greffe par le TMCS apporte de nombreuses données en réponse aux différents besoins de notre étude. Les isothermes d'adsorption ont été obtenues successivement pour des solutions aqueuses de phénol, de 4AHB et du mélange phénol - 4AHB.

La représentation de ces isothermes est applicable au modèle de Langmuir et Freundlich avec une capacité d'adsorption maximale.

Les deux espèces s'adsorbent de façon analogue avec des capacités d'adsorption très semblables, montrant une légère supériorité pour l'acide.

L'adsorption compétitive phénol - 4AHB met en évidence la nette supériorité du 4AHB, si bien que l'isotherme du phénol, obtenue à partir d'un mélange initial équimoléculaire, passe par un maximum assez marqué à très faible concentration d'équilibre.

La variation de la température, de 298 K° à 318 K°, a permis de calculer la chaleur d'adsorption du phénol (-11,95kJ/mol) et de 4AHB (-15,91kJ/mol) et de confirmer que les interactions avec le phénol et 4AHB sont de nature physique.

REFERENCES

[1] N.Coustel, F. Di Renzo, F. Fajula, "Improved stability of MCM-41 through textural control," *journal Chem Commun*, vol. 8, pp. 967-968, 1994.

[2] A. Cauvel, D. Brunel, F. Di Renzo, F. Fajula, "Organic lining of MCM-41-type silicas," *American Institute of Physics*, vol. 1, pp. 354-477, 1996.

[3] A. Cauvel, D. Brunel, F. Di Renzo, B. Fubini, E. Garrone, "Preferential grafting of alkoxysilane coupling agents on the hydrophobic portion of the surface of micelle-templated silica," *Langmuir,* vol. 24, no. 10, pp. 807-813, 2000.

[4] J.L. Shen, Y.C. Lee, Y.L. Liu, C.C. Yu, P.W. Cheng, C.F. Cheng, "Photoluminescence sites on MCM-48", *Microporous and Mesoporous Materials,* Vol. 64, pp. 135-143, 2003.

[5] F. Hoffmann, M. Cornelius, J. Morell, M. Froba, Angew, "Silica-based mesoporous organic-inorganic hybrid materials", *Chem. Int. Ed. Engl*, vol. 45, no. 20, pp. 3216-3251, 2006.

[6] X. S. Zhao and G. Q. Lu, "Modification of MCM-41 by surface silylation with trimethylchlorosilane and adsorption study," *Journal Phys. Chem. B*, Vol. 102, no. 9, pp. 1556-1561, 1998.

[7] A.R. Dincer, Y. Gunes, N. Karakaya, "Coal-based bottom ash (CBBA) waste material as adsorbent for removal of textile dyestuffs from aqueous solution ", *Journal of Hazardous Materials*, Vol. 141, no. 3, pp. 529-535, 2007.

[8] Z. Yaneva, B. Koumanova, "Comparative modelling of mono- and dinitrophenols sorption on yellow bentonite from aqueous solutions", *Colloid and Interface Science*, Vol. 293 , no. 2, pp. 303-311, 2006.

[9] Rengaraj, S., Moon S-H., Sivabalan, R., Arabindoo, B, Murugesan, V., "Removal of phenol from aqueous solution and resin manufacturing industry wastewater using an agricultural waste: rubber seed coat", *Hazardous Materials*, Vol. 89, no. 2, pp. 185-196, 2002.

[10] S. Lagergren, S. Vetenskapsakad, "About the theory of so-called adsorption of soluble substances," *Hand. Band*., Vol. 24, no. 4, pp. 1–39, 1898.

[11] Y. S. Ho , G. McKay, "Pseudo-second order model for sorption processes," *Process Biochemistry*, vol. 34, no. 5, pp. 451-465, 1999.

International Journal of Innovation and Applied Studies
ISSN 2028-9324 Vol. 3 No. 4 Aug. 2013, pp. 1125-1131

http://www.issr-journals.org/ijias/

Antihyperglycaemic and Antihyperproteinaemic Activity of Extracts of *Picralima nitida* Seed and *Tapinanthus bangwensis* Leaf on Alloxan-Induced Diabetic Rabbits

Bosede M. Adegoke[1] and Oyelola B. Oloyede[2]

[1]Department of Applied Sciences, Osun State Polytechnic,
Iree, Osun State, Nigeria

[2]Department of Biochemistry, University of Ilorin,
Ilorin, Kwara State, Nigeria

ABSTRACT: Coconut water extract of *Picralima nitida* seed and aqueous extract of *Tapinanthus bangwensis* leaf were investigated for their antidiabetic activities on some biochemical parameters (glucose, protein) associated with diabetes in both the serum and tissues of experimental animals using alloxan-induced diabetic rabbits as model. The rabbits were fasted overnight before they were given a single intraperitoneal injection of aqueous alloxan monohydrate (Sigma, USA) at a dose of 300 mg/kg body weight to make them diabetic. The experimental rabbits (chinchilla) were grouped into six and extracts administered orally, once daily for five weeks. Groups 1 and 2 (non-diabetic) received only distilled water and coconut water respectively, group 3 (diabetic) received 200 mg/kg body weight aqueous extract of *T. bangwensis* leaf, group 4 received 400 mg/kg body weight of coconut water extract of *P. nitida* seed, groups 5 and 6 (diabetic) received only distilled water and coconut water respectively. The results revealed that the extracts independently lowered significantly ($p<0.05$) the blood glucose and protein levels of the diabetic rabbits. Both extracts significantly ($p<0.05$) increased the tissue protein. Overall, aqueous extract of *T. bangwensis* leaf and coconut water extract of *P. nitida* seed independently possesses insulin-like properties as demonstrated by their antidiabetic actions, hence, may be good herbal extracts in the management of diabetes.

KEYWORDS: Alloxan, Antihyperglycaemic, Antihyperproteinaemic, Diabetes, *Picralima nitida*, *Tapinanthus bangwensis*.

1 INTRODUCTION

Diabetes mellitus referred to simply as diabetes, is a syndrome characterized by disordered metabolism manifesting abnormally high blood sugar (hyperglycaemia) resulting from insufficient levels of insulin, the principal hormone that regulates uptake of glucose from the blood into most cells primarily muscle and fat cells [1].

Diabetes is one of the world's commonest diseases today with about 171 million people being affected by the disease [2]. The figure is ever increasing and it has been predicted that by 2030, over 366 million people would be living with diabetes if current trend continues [3].

The orthodox approach of managing diabetes is faced with a lot of difficulties, this is partly because several of the drugs, aimed in managing diabetes pose a significant risk of inflicting heart disease and no pill or injection to date is able to address the problem of dying pancreatic beta cells, a fundamental dysfunction in diabetes.

The management of diabetes concentrates on keeping blood sugar levels as close to normal as possible, without causing hypoglycaemia.

Consequent upon the problems associated with orthodox approach in the management of diabetes, effort is now geared towards the traditional approach of curing/managing diabetes. It is assumed that this approach is safer and more natural.

Corresponding Author: Bosede M. Adegoke (abosedeadegoke@yahoo.com)

The use of herbal medicines for the treatment of diabetes mellitus has gained importance throughout the world. The World Health Organization also recommended and encouraged this practice especially in countries where access to the conventional treatment of diabetes is not adequate [4].

In Nigeria, many herbalists have claimed to use the coconut water extract of *Picalima nitida* (Akuamma) seed and aqueous extract of *Tapinanthus bangwensis* (Mistletoe) leaf for the treatment for various diseases, including diabetes. In Nigeria, several herbal preparations from leaves and twigs of mistle-toes e.g. *T. bangwensis* (Engl. and K. Krause] Danser have become popular for the treatment of variety of diseases, such as diabetes and hypertension, which have been reported to be on the increase in the country [5]. However, information is scanty in open scientific literature to support the folkloric use of these plants as antidiabetic agents.

2 MATERIALS

2.1 COLLECTION AND PROCESSING OF PLANT MATERIALS

The seeds of *Picralima nitida* (Stapf) T. Durand & H. Durand were purchased from herbseller at 'Baboko market', Ilorin, Nigeria while the leaves of *Tapinanthus bangwensis* (Engler & K. Krause) Danser from citrus tree (host plant) were obtained from a farm settlement in 'Ila-Orangun', Osun State, Nigeria. The plants were authenticated at Forest Research Institute of Nigeria (FRIN) Ibadan, Nigeria. Voucher samples were preserved in the Institute's Herbarium (FHI 109955 and FHI 109972 for *P. nitida* and *T. bangwensis* respectively). The seed coats of the *P. nitida* seeds were removed with the hand and the *T. bangwensis* leaves were washed free of sand and debris. The seeds and leaves of the *P. nitida* and *T. bangwensis* respectively were air- dried for two weeks at room temperature ($28^{o}C \pm 0.02$) and pulverized using an electric blender (Holt Star, Model BE 768-2, John Holt product, UK).

2.2 ANIMALS AND FEED

The experimental rabbits (36), (chincilla breed) of mixed sexes from Goshen rabbit farm, Osogbo, Nigeria were randomized into six groups of six animals each were used in this study. Rabbit pellets (a product of Guinea Feeds, Ibadan, Nigeria) and water were available to the animals *ad libitum* throughout the experimental period. The experimental rabbits were acclimatized for a week. Experimental animals were handled according to the stated guidelines of Ethical Committee on the ethical use of animals in research.

3 METHODS

3.1 PREPARATION OF PLANTS EXTRACTS

Solvent extract of pulverized seeds of *P. nitida* and leaves of *T. bangwensis* were prepared by separately suspending 500g each of the powdered samples in 1000 ml of coconut water and distilled water respectively using the modified method of Gray and Flatt [6]. The mixtures were left to infuse overnight and were thereafter vigorously shaken for 3 hours using a wrist hand shaker for thorough extraction. The extracts were filtered with Whatman No. 1 filter paper and the filtrates concentrated in a rotary evaporator to obtain semi solid extracts. Calculated amount of the extract was weighed and thereafter used to determine the concentrations of the extracts administered to the different groups of the experimental animals using the appropriate solvent.

3.2 INDUCTION OF DIABETES

The rabbits were fasted overnight before they were given a single intraperitoneal injection of aqueous alloxan monohydrate (Sigma-Aldrich, USA) at a dose of 300 mg/kg b. w. to make them diabetic. After 6 hours, they were given 5% D - Glucose solution to drink to counter the hypoglycaemic shock phase [7]. The fasting blood glucose level of blood samples drawn from the tail vein puncture was determined after 72 hours using Onetouch ultraeasy glucometer (Lifescan Johnson and Johnson Company, Milipitas). Rabbits showing blood glucose level greater than 180 mg/dL were selected for the study [8] to indicate diabetic rabbits.

3.3 Experimental Design and Extract Administration

The experimental rabbits (mix sexes) were grouped into six (6). Extracts were administered orally at the dose of 200 mg/kg and 400 mg/kg for *Tapinanthus bangwensis* and *Picralima nitida* respectively, once daily for five (5) weeks. The dosages were arrived at with series of preliminary studies to establish the concentration at which the extracts exhibited the safest and highest hypoglycaemic activities. The animals were grouped and treated as follows:

A: Non diabetic rabbits placed on distilled water only (NDDW)

B: Non diabetic rabbits placed on coconut water only (NDCW)

C: Diabetic rabbits placed on distilled water extract of *T. bangwensis* leaf (DDWT)

D: Diabetic rabbits placed on coconut water extract of *P. nitida* seed (DCWP)

E: Diabetic rabbits placed on distilled water only (DDW)

F: Diabetic rabbits placed on coconut water only (DCW)

3.4 Blood Samples Collection and Preparation

At the end of the fifth week of experimentation, the rabbits were anaesthetized with chloroform.The jugular vein was exposed and with a sterile knife, the rabbits were bled and whole blood sample was collected from each group of the animals into sterile plain bottles and allowed to clot for one hour and were thereafter centrifuged at 2000 rpm for 10 minutes [9] to obtain the serum which was then collected in universal sample bottles and stored in the freezer until required.

3.5 Collection and Weighing of Organs

The animals were dissected after the collection of the blood samples and each of their kidneys, hearts and livers were removed. The organs were blotted in clean tissue paper, weighed, and thereafter kept frozen until required for homogenization.

3.6 Homogenization of the Organs of the Experimental Animals

A known weight of each of the organ (liver, kidney and heart) of the experimental animals was put into the mortar and homogenized with pestle in an aliquot of ice – cold 0.25 M sucrose solution until a smooth homogenate was obtained.

3.7 Determination of Biochemical Parameters

Blood glucose concentrations were read using Onetouch ultraeasy glucometer (Lifescan Johnson and Johnson Company, Milipitas, CA) following the procedures as outlined by the manufacturer. Protein concentrations in the serum and tissue homogenates were determined as described by Gornal *et al*, [10].

3.8 Statistical Analysis

All data were subjected to analysis of variance using the model for randomized complete block design [11]. Significant differences between treatment means were determined at 5% confidence level using Duncan's Multiple Range Test (SPSS 16).

4 Results

The blood glucose levels in untreated diabetic rabbits (DDW, DCW) when compared with normal rabbits were significantly ($p<0.05$) raised (Figure 1). Administration of aqueous extract of *T. bangwensis* leaf and coconut water extract of *P. nitida* seed respectively decreased blood glucose level in diabetic rabbits (DDWV, DCWP).

Except for the extract treated rabbit groups (DDWT and DCWP), the untreated rabbit groups exhibited a significant increase ($p<0.05$) in the plasma protein concentration in comparison to those of the control (Figure 2).

There was also significant ($p<0.05$) reduction in the protein concentration in the organs of the diabetic untreated rabbits (DDW, DCW) (Figure 3) in comparison to those of the extract treated groups (DDWT and DCWP) though they also exhibited reduction in the protein concentration when compared with the control (NDDW and NDCW).

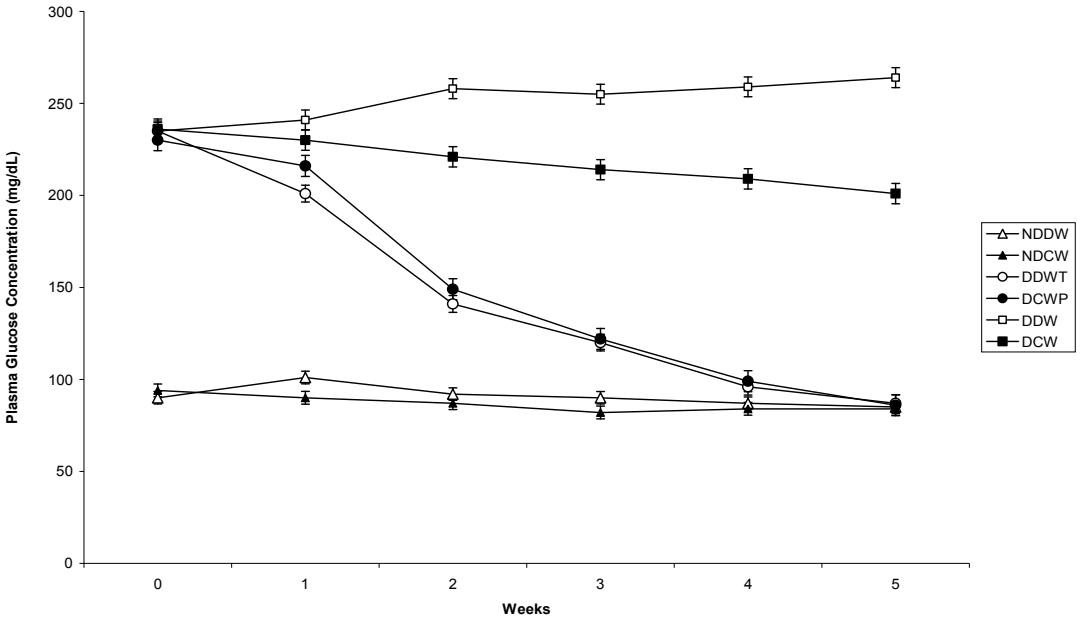

Fig. 1. Plasma Glucose (mg/dL) Concentration of Alloxan - Induced Diabetic Rabbits Placed on Aqueous Extract of T. bangwensis Leaf and Coconut Water Extract of P. nitida seed over a Period of Five Weeks

Values are Means of Six Determinations ± S. E. M.

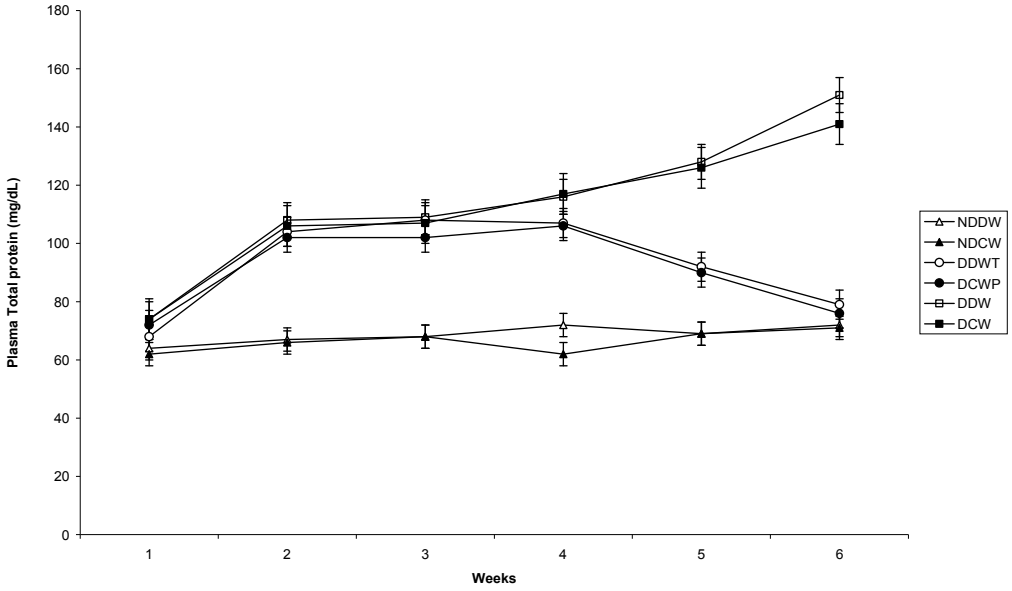

Fig. 2. Plasma Total Protein Concentration (mg/dL) of Alloxan–Induced Diabetic Rabbits Placed on Aqueous Extract of T. bangwensis Leaf and Coconut Water Extract of P. nitida seed over a Period of Five Weeks

Values are Means of Six Determinations ± S. E. M.

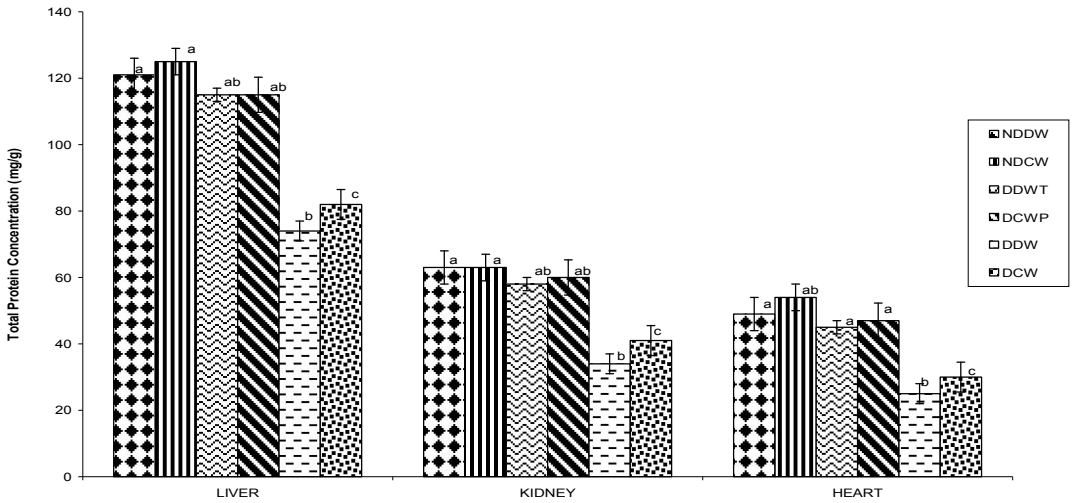

Fig. 3. Total Protein Concentration (mg/dL) of Alloxan –Induced Diabetic Rabbits Placed on Aqueous Extract of T. bangwensis Leaf and Coconut Water Extract of P. nitida seed over a Period of Five Weeks. Values are Means of Six Determinations ± S. E. M.

5 DISCUSSION

As a result of the effect of alloxan, leading to diabetes, as evidenced from the significant ($p<0.05$) elevation in the level of blood glucose in rabbits (Figure 1), an observation which had also been reported by several workers [12], [13], [14], there is also derangements in protein metabolism in the plasma as well as in some selected tissues (liver, kidney and heart) which are implicated in diabetes.

Blood glucose level usually returns to normal within two hours after ingestion of carbohydrates in normal individual, but, in diabetes, blood glucose reaches a high level of above 115 mg/dL and remains elevated for longer period of time [15]. The hyperglycaemia status in the diabetic untreated rabbits may be attributable to deficiency of insulin which is responsible for the uptake of glucose from the blood. However, administrations of aqueous extract of *T. bangwensis* leaf and coconut water extract of *P. nitida* seed respectively decreased the blood glucose levels in diabetic rabbits demonstrating antihyperglycaemic properties. Aqueous infusions of some medicinal plants (such as *Eleophorbia druifera* and *Amaranthus sp.*) had earlier been reported to have antihyperglycaemic properties [16], [17]. It had also been reported that the leaf and stem of European mistletoe contain water soluble natural product(s) which directly stimulate insulin secretion from clonal B-cells [18]. This is also in agreement with the report of Gray and Flatt [6]. However, Coconut water extract of *P. nitida* seed also produced the desired normoglycaemia (≥75 to ≤ 115 mg/dL) [15]. Possible hypoglycaemic effect had also been reported of aqueous extract of *P. nitida* seed [19]. Other probable mechanisms by which the extracts lowered blood glucose levels in diabetic rabbits might be by increasing glycogenesis, inhibiting gluconeogenesis in the liver, or inhibiting the absorption of glucose from the intestine [20]. The significant ($p<0.05$) reduction in the glucose level in the diabetic rabbit group placed on coconut water extract of *P. nitida* seed may in part be as a result of health benefits of coconut water which had earlier been documented to improve insulin secretion, improve utilization of blood glucose, being completely non- toxic and capable of relieving stress on pancreas [21]. The basis for the elevation of serum protein in diabetics is due to the fact that the serum is the medium through which the proteins and amino acids removed from the peripheral tissue are transported in the body [22]. However, the effects of insulin on protein metabolism (e. g. enhancement of amino acids uptake from the blood, protein synthesis and decreased protein degradation in tissue) is to decrease the level of protein in the serum [23]. When there is insulin deficiency as in diabetics, the reverse of the normal effects would occur and as shown in the present study (Figure 2) causing an increase in the serum protein level when compared with the control. It is possible that the hyperproteinaemia observed in this study may also be consequent upon damaged kidney and liver [24]. It is most likely that the test extracts which contain bioactive ingredients which possess insulin - like property which enhance normal protein metabolism.

Moreso, insulin inhibits proteolysis and vice versa in its absence. In insulin deficiency, glucose accumulates in the blood, hence, not absorbed by peripheral tissues thereby depriving cells of glucose for energy production and the body consequently, reverts to the use of protein for energy. In such situation, tissue proteins are degraded and the amino acids produced are used by the liver for energy production [15]. This may account for the reduction in protein level of the organs of the diabetic rabbits in this study (Figure 3). This is in agreement with the report of Zimmet *et al.* [25]. It is considered that

the test plant extract contain bioactive ingredients which tend to rehabilitate the protein levels in the selected organs under investigation. This may probably be by inhibiting gluconeogenesis and proteolysis in these organs thereby sparing protein for other metabolic activities instead of energy production.

6 CONCLUSION

The data generated from this study showed that diabetic rabbits were obtained using alloxan. The diabetic rabbits exhibited characteristics like hyperglycaemia and hyperproteinaemia. The extracts (aqueous extract of *T. bangwensis leaf* and coconut water extract of *P. nitida* seed) independently affected the diabetic rabbits as evident by the significant reduction in the levels of the serum and tissue biomolecules (blood glucose, protein) in the diabetic rabbits to almost the level in the control. Overall, the plant independently demonstrated to be efficacious as espoused by their antihyperglycaemic and hyperproteinaemic actions thus alleviating the biochemical disorders associated with diabetes and hence confirming the antidiabetic activity of the extracts.

REFERENCES

[1] L. M. Tierney, S. J. McPhee, and M. A. Papadakis, *Current Medical Diagnosis and Treatment*, International edition. New York: Lange Medical Books, McGraw-Hill, 2002.

[2] NHANES, *National Health and Nutrition Examination Survey 2002-2009*, India, 2009.

[3] World Health Organization, *World Health Statistics 2011: Facts and Figures about Diabetes,* WHO Statistical Information System, 2011.

[4] World Health Organization, *Report of The WHO Expert Committee on Diabetes Mellitus*, Technical Report Series 646, Geneva, vol. 66, 2000.

[5] E. O. Olapade, "Modern Ethnomedicine in Diabetes Mellitus," *Natural Cure Series*, 2: 120, 1995.

[6] A. M. Gray, and P. R. Flatt, "Insulin-Secreting Activity of the Traditional Antidiabetic Plant *Viscum album* (Mistletoe)", *Journal of Endocrinolog,* vol. 160, pp. 409–414, 1999.

[7] S. Lenzen, "The Mechanisms of Alloxan and Streptozotocin-Induced Diabetes," *Diabetologia*, vol. 51, no. 2, pp. 216–226, 2008.

[8] P. E. Lacy and M. Kostianosvky, "Method for the Isolation of Intact Islets of Langarhans from the Rat Pancreas," *Diabetes,* vol. 16, pp. 35-39, 1963.

[9] A. A. Adesokan, O. I. Oyewole, and B. M. S. Turay, "Kidney and Liver Function Parameters in Alloxan-Induced Diabetic Rats Treated with *Aloe barbadensis* Juice Extract", *Sierra Leone J Biomed Res.,* vol. 1, no. 1, pp. 33-37, 2009.

[10] A. C Gornal, C. J. Bardwell, and M. M. David, "Determination of Serum Protein by Means of Biuret Reaction", *J. Biol. Chem*., vol. 177 pp. 751-756, 1949.

[11] R. G. D. Steel, and J. H. Torrie, *Principles and Procedures of Statistics: A Biometric Approach*, 2nd ed., McGraw Hill Books Co., New York, USA, 1980.

[12] S. S. Gyang, D. D. Nyam, and E. N. Sokomba, "Hypoglycaemic Activity of *Vernonia amygdalina* (Chloroform extract) in Normoglycaemic and Alloxan-Induced Hyperglycaemic Rats," *J. Pharm. Bioresources*, vol. 1, no. 1, pp. 61-66, 2004.

[13] J. S. Kim, J. B. Ju, C. W. Choi, and S. C. Kim, "Hypoglycaemic and Antihyperglycaemic Effect of Four Korean Medicinal Plants in Alloxan Induced Diabetc Rats," *Am. J. Biochem. Biotech*., vol. 2, no. 4, pp. 154-160, 2006.

[14] P. E. Ebong, I. J. Tangwho, E. U. Eyong, C. Ukwe, and A. U. Obi, "Pancreatic Beta Cell Regeneration: A Probable Parallel Mechanism of Hypoglycemic Action of *Vernonia amygdalina* Del. and *Azadirachta indica*", *In the Proceeding of the 2006 International Neem Conference*, pp. 83-89, 2006.

[15] T. M. Delvin, *Textbook of Biochemistry with Clinical Correlations*, Sixth Edition. John Wiley & Sons, Inc. Publications, 2006.

[16] A. E. Eno, and E. H. Itam, "Hypoglycaemic agents in leaves of *Eleophorbia drupifera", Phytother. Res.*, vol. 10, pp. 680-682, 1996.

[17] O. A. Akinloye, and B. R. Olorode, "Effect of *Amaranthus spinosa* Leaf Extract on Haematology and Serum Chemistry of Rats", *Nigerian J. Nat. Prod. Med*., vol. 4, pp. 79-81, 2000.

[18] S. K. Swanston-Flatt, C. Day, C. J. Bailey, and P. R. Flatt, "Evaluation of Traditional Plant Treatments for Diabetes: Studies in Streptozotocin Diabetic Mice," *Acta Diabetologica Latin,* vol. 26, pp. 51–55, 1989.

[19] C. N. Aguwa, C. V. Ukwe, S. I. Inya-Agha, and J. M. Okonta, "Antidiabetic Effect of *Picralima nitida* Aqueous Seed Extract in Experimental Rabbit Model," *J. Nat. Remedies,* vol. 1, no. 2, pp. 135–139, 2001.

[20] A. K. Tiwari, and J. M. Rao, "Diabetes Mellitus and Multiple Therapeutic Approaches of Phytochemicals: Present Status and Future Prospects," *Curr. Sci*., vol. 83, no. 1, pp. 30-37, 2002.
[21] KI Rother, "Diabetes Treatment — Bridging the Divide," *N Engl J Med*, vol. 356, no. 15, pp. 1499–1501, 2007.
[22] N. J. Morrish, L. K. Stevens, J. H. Fuller, H. Keen, and R. J. Jerret, "Incidence of Microvascular Diseases in Diabetes Mellitus: The London Cohort of the WHO Multinational Study of Vascular Diseases in Diabetes," *Diabetologia*, vol. 34, pp. 534-589, 1999.
[23] F. G. William, *Review of Medical Pharmacology,* Mc Graw Hill, 20th Edition, 1999.
[24] L. Andrew, and J. Goslin, "Microalbuminuria: Yet Another Cardiovascular Risk Factor?," *Ann. Clin. Biochem*., vol. 36, pp. 700-703, 1999.
[25] P. Zimmet, G. Dowse and C. Finch, "Epidemiology and Natural History of NIDDM- Lessions from the Pacific," *Dialmet Rev*., vol. 12, pp. 121-134, 1996.

International Journal of Innovation and Applied Studies
ISSN 2028-9324 Vol. 3 No. 4 Aug. 2013, pp. 1132-1140

http://www.issr-journals.org/ijias/

A new analytical formulation for investigating in modern engineering for the harmonic distortion occurring at large vibration amplitudes of clamped-clamped beams: Explicit Solutions

H. Atmani[1], R. Benamar[1], and B. Harras[2]

[1]Laboratoire d'Études et de Recherches en Simulation, Instrumentation et Mesure, LERSIM, E.G.T,
École Mohammadia d'Ingénieurs, Université Mohammed V,
Rabat, Morocco

[2]UFR de mécanique, Laboratoire de Modélisation Numérique et Analyse des Structures, LAMNAS,
Université Sidi Mohamed ben Abdellah, Faculté des sciences et Techniques,
Fès-Saiss, Morocco

ABSTRACT: This work is a contribution to the numerical modeling and computer implementation of geometrically non-linear vibrations of the thin beams. The spatial distribution over the beam span of the harmonic distortion induced by large vibration amplitudes has been examined, and an analytical investigation has been elaborated to describe this aspect of non-linear vibration. This model allowed us to obtain the explicit analytical expressions for the non-linear response, including the contributions of various spatial functions, associated to the first and higher time harmonics. In the present work, devoted to this particular but practically very important aspect of non-linear vibration, a review is made of some important experimental and theoretical works on the subject. The model is based on an expansion of the transverse displacement function as a sum of series, each series being the product of a given harmonic time function by a series of chosen basic spatial functions, multiplied by the unknown contribution coefficients, to be determined. The explicit analytical expressions obtained for the function contributions corresponding to the first time harmonic are identical to those obtained in the previous works above assuming harmonic motion, which allows one to consider that the present model is a generalization of the previous ones. Also, the results of the model presented here, corresponding to the higher harmonics, are in a very close agreement with each other. They are also in a qualitative agreement with previously published numerical results, based on the hierarchical finite element method.

KEYWORDS: Vibration, non-linear, harmonic distortion, amplitude, multimode.

1 INTRODUCTION

The previous work was concerned with the non linear response of clamped-clamped beams to harmonic excitation exhibits, at large vibration amplitudes. In modern engineering problems, large vibration amplitudes of beam-like or plate-like structures very often occur [1], inducing a dynamic behaviour, which is different in many ways from that predicted by linear structural dynamics theories.

A theoretical model based on Hamilton's principle and spectral analysis has been developed and used to study the non-linear free and steady state periodic forced vibration of beams, homogeneous and composite plates [2], [3], [4], [5], [6], [7], [8], [9], [10] [11], [12]. The model developed in [9] has been extended to the non-linear free vibration of cylindrical shells. The effects of large vibration amplitudes on the first and second coupled transverse-circumferential mode shapes of isotropic circular cylindrical shells of infinite length have been examined in [13], [14],[15]. This model was used to calculate the second non-linear mode of fully clamped homogeneous rectangular plates with various values of the aspect ratio, and to analyse the

Corresponding Author: H. Atmani (atmanihassan@gmail.com)

effect of non-linearity on the induced bending stresses. In [16], the model presented in [2], [3], [4] was adapted to study the non-linear steady state forced periodic response of C-C and S-S beams; the results obtained were close to those obtained by other methods. More recently, this method has been extended to free vibrations of clamped circular plates and C-C-C-SS plates [17], [18]. Good agreement has been found in each case via comparisons with previous published works. In reference [19], the geometrically non-linear free vibration of symmetrically laminated rectangular plates with the fully clamped boundary conditions has been examined both experimentally and theoretically. The model was validated by comparison with experimental results.

In an improved version of the model, the spatial distribution of the harmonic distortion was also introduced in the analytical and numerical formulation and some results were obtained, which are presented in [20]. In [21], a practical simple "multi-mode theory " based on the linearization of the non-linear algebraic equations, written on the modal basis, in the neighbourhood of each resonance has been developed. Simple formulae have been derived, which is easy to use, for engineering purposes. The approach has been successfully used in the free vibration case to the first, second and third non-linear mode shapes of CC beams, and the first non-linear mode shape of clamped SS beam. It has also been applied to obtain the non-linear steady state periodic forced response of CC and clamped SS beams, excited harmonically with concentrated and distributed forces.

In reference [22], the fundamental mode shape of a clamped-clamped beam has been investigated experimentally at large vibration amplitudes, and least square polynomial approximation fitting procedures were used to numerically estimate its amplitude dependence, and determine its first and second spatial derivatives. Although the excitation was harmonic, the non-linear response of the beam exhibited a harmonic distortion, which was more accentuated near to the clamps, as shown in figures 6 to 8 in [22]. A careful examination of this effect was made via separation of harmonics performed using a B&K analyser. The spatial distribution of the third harmonic component was found to be quite similar to the second mode shape of the clamped-clamped beam, which should exist theoretically at three times the fundamental frequency, according to the linear analysis. This was attributed to a probable coincidence of the third harmonic, due to the non-linear effect, with the second resonance frequency of a clamped-clamped beam. It was also concluded, on the basis of experimental measurements, that the harmonic distortion of the induced strains in the clamped-clamped beam tested are influenced by two factors: non linear effects due to large amplitude oscillations, which change the mode shape, and the contribution of the axial strain to the resultant induced strain, which is dependent upon position along the beam. A laborious theoretical analytical model has been then constructed in an attempt to obtain a more detailed explanation for the behavior of the induced total strains observed in the experimental work. In [8], the amplitude dependant first three non-linear mode shapes of clamped-clamped beams, but the harmonic distortion effect was neglected.

In reference [10], experimental and theoretical investigations of the harmonic distortion of the induced strain components in clamped-clamped beams at large deflections were carried out. It was shown that the bending strain exhibited a significant harmonic distortion due to the considerable contribution of higher harmonics, such as two and three times the excitation frequency, in addition to the fundamental component. The axial strain signal showed much less harmonic distortion, and was basically composed of a component having twice the excitation frequency, with amplitude much larger than the other harmonics. This work showed also that the non-linear vibration due to large deflection amplitudes of a clamped-clamped beam significantly affected the fatigue life, due to the influence of the in-plane strain component. The harmonic distortion had a significant effect in reducing fatigue life than steady vibration at amplitudes of the order of the beam thickness. The experimental results for the particular beam tested showed a 60% reduction in fatigue life at a strain level double the endurance limit, and 75% reduction at three times the endurance limit

Analytical formulations and experimental studies have been concerned with the effects of large vibration amplitudes on the mode shapes and resonance frequencies of a CC beams [1], [23], [24], [25]. Experimental measurements [22], showed that the dynamic response of a clamped-clamped beam, at large deflections, exhibits a spatial dependence of harmonic distortion in the response. Experimental work, reported in [22], has shown that the response harmonic distortion, occurring at large vibration amplitudes, can have a significant influence on the fatigue life of structures undergoing large amplitudes of vibration [24], [25].

The objective of this study, being an extension of the model presented in [20], is to propose a new model for non-linear vibration of CC beams taking into account the harmonic distortion, which occurs at large vibration amplitudes. In the present work, a new approach is presented, based on appropriate simplifications, and allowing direct calculation of the harmonic distortion, via solution of a set of linearised differential equations.

2 FORMULATION OF NON-LINEAR FREE VIBRATION OF CC BEAMS

Consider transverse vibrations of an isotropic beam having an area of cross section S, a length L, a thickness H, a young's modulus E, a mass per unit length ρ and a Poisson's ratio ν. The total beam strain energy can be written as the sum of the strain energy due to bending denoted as V_b, plus the axial strain energy due to the axial load induced by large deflection V_a. Vb, Va and the kinetic energy T are given by [2], [13]:

$$V_b = \frac{1}{2}\int_0^L EI\left(\frac{\partial^2 W}{\partial x^2}\right)^2 dx \quad V_a = \frac{ES}{8L}\left(\int_0^L\left(\frac{\partial W}{\partial x}\right)^2\right)^2 \quad T = \frac{1}{2}\rho S\int_0^L\left(\frac{\partial W}{\partial t}\right)^2 dx \tag{1-3}$$

in which W is the beam transverse displacement.

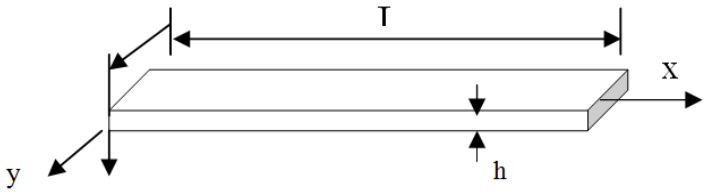

Fig. 1. Co-ordinates system for the beam

Using a generalized parameterization and the usual summation convention used in [9], the transverse displacement can be written as:

$$W(x,t) = q_i(t)w_i(x) \tag{4}$$

Substituting W in the expressions for V_b, V_a, T and rearranging leads to:

$$V_b = \frac{1}{2}q_i q_j k_{ij} \quad V_a = \frac{1}{2}q_i q_j q_k q_l b_{ijkl} \quad T = \frac{1}{2}\omega^2 \dot{q}_i \dot{q}_j m_{ij} \tag{5-7}$$

Where m_{ij}, k_{ij} and b_{ijkl} are defined in references [22]-[23] as:

$$m_{ij} = \rho S\int_0^L w_i(x)\,w_j(x)\,dx \;;\; k_{ij} = \int_0^L\left(\frac{\partial^2 w_i}{\partial x^2}\right)\left(\frac{\partial^2 w_j}{\partial x^2}\right)dx \tag{8-9}$$

$$b_{ijkl} = \frac{ES}{4L}\int_0^L\left(\frac{\partial w_i}{\partial x}\right)\left(\frac{\partial w_j}{\partial x}\right)dx\int_0^L\left(\frac{\partial w_k}{\partial x}\right)\left(\frac{w_l}{\partial x}\right)dx \tag{10}$$

The dynamic behaviour of the structure may be obtained by Lagrange's equations for a conservative system, which leads to:

$$-\frac{\partial}{\partial t}\left(\frac{\partial T}{\partial \dot{q}_r}\right)+\frac{\partial T}{\partial q_r}-\frac{\partial V}{\partial q_r}=0 \quad \text{r=1 to n} \tag{11}$$

Replacing in this equation T and V =(V_a +V_b) by their expressions given above, leads to the following set of non-linear differential equations:

$$\ddot{q}_i m_{ir} + q_i k_{ir} + 2q_i q_j q_k b_{ijkr} = 0 \quad \text{r=1,..., n} \tag{12}$$

Which can be written in matrix form as:

$$[M]\{\ddot{q}\}+[K]\{q\}+2\left[B\left(\{q\}\right)\right]\{q\}=\{0\} \tag{13}$$

Where [M], [K], [B] and {q} are respectively the mass matrix, the linear rigidity matrix, the non-linear rigidity matrix depending on {q} and the column vector of generalised parameters $\{q\}^T=[q_1\ q_2\ \dots\ q_n]$.

Now assuming a harmonic motion:

$q_i(t)=a_i \sin(\omega t)$ (14)

Substituting (14) in (13) and applying the harmonic balance method leads to:

$$2\left(\left[K\right]-\omega^2\left[M\right]\right)\{A\}+3\left[B(A)\right]\{A\}=\{0\} \quad (15)$$

In which {A} is the column vector of the basic functions contribution coefficients $\{A\}^T=\{a_1\ a_2 \dots a_n\}$.

To obtain non-dimensional parameters, we put, as in reference [22]:

$$w_i(x)=Hw_i^*(\frac{x}{L})=Hw_i^*(x^*) \quad (16)$$

$$\frac{\omega^2}{\omega^{*2}}=\frac{EI}{\rho SL^4}\ \ \frac{k_{ij}}{k_{ij}^*}=\frac{EIH^2}{L^3}\ \ \frac{m_{ij}}{m_{ij}^*}=\rho SH^2L\ \ \frac{b_{ijkl}}{b_{ijkl}^*}=\frac{EIH^2}{L^3} \quad (17\text{-}20)$$

Substituting these equations in equation (15) leads to:

$$\left(\left[K^*\right]-\omega^{*2}\left[M^*\right]\right)\{A\}+\frac{3}{2}\left[B^*(A)\right]\{A\}=\{0\} \quad (21)$$

Which may be written also, using the tensor notation as :

$$-\omega^{*2}a_i m_{ir}^*+a_i k_{ir}^*+\frac{3}{2}a_i a_j a_k b_{ijkr}^*=0 \qquad r=1 \text{ to } n \quad (22)$$

Equation (22) is identical to that obtained in reference [9] for the non-linear free vibrations of beams and plates using Hamilton's principle and integration over the range $[0, 2\pi/\omega]$. These equations are a set of non-linear algebraic equations, involving the parameters m_{ij}^*, k_{ij}^* and b_{ijkl}^* which have been computed numerically. In order to obtain the numerical solution for the non-linear problem in the neighbourhood of a given mode, the contribution of this mode is chosen and those of the other modes are calculated numerically using the Harwell library routine NS01A. For the first mode, the procedure consisted on fixing a1 and calculating the higher mode contributions from the system:

$$-\omega^{*2}a_i m_{ir}^*+a_i k_{ir}^*+\frac{3}{2}a_i a_j a_k b_{ijkr}^*=0 \qquad r>1 \quad (23)$$

in which ω^{*2} is obtained from the principle of conservation of energy as :

$$\omega^{*2}=\frac{a_i a_j k_{ij}^*+a_i a_j a_k a_l b_{ijkl}^*}{a_i a_j m_{ij}^*} \quad (24)$$

3 A NEW SIMPLIFIED MODEL FOR BEAMS NON-LINEAR VIBRATION TAKING INTO ACCOUNT THE HARMONIC DISTORTION

3.1 GENERAL PRESENTATION

The purpose of this subsection is to replace the solution process described in the above subsection, based on the harmonic motion assumption, use of the harmonic balance method, and the iterative numerical solution of the resulting set of non-linear algebraic equations, necessary to obtain the beam non-linear mode shapes and resonance frequencies at large vibration amplitudes, by an analytical model, using the assumption, based on experimental data and a recent theoretical work [2-4], that the first time function is predominant, compared to the higher order time functions i.e, $|q_1(t)| \geq |q_i(t)|$ for

i=2 to n. Then, assuming an expression for the first time function involving the first and third harmonics, which is conform to the known data, the resulting system of differential equations in time is analytically solved by superposition to obtain directly the higher order time functions. As stated in the introduction, this formulation has been developed with two objectives: 1) to develop a new approximate but efficient analytical method of solution of the multidimensional Duffing equation, which may be applicable to various non-linear systems. 2) To validate the numerical result of the first model. 3) To provide designers, needing accurate estimates of the structural fatigue life, with explicit analytical expressions, which may be easily implemented in their models, for the non-linear harmonically distorted response.

To obtain in [14] explicit solutions for the non-linear algebraic system (15), it was noticed that the results obtained iteratively in [13] allowed one to write the contribution vector $\{q\}^T$ as: $\{q\}^T = \sin(\omega t)\ [a_1\ \varepsilon_2\ \ldots.\ \varepsilon_n]$, with $\varepsilon i << a_1$, for i >1. Then, both first and second order terms with respect to εi were neglected in the term $a_i\, a_j\, a_k\, b^*_{ijkl}$ of equation (22), which has led to explicit expressions for εi, for i >1.

In the present work, a simple solution of the harmonic distortion problem is attempted, based on the assumption of an unknown, time dependent, contribution vector $\{q(t)\}^T = [q_1\ \zeta(t)_2\ \ldots.\ \zeta(t)_n]$, in which the time functions ζi's are assumed to be small, compared with $q^1(t)$. This allows, after simplifying equation (12), in a manner similar to that adopted in [14], to write the non-linear differential system (12) as:

$$\ddot{\zeta}_r(t)\, m^*_{rr} + \zeta_r\, k^*_{rr} + 2\,\zeta_1^3(t)\, b^*_{111r} = 0 \quad \text{for r=1,...,n} \tag{25}$$

So that if the solution for q_1 obtained from the first equation, corresponding to r = 1, is assumed, the remaining equations, i.e.:

$$\ddot{\zeta}_r(t) m^*_{rr} + \zeta_r k^*_{rr} = -2\zeta_1^3(t) b^*_{111r} \quad \text{for r=2,...,n} \tag{26}$$

appear as set of linear differential equations in ζr, with a right hand side forcing term, due to the non-linearity given by: $f_r(t) = -2b^*_{111r}\zeta_1^3(t)$.

The procedure adopted here was to solve first the first equation, i.e.

$$\ddot{\zeta}_{11}(t) m^*_{11} + \zeta_1 k^*_{11} + 2\zeta_1^3(t) b^*_{1111} = 0 \tag{27}$$

assuming a solution of the form:

$$\zeta_1(t) = a_1(\omega)\sin\omega t + a_1(3\omega)\sin 3\omega t \tag{28}$$

and using the harmonic balance method to calculate $a_1(\omega)$ and $a_1(3\omega)$. Then, this solution was injected in the linearised pseudo-forced system (26), which has been then directly solved by superposition, leading to the time functions $\zeta i(t)$, exhibiting the harmonic distortion due to the non-linearity.

3.2 ANALYTICAL RESULTS

Application of the procedure described above, has led for $a^1(3\omega)$ to:

$$a_1(3\omega) = \frac{1}{2}\frac{a_1^3(\omega) b^*_{1111}}{(9(k^*_{11} + a_1^2 b^*_{1111}) - k^*_{11})} \tag{29}$$

After substitution in (26), the solution obtained, restricted to the third harmonics for $\zeta i(t)$ was:

$\zeta i(t) = \varepsilon_i(\omega)\sin(\omega t) + \varepsilon_i(3\omega)\sin(3\omega t)$ (30)

where

$$\varepsilon_r(\omega) = -\frac{3a_1^3 b^*_{111r}}{2(-m^*_{rr}\omega^{*^2} + k^*_{rr})} \qquad \varepsilon_r(3\omega) = \frac{a_1^3 b^*_{r111}}{2(9(k^*_{11} + a_1^2 b^*_{1111}) - k^*_{rr})} \tag{31-32}$$

The first harmonic component of the non-linear free response, denoted as $W^{*}_{\omega}(x,t,a_1)$ can be explicitly expressed by the following series:

$$W^{*}{}_{\omega}(x,t,a_1)=\left[a_1 w^{*}{}_1(x)+\frac{3a_1^3 b^{*}_{1113}\, w^{*}{}_3(x)}{2((k^{*}_{11}+a_1^2 b^{*}_{1111})-k^{*}_{33})}+\cdots+\frac{3a_1^3 b^{*}_{1119} w^{*}{}_9(x)}{2((k^{*}_{11}+a_1^2 b^{*}_{1111})-k^{*}_{99})}+\frac{3a_1^3 b^{*}_{11111} w^{*}{}_{11}(x)}{2((k^{*}_{11}+a_1^2 b^{*}_{1111})-k^{*}_{1111})}\right]\sin\omega t \qquad (33)$$

The third harmonic component of the non-linear free response, denoted as $W^{*}_{3\omega}(x,t,a_1)$, can be explicitly expressed by the following series:

$$W^{*}{}_{3\omega}(x,t,a_1)=\left[-\frac{a_1^3 b^{*}_{1111} w^{*}{}_1(x)}{2(9(k^{*}_{11}+a_1^2 b^{*}_{1111})-k^{*}_{11})}+\frac{-a_1^3 b^{*}_{1113} w^{*}{}_3(x)}{2(9(k^{*}_{11}+a_1^2 b^{*}_{1111})-k^{*}_{33})}+\cdots+\frac{-a_1^3 b^{*}_{1119} w^{*}{}_9(x)}{2(9(k^{*}_{11}+a_1^2 b^{*}_{1111})-k^{*}_{99})}+\frac{-a_1^3 b^{*}_{11111} w^{*}{}_{11}(x)}{2(9(k^{*}_{11}+a_1^2 b^{*}_{1111})-k^{*}_{1111})}\right]\sin 3\omega t \qquad (34)$$

Expression (33) et (34) is an explicit simple formula, allowing direct calculation of the third harmonic contributions to the first non-linear beam mode shape, as functions of the assigned first mode contribution a_1 and of the known parameters k_{rr}, m_{rr} and b_{111r} computed numerically.

The results given in Table 1 correspond to the values of ε_1, ε_3, ε_5, .., ε_{11} corresponding to the third harmonic, obtained via the present new formulation for some assigned values of a_1 varying from 0.05 to 1.8, which corresponds to a maximum non-dimensional vibration amplitude at the beam centre varying from 0.0794 to 1.225. For each solution, the corresponding values of $\omega^{*}_{nl}/\omega^{*}_{l}$ and the curvature calculated at $x^{*}=0$ are also given. Comparison between Table 1, and data of table 2 taken from reference [9], based on another numerical approach, and the solution of a big set of numerical algebraic equations, shows that there exists a very good agreement between these results for finite amplitudes of vibration up to a displacement equal to the beam thickness, which corresponds to $a_1 \cong 0.67$. For higher values of the vibration amplitude, slight differences start to appear and increase with the amplitude of vibration, as can be seen in Figures 2-4.

Table 1. Explicit results obtained via the present formulation

$a_1(\omega)$	$\varepsilon_1(3\omega)$	$\varepsilon_3(3\omega)$	$\varepsilon_5(3\omega)$
0.05	-0.7061 E-5	-0.22 E-5	-0.20 E-6
0.3	-0.1401 E-2	-0.49 E-3	-0.44 E-4
0.55	-0.7205 E-2	-0.33 E-2	-0.28 E-3
0.8	-0.1755 E-1	-0.12 E-1	-0.87 E-3
1.05	-0.3087 E-1	-0.37 E-1	-0.20 E-2
1.55	-0.6115 E-1	-0.23 E-1	-0.69 E-2

Table 2. Numerical results, taken from reference [2], based on the iterative solution of a non-linear algebraic system

$a_1(\omega)$	$a_1(3\omega)$	$a3(3\omega)$	$a_5(3\omega)$
0.05	-0.7071 E-5	-0.2219 E-5	-0.2077 E-6
0.3	-0.1419 E-2	-0.4743 E-3	-0.4565 E-4
0.55	-0.7450 E-2	-0.2834 E-2	-0.2890 E-3
0.8	-0.1853 E-1	-0.8253 E-2	-0.9050 E-3
1.05	-0.3312 E-1	-0.1729 E-1	-0.2042 E-2
1.55	-0.6678 E-1	-0.4616 E-1	-0.6193 E-2

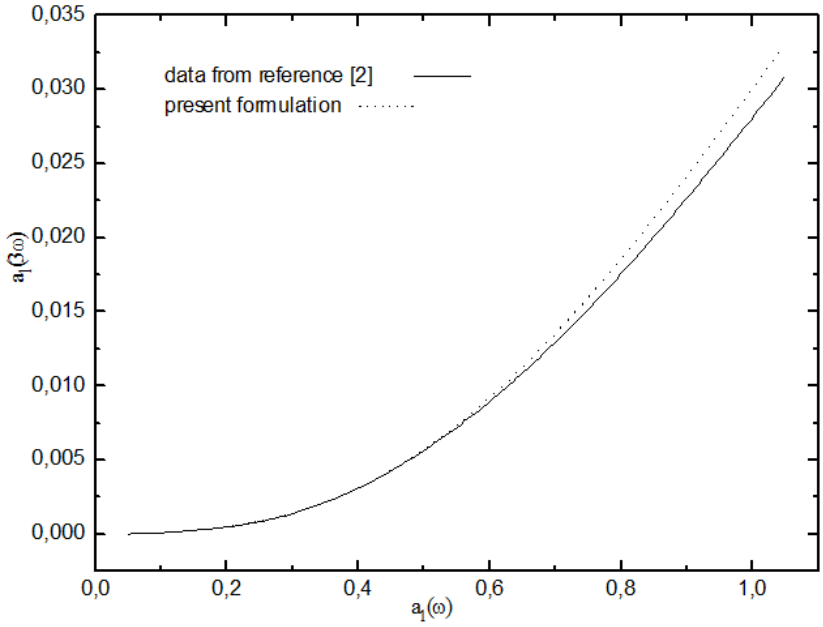

Fig. 2. Comparaison between the contribution $a_1(3\omega)$ of the data taken from reference [2] and the present formulation of the C-C beam

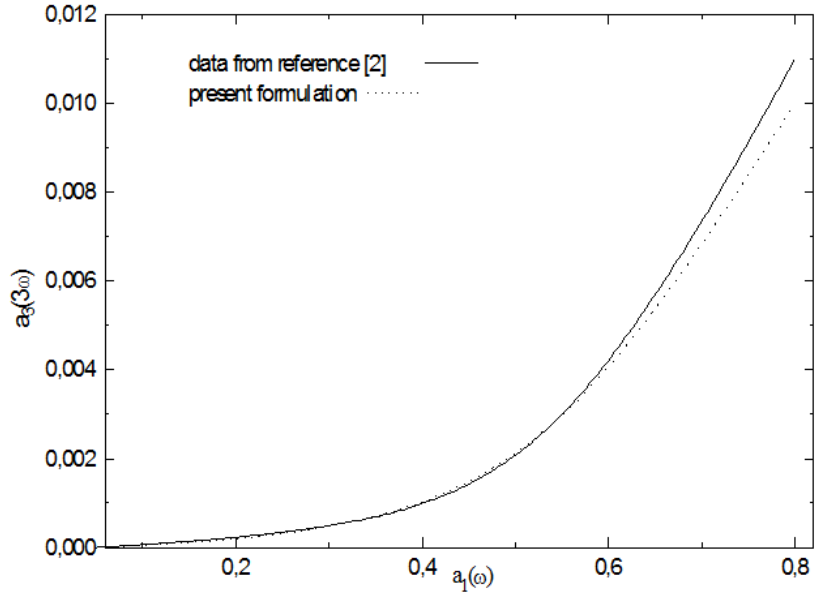

Fig. 3. Comparaison between the contribution $a_3(3\omega)$ of the data taken from reference [2] and the present formulation of the C-C beam

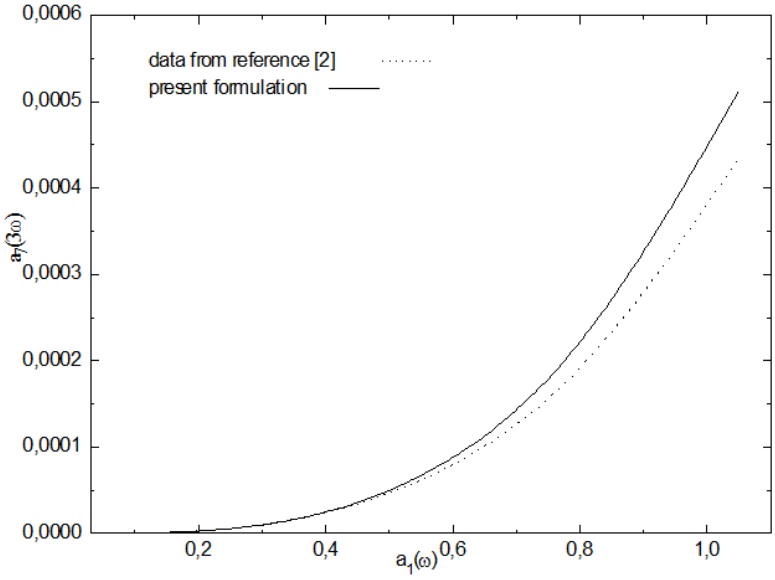

Fig. 4. Comparaison between the contribution $a_7(3\omega)$ of the data taken from reference [2] and the present formulation of the C-C beam

4 CONCLUSION

Considering the harmonic distortion occurring at large transverse vibration amplitudes, simple approximate analytical expressions for the higher mode contribution coefficients to the first and third harmonic of the response have been derived. It gives accurate results for moderate non-linearity, namely for vibration amplitudes up to 0.7 the beam thickness.

These analytical expressions for the harmonic distortion are expected to be very useful in developing new non-linear models for estimating the fatigue life of beams-like structures, undergoing high vibration amplitudes.

REFERENCES

[1] R. Benamar, M.M.K. Bennouna and R. G. White, "Non-linear mode shape and resonance frequencies of fully clamped rectangular beam and plate", *Proceeding of 7th International Modal Analysis conference Las Vegas, Nevada, USA*, 1989.

[2] H. Atmani, A. SEDDOUKI, B. Harras and R. Benamar, "A new approach to the geometrically non-linear dynamic behaviour of a glare 3 hybrid composite panel: explicite solutions", International *Journal of Research and Reviews in Mechatronic Design and Simulation (IJRRMDS),* Vol. 1, No. 3, pp. 49-59, 2011.

[3] H. Atmani, B. Harras and R. Benamar, "A new approach for investigating the spatial distribution and amplitude dependence of the harmonic distortion occurring at large vibration amplitudes of clamped-clamped beams", *the Fourth International Conference on Applied Mathematics and Engineering Sciences, Casablanca,* 23-25 October 2002, (CIMASI'2002).

[4] H. Atmani, B. Harras, and R. Benamar, "Numerically Simulation and Adaptation of a New Approach to the Geometrically Non-Linear Dynamic Behaviour of Fully Clamped Glare 3 Hybrid Composite", *International Journal of Artificial Intelligence and Mechatronics IJAIM*, Vol. 1, No. 6, pp. 156-162, 2013.

[5] H. Atmani, A. Seddouki, B. Harras and R. Benamar, "A new approach to the geometrically Non-Linear Dynamic Behaviour of a Glare 3 Hybrid Composite Panel: Explicit analytical solutions", *Acta Mechanica Slovaca,* No.1, pp. 39-53, 2005.

[6] H. Atmani, R. Benamar, M. Haterbouch and B. Harras, "Modelling and Analysis Multi-Harmonic Non-Linear Free Vibration of Clamped-Clamped Beams", *Second International Conference on Nonlinear Phenomena,* Errachidia, Morocco, 25-27 April, 2005.

[7] H. Atmani, R. Benamar, "The Simulation Modeling for the Non-Linear Free Vibration Taking into Account The Harmonic Distortion of Clamped-Clamped Beams*", International Journal of Artificial Intelligence and Mechatronics, IJAIM*, Vol. 1, No. 6 , pp. 151-155, 2013.

[8] Seddouki, H. Atmani, B. Harras and R. Benamar, "Determination of the geometrical nonlinear dynamic steady state periodic forced response of fully clamped thin rectangular isotropic plates", *Colloque International sur les problèmes non linéaires en Mécanique* Fès, Maroc, 2004.

[9] R. Benamar, M.M.K. Bennouna, and R. G. White, "The effects of large vibration amplitudes on the mode shapes and natural frequencies of thin elastic structures. Part I: simply supported and clamped-clamped beams", *Journal of Sound and Vibration,* vol. 149, pp. 179-195, 1991.

[10] R. Benamar, M. M. K. Bennouna, and R. G. White, "The effects of large vibration amplitudes on the fundamental mode shape of thin elastic structures, part II: Fully clamped rectangular isotropic plates", *Journal of Sound and Vibration,* vol. 164, no. 2, pp. 295-316, 1993.

[11] R. Benamar, M. M. K. Bennouna and R. G. White, "The effects of large vibration amplitudes on the fundamental mode shape of a fully clamped, symmetrically laminated rectangular plate", *Proceeding of the Fourth International Conference on Recent Advances in Structural Dynamics*, Southampton, 1990.

[12] F. Moussaoui, R. Benamar and R. G. White, "The effect of large vibration amplitudes on the mode shapes and natural frequencies of thin elastic shells. Part I: coupled transverse-circumferential mode shapes of isotropic circular shells of infinite length", *White Journal of Sound and Vibration,* vol. 232, no. 5, pp. 917-943, 2000.

[13] R. Benamar, M. M. K. Bennouna and R. G. White, "Spatial distribution of the harmonic distortion induced by large vibration amplitudes of fully clamped beams and rectangular plates", *Proceedings of the 8th International Modal Analysis Conference. Kissimmee,* Florida (2), pp. 1352-1358, 1990.

[14] R. Benamar, M. M. K. Bennouna, and R. G. White, "The effects of large vibration amplitudes on the mode shapes and natural frequencies of thin elastic structures, part III: Fully clamped rectangular isotropic plates-measurements of the mode shape amplitude dependence and the spatial distribution of harmonic distortion", *Journal of Sound and Vibration,* vol. 175, no. 3, pp. 377-424, 1994.

[15] M El Kadiri, R. Benamar and R. G. White, "The non-linear free vibration of fully clamped rectangular plates: second non-linear mode for various plate aspect ratios", *Journal of Sound and Vibration,* vol. 228, no. 2, pp. 333-358., 1999.

[16] L. Azrar, R. Benamar and R. G. White, "A Semi-analytical approach to the non-linear dynamic response problem S-S and C-C beams at large vibration amplitudes Part I: General theory and application to the single mode approach to free and forced vibration analysis", *Journal of Sound and Vibration,* vol. 224, no. 2, pp. 183-207, 1999.

[17] Z.Beidouri, "Contribution to a non-linear modal analysis theory. Application to continuous structures and discrete systems with localised non-linearities", *Doctorat Esciences Appliques, Ecole Mohammadia d'Ingénieurs*, Rabat, 2006.

[18] H. Haterbouch, R. Benamar and R. G. White, "The effects of large vibration amplitudes on the mode shapes and natural frequencies of clamped circular isotropic plates. Journal of Sound and Vibration", *Journal of sound and vibration,* vol. 265, pp. 123-154, 2003.

[19] Harras B., Benamar R., and White R. G., "Geometrically non-linear free vibration of fully clamped symmetrically laminated rectangular composite plates", *Journal of sound and vibration*, vol. 251, no. 4, pp. 579-619, 2002.

[20] R. Benamar " Non-linear dynamic behaviour of fully clamped beams and rectangular isotropic and laminated plates", *Ph.D. thesis, University* of Southampton, 1990.

[21] M. El Kadiri and R. Benamar, "Improvement of the semi-analytical method, for determining the geometrically non-linear response of thin straight structures. Part I: Application to clamped-clamped and simply supported-clamped beams", *Journal of Sound and Vibration,* vol. 249, no. 4, pp. 263-305, 2003.

[22] M.M.K. Bennouna and R. G. White, "The effects of large vibration amplitudes on the fundamental mode shape of a clamped-clamped uniform beam", *Journal of Sound and Vibration,* vol. 96, no. 3, pp. 309-331, 1984.

[23] M.M.K. Bennouna and R. G. White, "The effects of large vibration amplitudes on the dynamic strain response of a clamped-clamped beam with consideration of fatigue life", *Journal of Sound and Vibration,* vol. 96, no. 3, pp. 281-308. 1984.

[24] L.K Chunchung and S.Y Wu, "Non linear vibration of thin elastic plates", *Journal of Applied Mechanics,* Vol. 51, pp. 837-851, 1984.

[25] C. Mei, "A finite element method for non-linear forced vibrations of beams", *Proceedings of the second International Conference on Structural dynamics: Recent advance*s, Southampton, UK, 1985.